

**Proceedings
of the
Third Annual
WIRELESS Symposium**

FEBRUARY 13-17, 1995

SANTA CLARA CONVENTION CENTER, SANTA CLARA, CA

Sponsored by
Microwaves & RF Magazine



Proceedings of the Third Annual *WIRELESS* Symposium

**FEBRUARY 13-17, 1995
SANTA CLARA CONVENTION CENTER, SANTA CLARA, CA**

Sponsored by
Microwaves & RF Magazine

Copyright c 1995
Penton Publishing
All rights reserved

Penton Publishing
611 Route 46 West
Hasbrouck Heights, NJ 07604
TEL: (201) 393-6289
FAX: (201) 393-6297

Printed by **OMNIPRESS . . . "The Proceedings Printer"**
Madison, Wisconsin (800) 828-0305

ACKNOWLEDGMENTS

In a field that changes as rapidly as wireless electronics, organizing a technical program that furthers the education of WIRELESS conference attendees remains a formidable challenge. Yet, in assembling the papers for the Third Annual WIRELESS Symposium, the enthusiasm and energy of the authors and presenters always seems to make the task go quickly.

Special thanks are in order for all the WIRELESS authors and presenters. They often had to give up personal time to complete their articles by the deadline time, as well as prepare their presentations for the conference. In addition, in a field where time to market is everything, these authors spent valuable time traveling to Santa Clara for the WIRELESS conference.

Also, gratitude is due to all WIRELESS Program Chairpeople who, in varying degrees, helped organize and deliver the finest collection of WIRELESS Symposium technical papers yet. Their invaluable advice has helped shape WIRELESS as a true engineer's conference.

Last, but certainly not least, thanks are offered to all of you attending the WIRELESS Symposium & Exhibition. Your continued support and appreciation makes all the effort worthwhile.

Jack Browne

Technical Program Chairman

PROGRAM CHAIRPEOPLE

Paul Khanna, Hewlett-Packard Co., Communication Components Division (Santa Clara, CA)

Mark McDonald, Wireless Communications, National Semiconductor (Santa Clara, CA)

David L. Sprague, InMark—The Independent Marketing Corporation (Walnut Creek, CA)

Algis Juodikis, Juodikis & Associates (Los Altos, CA)

Ben Zarlingo, Hewlett-Packard Co., Lake Stevens Div. (Everett, WA)

Thomas Brinkoetter, Tektronix, Inc. (Beaverton, OR)

Mark A. Sturza, Teledesic Corporation, Communications Systems (Encino, CA)

Todd Westerhoff, Compact Software, Inc. (Paterson, NJ)

Chris Fisher, MicroWave Technology (Fremont, CA)

Victor Perrote, Microwaves & RF (Hasbrouck Heights, NJ)

Technical Proceedings of the Third Annual WIRELESS Symposium and Exhibition

WIRELESS DESIGN METHODS.....1

Digital modulation and methods to simulate the receiver/transmitter. George Kannell and William McGinn, Compact Software (Paterson, NJ).....	2
Spread-spectrum techniques for long-range non-licensed communications. Dean Gaston, Utilicom, Inc. (Goleta, CA).....	10
Comparative study of PPM and FQPSK modulations for infrared systems. Rafael Perez-Jimenez, Victor M. Melian, and Manuel J. Betancor, DET. ETSI Telecomunicacion, University of Las Palmas (Las Palmas, Spain); Francisco J. Lopez-Hernandez, DFT. ETSI Telecomunicacion, Ciudad University (Madrid, Spain); Kamilo Feher, Department of Electrical and Computer Engineering, University of California-Davis (Davis, CA).....	23
Clear-channel assessment for frequency-hopping-based WLANs. Charlie Jenkins, GEC Plessey Semiconductor (Scotts Valley, CA).....	29
GMSK, GFSK, and FQPSK implementations of Feher's patented-licensed technologies. Kamilo Feher, Digital & Wireless Communications Laboratory, Department of Electrical and Computer Engineering, University of California-Davis (Davis, CA).....	44
CDMA/SSMA approach to wireless local loops. S. Daniel Jebaraj, ITI Limited (Bangalore, India).....	72

CELLULAR TECHNOLOGIES.....74

Microcell propagation and antenna diversity measurements for non-line-of-sight communications at 900 MHz. Gregory A. DesBrisay and James D. DeLoach, Jr., Cellnet Data Systems (San Carlos, CA).....	75
RF radiation and radiation checker for cellular phones. A. Kumar, AK Electromagnetique, Inc. (Coteau Station, Quebec, Canada).....	80
A new standard for in-building personal communications service. John Avery, Matsushita Communication Industrial Corporation of America (Alpharetta, GA).....	88
A fast locking scheme for PLL frequency synthesizers. David Byrd, Craig Davis, and William O. Keese, National Semiconductor Corp., Wireless Communications Group (Santa Clara, CA).....	96
PCS-1900: GSM as a candidate for US PCS applications. Rupert Baines, Analog Devices, Inc., Communications Division (Wilmington, MA).....	101

WIRELESS-DATA TECHNOLOGIES.....113

Wireless LANs: Tradeoffs, implementations, and applications. Al Juodikis, Juodikis & Associates (San Jose, CA).....	114
So you want to design a radio for a wireless LAN? Ron Ruebush, Celeritek (Santa Clara, CA).....	115
IEEE 802.11 standards to boost rising WLAN markets in the mobile workplace. Jonathan Edney, Symbionics Networks Ltd. (Cambridge, England).....	116
A high-volume, low-cost, plastic-packaged, 2.4-GHz transceiver MMIC. Liam M. Devlin, B.J. Buck, A.W. Dearn, J.C. Clifton, A.A.G. Frier, and M.W. Geen, GEC-Marconi Materials Technology Ltd. (Caswell, Northants, England).....	121
2.4-GHz silicon RF integration for wireless LANs. Brian Matthews, Harris Semiconductor (Melbourne, FL).....	126
Synchronous FM discriminator for high-data-rate digital communications. Sheng H. Lee and Alvin Wong, Philips Semiconductors (Sunnyvale, CA).....	127

INTEGRATED-CIRCUIT SOLUTIONS.....133

Enabling personal communications through highly-integrated RF signal-processing functionality. John S. Brewer, Jr., Analog Devices, Inc. (Beaverton, OR).....	134
Wideband transceivers and universal base stations. Scott Behrhost, Analog Devices, Inc., Computer Labs Division (Greensboro, NC).....	148
A 1.5-V/25- μ A CMOS microcontroller with pager decoder for alphanumeric and numeric applications. Remy Pache, Centre Suisse d'Electronique et de Microtechnique (CSEM) SA (Neuchatel, Switzerland).....	156
Designing the virtual battery. Ray Waugh, Hewlett-Packard Co., Components Group (San Jose, CA).....	160
Monolithic gain blocks in mini-packages for DC-to-4000-MHz wireless handheld communications. Henrik Morkner, Nhat Nguyen, and Gary Carr, Hewlett-Packard Co., Communications Components Division (Newark, CA).....	169

MEASUREMENT SOLUTIONS.....175

Adjacent-channel power measurements and troubleshooting. Bob Cutler, Hewlett-Packard Co. (Everett, WA).....	176
Cost-effective frequency calibration in field environments. Stuart Jensen, Fluke Manufacturing Co. (Everett, WA).....	183
Testing data-communications systems. David W. Tarver, Telecom Analysis Systems, Inc. (Eatontown, NJ).....	193
Evaluating communications systems and components under multiple-signal conditions, Tim Carey, Hewlett-Packard Co., Video Communications Division (Santa Clara, CA).....	194
Wafer-probe technology for high-speed digital and RF IC testing. Ken Smith, Reed Gleason, and Eric Strid, Cascade Microtech (Beaverton, OR).....	200
Fast phase-noise measurements for high-volume design and manufacturing. Darryl Schick, RDL, Inc. (Conshohocken, PA).....	210
Quantifying the benefits of improved antenna performance in terms of microwave point-to-point link density. Gary Heane, Flann Microwave Instruments Ltd. (Bodmin, Cornwall, England).....	215

MONOLITHIC SOLUTIONS.....220

Study of the feasibility of 20-GHz multistage amplifiers with monolithic technology. Angelo Angelucci, P. Audagnotto, R. Comitangelo, P. Corda, and B. Piovano, Centro Studi e Laboratorio Telecomunications (Torino, Italy); E. Marazzi, M.C. & S.S.R.L. (Milan, Italy).....	221
A MMIC-compatible impedance transformer. Mark W. Ingalls and Eric D. Arnold, Dielectric Laboratories, Inc. (Cazenovia, NY); L. Christopher Henning, Motorola (Fort Lauderdale, FL).....	225
GaAs MMIC LNAs for commercial applications: A new product platform. Michael T. Murphy, Holly Laferrara, S. Smith, and S. Mitchell, M/A-COM, Microelectronics Division (Lowell, MA).....	229
Optimizing the performance of monolithic spread-spectrum receivers in low-power commercial applications. Alex Nadler and Victor Steel, RF Micro-Devices (Greensboro, NC).....	234
Half-rate GSM speech codec: True silicon complexity versus ETSI complexity evaluation. Chris Cavigioli, Analog Devices, Inc. (Wilmington, MA).....	249
Performance evaluation of a low-voltage monolithic FM/IF system for GMSK/GFSK applications. Yanpeng Guo and Alvin Wong, Philips Semiconductors (Sunnyvale, CA).....	264

CELLULAR/RFID APPLICATIONS.....274

- Advantages of mobile cellular-packet-data services for in-car navigation systems. Bernd Eschke, Robert Bosch GmbH (Hildesheim, Germany); Michael Mayer and Wolfgang Schulz, Department of Communications Engineering, University of Paderborn (Paderborn, Germany).....275
- Correlative channel estimation in DS-CDMA systems. Volker Kuhn and Michael Meyer, Department of Communications Engineering, University of Paderborn (Paderborn, Germany).....279
- Improving the reading distance of omnidirectional transponder-based systems. Boni Angelo and Massimo Montecchi, MED s.p.A. (Reggio Emilia, Italy).....285
- Fundamental constraints on RFID tagging systems. Peter H. Cole and David M. Hall, Department of Electrical and Electronic Engineering, The University of Adelaide (Adelaide, Australia); Michael Y. Loukine and Clayton D. Werner, Integrated Silicon Design Pty (Adelaide, Australia).....294
- Field-strength monitor receiver for remote-control applications. Rainer Perthold, Albert Heuberger, and Ludwig Wallrapp, Fraunhofer-Institut fur Integrierte Schaltungen (Erlangen, Germany).....304
- Integrated SAW oscillator in bipolar technology. Albert Heuberger and Eberhard Gamm, Fraunhofer-Institut fur Integrierte Schaltungen (Erlangen, Germany).....305

PERSONAL COMMUNICATIONS.....306

- Unlicensed PCS market acts as springboard into emerging mobile communications field. Henk Koopmans, Symbionics Communications Ltd. (Cambridge, England).....307
- Design of direct digital frequency synthesizers for wireless personal communications systems. Sang-Gon Lee, Eun-Taek Jeong, Yong-Ro Kim, and Heung-Gyoon Ryu, Department of Electrical Engineering, Chungbuk National University (Chungbuk, Republic of Korea).....311
- PCS designers turn to component manufacturers with systems engineering and integration experience. Kim Goryance, Allen Telecom Group, Allen Telecom Systems Division (Cleveland, OH).....318
- High-speed subcarrier data system (HSDS). Gary Gaskill and Ken Gray, SEIKO Telecommunication Systems, Inc. (Beaverton, OR).....322
- Multimedia support in personal communications networks. Kamran Ghane, Neda Communications, Inc. (Bellevue, WA).....341

MOBILE COMMUNICATIONS/WIRELESS DESIGN.....348

- The AC power line as a wireless medium. Michael Propp, Adaptive Networks, Inc. (Cambridge, MA).....349
- Wireless options abound. Wayne Stargardt, Pinpoint Communications, Inc. (Dallas, TX).....358
- An integrated power-amplifier/switch solution for 1.9-GHz personal communicators. Tom Schiltz, Bill Backwith, and Anju Kapur, Motorola Communications, Semiconductor Products Division (Tempe, AZ); Jean-Baptiste Verdier, Motorola Semiconducteurs S.A. (Toulouse, France).....363
- Mobile communications: High-frequency parts for GSM, PCN, DECT, and other systems, with special focus on GaAs MMICs and small-signal semiconductors. Ludwig Scharf and Jorg Lutzner, Siemens AG, Semiconductor Group (Munich, Germany).....370
- An improved PLL design method without ω_0 and ζ . Morris Smith, Motorola, Inc., MOS Digital/Analog IC Division (Austin, TX).....381
- Phase-prediction digital synthesizer for mobile communications. Young J. Jung and Young O. Park, Mobile Communications Technology Division, Electronics and Telecommunications Research Institute (Daejeon, Republic of Korea).....400

SATELLITE COMMUNICATIONS....401

The Teledesic satellite system: Overview and design trades. Mark A. Sturza, Teledesic Corporation (Encino, CA).....	402
MCPC-VSATs for rural communications. M.L. Sharma, ITI Limited (Bangalore, India).....	410
Automatic frequency control for VSAT networks. Cheol Sig Pyo, Jae Ick Choi, and Choon Sik Yim, Satcom Technology Division, Electronics and Telecom Research Institute (Yusong Gu, Daejeon, Korea).....	419
Performance of a PM HEMT-based LNA vs. temperature for VSAT applications. A. Caddemi, P. Livreri, and M. Sannino, Dipartimento di Ingegneria Elettrica, Universita degli Studi Palermo (Palermo, Italy).....	425
Direct digital synthesis of FM (chirp) waveforms. D. Cioppi, Micrel S.p.A. (Florence, Italy); P. Tortoli and F. Guidi, University of Florence (Florence, Italy).....	430

COMPONENTS FOR WIRELESS DESIGN....436

Design and implementation of low-noise discrete silicon bipolar transistors and GaAs FET devices in low-current commercial applications at 900 MHz and 2400 MHz. Al Ward, Hewlett-Packard Co., Communications Components Division (Richardson, TX).....	437
A 1-W, Class A, hybrid surface-mountable amplifier for ultralinear multicarrier wireless applications. Masa Omori, John Martin, and Chris Fisher, Microwave Technology, Inc. (Fremont, CA).....	444
Low-cost broadband GaAs RF IC amplifiers. Leonard Reynolds, Jr. RF Micro-Devices (Greensboro, NC).....	445
Unique VCO design for wireless applications. Shankar Joshi, Synergy Microwave Corp (Paterson, NJ).....	452
KTP: A new piezoelectric material for wireless communications. David K.T. Chu, EI DuPont, Central Research and Development Group (Wilmington, DE).....	453

MILLIMETER-WAVE COMPONENTS AND TECHNOLOGY FOR COMMERCIAL COMMUNICATIONS....454

Millimeter-wave communications: Current use and future trends. George Bechtel, Strategies Unlimited (Mountain View, CA).....	455
Microwave technology in 23- and 38-GHz PCN data-communications systems. Roberto Alm, Innova Corp. (Seattle, WA).....	458
Low-phase-noise transmitter sources at 23 and 38 GHz for PCN radio links. Roland Soohoo and Paul Khanna, Hewlett-Packard Co. (Santa Clara, CA).....	464
A heterostructure triple varactor device for a 40-GHz PCN radio source. Kathiravan Krishnamurthy and Robert G. Harrison, Department of Electronics, Carleton University (Ottawa, Ontario, Canada); Erik Boch, Lockheed Canada (Kanata, Ontario, Canada).....	468
Digital transmission over a millimeter-wave fiber-digital radio link. John Park and K.Y. Lau, Department of Electrical Engineering and Computer Sciences, University of California (Berkeley, CA); M.S. Shakouri, Hewlett-Packard Co., Microwave Communications Group (Palo Alto, CA).....	471

Wireless Design Methods

Session Chairperson: Todd Westerhoff,
Compact Software (Paterson, NJ)

Digital modulation and methods to simulate the receiver/
transmitter. **George Kannell and William McGinn,** Compact
Software (Paterson, NJ).....2

Spread-spectrum techniques for long-range non-licensed communi-
cations. **Dean Gaston,** Utilicom (Goleta, CA).....10

Comparative study of PPM and FQPSK modulations for infrared
systems. **Rafael Perez-Jimenez, Victor M. Melian, and Manuel J.
Betancor,** DET. ETSI Telecomunicacion, University of Las Palmas
(Las Palmas, Spain); **Francisco J. Lopez-Hernandez,** DFT. ETSI
Telecomunicacion, Ciudad University (Madrid, Spain); **Kamilo
Feher,** Department of Electrical and Computer Engineering,
University of California-Davis (Davis, CA).....23

Clear-channel assessment for frequency-hopping-based WLANs.
Charlie Jenkins, GEC Plessey Semiconductor
(Scotts Valley, CA).....29

GMSK, GFSK, and FQPSK implementations of Feher's patented-
licensed technologies. **Kamilo Feher,** Digital & Wireless Com-
munications Laboratory, Department of Electrical and Computer
Engineering, University of California-Davis (Davis, CA).....44

CDMA/SSMA approach to wireless local loops. **S. Daniel Jebaraj,**
ITI Limited (Bangalore, India).....72

Digital Cellular Mobile Design

By George Kannell and William McGinn
 Compact Software, 201 Mclean Blvd., Paterson, NJ, 07504

The time is upon us where the way that we communicate is changing more rapidly than ever before. In a few short years, we will be freed from the hard wired communications era. We will be able to stay in contact with one another from virtually any location. In the office, people will no longer be tethered to fixed extensions; rather, their extensions will be carried in their pockets. At home, the same is true and the phones will be pocket sized and transportable outside the home.

In 1993, there were over 20 million cellular subscribers and over 60 million cordless telephones in use [1]. The year 1993 alone saw the fabrication of 14 million cellular phones and several hundred thousand CT-2, DECT, and 902-928 MHz ISM hand held units [2].

The first cellular systems were FM modulated analog with users separated by frequency. These systems are limited in capacity by the allocated frequency band and the spacing between user channels. For example, the advanced mobile phone system (AMPS) used for many years mainly in North and South America has 25 MHz forward and reverse bandwidths. With a channel spacing of 30 KHz, 832 frequency channels will fit in this band.

Cellular communications systems using digital modulation techniques have many advantages over the analog networks. The most important is the improved spectral efficiency since digital techniques allow for a greater user capacity. In addition, digital modulation provides security since it is encoded. Most Frequency scanners sold before 1994 allow eavesdroppers to listen in on analog cellular transmissions. Other digital advantages include enhancements to voice

quality, voice recognition, and voice messaging services.

Tables 1 and 2 show both the analog and digital wireless systems for cellular and cordless telephones. It should be noted that some of the cordless telephones are actually small cellular systems.

Cellular Telephones	
Analog	Digital
AMPS Advanced Mobile Phone System	IS-54 North American Digital Cellular
TACS Total Access Communication System	IS-95 North American Digital Cellular
NMT Nordic Mobile Telephone	GSM Global System for Mobile Communications
	PDC Personal Digital Cellular

Table 1. Cellular Telephone Networks

Cordless Telephones	
Analog	Digital/PCN
CT0 Cordless Telephone 0	CT2/CT2+ Cordless Telephone 2
JCT Japanese Cordless Telephone	DECT Digital European Cordless Telephone
CT1/CT1+ Cordless Telephone 1	PHS Personal Handy Phone System
	DCS-1800

Table 2. Cordless Telephone Networks

Multiple Access Techniques

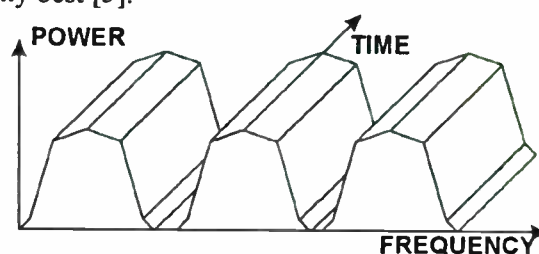
There are three main channelization methods that are used for subscribers to gain access to the cellular networks: frequency division multiple access (FDMA), time division multiple access (TDMA), and code division multiple access (CDMA). It is important to note that these techniques can be used alone or in combination. For example, The IS-54 cellular network uses a combination of FDMA and TDMA.

FDMA is the analog cellular standard [3]. FDMA is used exclusively in all of the analog systems listed in tables 1 and 2. These systems are generally older than the newer digital systems. Both analog and digital FDMA systems have a single user on each channel or frequency. This is illustrated in Figure 1 (a) showing the channels divided along the frequency axis. Since the capacity of these systems is limited by their allocated frequencies, newer digital schemes were developed to add more users for the same bandwidths.

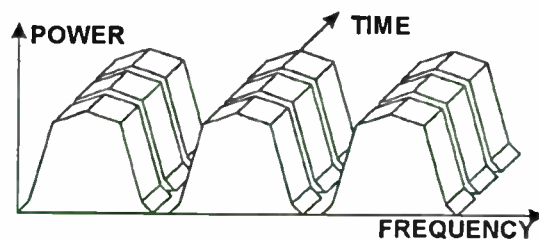
FDMA systems are often upgraded with TDMA techniques to include more than one user at each frequency. These networks have multiple users on each channel divided in time. This is illustrated in Figure 1 (b) showing channel divisions in the frequency and time axes. All of the digital networks in tables 1 and 2 use TDMA except for the IS-95 version of the NADC (to be discussed later). American and Japanese systems have begun with three time slots per frame, increasing the number of users threefold over their analog counterparts. For example, in order to increase capacity, the AMPS network using FDMA is being upgraded by the digital IS-54 system using TDMA. Although both share the exact same frequencies, the IS-54 has three times the capacity of duplex channels. Using more sophisticated voice CODECs and extended TDMA can further increase the capacity by 6 to 15 times [4].

CDMA is a direct sequence spread spectrum technique implemented through the IS-95

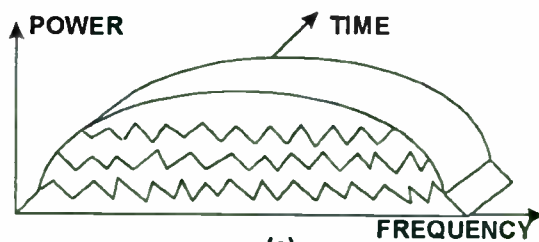
specification of table 1. With CDMA, frequency division multiplexing is still used; but, unlike TDMA, multiple users operate over the same band at the same time as shown in Figure 1. (c). Each user's channel is distinguished from the other through the use of correlative codes. CDMA is touted to have many advantages over other TDMA, the most important being a 6 to 7x increase in capacity. CDMA channels can be repeated in adjacent cells, negating the need for a frequency reuse pattern. These advantages are emphasized by the cluster sizes and number of channels in Table 3. Other touted benefits include CDMA's lower power levels and a lower number of cells. It should be noted here that there is still much controversy as to which technology is really best [5].



(a)



(b)



(c)

Figure 1.(a)FDMA (b)TDMA/FDM (c) CDMA

Digital Cellular Systems

Characteristics	Cellular Telephones			Cordless Telephones		
	IS-54	IS-95	GSM	CT2	DCS1800	DECT
Band (Forward)	869-894	869-894	935-960	864-868	1805-1880	1880-1900
Band (Reverse)	824-849	824-849	890-915	864-868	1710-1785	1880-1900
Bandwidth	50 MHz	50 MHz	50 MHz	2 MHz	150 MHz	20 MHz
Channelization	TDMA/ FDM	CDMA/ FDM	TDMA/ FDM	FDMA	TDMA/FDM	TDMA
Channel Spacing	30 KHz	1250 KHz	200 KHz	100 KHz	200KHz	1728 KHz
Channels/Carrier	3	55-62 ?	8	1	16	12
# of Channels	832 (3 users/ch.)	20 (798 users/ch.)	124 (8 users/ch.)	40	750 (16 users/ch.)	10 (12 users/ch.)
Duplex Method	FDD	FDD	FDD	TDD	FDD	TDD
Channel Bit Rate	48.6 kbps	1.2288 Mb/s	271 kbps	72 kbps	271 kbps	1152 kbps
Speech Codec	VSELP	CELP	RPE-LPT	ADPCM	RPE-LTP	ADPCM
Bit Rate (Voice)	8 kbps	1.2-9.6 kbps	13 kbps	32 kbps	13 kbps	32 kbps
Modulation	$\pi/4$ DQPSK	BPSK/ 0QPSK	GMSK	GFSK	GMSK	GMSK
Mobile Peak Pwr	.6-3 W	.2-2 W	2-20 W	10 mW	.25-2 W	250 mW
Mobile Avg. Pwr	.6-3 W	.2-2 W	.25-2.5 W	5 mW	.03-.25 W	10 mW
Cell Radius	30 miles	30 miles	1-5 miles	?	?	40-140m
Cluster Size (min)	7	1	3	N/A	3	N/A

Table 3. Comparison of Digital wireless network standards.

Cordless or Cellular Telephone?

The differences between the cellular and cordless telephone networks in Table 3 are not always clear since the cordless telephones can be implemented using cellular methods. For the sake of categorizing these two groupings into their respective applications, the following definitions are provided:

The cellular telephone networks are typically designed to handle mobile applications in large coverage areas. This is evident from the cell radius data of Table 3. Subscribers in moving vehicles place extra demand on these systems due to the rapidly changing conditions. This raises issues such as Doppler, multipath, changing distances or power levels, and hand-offs between cells.

The cordless telephones are typically designed for handheld use in small coverage areas. This is also evidenced by Table 3. Users are usually stationary or moving slowly within the confines of a home, building or office environment. These communications are comparatively short range. Multipath can be an important consideration since line-of-sight transmissions can't always be achieved. The attractive features of the cordless telephone are that they are simpler and the hardware is generally smaller and less expensive to consumers than their cellular cousins.

DECT

The digital European cordless telephone (DECT) is a cordless telephone that operates in the 1880-1990 MHz frequency range. It is a cellular network that uses much smaller cells than the large scale cellular networks. It is predicted that the DECT will have nine million subscribers by 1997 [6]. An important feature of the DECT is that it will provide wireless telephone using the private branch exchange (PBX) network.

Norwegian Telecom began testing the DECT in Forde, Norway last April [7]. One hundred

sixty base stations were placed within buildings and homes to provide coverage for an area slightly larger than one square mile. This will allow users to have telephone access from any location within this entire coverage area.

In addition to using TDMA and FDMA, the DECT also uses time division duplex (TDD). This duplex method alternates the RF link between transmit and receive modes over time and at the same frequency instead of separating them into two frequencies as in frequency division duplex (FDD). The DECT's TDD switching is achieved with a single-pole-double-throw switch located near the antenna port.

TDD is also illustrated in Figure 2 showing one DECT frame. The frame is divided into twenty-four time slots where the first twelve are for the forward link and the second twelve are for the reverse link. Thus, there are twelve users for each carrier.

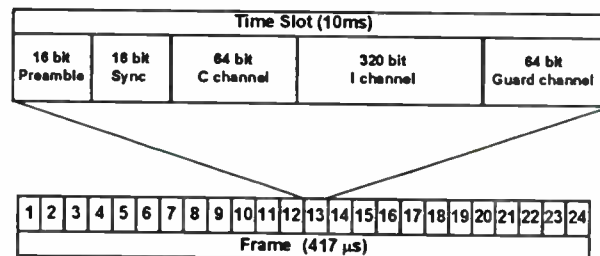


Figure 2. 1 of 24 time slots in a DECT frame

The DECT uses Gaussian frequency shift keying (GFSK) modulation. This is a form of filtered FSK where the data stream passes through a Gaussian shaped impulse response digital filter. This significantly reduces the amount of bandwidth needed for the data.

Simulation of the DECT System

Modern Computer Aided Design tools have evolved, or more correctly, have been engineered to the point that designing and simulating complete communication systems is now possible. Systems such as the DECT, which is our focal point here, can be captured into a CAD system in a meaningful schematic and then simulated for both digital and analog behavior. Among the parameters which can be examined are gain and noise figure of an LNA for example. Trade offs between two such parameters can be made and design improvements made with the help of the simulation. Nonlinear characteristics such as power compression and intermodulation distortion can also be simulated in order to better understand or fine tune a design. Considerations in the digital regime can also be looked at in current system simulation tools. Parameters such

as degradation to modulated carriers and bit error rate can be examined. In addition, Eye diagrams and constellation plots can be generated for the system simulation.

Design Approach:

In general the computer aided approach to system design involves capturing the properties of the components that make up the system and then simulating and optimizing until overall system design specifications are met. For example the basic design specifications for the DECT mobile unit are:

Dynamic Range at the antenna: -100 to -23dBm
 Signal to Noise Ratio at the output: min 9 dB
 Noise Figure: max 12 dB
 Third Order Intercept point: min -20.5dBm
 In Band Blocking: min 80 dB
 Out of Band Blocking: min 106dB

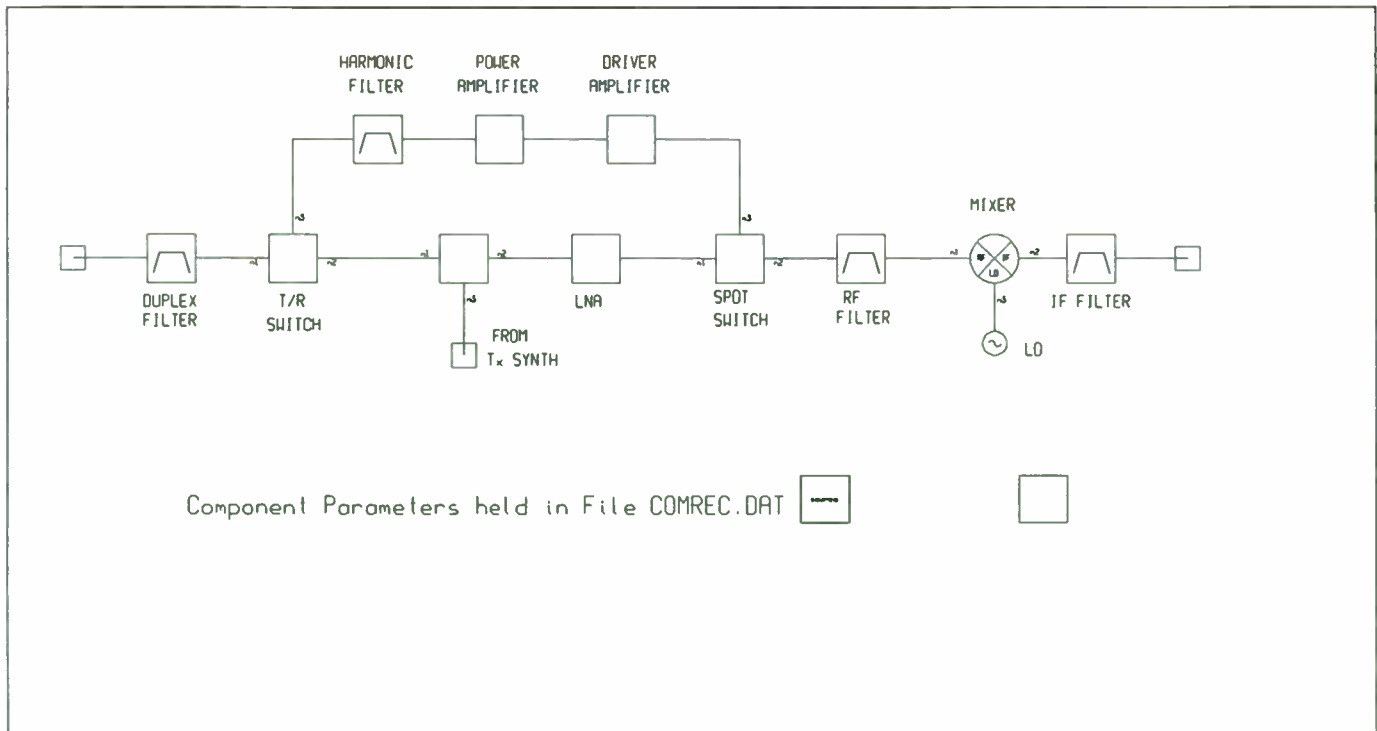


Figure 3. Block diagram of DECT transmit / receive mobile unit.

Component characteristics are entered into the simulator either by entering them directly into a netlist (network listing) or by building the system graphically in schematic capture software. Components are defined using system level or macro parameters. For example, the following defines the linear properties associated with a filter:

```
BBPF 100 99 N=5 ATT=1dB QU=1000
FL=1800MHZ FU=1885MHZ
```

This describes a bandpass filter connected between nodes 100 and 99 having an order of 5, with lower and upper 1dB attenuation frequencies of 1800 MHz and 1885 MHz respectively. The filter is a Butterworth with unloaded Q factors for all components of 1000. An example of defining a component with nonlinear properties follows:

```
MIXER 64 70 26 MS11=-10DB MS12=-60DB
MS21=12DB MS22=-10DB NF=10DB
IP3=10DBM P1DB=0DBM MAXO=10
MINF=.2GHZ MAXF=4GHZ MIX_1
```

This defines an active mixer having 12dB RF to IF conversion gain and a 10dB SSB Noise Figure. The maximum order of spurs to be used is 10 over the frequency range of 200 MHz to 4 GHz. In addition a mixer spur data table is referenced by the label MIX_1.

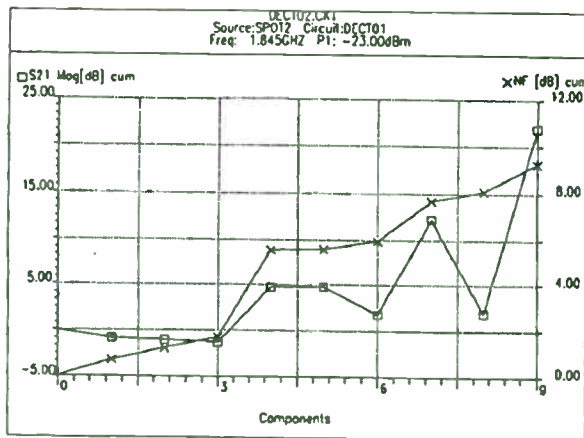


Figure 4. Budget plot showing individual component contributions.

The DECT system simulated is shown in Figure 3. Notice the T/R Switch, creating the different channels for the transmit and receive functions. As an example of design trade-offs simulated, we can consider the overall Noise Figure of the front-end. Figure 4 shows the gain and noise figure on what is termed a Budget plot. This plot displays system parameters as a function of components in the system chain. Figure 4 shows the case where the front-end gain is mainly concentrated after the mixer in an IF amplifier. The NF of the LNA was selected at 4dB and then in order to come in under the 12dB overall system spec, a mixer with 6dB NF was used.

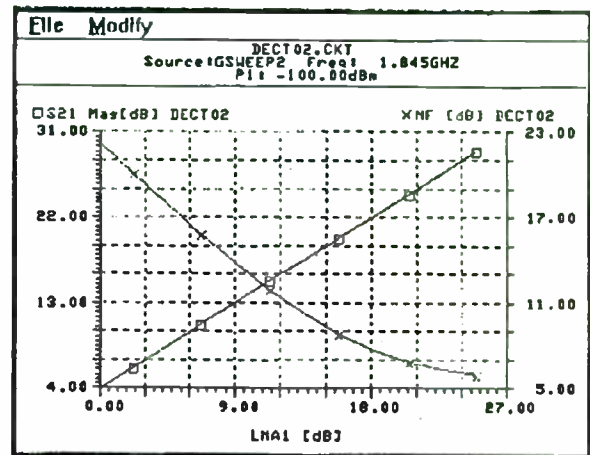


Figure 5. Swept Gain Plot - Passive Mixer

System trade-off analysis can also be performed on the mixer component. To do this, we use the simulator to sweep the gain of the LNA and then repeat the exercise for several different mixer types. In this way we can determine not only the appropriate mixer, but also get an indication of the gain needed from the LNA. Figure 5 shows both the gain and NF of the overall system as a function of the gain of the LNA for the case of a passive mixer with 6dB conversion loss.

Figure 6 shows the same parameters for the case of an active mixer with the same 6 dB NF but with 10 dB conversion gain. The clear indication here is to try to incorporate the active mixer into the system, although this will obviously have cost implications. In this sense, the simulator can also help evaluate the cost issues associated with

choosing one set of components over another. For low cost production it is mandatory that the performance of each circuit is reproducible and easy to achieve, resulting in high yield.

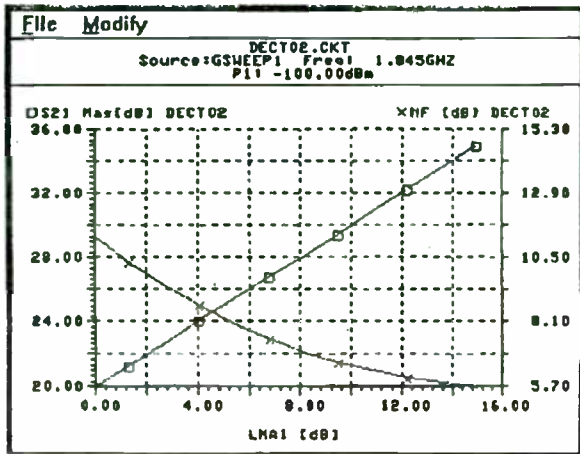


Figure 6. Swept gain plot - Active Mixer

Through simulation, we can also investigate parameters such as output power and gain. Furthermore, the ability to sweep the input power gives us the capability to examine the power compression and gain compression of the system. Figure 7 shows the output power of the system as a function of swept input power.

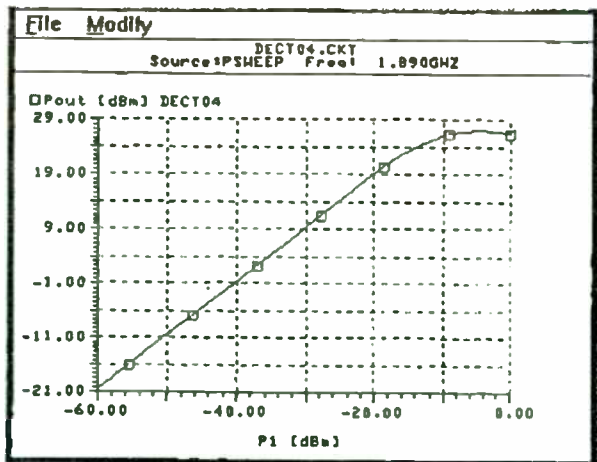


Figure 7. Power Compression.

We can clearly see the system begins to compress at about -15dBm input power. Figure 8 shows the gain compression for the same input power sweep.

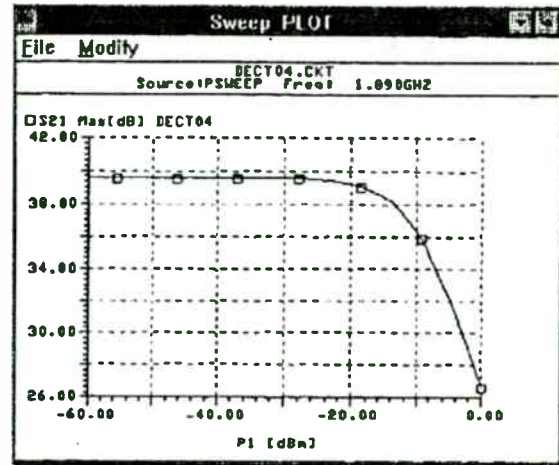


Figure 8. Gain Compression.

Summary

Design trade-offs can be quickly simulated using system level CAD tools and valuable information gained regarding the effect of component characteristics on system behavior. Sweeping parameters such as input power, input frequency and even the gain of a component in the chain can give the designer greater insight. In the case of the DECT transmit/receive section we were able to demonstrate important trade offs in mixer selection and LNA characteristics. Similar insights can be gained on other system parameters through the use of CAD tools.

Bibliography

- [1] J. Ortiz, Zavion, and Holmes, "RFIC Chip Set Targets 900 MHz Tranceivers," RF design, August, 1993, pp. 60-66.
- [2] C. Huang, "Where Do Integrated Circuits Replace Discretes?," Applied Microwaves and Wireless, Summer 1994, pp. 5-6
- [3] D. Balston and R. Macario, *Cellular Radio Systems*, Artech House, Boston, MA, 1993, pg. 31.
- [4] K. Fielhauer, "Using RF Channel Simulators to Test New Wireless Designs", RF design, January, 1994, pp. 56-60.
- [5] N. Stone, "Cellular Radio and the Modern Amateur", QST, March, 1994, pp. 50-55.
- [6] D. Larson, "Wireless Technology: How Test Fits In," Microwave Journal, January, 1994, pp. 63-74.
- [7] R. Woolnough, "More PCS Trials for the DECT," Electronic Engineering Times, February 14, 1994, pg. 20.

**Spread Spectrum Techniques
For Long-Range Non-Licensed Communications**

Dean Gaston
Utilicom Inc.

323 Love Place
Goleta, California 93117
(805) 964-5848 phone
(805) 964-5706 fax

1 ABSTRACT

The number of spread spectrum radios entering the commercial market is proliferating rapidly; however, practically all available systems are designed for high-data-rate LAN and related short-range applications, while long-range requirements remain essentially unexploited. The purpose of this paper is to discuss the application of design techniques to develop spread spectrum systems that can reliably achieve ranges in excess of 100 miles while complying with FCC rules for unlicensed operation. The paper will present practical examples demonstrating the long-range capability of spread spectrum, and specific applications will be described both for maximum-range systems and for shorter-range systems offering extreme robustness to serve critical needs.

2 REQUIREMENTS FOR A ROBUST LONG-RANGE SYSTEM

If an unlimited radio horizon is assumed, the range of a communication system – whether conventional or spread spectrum – is determined by maximum system gain, which must be at least equal to free space path loss plus link margin in the application environment. To facilitate the main discussion, the following paragraphs will define the terms system gain, free space path loss, link margin, and radio horizon.

2.1 System Gain

System gain is defined as:

$$\text{transmit power} + \text{transmit antenna gain} + \text{receiver sensitivity} + \text{receive antenna gain} - \text{feed line losses of the transmit and receive antennas} \quad (1)$$

The basic requirement for system gain is that it exceed the theoretical loss between communication stations by sufficient margin to allow for signal strength fluctuations due to multipath fading and anomalous propagation conditions. The theoretical loss consists of *free space path loss*, and the safety margin is called *link margin*.

2.2 Free Space Path Loss

Free space path loss is the loss of power in a signal as it travels between communication links located in free space. This loss, represented by A can be calculated from the following formula:

$$A_{dB} = [96.6 + 20 \log(\text{distance in miles}) + 20 \log(\text{frequency in GHz})] \quad (2)$$

Table 1 shows free space path loss for each of the ISM bands for various distances.

Table 1. Free Space Path Loss

Distance (miles)	Path Loss (dB) @ 915 MHz (L-Band)	Path Loss (dB) @ 2.4 GHz (S-Band)	Path Loss (dB) @ 5.8 GHz (C-Band)
10	116	124	132
50	130	138	146
100	136	144	152
200	142	150	158
300	145	154	162
400	148	156	164
500	150	158	166
1,000	156	164	172
10,000	176	184	192

2.3 Link Margin

Although free space path loss is by far the major cause of signal attenuation, additional attenuation results from multipath fading, caused by reflections from the ground and other objects, and from Fresnel effect fading.¹ These losses must be compensated for by *link margin*, which is defined as the amount of signal attenuation the system can withstand in excess of the free space path loss while maintaining the required bit error rate (BER). Link margins may range from 10 dB to more than 40 dB, depending on application and maximum acceptable BER.

2.4 Radio Horizon

Radio communications at the high-frequency bands allocated by the FCC for non-licensed spread spectrum communications are "line of sight," meaning that there must be an unobstructed path between communication links. (This does not apply at short ranges, where power may be sufficient to penetrate obstructions such as building walls and floors.) On flat ground, "line of sight" is obstructed by the horizon, which blocks communications; on irregular ground, topographic irregularities, such as hills, may limit communications to a much shorter range than the theoretical horizon.

The maximum radio horizon range for a given elevation of transmit and receive antennas above ground level can be calculated by the following formula

$$R = \sqrt{2h_T} + \sqrt{2h_R} \quad (3)$$

where

R = distance in miles between radio links

h_T = height in feet of the transmitting antenna

h_R = height in feet of the receiving antenna

To realize the extended range offered by enhanced system gain, the radio horizon must also be extended by elevating the antennas as required. If it is not practical to raise the primary transmitter or receiver antenna, repeaters can be placed at elevated locations to extend the range.

In the special case of earth-to-satellite or earth-to-balloon links, communications are possible only when the satellite or balloon is above the horizon; at such times, range is limited only by system gain.

3 INCREASING RANGE BY IMPROVING SYSTEM GAIN

Since range and reliability depend on system gain – given an unlimited radio horizon – increasing range or reliability requires that system gain be improved. This can be done by one or more of the following techniques:

- (1) Increasing transmitter power.
- (2) Increasing receiver sensitivity and processing gain.
- (3) Increasing transmitter antenna gain.
- (4) Increasing receiver antenna gain.
- (5) Reducing antenna feed line losses.

Each of these techniques will be discussed in turn.

3.1 Increasing Transmitter Power

Because the systems under discussion must comply with FCC rules for unlicensed operation, transmitter power is limited to 1 watt (30 dBm) and effective radiated power to 4 watts (36 dBm). Therefore, once either of these limits is reached, further transmitter power increase is ruled out, and this technique is no longer available as a means of improving system gain.

3.2 Increasing Receiver Sensitivity and Processing Gain

For a direct sequence spread spectrum system, receiver sensitivity (S_{dBm}) at ambient temperature is determined by the following equation. (Note that receiver sensitivity is the minimum signal level detectable by the receiver; the lower the number, the better the sensitivity.)

$$S_{(dBm)} = -174_{(dB)} + NF_{(dB)} + 10 \log(BW) - G_p + \frac{E_b}{N_o} \quad (4)$$

where

$$NF = \text{the receiver's noise figure} \quad (5)$$

$$BW = \text{IF bandwidth} = 2 \times \text{code rate (typically)} \quad (6)$$

$$G_p = \text{processing gain} = 10 \log \left(\frac{\text{P/N code rate}}{\text{data rate}} \right) = 10 \log [\text{number of P/N chips per data bit}]^{\text{note 2}} \quad (7)$$

$$\frac{E_b}{N_o} = \text{bit energy-to-noise ratio, 11.2 dB for } 10^{-6} \text{ BER with differential non-coherent BPSK modulation} \quad (8)$$

As the equations indicate, the lower the data rate, the higher the receiver sensitivity and processing gain.

3.3 Increasing Transmitter Antenna Gain

Like transmitter power, maximum transmitter antenna gain is limited by FCC rules for unlicensed spread spectrum operation, which allow a maximum effective radiated power (ERP) of 4 watts (36 dBm). Thus if the maximum allowed transmitter power of 1 watt is used, transmitter antenna gain can not exceed 6 dBi. Within this limit, best results can be obtained for omnidirectional coverage with a 6-dBi collinear antenna with a uniform over-the-horizon coverage of 360°.

For point-to-point operation, it is highly advantageous to reduce transmitter power in conjunction with the use of a high-gain directional antenna. For example, at 2.4 GHz, a 4-foot dish with 27 dBi gain could be used with 9-dBm transmitter power to achieve the ERP limit of 36 dBm. This offers the advantage of courtesy to other users of the band, since energy is focused to a 3-dB beam width of 7°, reducing the chance of interference with other services.

3.4 Increasing Receiver Antenna Gain

Since there is no regulatory limit on receiver antenna gain, it can be increased as desired within the limits of required directionality. For omnidirectionality, 6-dBi gain can be realized by use of a collinear antenna with uniform 360° coverage. For point-to-point applications, narrow-beam antennas can offer substantial gain, as in the example of the 4-foot dish discussed in the previous paragraph. In addition to increasing gain, such an antenna offers a secondary advantage in decreasing total interference levels, since interference outside the 3-dB beam width of 7° is reduced.

3.5 Reducing Antenna Feed Line Losses

Antenna feed line losses can be minimized or eliminated by including a transmitter power amplifier and a low-noise receiver amplifier as part of the antenna assembly. Any line losses between the amplifiers in the antenna and the remainder of the radio system are easily compensated.

3.6 Summary of Techniques for Improving System Gain

Of the techniques available for improving system gain, transmitter power and antenna gain increases offer little potential because of FCC regulations. Best use must be made of the remaining three techniques: Receiver sensitivity can be increased within the limits of minimum acceptable data rates, receiver antenna gain can be increased within the limits of directionality requirements and maximum size constraints, and antenna feed line losses can be eliminated as a factor limiting system gain. Implementation of these techniques in designing a robust direct sequence link will be discussed in the next section.

4 EXAMPLES OF ROBUST SPREAD SPECTRUM LINKS

This section discusses examples of design implementation for two spread spectrum links, one using direct sequence techniques and the other a hybrid of direct sequence and frequency hopping.

Communication range of systems using these receivers is discussed below in the section titled "Maximum Range Capabilities."

4.1 Robust Direct Sequence Link

With the recent introduction of highly integrated high processing-gain ICs, such as the Unisys PA-100 Spread Spectrum Baseband Receiver, it is now possible to implement robust direct sequence receivers with off-the-shelf components.

The PA-100 can operate with code rates to 32 Mchips and can be programmed for code lengths to 64,000 chips, thus providing a maximum processing gain of 48 dB. Using a code rate of 6.4 Mchips and the full 64,000 code length provides a data rate of 100 bits/second:

$$\frac{6.4 \text{ MCHPS}}{64,000 \text{ CHIPS}} = 100 \text{ bits/second} \quad (9)$$

Processing gain is 48 dB:

$$G_p = 10 \log 64,000 = 48 \text{ dB} \quad (10)$$

Assuming a noise figure of 3 dB and $\frac{E_b}{N_o} = 11.2$ dB for non-coherent differential BPSK modulation, sensitivity will be

$$\begin{aligned} S &= -174 + 3 + 10 \log(12.8 \text{ MHz}) - G_p + 11.2 = \\ &= -174 + 3 + 71 - 48 + 11.2 = -136.8 \text{ dBm} \end{aligned} \quad (11)$$

4.2 Robust Hybrid Link

A hybrid system using both direct sequence and frequency hopping techniques can be used for extremely reliable performance in low data rate applications. However, the use of frequency hopping requires that special attention must be given to direct sequence synchronization time. This is because FCC regulations limit dwell time at each frequency to 400 ms, ruling out the use of a conventional sliding correlator, which can consume a substantial part of this time. Only a digital matched filter design can serve efficiently in this application.

An off-the-shelf ASIC, the STEL-2000A Digital Spread Spectrum Processor developed by Stanford Telecom, can be used to implement such a system. (This ASIC is second-sourced by Zilog as the Z2000A.) An extremely robust hybrid system based on this ASIC can be achieved with the following architecture:

Selecting a 6.4-kchip code rate and the maximum code length of 64 chips yields a 100-bit/second data rate:

$$\frac{6.4 \text{ kchips}}{64 \text{ chips}} = 100 \text{ bps} \quad (12)$$

Processing gain will be

$$G_p = 10 \log 64 = 18 \text{ dB} \quad (13)$$

and band width will be

$$BW = 2 \times \text{code rate} = 12.8 \text{ kHz} \quad (14)$$

Using equation (4) and assuming a noise figure of 3 dB and $\frac{E_b}{N_o} = 11.2 \text{ dB}$ for non-coherent BPSK modulation gives a receiver sensitivity of:

$$S = -174 + 3 + 10 \log(12.8 \text{ kHz}) - 18 + 11.2 = -136.8 \text{ dBm} \quad (15)$$

This receiver has the same data rate and sensitivity as the direct sequence receiver in the previous example; however, it can not be used in a fixed-frequency direct sequence system, since its RF band width does not meet the FCC's 500-kHz minimum band width requirement for direct sequence. With the addition of frequency hopping, however, the design does meet FCC frequency hopping requirements of 500 kHz maximum band width per channel in the 900-MHz band and 1 MHz in the upper bands.

This system provides interference suppression with 18 dB processing gain contributed by direct sequence and interference avoidance contributed by frequency hopping.

Since RF bandwidth is only 12.8 kHz, a large number of non-overlapping hopping channels are available in each band:

Band	Number of Channels
915 MHz	2031
2.4 GHz	6523
5.8 GHz	9765

However, using a large number of hopping channels places a burden on synchronization time; nevertheless, even with the minimum number of channels allowed by the FCC, the system can maintain its robustness, provided adaptive hopping channel selection is used. (The minimum number of hopping channels required by the FCC is 50 in the 900-MHz band and 75 in the 2.4- and 5.8-GHz bands.)

4.3 Maximum Range Capabilities

The following paragraphs discuss maximum ranges attainable in point-to-point and multipoint applications for both the direct sequence and hybrid receivers discussed above. Note that maximum range is the same for both receiver types, since both have the same data rate and receiver sensitivity.

4.3.1 Maximum Ranges in Point-to-Point Communications

In calculating system gain in point-to-point communications, the following assumptions are made:

- (1) No feed line losses.
- (2) Operation in the 2.4-GHz band.

- (3) Use of 4-foot dish antennas with 27 dBi gain. (Transmit power is limited to 9 dBm, providing maximum allowable ERP or 36 dBm.)

Under these condition, system gain is:

$$S_{dBm} = xmt\ pwr + xmt\ ant\ gain + rcv\ sens + rcv\ ant\ gain = 9 + 27 + 136.8 + 27 = 199.8\ dBm \quad (16)$$

If a 20-dB link margin is assumed, maximum allowable free space path loss is 179.8 dB. In the 2.4-GHz band, this allows a maximum line-of-sight range of 6166 miles, offering the possibility of unlicensed satellite communications, particularly with low earth orbiting satellites (LEOs), whose orbits typically range from 325 to 865 miles.

The comparatively short ranges to LEOs offers the possibility of trading off range for increased data rate; table 2 shows ranges corresponding to various data rates.

Table 2. Data Rate vs. Range, Point-to-Point 2.4-GHz Link with 27-dBi Antenna

Data Rate (bps)	Range (miles) With 20-dB Link Margin
100	6,166
1,000	1,950
10,000	616
100,000	195

It is very important to note that communication ranges for this point-to-point application are identical for all ISM bands for a dish antenna of a given size. This is because the gain of a dish antenna increases with frequency at approximately the same rate as free space path loss, as shown in table 3.

Table 3. Dish Antenna Gain and Attenuation for the ISM Bands

ISM Band	Antenna Gain (dB), 4-Foot Dish	Attenuation (dB) At 1 Mile	Gain Minus Attenuation (dB)
915 MHz	18.5	95.8	-77.3
2.4 GHz	27.0	104.2	-77.2
5.8 GHz	35.0	111.9	-76.9

As the fourth column shows, antenna gain minus attenuation remains virtually the same in all three bands.

4.3.2 Maximum Ranges in Multi-Point Communications

For multipoint communications, the requirement for horizontal omnidirectionality essentially limits antenna gain to approximately 6 dBi. Vertical collinear antennas of practical sizes offer the required performance in all ISM bands. Even in the 900-MHz band, which requires the largest antenna, height does not exceed approximately 4 feet.

Because increased attenuation in the higher bands can not be compensated by increasing antenna gain for multi-point applications, longest ranges are attained in the 900-MHz band.

Table 4 shows maximum ranges for various data rates in each of the bands. A 20-dB link margin is used for the calculations.

Table 4. Maximum Ranges, Omnidirectional Communications with 6-dBi Antenna Gain and 20-dB Link Margin

Data Rate (bps)	Maximum Range (Miles)		
	915 MHz Band	2.4 GHz Band	5.8 GHz Band
100	1412	490	221
1,000	467	155	70
10,000	141	49	22
100,000	46.7	15.5	7

5 DATA RATE VS. SYSTEM GAIN TRADEOFFS

Since receiver sensitivity is a dependent variable of data rate (equations [4] and [7]), increasing data rate results in a reduction of receiver sensitivity and therefore a reduction of system gain. The tradeoffs between data rate and system gain are discussed in this section.

Increases in data rate can be implemented in conjunction with increases of P/N code rate to maintain the ratio in the term

$$\frac{\text{P/N code rate}}{\text{data rate}}$$

in equation (7), leaving processing gain unchanged. However, band width is increased in proportion to code rate ($BW = 2 \times \text{code rate}$). This increases the term

$$10 \log(BW)$$

in equation (7), decreasing receiver sensitivity.

Conversely, leaving the code rate unchanged while increasing data rate reduces processing gain by decreasing the term

$$\frac{\text{P/N code rate}}{\text{data rate}}$$

In either case, receiver sensitivity is decreased.

In deciding whether to increase code rate along with data rate, the designer must consider the following: Maintaining high processing gain by increasing code rate maintains interference rejection, which may be desirable. However, code rate increases are limited by maximum band width allowed by the FCC, and the designer may want to keep band width well below this limit to allow for selective frequency hopping, which makes it possible to avoid narrow-band interference signals that may exceed the system's jamming margin.³

The following parameters can be used in a design offering 1000 bps data rate with selective frequency hopping:

code rate: 12.8 Mchips

code length: 12,800 chips

data rate: $\frac{12.8 \text{ Mchips}}{12,800 \text{ chips}} = 1000 \text{ bps}$

$G_p: 10 \log 12,800 = 41 \text{ dB}$

occupied BW: $2 \times \text{code rate} = 25.2 \text{ MHz}$

In the 5.8-GHz band, this system uses five non-overlapping sub-channels for interference avoidance.

6 PRACTICAL APPLICATIONS

There are a number of practical applications for the high-gain systems described above, some requiring maximum range, others requiring higher data rates at moderate ranges, and still others requiring maximum reliability at shorter ranges. This section discusses typical applications for which these systems are excellent candidates.

Long-Range Sensing and Control

Various utility providers have the need to set up remote control and sensing systems in areas without telephone lines where licensed channels may be unavailable or difficult to obtain. For example, water companies may need to monitor well levels and control pumps in such areas. Electric companies may need to regulate load distribution and, in the future, may be able to control power to residential electrical appliances to minimize peak demand. Gas companies may need to control shutoff valves along distribution pipelines and in the future may want to install remote residential gas shutoffs for use in earthquakes.

Other applications for remote long-range sensing and control systems include automatic irrigation in large agricultural installations, environmental monitoring networks (weather and pollution), and seismic monitoring networks.

Short-Range Alarm and Security

Instead of providing long range, a high system-gain radio link can offer very high reliability in critical short-range applications. For example, a one-mile terrestrial radio link may have a link margin as high as 90 dB, providing extremely robust communications ideal for such applications as fire alarm and security systems in high-rise buildings. With its high system gain, the link would reliably penetrate floors and walls, and a 100-bit/second data rate would be adequate, since the only data requiring transmission would be location (room ID) where a fire has started or security has been violated.

Other applications of such a system include back-up elevator alarms, traffic signal controls to be exercised by emergency vehicles, and other critical alarm and emergency monitors and controls.

7 A LONG-RANGE DATA TRANSMISSION APPLICATION UNDER DEVELOPMENT

Utilicom Inc. has been tasked by the Astrophysics Group of the Department of Physics at the University of California at Santa Barbara to provide a non-licensed spread spectrum link for a sophisticated equipment package designed to record and report cosmic background radiation from the early universe. The equipment is carried aboard a NASA-launched balloon cruising at altitudes to 130,000 feet.

During a number of successful flights which have already taken place, a licensed narrow band FM communication link has been used in a 416-MHz UHF channel at a 4.8-kbps data rate. These flights were restricted to a sub-orbit, allowing data to be downloaded on an uninterrupted basis. However, the next flight, scheduled for June 1995, will place the balloon in full earth orbit; data will be collected and recorded throughout the flight, but transmission of the data to earth can take place only while the balloon is above the horizon with respect to a single earth station. For the balloon's altitude, the radio horizon will be approximately 300 miles.

Because the time for data transmission is limited, data rate of the down link must be increased to 256 kbps, 50 times higher than the 4.8-kbps link used for earlier flights, and the 416-MHz radio link can not handle the task. However, the up link, which is used primarily for transmitting a limited number of commands to the balloon, can continue to operate at the lower data rate, and 416-MHz radio link will be retained for this purpose.

For the down link, Utilicom has designed an optimized frequency-agile transmitter operating with 1 W power output in the 5.6-GHz ISM band. A broad-pattern antenna with 6 dBi gain will be used for optimum coverage in the direction of the earth. Thus ERP will be 36 dBm, the maximum allowed by the FCC for non-licensed spread spectrum communications.

Offset QPSK (OQPSK)⁴ modulation will be used for band width efficiency and minimized power consumption, since the balloon's power resources are limited. QPSK offers twice the data rate of BPSK within the same band width, and the offset mode is less demanding of linearity than conventional QPSK, improving the efficiency of the transmitter and the bit error rate (BER) of the receiver.

A code rate of 32.64 Mchips has been selected, since this is just about the upper limit for highly integrated off-the-shelf ASICs. Code length is 255-chip-per-bit maximal sequence, providing a processing gain of $10 \log 255 = 24$ dB. For QPSK, these parameters yield the desired data rate of 256 kbps:

$$\text{data rate} = 2 \times \frac{\text{code rate}}{\text{code length}} = 2 \times \frac{32.64 \text{ Mchips}}{255 \text{ chips}} = 256 \text{ kbps} \quad (20)$$

Using equation (4) and assuming the following parameters, sensitivity of this design will be -104.1 dBm:

$$N_F = 3.5 \text{ dB}$$

$$BW = 42 \text{ MHz note 5}$$

$$G_p = 24 \text{ dB}$$

$$\frac{E_b}{N_o} = 14.2 \text{ dB for QPSK}$$

thus

$$\text{sensitivity} = -174 + 3.5 + 10 \log(42 \text{ MHz}) - 24 + 14.2 = -104.1 \text{ dBm} \quad (21)$$

At the earth station receiver site, an 8-foot dish antenna with a gain of 41.5 dB will be used. Calculating system gain from equation (2), we get

$$30 + 6 + 104.1 + 41.5 = 181.6 \text{ dB}$$

From equation (2), free space attenuation (A) at 5.8 GHz for 300 miles is

$$96.6 + 20 \log 300 + 20 \log 5.8 = 161.4 \text{ dB}$$

and available link margin is

$$181.6 - 161.4 = 20.2 \text{ dB}$$

Since the earth station is located in a remote and desolate area where multipath fading is expected to be minimal, a link margin of 20.2 dB should be adequate.

Although no interference is expected at the earth station site, the system will incorporate frequency agility to increase interference protection beyond that provided by the processing gain. The receiver will automatically scan the 5.8-GHz band in 1-MHz increments, select the sub channel with the lowest noise, and transmit the channel ID to the balloon through the 416-MHz link. In response, the 5.8-MHz balloon transmitter will switch to the identified sub channel for its data transmission.

This example demonstrates a case in which increased data rates are attained in a system that maintains high reliability at long ranges. In addition, it illustrates that range limitations in non-licensed spread spectrum communications are not the result of FCC transmit power limits, but rather the radio horizon. If such means as high antenna locations or the use satellites or balloons are available to extend or eliminate the radio horizon, substantial ranges can be attained even with the 4-watt ERP limits imposed by regulation.

8 SENSITIVITY COMPARISON: NARROW BAND VS. SPREAD SPECTRUM RECEIVERS

The receiver sensitivity of a narrow-band radio system is given by the equation

$$S_{(\text{dBm})} = -174_{(\text{dB})} + NF_{(\text{dB})} + 10 \log(BW) + \frac{E_b}{N_o} \quad (22)$$

This is identical to equation (4), which gives receiver sensitivity for a direct sequence spread spectrum system, except for the elimination of processing gain (G_p) from the calculation.

The inclusion of processing gain may lead one to conclude erroneously that a direct sequence spread spectrum system offers higher receiver sensitivity than a conventional narrow band system. This is not the case, as the following example illustrates. In this example, we calculate the receiver sensitivity of a narrow-band system having the same data rate – 100 bps – and using the same modulation technique – BPSK – as our spread spectrum system (equation [11]). With the following parameters

$$NF = 3.0 \text{ dB}$$

$$\frac{E_b}{N_o} = 11.2 \text{ dB}$$

$$BW = 2 \times \text{data rate} = 200 \text{ Hz (no spreading)}$$

receiver sensitivity is

$$S_{(\text{dBm})} = -174 + 3.0 + 10 \log 200 + 11.2 = -136.8 \text{ dB} \quad (23)$$

which is the same as obtained in equation (11) for the spread spectrum system. The reason for this is that the term

$$10 \log(12.8 \text{ MHz}) - G_p$$

in equation (11) is equal to the term

$$10 \log 200$$

in equation (23), with both values equal to 23. Since there is no energy spreading in the narrow band system, the loss in receiver sensitivity due to band width is reduced. In the spread spectrum system, this loss is greater because of the spreading, but it is compensated by the processing gain.

Consequently, under conditions of no interference, the communication range should be identical for a narrow-band and a spread spectrum system with the same transmitter power, data rate, noise figure, and $\frac{E_b}{N_o}$. However, under interference conditions, the processing gain of the spread spectrum system ensures longer ranges.

Concern has lately been expressed about increasing use of the spread spectrum bands and the consequent rising of noise floors. For example, a prospective user recently stated that he had measured the noise floor in the 900-MHz band in his locale and found it to be around -80 dB. He concluded that receiver sensitivity greater than this would be wasted.

In the case of narrow-band systems, this conclusion is correct, but it overlooks the strong point of spread spectrum systems, i.e., that they can cope with interference and operate reliably well below the noise – provided that they have been designed with sufficient processing gain.

As more and more users enter the ISM bands, higher processing gains will be required, along with “smart” adaptive frequency hopping techniques that will select the sub band with the lowest noise floor.

9 CONCLUSION

While short-range high data-rate requirements are being well served by commercial spread spectrum manufacturers, other requirements have been neglected.

The technology is now available to exploit the full potential of spread spectrum communications within the limits set by the FCC to provide super long-range systems serving low data-rate requirements, moderate-range systems providing higher data rates, and short-range systems offering the reliability required by critical emergency and alarm systems.

The key to serving these requirements is to take advantage of the means available for increasing system gain, namely improving receiver sensitivity and processing gain, eliminating antenna line losses, and increasing receiver antenna gain. With these techniques, it is possible to attain ranges exceeding 6000 miles with 20-dB link margin at a data rate of 100 bps in the 2.4-GHz band or to attain a link margin of 90 dB at short range (1 mile) for ultra reliability.

With the appropriate tradeoff of parameters and the use of these techniques, a combination of high data rate, high reliability, and long range is currently being incorporated in a one-way link between an earth station and a high-altitude balloon, demonstrating the diverse potential of non-licensed spread spectrum communications

FOOTNOTES

¹Roger L. Freeman, *Radio System Design for Telecommunications* (John Wiley & Sons, 1987), p. 13.

²For a discussion of processing gain, refer to Dean Gaston, "Spread Spectrum Systems: Evaluating Performance Criteria for Your Application," *Proceedings of the Second Annual WIRELESS Symposium* (Penton Publishing, New Jersey, 1994), p. 496.

³Gaston, p. 496.

⁴Robert C. Dixon, *Spread Spectrum Systems with Commercial Applications* (John Wiley & Sons, 1994), pp. 288–289, 438.

⁵Band width can be limited to 1.3 x code rate, since OQPSK is less vulnerable than QPSK to receiver non-linearity.

Comparative Study of PPM and FQPSK modulations for Infrared Systems

Rafael Pérez-Jiménez¹, Victor M. Melián¹, Manuel J. Betancor¹,
Francisco J. López-Hernández² and Kamilo Feher³

¹DET. ETSI Telecomunicación, Univ. Las Palmas. Campus Univ. de Tafira, 35017 Las Palmas, Spain.

Tlf: +3428 452865, Fax +3428451243, e-mail:rperez@cibeles.teleco.ulpgc.es

²DTF. ETSI Telecomunicación, U.P. Madrid, Ciudad Univ. S/N, 28040 Madrid, Spain.

³DCRL. Dpmt. of Electrical & Computer Engineering, University of California-Davis,
95616 Davis CA, USA

Abstract

The main characteristics of the leading modulation techniques for IR wireless application links (16PPM, 4PPM, OOK and FQPSK) and for different baud rates (from 1Mb/s until 10 Mb/s) are analyzed. One of the most important factors for wireless LAN systems is DC power consumption. To calculate DC power consumption frame energy (which is the energy needed to transmit a frame) rather than the bit energy is considered. In these measurements, the most important factor taken into account is the electrical current demanded by the optical emitter (IRED). For a frame of 20 bits and an ON time T_{on} used for calculating power consumption for each modulation, L-PPM consumes more power than OOK or FQPSK for the same baud-rates. It is also concluded that for the IR-PHY proposal, and for the practical IR diode bandwidth of 30 MHz, only FQPSK is a viable option for the 4 and 10 Mb/s rates.

I. Introduction

The aim of this paper is to show the power efficiency (DC power) and other characteristics of some of the most popular modulation schemes for IR Wireless High-Speed Data Links. It is usually assumed that PPM is the most power efficient technique, in this submission we demonstrate that this is not true. We shall compare the DC power consumption (as well as other characteristics) of four modulation and codification schemes: 16-PPM, 4-PPM, OOK and FQPSK [1], and for different baud rates (from 1Mb/s until 10 Mb/s).

A realistic approach to the energy problem should be based on frame energy, i.e., the energy needed to send a frame of data, not on the power needed to send a single bit. According to this, the

most important factor taken into account is the electrical current demanded by the optical emitter (IRED, Infrared Emitter Diode), other consumptions can be neglected because they represent less than 10% of the total power consumption. The actual power consumption depends on the time that the IRED is in the ON state [2]. This time is, for the studied modulations, and for a frame of data as depicted in figure 1.

Table I: T_{on} of an IRED for different modulation schemes. For OOK FQPSK the frame is considered to have the same number of "1" and "0".

Modulation	Baud-Rate	T_{frame}	T_{ON} (IRED)
16-PPM	1 Mb/s	20 μ s	1.25 μ s
4-PPM	1 Mb/s	20 μ s	5 μ s
	2 Mb/s	10 μ s	2.5 μ s
	10 Mb/s	2 μ s	1 μ s
OOK-FQPSK	1 Mb/s	20 μ s	10 μ s
	2 Mb/s	10 μ s	5 μ s
	4 Mb/s	5 μ s	2.5 μ s
	10 Mb/s	2 μ s	1 μ s

For these power consumption measurements, as a first approach, we can consider that OOK and FQPSK have similar T_{on} for baseband communications. The amplitude of these signals varies in order to assure that they have the same average energy per symbol. So for an L-PPM modulation, each pulse should have a voltage $L/2$ times greater than in OOK.

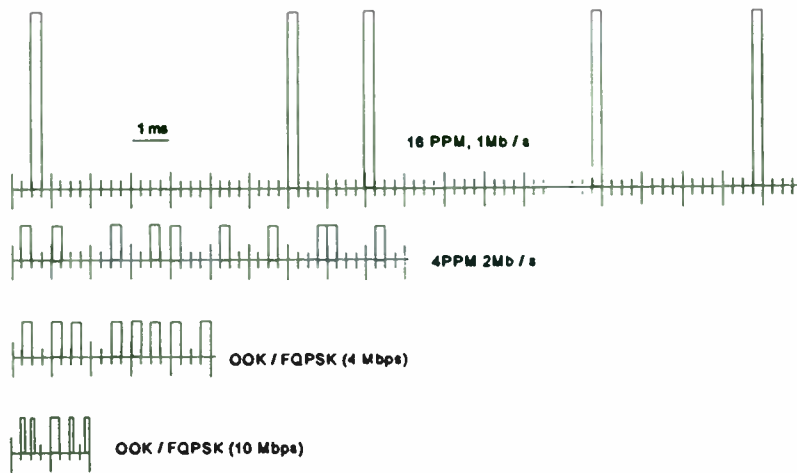


Figure 1: Wave shape of the considered signals (we have considered OOK and FQPSK similar for a first approach of power consumption).

This communication is organized as follows: in the following section the measurements of DC power consumption for PPM and FQPSK modulation are presented, in section III the spectral efficiency, synchronization and other related characteristics of these schemes for infrared wireless communications. In section IV a comparison between the performances of these two systems and final conclusions are also given.

II. Measurements of DC Power Consumption

We have measured the power consumption of these modulation schemes over the circuits depicted on figures 2 and 3. Those are drivers for the Siemens SFH477 high-power emitting diode. The only difference between the drivers is the input logical gate for the PPM, removed for FQPSK so as to guarantee its filtered waveform. It is easily seen that the actual value of the power consumption (DC) across the diode can be obtained by multiplying the current amplitude by the direct voltage on the IRED and by the time while the diode is ON. In order to assure a linear ratio between the power consumption and time that the diode is "ON", we have designed the driver to emit only when the

signal is "1", with the transistor cut-off for the "0" state. We have used separate power supplies for the diode branch and for the IC. The power consumption on the diode branch is always over 94% of the total power consumption, and the DC current on the logic gate is almost constant with the baud rate.

First of all, we establish the DC current consumption for an OOK modulation while varying the baud rate. We use, as a first approach, a linear amplifier configuration. These results can be directly translated to non-linear amplifiers configurations. This DC current is nearly constant and about 120mA (in the diode) from 1Mb/s to 4Mb/s. If we increase the baud rate the power consumption decreases (as well as the total amount of emitted optical power). For the L-PPM signal we shall need $L/2$ -times more peak-to-peak voltage in the output signal. So, as the logic gate limits the base current in the transistor, we have to use a theoretical approach. We can consider that while the voltage (DC) in the diode (V_d) is nearly constant for the measured values in OOK (about 1.2V). The instant peak-to-peak current will rise to $L/2$ -times the value of The OOK signal (considering a linear behavior in the diode, as can be seen in the manufacturer data sheets for the SFH477). So for a frame of 20 bits and multiplying for the T_{on} calculated for each modulation, we obtain the power results given

in table II (considering only the power consumption in the diode).

We have also measured a 2Mb/s FQPSK link [3] using the emitter depicted in figure 3 and for the configuration on figure 4. In figure 5 the obtained eye diagram for the received signal, before the filter, can be observed. The power consumption is similar to the OOK signal for the same baud rate. This confirms the assumption we made of considering the same approach for calculating T_{on} on OOK and FQPSK. The values given for PPM were measured using the driver of figure 2, with the signal entering by the base of the transistor.

So we have that, for the emitter, L-PPM schemes consume the same power than OOK or FQPSK for the low baud-rates, and more for high rates. In the receiver side, obviously, if the baud-rate is higher, we would have less power consumption, as less time required for receiving a frame.

Table II: Power consumption of the IRED driver for different modulation schemes. For OOK/FQPSK the frame is considered to have the same number of "0" and "1"

Modulation	Baud-Rate	T_{ON} (IRED)	DC Power
16-PPM	1Mb/s	1.25 μ s	1.44 μ W
4-PPM	1Mb/s	5 μ s	1.44 μ W
	2 Mb/s	2.5 μ s	0.72 μ W
	10 Mb/s	1 μ s	0.28 μ W
OOK-FQPSK	1 Mb/s	10 μ s	1.44 μ W
	2 Mb/s	5 μ s	0.72 μ W
	4 Mb/s	2.5 μ s	0.36 μ W
	10 Mb/s	1 μ s	0.14 μ W

III. Spectral Efficiency and Synchronization

It is well-known that FQPSK is more spectrally and power-efficient than L-PPM or OOK for the same baud rate [4]. The spectral efficiency of 4-PPM is 0.4 b/s/Hz, for the considered -20dBm bandwidth of the 802.11 standard proposal, while FQPSK has a spectral efficiency more than 1b/s/Hz. The resulting power spectra of these modulation

schemes are shown in figures 6 and 7. 4-PPM 1Mb/s requires 2.5 MHz of bandwidth for 20dBm of spectral attenuation. For 16-PPM 1Mb/s the required bandwidth is even greater. This factor introduces another penalty over the signal, due to the IR-Transmitted power requirement in order to achieve the same S/N ratio in the compared systems, for assumed same receiver bandwidth and BER.

Considering the increase on BER due to synchronization errors, L-PPM is also higher depending on a correct synchronization than FQPSK. This is because the PPM 2Mb/s pulse is defined in 250ns, while in FQPSK, at 4Mb/s the definition time for the symbol is 500ns. This is a very important factor in the extremely jittery IR-wireless channels.

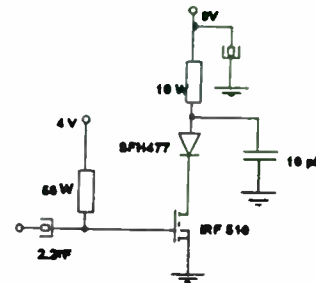


Figure 2: Driver for the FQPSK measurements

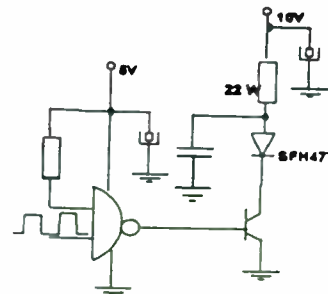


Figure 3: Driver configuration for the PPM signal.

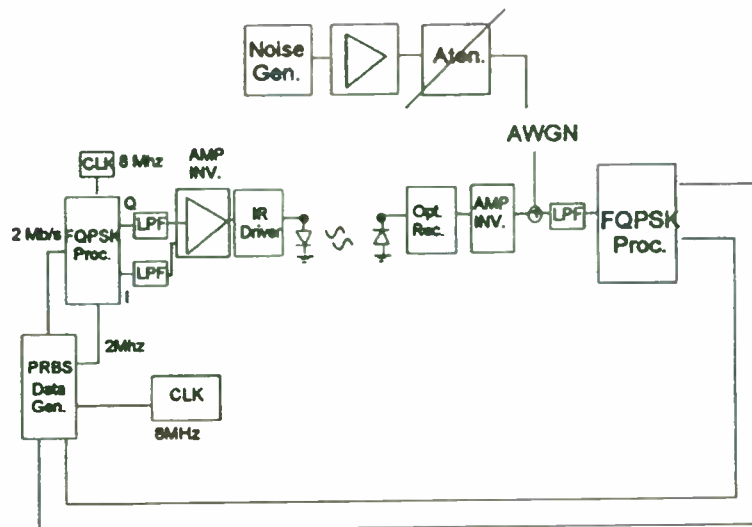


Figure 4: configuration used for testing a FQPSK infrared 2 Mb/s modem

In the other hand FQPSK is less robust against multipath propagation induced penalty than PPM, but more robust than OOK. This problem can be easily avoided using quasi-diffuse optical systems, which reduces the rms delay-spread of the signal until 5-6 ns.

Another consideration also due to the higher spectral efficiency of the FQPSK modulation compared to L-PPM or OOK, is that FQPSK can be easily used on

a carrier-based system [5]. This should avoid problems of interference between distinct emitters and receivers and produce a more efficient use of the IR-spectrum.

IV. Improving the Performances of the PPM Systems

In previous sections we have compared the performances of PPM and FQPSK schemes for IR-WLAN. We can improve some characteristics (particularly, its spectral efficiency) of the PPM systems simply changing its pulse shape. We propose the use of a semi-sinusoidal pulse instead of the square pulse. This new shape reduces the high frequency components of the power spectral density of the transmitted signal. In figure 8 the power spectral density of the basic 4-PPM, 2Mb/s baud rate signal is compared against the spectrum of the modified (we call it *reduced-power 4-PPM*) scheme, also with a baud rate of 2Mb/s. These results, for a quality bandwidth of -21dB, and for the IEEE 802.11 requirements, show an important improvement on the spectral efficiency. Using this alternative pulse shape, we can still recover the signal with the same structures for the standard PPM. The receiver is based on block detection, with maximum likelihood criteria. Its performances on BER can be also improved using a dual feedback equalizer (DFE) structure.

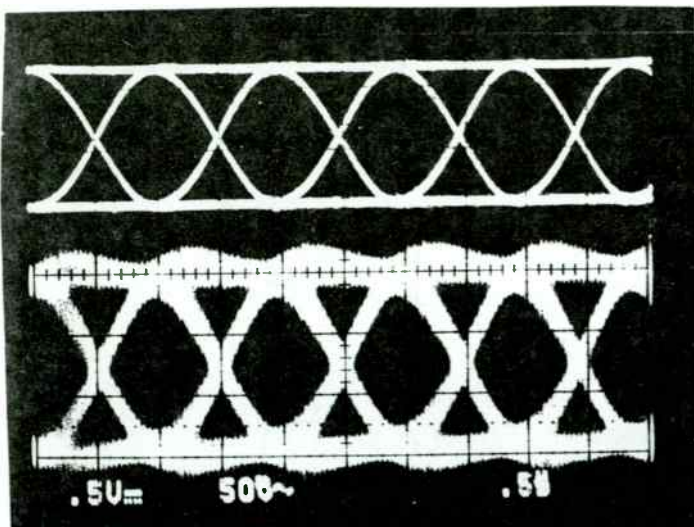


Figure 5: Eye diagram of the transmitted and received FQPSK signal (Channel Q), for baud rate of 2Mb/s

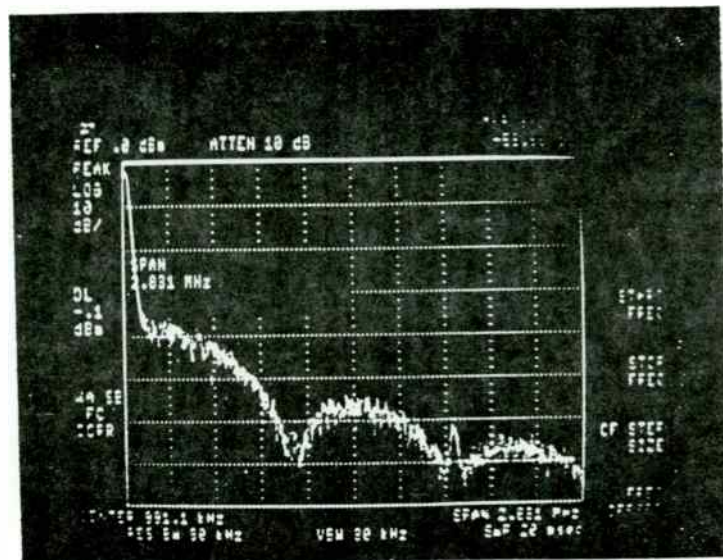


Figure 6: measured PSD of the IR-FQPSK received Q channel

V. Conclusions

In this paper we have compared the performances of L-PPM, OOK and FQPSK modulation schemes for IR Wireless communications systems. The main factor for calculating the power consumption of the communications system is the DC power consumption in the infrared emitting diode. It has been demonstrated that FQPSK and OOK needs less energy to work than L-PPM, working on a higher baud rate. This increase the system performance and is a very important factor for the battery-powered portable notebooks. We have also studied an alternative PPM-based scheme trying to improve the spectral efficiency of the basic PPM system. It is also shown that FQPSK is more spectrally efficient, more robust against jitter than L-PPM, and more robust against multipath propagation than OOK.

References

- [1] Kato, S., Feher, K.: "Correlated Signal Processor". U.S. Patent No. 4,567,602. Issued January 28, 1986. Canada Patent No. 1211-517. Issued September 16, 1986.
- [2] Lopez-Hernandez, F.J., Betancor, M.J., Just, H., Kindl, H.: "Low Power IR-4 Mb/s and 10 Mb/s FQPSK and 1 Mb/s and 2 Mb/s PPM Components and Systems". IEEE 802.11 94/151. May, 1994.
- [3] Kanh, J., et alius: "Non-Directed Infrared Links for High-Capacity Wireless LANs". IEEE Personal

Communications. Second Quarter, 1994.

- [4] Feher, K.: "EXIRLAN-Infrared FQPSK-Based Proposed Standard". IEEE 802.11 94/55. March 1994
- [5] Pérez-Jiménez R., Melián V.M., Betancor, M.J. "Analysis of multipath impulse response of diffuse and quasidiffuse optical links for IR-WLAN" Accepted for INFOCOM'95, Boston, Mass, Apr. 1995

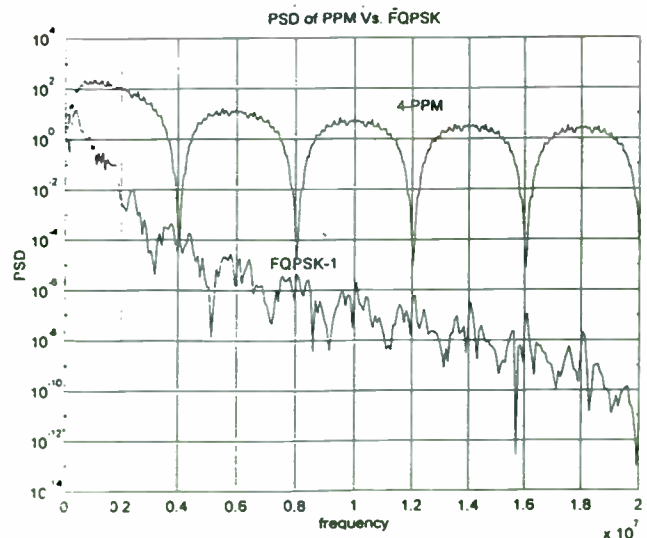


Figure 7: comparison between the received 4-PPM and FQPSK power spectral densities

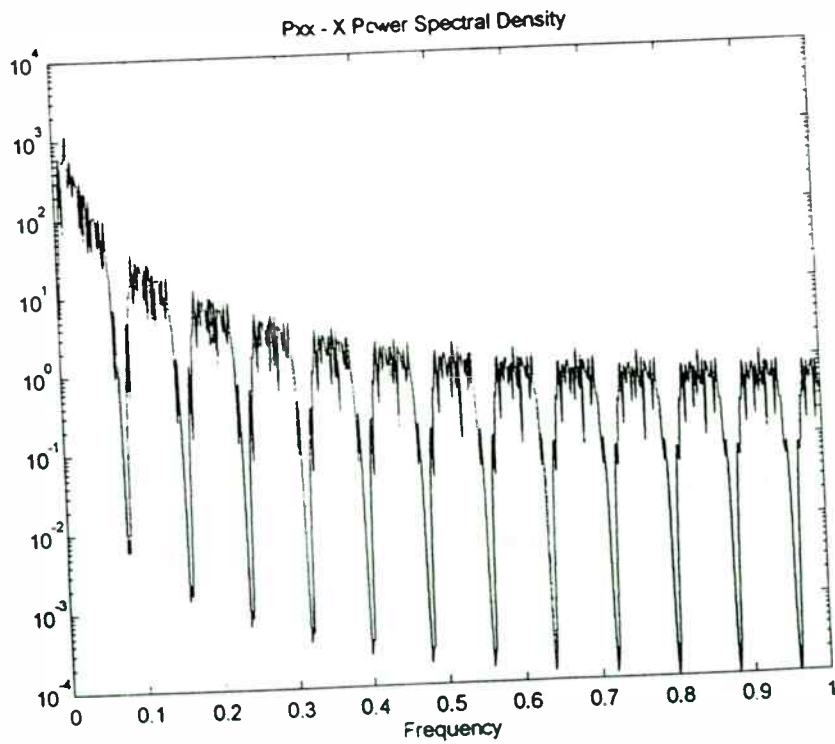
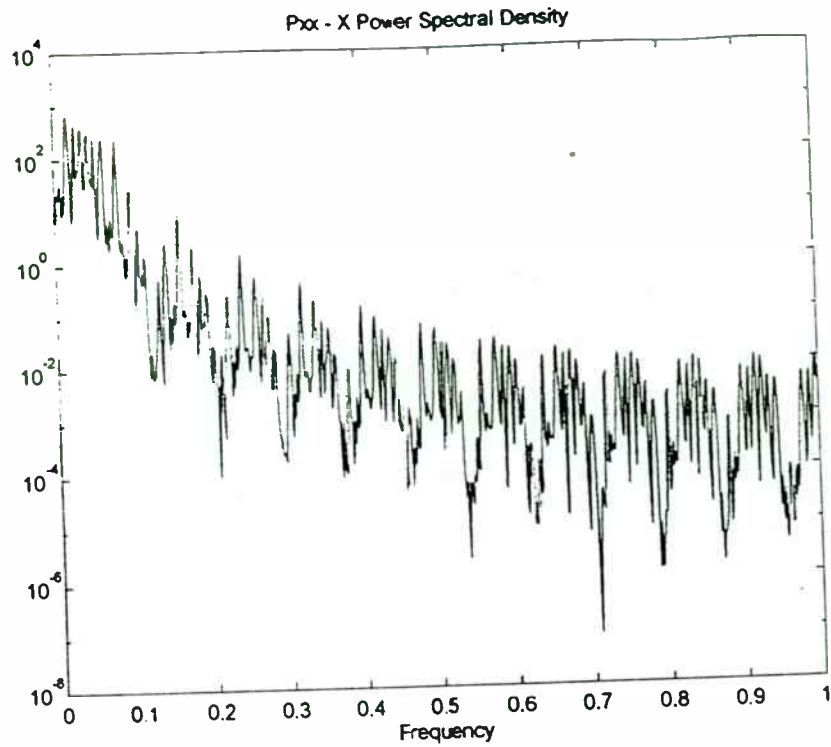


Fig 8: Simulated power spectral density for two PPM configurations: Reduced-Power 4-PPM (above) and basic 4-PPM (below) both of them are presented for frequency 1-50 MHz.

CLEAR CHANNEL ASSESSMENT FOR FREQUENCY HOPPING BASED WLANS

Charlie Jenkins
Wlan System Engineer
Gec Plessey Semiconductor
San Jose, Ca
Ph: 408 451-4734, Fax: 408 451-4710
charlie@sv.gpsemi.com

Abstract... This paper presents a method of Clear Channel Assessment (CCA) based on the human model, a subconscious paradigm by which we communicate each day. The method uses a hybrid approach of both energy and transition detectors that minimizes collisions, is fast and proven in practice. The benefits are threefold:

1. 50% faster than packet detect thus maximizing throughput while minimizing collisions
2. 77% better hidden node detection due to lower CCA sensitivity requirements
3. Ability to pass multiple parameters to MAC layer for higher quality adaptive decisions

The document begins with background information covering scenarios for single and multiple network topologies and then presents the classic approaches to CCA graphically. Next a proposal for a more intuitive CCA approach based on the human model of 'listen before talk' is discussed. This model is then transformed into a CCA approach for WLANs by stepping through the cases that make up the model. A comparison of acquisition times between this and the classical methods is given. Finally, different data modulation types are discussed with their effects on acquisition times.

1. Single Network Scenarios

The purpose of Fig. 1 is twofold:

1. Provide the reader with an appreciation of single network scenarios.
2. Highlight the benefits of a low sensitivity CCA with respect to hidden nodes.

The range of a single transceiver as a receiver is diagrammed in Fig 1. It assumes isotropic antennas, ideal indoor propagation patterns, transmitters of equal power and a receive sensitivity of 80dBm for 10E-5 BER without fading^[1]. Note the 2x increase in range for a BER of 10E-1 versus 10E-5 and a .5x decrease in range for a power output of 10 dBm versus 20 dBm.

The usable range of a two node network is shown in Fig. 1B and is equal to the minimum range of either receiver (1x @ 100mw & 10E-5). Therefore the radius of a transceiver's range is equal to the diameter of the usable network range. Note that transceivers on the perimeter of the circle defined by the range diameter should use a power output of 20dBm whereas transceivers within a circle defined by 1/2 the range diameter could use the 10dBm output assuming a CCA sensitivity requirement for a BER << 10E-5.

Fig. 1C shows the range of a multinode network with a hidden node. Although the node is hidden from all but its nearest neighbor at a BER of 10E-5, if a node is less than 2x from any other network node, it is not hidden at a BER of 10E-1.

Fig. 1D compares a network's range with its RF energy shadow. In set notation, the RF shadow is the union of all individual transceiver ranges whereas the usable network range is the intersection thereof. The 1x dimension defines a network area without hidden nodes. The 3x dimension defines an area where communication is possible with some nodes. The 5x dimension defines the limit of any communication. Rayleigh fading will cause an additional 20dB of loss without antenna diversity (-12dB with diversity) in the network range.

2. Multiple Network Scenarios

The purpose of Fig. 2 is twofold:

1. Provide the reader with an appreciation of on channel interference issues in multiple network scenarios, particularly reliability/throughput during collisions.
2. Highlight a benefit of antenna diversity in avoiding collisions.

The dimensions required for independent operation of two networks (any node to any node) on the same channel without fading is 2x, as pictured in Fig 2A. This spacing is analogous to cell repetition (i.e., spatial diversity) in cellular based systems. Figures 2B-D show progressively higher levels of network overlap with increasing levels of on channel interference. Adjacent and alternate channel levels are also affected to a lesser extent depending on the selectivity of the receiver.

Although a FHSS network inherently provides tolerance to off channel interference, there is a requirement that the network remain operationally intact during on channel interference scenarios including collisions, if reliability and throughput are to be maintained^[4]. Lab tests indicate that significant on channel and adjacent channel interference at a receiver is caused, when 2 nodes transmit on the same channel, if their received power is within 15 dBm (without antenna diversity and within 10dBm with diversity). This channel interference appears as a mix of data and noise transition widths and could easily be false detected as noise albeit at a relatively high RSSI level. A transceiver using packet detect CCA would most definitely signal a clear indication and begin transmission, worsening the existing collision problem - 'I5 in the fog'.

3. CCA Approaches Versus Received Power Level and BER

The purpose of Fig. 3 is twofold:

1. Provide the reader with an appreciation of CCA methods with respect to the power level and BER.
2. Highlight the sensitivity of false detection for each method.

The diagram covers various approaches to CCA (ranging from a simple power detect to a rigorous packet detect) with respect to the required power level at the receiver and the approximate BER of the data received^[2].

Three areas are important:

1. Probability of false sensing (false deferral),
2. Probability of missed sensing (false transmit or collision avoidance) and
3. Ability to detect collision.

Collision avoidance (CA) is important to keep the network throughput high and is best achieved with the lowest CCA sensitivity level (i.e., fewest hidden nodes)^[3,4]. Collision detection (CD) is important for network reliability and can be achieved with a power detect of moderate level in conjunction with a detector looking for a simple data pattern (like sync). The obvious effect of no CD is 'I5 in the Fog' - most data would be corrupted and the network would be down until the next channel slot. The benefit of CD is that the fewer transmitters involved, the more likely that transmissions will get to their destinations uncorrupted (Data at the destination receiver is likely to be corrupted if the received power is within 15dBm without diversity and 10dBm with diversity).

Table 1 - CCA method Vs Sensitivity to Missed Sensing

	<u>Power</u>	<u>Clock</u>	<u>Hybrid</u>	<u>Sync</u>	<u>Packet</u>
avoidance	poor	best	poor	good	fair
detection	good	good	best	fair	poor

Although a higher level has been suggested (12 dBm above 10E-5), the power detect method shown has a more conservative -75 dBm level to better avoid collisions (It still has the worst collision avoidance of these methods) and is inherently efficient at collision detection. The power level can be determined in conjunction with antenna diversity with a 10 bit increase in acquisition time.

The clock detect has the lowest required energy for acceptable performance including the best collision avoidance, the best acquisition time but only fair collision detection.

The hybrid version shown combines power detect AND clock detect in an undesirable way that may aggravate an existing collision. A proposal for a hybrid "human model" CCA with much better characteristics, will be discussed in the next section.

The SYNC method requires more energy and more time but implies a higher false deferral confidence factor than clock detect alone. Likewise packet detect takes even higher energy, BER ~ 10E-4 and significantly more time particularly during asynchronous operation. Table 3 compares the acquisition times for these methods.

A look at these methods gives some insight into desirable CCA characteristics:

1. A CCA approach with the minimum detection level has the greatest ability to detect hidden nodes^[3]. The 10E-1 BER level had a range large enough to detect all hidden nodes for a network [see Fig. 1]
2. CCA should attempt to avoid collisions to keep the throughput high and detect collisions to keep the network reliability intact^[4].
3. The quicker the method, the more opportunities (slots) are provided for access without collisions during the contention period. There is an added benefit of power savings for applications which are generally asynchronous in nature.

4. Proposed Hybrid Method of Clear Channel Assessment

A combination of energy and transition detectors would determine channel assessment in P bit times - where P is a protocol factor to allow time for clock recovery, synchronization and framing using different data encoding methods (about 36 bits for NRZ/16). Further M, the maximum run length in bits must be less than P (17 bits for NRZ/16^[5]). Diversity would increase the probability of a correct assessment in a total time less than 52 bits (16 bits for diversity + 36 bits for transition)^[3]. Table 2 shows a wireless CCA model as compared to the six case "Listen before Talk" human model. Figures 4 - 9 step through the 6 cases.

TABLE 2 - Proposed Hybrid Method Based on LBT Human Model

Human Model		Wireless Model			
Case.	Observation	Action	Observation	Action	CCA Detection Method
1.	quiet	Speak	minimal RF energy	Clear	ED < TH1
2.	sounds	Speak	Th1 < non802 < Th3	Clear	Th1 < ED < Th3 & TD = No trans
3.	background noise	Speak	AWGN	Clear	Th1 < ED < Th2 & TD = Noise
4.	foreground voices	Defer	possible collision	Busy	Th2 < ED < Th3 & TD = Noise
5.	voice	Defer	Th1 < 802 Data < Th3	Busy	Th1 < ED < Th3 & TD = Data
6.	loud racket	Defer	RF energy above Th3	Busy	ED > Th3

NOTES:

1. The Tx/Scan terminology used in the text and diagrams means "clear to transmit" and "channel busy" and is one of several indications/parameters which the MAC layer may use to determine whether to Transmit or Defer. Parameters from the transition detector would be Data, Noise, Notrans and from RSSI would be the power level.
2. N is the number of bits detected - one less than the number of transitions detected.

where:

ED = Energy Detect with example programmable thresholds:

- Th1 = -85 dBm Set based on an extremely low ambient RF (data or noise) signal level which indicates that traffic is distant (BER << 10E-5) or nonexistent. Analogy would be traveling a deserted desert highway.
- Th2 = -50 dBm Set based on a high ambient RF noise signal level unlikely to occur during normal loads and signifies a possible collision already in progress. Analogy would be flares/skid marks on freeway indicating an accident.

Th3 = -20 dB Set based on a desensitizing signal level and is intended to avoid potential collisions which may occur when strong RF signals are present. Analogy might be poor visibility at an airport .

TD = Transition Detect with programmable jitter tolerance and % of occurrences:

Data = $1.0\mu s \times N \pm J_t$ (Jitter tolerance) for $N < M$ (maximum run length in bits)

Noise = % of occurrences of invalid vs valid data widths (0 % indicates data)

No trans = 0 or 1 transition within M bits

For all cases, energy detection is obtained as part of the antenna diversity decision. The existing antenna is sampled, converted and compared to the second antenna level. The higher level is stored and the antenna switched in less than 15 us. The transition detector is about 500 gates and uses programmable transition timings (jitter tolerance and percentage of occurrences) to determine either data, noise or no transitions as defined above. For NRZ data, the acquisition times are shown in Table 3. Other data modulation methods can significantly shorten these times.

Case 1 - Low Power Threshold

This case says clear to transmit below this threshold. This level is more of a reference point than a fixed value since other cases will cover both higher and lower energy levels.

Case 2 - Non 802 Communications

This case says clear to transmit if the channel does not look like 802 FH data. It is the equivalent of speaking in spite of a dog barking or jet overhead (i.e. intelligent life not inanimate noise). The transition detector sees less than two transitions over the run length window M. The peak power outputs of a microwave fall into this category.

Case 3 - RF Noise

This case says clear to transmit if the channel looks like noise. It is the equivalent of speaking in spite of the wind blowing or a cooling fan. The transition detector sees a higher percentage than that programmed for non valid vs valid data widths.

Case 4 - Potential 802 collision detected

This case says busy if the channel looks like noise and is above some moderate energy threshold. It is the equivalent of deferring when several people speak at once. The transition detector sees a higher percentage of transitions [than that programmed for non valid vs valid data widths] AND the power is above a potentially moderate level. My research shows this is a viable case and could avoid "I5 in the fog".

Case 5 - 802 data detected

This case says busy if the channel looks like data. It is the equivalent of deferring when another person speaks. The transition detector sees a lower percentage than that programmed for non valid vs valid data widths.

Case 6 - Extreme Interferer detected

This case says busy if the channel energy is quite high. It is the equivalent of not speaking when a jet engine or rock concert is going! The energy detector sees a high desensitizing radio level which may cause CCA miscues in the network. The reliability of the network is in jeopardy unless "the airport closes for a limited time" (until the next channel hop). The MAC layer may desire to adjust the level over time for an adaptive type CCA.

Table 3 - CCA Bit Delay vs Method

Assumptions: NRZ data bit stuffed as indicated, 80 bit mark/space sync pattern, 16 bit frame, 32 bit header

CCA Method	faster \longrightarrow				^ (faster) ^
	NRZ32 (<u>async</u>)	NRZ32 (<u>sync</u>)	NRZ16 (<u>async</u>)	NRZ16 (<u>sync</u>)	
Energy	4	4	4	4	
Energy w/ div.	16	16	16	16	
CK	71	2	35	2	
SYNC	71	9	35	9	
* TD = DATA	71	9	35	9	
* TD = NOISE	71	9	35	9	
* TD = Notrans	71	9	35	9	
FRAME	80+16	80+16	80+16	80+16	
PACKET	10ms	80+16+32	10ms	80+16+32	

Notes:

1. All units are bit times unless noted
2. TD = Transition Detector as defined on previous page.
3. Synchronous operation assumes CCA detect during preamble
4. Other modulation types can have considerably shorter times for asynchronous operation
5. MAC CCA Target ~ 50us

5. Other Modulation Types

Data modulation encoding other than NRZ may be used to limit the run length between transitions (reducing variable M) and thus reduce the acquisition time ($P > 2 \times M$), particularly with respect to asynchronous operation. A modulation run length limited to 8 bits would need at least 2 times 8 bits to guarantee at least 2 transitions (1 valid bit duration = $1.0\mu s \times N \pm Jt$). There are modulation types which limit run length to 2 bits for any data stream and provide positive benefits for radio operation as well.

6. Summary

This paper presented/discussed three desirable characteristics for CCA:

1. An approach with the minimum detection level has the greatest ability to detect hidden nodes [2].
2. The ability to avoid and detect collisions keeps the network throughput and reliability intact [4].
3. At the MAC layer, the faster the CCA acquisition, the more access slots are available during the contention period.

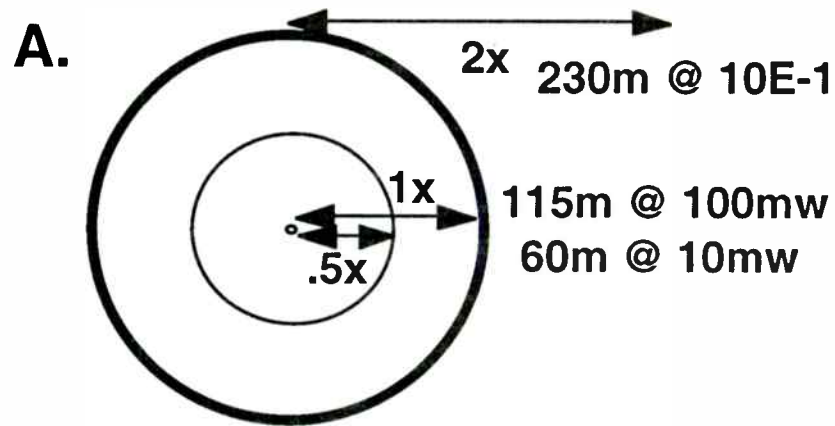
The proposal for a hybrid FH CCA based on the human model using energy and transition detectors provides three major benefits:

1. Very fast acquisition time (sync or async).
2. Maximum hidden node detection.
3. Higher quality decision by obtaining/passing multiple parameters (A singular CCA decision could be made in Phy or Mac layer)

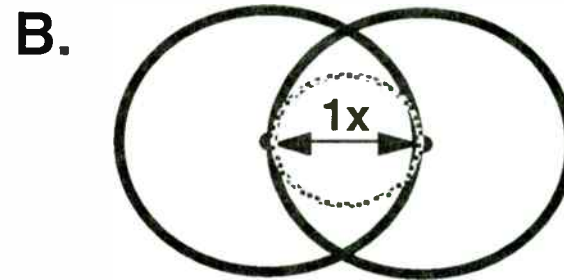
REFERENCES

- [1] GEC Plessey Semiconductors, RF Propagation Considerations For WLAN Applications, Apl Note 145, November 1993
- [2] Jim MacDonald, Proposal For the Use of Packet Detection in Clear Channel Assessment, P802.11-94/79...Proceedings of IEEE802.11, Motorola, March 1994
- [3] Dean Kawaguchi, Carrier Sense with Diversity Model for FH PHY, P802.11-94/70...Proceedings of IEEE802.11, Symbol Technologies, March 1994
- [4] Carlos Puig, RF MAC Simulation Highlights, P802.11-94/20...Proceedings of IEEE802.11, Apple Computer, March 1994
- [5] Ed Geiger, DC Balance and Edge Transitions-Their Impact on Data Recovery and Overall LAN Performance, P802.11-94/72...Proceedings of IEEE802.11, Apple Computer, March 1994

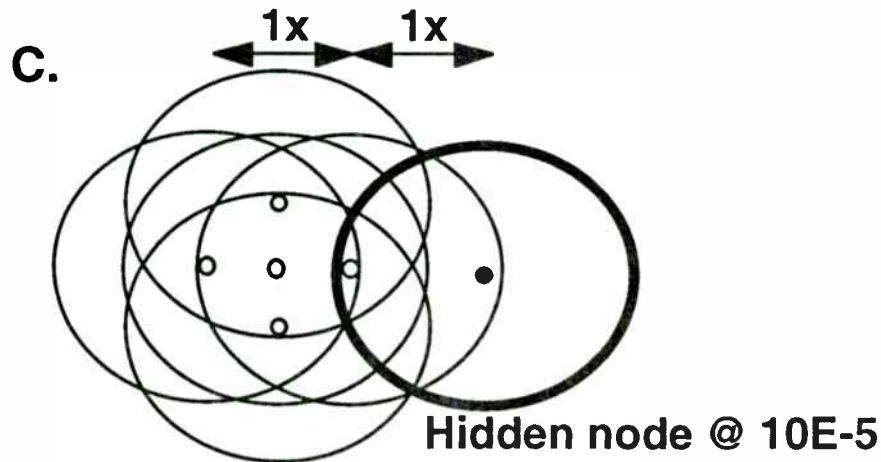
FIG 1 - CCA IN IDEAL SINGLE NETWORK SCENARIOS



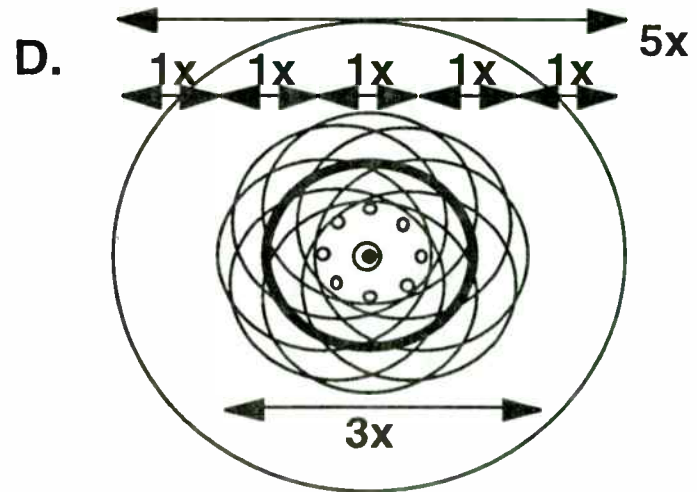
35 Range (radius) of Rx node [1]
(-80dBm Sens @10E-5, no fade)



Range (diameter) of network =
range (radius) of Rx node

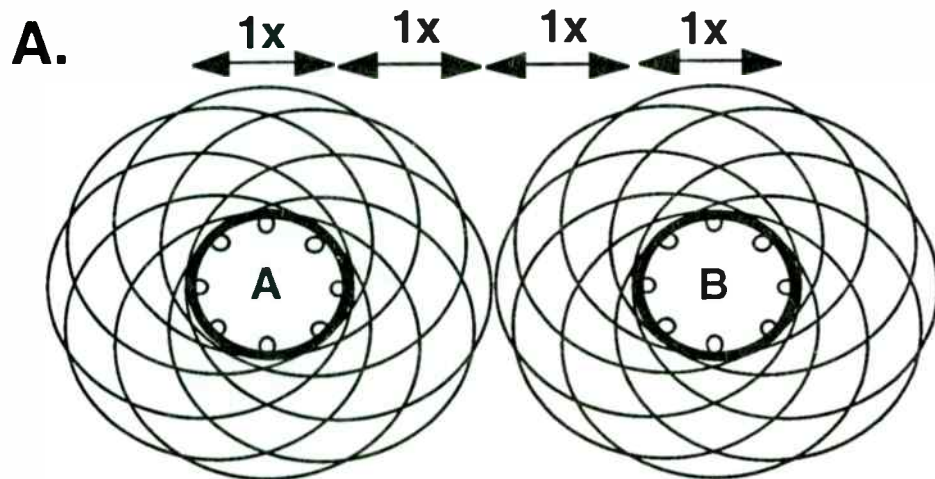


Any node to node separation > 1x

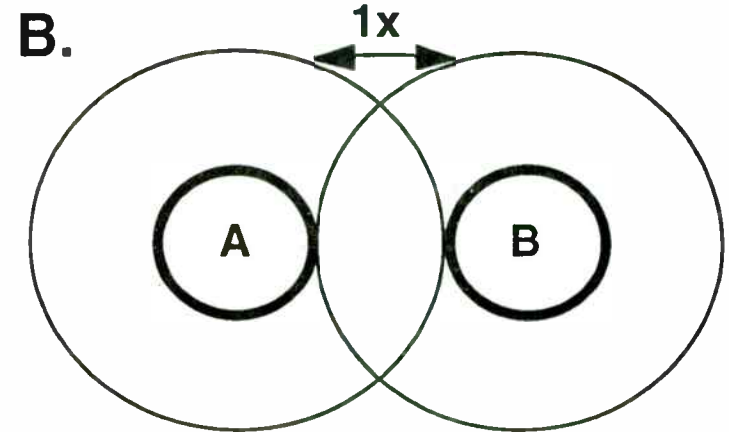


Network's RF Shadow -
10E-5: 3 x range, 9 x area
10E-1: 5 x range, 25 x area

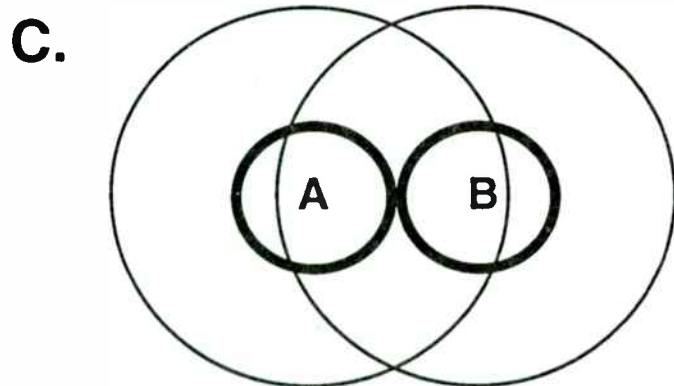
FIG 2 - CCA IN IDEAL MULTIPLE NETWORK SCENARIOS



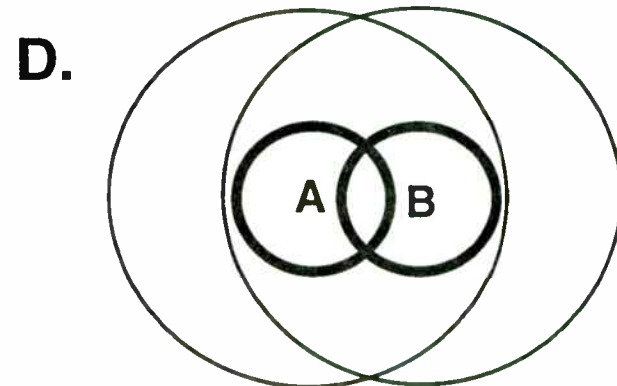
36 If Separation of all A nodes to all B nodes $> 2x$
No Interference



$1x < \text{Separation} < 2x$
Some Interference on Channel



$0 < \text{Separation} < 1x$
Significant Interference on & adj channels



Overlapping Networks
Destructive Intrfr. on & adj channels

Note: shadows based on $10E-5$, no fading

FIG 3 - CCA METHODS VS RF POWER & BER [2]

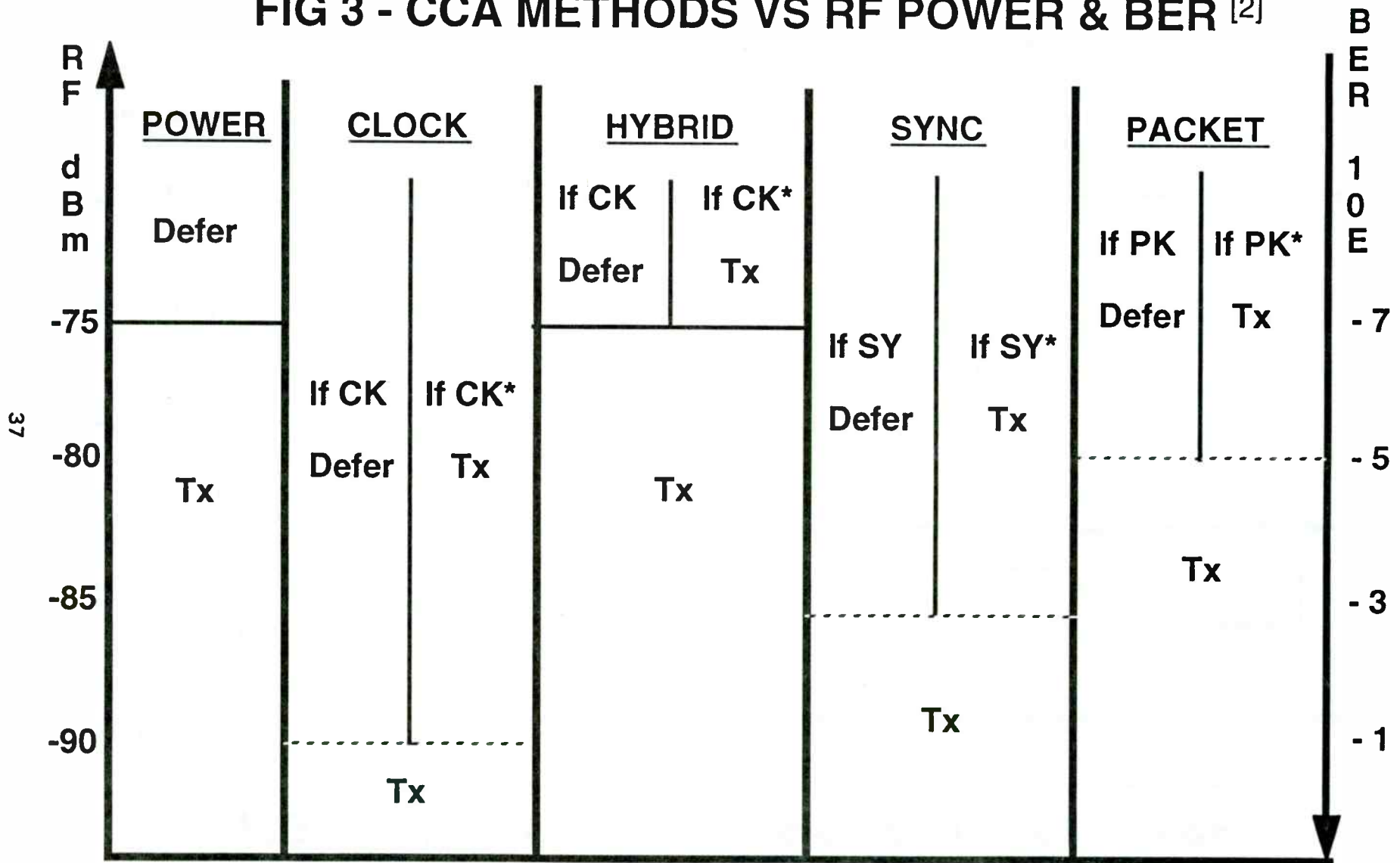


FIG 4 - HUMAN MODEL VS CCA MODEL: CASE #1

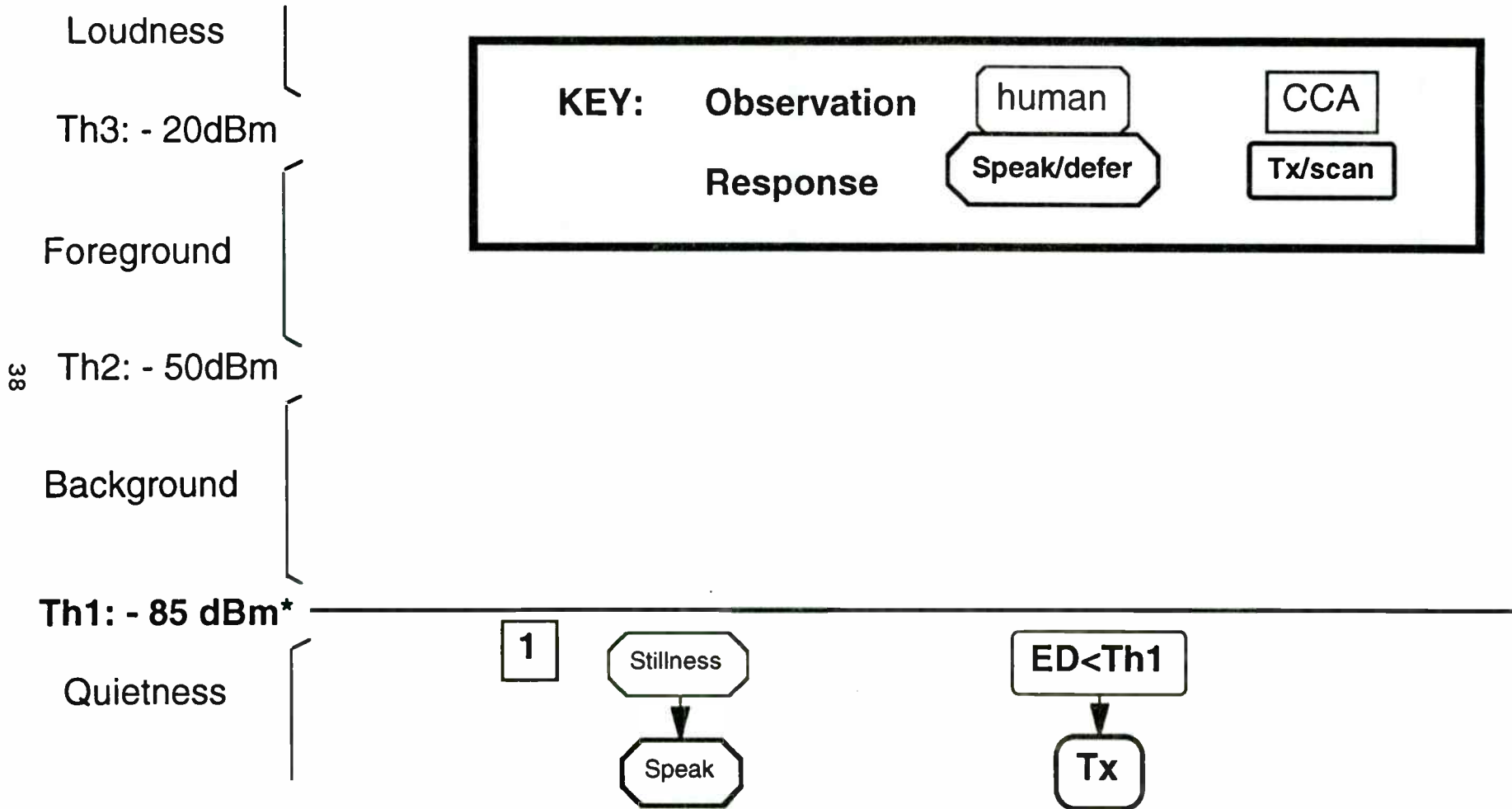


FIG 5 - HUMAN MODEL VS CCA MODEL: CASE #2

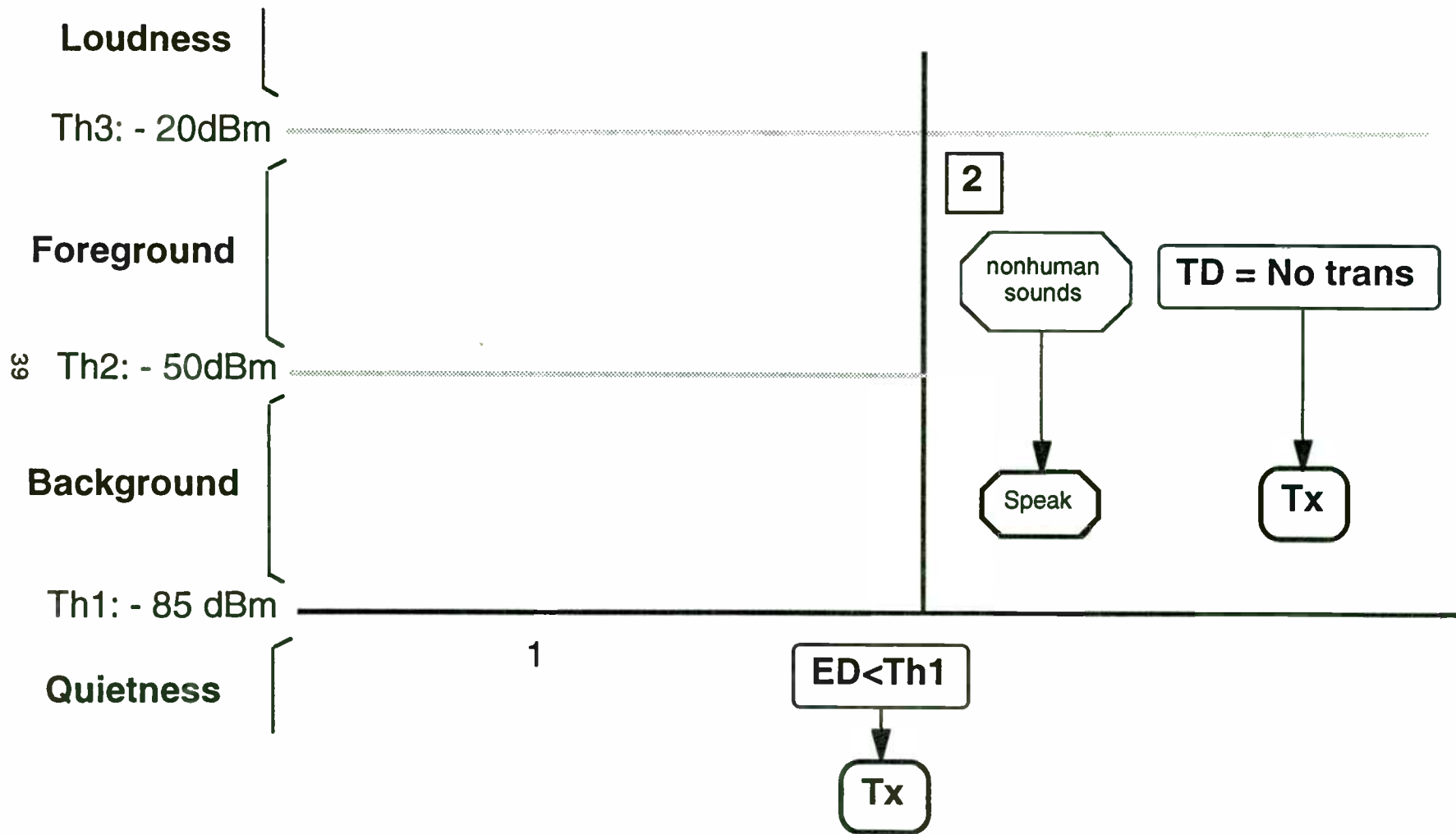


FIG 6 - HUMAN MODEL VS CCA MODEL: CASE #3

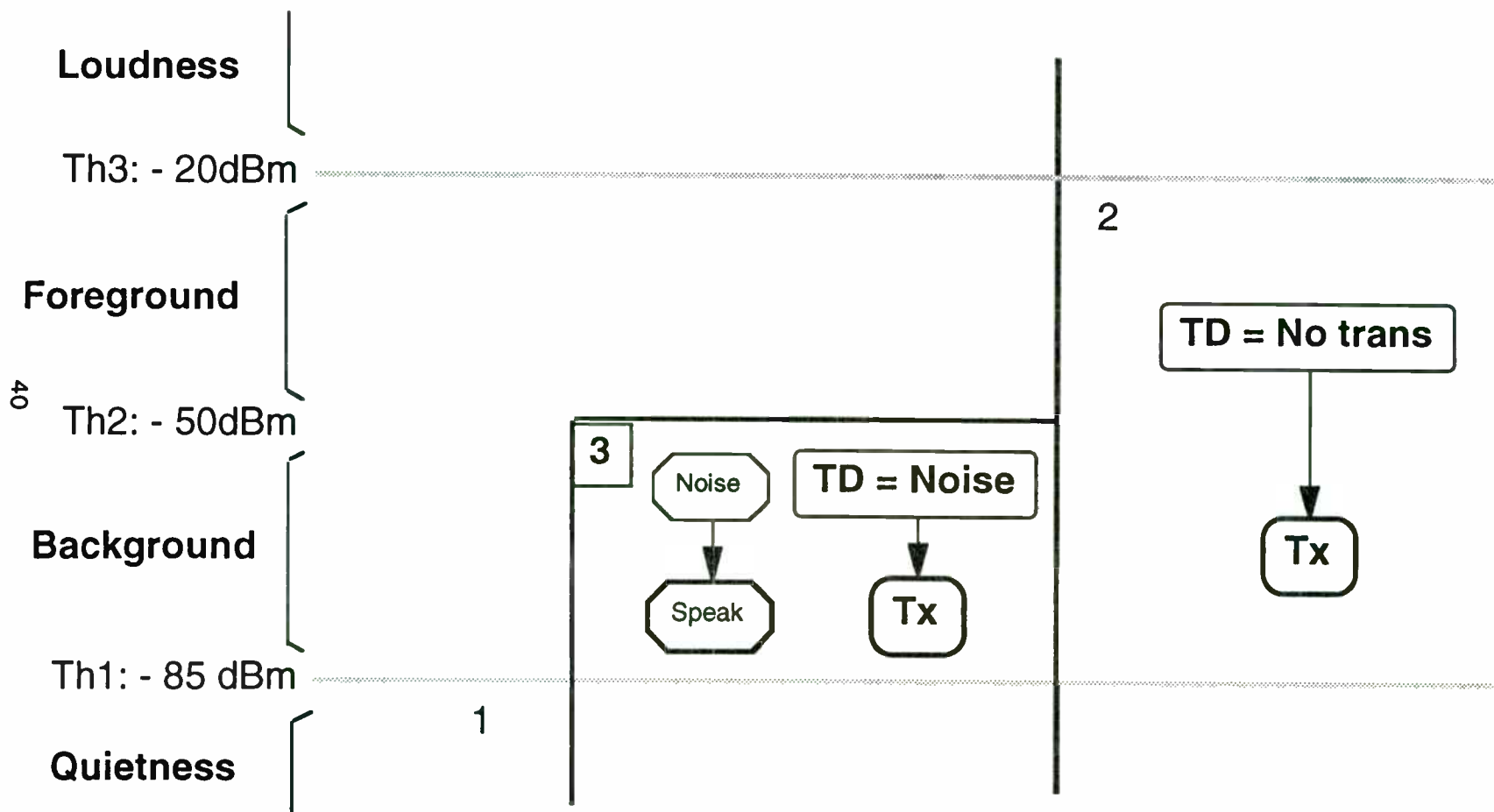


FIG 7 - HUMAN MODEL VS CCA MODEL: CASE #4

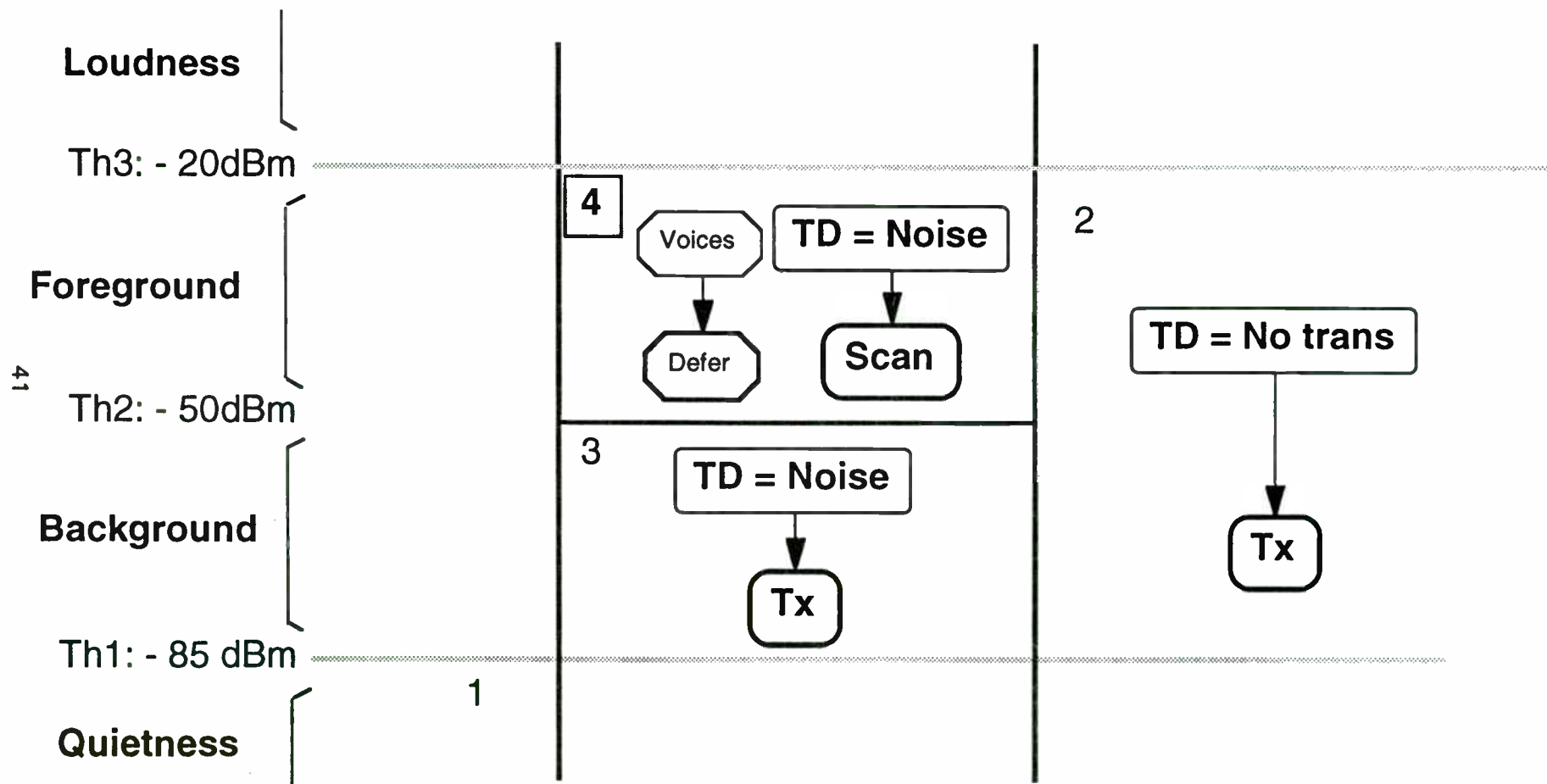


FIG 8 - HUMAN MODEL VS CCA MODEL: CASE #5

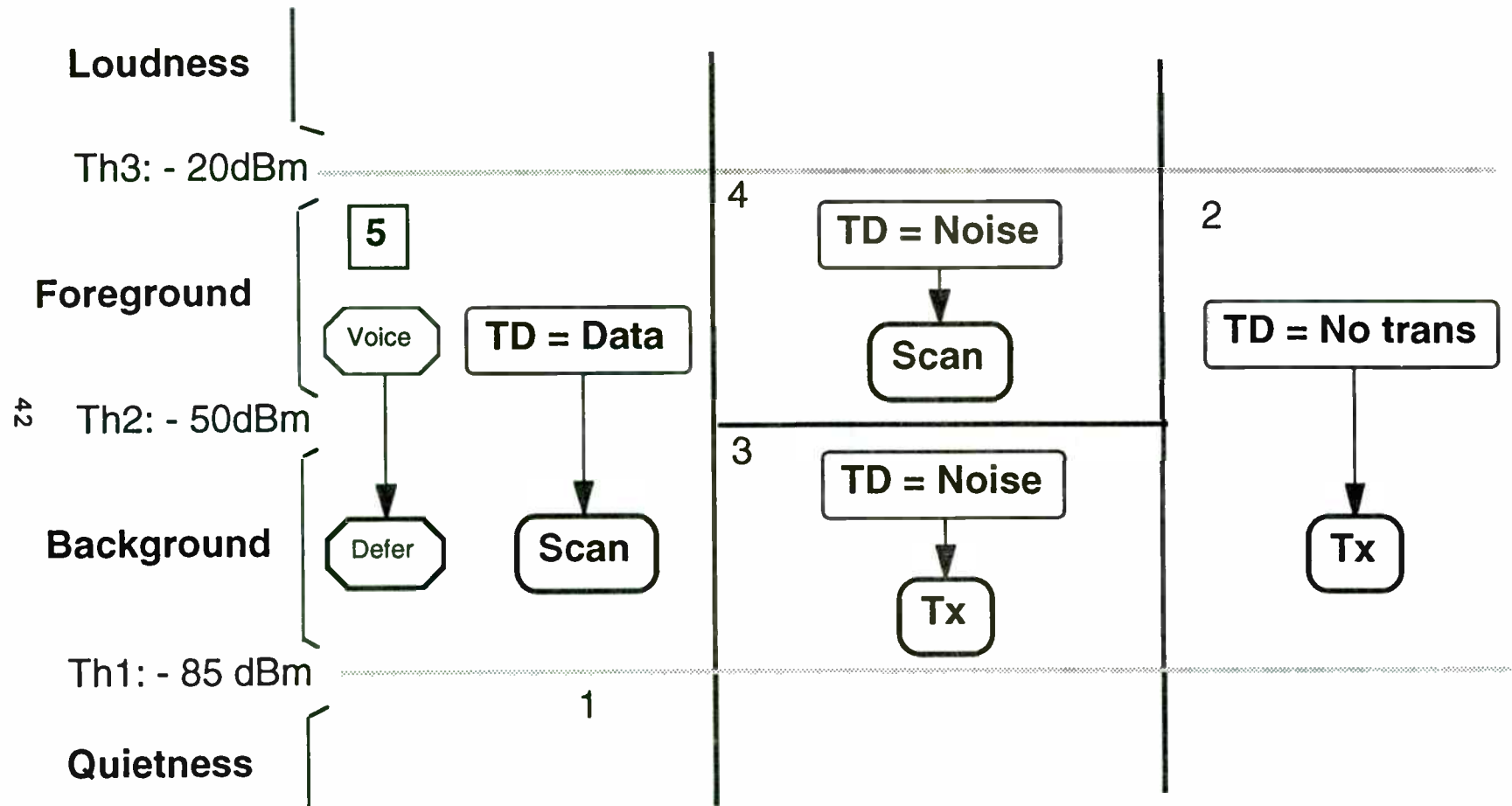
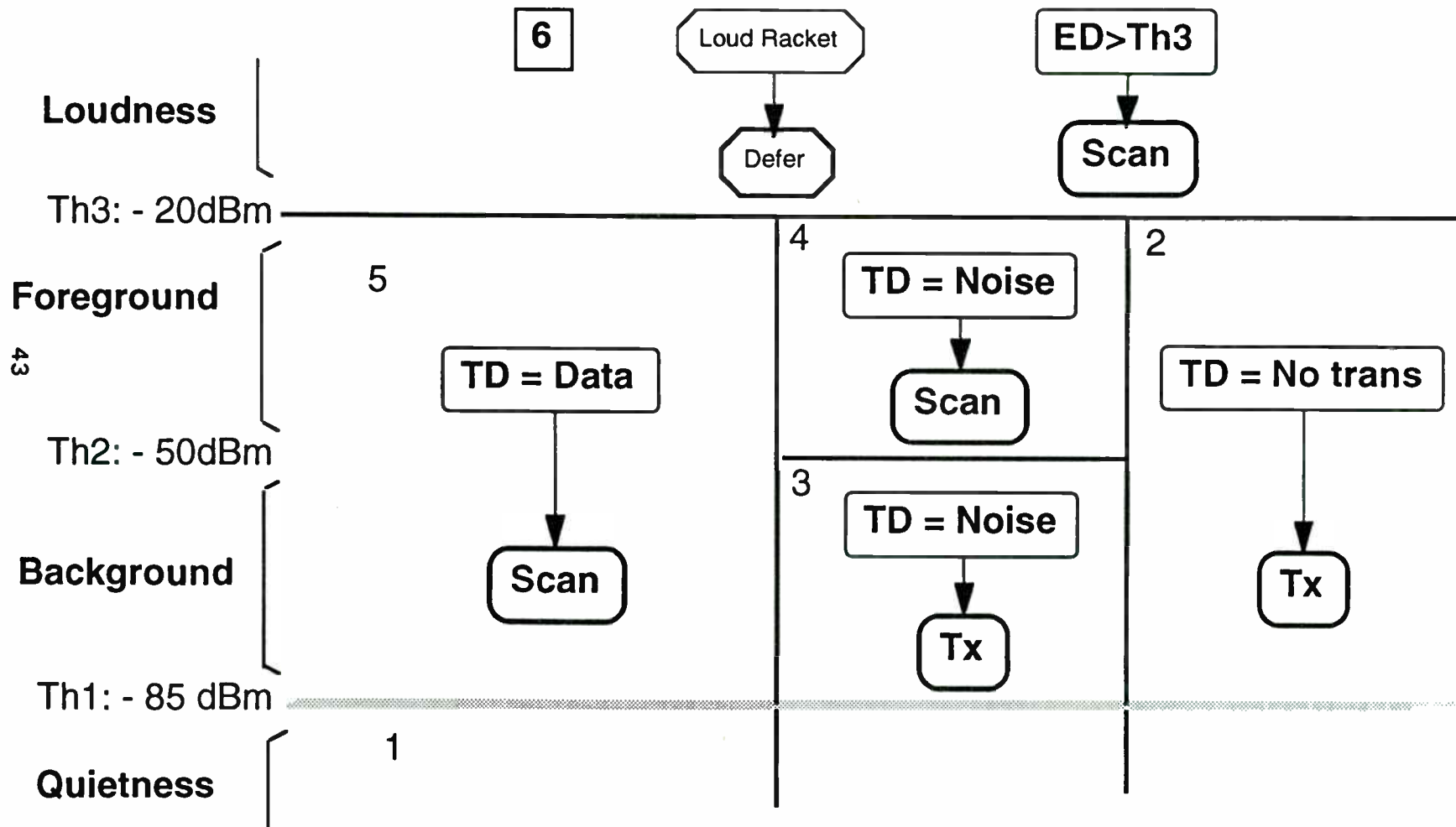


FIG 9 - HUMAN MODEL VS CCA MODEL: CASE #6



GMSK, GFSK and FQPSK Implementations of Feher's Patented-Licensed Technologies*

Dr. Kamilo Feher

Director, Digital & Wireless Communication Laboratory
Professor, Electrical and Computer Engineering Dept.
University of California, Davis, Davis, CA 95616 USA
(916) 752-8127 FAX: (916) 752-8428

President, Consulting & Licensing Group, DIGCOM, Inc.
FQPSK Consortium-Dr. Feher Associates
(916) 753-0738 FAX: (916) 753-1788

A.1 Abstract

The extraordinary impact of two landmark inventions on filter, modulation, and overall wireless system design is described in this paper. Feher's "Filter" (FF) patent led to new generations of reduced power/size, cost-efficient, and increased speed FPGA and ROM look-up table-based filter designs and to more spectral- and power-efficient modulated GFSK, FQPSK, and FBPSK systems. The abbreviations FQPSK and FBPSK are for Feher's patented QPSK and BPSK systems. New generations of GMSK quadrature modulator IC baseband processor chips use the "Correlated Signal Processor" means of the Kato/Feher (KF) patent. The described patented/licensed technologies have been used in the Global Mobile System (GSM), DECT, PCS-1900, and other standardized and non-standard wireless and cable system applications. Standard compatible and interoperable FQPSK and FBSK inventions increase the power and spectral efficiency of conventional QPSK, $\pi/4$ -DQPSK, and GMSK systems by 300%.

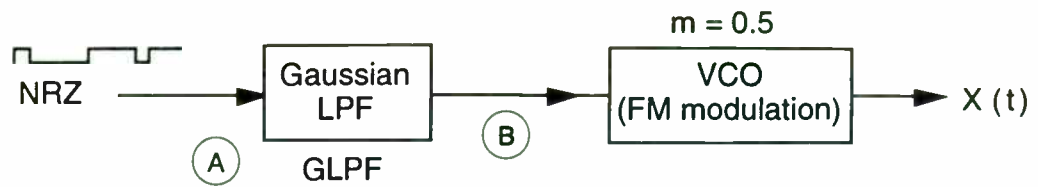
***A.2 Copyright Statement**

Material contained in this paper is based on and is closely related to previously copyrighted material by Dr. Feher-Digcom, Inc. It is submitted on a non-exclusive basis for publication in the *Proceedings of the Third Annual Wireless Symposium and Exhibition*, February 14, 1995, San Jose, CA. Most parts will also be published in journal/magazine publications and in Feher's forthcoming book (April 1995):

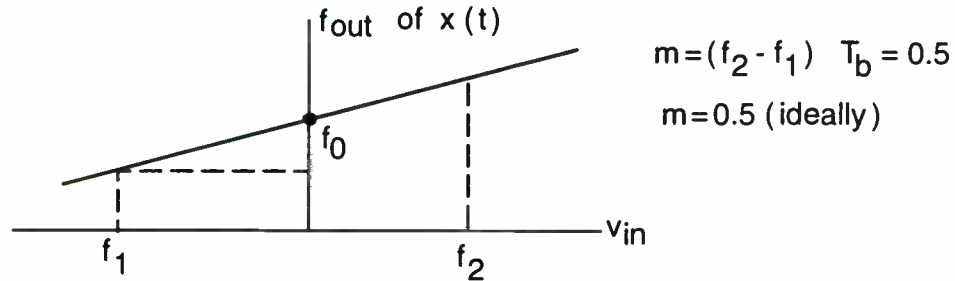
K. Feher: "Wireless Digital Communications: Modulation and Spread Spectrum Applications," Prentice Hall, Englewood Cliffs, NJ 07632, 1995.

A.3 Feher's Patented Filter, DSP, and Correlated Modulation/RF Amplification Means. GFSK and GMSK Applications. FQPSK Consortium/Licensing.

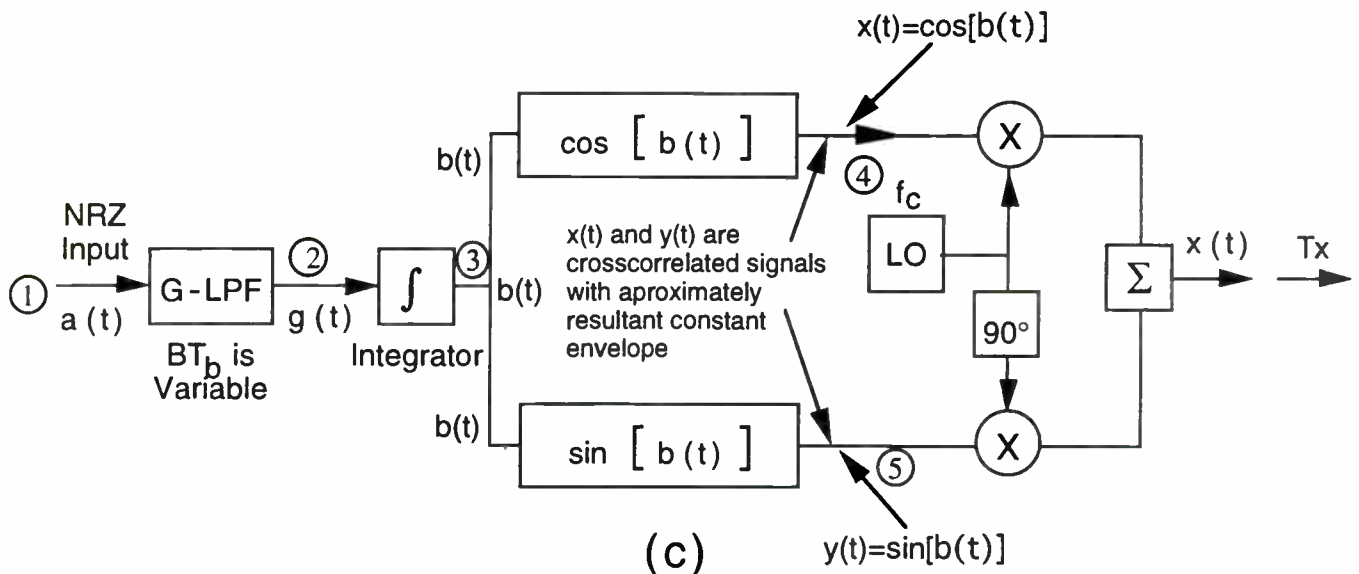
Filter and Digital Signal Processing (DSP) theory, development and design techniques have been documented in numerous authoritative publications and books. Many patents have been issued for original and truly outstanding principles, implementations and design structures/architectures and/or "means" (a term frequently used in patents). Until



(a)



(b)



(c)

Figure A.3.1

GFSK and GMSK implementation/architectures. (a) Filtered binary FM architecture: the simplest and most efficient Gaussian LPF (low-pass filter) design is by means of the licensed Feher filter (US Patent No. 4,339,724); (b) transfer function of a voltage controlled oscillator (VCO) based binary FM modulator; and (c) a frequently used “crosscorrelated signal processor” architecture implementation of GMSK, based on Kato/Feher US Patent No. 4,567,602 licensed by Dr. Feher Associates/Digcom, Inc.

the 1980s inventors devoted their attention to "linear" filter implementation means, including analog (passive and active) and digital DSP filters. The DSP filters are based on Infinite Impulse Response (IIR) and Finite Impulse Response (FIR) designs. These "linear transversal filter structures" are in extensive use.

In this paper, two landmark inventions (patents) are highlighted. The **Feher "Filter"** patent, or "**FF**" for short, contains a new and completely different principle from that of linear filter theory and design. Feher's Filter Patent includes "nonlinear" or "synthesized wave" store-readout/switching filter and comparison means.

Another extraordinary discovery described in this chapter is the **Kato/Feher** or "**KF**" "**Correlated Signal Processor**" Patent. This invention could be described as **an invention which is "against" the well-established wisdom of classical linear communication system theory and principles**. Digital communications textbooks and prestigious research publications contain detailed justifications in regard to the need of having **independent or uncorrelated** in-phase (I) and quadrature (Q) baseband signals. Independent I and Q signals lead to optimum quadrature modulated performance. Cross-correlation between the I and Q baseband transmit signals would be a cause of crosstalk and thus detrimental to performance. Therefore communication theory, developed for linear systems, demonstrates that cross-correlation is not desired and that for optimum performance it must not exist.

The KF Correlated Signal Processor patent demonstrates, contrary to previous theoretical and practical achievements, that correlation between the I and Q channels can be of substantial benefit.

A.3.1 A Review of Two of Dr. Feher Associates' Patents

Some of the reasons for the worldwide impact of these inventions/patents, technology transfer, consulting and professional training courses, and license arrangements on new generations of products are discussed. These include digital and analog filters, Digital Signal Processing (DSP), correlated baseband processor, combined modulation and Radio Frequency (RF) Integrated Circuit (IC), cable and other wireless technology and continued Research and Development (R&D). An informal discussion follows. This paper is merely a brief description of some of the patent claims. **It is not a legal and contractual licensing arrangement or technical/legal interpretation of the patents described herein.** For a complete text of these patents and of other Dr. Feher Associates patents, a detailed study of the complete patents and Feher's more recent patent disclosure documentations is recommended.

We limit this paper to the informal discussion of only two of our patents and to only one claim per patent. Detailed study of the entire patents will give you an insight into the value of these technologies for your research, ongoing product developments, and licensing. For licensing and technology transfer arrangements write to:

Kamilo Feher
c/o Dr. Feher Associates/Digcom, Inc.-Digital and Wireless Communications
US and International Consulting/Training and Licensing Group
44685 Country Club Drive, El Macero, CA 95618, USA
Tel 916-753-0738, Fax 916-753-1788 or
Dr. K. Feher at University of California, Davis Tel 916-752-8127

**A.3.2 Patents: Feher: "Filter", USA No. 4,339,724, July 13, 1982
Abbreviated "FF" and Kato/Feher: "Correlated Signal Processor" USA No. 4,567,602, Issued January 28, 1986, Abbreviated "KF"**

Our patent claims, as well as patent claims of inventors include a text related to other embodiments and variations which utilize the principles described in the awarded patents. Such a text may state: . . . "A person understanding this invention may now conceive of changes or other embodiments or variations, which utilize the principles of this invention. All are considered within the sphere and scope of the invention as defined in the claims appended hereto . . ."

A.3.3 A Brief Historical Perspective of the FF (Feher Filter) Patent Technology and of Other Signal Filtering Methods

Assume that around 1980 you were given a task to design a "Gaussian" or "raised-cosine" filter having a 3 dB bandwidth of approximately 500kHz for a 1Mb/s rate digital communication system. Probably you would accomplish this task by means of analog (active or passive) traditional filter design or by transversal IIR or FIR filters which use mixed digital and analog components (flip-flops and discrete resistors or other gain coefficients served as multipliers). For your power and cost-efficient design during 1980 it would not be obvious to use a filter with several thousand logic gates instead of one operational amplifier or a couple of low-cost LC components.

Transversal filter structures include "IIR" or Infinite Impulse Response and "FIR" or Finite Impulse Response digital and/or mixed analog-digital implementations. Design of these types of digital filters has been extensively covered in numerous references. Many Digital Signal Processing (DSP) IIR and FIR filters/DSP Integrated Circuits have been manufactured during the late 1980s and 1990s. These IIR and FIR architectures have a drawback, namely that they may require a relatively large number of "multiplier" coefficients and adders. Each multiplier requires many gates. For high speeds such DSP-based filters could be very "power hungry," require far too many gates, and be expensive.

Principles of the more efficient ROM look-up table and/or FPGA nonlinearly synthesized or switched filters are described in Feher's books and publications and in the original discoveries-pioneering patents.

During the 1990s, Feher's Filter (FF) family products have been implemented with ROM and FPGA control-based DSP architectures. The scheme may work at a sampling rate nf_b where n is an integer and f_b is the bit rate. Thus n is the number of samples per bit period. To have an acceptably small aliasing error " n " is frequently chosen to be larger than 4. In the ROM various signal shapes, e.g., $s_1(t)$..., $s_{16}(t)$ are stored or it is arranged that the ROM is used as a waveform selector/generator/switch. Depending on the data input, the difference between data patterns, these stored waveforms are "read out" or switched to the D/A converter, converted into an analog wave and transmitted.

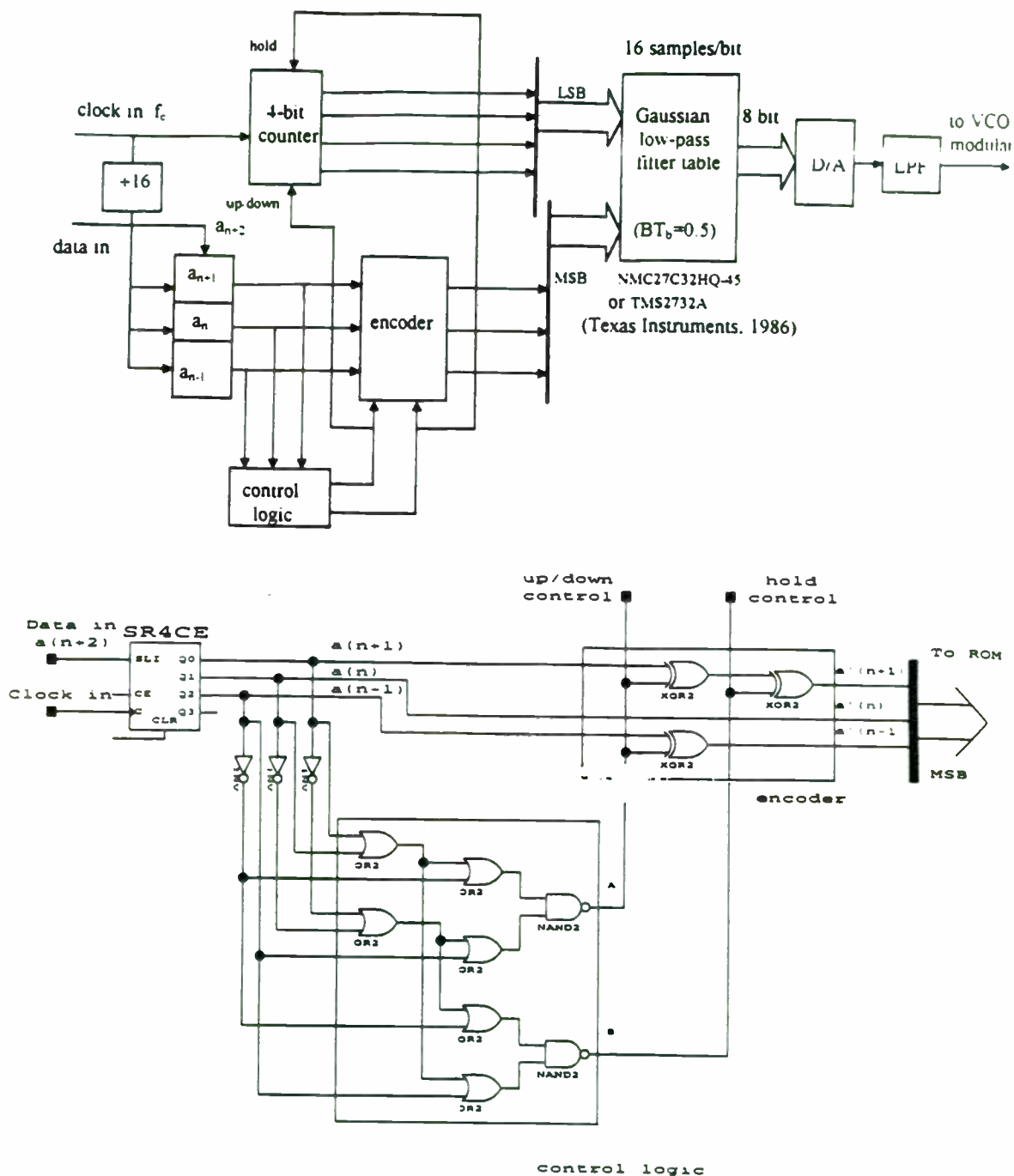
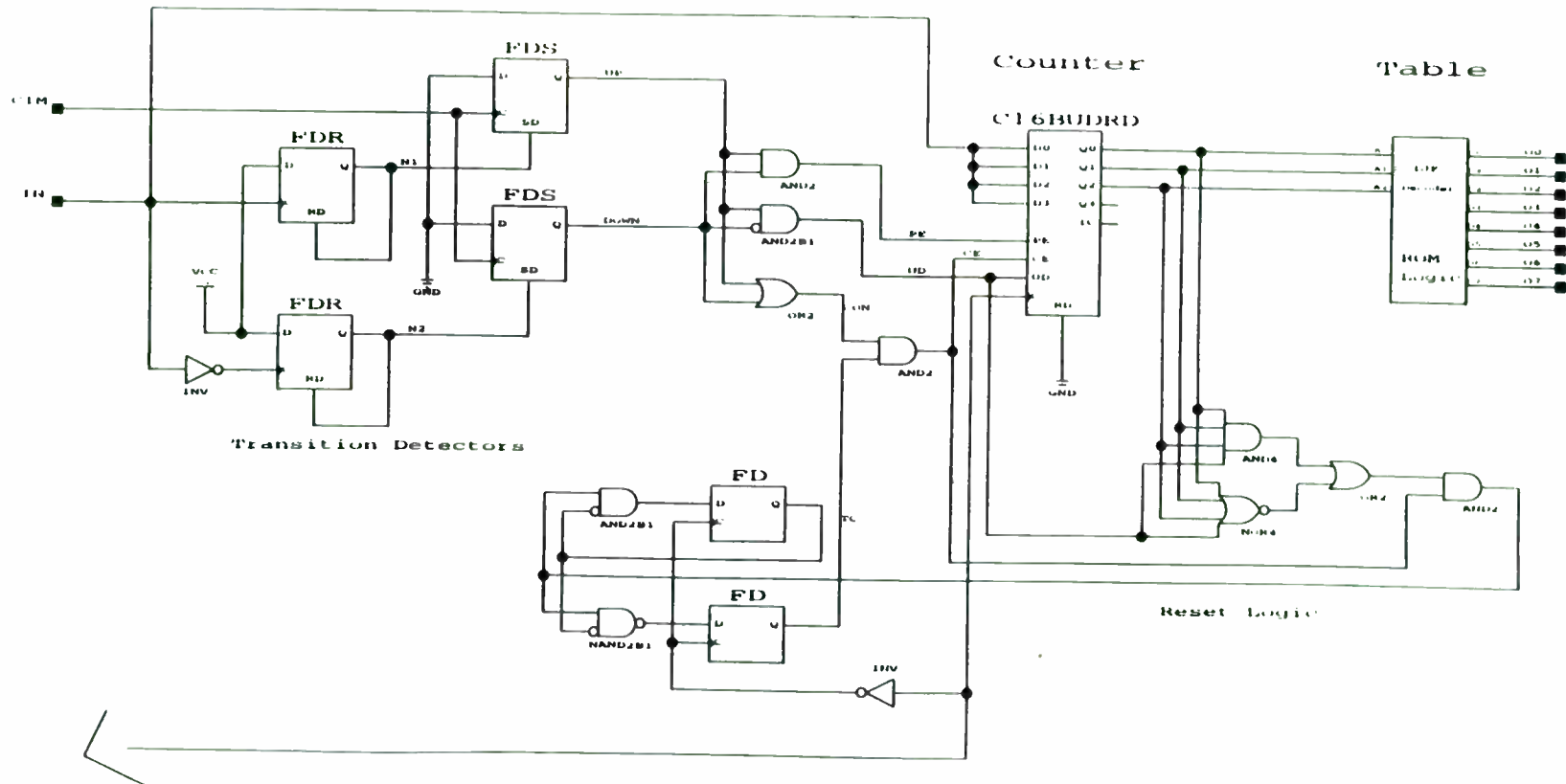


Figure A.3.2
Gaussian low-pass filter (GLPF) illustrative circuit diagram implementation by the Feher filter (FF) US Patent No. 4,339,724. This GLPF has a $BT_b = 0.5$. The "comparing means" of the FF lead to a simple design and a phenomenal hardware/software reduction. Courtesy of G. Wei.

IJF - Filter (8 samples per symbol)



49

Figure A.3.3
Circuit diagram of an illustrative FQPSK-1 baseband processor by means of the Feher filter

A.3.4 An Interpretation of the Principles and/or of Claim No 1 (of 7 claims) Based on the "FF" (Feher's Filter) USA Patent No. 4,339,724:

I claim:

"A filter having an input for receiving a pulse signal form of binary information and an output for providing a synthesized output signal correlated to the input signal comprising:

- a. means for comparing the output signal with the input signal one bit at a time
- b. means connected to said comparing means and said output for generating a first predetermined output signal waveform when the output signal bit is different from that of the input signal and the input signal is binary "1,"
- c. means connected to said comparing means and said output for generating a second predetermined output signal waveform when the output signal bit is different from that of the input signal and the input signal is binary "0,"
- d. means connected to said comparing means and said output for generating a third predetermined output signal waveform when the output signal bit is the same as that of the input signal and the input signal is binary "1,"
- e. means connected to said comparing means and said output for generating a fourth predetermined output signal waveform when the output signal bit is the same as that of the input signal and the input signal is binary "0,"

in which the predetermined output signals are continuous, whereby the spectra and sidelobes of the output signal which is correlated to the input signal are controlled to a predetermined extent."

An informal discussion and interpretation follows.

In Claim #1, "means for comparing the output signal with the input signal one bit at a time" are claimed. In a sequence of serial bits at the input of a processor the **first input bit**, relative to the **second input bit**, which has been previously processed is defined as the "**output signal**" or output bit. As described in the body of the patent (including Section 2, lines 65 to 68 and Section 3, lines 1 to 19) consecutive bits A_i and A_{i-1} are compared. This comparison is interpreted as a **1 or multibit memory system**. Based on the bits which are being processed, various predetermined signals are "read-out" to the transmission system. In particular, means for generating four (4) distinct and separate time-limited pulses

$S_1(t)$, $S_2(t)$, $S_3(t)$ and $S_4(t)$

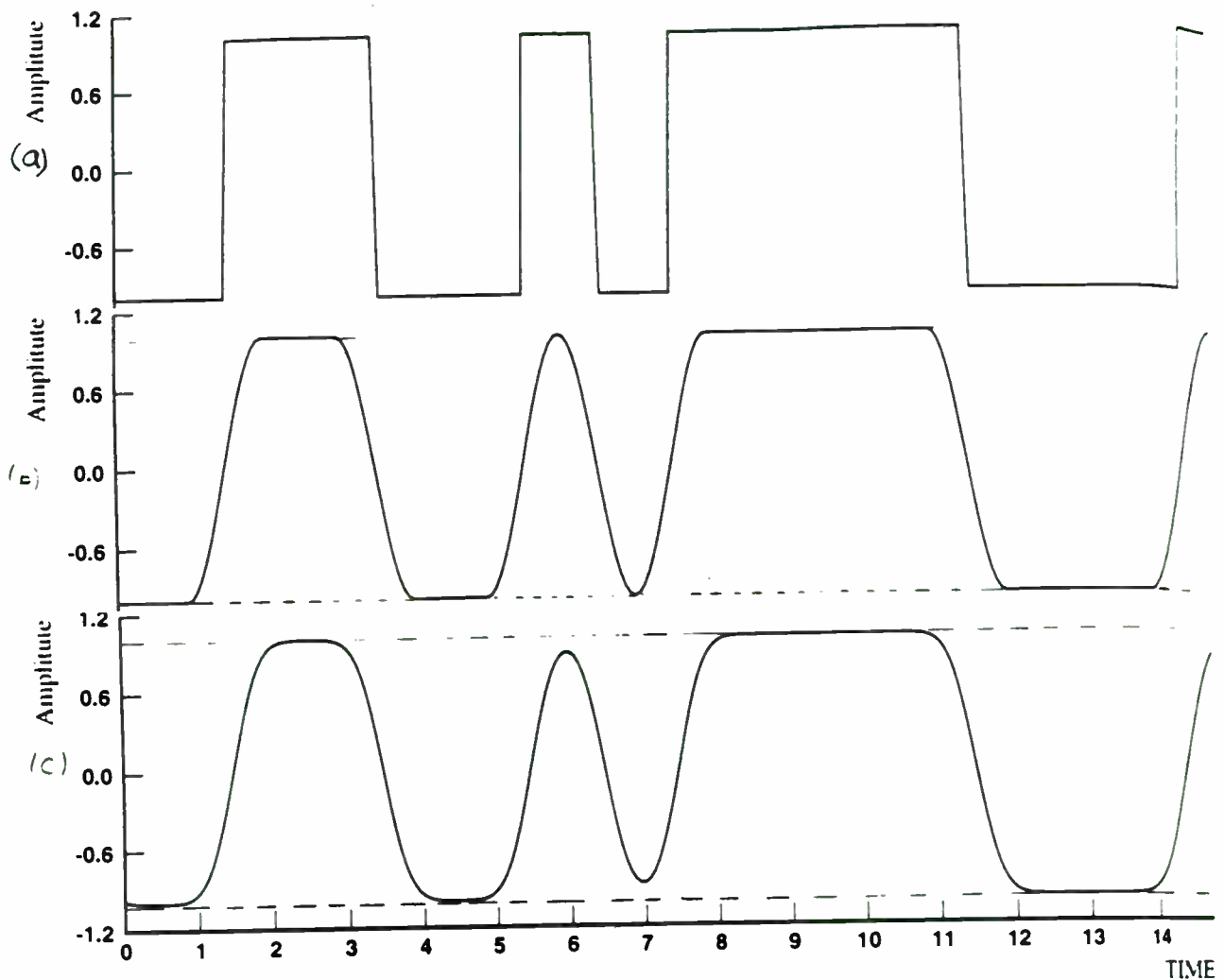
are generated. Whether we choose the "first or second" or other signals depends on the logic control bits comparing means of consecutive bits. Extension of the "four" (4) signal "storage" or "generation" and "read-out" principle to "eight" (8) or more signals generated, and read out from a memory, is obvious.

The first embodiment of this "FF" patent was described in the Canadian priority date filing during 1979. This embodiment as described in the patent uses nonlinearly switched and thus synthesized waveforms dependent on the comparing means of correlated bits. The switched waveforms are read out from separately stored or generated functions by means of selection. Means for Intersymbol Interference and Jitter Free (IJF) waveshape generations are also claimed in this patent.

The means of the Feher Filtering (FF) can be achieved through the use of a ROM and digital-to-analog converter (ROM-DAC filter). In this implementation of the filter, the possible amplitude or possible phase-transitions and values of the transmit data are stored in a ROM and read out based on addresses formed by the transmit data. The addresses are based on comparative means of input data patterns. For example with 2 bits, 4 different signal patterns can be read-out from the memory, with 3 bits 8 pulse shapes are synthesized, et cetera.

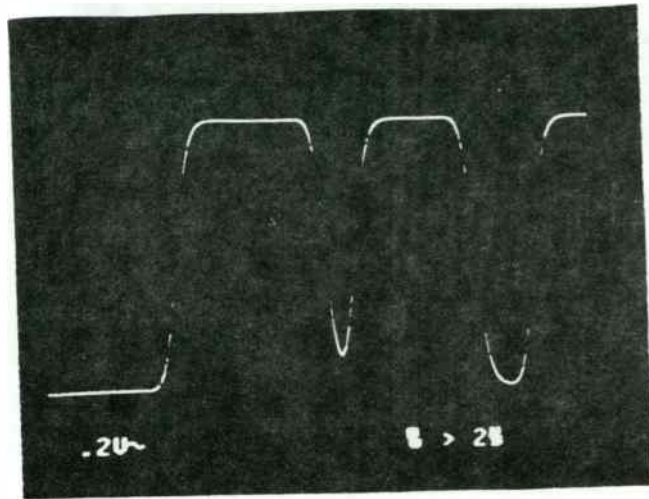
In Fig. A.3.1 to Fig. A.3.8, GFSK, GMSK architectures, Gaussian and "FQPSK-1," Intersymbol Interference and Jitter Free (IJF) circuit diagrams, time domain response, and eye diagrams are illustrated. The bit-by-bit "comparing means" of the Feher Filter (FF) patent led to many implementations. The circuit diagrams illustrate that by the FF comparing means the number of stored signals of a Gaussian $BT_b = 0.5$ filter can be reduced from $s_1(t) \dots s_8(t)$ to only two signals $s_1(t)$ and $s_2(t)$, thus a **4 times (400%)** hardware/memory saving is obtained.

A careful and thorough study of the awarded claims of the FF patent and of ROM or other stored waveform and controlled read-out means of input data patterns leads to the conclusion that the ROM or FPGA based filter implementation is a non-linear filter waveform synthesis method. It has not received nearly as much attention in the literature as the so-called IIR (infinite impulse response) and FIR (finite impulse response) DSP implementation which has also been known under the category of "transversal filters." These types of filters have been implemented by several corporations since 1984. It is our belief that the ROM-based filter implementation is more cost and power efficient than the conventional IIR and FIR "transversal" DSP structures and leads to significant reduction of gate counts because this approach does not require multipliers and is based solely on ROM-driven waveform synthesis. Our survey of some leading DSP and filter IC products indicates that the trend and particularly for higher speed systems is towards the implementation of nonlinearly switched waveform-synthesized filters which are implemented by the ROM or FPGA technology and means of the FF patent.

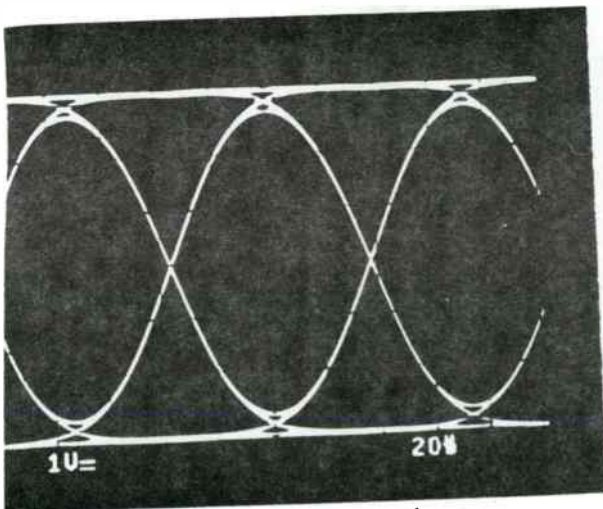


Time Domain Wave Form

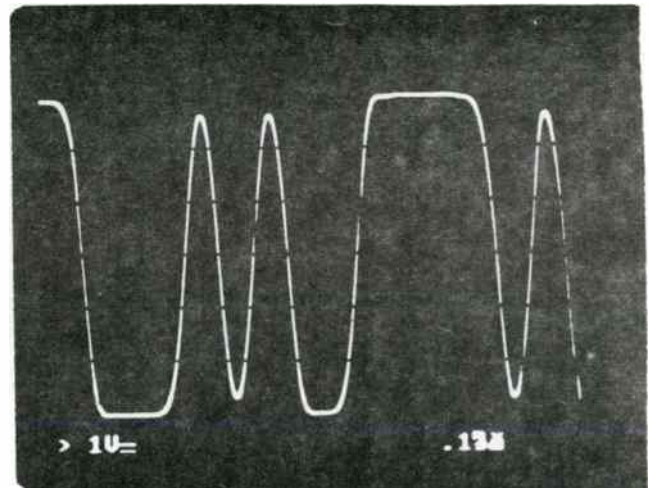
Figure A.3.4
 GFSK and FQPSK-1 signal patterns generated by Feher's filter (FF) US Patent No. 4,339,724:
 (a) NRZ unfiltered sample data pattern; (b) "FQPSK-1" of the I-channel baseband modulator or of FQPSK Feher patent -
 means based GFSK-equivalent generator; and (c) Gaussian filtered ($BT_b = 0.5$) signal generated by the FF patent. In both
 digital ROM based implementations, only one- and two-bit memory comparison circuits were required.



(a)



(b)



(c)

Figure A.3.5
 GFSK experimental "eye diagrams" and sample filtered (Gaussian $BT_b = 0.5$) pulse pattern responses. (a) National's LMX 2411 at DECT standardized $f_b = 1.152$ Mb/s rate. (b), (c) implementations based on Feher filter (FF) US Patent No 4,339,724 with reduced gate count reduced power

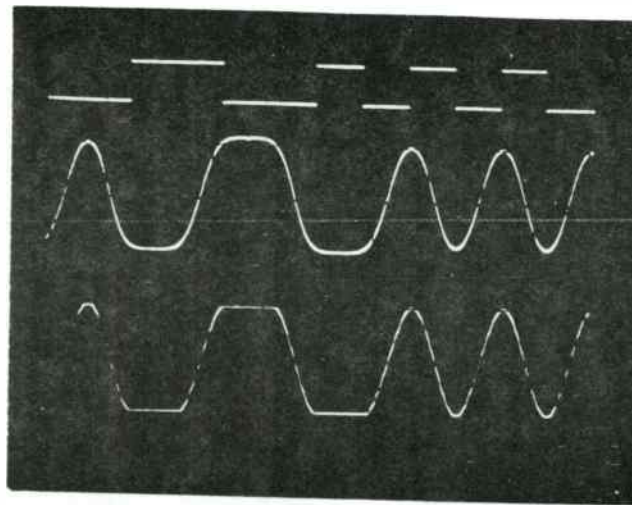
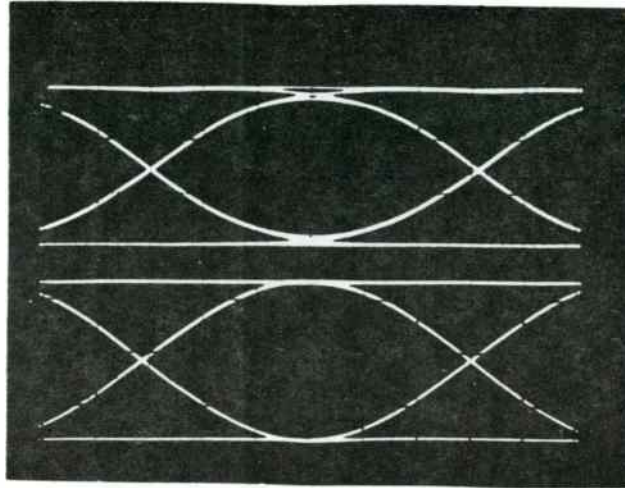


Figure A.3.6

Eye diagrams and sample data pattern diagrams of Gaussian ($BT_b = 0.5$) filtered and of "FQPSK-1" baseband processed signals. The upper eye diagram and time response of GFSK has approximately 10% ISI (intersymbol interference). The lower diagrams correspond to FQPSK-1 are intersymbol interference and jitter free (IJF). Both implementations are extremely simple and use the technology and principles of the Feher filter (US Patent No. 4,567,602).

A.3.5 An Interpretation of the Principles and/or of Claim No. 6 (of 14 claims) from the "KF" (Kato/Feher "Correlated Signal Processor") USA Patent No. 4,567,602. Implementation of GMSK and of Other Transmitters with Baseband Cross-Correlated Signals

We claim:

A cross-correlated signal processor comprising:

- a. means for providing in-phase and quadrature phase shifted NRZ signals from an input signal,
- b. means for cross-correlating the in-phase and quadrature shifted signals,
- c. means for generating in-phase and quadrature shifted intersymbol-interference and jitter free(IJF) encoded output signals having amplitudes such that the vector sum of the output signals is approximately the same at virtually all phases of each bit period,
- d. and means for quadrature modulating the in-phase and quadrature output signals, to provide a cross-correlated modulated output signal.

An informal discussion and interpretation follows:

A simplified interpretation of one of the independent claims, Claim #6 of the "KF" patent, indicates that we were awarded claims for principles and implementations of cross correlation between the in-phase and quadrature channels of a quadrature (QUAD) modulation structure and the generation of bandlimited signals of constant modulated envelope with intersymbol interference and jitter-free (IJF) **crosscorrelated** capability.

A closer examination of some of the modern quadrature GMSK integrated circuit architectures and products indicates that the I and Q baseband signals are obtained from an original NRZ signal which is Gaussian filtered and integrated, e.g., see Fig. A.3.1(c). This resultant filtered signal is split into a "cos () and sin() ROM-based look-up table and in turn is used as the I and Q baseband drives of the quadrature modulator. One of the key principles is that the final I and Q outputs are cross-correlated over an interval of one or more bits. In fact the Q signal is mathematically related or "cross-correlated" to the I signal. You may note that the term "correlated" means "predictable, calculable." In a QUAD-based ROM implementation, the I and Q signals are cross-correlated and they lead to a constant envelope signal which is bandlimiting the original NRZ signal. Additionally this constant envelope transmitted signal, after demodulation, has a practically IJF property and in particular if the BT_b product is 0.5. Illustrative experimental photographs demonstrate this fact in several well-known references and also Fig. A.3.8. Bandwidth products $BT_b = 0.5$ is specified in systems such as the European Standard DECT and others. For a reduced $BT_b = 0.3$, such as specified for the **GSM Standardized GMSK** system the **I and Q crosscorrelated eye diagrams exhibit Intersymbol Interference**, see Fig. A.3.7. Claim No. 1 and other claims of our KF patent (U.S. Patent No. 4,567,602 Kato/Feher) include signals with Intersymbol Interference, e.g., Claim 1 (ii): "When the in-phase channel signal is non-zero, the maximum magnitude of the quadrature shifted signal is reduced from normalized to A, where $1/\sqrt{2} \leq A \leq 1$."

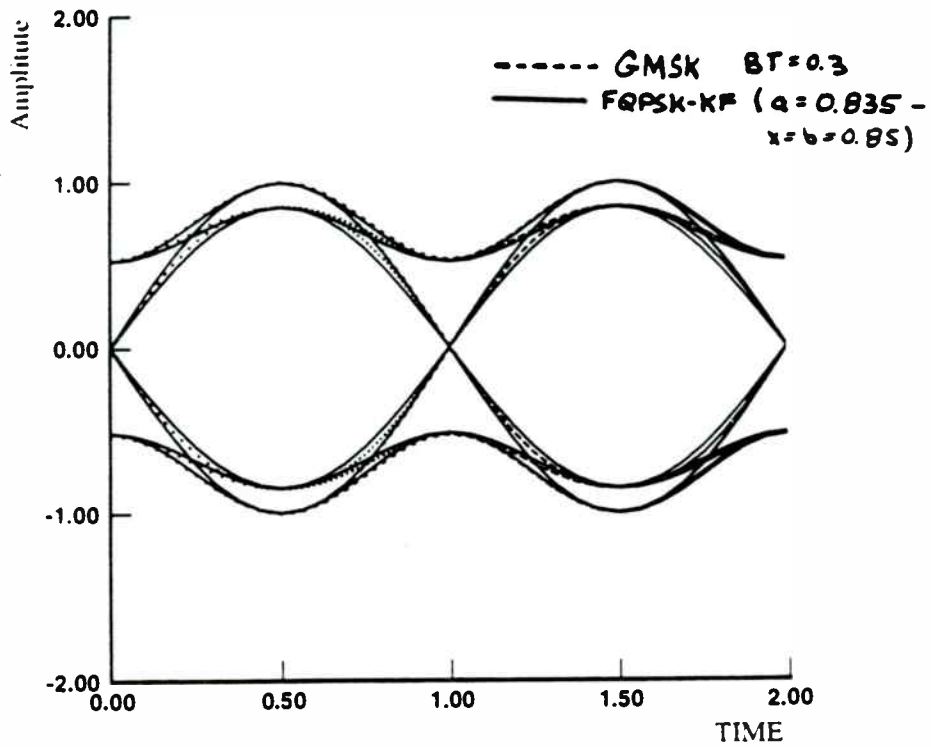


Figure A.3.7
 GMSK ($BT_b = 0.3$) and FQPSK-KF equivalent eye diagrams. The GMSK (dotted lines) as well as the FQPSK-KF (solid lines) are generated by the Kato/Feher (KF) US Patent No. 4,567,602. The licensed KF technology for GMSK as well as FQPSK applications, leads to simpler hardware than alternative GMSK implementations.

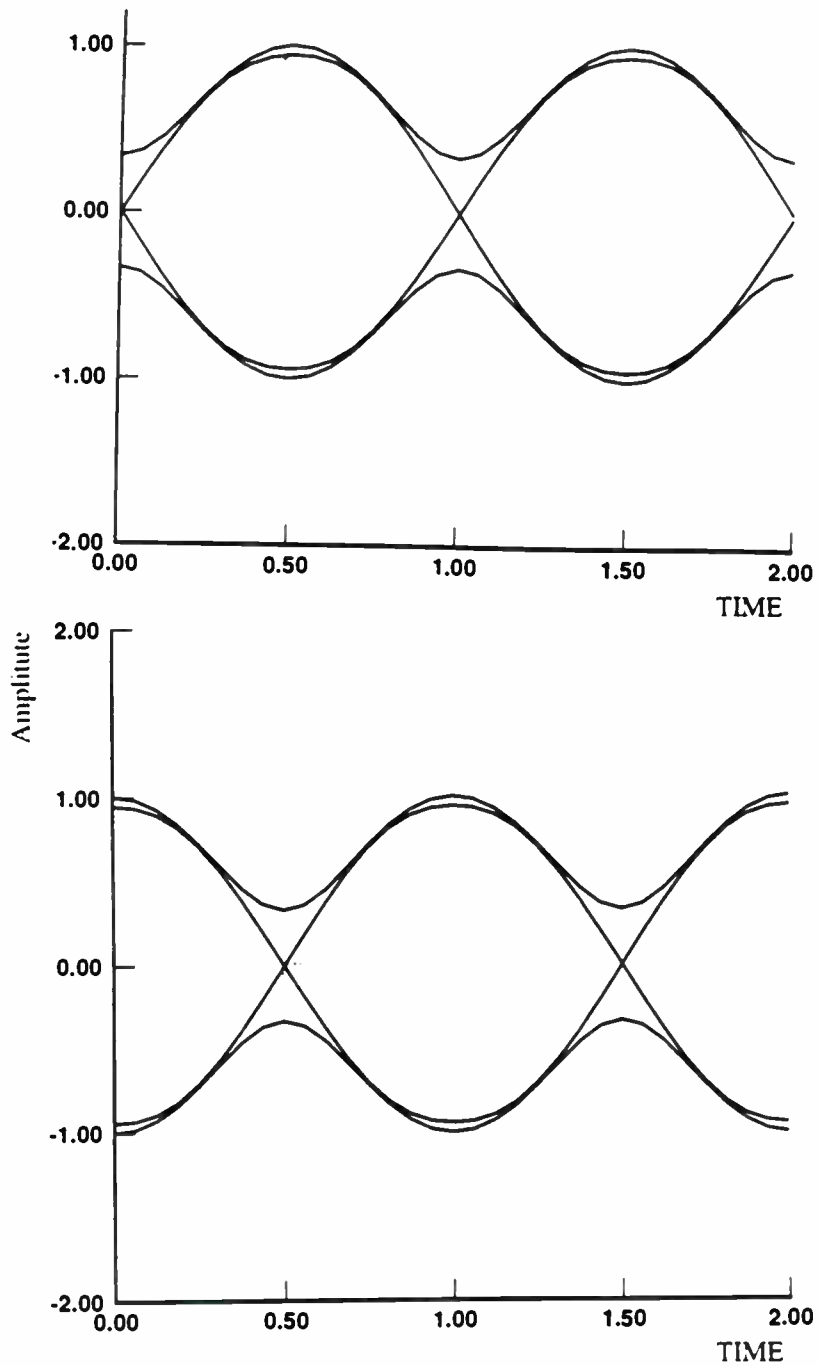


Figure A.3.8
 GMSK eye diagrams with $BT_b = 0.5$ of a quadrature modulator generated by the Kato/Feher (KF) US Patent No. 4,567,602. Note from Figure A.3.1(c) that the I and Q signals are crosscorrelated, are virtually intersymbol interference and jitter free (IJF), and their quadrature modulated signal has a constant envelope. These specifications are identical to some of the claims of this patent.

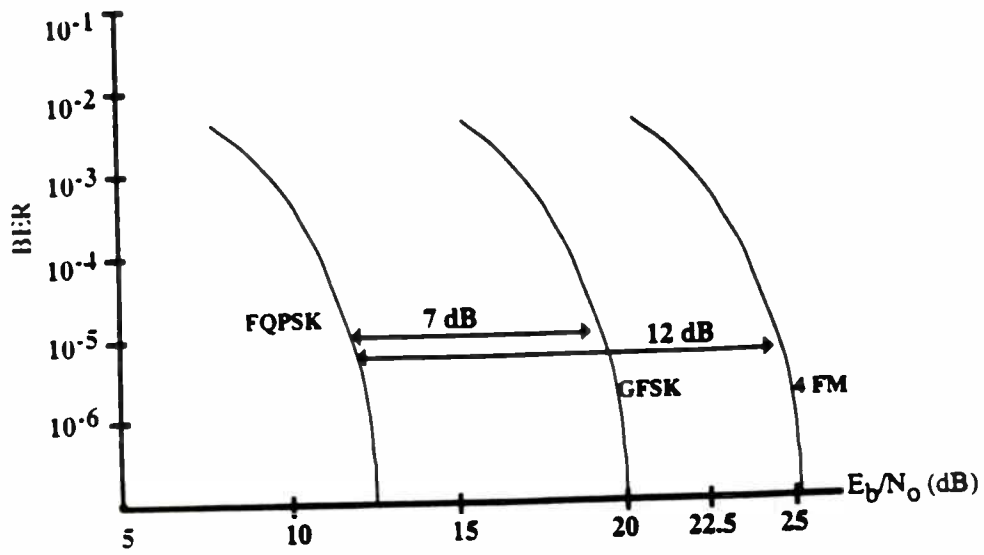
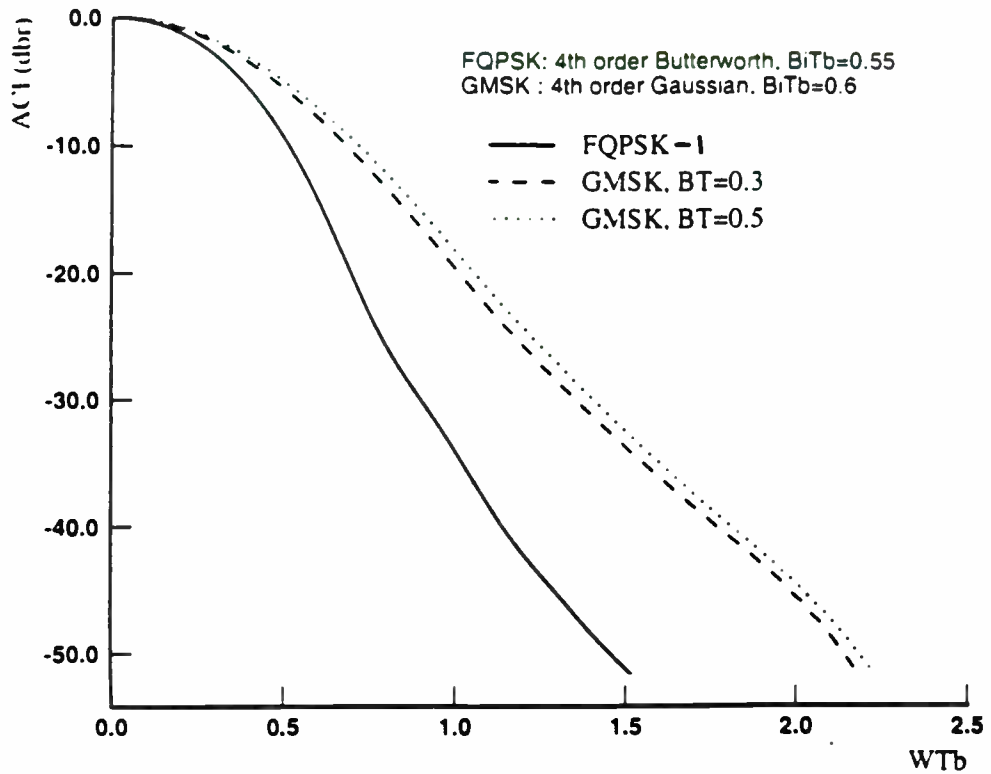


Figure A.3.9

Measured $BER = f(E_b/N_0)$ curves of several "C-class" RF IC-nonlinearly amplified modulated systems at $f_b = 1$ Mb/s and 2 Mb/s rate. FQPSK, GFSK with 160 kHz deviation, and digital 4FM shown. Illustrative experimental data as submitted to WLAN and PCS standardization committees such as IEEE 802.11 and TIA/JTC. The experimental data show that at the specified $BER = 10^{-5}$, FQPSK is 7 dB and 12 dB more robust than GFSK and 4FM, respectively. Such dramatic performance improvement in an interference controlled environment, e.g., FCC-15, can increase the throughput rate about 100 to 1000 times.



ACI of FQPSK & GMSK

(a)

Figure A.3.10

Power spectral density advantage of "FQPSK-1" over GMSK. Integrated adjacent channel interference (ACI) is illustrated in Fig. A.3.10(a). Even more significant spectral compression and efficiencies can be attained with FQPSK-KF, as illustrated in Fig. A.3.10(b) and Fig. A.3.10(c).

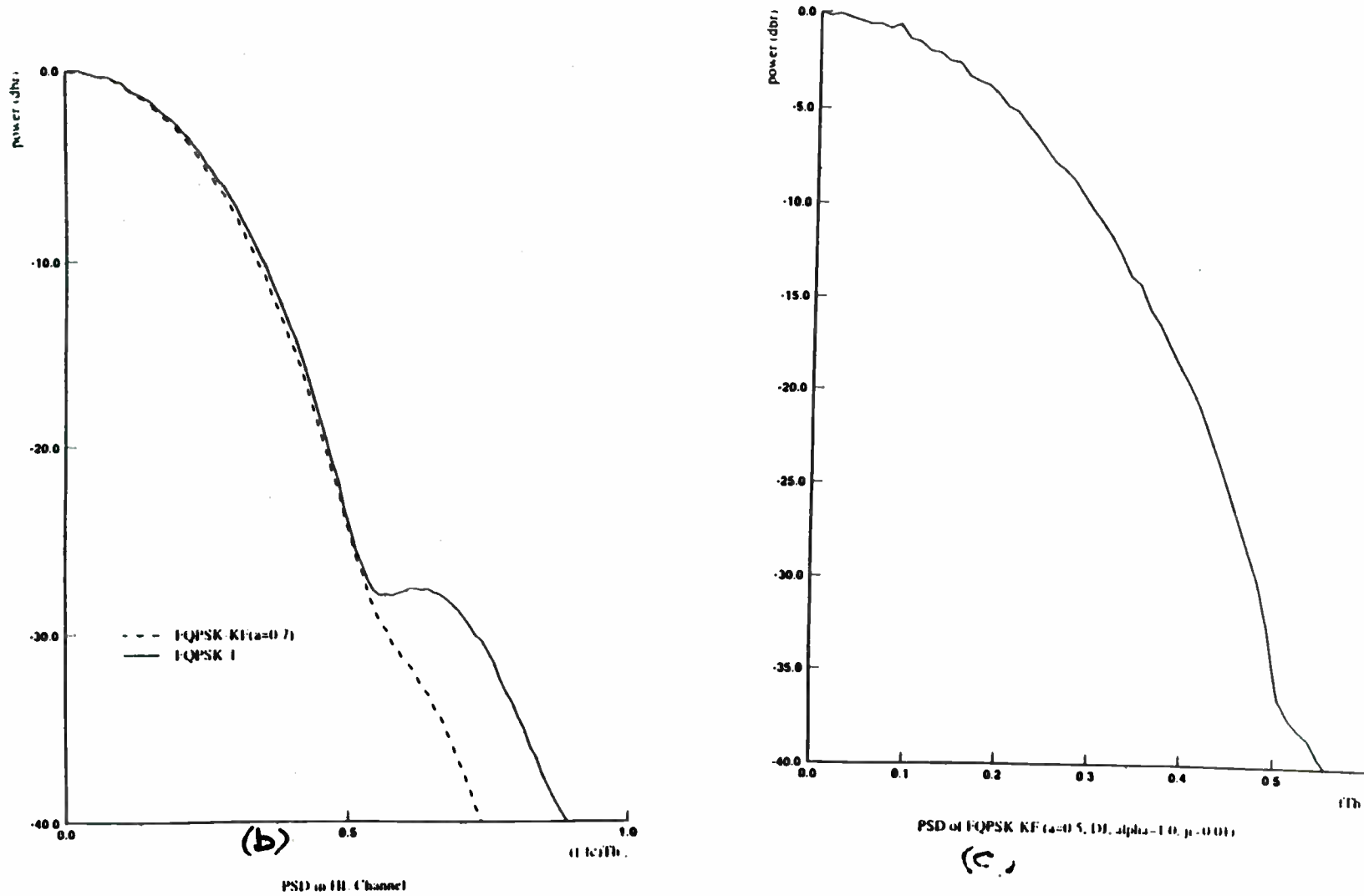


Figure A.3.10

Power spectral density advantage of "FQPSK-1" over GMSK. Integrated adjacent channel interference (ACI) is illustrated in Fig. A.3.10(a). Even more significant spectral compression and efficiencies can be attained with FQPSK-KF, as illustrated in Fig. A.3.10(b) and Fig. A.3.10(c).

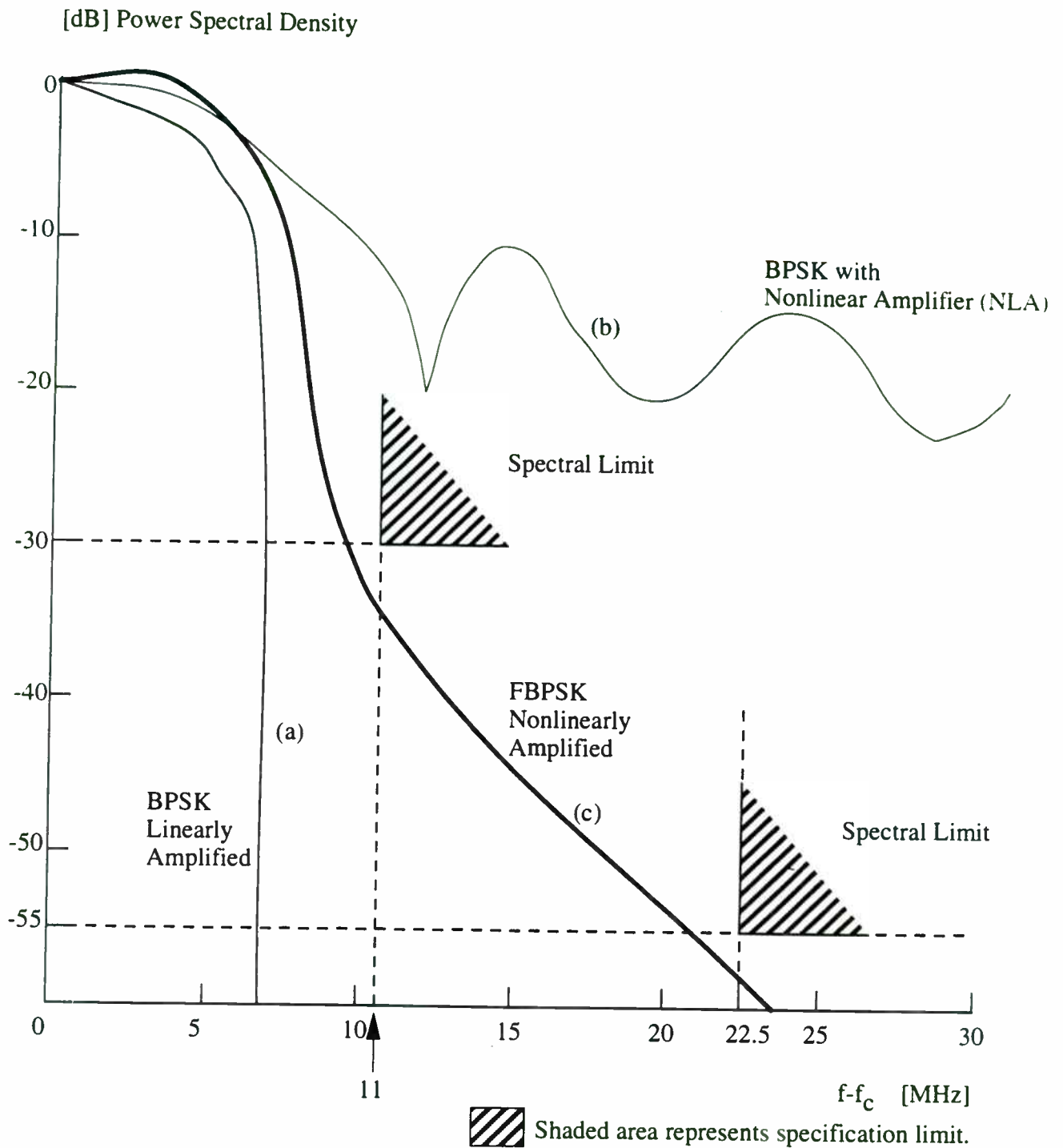


Fig. A3.11 Power spectral density of $f_c = 11$ Mchips/second rate direct sequence spread spectrum BPSK systems.

- (a) BPSK - bandlimited, linearly amplified
- (b) BPSK - bandlimited and nonlinearly amplified
- (c) FBPSK - bandlimited and nonlinearly amplified

GMSK implementations based on traditional passive component Gaussian filter design, followed by FM modulator (VCO) do not necessarily use the means of the FF and KF patents. However GMSK structures which implement the comparison-based ROM Gaussian filter, integrator, or other functions, including quadrature modulation with crosscorrelation, use the claims of the FF patent as well as that of the KF patent. Additionally the $\sin(\)$ and $\cos(\)$ derived from the same input signal to drive the IQ processors has cross correlation and in particular correlation to attain fully-constant envelope. Careful examinations of the claims as well as of the text of the KF patent may reveal that our claims in the KF patent have also been used.

A.3.6 What are Feher's FQPSK, FBPSK, FQAM, FGFSK and FGMSK? Are All of These Systems Patented?

Conventional (coincident transition or "non-offset") and offset QPSK as well as other filtered systems which use one or more of Dr. Feher and Associates' patented filters and correlators are part of the FQPSK family of inventions and products. The broad "FQPSK" term may include Feher's patented BPSK or FBPSK, patented baseband, and/or FSK signals, see Fig. A.3.11 in regards to FBPSK advantages over conventional BPSK. The implementation of Feher's filter or processors is much simpler than that of conventional raised-cosine, Gaussian, Chebychev, Butterworth filters. FF patented filters operate with less DSP power and they lead to dramatic combined modem-RF advantages. See Fig. A.3.9. The ROM and FPGA based "Feher Filter (FF)" patent advantages were discussed previously in this paper.

The implementations of conventional FSK systems (coherent or noncoherently demodulated) including GFSK and GMSK may or may not be patented. For example, if a GFSK transmitter utilizes a filtered ROM generated signal, then the conventional GFSK system may be protected by Intellectual Property. In the case of BPSK-compatible FBPSK, which is suitable for power-efficient low-cost nonlinear amplifications with a 5dB to 7dB power advantage, the implemented BPSK may also be in the category of our patented systems, see Table A.3.1. Similarly, if a conventional GMSK system is implemented based on one of our patents, e.g., ROM-based filter and/or I and Q transmit quadrature baseband correlation (quadrature) then the product, unless licensed, may infringe our patents.

To designate that GFSK, GMSK, BPSK, QPSK, or QAM systems use the means and claims of Feher Associates patents we call them "FGFSK," "FGMSK," "FBPSK," "FQPSK," or "FQAM."

A.3.7 Correlated and crosscorrelated in-phase (I) and quadrature (Q) signals of GMSK transmitters. An informal tutorial discussion in regards to the use of Kato/Feher U.S. Patent No. 4,567,602 for GMSK applications and in particular of the GSM standard.

A demonstration of the fact that the in-phase (I) and Quadrature (Q) signals in a GMSK transmitter are crosscorrelated (Kato/Feher, U.S. Patent No. 4,567,602) follows. In Figure A.3.1(c), we refer to the input NRZ signal $a(t)$ at point 1, Gaussian low-pass filtered signal $g(t)$ at point 2, integrated and Gaussian filtered signal $b(t)$ at point 3, and cosine and sine values of the $b(t)$ signal, designated as $x(t)$ and $y(t)$ at points 4 and 5 of Fig. A.3.1(c). Signals for the implementation means of Fig. A.3.1(c) have been generated for the Global Mobile System (GSM) international standard specifications. These specifications stipulate a GMSK modulator with $BT_b = 0.3$. A brief explanation of the generated signals of Fig. A.3.1(c) and of the corresponding eye diagrams follows.

The Gaussian ($BT_b = 0.3$) filtered output signal at point 2 in Fig. A.3.1(c) of an input Non-return to Zero (NRZ) signal for a typical random pattern is illustrated in Fig. A.3.12. Note that this Gaussian filtered NRZ signal pattern, designated $g(t)$, exhibits substantial Intersymbol Interference (ISI). The ISI-free maximal amplitude values are normalized to +1 and -1. After integration, the filtered and integrated signal at point 3 is shown in Fig. A.3.13. This random-like data signal, signal $b(t)$, is **not** a “sinusoidal” signal. At point 3, this signal is split into the “in-phase” (I) and “quadrature” (Q) channels. Thus the **same** $b(t)$ signal appears in the I and Q channels. The presence of the “same” I and “Q” is a fundamental difference between MSK, OQPSK, QPSK, and GMSK quadrature implementations in which a serial to parallel converter provides independent and **not correlated** binary data into the I and Q branch of the modulator. Thus splitter, point 3, with its connecting wires provides the same $b(t)$ signal into I and Q. Evidently these I and Q signals are **100% correlated and crosscorrelated** as they are the same. An interesting implementation means (to **split the same signal into I and Q**).

Following the $\cos[b(t)]$ and $\sin[b(t)]$ processors at points 4 and 5, the generated signal patterns are shown in Fig. A.14 and on an expanded time scale in Fig. A.15. These resultant bandlimited processed NRZ signals are designated $x(t)$ and $y(t)$ in Fig. A.3.1(c). Points 4 and 5 serve as the in-phase and quadrature drives of quadrature modulators. These $x(t)$ and $y(t)$ random data signal patterns are “nonsinusoidal” in nature, i.e., they are not periodic sinusoidal waves. The $x(t)$ and $y(t)$ signals are crosscorrelated, in fact, they are related by equations.

$$x(t) = \cos[b(t)] \quad (1)$$

$$y(t) = \sin[b(t)] \quad (2)$$

Thus, the “predictability” or crosscorrelation of $y(t)$ from $x(t)$ is defined. In this case,

$$y(t) = \sin[\cos^{-1}x(t)] \quad (3)$$

In other words, to generate $x(t)$ and $y(t)$ we use a mathematical relation of “crosscorrelation” between these terms.

In Fig. A.16, the respective “eye diagrams” of these crosscorrelated $x(t)$ and $y(t)$ signals are displayed. Note that these crosscorrelated signals are data transition jitter free and the maximum magnitude of the quadrature (alternatively in-phase) signal is reduced when the in-phase channel signal is non-zero. A careful examination of Claim 1a, 1b (i-iv), 1c, and/or of other claims of U.S. Patent No. 4,567,602 leads to our conclusion that the GMSK system quadrature implementation is using the means of our inventions.

A.3.8 Field-Proven? Can We Get Patented GFSK, GMSK, FBPSK, FQPSK, or FQAM Chips? Bit Rates?

Since the early 1980s, generations of products benefited from Dr. Feher Associates patented/licensed technologies. Many products have been developed. During the last quarter of 1994, one of the largest and most profitable American corporations completed the design of FQPSK-based licensed systems for a production run of **several million subscriber units**. For power efficient **satellite** systems at 6GHz and 14GHz, relatively low bit rate (less than 500Kb/s) have been implemented and operate in the USA and internationally. For cable systems including digital **cable TV**, a wide variety of products use our filter and processor technologies for FQPSK and FSK applications.

Signal Pattern

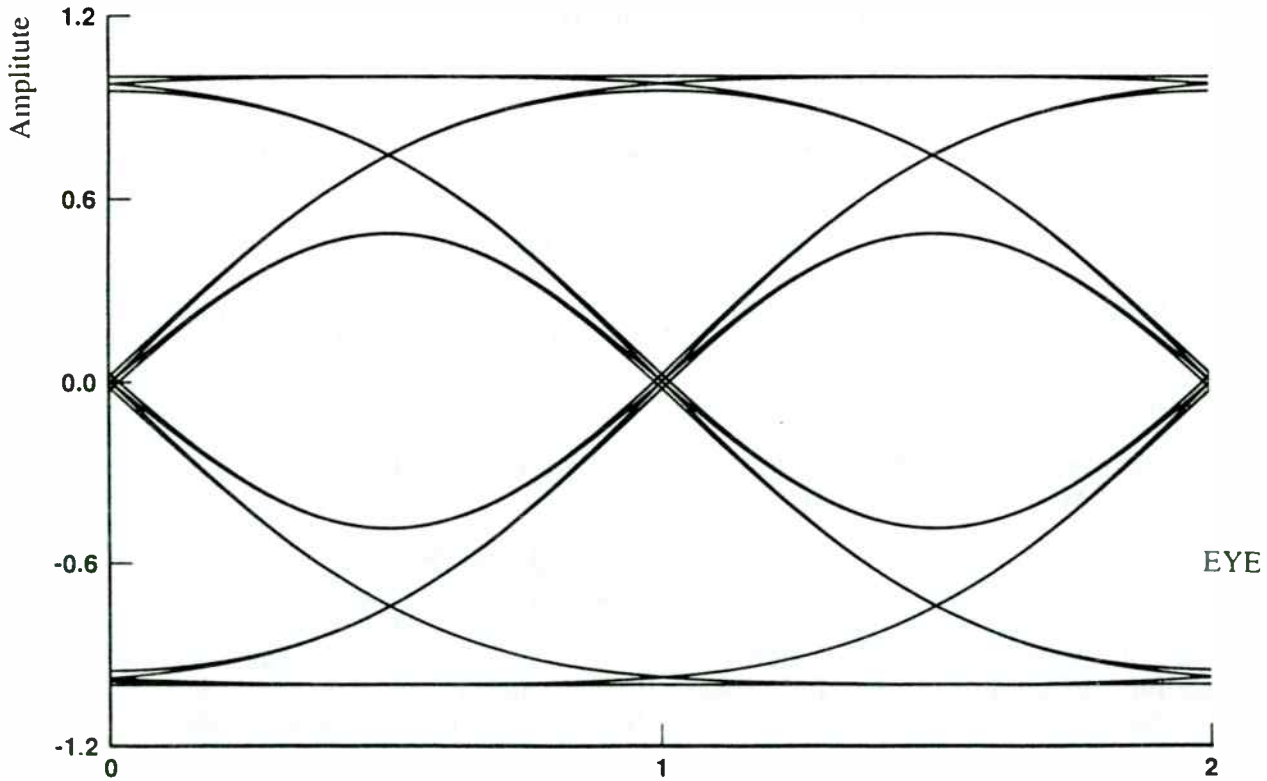
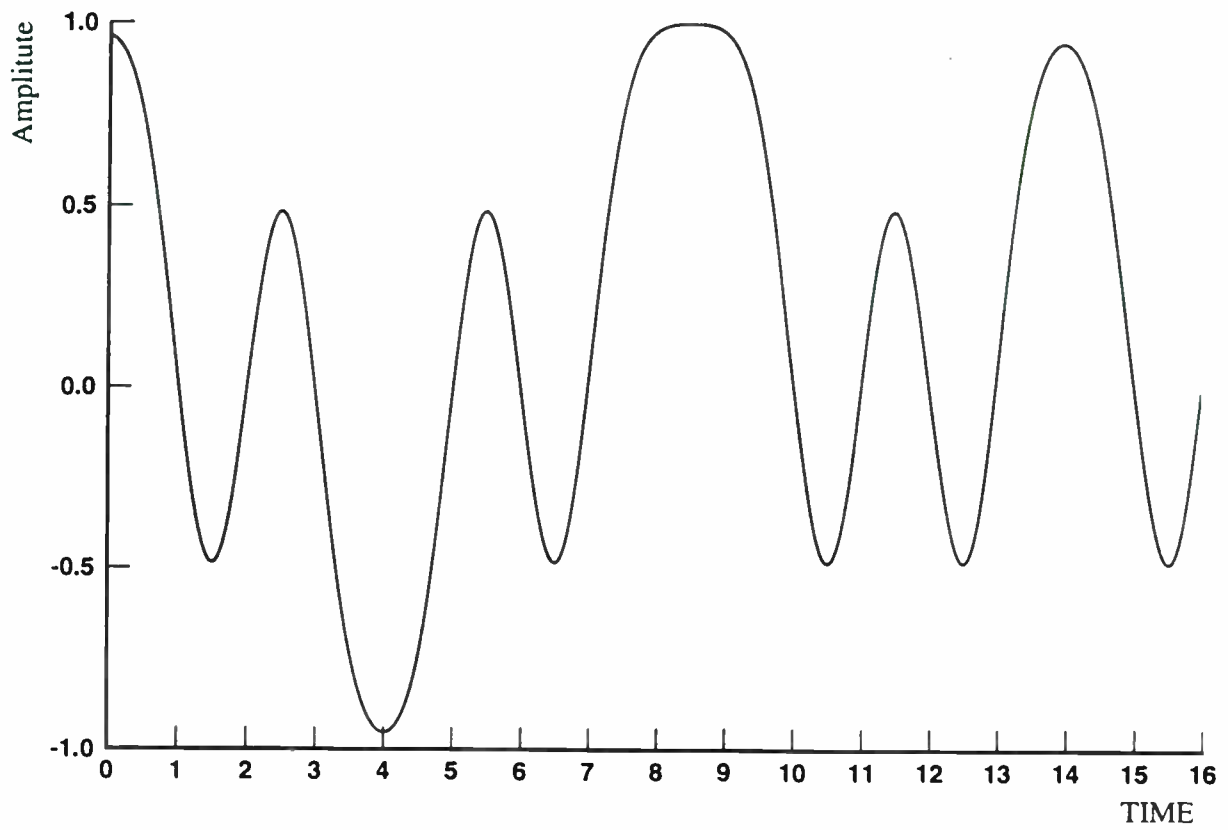
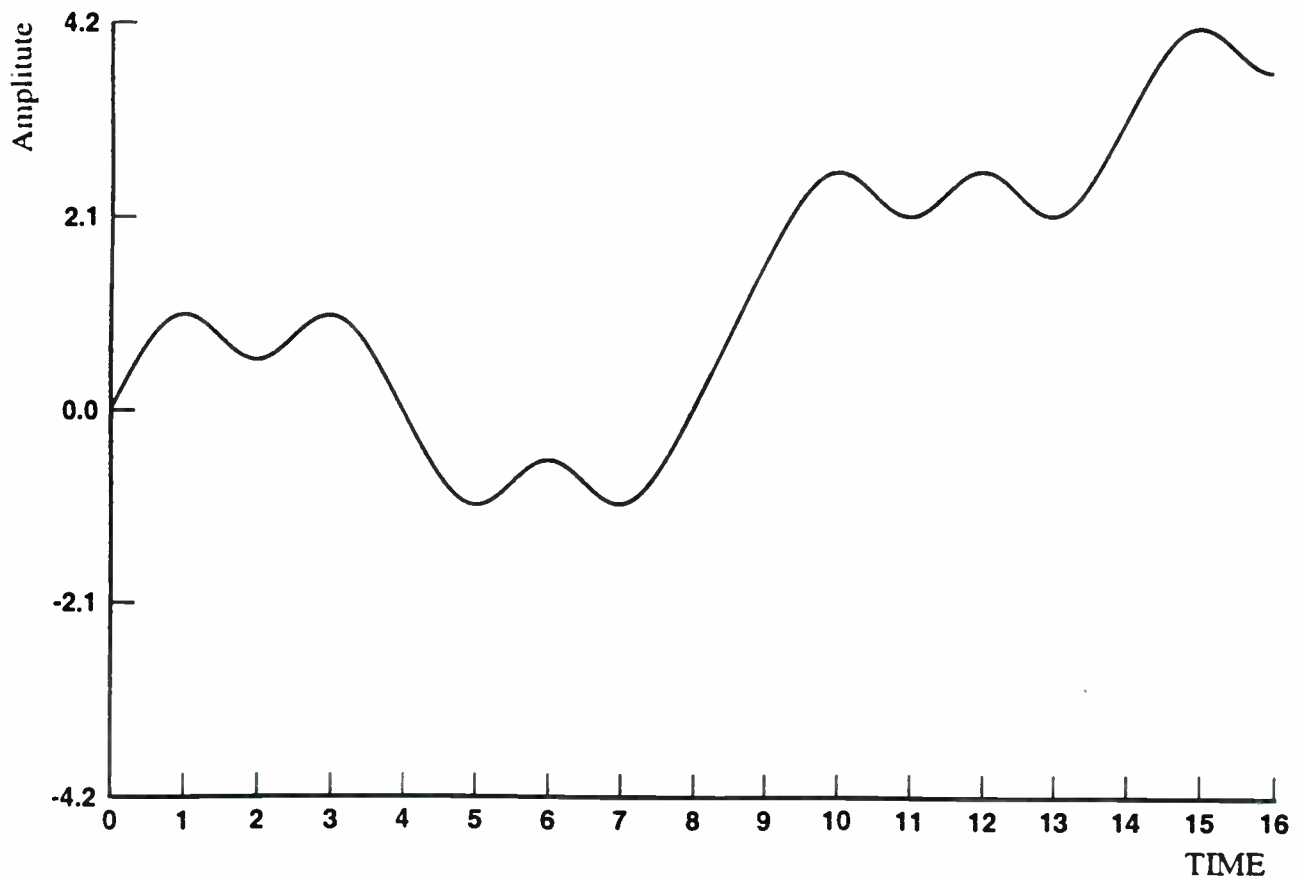


Fig. A.3.12 Gaussian filtered Non-return to Zero (NRZ) random data signal pattern at point 2 of Fig. A.3.1(c) and corresponding eye diagram for $BT_b = 0.3$ specified by the GSM standardization committee.

	DBPSK, DQPSK and $\pi/4$ -DQPSK	FQPSK and FBPSK	Improvement achieved by FQPSK and FBPSK
Measured maximum RF output power at 2.4 GHz	18.5 dBm	23.5 dBm	300%
Power efficiency	10%	20%	100%

Table A3.1 Maximal output power of illustrative 2.4 GHz integrated circuit amplifiers, suitable for PCMCIA cards with 3 V battery supplies and power efficiency comparison of DBPSK, DQPSK, $\pi/4$ -DQPSK vs. FQPSK and FBPSK.

Fig. A.3.13 Integrated Gaussian ($BT_b = 0.3$) filtered signal pattern $b(t)$ at point 3 of Fig. A.3.1(c).



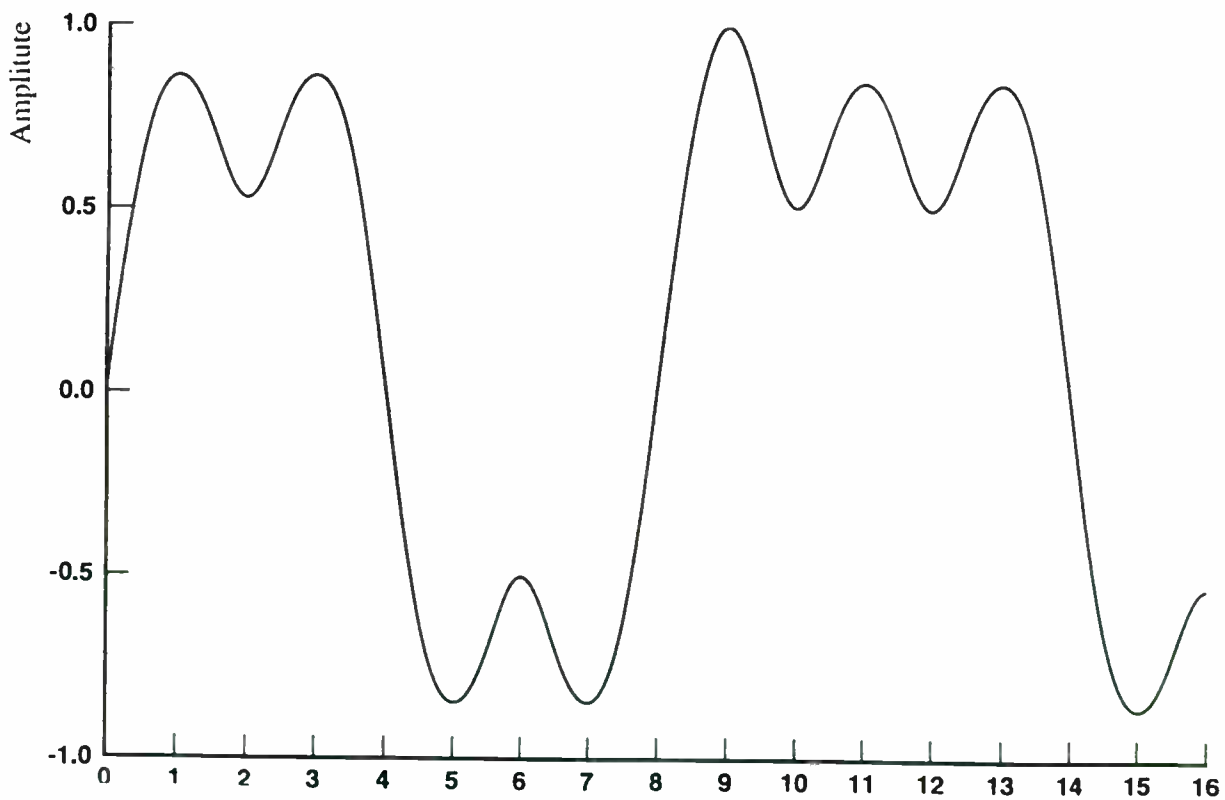
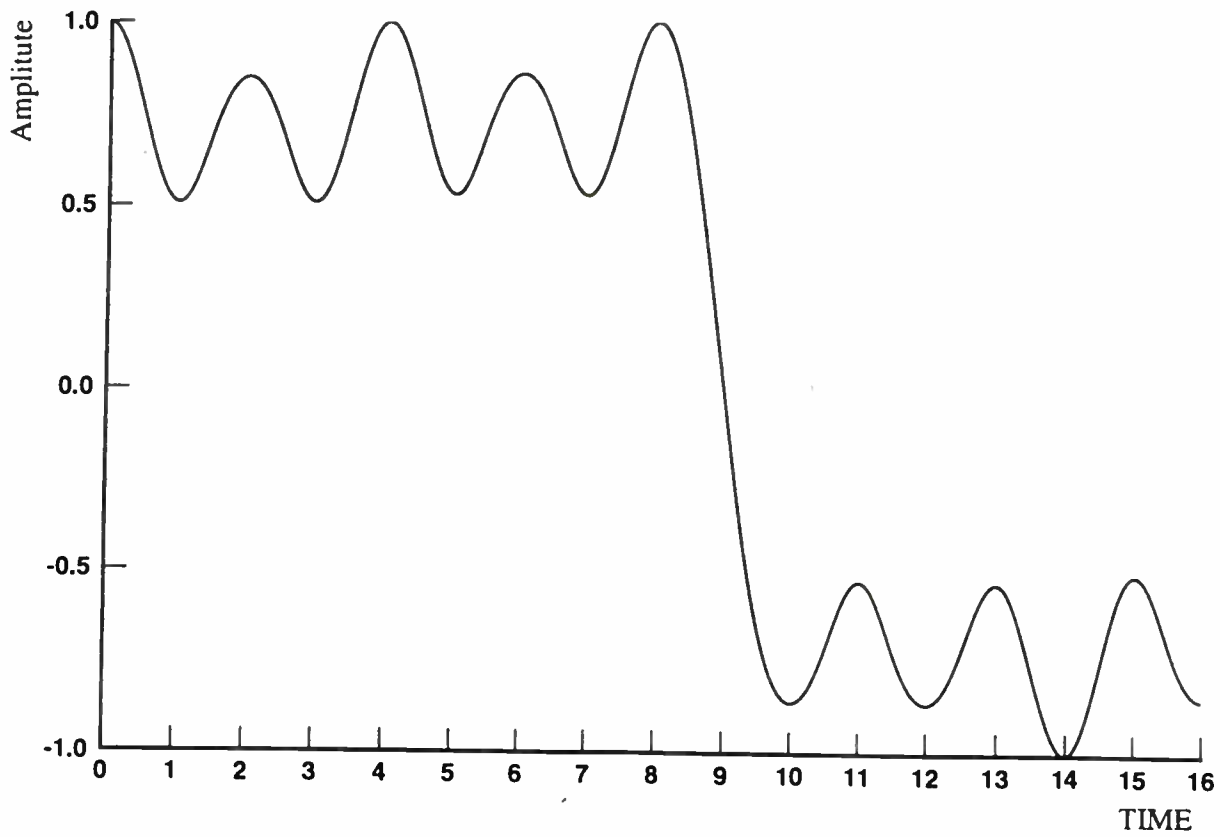


Fig. A.3.14 Signal patterns $x(t)$ and $y(t)$ corresponding to the outputs of the baseband processor I and Q drive signals. These crosscorrelated "outputs" are the "inputs" of the quadrature modulator, see points 4 and 5 in Fig. A.3.1c

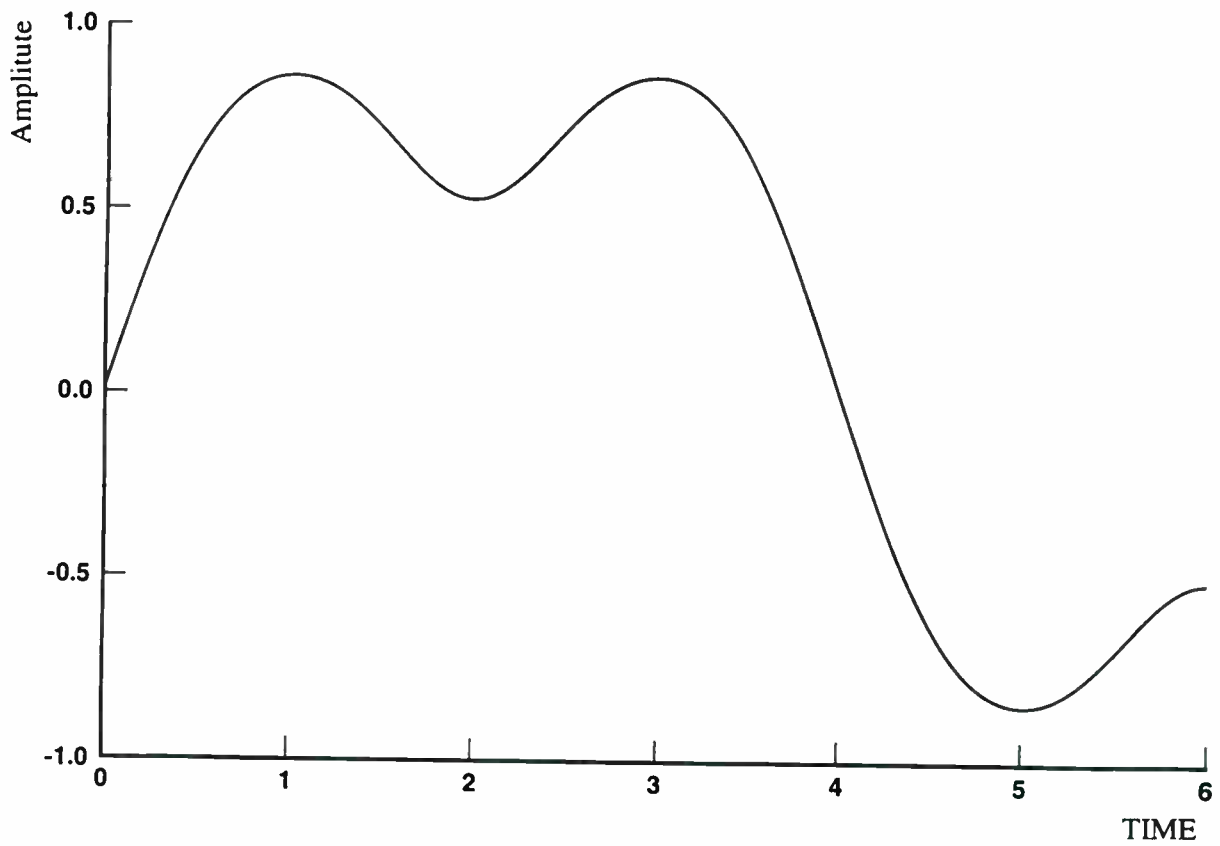
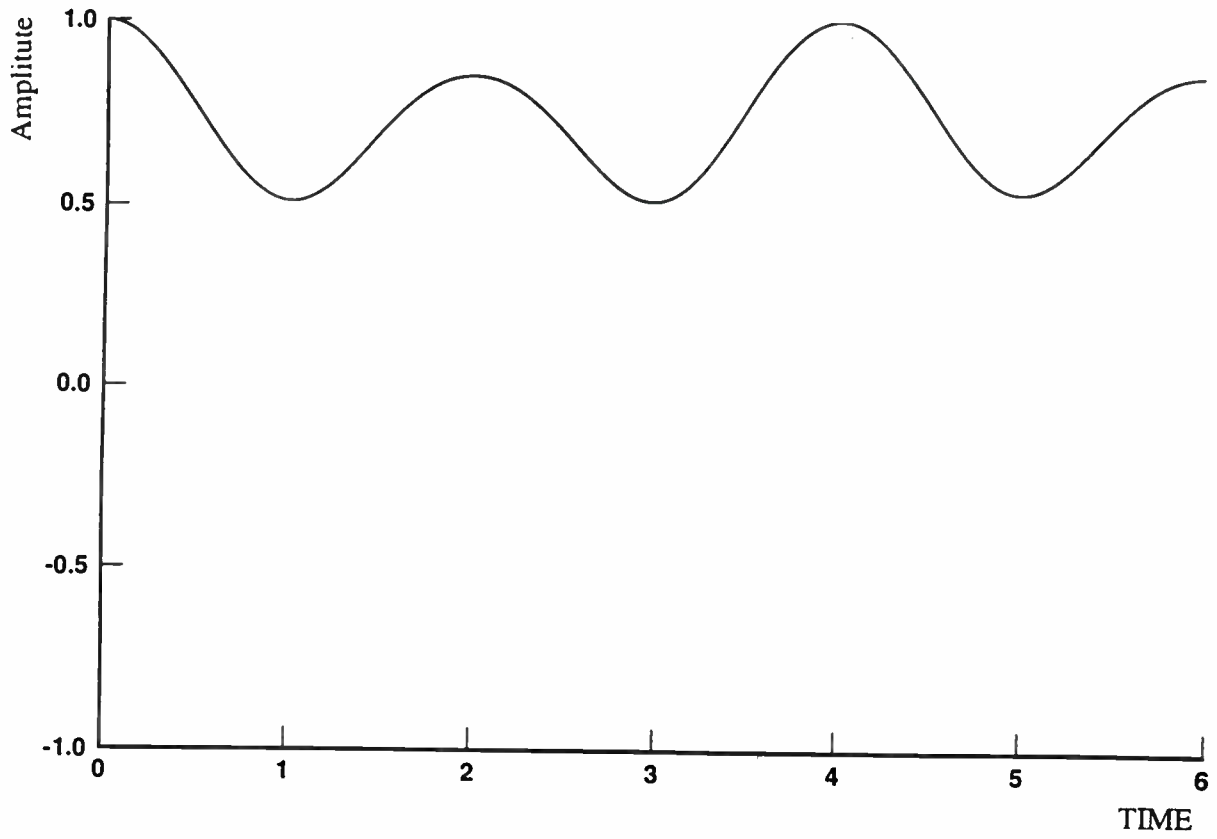
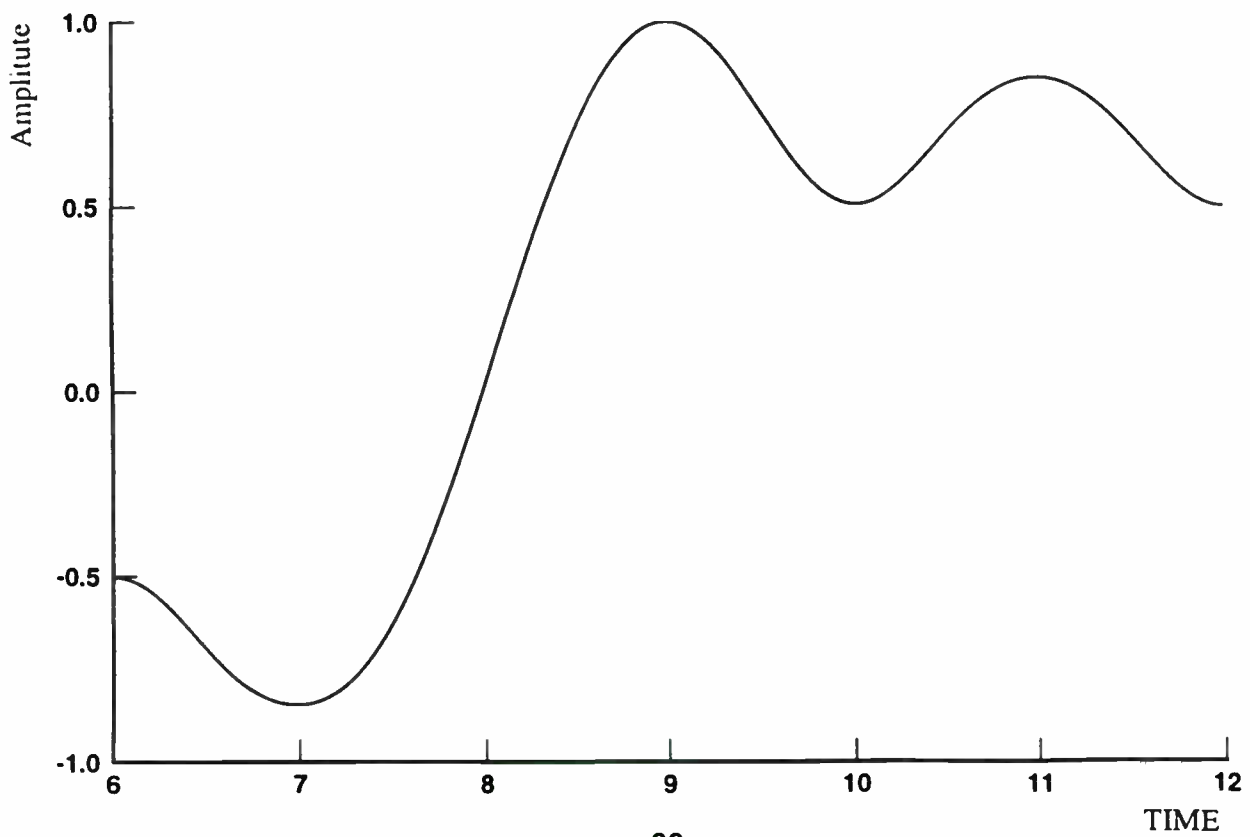
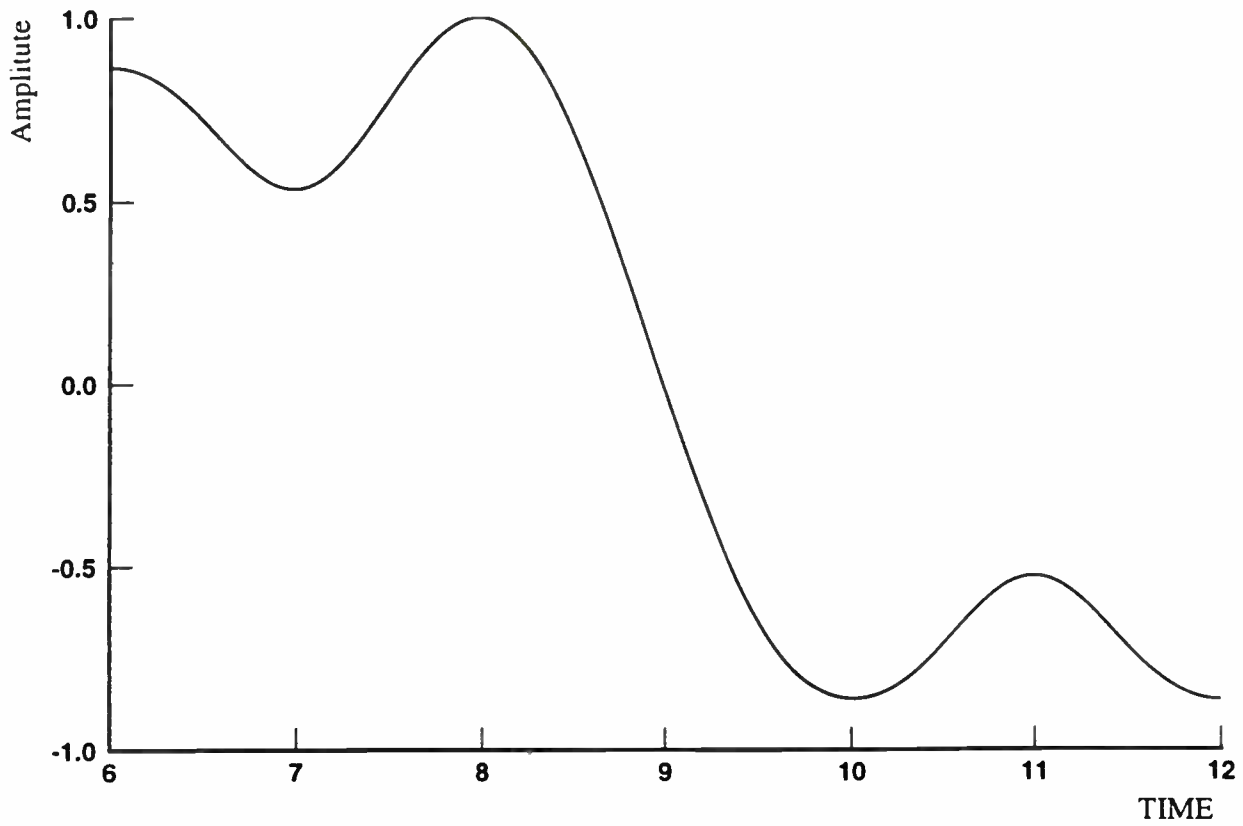


Fig. A.3.15 Time scale expanded signal outputs of $x(t)$ and $y(t)$ (otherwise same as Fig. A.3.13).

Fig. A.3.15 Time scale expanded signal outputs of $x(t)$ and $y(t)$ (otherwise same as Fig. A.3.13).



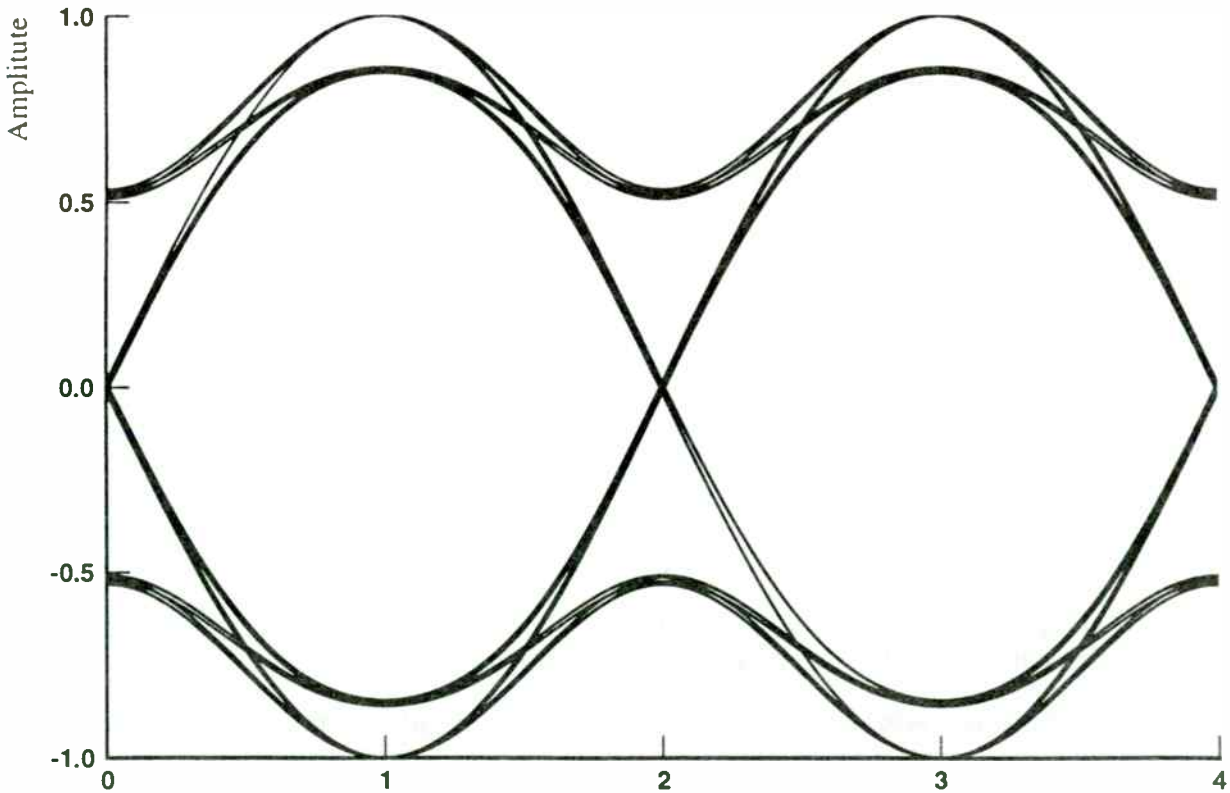
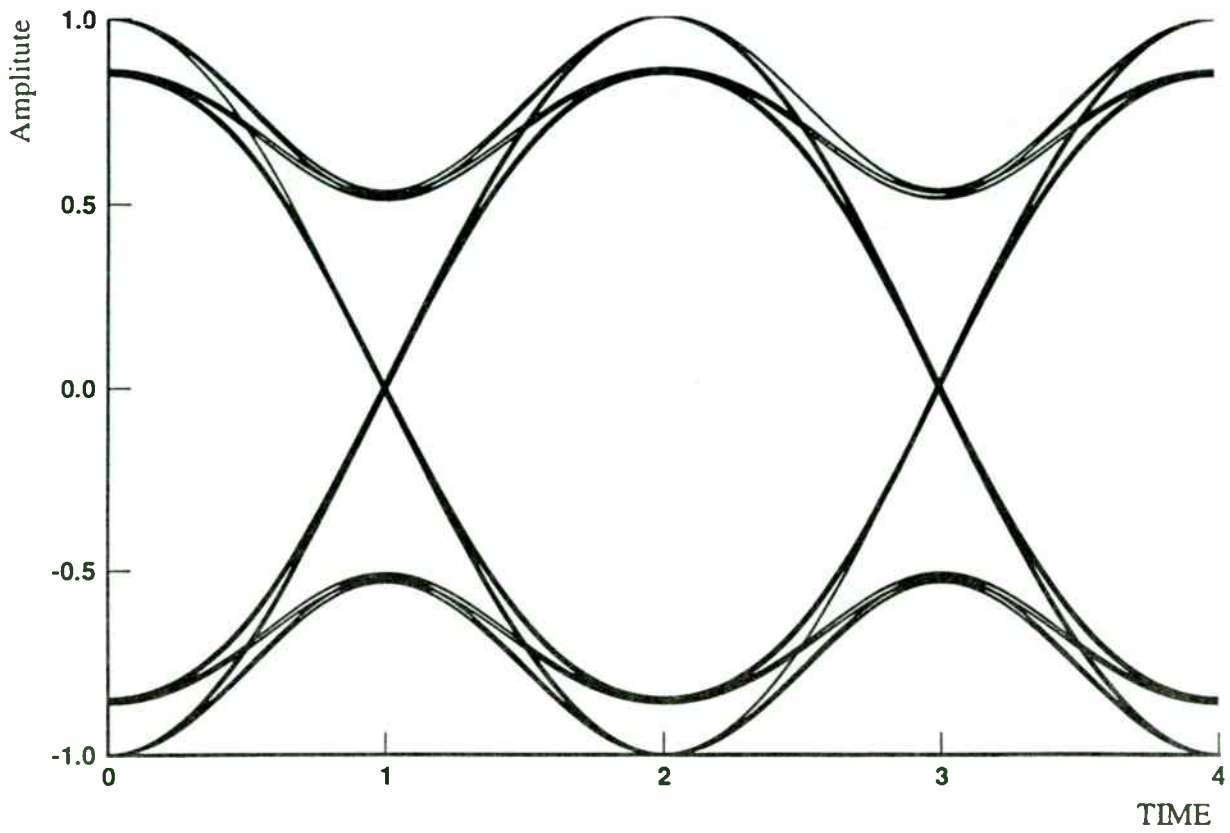


Fig. A.3.16 Crosscorrelated in-phase (I) and quadrature (Q) eye diagrams of the $x(t)$ and $y(t)$ signals displayed at points 4 and 5 of Fig. A.3.1(c).

Our filter “FF” patent meets the **Token-Passing Bus Local Area Networks** ISO/IEC/IEEE Standard 802.4-1990 specifications. Our “KF” patent claims the quadrature correlation based implementation of GMSK systems such as used in the **Global Mobile Systems (GSM)** standard. We have other patent disclosures and intellectual property (IP) (not listed in this paper) which are for new FBPSK and 4-FM and GFSK systems. On Motorola, Teledyne, MiniCircuits, and other RF ICs at 900MHz and 2.4GHz we demonstrated with our chips at 1Mb/s and 2Mb/s the spectral and power performance advantages of our wireless technologies, e.g., see Table A.3.1. FQPSK, FBPSK, FGFSK and FGMSK sample chips and/or technology transfers are available to members of the FQPSK Consortium. These chips operate in the 64Kb/sec to 10Mb/sec range. On infrared (IR) systems we demonstrated successful operation at 2Mb/s to 10Mb/s bit rate baseband and FQPSK.

A.3.9 Are the filter, correlation, GMSK, GFSK, FQPSK, FBPSK and FSK filter/processor patents and licensed product advantages truly revolutionary?

- a) **Robust BER** performance is essential in interference and/or noise controlled environments. Examples include FCC-15 authorized ISM bands, cellular and PCS cochannel controlled systems. In Fig. A.3.9 the experimental $BER=f(E_b/N_o)$ results demonstrate the **7dB to 12dB advantage** of robust FQPSK as compared to standardized GFSK and 4-FM systems. Such unparalleled improvements, as demonstrated in several IEEE 802.11 submissions **increase throughput and reduce delay at least 1000 times.**
- b) **RF IC power advantages** are illustrated in Table A.3.1. By comparing the average power output of some of the newest generations of 2.4GHz (and other RFIC frequency) chip sets note that FQPSK and FBPSK provides +23.5dBm while with the same device and same 3V battery dc power consumption, conventional BPSK and QPSK provide only +18.5dBm. The tremendous **5dB (300%) power advantage** of our technology is attained by patented simple baseband filters which enable the use of saturated "C-class" amplifiers instead of linearly operated RFIC amplifiers used in the cases of conventional BPSK and DQPSK spread spectrum, which require significant output back-off. **Note that FBPSK is fully compatible with conventional BPSK while FQPSK is compatible with OQPSK and GMSK.**
- c) **Spectral efficiency advantage** over standardized GMSK is illustrated in Figure A.3.10. The integrated out-of-band Adjacent Channel Interference of C-class amplified (saturated systems) demonstrate that the spectral efficiency of FQPSK is about 80% higher than that of GMSK or of GFSK. For example, in an authorized bandwidth of 1MHz you can transmit 1.5Mb/s with FQPSK-KF instead of 800kb/s with GMSK, **a real throughput advantage.** The compatibility and identical quadrature mod-demod structures of GMSK enable interoperability of these systems with FQPSK. Increase transmission speed and capacity of GMSK by nearly 200%!
- d) **"Talk time"** increased with simpler, smaller and reduced battery power filter implementations and more efficient RF IC operation.
- e) **Radiation is reduced.** Nonlinearly amplified FQPSK and FBPSK wireless systems have a 6dB to 8dB lower peak radiation than standardized DBPSK, DQPSK and p/4 DQPSK.

- f) **Gate count reduction of over 5 times (500%) with Feher's Filter/Correlation** based on look-up table ROM or FPGA enables design of much simpler quadrature implementation.

A.3.10 Is Reduced Peak Radiation an Essential Requirement?

New PCS and wireless regulations could stipulate limits on peak radiation. For such applications you could transmit with the FQPSK family of radio systems 6dB or more power than with conventional QPSK because of the reduced peak factor and envelope fluctuation of our technologies. FQPSK's reduced peak radiation is an additional advantage of this powerful technology.

A.3.11 Benefits of Joining the FQPSK International Consortium

To introduce, manufacture and market power and spectrally efficient cost-competitive wireless -RF, cable, infrared satellite microwave and other systems and components, you may wish to become knowledgeable and **have the license to participate** in some of the most exciting technical achievements and product implementations, including standardized GMSK quadrature modulated systems, GFSK, FQPSK, FGFSK, FGMSK, and FBPSK product designs. You could obtain technology transfer and license for FPGA and ROM based "FF" and Kato/Feher "KF" correlation, e.g., GMSK revolutionary implementation technology. By joining the FQPSK Consortium your products could become compatible with standardized wireless systems and be ahead of the "just barely meets" standard requirements. Your organization may also benefit from potentially new "de facto" leading and emerging standards which could have significantly superior performance, increased speed, longer "talk time" (reduced battery power consumption) than compatible conventional systems.

Resume of DR. KAMILO FEHER

Dr. Kamilo Feher, Fellow of IEEE, Professor at University of California, Davis, author of 6 books and of more than 300 R&D papers, is co-inventor of analog and digital filter, signal processing and modulation patents licensed for digital wireless, cable, satellite and other communication systems. His U.S. Patents include No. 4,339,724 and No. 4,567,602; these are used for ROM and digital synthesized FPGA-related and ASIC Gaussian (e.g., GMSK and GFSK) and raised cosine $\pi/4$ -QPSK as well as other filter and system implementations. Feher's FQPSK, FBPSK, and "F-Modulation" patent disclosure family of patented nonlinearly amplified, combined modulation/RF and infrared wireless systems increase by 300% the throughput of WLAN standardized and other GFSK and GMSK systems and have been proven to triple the RF output power and increase dramatically the battery power efficiency of QPSK types of systems. Through Dr. Feher Associates and as President of Digcom Inc. and of the international FQPSK Consortium he is active in technology transfer, consulting and licensing of power and spectrally efficient wireless, cable and other filter/modulation RF products. At UC Davis he is directing one of the most active and best-equipped experimental digital and wireless communications university-based laboratories in the U.S. in the fields of CDMA, TDMA, modulation and IF-RF design. His newest book, K. Feher: "Wireless Digital Communications: Modulation and Spread Spectrum Applications," published by Prentice-Hall, will be available during the Spring of 1995.

CDMA/SSMA APPROACH TO WIRELESS LOCAL LOOP

by

S.DANIEL JEBARAJ & B.S.KRISHNA SHASTRY, ITI Ltd, BANGALORE.

ABSTRACT

Wireless Communication is developing at a rapid pace in many walks of life today. The demand for scarce radio spectrum is ever increasing, as data and voice communication has become very essential for global information exchange. The various modulation techniques with different media access techniques which are in vogue have not been able to cope with the ever increasing demands of the radio spectrum. The code division multiple access technique (CDMA) promises to meet the large demand of the radio spectrum by the ever increasing users. The CDMA allows for large number of users to simultaneously access the same bandwidth, without degrading the quality of service.

The Wireless Telephone Systems like Wireless Local Loop, Cellular mobile radio etc, which are in operation today, use FDMA, TDMA with analog and digital modulation techniques. This paper presents a novel Line-of-sight (LOS) CDMA approach to the wireless local loop for secondary switching areas in developing countries. The CDMA Wireless Local Loop (CWLL), consists of a switching centre, a radio Base station and fixed Remote subscriber units. The switching centre interconnects the PSTN to the Radio Base station over a serial link for control and voice circuits for speech.

The CWLL uses the radio control channel with an unique PN sequence adopting Adaptive Time Division Multiplexing (ATDM) for signalling. The voice channels which are 32 Kbps ADPCM use different PN sequences for different users. The CWLL uses radio concentration of 10:1 which meets the traffic requirements of the secondary switching areas.

The CWLL proposal is an ideal solution to low power efficient spectrum utilisation amongst various users. The network has inherent immunity to interference, anti-jamming and security from eaves-droppers. The system can also be used as a captive network for police and military applications. The system proposal uses UHF band with low power (less than one watt) transmission with a range of 10 km. using directional antennae for fixed terrestrial application.

Cellular Technologies

Session Chairperson: David Sprague,
INMARK—Independent Marketing Corp. (Walnut Creek, CA)

Microcell propagation and antenna diversity measurements for non-line-of-sight communications at 900 MHz. **Gregory A. DesBrisay and James D. DeLoach, Jr.,** Cellnet Data Systems (San Carlos, CA).....75

RF radiation and radiation checker for cellular phones. **A. Kumar,** AK Electromagnetique, Inc. (Coteau Station, Quebec, Canada).....80

A new standard for in-building personal communications service. **John Avery,** Matsushita Communication Industrial Corporation of America (Alpharetta, GA).....88

A fast locking scheme for PLL frequency synthesizers. **David Byrd, Craig Davis, and William O. Keese,** National Semiconductor Corp., Wireless Communications Group (Santa Clara, CA).....96

PCS-1900: GSM as a candidate for US PCS applications. **Rupert Baines,** Analog Devices, Inc., Communications Division (Wilmington, MA).....101

Microcell Propagation and Site Diversity Measurements for Non-LOS Communications at 900 MHz

Gregory A. DesBrisay and James D. DeLoach, Jr.

CellNet Data Systems, 125 Shoreway Road, San Carlos, California 94070 USA

Abstract—New microcell systems are being deployed to provide communications to low-cost, low-power data transmitters for telemetry devices (e.g. electric, gas, and water meters; vending machines; and paging devices). In order to characterize propagation conditions for those microcell systems, radio propagation measurements were conducted in the 902-928-MHz band in suburban areas of San Rafael, California and in Kansas City, Kansas where spread-spectrum transmitters are located in electric power meters on the sides of homes, apartment buildings, and office buildings; and receivers are mounted on power poles. Line-of-sight propagation paths are rare for those installations.

This paper also reports on the influence of site diversity on the coverage area of the microcell base-station receivers.

1. Introduction

New microcell systems are being deployed to provide communications to low-cost, low-power data transmitters for telemetry devices (for example, electric, gas, and water meters; vending machines; and paging devices). In order to characterize propagation conditions for those microcell systems, radio propagation measurements were conducted in the 902-928-MHz band in suburban areas of San Rafael, California and in Kansas City, Kansas.

Xia *et. al.* [1, 2] report that propagation paths in microcells for communications to vehicles in streets contain significant line-of-sight components out to the distance where the ground just begins to disrupt the first Fresnel zone (depending on terrain, distances of 100 to 900 m are indicated in their papers).

Propagation in microcells for services to homes and office buildings is somewhat different. As might be expected, we find that line-of-site (LOS) propagation paths are rare in such microcells, and blockage creates large variations in path loss.

Section 2 of this paper contains a description of the system that was the motivation for conducting the measurements described here.

Section 3 contains data from path-loss measurements in the 902-928-MHz band in two suburban communities.

Section 4 contains a comparison of the coverage percentages for those communities with and without site diversity.

2. Background: The CellNet RF System Architecture

The CellNet wireless data communication system, illustrated in Figure 1, has a two-layer architecture: a wide-area network (WAN) macrocell layer and a local-area network (LAN) microcell layer.

The WAN macrocell layer enables electric, gas, and water utilities to remotely monitor and control points in their distribution systems, including voltage regulators, capacitor banks, line reclosers, sectionalizers, pressure monitoring points, and leakage detectors, among others.

The LAN microcell layer enables communications to low-cost, low-power data transceivers for telemetry applications such as electric, gas, and water meters; vending machines; and paging devices.

The microcells operate in the 902-928-MHz Part-15 spread-spectrum band in the United States. The microcell base stations (also known as microcell controllers) communicate to system controllers via the wide-area-network radios in the licensed 952/928-MHz multiple-address-services (MAS) band.

Radios in the local area network are direct-sequence BPSK spread-spectrum radios. The data rate for the local area network is 19.2 kbps. Radios in the wide-area network are narrowband 9-QPR digital radios deployed in a cellular frequency-reuse architecture.

Intelligence is distributed throughout the network. Microcell controllers collect, filter, and interpret data from telemetry devices. Data can then be relayed via the wide-area network to the system controller immediately, or it can be stored for periodic uploads.

As described in the next section, path-loss measurements for the local-area network radios were taken to enhance our ability to plan and deploy the microcells in this system so that they provide coverage to nearly all of the possible locations where meters and other telemetry devices will be deployed.

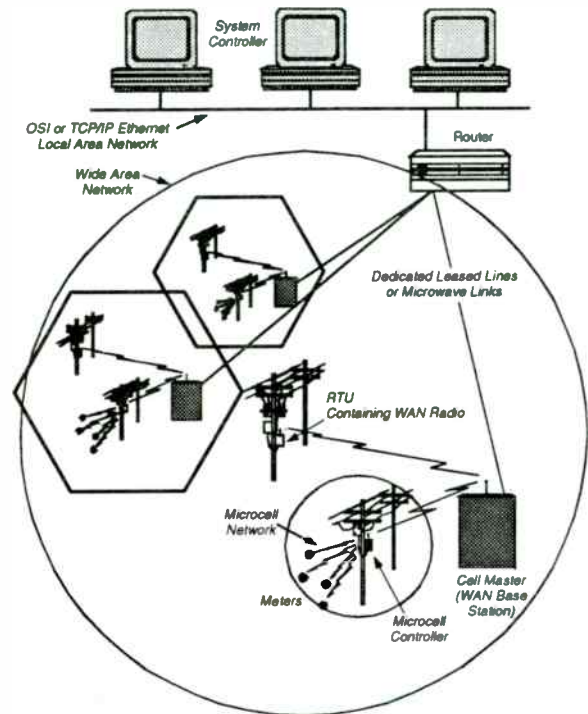


Figure 1. The CellNet wireless data communication system includes a local-area network layer for communication with low-cost, low-power telemetry devices like power meters, and a wide-area network layer for communication with microcell controllers and control devices for electric, gas, and water utilities.

3. Path-Loss Measurements

The microcell propagation measurements described here were gathered from two network installations, one in San Rafael, California, and another in Kansas City, Kansas. Both networks use 902-928-MHz spread-spectrum 200-mW transmitters imbedded in electric power meters to provide automated meter reading services in those cities.

The San Rafael deployment is located in central San Rafael, California. Structures in the area include single-family one- and two-story wood-frame homes, two- and three-story reinforced-concrete apartment buildings, and one- and two-story masonry and reinforced-concrete commercial structures.

The Kansas City deployment is located in parts of Overland Park and Prairie Village, suburbs of Kansas City, Kansas. Structures in the area include mostly single-story, wood-frame homes, with some moderate-density apartment structures.

To produce the path-loss data presented in Figures 2 and 3, 1000 meters in San Rafael and 5000 meters in Kansas City were used.

The power meters in these two communities are usually mounted outside on the sides of houses. In apartment buildings, however, meters are often mounted in underground parking garages. Microcell controllers are mounted on power poles or light poles at heights of 18 to 25 feet. The antenna gain for the microcell controllers is +5 dBi. The antenna gain for the transmitters imbedded inside the electric meters is estimated to be about -6 dBi (a figure that is being improved upon as a result of these measurements). The microcell controller antennas are vertically polarized in these areas of San Rafael and Kansas City. The electric meter antennas exhibit a mix of horizontal and vertical linear polarization.

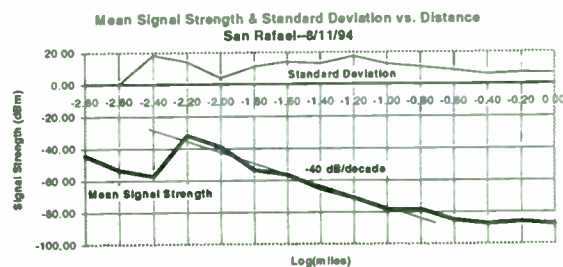


Figure 2. The overall path-loss slope is roughly 40 dB/decade, and the standard deviation is about 14 dB in San Rafael, California

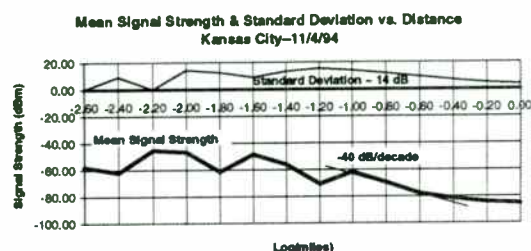


Figure 3. The overall path-loss slope is also about 40 dB/decade, and the standard deviation is about 14 dB in Kansas City, Kansas, but the path-loss intercept is different.

As shown in the figures, the overall mean path-loss slope for both communities is about 40 dB/decade. The mean path-loss slope for individual microcells in those communities has been found to vary from 30 to 60 dB/decade.

The standard deviation of path loss in microcells was found to be about 14 dB in both communities. *That standard deviation includes the effects of blockage by buildings and terrain, along with the effects of the essentially random orientation of meters and their antennas with relation to the microcell controllers.*

Note that in these two microcell environments there are no discernible LOS regimes. Undoubtedly that is because very few LOS paths exist when transmitters are affixed to the sides of buildings.

4. Coverage and Site Diversity

Packet-error-rate (PER) data was collected along with the path-loss data and was used to determine the coverage percentage for microcells as a function of distance for the test area in Kansas City.

The protocols in the CellNet local area network can tolerate very high packet error rates because of the extensive use of redundancy and error checking. The exact PER requirements are a function of the reliability requirements of the telemetry applications for which the network is intended. For example, once-per-day electric power meter reading can be accomplished with very high packet error rates, while load-profile metering requires lower packet error rates. (Load-profile metering requires readings every 2.5-minutes.)

As shown in the previous section, path loss for these microcells is highly variable. Site diversity (the ability to receive a transmission at any of the several neighboring microcell controllers) increases the coverage percentage in each microcell and allows larger microcells to be used.

Figure 4 shows the coverage percentage (that is, the percentage of meters heard) as a function of microcell size for a range of packet success rate (PSR = 1 - PER) thresholds when site diversity is *not* used.

Figure 5 shows the coverage percentage as a function of microcell size when site diversity *is* used.

In the area of Kansas City where this data was gathered, the spacing between microcell controllers is roughly 0.2 miles.

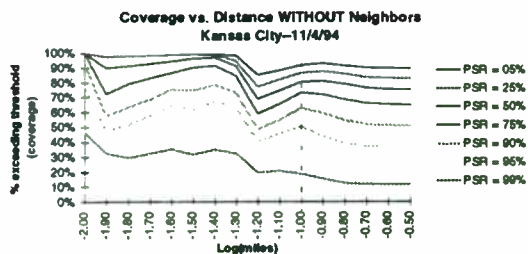


Figure 4. Coverage percentage as a function of distance and packet-success-rate threshold without the benefit of site diversity.

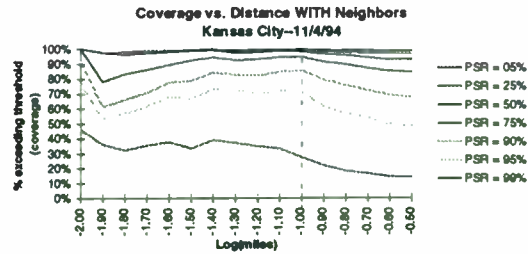


Figure 5. At the boundary between microcells (0.1 mi. or -1.0 log-miles in this plot) the coverage percentage for most levels of packet success rate is improved by around 20% when site diversity is used in this Kansas City LAN. (Microcell Controller spacing is roughly 0.2 mi.)

The figures show that site diversity has a large effect. At the boundary between microcells (at a distance of 0.1 mi. or -1.0 log-miles in this area of Kansas City) the coverage percentage for most levels of packet success rate is improved by around 20% when site diversity is used. For example, at a PSR of 75%, the coverage percentage increases from 73% without site diversity to 95% with site diversity. Furthermore, out of 5000 transmitters, only 3158 transmitters are seen best by the closest microcell receiver; the others are heard best by a neighboring microcell receiver.

The figures shown above are derived from the combined data for 5000 transmitters in 35 microcells. Figure 6 below illustrates the variability of coverage area from one microcell to another. The curves represent the coverage without the benefit of site diversity as a function of distance for each individual microcell. (The PSR threshold for all the plots in Figure 6 is 75%.)

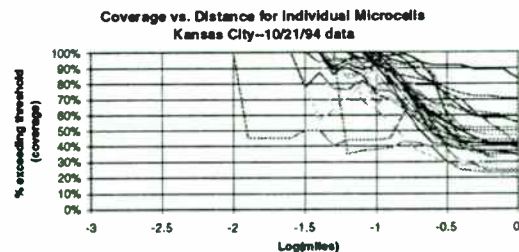


Figure 6. Coverage percentage as a function of distance is variable from one microcell to another.

5. Conclusions

Microcell path-loss measurements from two suburban areas in San Rafael, California and Kansas City, Kansas have been presented.

The typical mean path-loss slope for those two locations is 40 dB/decade, although it varies between 30 and 60 dB/decade for individual microcells. The standard deviation for path-loss in both locations is about 14 dB. That variation includes the effects of blockage by buildings and terrain, along with the effects of the essentially random orientation of meters and their antennas with relation to the receivers.

In this microcell environment there is no discernible LOS regime. Undoubtedly that is because very few LOS paths exist when transmitters are affixed to the sides of buildings.

Blockage creates extremely large variations in path loss, especially when meters are installed in apartment buildings and other metal-inclusive structures.

Site diversity mitigates the effects of blockage to a significant extent allowing improved coverage percentages and larger microcells.

6. References

- [1] H.H. Xia , H.L. Bertoni, L.R. Maciel, A. Lindsay-Stewart, and R. Rowe, "Radio Propagation Characteristics for Line-of-Sight Microcellular and Personal Communications," *IEEE Transactions on Antennas and Propagation*, Vol. 41, No. 10, October 1993, pp. 1439-1447.
- [2] H.H. Xia, L. Grindstaff, and H.L. Bertoni, "Microcellular Propagation Characteristics," *Proceedings of ISAP '92*, Sapporo, Japan, pp. 425-428.

RF RADIATION AND RADIATION CHECKER FOR CELLULAR PHONE

A. Kumar
AK Electromagnetique Inc.
30 Rue Lippee
Coteau Station
Quebec
Canada JOP 1EO

ABSTRACT

This paper summarizes the effects of radiation and it has been explained that available data on the effects of radiation varies in every human. The radiation standard data for the United States and Canada have been provided. Electromagnetic coupling effects on a operator of a cellular phone has been discussed and computed results are compared. Applications of a low-cost cellular phone radiation checker are presented. The radiation checker provide a fullproof means of testing for potential health hazards from excessive non-ionizing radiation for the general public and should be used by the operator of a cellular phone.

1.0 Introduction

There is a great deal of concern on the part of the public about the purported biohazards of RF electromagnetic radiation. RF electromagnetic fields have special biological significance since they can readily be transmitted through, absorbed by, and reflected at biological tissue boundaries in varying degrees, depending on frequency, physical and chemical properties of the body tissue. The effect of RF electromagnetic radiation on the biological system may be categorized into two classes: 1) the thermal effects resulting from high-level RF power, and 2) the non-thermal effects due to low-power. Thermal effects (cataracts, male infertility, etc.) have been identified, but these require high power level. Low power RF electromagnetic radiation do not have enough energy to damage cells in the same manner as nuclear (ionizing) radiation or certain chemicals. However, very low-power level RF electromagnetic fields do not produce cancer but rather influence or enhance the development of natural and spontaneous cancers.

At present, cellular phones have been extensively used by the world. The portable handset cellular phone operates in the frequency range of 824 to 896 MHz. The operator of the portable handset cellular phone is very near to the transmitter and radiating antenna. Many researchers [1] - [5] have reported on the RF exposure of a human body in the near field of a dipole antenna. However, the detailed effects of the RF field due to a human body and radiating element at cellular band have been unavailable. Recently, Kumar [6] has analyzed the specific absorption rate (SAR) on a model

of the human head. Chuang [7] has reported the effect of the electromagnetic coupling and body absorption on the antenna radiation pattern of a cellular phone at 840 MHz.

In this paper, we have compared the radiation data reported by various researchers at UHF-band (cellular frequency band). The radiation standard for general public is compared with available data. Application of a low cost radiation checker is discussed for the general public.

2.0 MECHANISIM ON EFFECTS OF ELECTROMAGNETIC RADIATION

The effects of RF electromagnetic radiation are same in every human. There are more than thosand papers and reports are published on the subject, but their findings are not same. To a large extent, this is because the low-power RF electromagnetic field do not have enough energy to produce large amount of defective (bad) cells.

The human body produces a number of defective cells per day as a result of exposure to x-rays, cosmic rays, nuclear radiation, and certain chemicals. Ames et al. [8] Kinzler et al. [9], and Hoeft [10] have reported that cancers or metastasizing tumors originate in a cell with defective genetic material (DNA). The human body produces a number of defective cells per day as a result of mutagenic and/or carciogenic agents. These agents are produced by certain chemicals, ionizing radiation and accients (perhapes thermal-ly induced). Usually, defective cells are destroyed by the immune system before it can reproduce the bad cell. However, in presence of a low power electromagnetic radiation the cell division rate increases results in more bad cells. There is a probability that the electromagnetic radiation is present very close to the body part where bad cells already exist and therefore, an increase in rate of production of bad cells become very high. Hoeft's another model [10] describes that the physiological stress produced by the low power RF electromagnetic field adversely affects the immune system and therefore, the immune system reduces the ability to destroy bad cells. In both cases low power RF electromagnetic field do not produce cancers, but rather enhance or influence the development of bad cells which produces natural or spontaneous cancers. Experimental data show that the immune system and cell rate division varies human to human.

3.0 MAXIMUM PERMISSIBLE EXPOSURE

Exposure associated with an uncontrolled environment is the exposure of individuals (general public) who have no knowledge or control of their exposure. The exposure may occur in living places or work places where there are no expectations that the exposure levels may exceed those shown in Table 1 [11] - [12]. The maximum permissible specific absorption rate (SAR) limits are shown in Table 2 [11] - [12].

Table 1

Maximum Permissible Exposure for an Uncontrolled Environment

Country	Frequency Range (MHz)	Power Density (mW/cm ²)	Average Time (Minutes)
United States	300 - 3000	f/1500	6
Canada	300 - 1500	f/1500	6

f is the frequency of radiation in MHz.

Table 2

Maximum Permissible SAR Limits for Uncontrolled Environments

Country	Conditions and Limits
United States	<ol style="list-style-type: none"> 1) Below 0.08 W/kg (averaged over whole body). 2) Maximum peak below 1.6 W/kg, as averaged over any 1 gm of tissue. 3) Below 4 W/kg for hands, wrists, feet, and ankles (averaged over 10 gm of tissue). 4) The above limits and conditions (1 to 3) are valid at frequencies between 100 kHz and 6 GHz.
Canada	<ol style="list-style-type: none"> 1) Below 0.2 W/kg, as averaged over any 0.2 of the body mass. 2) Below 0.2 W/kg for the eye. 3) Maximum peak below 4 W/kg, as averaged over any 1 gm of tissue. 4) Below 12 W/kg at the body surface and in limbs (averaged over 10 gm of tissue)

4.0 COMPUTED RESULTS

A computer model and numerical simulation scheme are constructed to study the detailed human head coupling effects on the cellular phone antenna. The total electromagnetic field in free space is the sum of the incident field of the antenna, the absorbed field and the scattered field by the human head model.

$$E_T, H_T = E_I, H_I + E_A, H_A + E_S, H_S \quad (1)$$

where E_T, H_T are the total electric and magnetic field vectors,

E_i , H_i are the incident electric and magnetic field vectors, and E_A , H_A are the absorbed electric and magnetic field vector by the model of human head and E_s , H_s are the scattered electric and magnetic field vectors by the model of the human head. It is assumed in the calculation that there is no other losses in the electric and magnetic field vectors except in the model of the human head. The antenna current distribution of a z-oriented linear dipole antenna and the total induced electric current inside the model (human head) can be written as a pair of coupled integral equations by the dyadic Green's function techniques. A detailed description of the equation has been given in by Karimullah et al. [13]. The method of moments [14] has been used to solve the coupled integral equation. The total electromagnetic field in space is the sum of the incident field of the antenna and the absorbed power (including scattered power) by the human head model. It is assumed that there is no loss of power in the antenna.

A cellular phone is located in front of the right ear and the whole head is partitioned into thousands of non-uniform cubic cells for numerical analysis. The thin wire dipole antenna of the cellular phone is partitioned into 80 segments. In a typical telephone conversation, the dipole antenna is about 3 cm away from the right side of the head. A software is developed to calculate the radiated power, radiation efficiency and absorbed power by the head. These calculations were made for the antenna location at a distance of 1 cm, 2 cm, 3 cm, and 4 cm from the right side of the head. The relative permittivity and conductivity of the human head model are shown in Table 3 [15]. The phantom muscle of the human head model consisted of 74% pure water, 15% polyethylene, 9% TX150, and 2% salt.

Table 3

Relative permittivity of conductivity of the human head phantom muscle model at 835 MHz

	Relative Permittivity	Conductivity
Phantom muscle	54	1.6

Computed results for the model are summarized in Table 4. There is a variation of power with the distance. Recently, Chuang [7] published the work on the human operator coupling effects of a portable communication dipole antenna. Table 5 shows the computed results by Chung. Table 4 shows slight higher values of absorption than Table 5. The relative permittivity and conductivity values are slightly higher for the result shown in Table 4. The number of cells and the method of numerical calculations are slightly different.

Table 4

Computed results at 835 MHz when antenna is placed right side of the head and antenna radiates 1 W of power

Characteristic	Free space	Distance to the antenna			
		1 cm	2 cm	3 cm	4 cm
Radiated power into free space	1 W	0.30	0.45	0.55	0.65
Radiation efficiency (%)	100	30	45	55	65
Head absorbed power	-	0.70	0.55	0.45	0.35

Table 5

Computed results by Chung [7] at 840 MHz when cellular antenna is placed in front of the head with an antenna radiating power in free space is 1 W

Characteristics	Antenna in front of the head				
	1 cm	2 cm	3 cm	4 cm	5 cm
Radiated power into free space	0.219 W	0.427 W	0.505 W	0.634 W	0.723 W
Radiation efficiency (%)	21.9	42.7	50.5	63.4	72.3
Full body absorbed power	0.720 W	0.590 W	0.510 W	0.384 W	0.289 W
Head absorbed power	0.650 W	0.501 W	0.440 W	0.324 W	0.243 W
Peak SAR (averaged over 1 gm of tissue)	2.241 W/kg	1.501 W/kg	0.777 W/kg	0.530 W/kg	0.356 W/kg
Full body average SAR	0.0077 W/kg	0.0063 W/kg	0.0055 W/kg	0.0041 W/kg	0.0031 W/kg
Head average SAR	0.1192 W/kg	0.0976 W/kg	0.0844 W/kg	0.0636 W/kg	0.0478 W/kg

5.0 RADIATION CHECKER FOR CELLULAR PHONE

A low-cost radiation checker has been developed [16] - [17] to check the radiation through cables, connectors, antennas, and power amplifiers in the vicinity of human presence. The checker operates without batteries, powered by the strength of radiated electromagnetic field that it is measuring. An operator simply turns on the cellular phone, holds the radiation checker near source under test, and moves the checker around the operating area for maximum deflection. The back of the checker should face the expected source of radiation. Results are shown in mW/cm^2 on the dial of a meter (see Figure 1). Specifications of the radiation checker is summarized in Table 6.

Table 6

Specifications of the cellular phone radiation checker

- | | |
|---|--|
| (1) Frequency of operation: | UHF Cellular band
(824 to 896 MHz) |
| (2) Exposure limit for
general public: | $f/1500$ (IEEE C91.1)
For 824 MHz = $0.55 \text{ mW}/\text{cm}^2$ and
896 MHz = $0.6 \text{ mW}/\text{cm}^2$. |
| (3) Calibration: | 0 to $0.6 \text{ mW}/\text{cm}^2$. |
| (4) Physical size:
(Length x Width x depth): | 6 cm x 6 cm x 6 cm (approx.) |
| (5) Weight: | 80 gm (approx.) |
| (6) Casing: | Transparent plastic cover in
the front face of the checker
and plastic cover in the back. |
| (7) Maintenance: | Maintenance free (it does not
require any batteries). |
-

6.0 DISCUSSIONS AND CONCLUSIONS

Tables 4 and 5 show that the radiated power exceeds the limit for distances of 1 cm and 2 cm from the head. Experimental results of Guy et al. (Table IX of ref. [18]) show that the value of power density is $0.6235 \text{ mW}/\text{cm}^2$ per W for a woman standing 9.7 cm away from a truck mounted antenna. A low-cost radiation checker provide a full-proof means of testing for excessive non-ionizing radiation.

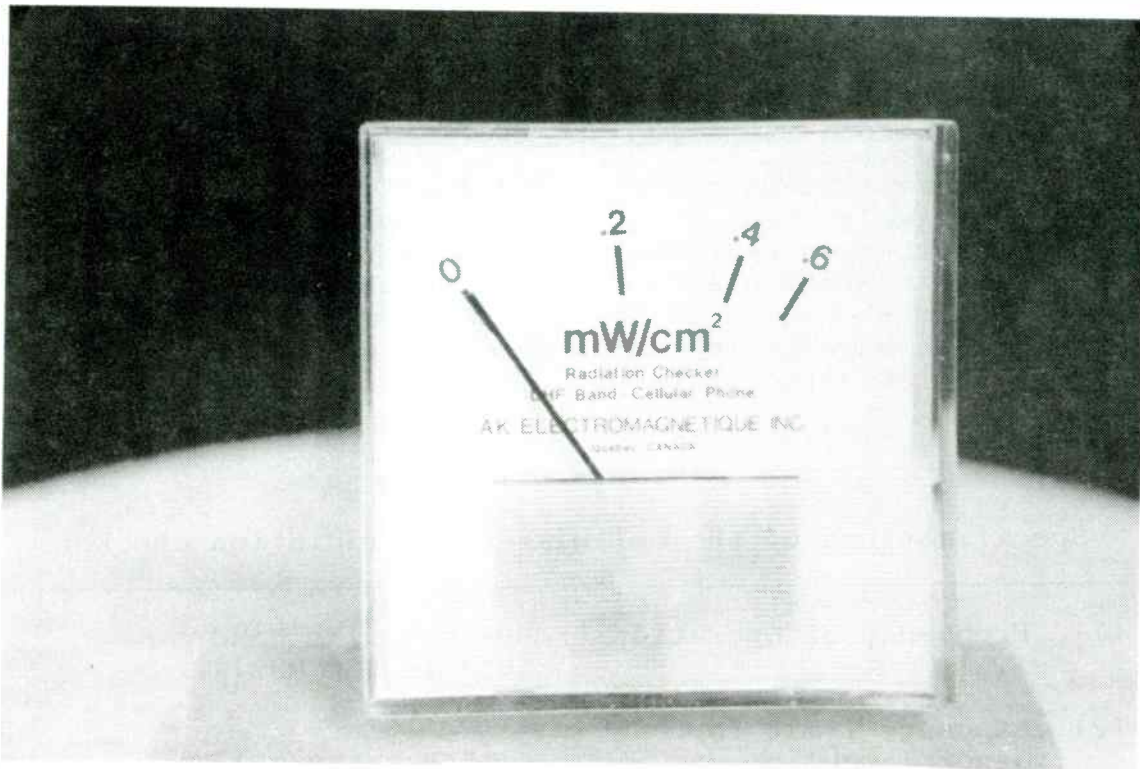


Figure 1 A photograph of a cellular phone radiation checker.

REFERENCES

- [1] I. Chatterjee, M. J. Hagmann, and O. P. Gandhi, "Electromagnetic energy deposition in an inhomogeneous block model of man for near-field irradiation conditions", IEEE Trans. Microwave Theory Techn., Vol. MTT-28, 1980, pp. 1452-1459.
- [2] M. A. Stuchly, R. J. Spiegel, S. S. Stuchly, and A. Kraszewski, "Exposure of man in the near-field of a resonant dipole: comparison between theory and measurements", IEEE Trans. Microwave Theory Techn., Vol. MTT-34, 1986, pp. 26-31.
- [3] A. W. Guy and C. K. Ckou, "Specific absorption rates of energy in man models exposed to cellular UHF mobile antenna fields", IEEE Tran. Microwave Theory Techn., Vol. MTT-34, 1986, pp. 671-680.
- [4] A. Kumar, "Microwave radiation, calculations and shielding", Proc. Canadian Conf. Elect. Comp. Eng., Montreal, Sept. 1989, pp. 922-925.
- [5] C. M. Furse, J. Y. Chen, and O. P. Gandhi, "The use of the frequency-dependent finite-difference time-domain method for induced current and SAR calculations for a heterogeneous model of the human body", IEEE Trans. Electromagn. Compat., Vol. 36, 1994, pp. 128-133.
- [6] A. Kumar, Calculation of SAR of the model of human head, Research Report, AK-47-93, AK Electromagnetique Inc., 1993.

- [7] H. R. Chung, "Human operator coupling effects on radiation characteristics of a portable communication dipole antenna", IEEE Trans. Antennas Propagat., Vol. AP-41, 1994, pp. 556-560.
- [8] B. N. Ames and L. S. Gold, "Too many rodent carcinogens: mitogenesis increases mutagenesis", Science, Vol. 249, 1990, pp. 970-971.
- [9] K. W. Kinzler, M. C. Nilbert, B. Vogelstein, T. M. Bryan, D. B. Levy, K. J. Smith, A. C. Preisinger, S. R. Hamilton, P. Hedge, A. Markham, M. Carlson, G. Joslyn, J. Groden, R. White, Y. Miki, Y. Miyoshi, I. Nishisho, and Y. Nakamura, "Identification of a gene located at chromosome 5q21 that is mutated in colorectal cancers", Science, Vol. 251, 1991, pp. 1366-1370.
- [10] L. O. Hoefft, "A model for possible effects of electromagnetic fields on occurrence of cancer", Proc. IEEE Int. EMC Symp., Anaheim, California, 1992, pp. 266-268.
- [11] IEEE Standard for safety levels with respect to human exposure to radio frequency electromagnetic fields, 3 kHz to 300 GHz, IEEE C95.1-1991, April 27, 1992.
- [12] Limits to exposure to radiofrequency fields at frequencies from 10 kHz - 300 GHz, Safty code 6, Health and Welfare Canada, Ministry of Supply and Services Canada, 1991.
- [13] K. Karimullah, K. M. Chen, and D. P. Nyquist, "Electromagnetic coupling between a thin-wire antenna and a neighboring biological body: theory and experiment", IEEE Trans. Microwave Theory Techn., Vol. MTT-28, 1980, pp. 1218-1225.
- [14] R. F. Harrington, Field Computation by Moment Methods. New York: Macmillan, 1968.
- [15] A. Kumar, "Complex permittivity and conductivity of TX150, Polyethylene power, water, and salt (model of phantom muscle)", Presented in the Symp. on Electronics, 1978, Higher Inst. of Electronics, Hal-Far, Malta.
- [16] A. Kumar, Microwave Oven Leakage Checker, U. S. and British Patent Pending, 1994.
- [17] A. Kumar, Low-cost Radiation Checkers, Research Report AK Electromagnetique Inc., Quebec, Canada, 1993, and Canadian Patent Pending, 1994.
- [18] A. W. Guy and C. K. Chou, "Specific absorption rates of energy in man made models exposed to cellular UHF mobile antenna fields", IEEE Trans. Microwave Theory Techn., Vol. MTT-34, 1986, pp. 671-680.

A new standard for In-building Microcellular Personal Communications Service

John Avery
Phone/fax: 404-713-0541
E-mail: 73762.1734@compuserve.com

Matsushita Communication Industrial Corporation of America (MCC/Panasonic)
2001 Westside Parkway
Alpharetta, GA 30201

ABSTRACT

The 1988 Amendments to Parts 2 and 22 of the Federal Communications Commission's (FCC) GEN. Docket No. 87-390 allow cellular operators to provide auxiliary services within the cellular spectrum. This paper outlines the development of a new standard for Cellular Auxiliary Personal Communications Service (CAPCS) designed to operate under these guidelines. It also discusses preliminary results of frequency availability tests performed in a dense urban environment.

I. INTRODUCTION

To compete effectively with the 1.8 GHz PCS service providers, cellular operators in the United States are looking for ways to provide PCS services using their existing frequency allocation. The FCC allows for this possibility in GEN. Docket No. 87-390 [1]. In this docket, the FCC mandates that an "auxiliary" system operating in the cellular spectrum must meet the following requirements:

1. The auxiliary system must not transmit on any of the 21 cellular control channels of either cellular system (A or B side).

2. The cellular operator must continue to devote sufficient spectrum to conventional cellular service to satisfy demand.

3. The auxiliary system must operate on a "secondary" basis with conventional cellular service.

4. The auxiliary system must remain under control of the cellular licensee.

5. The FCC must be made aware of the implementation of auxiliary services with an analysis of potential interference.

A wireless PBX adjunct system based on the existing EIA/TIA-553 AMPS standard [2] meets these requirements and provides the following advantages:

1. The spectrum is managed by the cellular license holder, which minimizes the chance of interference.

2. The in-building microcellular PCS design is based on a proven technology with a large installed base of equipment. This results in shorter

development time and quicker availability of equipment.

3. The capacity of the cellular system is increased by shifting some of the load to the in-building microcellular PCS [3].

4. A common handset can be used for both the in-building microcellular PCS and the cellular system.

However, modifications were needed to the EIA/TIA-533 AMPS standard to resolve the following issues:

1. The FCC in GEN. Docket 87-390 requires that auxiliary systems not use the standard cellular control channels of either cellular system (A or B side).

2. EIA/TIA-553 does not provide any way to deny registration of a handset making support for closed user groups difficult.

3. EIA/TIA does not support low transmit power operation generally needed by CAPCS Systems.

The new standard for CAPCS was submitted to the United States Telecommunications Industry Association (TIA) by Matsushita in 1993. After several months of deliberations it was approved and designated TIA/EIA/IS-94 [4].

II. DESCRIPTION OF THE SYSTEM AND CAPCS STANDARD

Because PCS systems operate in the cellular band, they must be authorized and controlled by a licensed cellular operator within its service area. They are also designed to co-exist with existing cellular systems. This is accomplished by using low power and cellular frequencies that are not used in the vicinity of the PCS.

Figure 1 illustrates the main hardware components of one CAPCS system. The main function of these components is described below.

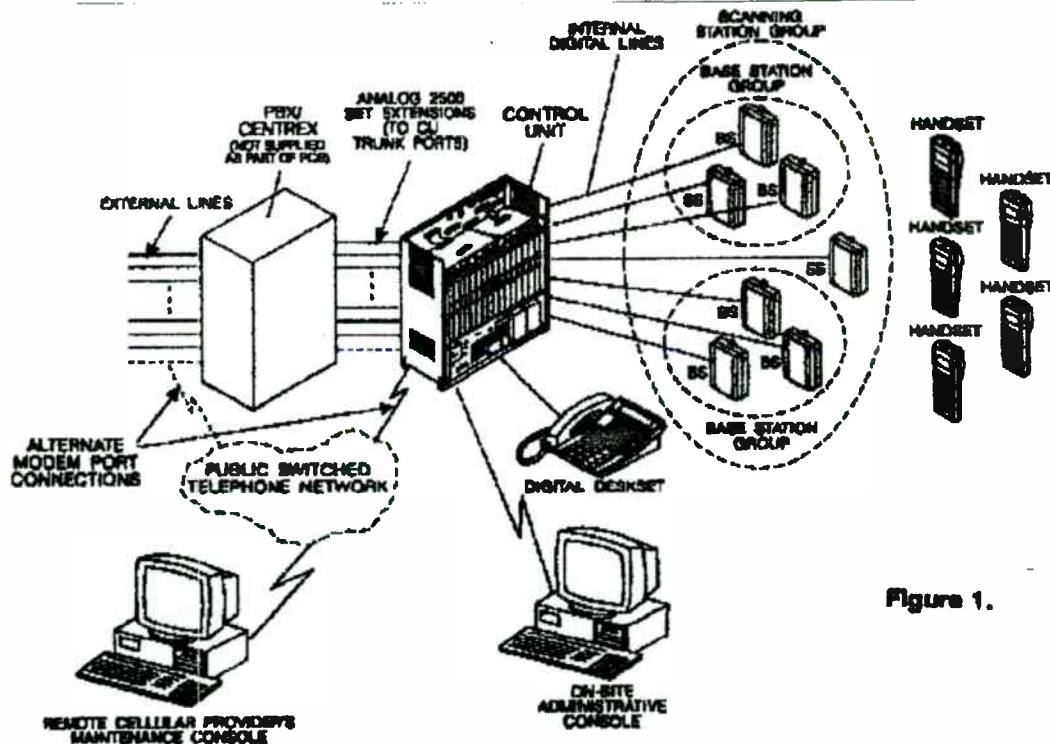


Figure 1.

1. Control Unit (CU)-The Control Unit performs all control functions such as configuration, call processing, authentication and base station control. The CU connects to the PBX or Centrex using standard 2500-set extensions, essentially making these extensions wireless.

2. Base Stations (BS)-Base Stations are low power radio transceivers that provide the wireless link to the handset.

3. Scanning Station(s) (SS)-The Scanning Station continuously monitors the cellular system to determine which channels can be used by the PCS system. Several Scanning Stations may be used in large coverage areas since available channels may vary from zone to zone.

4. Handsets (Mobile or Wireless stations)-can operate as standard cellular phones or wireless extensions.

5. Administrative Console (AC)-The Administrative Console is an IBM PC program that simplifies configuration and administration of the system.

6. Cellular Operator Maintenance Console (MC)-The Cellular Operator Maintenance Console is an IBM PC program that performs remote system control, maintenance, and billing retrieval functions.

Base Stations are combined into groups which operate like cell sites in a standard cellular system. Any base station in the group can work as a voice channel or control channel at any given time. One base station in the group is always serving as a control channel (unless all are busy handling conversations).

A Scanning Station group is a collection of Base Station Groups that shares the frequency availability information provided by a single Scanning Station. This allows the number of Scanning Station Groups to be adjusted independently of the number of Base Station Groups. Using Multiple Scanning Station Groups provides an efficient re-use of the available cellular channels.

To satisfy FCC mandates that an auxiliary system not use the standard cellular control channels, control channels in the cellular voice band must be deployed. Placing the control channels in the voice band represents a compromise between system deployment flexibility and scan time for the handsets. The CAPCS standard achieves flexibility by allowing each system to tell the handset the control channel block size for that system.

The CAPCS control channels are allocated to the voice channels adjacent to the standard cellular control channels starting with channel 301 for the A side and channel 366 for the B side. When a handset is activated for the first time, the control channel block size is initially set to 127. Once the handset has registered in a CAPCS system, the block size is continually updated by the received System Parameter Overhead Message (SPOM). When the handset is deactivated, the block size is retained in memory until it is reactivated.

The handset will only allow the block size to become larger. This is to allow a handset that roams between systems (one with a small block size and the other with a large block size) to continue operating correctly in each system. In some cases, a small block size may be unable to locate a system

with a larger block size because the latter may not have control channels in the small block size band. In this case, user intervention is required.

Once the block of potential control channels is identified, the handset scans each channel and determines if Word-Sync can be achieved. If so, the channel number and signal quality are stored. Starting with the strongest Word-Sync channel, the handset searches for a valid control channel. Once it finds one, the handset attempts to register in the CAPCS system.

To compensate for the EIA/TIA-553 AMPS cellular standard's lack of handset registration denial methods, additional messaging was added to IS-94. This allows a handset to request a CAPCS registration, and enables a CAPCS system to deny such a registration request if the handset is not authorized for that system.

If the handset is denied CAPCS registration, it will log which system denied it and will attempt to locate another system. The handset will not attempt a CAPCS registration again on the denying handset until its power is cycled.

To reduce the number of "nuisance" registrations, the handset contains a list of home Auxiliary System IDs (ASIDs) in its NAM. It will also remember the ASIDs of systems that have granted CAPCS registration in the past (in FIFO order). The handset will only attempt CAPCS registration on ASIDs in these lists. There are two exceptions to this rule:

1. At power-up the handset will attempt CAPCS registration on any ASID that it finds.
2. If the SPOM has the Always Register (AR) bit set to "1" the handset will always attempt to register. This bit is provided so that a system can provide service to any handset in its coverage area by overriding the handset's normal registration logic.

To enable support of low transmit power operation, Power Class IV is used. Power Class IV allows three additional power levels (8, 9, and 10) of which the lowest (10) is -34 dBW. To support these three other power levels, an additional bit is added to the messaging.

Messaging that allows a CAPCS system to transmit an extension number to a handset after the handset has registered, was also added to the standard.

III. INTERFERENCE CONTROL IN A CAPCS FIELD TRAIL

To comply with FCC regulations, cellular auxiliary PCS has many features that reduce the possibility of interference to the external cellular network.

1. The Scanning Stations detect new cellular channel usage and rapidly remove them from the PCS frequency lists. Furthermore, the Scanning Stations do not add channels to the PCS frequency list until they have been idle for a sufficiently long period of time.
2. Each base station makes sure the channel is clear immediately before using the channel in voice mode.
3. If a control base station detects SAT from a mobile station, it reports the interference and stops using the channel.
4. If a base station detects the wrong SAT during a conversation, it will report the interference and attempt to hand-off to a new idle voice channel.

The cellular operator maintains control of the system in the following ways:

1. The cellular operator can dial into the system and shut it down at any time.
2. The cellular carrier must periodically connect to the system to authorize it to continue operating. The system will automatically shut down if this "keep-alive" message is not received.
3. If the system detects that it is operating under a different cellular system than the one originally programmed (different SID), the system will automatically shut down.

There are two potential ways that the external cellular system can interfere with the CAPCS system. In the first, the base stations that belong to the external cellular system interfere with the forward link from the CAPCS base stations to the CAPCS handsets. In the second, the handsets that belong to the external cellular system interfere with the reverse link from the CAPCS handsets to the CAPCS base stations.

In order to determine the extent of this interference and how it limits the capacity of the CAPCS system, Matsushita, with the cooperation of several cellular service providers, conducted a field trial of an in-building microcellular PCS based on the TIA/EIA/IS-94 CAPCS standard.

The purpose of the field trial, conducted at the New York Marriott Marquis in midtown Manhattan, was to test the CAPCS system in an urban, high RF interference, high-rise environment and determine its ability to operate in such an environment. Data was also gathered in the hope that it could be used to develop guidelines for the deployment of CAPCS in such an environment in the future.

The New York Marriott Marquis is located at 45th and 46th Streets, between

Broadway and Eighth Avenue. The atrium-type building with forty-six floors and two basement levels, three sides (45th Street, 46th Street, and Broadway) faces nearby cell sites. The fourth side, which faces Eighth Avenue, is blocked by a building.

To determine the extent of interference and how it limited the capacity of the CAPCS system, receivers (scanning stations) were installed on the 45th Street, 46th Street, and Broadway sides of several floors of the hotel between the first to the forty-fifth floors.

The scanning station consisted of a receiver capable of being tuned to any forward or reverse cellular channel to measure the signal strength on that channel. The channel the receiver was tuned to was controlled by a personal computer, which also stored signal strength information. The scanning station was programmed to:

- scan both the forward and reverse cellular channels on either the A or B side N times per hour;
- to measure the received signal strength on each channel;
- and to maintain a count of how many times each channel's signal strength fell into a particular power range.

Power ranges from -65 to -113 dBm in 1 dB increments were used. Any signal measurements greater than -65dBm or less than -113 dBm were assigned to the 65 dBm and -113 dBm power ranges, respectively. At the end of each hour of active scanning a file was generated which contained the number of times the signal strength for each channel fell into each power

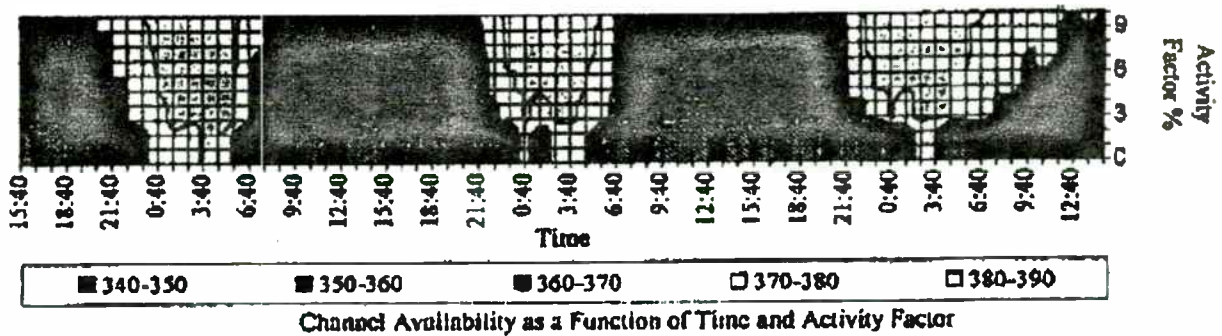
range. A scanning station was placed in a hotel room and left to gather and store data undisturbed for twenty-four to seventy-two hours.

After scanning stations had been in place long enough to gather and store the desired amount of data, the resulting files were processed off-line to determine how many cellular channels are available for the CAPCS system to use. First, the forward and reverse link data for each channel was combined by taking the larger of the counts for each channel. Next, a cellular channel was said to be available during a particular hour if the signal strength on that channel did not exceed a certain threshold more than a certain percentage of the time during that hour. This algorithm for determining channel availability was used (rather than one based on just a signal strength threshold) because it was felt that it is reasonable to use channels that are above a signal strength threshold for a small percentage of the time.

IV. FIELD TEST RESULTS

The signal strength threshold is referred to as the Voice Channel Threshold. The percentage is referred to as the Activity Factor. The following figures show some channel availability results for the CAPCS field trial. Figure 2 shows how the channel availability varies as a function of time and activity factor. This figure was the result of processing seventy-two hours of data taken on the Broadway side of the hotel's first floor. The Voice Channel Threshold used was -98 dBm. Note the higher channel availability during the midnight to 6 A.M. hours, compared to the daytime and early evening hours. This is due to a lighter load on the external cellular system from midnight to 6 A.M., a load that makes more channels available for the CAPCS system.

Figure 2.



Figures 3, 4, and 5 all show combined channel availability as a function of Voice Channel Threshold and Activity Factor. All three figures are the result of processing one hour of data taken from approximately 5:30 to 6:30 P.M. on the Broadway side of the hotel. Figure 3 is from first floor data. Figure 4 is from twentieth floor data, and Figure 5 is from fortieth floor data.

The data for each of these three figures was gathered during the same time of day, but on different days. Note the higher channel availability on the first floor versus the twentieth and fortieth floors. This is due to the increase in the number of external cellular system base stations and handsets seen by the scanning station on the higher floors. Even with this effect, Figure 5 shows the availability of over 100 channels on the fortieth floor with the proper combination of Voice Activity Threshold and Activity Factor.

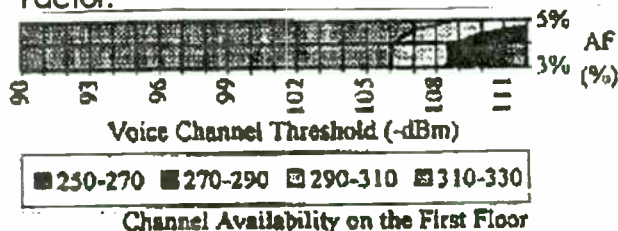


Figure 3.

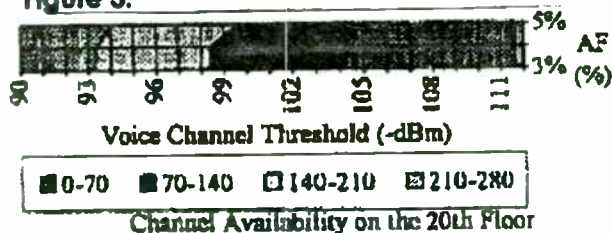


Figure 4.

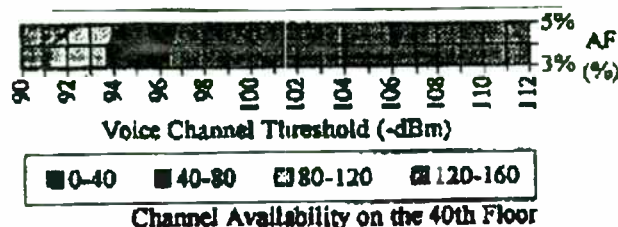


Figure 5.

V. CONCLUSIONS

Competition from the 1.8 GHz PCS and other services continues to grow. As a result, it is increasingly important for cellular carriers to compete with these services using their existing frequency allocation.

The FCC allows cellular carriers to offer new services in their spectrum as long as they comply with specific "auxiliary" system regulations. The TIA/EIA/IS-94 CAPCS standard allows for an in-building PCS application that gives cellular carriers the opportunity to extend and enhance the capability of their existing cellular service, while complying with existing regulations.

At the same time, Preliminary results from a field trial of an in-building microcellular PCS based on the TIA/EIA/IS-94 standard indicate that even in an urban, high RF interference, high-rise environment, sufficient channels are available to support a CAPCS system.

The TIA is presently looking at future revisions to TIA/EIA/IS-94. It is fairly certain that such revisions will include authentication, short messaging, and voice mail functions.

VI. REFERENCES

- [1] Federal Communications Commission, GEN. Docket No. 87-930, 1987.
- [2] Telecommunications Industry Association (TIA), EIA/TIA-553, "Mobile Station-Land Station Compatibility Specification," September 1989.

[3] Y. Kinoshita, T. Hamada, M.A. Henriques, and Y. Izawa, "Advanced Common Air Interface Between Indoor and Urban Cellular Telephone: Spatial Frequency Reallocated Systems," Proceedings of the 4th IEEE International Symposium on Personal, Indoor and Mobile Radio Communication. September 1993, pp. 696-700.

[4] TIA/EIA/IS-94. Mobile Station-Land Station Compatibility Specification for Analog Cellular Auxiliary Personal Communication Service, Telecommunications Industry Association (TIA), May 1994.

[5] Matsushita Communications Industrial Corporation of America (MCC/Panasonic), "A Proposed Common Air Interface for Cellular Band Personal Communication Systems," April 1993.

A Fast Locking Scheme for PLL Frequency Synthesizers

David Byrd, Craig Davis, William O. Keese
National Semiconductor Corporation, Wireless Communications Group
2900 Semiconductor Drive, Santa Clara, CA 95052

Abstract

Frequency synthesizers are used in a large number of time division multiplexed (TDMA) and frequency hopping wireless applications where quickly attaining frequency lock is critical. A new frequency synthesizer is described which employs a scheme for reducing lock time by a factor of two using a conventional phase locked loop architecture. Faster lock is attained by shifting the loop filter's zero and pole corner frequencies while maintaining the PLL's gain/ phase margin characteristics.

Introduction

RF system designers of TDMA based cellular systems, such as PHS, GSM and IS-54, need local oscillator (L.O.) or frequency synthesizer blocks capable of tuning to a new channel within a small fraction of each time slot. The suppression of reference spurs and phase noise is also critical for these modern digital standards. Base station and data transmission applications are now striving to utilize all the time slots available in each frame using a single synthesizer. This push towards a 'zero blind slot' solution has put stringent demands upon the radio frontend's L.O. section.

The communication systems channel spacing determines the upper bound for the synthesizer's frequency resolution and loop filter bandwidth. More closely spaced channels dictate that the synthesizer's frequency resolution be finer, which in turn means the loop makes frequency corrections less often. A wider loop filter bandwidth would make it easier to attain lock within a given time constraint, but the price paid is less attenuation of the reference frequency sidebands and a higher integrated phase noise for the locked condition. An examination of the equations which govern the responsiveness of a closed loop system will provide some solutions to this dilemma.

Closed Loop Operation

The basic phase-lock-loop configuration we will be considering is shown in Figure 1. The PLL consists of a high-stability crystal reference oscillator, a frequency synthesizer such as the National Semiconductor LMX2335TM, a voltage controlled oscillator (VCO), and a passive loop filter. The frequency synthesizer includes a phase detector, current mode charge pump, as well as programmable reference [R] and feedback [N] frequency dividers. A passive loop filter configuration is desirable for its simplicity, low cost, and low phase noise.

The VCO frequency is established by dividing the crystal reference signal down via the R counter to obtain a frequency that sets the tuning resolution of the L.O. This reference signal, f_r , is then presented to the input of a phase detector and compared with another signal, f_p , the feedback signal, which was obtained by dividing the VCO frequency down by way of the N counter. The phase detector's current source outputs pump charge into the loop filter, which then converts the charge into the VCO's control voltage. The phase/frequency comparator's function is to adjust the voltage presented to the VCO until the feedback signal's frequency (and phase) match that of the reference signal. When this 'phase-locked' condition exists, the VCO's frequency will be N times that of the comparison frequency.

Increasing the value of the N counter by 1 will cause the phase comparator to initially sense a frequency error between the reference and feedback signals. The feedback loop responds and eventually shifts the VCO frequency to be N+1 times the reference signal. The VCO's frequency has in effect increased by the minimum tuning resolution of the PLL. The rate at which the transition to the new operating frequency occurs is determined by the closed loop gain and stability criteria.

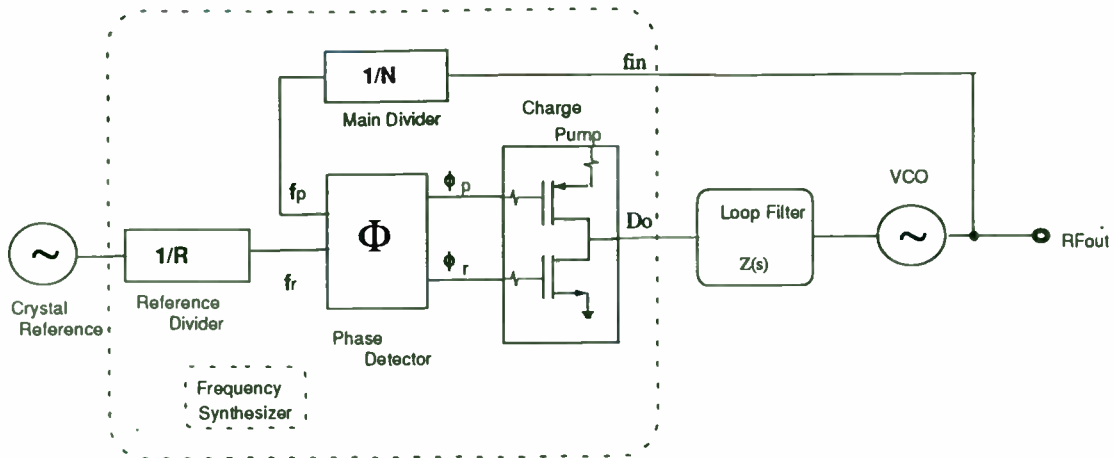


Figure 1. Conventional PLL Architecture

Loop Gain Equations

A linear control system model of the phase feedback for a PLL in the locked state is shown in figure 2. The open loop gain is the product of the phase comparator gain (K_{pd}), the VCO gain (K_{vco}/s), and the loop filter gain $Z(s)$ divided by the gain of the feedback counter modulus (N). The passive loop filter configuration used is displayed in figure 3, while the complex impedance of the filter is given in equation 2. [Ref 5]

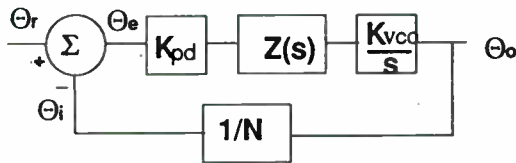


Figure 2. PLL Linear Model

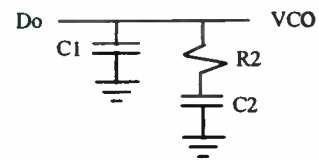


Figure 3. Passive Loop Filter

$$\text{Open loop gain} = H(s) G(s) = \Theta_i / \Theta_e = K_{pd} Z(s) K_{vco} / Ns \quad (1)$$

$$Z(s) = \frac{s(C2 \cdot R2) + 1}{s^2(C1 \cdot C2 \cdot R2) + sC1 + sC2} \quad (2)$$

The time constants which determine the pole and zero frequencies of the filter transfer function can be defined as

$$T1 = R2 \cdot \frac{C1 \cdot C2}{C1 + C2} \quad (3a) \quad \text{and} \quad T2 = R2 \cdot C2 \quad (3b)$$

The 3rd order PLL Open Loop Gain can be calculated in terms of frequency, ω , the filter time constants $T1$ and $T2$, and the design constants K_{pd} , K_{vco} , and N .

$$G(s) \cdot H(s) \Big|_{s=j\omega} = \frac{-K_{pd} \cdot K_{vco} (1 + j\omega \cdot T2)}{\omega^2 C1 \cdot N (1 + j\omega \cdot T1)} \cdot \frac{T1}{T2} \quad (4)$$

From equation 3 we can see that the phase term will be dependent on the single pole and zero such that the phase margin is determined in equation 5.

$$\Phi(\omega) = \tan^{-1}(\omega \cdot T2) - \tan^{-1}(\omega \cdot T1) + 180^\circ \quad (5)$$

A plot of the magnitude and phase of $G(s)H(s)$ for a stable loop, is shown in figure 4 with a solid trace. The parameter ϕ_p shows the amount of phase margin that exists at the point the gain drops below zero (the cutoff frequency ω_p of the loop). In a critically damped system, the amount of phase margin would be approximately 45 degrees. Given the pressure to minimize lock time, the cutoff frequency of the loop would be selected just wide enough to suppress the PLL's reference frequency spurs to a tolerable level.

If we were now to redefine the cut off frequency, ω_p' , as double the frequency which gave us our desired level of spurs, ω_p , the loop response time would be approximately halved. Because the filter attenuation at the comparison frequency also diminishes, the spurs would have increased by approximately 6 dB. In the proposed fast lock scheme, the higher spur levels and wider loop filter conditions would exist only during the initial lock-on phase--just long enough to reap the benefits of locking faster. The objective would be to open up the loop bandwidth but not introduce any additional complications or compromises related to our original design criteria. We would ideally like to momentarily slight the curve of figure 4 over to a different cutoff frequency, illustrated by the dotted line, without affecting the relative open loop gain and phase relationships. To maintain the same gain/phase relationship at twice the original cutoff frequency, other terms in the gain and phase equations 4 and 5 will have to compensate by the corresponding "1/w" or "1/w²" factor. Examination of equations 3 and 5 indicates the damping resistor variable R2 could be chosen to compensate the "w" terms for the phase margin. This implies that another resistor of equal value to R2 will need to be switched in parallel with R2 during the initial lock period. We must also insure that the magnitude of the open loop gain, $H(s)G(s)$ is equal to zero at $\omega_p' = 2\omega_p$: K_{vco} , K_{pd} , N , or the net product of these terms can be changed by a factor of 4. to counteract the w^2 term present in the denominator of equation 3. Altering K_{vco} could be difficult at best, however, both N and K_p gain terms are readily available in an integrated PLL IC. The K_{pd} term was chosen to complete the transformation because it can readily be switched between 1X and 4X values. This is accomplished by increasing the charge pump output current from 1mA in the standard mode to 4 mA in fast lock. Changing the N gain term could also have been chosen to accomplish our objective. In fact, doing so causes the PLL's reference frequency to be pushed over in the frequency domain along with the loop cutoff frequency. Unfortunately changing N also means changing the R counter value by the same factor. And while this is feasible, it probably means employing fractional counter techniques along with all the associated problems of this approach, as an $N/4$ term may no longer be an integer.

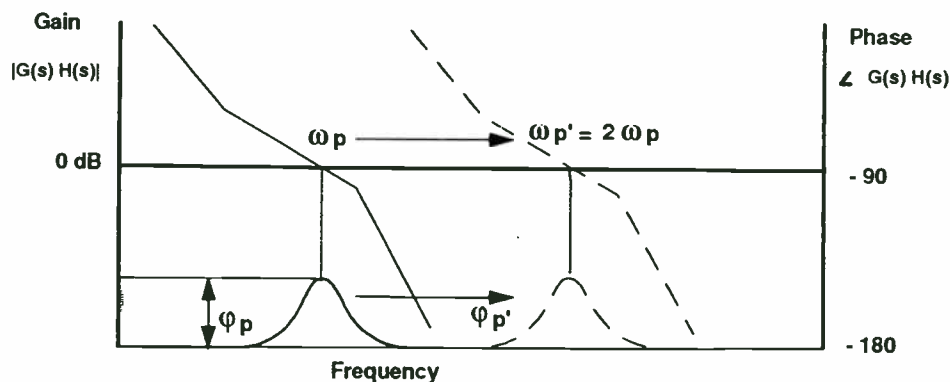


Figure 4. Open Loop Response Bode Plot

Circuit Implementation

A diagram of the fast-lock scheme as implemented in National Semiconductors LMX2335 PLL is shown in figure 5. When a new frequency is loaded, the charge pump circuit receives an input to deliver 4 times the normal current per unit phase error while an open drain NMOS on chip device switches in a second R2 resistor element to ground. The user calculates the loop filter component values for the normal steady state considerations. The device configuration ensures that as long as a second identical damping resistor is wired in appropriately, the loop will lock faster without any additional stability considerations to account for. Once locked on the correct frequency, the PLL will then return to standard, low noise operation. This transition does not affect the charge on the loop filter capacitors and is enacted synchronous with the charge pump output. This creates a nearly seamless change between fast lock and standard mode.

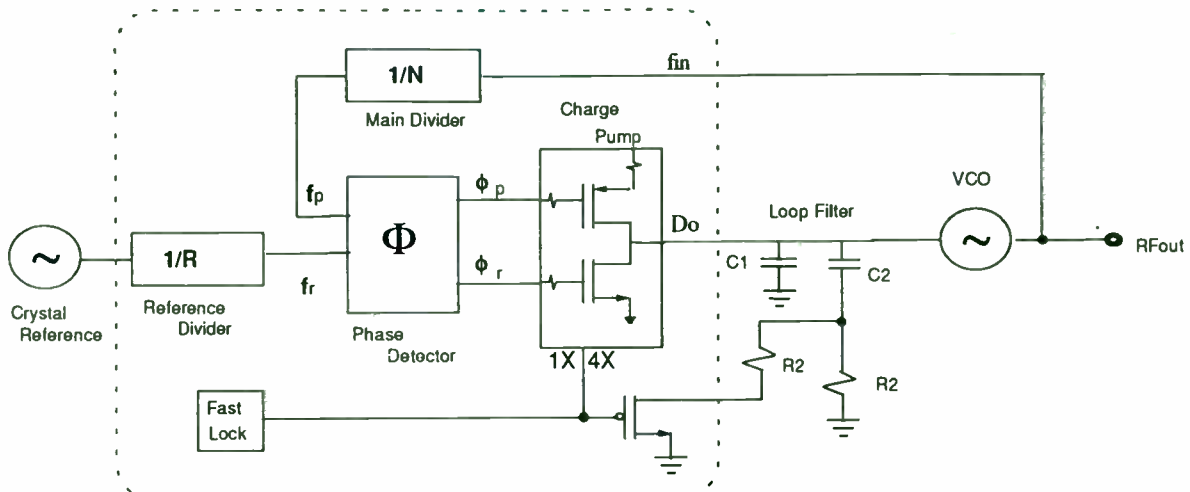


Figure 5 Fast Lock PLL Architecture

Results

An LMX2335 PLL was utilized to address the following IS-54 application constraints:

$$f_{vco} = 900 \text{ MHz}, K_v = 20 \text{ MHz/V}, \text{ Channel spacing} = 30 \text{ kHz.}$$

The PLL's device attributes were as follows:

$$K_{pd} = 1 \text{ mA}/2\pi, N = 30,000, f_{ref} = 30 \text{ kHz}, F_o = 3 \text{ KHz.}$$

The loop filter values used were:

$$C_1 = 1800 \text{ pF}, R_2 = 12 \text{ k}\Omega, C_2 = 0.012 \text{ }\mu\text{F}$$

The modulation domain analyzer graphs in figures 6-9 show the transient lock responses for the normal 1mA mode condition side by side with the response for the fast lock mode. The fast lock operation in figure 9. shows lock being attained within 1 msec (to within +/- 1 khz) for a frequency jump of 50 Mhz., compared with 1.8 msec for the standard condition (figure 8). As much as a 2 kHz frequency disturbance can result when switching back to normal operation after steady state is fully attained. By switching out of the fast lock mode when the PLL has settled to near the desired frequency tolerance, almost the entire 2X increase in lock time can be achieved.

Summary

The fast lock circuitry of the LMX2335 frequency synthesizer provides a means of improving TDMA channel switching speed, without compromising reference spur quality or phase noise. Zero blind slot RF synthesizer designs can more easily be attained through this technique, without compromising reference spur quality or phase noise.

References

- [1] W. Shepherd, *Phase Locked Loop*, U.S. patent #4,980,653 , 1990.
- [2] Eitan Sharoni, *Digital Control Speeds Synthesizer Switching*, *Microwaves & RF*, PP. 107 -112, 4/1987.
- [3] S. Swisher, et. al., *Synchronized Frequency Synthesizer with High Speed Lock*, U.S. Patent #4,330,758, 1982.
- [4] K. Arnold, *Low Noise Frequency Synthesizer Using Half Integer Dividers and Analog Gain Compensation*, U.S. patent #5,307,071, 1994
- [5] Keese, W.O., *An analysis and Performance Evaluation of a Passive Filter Design Technique for Charge-Pump Phase-Locked Loops*, RF Expo West, January 1995.
- [6] Barker, Cynthia, *Introduction to Single Chip Microwave PLLs*, National Semiconductor Application Note, AN885, March 1993

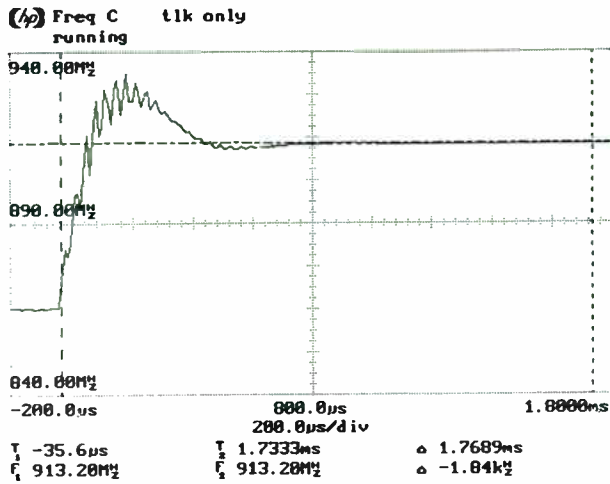


Figure 6. Normal Switching Waveform

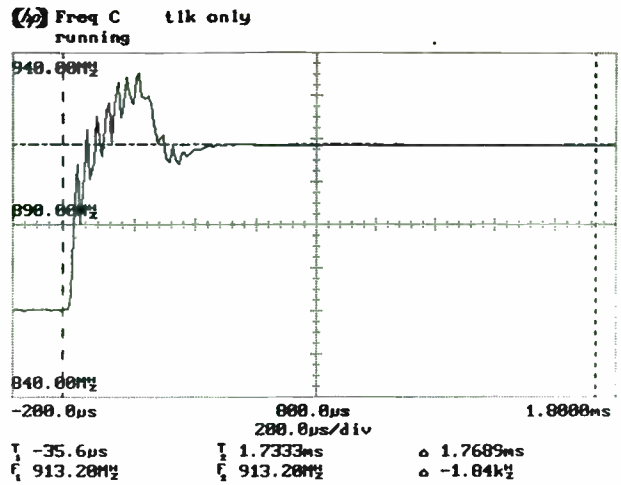


Figure 7. Fast Lock Switching Waveform

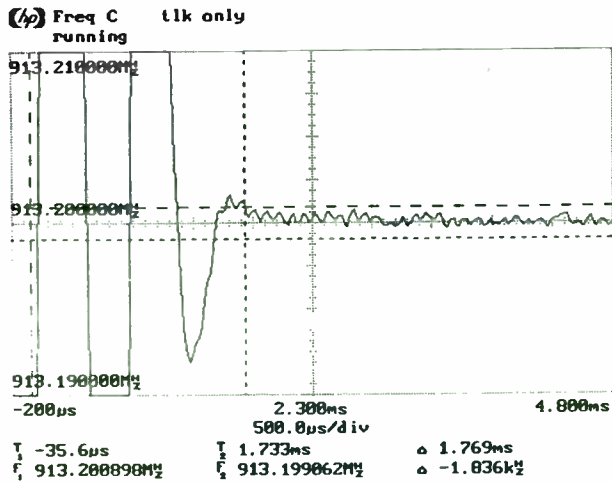


Figure 8. Normal Mode Lock Time

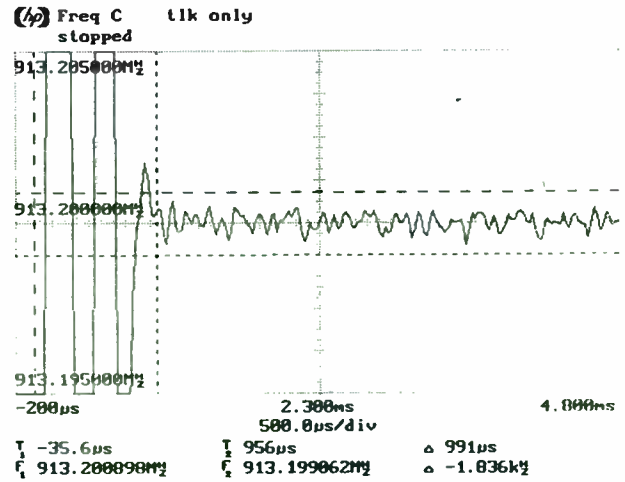


Figure 9. Fast Lock Mode Lock Time

PCS1900: GSM as a candidate for US PCS Applications

Rupert Baines

*Analog Devices, Communications Division
Wilmington, MA 01887*

Abstract

This paper describes the proposed PCS1900 standard (aka DCS1900), a variant of the international GSM (Global System for Mobile communications), and discusses its suitability for the US PCS market. By leveraging existing standards and manufacturing scale, this offers network providers the opportunity to offer more services, at lower prices. The paper describes the GSM standard, & the differences required for a PCS implementation. It will also discuss the differences between the roaming/call-management operations of US IS41 and GSM's MAP. Finally, it will discuss implementation aspects.

Keywords: Digital Cellular; Personal Communications Systems; GSM

1 Introduction

"Toll quality voice, anywhere, any time." Personal Communication System (PCS) is not so much a technology or a particular standard; it is more the *market* for small, individual telephones; whether the descendants of domestic cordless, or the miniaturization of cellular systems, PCS is forecast to be an incredibly fast-growing market.

Within the US., the 1.9 GHz band has been allocated for PCS systems; the allocated spectrum is 120 MHz wide (1850MHz to 1970MHz), divided into 30 and 10MHz sections for different regions and population centres.

There are at least seven suggested systems for use in PCS: three are variants on existing digital cellular standards - GSM, TDMA and CDMA (based on IS-54 and IS-95); broadband CDMA (supported by OKI and InterDigital), DCTU (Digital Cordless Telephone U.S.- a version of DECT), Omnipoint and PACS (Personal Access Communication System).

The would-be providers of PCS are currently gearing up to bid for operating licenses and build their networks. These are difficult enough requirements; the narrow-band (paging) auctions set a target of \$80 / Hz of spectrum, valuing a full PCS band hundreds of millions of dollars, while the network is required to be fully developed and 'rolled out' within just 18 months of the completion of the auction.

But beyond these, which confront all of the bidders, is the need to gain customers. The challenge for the providers will be to compete against existing cellular services (analog and emerging digital); they must prove that PCS is more than just cellular at 1900MHz. Rather than focusing on the technology *per se* (who cares that a carrier is at nineteen rather than nine hundred MHz ?), the networks must emphasize user-benefits such lower price, smaller, lighter handsets, superior speech quality and more features.

One possible way of achieving all of these benefits - as well as lower prices and easier access to infrastructure for the operators - is to leverage from an existing, established standard; GSM. This has the advantage of a ready developed, sophisticated technical specification and structure well suited to the needs of the PCS application. Moreover, as a world-wide standard there is the high-volume manufacture in place; forcing the cost of equipment down, while functionality increases.

PCS1900 is a proposed variant of the GSM standard. The GSM started as a conventional digital cellular system, operating around 900MHz region, with a transmitter power of typically 2W (a "Class 4 handset") and a range measured in miles. Within Europe a lower power variant was developed, with a few changes intended for reaching higher densities of people with shorter range for urban areas - DCS1800 (Digital Communications System at 1800MHz). PCS1900 (some people call it DCS1900) is a further development of this existing system¹.

This paper describes the technology of the GSM standard (in terms of lower layer functionality, radio interface and system electronics), and the (higher level) MAP mobility management protocol, comparing it to the American IS41 standard. It then discusses the business issues.

2 The GSM / DCS1800 Standard

GSM has the best claim to being the Global System for Mobile communications its name now proclaims it to be (a change from its previous Groupe Speciale Mobile). Although initially a European standard, developed by ETSI, the world (with the exceptions of America, Japan and South Korea) seems to have settled on this as a standard protocol for digital cellular communications.

The movement to digital communications standards has been propelled by a number of different forces. One significant reason is that the analog systems have been a victim of their own success and in many areas are overloaded. Although a raw digital signal requires more bandwidth than a analog signal of the same quality, digitisation offers designers several attractions. In particular, digital compression increases data efficiency, and discontinuous transmission improves spectral efficiency.

Although spectral over-crowding was a major motivation in the US, it has not yet been enough in itself for a switch to the new digital standards, as there are other, potentially cheaper remedies. In Europe, the additional motive was the need to develop a common system that would operate throughout the twenty or so countries without problems or incompatibilities. Given the need to develop a system from scratch and the severe bandwidth limitations (remember, most European countries are small and densely populated), an efficient and "smart" digital standard was the only way to go. Once the system had been established, it has been a great success: already more than one million handsets are in use, and even conservative forecasts for 1995 predict five million users. (ironically, while Europe went from many analog standards to a unified digital system, while the US went from a single analog AMPS standard to several incompatible digital ones). This user base makes the standard attractive for other nations considering a system,

¹ Increasingly "GSM" refers to the family of systems, at all frequencies, sharing common protocol. The cellular (900MHz) implementation specifically is GSM900; the companion to DCS1800 and PCS1900.

as it is both technically proven and comparatively cheap (existing volume manufacture drives production costs down). As a result, many nations have adopted the GSM system.

3 GSM - Technical Description

The sequence of actions in GSM, as in most digital standards is: Speech coding, channel coding, block formatting and modulation for transmission. At the receiver, the operations are done in reverse.

GSM is usually classified as a TDMA (Time Division Multiple Access) system - although to be more accurate it is TDMA/FDMA with frequency hopping. A few users access each channel, and a number of channels share a given cell at different frequencies, which hop at after each burst². FDMA is used to share the spectrum between channels within a cell, and is of a medium bandwidth type - 200kHz wide (*cf* the 30kHz of AMPS or IS54). The basic TDMA scheme allows for 8 calls (standard voice or 9600bps data) within a given 200kHz channel, although this is shortly to be increased to 16 now the new half-rate speech algorithm has been determined.

The GSM modulation scheme is 0.3 GMSK (Gaussian minimum shift keying, with $BT=0.3$). This was chosen as a compromise between spectral efficiency, and demodulation complexity.

The RF channels are spaced 200kHz apart, starting 200kHz away from a band border. In principle, this would allow for 149 channels in a 30MHz band (or 49 in one of the 10MHz bands). However, the modulation spectrum is somewhat wider than 200kHz (more exactly, it is only some -40dB at 200kHz spacing - higher than is usually accepted in radio channels), so to avoid interference with other applications the outermost channels of a band are left empty. As a result, there are 147 (or 47) usable channels in a PCS band (each carrying 8 or 16 calls).

The time arrangement of GSM transmissions can get *very* complex, and only the simplest situation is described here. The basic unit of a GSM call is a "burst" - 142 bits lasting 577 μ s. During this period it starts at an initial value of 0 (-70dB), rises to its nominal value (0dB); the signal phase is modulated to transmit a packet of bits, before the amplitude decreases to 0 again. The 'normal burst' two packets of 58 data bits, separated by a training sequence (or midamble) of 26 bits and three tail bits at either end. This block is sent in a particular time and frequency window - a "slot". Eight different calls will share a given radio channel (TDMA), with each call placing one burst into a time slot in sequence. A 'frame' is the sequence of 8 bursts (ie it lasts $8*0.57ms=4.6ms$), before returning to the first call. A 'multiframe' (or cycle) allows for 26 successive bursts on a call (24 with information, one control, and one idle); it therefore lasts $26*4.6ms = 120ms$. In this period 8 users have each sent 24 packets of modulated data; in essence this multi-frame is treated as a unit by the base-station..

For compatibility with ISDN (GSM was described as "mobile ISDN"), it is important to have a synchronisation which is some multiple of 20ms; hence the 120ms for a cycle. (This explains the strange value of a slot period - 0.577ms is derived from 120ms shared by 26

² To be *really* pedantic, it is TDMA/FDMA/SDMA; as any cellular system it employs spatial allocation, using physically separate cells and power control, to allow different users to share a given frequency.

frames each with eight slots; ie $120/(26*8) = 0.577\text{ms}$). In fact, there are other types of multi-frame, (eg a 51 multi-frame) and these are cascaded to form superframes and hyperframes, but that's not important right now.

The final ingredient of the radio protocol is frequency hopping, where each transmission burst (100 odd bits, $577\mu\text{s}$ long) between a mobile and basestation is at a different frequency (because this is much less than the modulation rate it is *slow* frequency hopping, as opposed to a spread spectrum FH system). This reduces the effects of Rayleigh fading, as each frequency is affected differently and can be considered independent; so overall immunity improves (this gain has been estimated at 6.5dB). A second advantage is in interferer diversity - even if calls from adjacent cells do interfere on a given frequency slot, this will not cause problems as the calls will soon shift to a new, non-interfering frequency. To a degree, the re-use factor thus increases, as with CDMA.

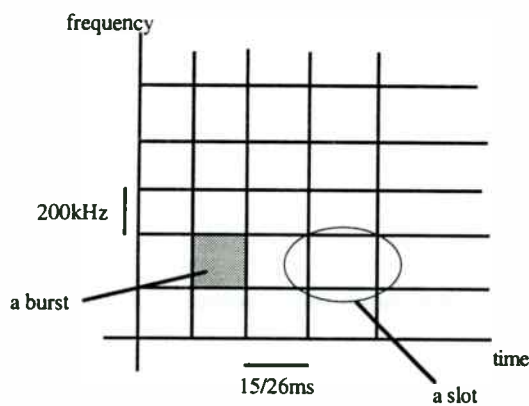


Figure 1. A GSM transmission unit (a "burst") lasts $577\mu\text{s}$, with a 200kHz channel bandwidth

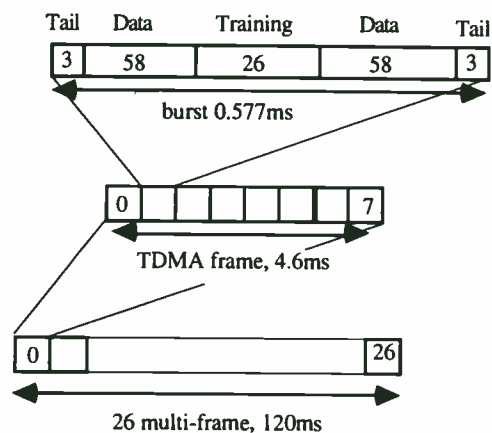


Figure 2. The hierarchy of bursts, frames and multiframes.

Each burst contains two sets of 58 information bits, representing the encoded speech. In the current standard (full rate GSM or GSM-FR), the voice signal is sampled with 13 bit resolution at 8kHz, to give raw data rate of 104kbps. The compression algorithm is based on a version of linear predictive coding (LPC) with long term prediction (LTP) and regular pulse excitation (RPE) to improve the quality of the encoded speech (and to give the hideous acronym of RPE-LTP LPC). This gives an encoded rate of 13kbps; the standards committee have recently selected an algorithm for half rate ($\approx 7\text{kbps}$) code, doubling capacity. In contrast, both the Japanese and American systems are based on VSELP (Vector Sum Excited Linear Predictive coding), which has an effective data rate of 8kbps.

The encoded speech is then passed on for channel coding, which introduces redundancy into the bit-stream, to help with error detection and correction. The different codes are used, with increasing protection for critical data (eg control signals) - a degree 40 Fire code, to detect and correct "bursty" errors, a degree 4 block convolutional code, and parity codes. The output of this stage is a flow of code words, each 456 bits long, with an overall bit rate of 22.8kbps. The bits within one window, and the redundant ECC bits, are spread

across several windows for redundancy - 'interleaving'; 57 bits in each of 8 bursts. These are then encrypted (an intrinsic part of the GSM specification, improving on security), formatted, and sent as bursts to the radio.

The receiver is more complex, for it must cope with decoding not an ideal signal but a weak one, corrupted by noise (from natural sources and other channels) and with distortion - especially that caused by multi-path propagation. The demodulator must estimate the most probable sequence of data, given the received (distorted) signal. In order to help this task, a portion of the received burst includes a known pattern - the midamble or training sequence, which allows the receiver to estimate the distortion and multipath properties, and then recover from them.

No formal definition of the receiver is specified, only required performance. For example, one serious constraint is that the receiver must cope with two multipath signals of equal power, separated by up to $16\mu\text{s}$ ie 4 bit periods. To recover this requires a powerful equaliser; typically a Viterbi equaliser with a path length of 5 bit periods.

Another tool to boost efficiency is discontinuous transmission, where the transmitter shuts down for pauses between words and phrases (in an average conversation, each speaker talks for about 40% of the time). Not only does this save power, it improves capacity by reducing interference and allowing different users to share channels (an 8:3 compression is typical). In order to do this the digital processor detects when speech is present and switches on and off; the receiver then fills in the gaps between speech with "comfort noise", an average background signal, so the listener does not notice the breaks.

Obviously, the processor needs to perform all these encoding/decoding, compression/expansion, error correction and discontinuous transmission functions within a given 20ms window. These demanding requirements help explain why digital mobile radio has only recently been used - even now these functions demand processors that are on the edge of commercially available technology. Fast DSP is an absolute requirement; one estimate is that each channel coding function requires about 18 MIPS of processing power. The DSP may also be used for tone generation, echo cancellation etc.

4 Suitability for PCS

While the US cellular industry is debating the relative merits of TDMA and CDMA, a critical point is being missed; the need for differentiation and additional services. The success of PCS will depend not on the air interface, but on whether or not the technology can deliver to users the features they desire. Essentially, PCS providers have three choices; they can offer subscribers "up-banded" cellular services, relying on existing (US) technology and standards, they can adopt a GSM-based standard that benefits from existing experience, or they can start from scratch.

Given the huge complexity of communications standards (man-centuries of work to develop, codify and test), and the need for rapid roll-out and reliable operation, it does not seem likely that a wholly new system could be developed in time, or be acceptable from a manufacturing or marketing point of view.

The alternative, is to adopt an existing system, and adapt it to the particular requirements of PCS for smaller, lighter handsets, with reduced range. But if PCS manufacturers use current cellular standards to build their system infrastructure and control call operations,

they will immediately run into the problem of differentiating the offering from the existing services; by definition their feature set cannot be any larger than those already offered.

In particular, the services and features offered will be limited. All US cellular systems use the IS41 standard mobility management protocol, which governs roaming capabilities, additional features and security. GSM, on the other hand, uses a different protocol - the Mobility Applications Part or MAP (strictly, MAP is a family of protocols handling different services or "interfaces", MAP/B through to MAP/G). MAP is compatible with the standard Signaling System 7, and what modifications or interfacing may be required is being handled by the Telecommunication Industry Association's TR46 committee.

In terms of features, a PCS system based on GSM and MAP offers everything that IS41 based networks offer - and much more. Some of these services are summarised below.

Some of these services are standard (call forwarding) or familiar from wired services (calling line ID). However some are much more interesting, and offer features to operators that are potentially very attractive to subscribers.

The short messaging service allows customers to receive and send short text messages, of up to 160 characters. It is more akin to e-mail than a standard pager; not only is it bi-directional, but messages can be stored - they can even be delivered while the user is having a separate conversation. Because it is managed by the network, messages can be held in the network until a handset is reachable, and repeated then; the sender can receive notice that the message was successfully delivered.

An extension of the message service is cell broadcast, allowing all handsets in an area to receive text messages automatically; a classic example is road traffic information.

More innovative, and potentially very attractive is the SIM card (Subscriber Identification Module); a credit card size card owned by a subscriber, who can put it into any GSM handset, anywhere in the world, to transform it into 'their' phone. It will ring when their unique phone number is dialed ("*The number belongs to a person, not a place*") ; calls made will be billed to their account; all options and services are enabled and configured; voicemail can be collected and so on. The SIM stores abbreviated speed-dial numbers etc³. People can share one 'physical' handset, turning it into several 'virtual' handsets, one per SIM. One commentator describes this as "In effect, the GSM phone becomes as small and as light as your credit card. The SIM is all you need to carry." It is hard to envisage any system more truly implementing the idea of *personal* communication system. In principle any PCS standard (or even any cellular standard) could adapt the SIM; however, it is obviously much easier to use the standard as a whole, with guaranteed compatibility.

The obvious complement to this, is the 'roaming' agreement, by which network operators agree to recognize (and accept) subscribers from another network, as phones (or SIMs) move. Vodafone, the British operator recently announced that they had added roaming agreements with Hong Kong and South Africa to their list. So, a British subscriber could drive to France and Germany, fly to South Africa or Hong Kong—and use their GSM

³ There are proposals that the - standardised - SIM could be used for other individual purposes; eg as a ATM card, toll gates, debit card for cash transactions, vending machines etc.

phone to make and receive calls (on their same UK number), with as much ease as American an businessman can use a phone in Boston, Miami, or Seattle.

	IS41	GSM
Features		
Call forwarding always	X	X
Call forwarding on busy	X	X
Call forwarding no answer	X	X
Call forwarding not reachable		X
Call waiting	X	X
Call hold		X
Multiparty	X	X
Advice of charge		X
Outgoing call barring	X	X
Outgoing international call barring	X	X
Outgoing international call barring (except to home network)		X
Incoming call barring	X	X
Incoming call barring (while outside home network)		X
Calling line ID		X
Connected line ID		X
Services		
Telephony	X	X
Emergency Calls	X	X
Short message Service		X
Short message (cell broadcast)		X
Videotex Access		X
Teletex access		X
Alternate speech/G3 fax		X
Automatic G3 fax		X
Data Services		X
Alternate Speech Data		X
SIM card		X

Figure 3 Comparison of MAP and IS41

5 Economic Issues

The best standard in the world is useless if consumers prefer something cheaper, or manufacturers do not support it. For PCS service to survive, let alone to flourish, it is essential that the system be affordable - for both handsets (to consumers)⁴ and infrastructure.

Two determinants of the costs of an electronic system are its complexity and the volume manufactured (economies of scale, experience curve, amortising initial costs etc).

⁴ Although subsidies on purchase are significant and can affect the initial price dramatically.

Given that virtually any PCS system, of any technology, will have a lot in common - the electro-mechanical components, radio stage, controller, sophisticated DSP, it is unlikely that any "cheaper" design can be relied on. Instead, the economies must - as in most consumer electronics application - rely on better manufacture and greater integration of VLSI technology. But, in turn, this is only feasible given volume manufacture. So, once again, we conclude that the lowest cost system is likely to be well-correlated with the most-manufactured system. And, of all the systems under discussion, GSM (and siblings) is head-and-shoulders above the rest.

	1993	1994	1995	1996	1997	1998	1999	2000
CDMA (IS95)	0	4	30	178	668	1350	2394	3322
TDMA (IS54)	21	66	173	534	1091	1497	1958	2406
GSM	2000	3000	4800	7900	6500	10200	12100	16000

Source: BIS Strategic Decisions, ADI internal.

Figure 4. Comparative Digital Cellular Standard, Worldwide, Figures in thousands

The table does not include PCS in any form, but clearly demonstrates that the global GSM standard has a lot more users - especially in the early years. This is essential - any system must rely on initial volume to bring the price down early, if it is to survive to gain users in the long term. Any system with low initial volumes, will remain costly, and is unlikely to survive long enough to gain customers⁵.

If you consider the importance of volume on manufacturing cost of ICs, then there are clear attractions. When you realise further that such volume forces faster development, then it is highly likely that GSM chip-sets will be more developed than alternatives - making the handsets smaller, cheaper with longer battery life.

Some argue that CDMA (IS95) will be significantly less expensive than TDMA technology (of which GSM is an example), partly as it is more 'digital' and can use less expensive processes, but primarily as it requires fewer cell-sites and (expensive) basestations.

At this point in time, the argument is still theoretical; there have been no real-world CDMA systems operating, and it is difficult to assess how much the infrastructure will cost. Moreover, this argument also ignores the effect of volume manufacture (as do handsets, GSM basestations benefit from economies of scale in manufacture) and the effects of technical advances may change the balance (eg the advent of wideband receivers dramatically reduces the cost of a BTS).

A related issue is that of risk. The PCS licences will be very expensive, and providers have only a short window to roll-out the network; the penalty for delays in construction could be forfeiture of the licence and licence fee! With that kind of capital at stake, risk-reduction is highly attractive. And many are likely to be wary of using this opportunity to

⁵ Again, subsidies cloud the issue. But it is obviously advantageous for all concerned to have a cheaper handset that requires less subsidy!

perform field-trials on still unproven technology; the idea of using 'off-the-shelf' equipment, readily available in volume has its attractions.

Several vendors have announced their support for PCS1900 and are conducting trials. For basestations, NMT (Northern Telecom / Matra), Motorola and Nokia have all announced suitable systems; while Nokia have launched their 2191, a very attractive handset for PCS1900. Indeed, Nokia's announcement (in Austin, Texas in August) demonstrated both speech and data services using the 2191 and a Nokia basestation.

6 US Concerns

The two primary concerns that have been raised about deploying GSM variants in the US are inter-operability (with respect to the existing IS41 and SS7), and the intellectual property rights policies of ETSI.

To address the first issue, the TIA TR-46 group is working to define the interoperability specifications, and has moved to ballot before being ratified as an ANSI standard (document PN3342). The group includes representatives from AT&T, Alcatel, Ericsson, Motorola, Nokia, Northern Telecom and Siemens Stromberg-Carlson. Given that GSM has been designed to be fully ISDN compatible, this should not be too hard. A consortium (involving Northern Telecom and Matra) are currently implementing a trial system.

On the question of ETSI's IPR, some have argued that it would not be possible to use GSM without allowing ETSI to control patents and - possibly - operating policies. In fact, the Secretary-General of ETSI wrote (in March '94) to the T1 standards committee in which he explicitly stated that ETSI has no interest or desire to exercise any control over GSM in the US. Indeed, it is hard to see what IPR issues could possibly exist that would make a standard already in use in 47 countries suddenly become unusable only in the US⁶. ETSI recently changed its IPR policy (on company licences), in a way which has gained support.

Indeed, it is a requirement of ANSI standards that IPR be available in a defined way, with a policy of non-discrimination and at 'fair and reasonable' terms to all comers.

Finally, there has been criticism of the speech quality of GSM. To address this, the proposal allows for up to 16 different speech coding schemes to be supported. This would make the software for basestations more complex, but not handsets (handsets need speak only their own dialect; BTSs need to understand all schemes and translate to standard ADPCM for the PSTN). In practice the existing codec will be used as a common default.

7 Implementation in Silicon

One of the principle advantages PCS1900 has, is the ability to leverage experience and manufacturing gained from other GSM markets. Despite the different carrier frequencies (900-1800-1900MHz), most of the content of a phone will be common, reducing cost and benefitting from experience.

The designer of a handset wants the particular configuration of devices that will implement the standard, together with all the special features that will make their handset unique, in the

⁶ Although similar concerns exist over IS95, as Qualcomm own many of the key CDMA patents.

cheapest and most convenient way. Often, they would like to have a number of competitive sources for standard elements, as this reduces both the risk and, with competition, the price of a given function. Some of the larger phone manufacturers have within their own companies, a division producing suitable components in-house, and they may prefer to use these. Others will tend to be reluctant to use devices designed and manufactured by a company which competes in the handset market.. The largest of the handset designers have the option of commissioning custom chips from foundries to implement their own custom designs, whilst the smaller companies, or those manufacturing “clone” phones will prefer to use standard parts, widely available and simple to use.

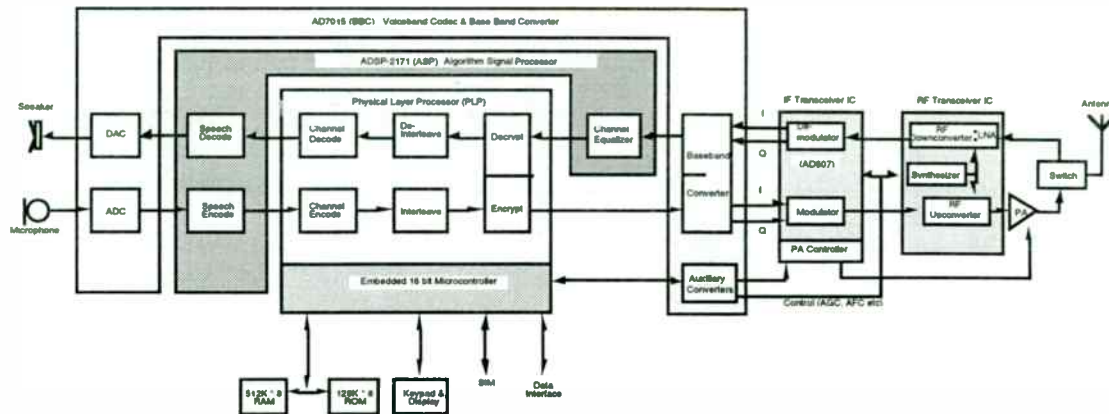
In many respects, the fewer devices required, the better. In addition, if all a handset manufacturer needs do to design a product is hook a keyboard, screen, microphone and earpiece to the “wonder processor”, their life becomes very simple! However, there are complications; for a start, many manufacturers want to have some involvement in the design of their product, otherwise how will they differentiate and compete? Secondly, such a single-chip device would be extra-ordinarily complex and require a large area of silicon; manufacturing yields would be so low as to make this extravagantly expensive.

There are design issues too; noise prevents the easy mixing of high frequency transmitters with fast digital chips and the sensitive signals of the audio converters. For the digital stages, layout is not critical but the need to cram large amounts of circuitry into a small area is. Conversely, for RF devices the power dissipated may limit the number of devices, whilst the requirements of circuit geometry and matching place constraints on layout.

As an example, ADI have announced a GSM chip-set (developed in co-operation with British consultancy TTP), that integrates all the baseband functions, including hardware and software (into three device set). One device is a DSP, that performs the speech coding and Viterbi equaliser, another is a controller, that integrates the channel coding, interleaving etc with a micro-controller (to manage the screen, keyboard etc), while the third is a mixed-signal device that includes the voiceband and baseband codecs, as well as a number of auxiliary converters for control and measurement functions.

A two chip radio stage is currently under development (excluding the power amplifier). Incidentally, it is worth mentioning that modern silicon processes are almost certainly fast enough for use in the radio stage of a PCS system, without the need for GaAs - allowing high integration. In addition, the use of high efficiency SiGe HBTs is a highly attractive possibility.

Analog Devices & The Technology Partnership - GSM Phase 2



The AD20msp410 chipset consists of:
 AD7015 Baseband converter (BBC)
 ADSP-2171 Algorithm Signal Processor (ASP)
 ADSP-TTP01 Physical Layer Processor (PLP)
 Software for Protocol Stack Layer 1

Radio Stage - Reference design now available.
 Three-IC set under development (IF Transceiver, RF Transceiver, PA)

The illustration shows a typical wireless handset (a GSM system, based around the Analog Devices architecture and AD20msp410 chipset). This system was developed by Analog Devices and The Technology Partnership.

Key elements are: The RF (radio) stage, the DSP (or "Algorithm Signal Processor"), the mixed signal section, voice band CODECS, Baseband CODECs and auxiliary converters, and the PLP (physical layer processor). This last stage contains the complex logic and firmware for the communications protocol. In the Analog Devices architecture, the control microprocessor is integrated into the same silicon as other parts of the PLP. Other approaches use a separate micro-controller.

Figure 5 - An Example of a GSM Implementation, suitable for PCS systems

8 Conclusion

The market forecasts for PCS are nothing short of staggering; unfortunately, the risks and costs are commensurate. If operators are to seize this opportunity they must do so in a way that has more to do with skilled marketing and clear benefits, rather than technology per se. PCS1900 offers the prospect of allowing providers to offer services and features that clearly differentiate their offering from existing cellular services (analog or digital). In addition, the system will be cheaper, have more user-base (global standard) and better manufacturer support than any purely domestic candidate. Finally, as a sibling to a mature system, it offers the simultaneous benefit of reducing the risks to the PCS provider and costs of both infrastructure & handsets.

9 References

Mouly & Pautet, The GSM System For Mobile Communications, private printing, ISBN2-9507190-0-7

Mobile Radio Communications, Raymond Steele, Pentech Press, 1992

"GSM: The Potential for PCS ?" Van Cullens, Telephony, 20 June 1994, p30-33

PN3389: PCS - Air Interface Specification - JTC (TAG#5)

PN3342: PCS - PCS Interoperability (System based on DCS1800) - JTC (TAG#5)

	CT2	UD-PCS	DECT	PHP	PCS-1900
Frequency Band MHz	864/868		1880-1990	1895-1907	1850-1890 1890-1930 1930-1970
Radio access method	FDMA	TDMA/ FDMA	TDMA/ FDMA	TDMA/ FDM	TDMA/ FDMA
RF channel	100 KHz	700 KHz	1.728 MHz	300 kHz	200 KHz
Modulation	0.5 GFSK ±14; .4- 25.2kHz		GFSK ±202-403 kHz 2 bits/symbol	$\pi/4$ DQPSK 2 bits/symbol $\alpha=0.5$	0.3 GMSK
Channel rate	72 Kb/s	514 Kb/s	1.152 Mb/s	384 Kb/s	270.8 Kb/s
Number of RF Channels	40		10	77	147
Voice channel per RF channel	1	10	12	4	16
Duplex voice channel size	100 Khz	70 Khz	144 Khz		50 Khz
Voice bit rate	32 Kb/s	32 Kb/s	32 Kbp/s		6.5Kb/s (GSM-Half Rate)
Speech CODEC	ADPCM	ADPCM ?	ADPCM	ADPCM	RELp-LTP
Phone xmit pwr max/avg mW	10/5	100/10	250/10	250/10	250/10
Max cell	100 m	500 m	500 m	500m	500m
Source:	MPT 1375 CAI	Bellcore	prTBR 6 (final draft)	RCR Spec Std 28	prl-ETS 30 176 prETS 300 175-2

CT2 is a second-generation digital cordless system that supports telepoint service (i.e., a handset can initiate, but cannot receive calls). **Universal Digital Personal Communications System (UD-PCS)** is an alternative system that has been proposed by Bell Communications Research (Bellcore) for in-building cordless phone service. **DECT** is the Digital European cordless Telephone - intended as both wireless PBX and PCS; a variant, "DCTU" has been discussed for the US market. **PHP** is the Japanese Personal Handy Phone system. **PCS1900** is a variant of GSM, with lower power and higher carrier frequency, intended for PCS (very similar to the current DCS1800 standard).

Figure 6 Comparison of Digital Communications Systems in Use/Proposed

Wireless-Data Technologies

Session Chairperson: Al Juodikis,
Juodikis & Associates (San Jose, CA)

Wireless LANs: Tradeoffs, implementations, and applications. **Al Juodikis,** Juodikis & Associates (San Jose, CA).....114

So you want to design a radio for a wireless LAN? **Ron Ruebush,** Celeritek (Santa Clara, CA).....115

IEEE 802.11 standards to boost rising WLAN markets in the mobile workplace. **Jonathan Edney,** Symbionics Networks Ltd. (Cambridge, England).....116

A high-volume, low-cost, plastic-packaged, 2.4-GHz transceiver MMIC. **Liam M. Devlin, B.J. Buck, A.W. Dearn, J.C. Clifton, A.A.G. Frier, and M.W. Geen,** GEC-Marconi Materials Technology Ltd. (Caswell, Northants, England).....121

2.4-GHz silicon RF integration for wireless LANs. **Brian Matthews,** Harris Semiconductor (Melbourne, FL).....126

Synchronous FM discriminator for high-data-rate digital communications. **Sheng H. Lee and Alvin Wong,** Philips Semiconductors (Sunnyvale, CA).....127

WIRELESS LANs -- TRADEOFFS, IMPLEMENTATION, AND APPLICATIONS

Abstract

The application of Spread Spectrum wireless technology in communications, entertainment, and information industries has created a great demand for innovations in components, systems architecture, hardware, application software and networking compatibility. Many view wireless as an adjunct to existing wire based technologies. The perceived ultimate goal of hardware and service providers is to outfit at least 50 million users with a personal communicator capable of video, audio, voice, and data, retrieval and transmission anywhere in the world, sans any "wired" connection. This presupposes some agreed to standardization and network in place ready and able to provide instant access to each personal communicator. Before all this becomes a reality via Gates' 680 satellite system, Motorola's Iridium, ARDIS, RAM, CDPD, or carriers implementation of PCS networks, spread spectrum technology will get a workout in "Wireless LANs" in the office and industrial environment. This paper deals with a number of issues surrounding the successful implementation of wireless LANs. Systems issues as well as implementation considerations are explored. Applications, tradeoffs, interoperability with existing wired LANs, and who's who in the business today are discussed. Effects of standardization and spectrum allocation by the FCC are reviewed and implications extrapolated. A number of Spread Spectrum manufacturers that allow wireless access to LAN networks, as well as peer to peer and some of their features and benefits are described. Chipset suppliers are included for that adventurous manufacturer who wants to do in-house design, develop, and integrate radio and computer technology. For those not so adventurous, some development facilities that will integrate these various technologies specific piece of hardware and software, are also included.

Biographical data of speaker

Name: Al Juodikis
Title: Managing Director
Company: Juodikis & Associates
Address: 3584 Sunnyhaven Drive
City, State Zip: San Jose, Ca 95117
Tel: 408.984.7269
FAX: 408.296.4147

Biography

Mr. Juodikis provides management consulting services in wireless technology design, development, applications, marketing, and manufacturing. He has over 30 years global experience in high tech business development, strategic planning, product development, program management, and system integration. He has held accountable positions in engineering, marketing, sales, and management, with Fortune 500 as well as start up companies. Mr Juodikis earned a MSEE degree from Caltech, Pasadena.

"So You Want to Design a Radio for a Wireless LAN."

The availability of unlicensed spectrum in the form of FCC specified ISM bands has created an unprecedented level of radio design activity. Companies designing radios today range from those who are experts in the field to total novices whose primary experience is in the digital world. This paper will explore critical design issues that must be addressed by the system designer in the successful development of a wireless LAN. Starting with system definition and anticipated operating environment, this paper addressed the tradeoffs that must be made before the design begins. Once the definition is complete, further design decisions are necessary in the selection of a radio architecture that will allow robust operation over a wide range of end-use scenarios. After an architecture is chosen, actual component selection must be made by balancing a broad list of factors: cost, development time, performance, size, power dissipation, component availability, and others. Upon completion of the design, obtaining FCC type approval presents many challenges for the uninitiated. However, the pay off at the end of the process is real and the wide variety of end use applications that will be explored speak highly of the FCC's original strategy in the ISM bands of fostering innovation through a reduction in regulation.

Biographical Data of Speaker

Name:	Ron Ruebusch
Title:	Vice President, Semiconductor Product Dev.
Company:	Celeritek, Inc.
Address:	3236 Scott Blvd.
City, State, Zip:	Santa Clara, CA 95054
Phone:	(408) 986-5060 x251
Fax:	(408) 986-5085

Biography

Mr. Ruebusch is Vice President, Semiconductor Product Development of Celeritek, Inc. In this capacity he is responsible for all of the company's semiconductor product definition, marketing, and engineering. He has 22 years experience in semiconductor marketing and operations in communications components. His background includes analog, mixed signal, and digital components in both Gallium Arsenide and Silicon technologies. He was previously employed by National Semiconductor, Pacific Monolithics, and Advanced Micro Devices. Mr. Ruebusch holds a BSEE, MSEE, and MBA degrees from Santa Clara University.

IEEE 802.11 Standards to Boost Rising Wireless LAN Markets in Mobile Workplace

by Jon Edney, General Manager
Symbionics Networks Ltd.
St. John's Innovation Park
Cowley Road, Cambridge, CB4 4WS, UK

ABSTRACT

Mandates of mobile work environments require immediate, flexible and wireless access to an organization's local area network. Proprietary systems for wireless LANs exist, but the current lack of standards makes wireless LANs impractical and expensive, except for highly specialized applications. The Institute of Electronic and Electrical Engineers 802.11 standard, approaching completion, will change those factors by defining interconnection between disparate systems and enabling expansion of wireless LAN markets.

IEEE 802.11 standards will address both radio and infrared physical media with a common media access control protocol. The standards group's terms of reference are bound by a set of general IEEE 802 functional

requirements and guidelines. The guidelines and requirements specify a range of architectural and performance-related criteria that the standard should meet.

Availability of the standard will raise customers' confidence in the technology and reduce the danger of obsolescence and vendor dependence. Furthermore, the availability of the standard will open up wider marketing channels such as large retail computer distribution chains and will allow smaller businesses to purchase the technology directly.

Edney will define the importance of the current standards, which still are in development. Edney also will explore the impact standards will have on the proliferation of wireless LANs.

I. WIRELESS LANS TODAY

Companies specializing in wireless data communications are selling wireless local area network products based on individual proprietary technologies. For the assorted radio systems, there are technical similarities among each company's package. These similarities stem from requirements to conform with federally-mandated radio rules and regulations. However, each company implements its own communications protocol. The exclusive nature of these protocols offer little possibility of interoperability with wireless LAN products from secondary sources. This limitation provides no competition in

pricing and forces customers to become dependent on one vendor for service or additional products. Because of these deterrents, the total market for wireless LAN products today is considered small. However, many predict the market for wireless LANs will develop rapidly once a standard is established. Standards, such as those under development by the Institute of Electronic and Electrical Engineers, are important because they ensure interoperability between products from different manufacturers. Access to multiple manufacturers creates a competitive climate that drives down market prices.

II. STARTING POINTS FOR THE IEEE 802.11 STANDARDS

Any technology capable of passing information over short distances without a physical connection is a candidate for wireless LAN communications. The two most practical technologies for wireless LANs are infrared light and radio. Today, both of these technologies are characterized by the capability to send data across short distances within a defined area, such as a building or a room, at speeds of 1 to 10 megabits per second. Neither technology requires a license from regulatory agencies to operate, and there are no outside charges for this service once the equipment is purchased.

A. Infrared technology

Infrared light, a technology commonly used for television remote controls, can be used for wireless LAN data transmissions. The distance of non-directional infrared systems is limited to 15 to 30 feet. A line-of-sight connection is preferred, but some infrared systems can

work using reflected light. Infrared systems are blocked easily by anything that interrupts the light beam. Transmissions are limited to a single room or through windows. Infrared's advantage as a wireless LAN medium stems from a lack of governmental restrictions on its spectrum use. Therefore, individual manufacturers can implement whatever modulation scheme they deem best. The modulation scheme is the method where data bits are encoded on the transmission medium. Infrared wireless LANs modulate light from an infrared light emitting diode (LED). Brightness of the light is changed, usually between on and off, to encode the data. The light is seen by a receiver and converted to data, with higher data rates requiring more complex modulation schemes similar to those used in analog modems. Because of the high potential for complexity, however, infrared systems may not be any less expensive than radio methods to achieve a wireless LAN environment.

B. Radio

In principle, sending data over radio is fairly simple. However, the technology is complicated with limitations imposed by governmental allocation of radio spectrum and the need to avoid interference with other radio system users. When governmental regulatory bodies, such as the Federal Communications Commission, allocate radio spectrum, they do so with a particular use in mind. Rules are set governing the technical specifications of radio systems to ensure users in different frequency bands do not interfere with each other. Within each band, a method of spectrum allocation must be chosen, again to limit interference among users. One approach is to make the spectrum available to many users but set technical rules so multiple users can share fairly the unlicensed band. In the 2.4 gigahertz industrial, science and medical (ISM) band, the most internationally available for wireless LANs, FCC rules place

severe constraints on system operations. The rules limit the allowable power transmission to one watt and specify that systems must be spread spectrum. The bands most widely used for wireless LANs in the United States are as follows: 1) 902-928 megahertz ISM band (spread spectrum); 2) 2.400- 2.4835 GHz ISM band (spread spectrum); 3) 5.725- 5.850 GHz ISM band (spread spectrum); 4) an 18 GHz licensed band that is used by Motorola systems. Users should not be concerned with the frequency of their equipment, but they should be concerned with the features that are affected by frequency, including: data rate, range, cost, interference susceptibility, international availability of the band, and options such as voice support. The availability of the IEEE 802.11 standard will simplify buying decisions for consumers. Standards eliminate concerns over the technical radio details. Users can choose products of similar function and performance based on cost, support and availability.

III. APPLICATIONS FOR THE IEEE 802.11 STANDARDS

The two types of connections for wireless capabilities in LAN networks include the access application, which is located at the edge of the network, and the trunk application which is part of the internal network fabric. The access connection is characterized by portable devices requiring flexible access to the LAN from anywhere in the office. Key requirements for access products are low cost, the PC card format, and standards. Trunk applications are typically building-to-building or from a central point to network islands. Wireless trunks may be used when it is too difficult or expensive to install or rent cable connections when the LAN islands are relocate physically. Key requirements for a wireless trunk are high data rates and reliability.

A. Standards mean interoperability

The IEEE 802.11 committee will establish the standards that will define interconnection for access applications among various systems. Although there are no statutory requirements for compliance, these standards will enable expansion of the wireless LAN market through interoperability. The IEEE 802.11 standards address both radio and infrared physical media with a common media access control protocol. The standards group's terms of reference are bound by a set of general IEEE 802 functional requirements and guidelines. These requirements and guidelines specify a range of architectural- and

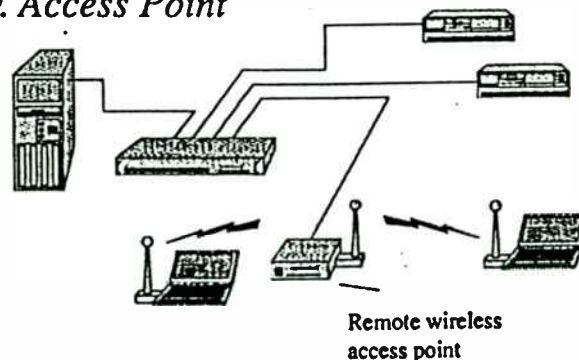
performance-related criteria that the standard should meet. This criteria includes a data rate of between 1 and 20 Mbps, compatibility with services provided by other IEEE 802 standards, and some support for digital voice applications. The standards group now recommends radio operation in the 2.4 GHz spread spectrum band and infrared light systems. Based on the current draft of the standard, IEEE 802.11 radio systems will have a range of approximately 200-300 feet and will have a data rate of 2 Mbps. The option to reduce the data rate to 1 Mbps will improve range or improve transmissions in difficult radio environments. Protocols are designed to interface easily to existing LAN systems so that wireless LANs can be incorporated seamlessly and transparently into conventional Ethernet and other LAN systems. This simplicity of installation is one of the key benefits that standards brings to the consumer. Products from different vendors that conform to the IEEE 802.11 standard will operate with each other. While the focus is on interoperability, consumers must still choose which physical media to use for transmissions. For instance, an infrared light system will not communicate with a radio-based system. It is also important to remember that although standards-based products will be interoperable, there still may be differences in valued-added features such as management. Each product will offer unique features available only on

that brand. However, by choosing IEEE 802.11 standards-based products, users will know that if they change to another vendor their existing investment is still usable.

B. Using access points for wireless LAN connectivity

In the access application, data is sent between portable computers and a file server through a wireless access point. The access point appears to the server like a bridged Ethernet segment or lower hierarchy LAN hub. Access points handle conversions between 802.3 (Ethernet) and 802.11 protocols. A similar scenario would apply in the case of 802.5 (token rings) protocol. This type of network would give portable computer users access to servers on the LAN as if they were directly connected to it. Portable computer users could access the network as long as they remained within 100 to 300 foot radius of the access point because radio signals travel through walls and partitions. Multiple access points with overlapping coverage areas could be used to extend the range by using a technique called roaming. When portable users move from one area to another, the access points automatically coordinate the signal hand off. IEEE 802.11 standards allow for the creation of ad hoc networks where laptops or personal digital assistants can communicate directly with each other rather than through a file server.

Hybrid W-LAN w. Access Point



IV. WIRELESS LAN MARKETS

A decision on industry standards is one of the major driving factors for new LAN connectivity products, especially wireless. The availability of the standard will raise customers' confidence in the technology and reduce the danger of obsolescence and vendor dependence. Market drivers will include users who need mobility in the office as well as users who need a convenient way to extend existing LANs or use wireless systems instead of installing a wired LAN. Furthermore, the availability of standards will open more marketing channels such as large retail computer distribution chains and will allow smaller businesses to purchase the technology directly. Other vertical markets will include: point-of-sale transactions, hospital/medical environments, warehouse environments, and utility companies. Until this year, the cost of wireless LAN adapters has been

expensive when compared to the expense of wired LANs. If the expense of cabling is considered, expenditures for wireless technology can be cost justified. However, most buildings, particularly new structures are pre-wired to avoid the cost of cable installation. The cost ratio is set to change this year because of the availability of standards-based silicon and radio components. Wireless LAN adapter costs will decline sharply to a consumer price of \$300 by the end of 1995 and down to \$200 by the end of 1997. Wireless LAN adapters always will cost more than simple Ethernet adapters. However, by the end of the decade, the difference will be small enough to entice many users into selecting wireless technology as a first choice for LAN connection because of benefits, such as convenience and flexibility, that mobility and portability have to offer.

A High Volume, Low Cost, Plastic Packaged 2.4GHz Transceiver MMIC

L M Devlin, B J Buck, A W Dearn, J C Clifton, A A G Frier, M W Geen

GEC-Marconi Materials Technology Ltd
Caswell, Northants
NN12 8EQ

Telephone: +44 1327 350581
Facsimile: +44 1327 356775

Introduction

Unlicensed transmission of spread spectrum signals is allowed in the Industrial Scientific and Medical (ISM) bands. GMMT have developed a high volume, low cost, plastic packaged transceiver for use in the 2.4 - 2.483GHz ISM band. The single chip GaAs IC is a production version of a prototype circuit, originally presented at the First Annual Wireless Symposium (1). Chip area has been reduced from 17mm² to 9mm² and through GaAs vias have been eliminated. The part is packaged in a low profile, TQFP-32 plastic package and has been used in a commercially available radio product, which has passed ETS 300328 type approval.

Circuit Design

A block diagram of the transceiver is shown in Figure 1. Particular effort was paid to ensuring the design would be tolerant to the common lead inductance associated with the low cost plastic package (2). To this end, differential circuitry has been used where possible to dispense with the need for RF/IF grounds. To avoid realising the LNA as a re-entrant gain structure, the image reject filter is realised on chip. The power amplifier has been limited to single stage, to keep the re-entrant gain at a manageable level. Also, no external VCO tuning or resonator components are used which helps keep LO leakage to a minimum.

A common local oscillator is used in both transmit and receive mode. The oscillator is a fully differential Clapp type VCO, with all resonator and varactor circuitry on-chip. The differential outputs are used to drive the gates of the quad ring, double balanced mixer.

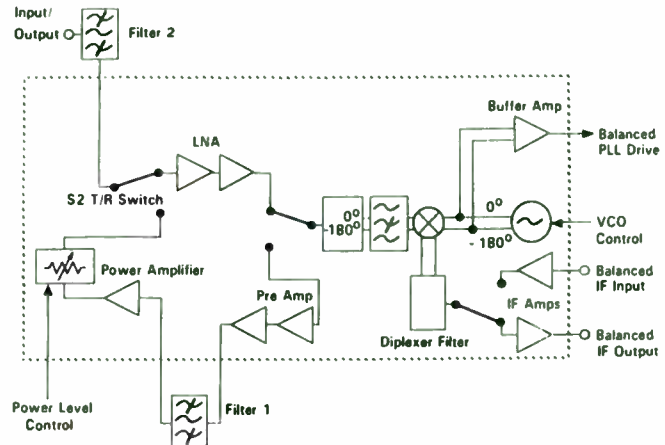


Figure 1 Block Diagram

Signals entering the chip in receive mode are routed into a two stage stacked bias LNA. A passive balun converts the single ended signal to differential, after which the on-chip, band stop filter is used to reject image frequency noise. The quad ring double balanced mixer generates a differential IF output which passes through a diplexer filter and an IF amplifier before being routed off chip as a balanced IF output.

In transmit mode, the IF input is boosted in level by a two stage amplifier. Active biasing is used to avoid large IF bias chokes. The signal is then routed through the diplexer filter, which reduces any harmonic output, and into the quad ring mixer. LO drive to the mixer is common to both transmit and receive modes. The differential RF output of the mixer passes through the image reject filter, which suppresses the unwanted sideband. The passive balun converts the differential RF signals into a single ended signal. This is amplified by the two stage preamplifier before leaving the chip. An external filter is used to suppress the unwanted sideband, any unwanted spurious and the already low LO

leakage. The signal is then routed back on chip through a single stage power amplifier. A 10dB single step level control is placed after the power amplifier. This ensures an accurate 10dB power step and avoids the increased harmonic output which will result if the power stage is simply biased down to reduce the gain.

Fabrication and Packaging

A photograph of the 3.0 x 2.9mm chip is shown in Figure 2. The GMMT F20 process is used, minus the through GaAs via process step. Active devices are depletion mode MESFETs with 0.5µm gate lengths. Final substrate thickness is 200µm and wafer diameter is 3". A two layer metallisation, with dielectric crossovers, allows redefinition of the top layer metal, for adjustment of resonator size or bias level, with a single mask plate. The simple 8 mask process is ideally suited to volume manufacture.

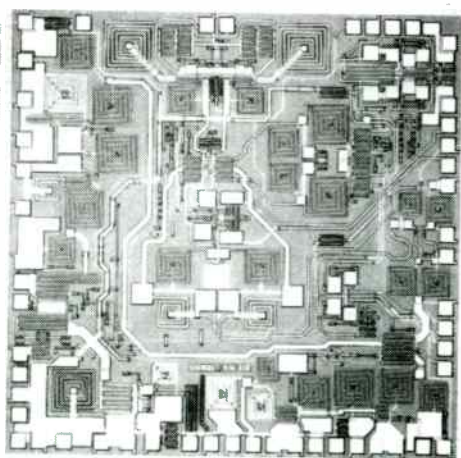


Figure 2 Chip Photograph

Wafers are RFOV measured at their unthinned stage, when the wafer is 600µm thick and more robust. All failed circuits are inked, Figure 3, and the wafer is thinned down to 200µm. The complete wafer is then shipped direct to the packaging company. Wafers are sawn and packaged in TQFP-32 plastic packages, Figure 4. The low profile (1.4 mm) and small area (7mm square body outline) make this package ideally suited for PCMCIA applications where space is at a premium.

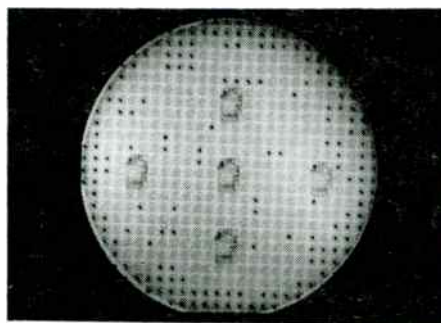


Figure 3 An Inked Wafer

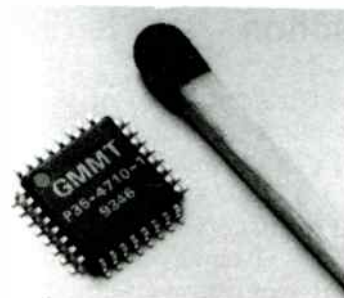


Figure 4 Photograph of One Packaged Transceiver

On Wafer Measurements

Although the absence of through GaAs vias means conventional RF on Wafer (RFOV) probing is not possible, it is still possible to carry out full functional RF testing of the circuit directly on wafer. This is facilitated by a meandering metal track interconnecting each ground bond pad, in the dicing street. The track is cut at the sawing stage and plays no part in the packaged chip functionality. A custom set of mixed DC and RF probes are used to make contact to all necessary bond pads (Figure 5). Ground signal connections are used for all RF signals. IF inputs and outputs use a pair of DC needles with an off chip, co-axial, IF balun positioned close to the probes.

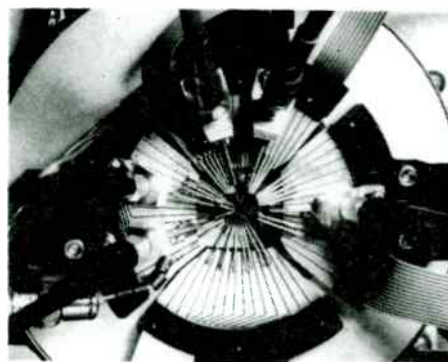


Figure 5 RFOV Probing of Transceiver

Figure 6 shows the measured receive mode conversion gain across one wafer. The measurement is not intended to be a definitive statement of the performance of the packaged part but is perfectly adequate for determining RF functionality. IF port impedance is not matched for this measurement and an additional 4dB of gain is available by presenting an 800Ω differential IF load. RF output power in transmit mode, for an IF input of -10dBm from a 600Ω differential source, is also measured. Performance across one wafer is shown in Figure 7. Other parameters which are currently measured on wafer for 100% of sites include, VCO tuning range, PLL reference output power, level control, standby, receive and transmit supply currents and a selection of monitoring voltages.

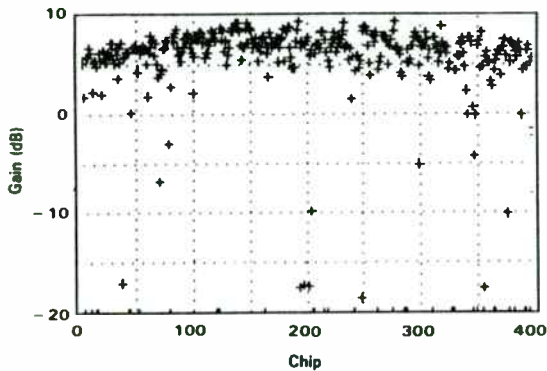


Figure 6 RFOV Measured Receive Mode Conversion Gain (No IF Matching)

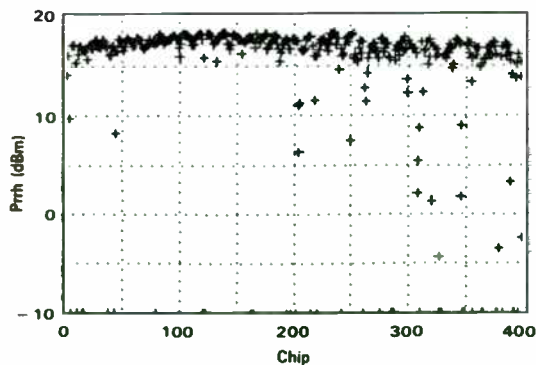


Figure 7 RFOV Measured Output Power

Figure 8 shows the mean LO frequency at tuning voltages of 1V and 2V for over 50 wafers fabricated using the current design. A shift down in frequency and a slight reduction in bandwidth is observed between on wafer and packaged performance. The 0.5 to 4V tuning range of packaged devices is specified to cover the 2050MHz to 2150MHz range. Devices typically have a bandwidth of 200MHz and centring of the on chip resonator

value to maximise the yield of devices to this parameter has been carried out.

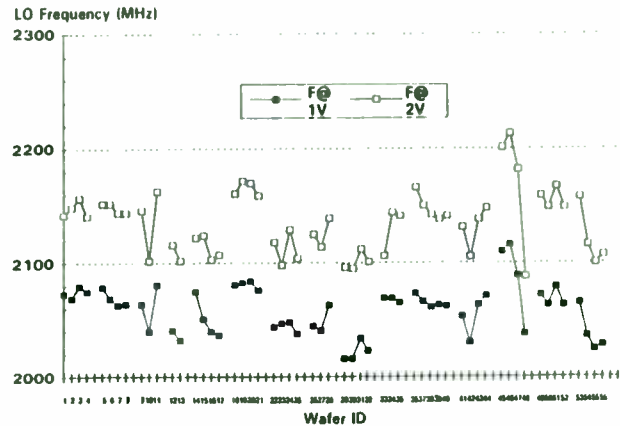


Figure 8 Mean LO Frequency Versus Wafer

Measured Performance of Packaged Devices

All packaged parts are re-measured to confirm RF functionality and to gather statistical data about the performance variation with production spread. The results presented here are for a typical assembly batch of devices.

The standby mode current drawn from the +5V supply is shown in Figure 9 and is typically 0.5mA. Receive mode current is shown in Figure 10 and is typically 35mA.

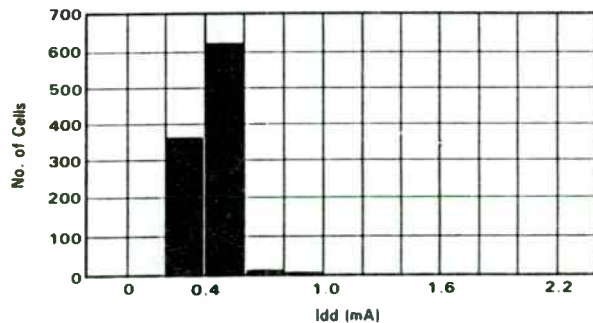


Figure 9 Standby Current

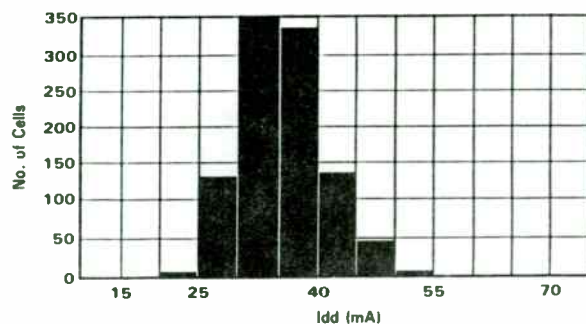


Figure 10 Receive Mode Current

Conversion gain into an IF load of 800Ω differential is shown in Figure 11. The typical available gain is 8.5dB. Although all bias voltages are set on chip, it is possible to adjust the bias with an external resistor to achieve more gain at the expense of current. Parts are measured in this increased gain/current mode using a $10k\Omega$ external resistor (receive mode 2). The current spread is shown in Figure 12, typical values are in the region of 45mA.

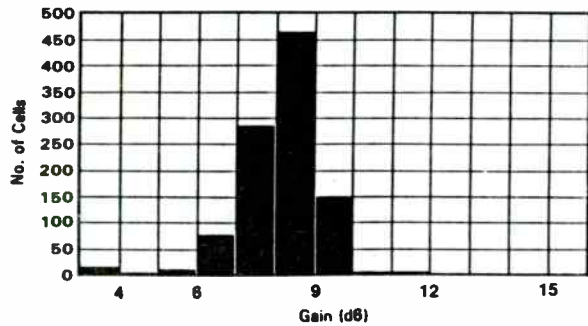


Figure 11 Receive Mode Conversion Gain into 800Ω Differential Load

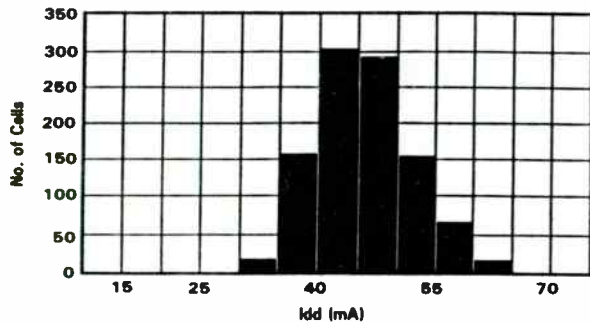


Figure 12 Receive Mode 2 Current

Figure 13 shows the gain spread, the mean available gain is 10.5dB and the typical SSB noise figure in this case is 6dB.

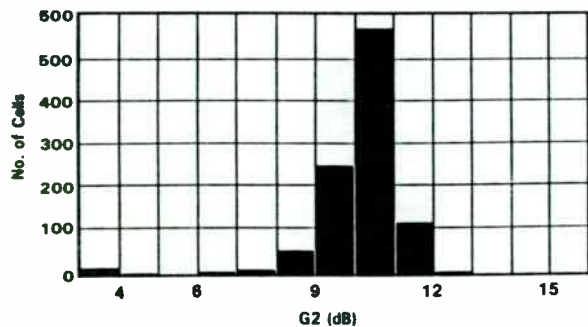


Figure 13 Receive Mode 2 Conversion Gain into 800Ω Differential Load

Transmit mode currents are plotted in Figure 14, the mean value is 180mA. IF input is -10dBm from a 600Ω differential source. A bandpass filter with an insertion loss of around 1.5dB was placed between the preamplifier output and the power amplifier input (filter 1 in figure 1). The RF output power level is shown in Figure 15, a typical value of 14dBm was measured.

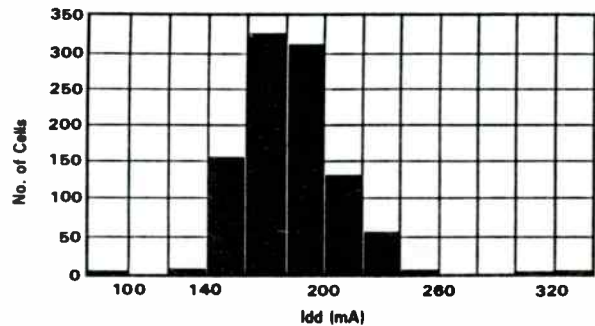


Figure 14 Transmit Mode Current

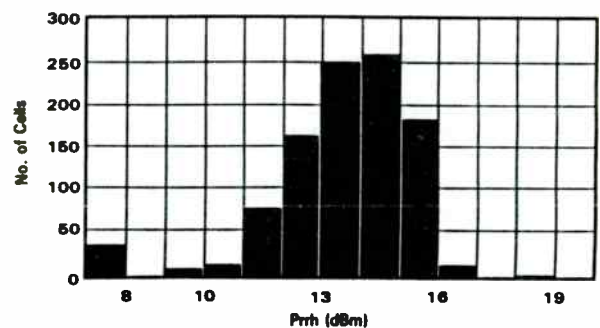


Figure 15 RF Output Power

LO tuning range is also measured on all devices. The spread of frequencies at $V_{tune} = 0.5V$ is shown in Figure 16. A typical tuning

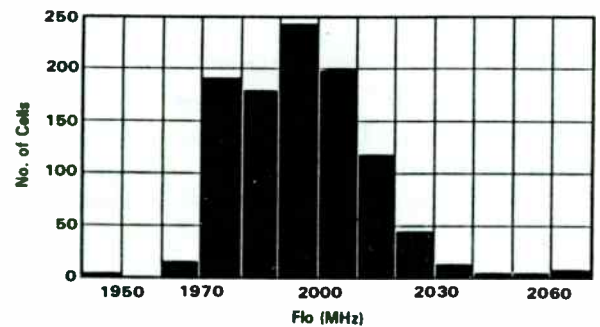


Figure 16 LO Frequency at $V_{tune} = 0.5V$

curve for one device is shown in Figure 17, with linearity better than 2:1 over the specified 2050MHz to 2150MHz tuning range.

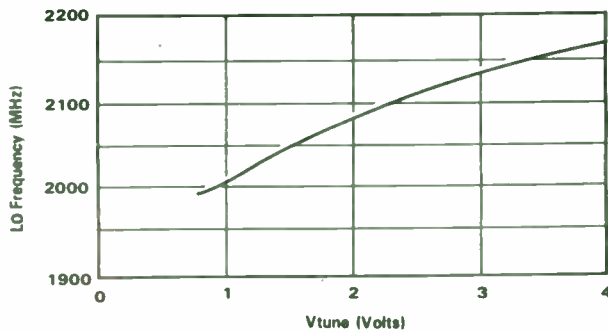


Figure 17 Typical Measured Tuning Curve of One Device

Application

A direct sequence spread spectrum radio, using the P35-4710-1, has been designed by RN Electronics. Figure 18 shows a photograph of the radio board. Typical sensitivities of -85dBm are achieved in production and line of site ranges in excess of 200m have been demonstrated. The radio is used in an industrial and retail stock control system produced by Symbol Technologies Ltd. Figure 19 shows one Laser Radio Terminal (LRT) which allows wireless transmission of data to/from a base station. Warehouses of up to 25,000 square feet have been successfully covered with a single base station. The radio has passed ETS 300328 type approval.

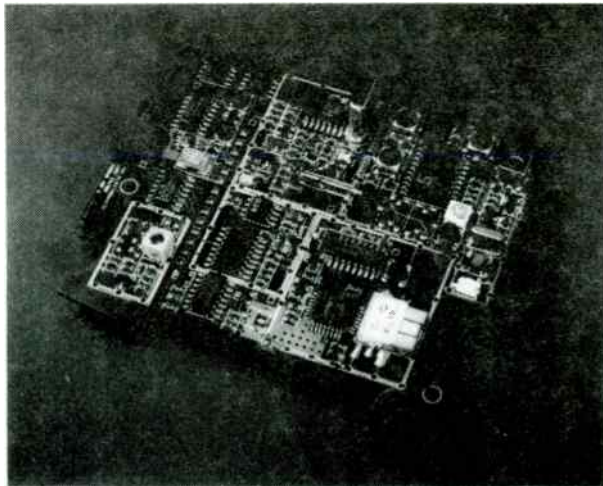


Figure 18 An LRT Radio Board



Figure 19 A Symbol Laser Radio Terminal

Conclusion

GMMT have developed a low cost, high volume, plastic packaged transceiver for use in the 2.4 - 2.483GHz ISM bands. A direct sequence spread spectrum radio for a commercially available product has been designed using the part. Low current consumption and negligible standby current make the part ideally suited to battery powered applications. The low profile, small area TQFP-32 plastic package is well suited to applications, such as PCMCIA radios, where space is at a premium.

Acknowledgements

The authors would like to thank the numerous staff at GMMT who have helped with the development of this part. The authors would also like to thank Symbol Technologies Ltd for allowing the use of the LRT and radio board photographs and RN Electronics and Silicon Communications Ltd for their co-operation during the development.

References

1. Devlin L.M, Buck B.J, Clifton J.C, Dearn A.W, Long A.P, "A 2.4GHz Single Chip Transceiver", Proceedings fo the First Annual Wireless Symposium, January 1993 pp 395 - 402.
2. Devlin L.M, Buck B.J, UK Patent Application No. 9309206

2.4GHz Silicon RF Integration for Wireless LANs

Abstract

R&D is underway to develop silicon bipolar ICs for 2.4GHz applications. The debates between MMIC technology vendors regarding whether GaAs FET, GaAs HBT, or Silicon Germanium HBT processes will be best for 2.4GHz RF generally dismiss the notion that silicon will be used for these applications. However, silicon historically is used wherever it can successfully perform the required function. This has been seen in high-speed digital circuits as well as other functions such as fiber optic transmitter and receiver circuits. By utilizing a unique silicon process technology and extreme care in design, it can be shown that producing 2.4GHz silicon bipolar ICs for portable Wireless LAN applications is entirely feasible. This paper will describe the attributes of the 2.4GHz band to explain why the industry is focused on providing solutions for this band. Also, some of the benefits of choosing silicon for this application will be illustrated. A review of some of the design challenges and constraints imposed on this design will be followed by an explanation of the design approach. A brief description of the underlying silicon process technology will help explain how it is possible to enhance silicon for 2.4GHz applications enabling the performance which is indicated in design predictions and simulation results. The paper will close with a description of design verification plans and issues to be resolved in transferring these devices into high-volume production.

Outline:

- I. Why Use the 2.4GHz Band?
- II. Pros and Cons of Silicon RF ICs
- III. Design Challenges
 - A. FCC Part 15
 - B. PCMCIA
 - C. IEEE802.11
 - D. Portability
- IV. Design Approach
 - A. Integrated CAD Environment
 - B. Parallel Design Tool Utilization
 - C. Technology Modeling
 - D. Accounting for Unwanted Parasitics
 - E. Package Modeling
 - F. Electromagnetic Simulation
- V. Technology Attributes
 - A. RF Transistor Performance
 - B. Passive Elements
 - C. Substrate Characteristics
- VI. Design Predictions
- VII. Design Verification and Production Transfer Plans
- VIII. Conclusions

Biographical Data of Speaker

Name: Brian D. Mathews
Title: Wireless Product Manager
Company: Harris Semiconductor
Address: P.O. Box 883 MS 58-96
City, State, Zip: Melbourne, FL 32902
Telephone: (407) 724-7585
Fax: (407) 729-5331

Biography

Mr. Mathews is responsible for the Wireless Products at Harris Semiconductor including Business Strategy Planning, New Product Development, Manufacturing Planning, and Marketing Programs. A 10 year veteran at Harris, Mathews has held various positions including Design, Applications, Product Engineering Management, and Strategic Marketing. Mr. Mathews holds a BSEE from California State Polytechnic University - Pomona.

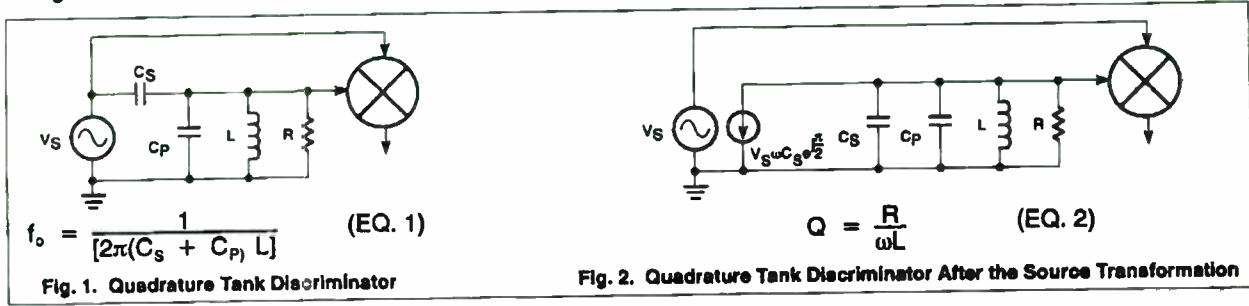
Synchronous FM Discriminator for High-Data-Rate Digital Communications

Sheng H. Lee, Philips Semiconductors

Abstract— A new type of FM discriminator uses dual resonators to adjust the allowable frequency deviation independent of demodulated amplitude, which is more appropriate for today's high-data-rate digital communications. Yet, it remains compatible with the ICs that were designed for quadrature tank discriminator.

I. INTRODUCTION

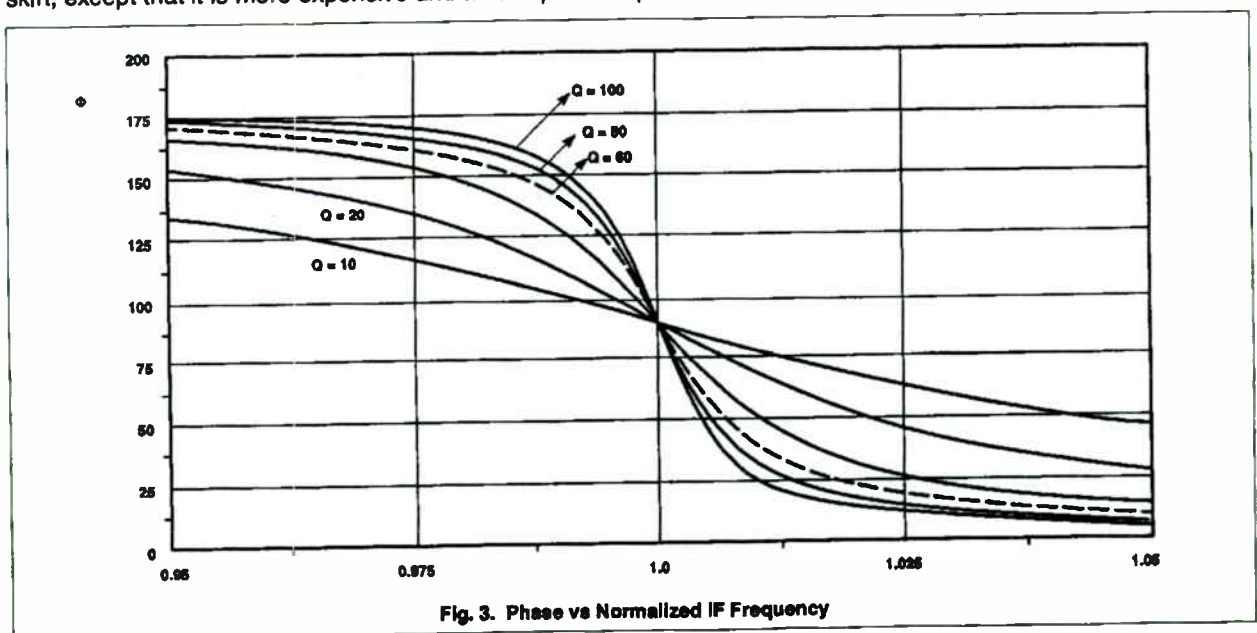
Quadrature tank discriminator is ideally suited for FM receiver ICs, thanks to its excellent performance and simple structure. The operation starts with the FM-to-PM conversion through the quadrature tank, which not only generates a high phase slope, but also provides a 90° phase offset at the center frequency; then followed by the phase detection that usually consists of a Gilbert-cell multiplier. A typical quadrature tank structure is shown in Fig. 1, and is redrawn in Fig. 2 after the source transformation to highlight its operation principle.

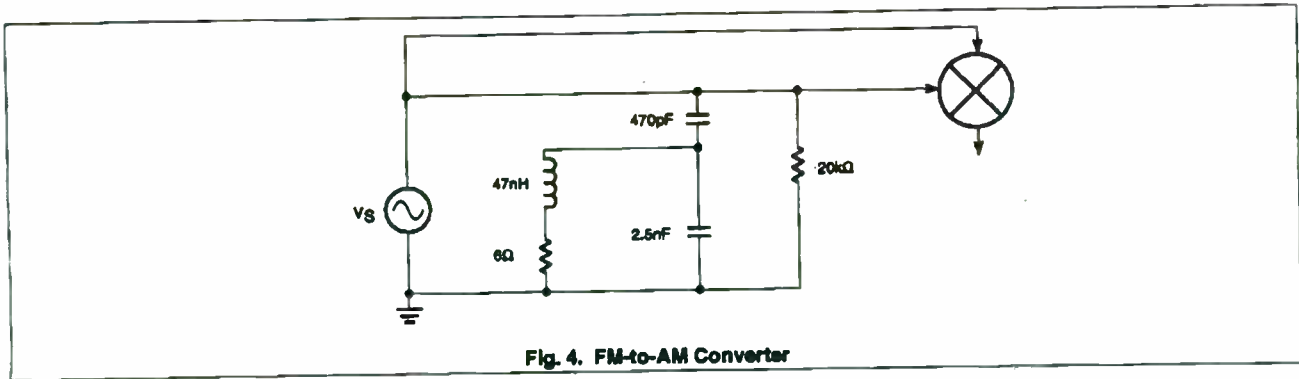


With the source transformation, the inherent 90° phase offset is clearly understood. In the meantime, the resonator provides a rapid phase shift according to the Q of the tank. Fig. 3 shows such phase shifts as functions of different 'Q's [Ref. 1], which allows the users to optimize the Q for each operating condition: a low-Q tank for the wide deviation; a high-Q for the narrow deviation, for the same distortion. But we also observed that the transformed source in Fig. 2 has a Q-dependent amplitude. As a result, high-data-rate transmission always suffered in output amplitude.

It is the intention of this article to remove the constraint by performing an FM-to-AM conversion, followed by a pseudo synchronous AM detection. In doing so, a relative constant output amplitude is achieved.

Since an ideal FM-to-AM converter requires a linear and steep gain slope, a high-Q bandpass filter is adopted to match the steep gain slope. Furthermore, a series capacitor of 470pF is added to the original filter to improve the linearity at the left skirt, which is shown in Fig. 4. An inductor can substitute for the extra capacitor to linearize the right skirt, except that it is more expensive and takes up more space.





After the FM-to-AM conversion is done, a high quality AM detector is still needed to complete the task. And the synchronous AM detection is chosen based on its superior performance. EQ. 3 lists a typical AM signal, while EQ. 4 shows how synchronous AM detection works. In the past, the synchronous AM detection is not popular only because of the complexity in providing an in-phase carrier.

$$[1 + m(t)] \cos \omega t \tag{EQ. 3}$$

$$[1 + m(t)] \cos \omega t \cos \omega t = [1 + m(t)] \frac{1}{2} (1 + \cos 2\omega t) \tag{EQ. 4}$$

where $m(t)$ is the baseband signal and ω is the carrier frequency. According to this new approach, the unconverted FM signal can serve as the carrier, although it will not be perfectly phase-aligned. EQ. 5 lists a typical FM signal, while EQ. 6 indicates that signal after such FM-to-AM conversion, including the associated phase shift from the filter.

$$\cos \left[\omega t + \int m(t) \right] \tag{EQ. 5}$$

$$C_1 [1 + m(t)C_2] \cos \left[\omega t + \int m(t) + \phi \right] \tag{EQ. 6}$$

where C_1 is a constant depending on the operating point; C_2 is a constant depending on the slope of the transfer function.

If we combine EQ. 4 and EQ. 6 together, there will be a cosine modulation on the amplitude as shown in EQ. 7.

$$C_1 [1 + m(t)C_2] \frac{1}{2} (\cos \phi + \cos [2\omega t + \phi + 2 \int m(t) dt]) \tag{EQ. 7}$$

However, this is not a cause for concern because the cosine modulation can be included in the slope linearization. Fig. 5 and 6 show the simulated gain and phase response, respectively, of the filter including the loss; Fig. 7 combines gain and phase information for the overall transfer function.

Fig. 8 compares the measured S-curves between Synchronous FM discriminator and Quadrature Tank discriminator, and the results are in excellent agreement with Fig. 7.

Normally, the S-curve was measured by stepping the input frequency at a small increment, then recording the DC voltage at the output of the discriminator. The process is tedious even if it is automated, because the tuning and testing are not coincident in time. So, a more efficient method was developed in this test, by FM-modulating the source with a sawtooth waveform to produce a linear time-varying RF frequency. Many newer HP signal generators have built-in sawtooth waveform capability such as HP8645A and HP8664A, etc. The test block diagram is shown in Fig. 9. However, even those newer signal generators have their limitations, i.e., they cannot generate 30kHz deviations at a center frequency of 455kHz. So an extra down-conversion was used to circumvent the problem.

Finally, a 45MHz demoboard incorporating the SA606 FM receiver IC from Philips Semiconductors was selected for the experiment, with the Mixer output modified to feed the Limiter Amp directly as shown in Fig. 10. Which will allow the user to achieve tune-on-the-fly for the S-curve measurement. And the complete application circuit is shown in Fig. 11.

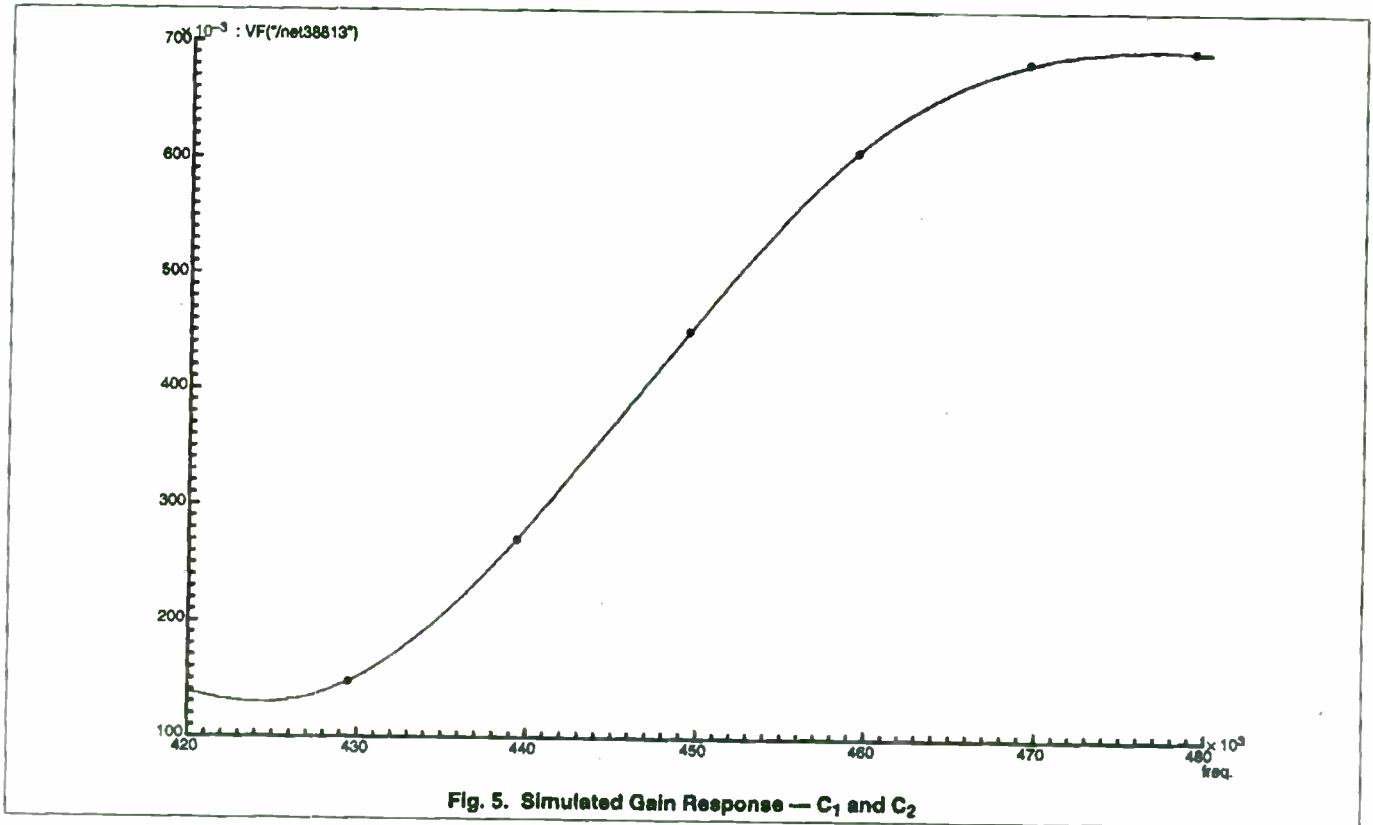
II. CONCLUSIONS

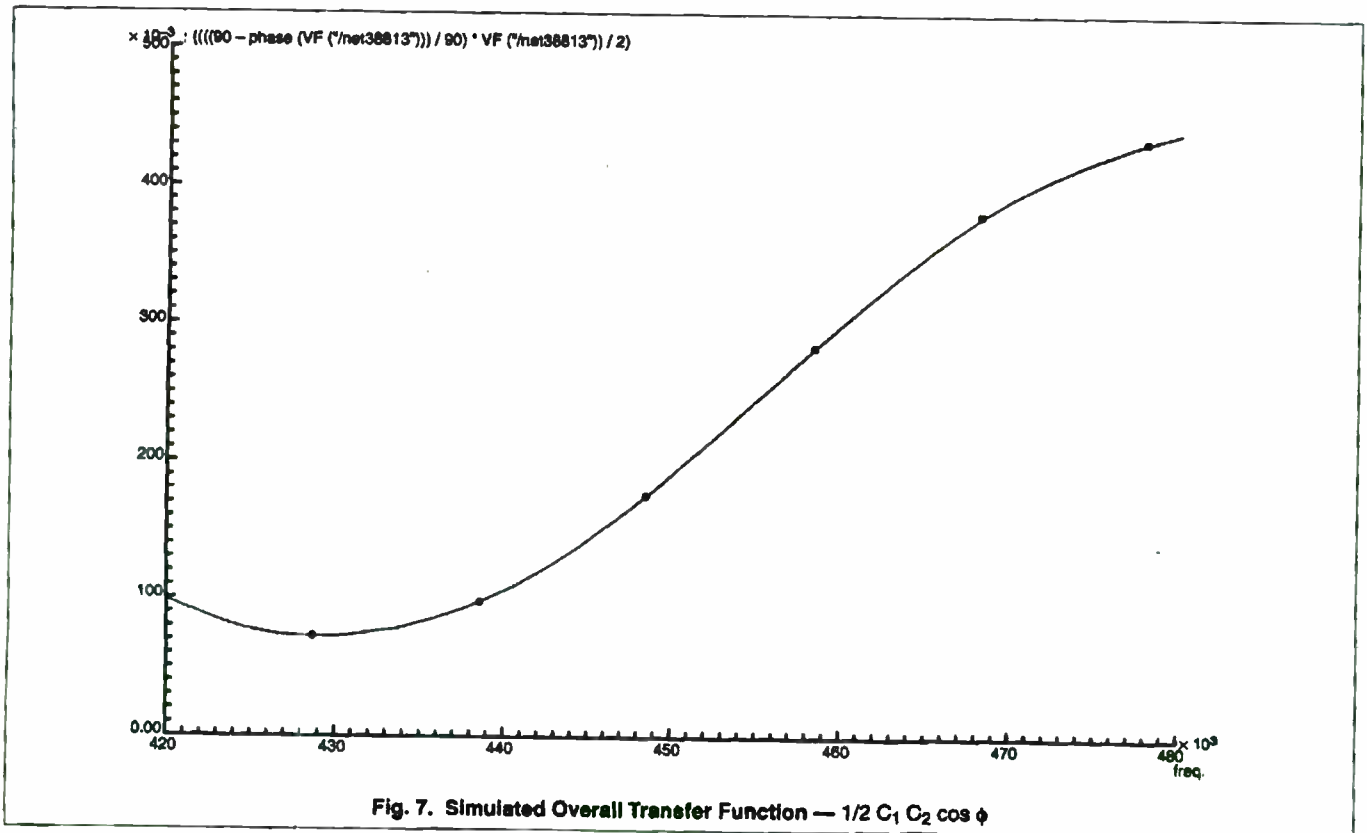
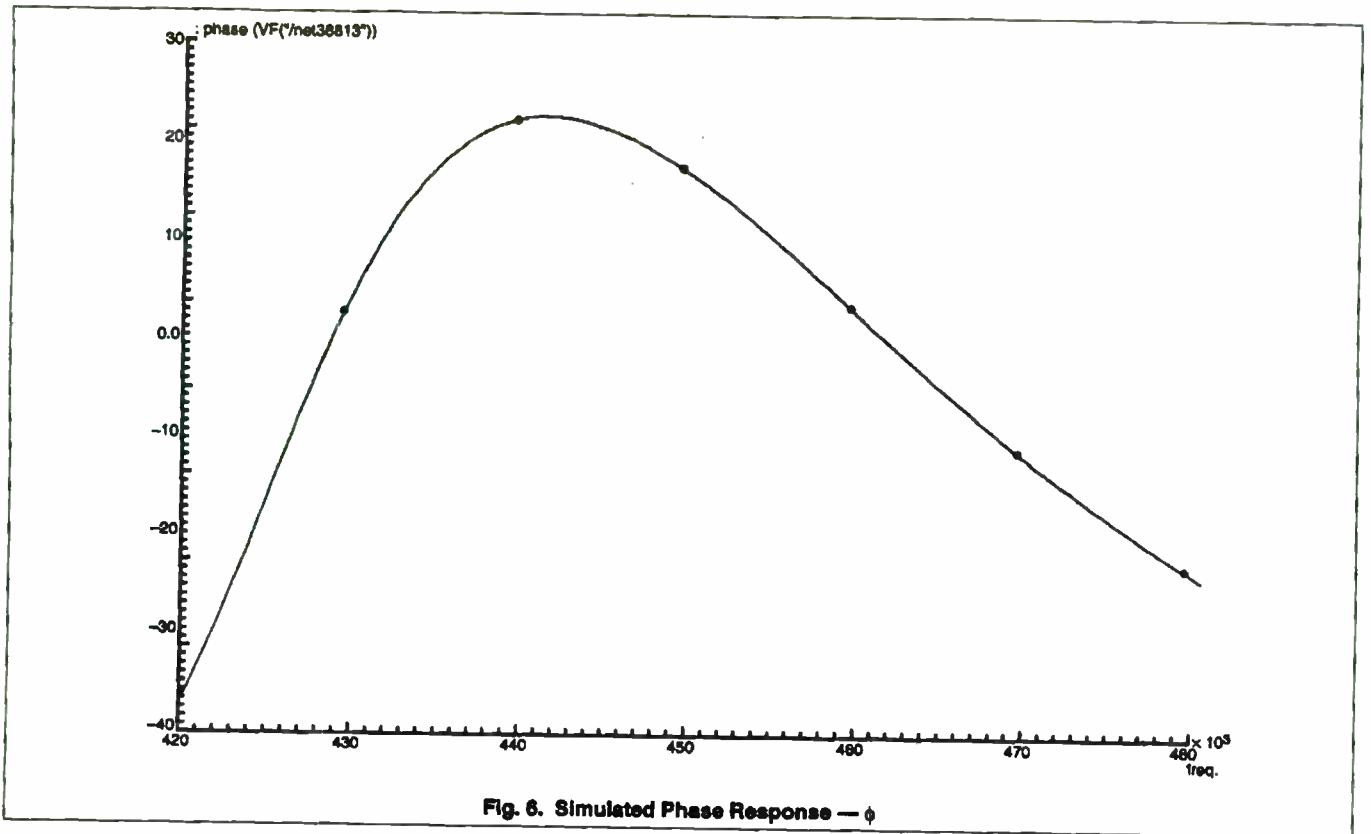
The advantage of this design becomes obvious when we review Fig. 6 for the transfer function; i.e., the vertical scale only depends on components' Q instead of system's Q. Which means the users can adjust the horizontal scale to accommodate different deviations without changing the demodulated amplitude.

However, limited by the available hardware, only the standard AMPS demoboard was modified to verify the concept. The results were 42dB SINAD at -68dBm and -119.5dBm sensitivity for the 12dB SINAD, which was about 1dB worse comparing to the standard quadrature tank discriminator. Since the front-end provides no less than 10dB gain in general, so the 1dB shortfall in sensitivity from the IF Strip is not discernible. The author wishes to thank Dr. Saeed Navid and Mr. Alvin Wong for reviewing the accuracy of this article.

III. REFERENCE

[Ref. 1] Philips Semiconductors, "High performance low power FM/IF system — NE/SA604A", Philips 1994 RF/Wireless Communications Data handbook, pp. 273.





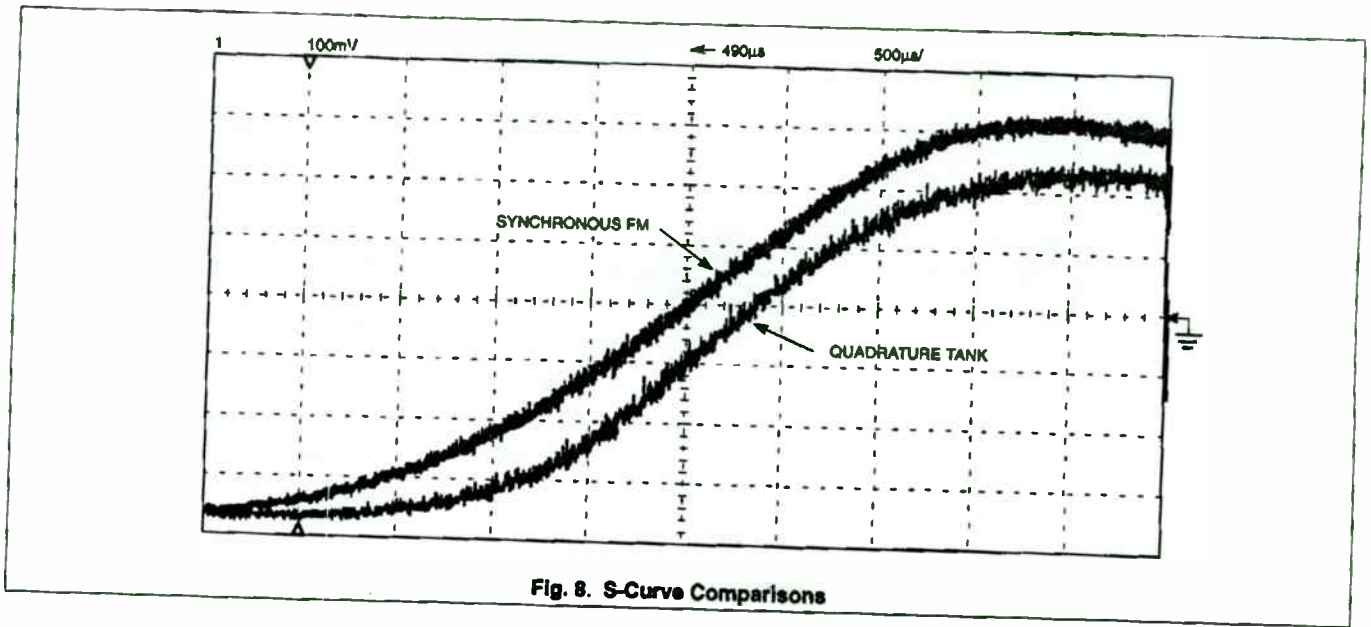


Fig. 8. S-Curve Comparisons

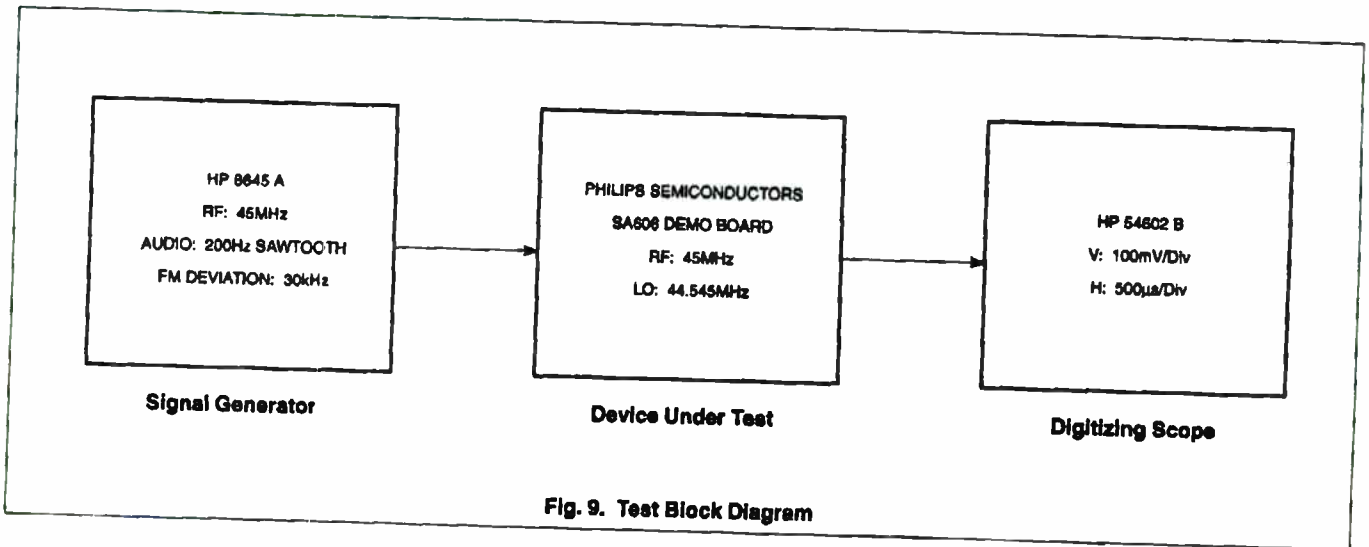


Fig. 9. Test Block Diagram

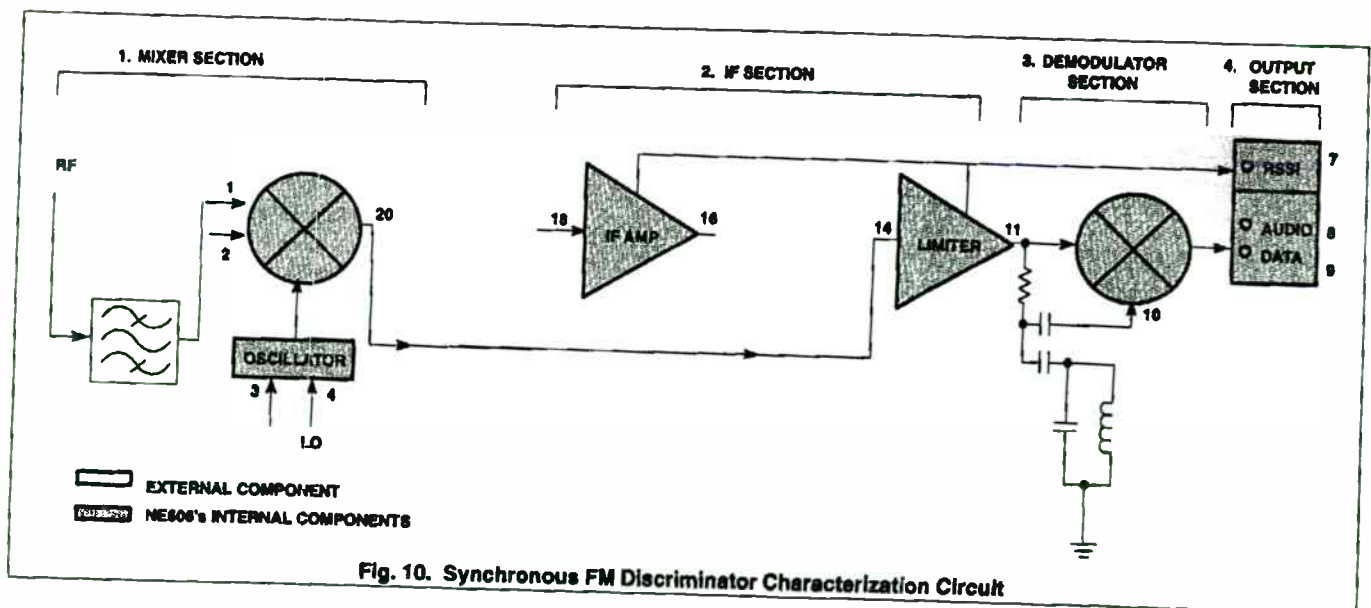
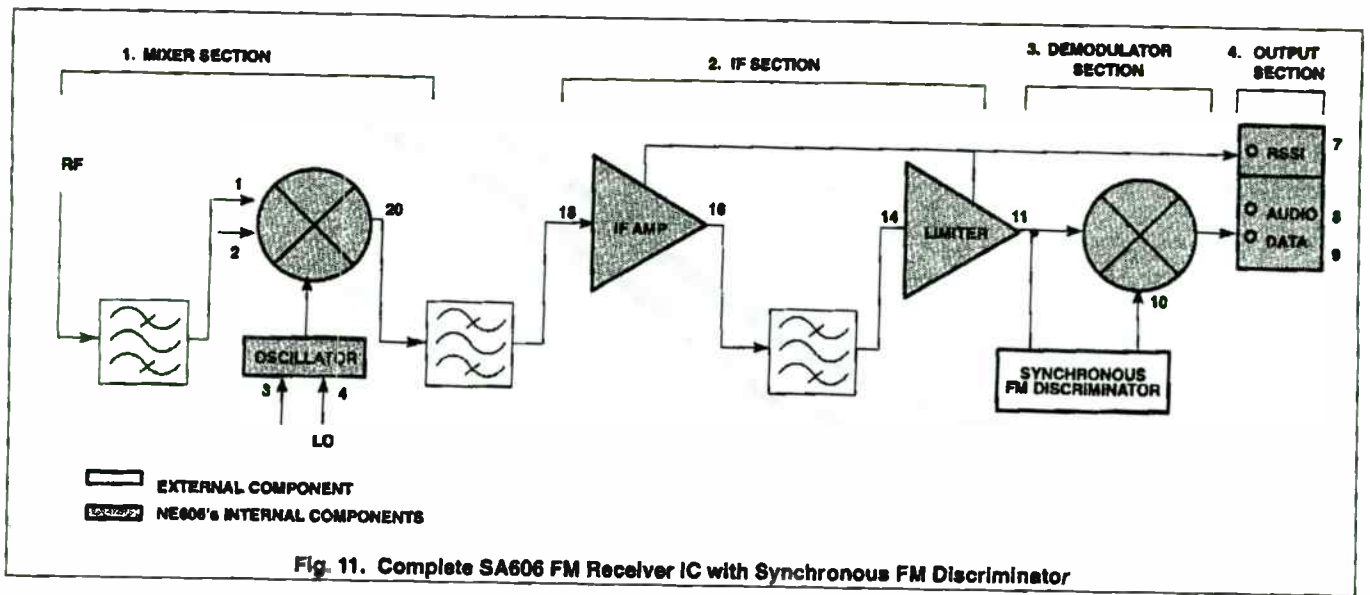


Fig. 10. Synchronous FM Discriminator Characterization Circuit



Integrated-Circuit Solutions

Session Chairperson: Mark McDonald,
Wireless Communicatios, National Semiconductor (Santa Clara, CA)

Enabling personal communications through highly-integrated RF signal-processing functionality. **John S. Brewer, Jr.,** Analog Devices, Inc. (Beaverton, OR).....134

Wideband transceivers and universal base stations. **Scott Behrhost,** Analog Devices, Inc., Computer Labs Division (Greensboro, NC).....148

A 1.5-V/25- μ A CMOS microcontroller with pager decoder for alphanumeric and numeric applications. **Remy Pache,** Centre Suisse d'Electronique et de Microtechnique (CSEM) SA (Neuchatel, Switzerland).....156

Designing the virtual battery. **Ray Waugh,** Hewlett-Packard Co., Components Group (San Jose, CA).....160

Monolithic gain blocks in mini-packages for DC-to-4000-MHz wireless handheld communications. **Henrik Morkner, Nhat Nguyen, and Gary Carr,** Hewlett-Packard Co., Communications Components Division (Newark, CA).....169

Enabling Personal Communications through Highly Integrated RF Signal Processing Functionality

John S. Brewer, Jr.
Analog Devices, Inc.

“...to come up with new products we are going to have to understand our customers’ system problems, and often understand them better than they do. If we do, then we can address them in a way that will give us some long-lasting components.”

Paul Brokaw, ADI Fellow
quoted in “The Magic of Analog Design”,
Electronic Design, 25 November 1992

Communications Division
RF Products Group



Outline

Why is Integrating RF Signal Processing Functionality Important?

What Barriers Exist to Achieving Highly Integrated RF Signal Processing?

- Circuit/System Design
- Commercial Risk Mitigation
- Manufacturing Technologies

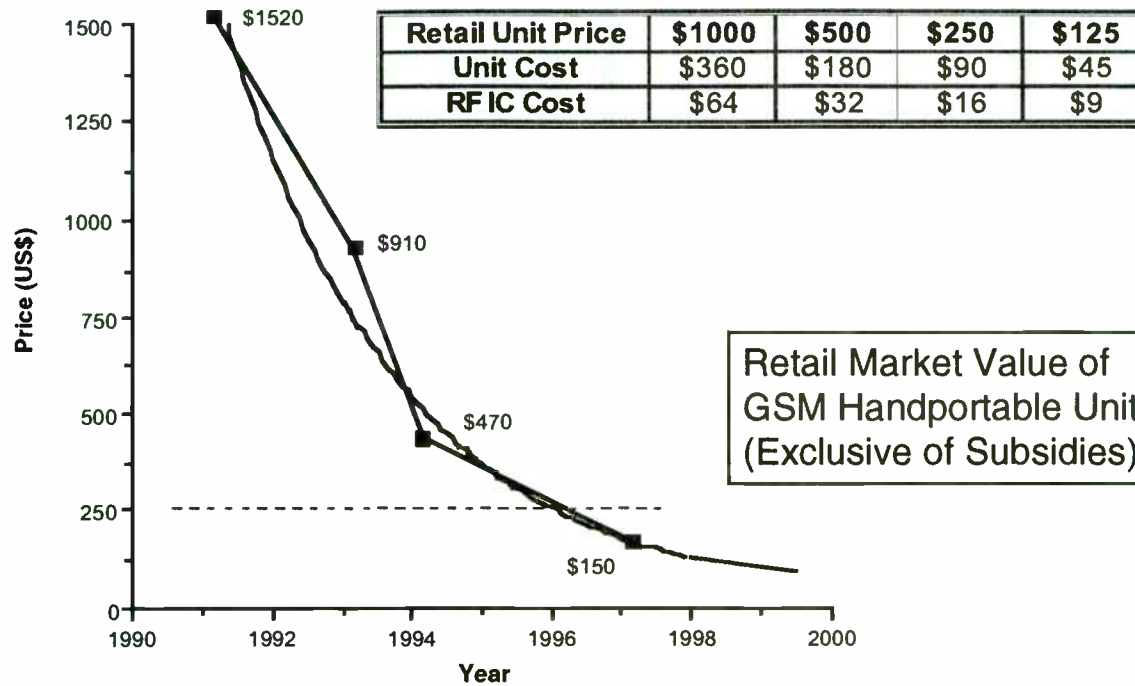
Current Status of Integrated RF Signal Processing

Conclusions

Communications Division
RF Products Group



Value of Integrated RF Signal Processing



Past: RF (discrete) well-understood; Baseband (DSP) was bottleneck.

Now: Baseband is understood, becoming more integrated...

∴ RF signal processing components enter the critical path for system cost and increasing market acceptance => Integration needed

Communications Division
RF Products Group



Outline

Why is Integrating RF Signal Processing Functionality Important?

What Barriers Exist to Achieving Highly Integrated RF Signal Processing?

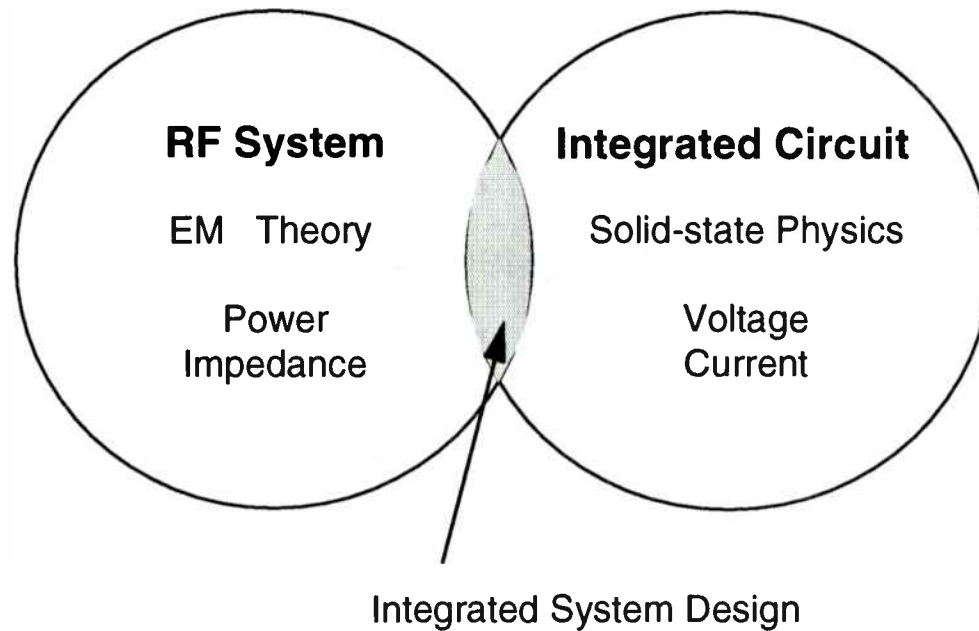
- Circuit/System Design
- Commercial Risk Mitigation
- Manufacturing Technologies

Current Status of Integrated RF Signal Processing

Conclusions

Key Issues in Integrated RF Signal Processing

Circuit/System Design Capabilities - Two Different Worlds...



- The “Reference Design” Fallacy: “An RF Signal Processing System designed for Discrete Implementation is not significantly different from the same system designed for Integrated Implementation”

Integrated Vs. Discrete RF Signal Processing Design

Underlying Theory Differs - Solid State vs. Electromagnetics

Emphasis on System Architecture - less on Circuit Design

- Minimize Performance Requirements of Channelization Filters
- Use Integrated Signal Processing (eg. RF/IF Image-Reject Mixers, PLL Demodulation)
- Integration “devalues” the RF transistor

Emphasis on Product Manufacturing Technology

- Proper mix of device (HEMT, HBT, BJT) and manufacturing (Si, SiGe, GaAs) technologies is critical for success
 - Optimum combination of signal processing function and manufacturing technology

Lack of Well-Defined Impedances

- Leads to Voltage/Current orientation

Non-Traditional Circuit Structures affect System Architecture

- Fully Differential Signal Path
- Filters, Mixers with Gain
- New Sources of Performance-Dominating Noise

Commercial Issues -- Integrated RF Signal Processing

Equipment Manufacturers

- Time-to-Market: Highly integrated RF ICs have relatively long development cycles (cf. discrete designs)
- Cost: Fiercely competitive consumer market
- Exclusivity/Sole-Source: RF ASICs, ASSPs contain intellectual property, dependent upon one supplier

Semiconductor Manufacturers

- RF is an Enabling Technology -- leading equipment manufacturers do not want to use the same RF as their competitors
- Exclusivity: Custom designs rely on the market success of one equipment manufacturer -- market risk for semiconductor supplier is high
- Requires significant initial investment (process modeling, characterization equipment, state-of-the-art simulation tools, ongoing process development)

Equipment and Semiconductor Manufacturers must share Technology, Intellectual Property, Commercial Risks as well as Rewards

- Avoid technology discontinuities which limit performance, increase cost (Computer industry "x86/OS" model)

Manufacturing Technologies -- Silicon

Until late 1980s, Silicon Technology lagged behind RF industry

- Lack of bandwidth dictated insufficient dynamic range, power consumption performance
- Most processes suitable for RF were prohibitively expensive
- Insufficient momentum towards RF from “high-speed analog” manufacturers

New Process Developments Worldwide Establish Silicon as Current, Future Technology for integration of RF Signal Processing

- More than 10 Si BJT IC processes with $f_T > 20$ GHz, $f_{max} > 25$ GHz are commercially available today
- Experiments with SiGe HBTs are ready for commercial introduction in 1995
Results in increased device BW, increased efficiency in power amplifier performance
- Continual advancements in BiCMOS technology facilitate increases in efficiency of integrated RF signal processing
Combination of SiGe, 0.5 μ CMOS into a single process

Manufacturing Technologies -- GaAs

Limited Potential for Functional Integration

- $f-1$ Noise of GaAs MESFET Limits Usefulness
- Small (expensive) wafers with relatively low (~35-50%) defect yields
- Application Limited to >100 mW Power Amp, RF Switch
- Significant Levels of Integrated Functionality are beyond capabilities of existing GaAs-based processes

“But what about the ‘0.5 dB LNA’?”

- Who needs it ?
- Performance of most Cellular/PCS communications systems (i.e. GSM, DECT, IS-95, IS-54, etc.) is limited by dynamic range, not sensitivity
- 1.7-2.0 dB NF/15 dB Gain LNA is sufficient

Satellite Communications Systems (eg. Inmarsat, Iridium) are exceptions due to the nature of their signal environment; however, migration of terrestrial wireless communications systems to the 2 GHz range increases the need for dynamic range performance in satellite-based systems

Outline

Why is Integrating RF Signal Processing Functionality Important?

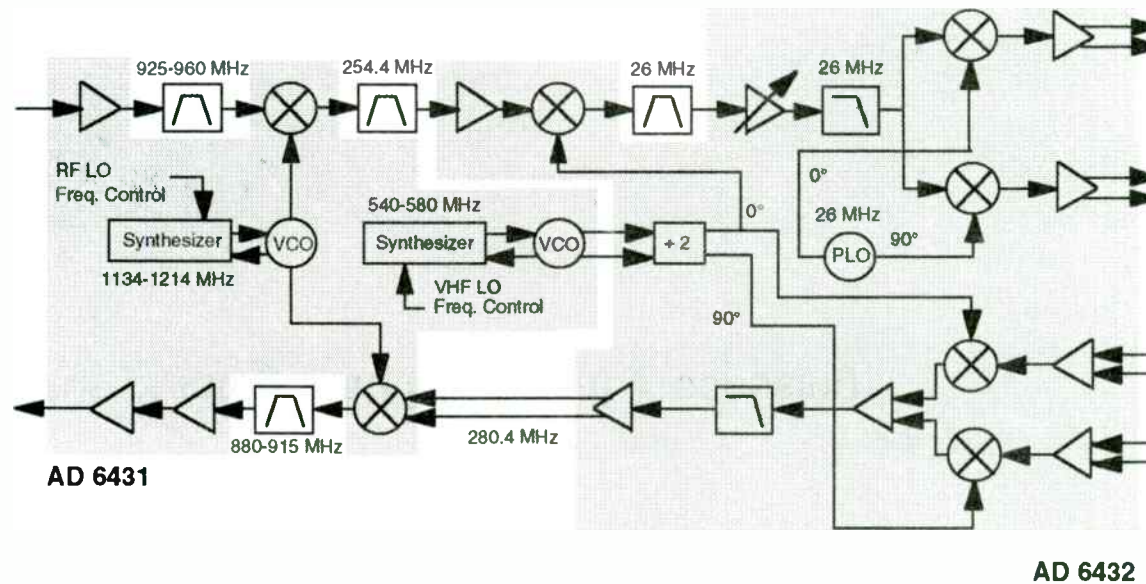
What Barriers Exist to Achieving Highly Integrated RF Signal Processing?

- Circuit/System Design
- Commercial Risk Mitigation
- Manufacturing Technologies

Current Status of Integrated RF Signal Processing

Conclusions

Example of Integrated RF Signal Processing



ADI GSM Transceiver

- 25 GHz NPN technology for RF
5 GHz complementary technology for IF
- Cost, size, power consumption represent quantum improvements
- Combines US\$35 of discrete RF functionality into a 2-chip set - US\$20
- Paired with ADI GSM Baseband chipset, AD6431/2 enables entry to GSM market for consumer electronics manufacturers without substantial RF skills

Outline

Why is Integrating RF Signal Processing Functionality Important?

What Barriers Exist to Achieving Highly Integrated RF Signal Processing?

- Circuit/System Design
- Commercial Risk Mitigation
- Manufacturing Technologies

Current Status of Integrated RF Signal Processing

Conclusions

Communications Division
RF Products Group



Conclusions

Integration is essential

- But Requires New Skills, Design Approaches (“Two Domains”)
- Merging Bipolar and CMOS is inevitable
- Silicon is here now, SiGe coming, GaAs is waning

Co-Operation needed

- Both Handset Manufacturers & IC Suppliers *must* work together - reduce risk to both
 - Handset manufacturer needs time-to-market, cost
 - IC vendor needs volume
 - Integration, joint design crucial

Integrated RF Products Enable Affordable PCS Terminals

- The sub-US\$250 PCS terminal requires RF signal processing for <US\$15

Digital Radios and Next Generation Receivers for Base Stations

Scott V. Behrhorst
Analog Devices, Inc.
Communications Division
7910 Triad Center Drive
Greensboro, NC 27409

Traditionally, base station designs been related to portables - both must implement the same air interface and protocol after all. This approach relied on the similarity in transceivers, using common architectures and components to get somewhat of a "free ride", as technology developed for handsets applied directly to base stations. In principle, the volume and competitive nature of consumer products should drive price targets for base stations. A completely different outlook is to contend that cellular "chip-sets" will not solve the problems unique to base stations; instead, the concentration of multiple channels for increased capacity drives new designs. Fueling this discussion is the knowledge that cellular base stations must reduce in size and cost for the personal communications infrastructure to become a reality.

A parallel development is the proliferation of standards (the arrival of NAMPS, two digital cellular standards, up to seven PCS protocols...). New design approaches promise the opportunity to develop a base station that is flexible, as well as compact. A transceiver that could be "programmed" to accommodate analog, TDMA, CDMA, or a combination, would allow operators to redistribute capacity from one standard to another, with little if any hardware changes. Integrated circuit (IC) manufacturers are now providing the technology necessary to make such "universal" base stations a realistic alternative. Clearly there are many ideas about what "universal" means, however. Wideband converters, programmable DSP, "smart antenna", linear PAs, the list of enabling technologies is long and fascinating.

This paper examines multiple architectures and relates some applicable IC technologies to each design. The technologies discussed in this paper will also apply to other digital transceiver designs, such as satellite terminals, digital modems, and wireless LANs.

Traditional Digital Base Station

Figure 1 is a simplified block diagram of a traditional digital base station transceiver. The variable frequency synthesizer selects one narrowband channel from an operating range that typically spans many megahertz. For European digital cellular systems based on the GSM standard, the channel width is 200 kHz, and the total operating band ranges from 25 MHz (standard GSM) to 75 MHz (DCS1800). U.S. analog cellular and the IS-54 dual standard both operate with 30 kHz channels within a 25 MHz band.

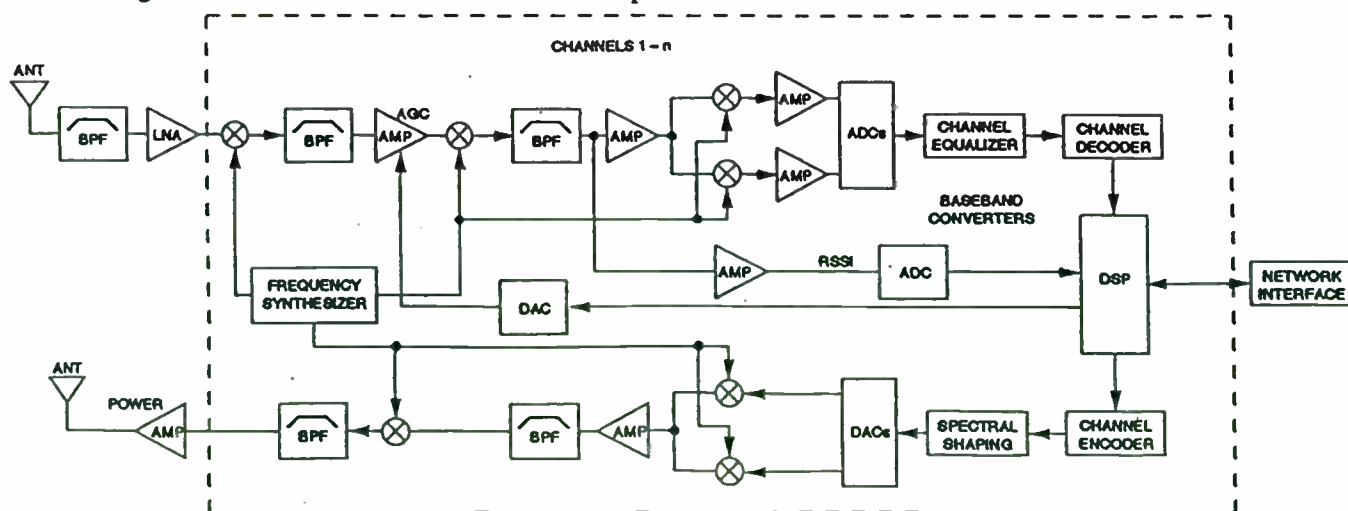


Figure 1. Traditional Digital Basestation Architecture

The design of the frequency synthesizer for base stations can be quite complex. For example, using conventional PLL design, first generation GSM stations normally use two synthesizers in parallel to drive the LO input of the receive RF mixer: while one synthesizer selects the current channel, the second pre-tunes to the next channel. This "ping-ponging" of synthesizers compensates for each tuner's long loop settling time. Besides the additional complexity, dual-synthesizer multi-loop designs take up a lot of valuable board space.

One way designers are reducing complexity in the synthesizer section is by using available direct digital synthesis (DDS) technology (Fig. 2). Direct digital synthesizers derive fine frequency resolution and accuracy using digital techniques: an external clock drives a phase accumulator/sine-ROM combination. A digital-to-analog converter then converts the digital sinewave to the analog domain. Although most DDS's do not output the desired frequency directly (i.e. 900 MHz), when used as part of an indirect method, a fast switching synthesizer can be realized for frequencies in both cellular and cordless bands. For example, the AD9955 32-bit CMOS DDS combined with an AD9721 10-bit DAC offers a wide-band solution which can tune over 30 MHz. This DDS/DAC combination lends itself to an "offset PLL" configuration which could select channels in the 900 MHz range (i.e. 824 to 849 MHz for NADC systems). A highly integrated DDS/DAC solution is the AD7008, which is well-suited for tuning over narrow bands; this monolithic contains the digital sinewave generator plus a 10-bit digital-to-analog converter in one 44-pin PLCC package.

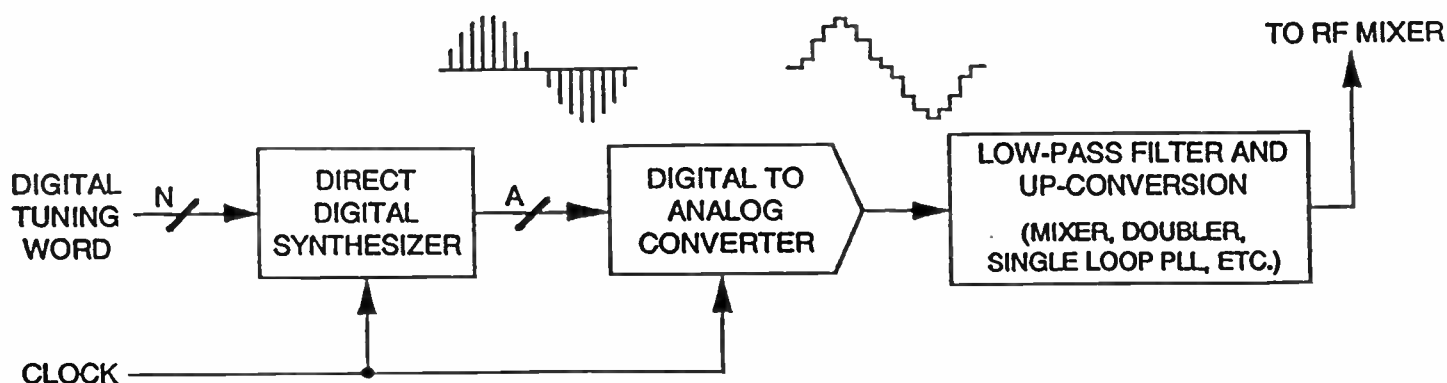


Figure 2. DDS-Based Local Oscillator

Receivers must be able to accurately recover "weak" signals as well as "strong" signals. For the single channel architecture, a variable gain amplifier (VGA) provides automatic gain control (AGC) to boost weak signals and attenuate large signals; a Received Signal Strength Indicator (RSSI) signal ultimately feeds back to the gain adjust on the VGA. The feedback path shown in Figure 1 works fine for some applications. However, failure to adjust gain quickly can result in saturation of subsequent processing stages, and designers are sometimes forced to implement fast, dedicated logic to complete the AGC loop.

In the traditional architecture the final intermediate frequency (IF) is processed by an analog quadrature demodulator. This circuit separates in-phase and quadrature (I and Q) signals and down-converts each to baseband. The demodulator must match amplitude and phase of the I and Q signals which becomes difficult as higher order modulation schemes are used. IC manufacturers are reducing the complexity of IF processing by integrating mixers, gain control, amplifiers, and RSSI functions. The AD607 RF/IF subsystem is a good example; this chip accepts differential RF input signals up to 300 MHz and outputs in-phase and quadrature baseband signals.

Baseband ADCs and subsequent digital processing complete the received signal path. Baseband I/O ports such as the AD70XX family integrate much of the baseband processing such as a-d and d-a conversion, pulse shaping, digital filtering and programmable gain. In some instances these parts include uncommitted DACs for auxiliary functions in the system. For example, the new AD7015 integrates both voiceband and baseband CODECs, together with a GMSK modulator, four auxiliary multiplexed converters and interfaces, all into a single compact monolithic device. Products like this, although designed for GSM "mobile" phones, will also be useful to reduce size, complexity and cost of GSM base stations.

The Undersampling Narrowband Receiver

An alternative architecture for the receive section of a base station transceiver is shown in Figure 3. In this case, a single ADC and DSP replace the analog demodulator: mixers, amplifiers, and matched filters.

An IF signal is applied directly to the input of a wide bandwidth ADC; the ADC's internal sample-and-hold amplifier acts as a mixer or downconverter, while the DSP performs I and Q separation in the digital domain. This approach can yield an improvement in overall signal-to-noise ratio by eliminating a complete stage of analog mixing, filtering, and amplification. Also, by employing DSP, the ADC sampling rate can be shifted to tune the exact position of the signal within the baseband. Positioning the signal so that it does not extend all the way to 0 Hz reduces the effect of $1/f$ noise on the detected information. This architecture is made possible by the concept of undersampling or *IF sampling*.

Sampling theory states that to recover a signal of bandwidth B, the sample rate of the digitizer or ADC must be greater than or equal to $2B$. A baseband signal from dc to 456 kHz thus requires a sample rate of at least 912 kSPS (2×456) to avoid losing information. In this instance, a 1 MSPS ADC would satisfy the "Nyquist criterion", $f_s \geq 2B$. The consequence of sampling at less than the $2B$ rate is "aliasing". Sampling a 900 kHz sinewave at 1 MSPS generates the same digital data as sampling a 100 kHz (i.e., $1 \text{ MHz} - 900 \text{ kHz} = 100 \text{ kHz}$) sinewave at 1 MSPS. Stated another way, the ADC cannot distinguish between a 100 kHz sine wave and a 900 kHz sinewave at a 1 MSPS digitization rate. Therefore the analog-to-digital conversion process can introduce errors into the digital data by digitizing frequencies too high for the sample interval. These out-of-band frequencies are translated in-band by the sampling process and corrupt the amplitudes of the desired frequency components.

IF sampling, also called bandpass sampling, is the digitization of a *bandlimited* spectrum whose frequency components are higher than the sample clock rate. IF sampling is possible because ADC sample rates do not have to be greater than a signal's *highest frequency component* to satisfy the Nyquist criterion. The sample rate does have to be greater than twice the signal's *bandwidth*, however. For example, the 1 MSPS ADC sampling a 456 kHz signal described above, can theoretically recover the information even if the signal is centered at 10.7 MHz, provided that the signal is bandlimited to $< 500 \text{ kHz}$. In receivers, the bandpass filter which follows the IF mixer is used to bandlimit the IF to less than one half the ADC

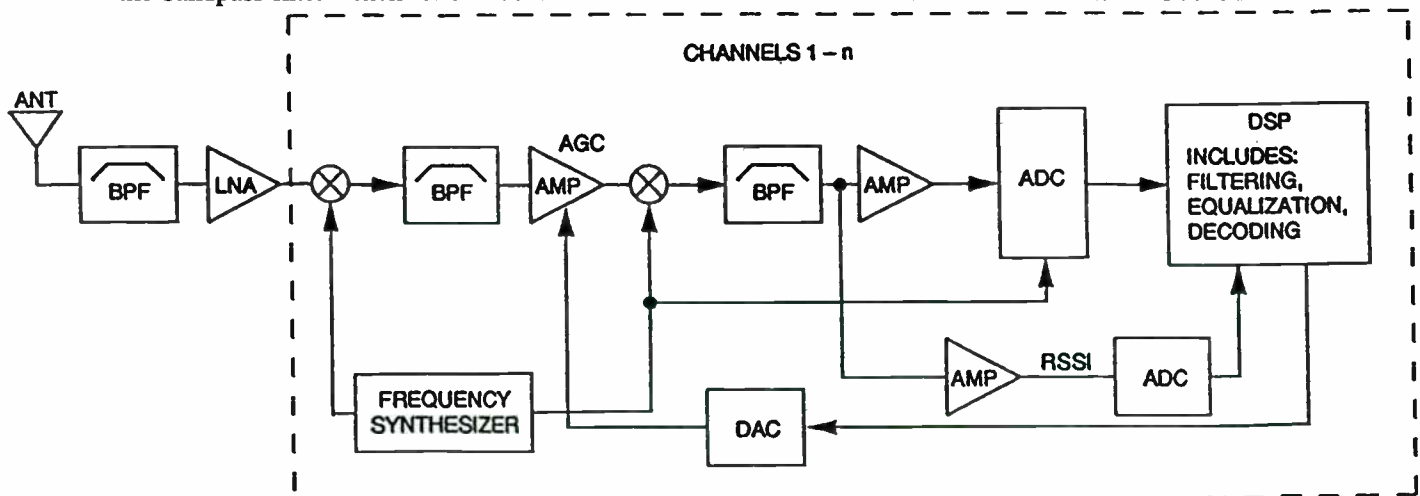


Figure 3. Undersampling Narrowband Receiver Architecture

sample rate. Aliasing can still occur with IF sampling even if the IF spectrum is bandlimited to less than half the sample rate. To avoid aliasing, the sample rate must be properly chosen by comparing the highest frequency component in the signal to the signal's bandwidth. This rate will never be more than four times the signal's bandwidth. Figure 4 shows how an IF signal in the 6 to 7 MHz band is translated to the dc to 1 MHz band by the undersampling technique.

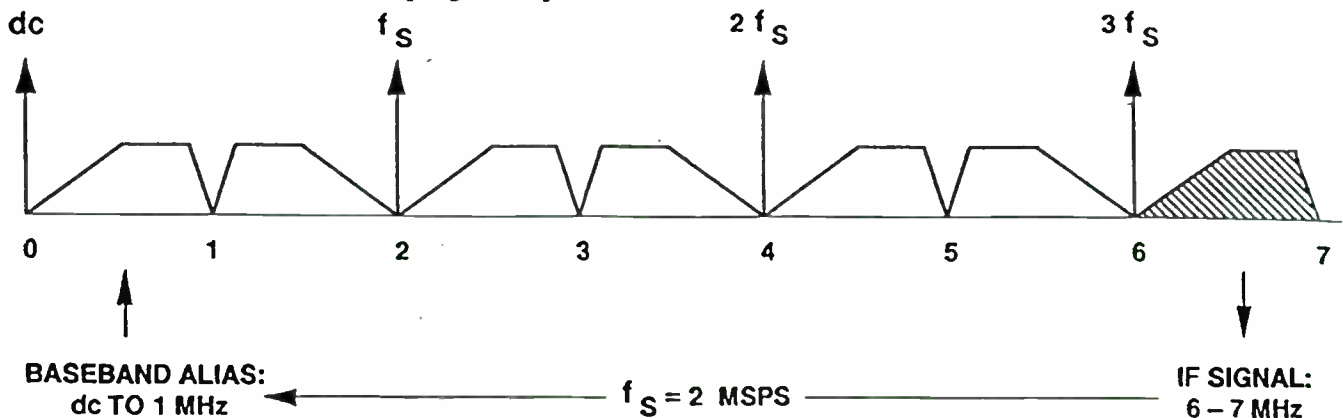


Figure 4. Intermediate Frequency (IF) Between 6 and 7 MHz is Aliased Between dc and 1 MHz by Sampling at 2 MSPS

An obvious consequence of the IF sampling approach is the added burden placed on the ADC input bandwidth. The ADC must now be able to digitize signals accurately outside a dc-to- $f_s/2$ Nyquist bandwidth. Special techniques and new IC processes are available which can extend the dynamic range of ADCs to intermediate frequencies. An important specification for such a system is spurious-free dynamic range, or SFDR. SFDR is defined as the difference in signal strength (i.e. power) between the signal of interest and any other in-band signal. Because harmonics almost always limit SFDR, ADC manufacturers often specify *worst-case harmonic distortion* to indicate SFDR. For many base station designs, it is desirable to maintain SFDR of 60 - 90 dB at the IF frequency. Unfortunately, this requirement cannot be met with standard Nyquist-sampling ADCs due to degradations which occur at high input frequencies.

An external wide-bandwidth, low distortion sample-and-hold amplifier (SHA) such as the AD9100, can be used to extend the dynamic range of the ADC at the higher input frequencies. In this configuration, the timing of the SHA clock relative to the ADC clock must be optimized. Ideally, the SHA would acquire a point on the input signal instantaneously, allowing a full sample period for track-to-hold transients to settle. In reality, after a hold-to-track command, the SHA needs "acquisition time" to reacquire the analog input to the desired accuracy. For the AD9100, 20 ns allows the device to acquire a new sample to .01 % accuracy. Performance is optimized by not clocking the ADC until just before the SHA goes back into track mode. This clocking scheme maximizes the amount of time allotted for the SHA output to settle to a steady-state value.

When selecting a SHA for IF sampling applications, make sure to check specifications for hold mode dynamics. Specifically, what is the signal distortion in the hold mode when the SHA is operating dynamically (i.e. switching back and forth between track and hold)? Characterization of the AD9100 at 10 MSPS clock reveals that for input levels of 2 V p-p, the SFDR rolls off quickly for input signals above 20 MHz. Lowering the signal amplitude to 200 mV p-p however, allows the SHA to maintain 70 dB SFDR for a 70 MHz input signal. Since the AD9022 (12-bit, 20 MSPS ADC) has a fullscale input range of 2 V p-p, an amplifier with gain = 10 placed after the AD9100 will preserve the overall dynamic range. This post amplifier should feature fast settling and low noise, as this stage could potentially lower the overall system signal-to-noise ratio. Characterization of the overall system helps the receiver designer make a tradeoff between the SHA input level, which affects SFDR, and the post amplifier gain, which affects SNR. To simplify this trade-off, the AD9101 "sampling amplifier" integrates a wide-bandwidth track-and-hold with a gain-of-four post amplifier.

The Universal Base Station

Personal Communications Services (PCS) is intended to be a competitive marketplace in the United States, as evidenced by the FCC's strategy to open up smaller chunks of spectrum to numerous potential operators. Combine multiple operators with the fact the PCS sites will output less power than cellular, and the result will be large numbers of PCS sites serving each metropolitan area. A PCS scenario was developed for Atlanta, GA which concluded that one operator would need over 2000 sites to provide complete coverage. Multiple PCS operators competing with cellular and enhanced specialized mobile radio (ESMR) services could result in many thousands of fixed base stations in one city. Scenarios like this will encourage operators to make the most of whatever fixed station sites they are able to secure for their infrastructure. Base stations that can easily accommodate multiple standards while maintaining small size will be highly sought after.

Wideband ADCs

Figure 5 illustrates one concept for a common hardware or "universal" base station. This architecture is a multi-channel transceiver design, in which one wideband ADC digitizes multiple channels in the receive path, and one wideband DAC converts multiple channels on the transmit side. Individual channel selection, down conversion to baseband, and filtering is done in the digital domain for receive. Likewise, modulation, carrier multiplexing and summation is done digitally for transmission. Narrowband channel characteristics such as bandwidth, passband ripple, and adjacent channel rejection, can be controlled with changes to digital device parameters (i.e filter coefficients). Such flexibility is not possible when narrowband analog filters are in the receive and transmit paths as in the previous two architectures.

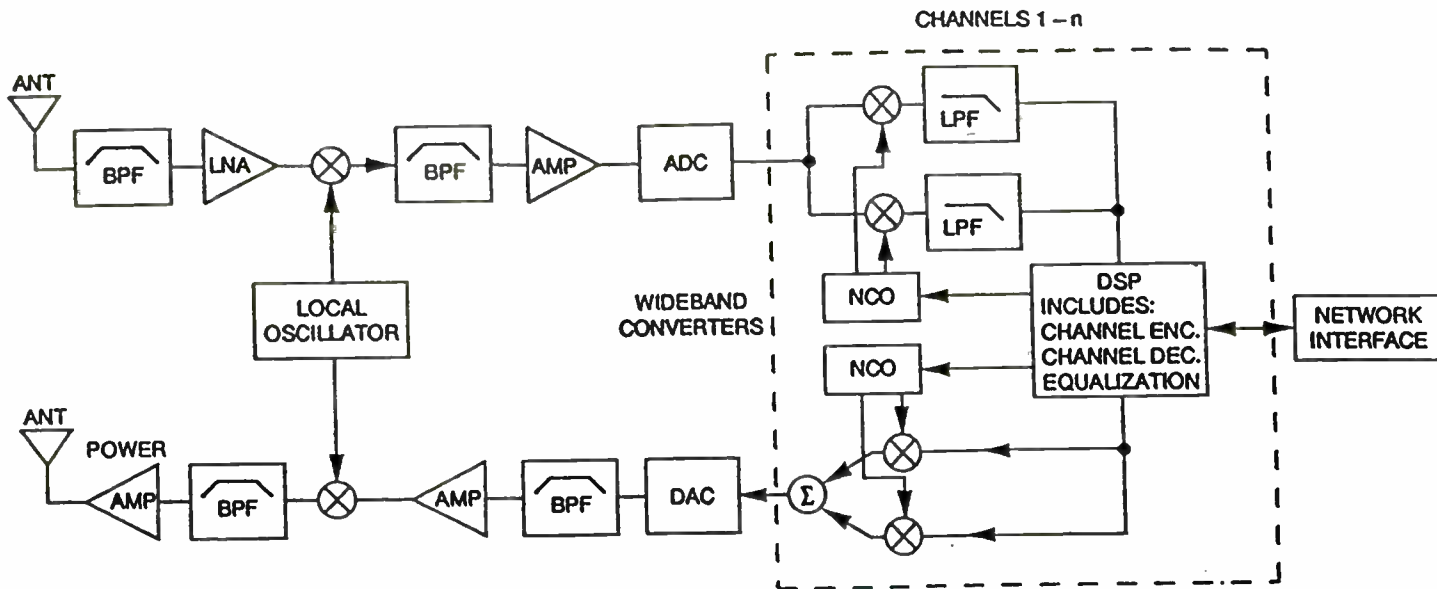


Figure 5. Universal Base Station Architecture

Figure 6 illustrates the kind of input spectrum an ADC must digitize in a multi-channel design. The spectral lines represent narrow-band signal inputs from a variety of signal sources at different received power levels. Signal "C" could represent a transmitter located relatively far away from the signal sources "A" and "B". However, the receiver must recover all of the signals with equal clarity. This requires that distortion from the front-end RF and IF signal processing components, including the ADC, not exceed the minimum acceptable level required to demodulate the weakest signal of interest. Clearly, third order intermodulation distortion products generated by "A" and "B" ($2 \times B - A$) will distort signal "C" if the nonlinearities in the front-end are severe. Strong out-of-band signals can also introduce distortion; signal "D" in Figure 6 shows a large signal that is partially attenuated by the filter. In many systems the power level of the individual transmitters is under control of the base station; this capability helps to reduce the total dynamic range required.

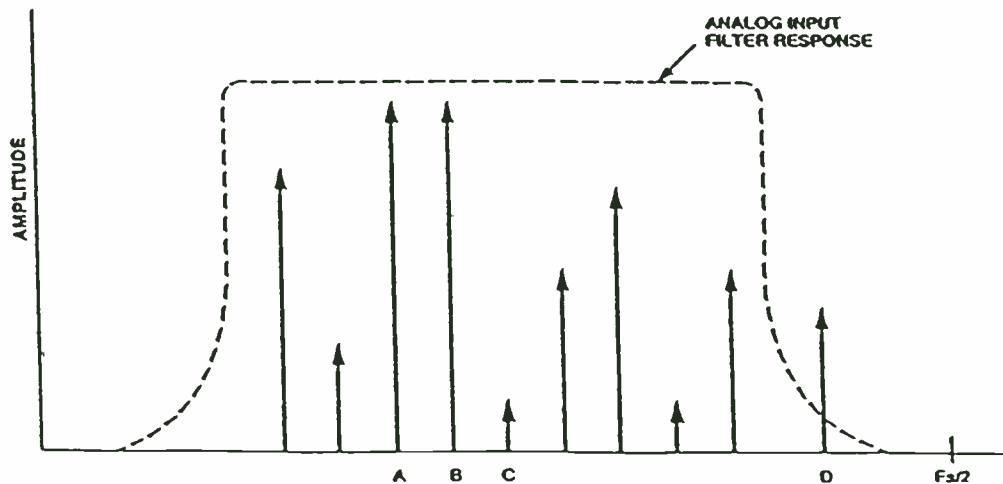


Figure 6. ADC Analog Input Spectrum

The sample rate required must cover the entire band of interest, and with resolution adequate for the channel. One 'magic number' is 30.72 MSPS - allowing 1024 samples of a 30 kHz channel (as used in AMPS). Other standards require different rates (eg 38.88 MSPS for IS-54, 39 or 52 MSPS for GSM); these fast sample rates result in processing gain on individual RF channels (27 dB increase in SNR for the AMPS example above) .

The "universal" architecture has not been widely applied because suitable data converters have not been available. Historically ADCs designed for multi-carrier environments were board level or hybrid designs, developed for military and radar applications. These converters were typically expensive and power hungry, neither trait desirable for cost-conscious commercial designs.

This is changing; last year Analog Devices released the AD9027, a 31MSPS 12-bit converter with the SFDR and IMD required for digital receiver applications. Later this year, its successor, the AD9042 will be released. This is a 12 Bit A/D converter that provides 80dB SFDR for a 20MHz analog input at 41 MSPS while dissipating only 575mW. It is based around a two step architecture (coarse-fine) and a novel "Magamp" design. This reduces pipeline delay, and allows precise matching to reduce distortion.

Crucially, these devices are designed and tested using multi-tone signals, representative of the 'wideband' environment. (Traditionally ADCs were only characterised using one-tone tests, two tone at the most. Some of the testing required for the wideband approach use a deliberately 'nasty' 48 tone-composite signal).

Figure 7 shows an FFT plot of AD9042 performance for a fullscale 18.4 MHz analog input at a 50 MSPS encode rate. The total RMS thermal noise is 0.33 LSB's; this results in only a 2dB loss in SNR with respect to an ideal ADC. SFDR on this device is > 80 dBc which represents a 6-7 dB improvement over the recently released AD9027.

If the distortion introduced by the ADC is deemed too large, some system design techniques may be applied to decrease the amplitude of converter non-linearities. Dithering is one technique of improving the SFDR of an ADC at the expense of SNR. When noise is added to the input signal, non-linearities are "smeared" across the transfer function of the ADC. In the frequency domain, the average energy of spurious signals is reduced while the SNR is degraded. The additive noise reduces the total dynamic range available, since the peak signal which can be applied without clipping the ADC is now reduced. A refinement is often referred to as subtractive dithering. In this technique, the input noise source is generated by a DAC and the same value is then subtracted from the digital output. This method subtracts out the added noise, resulting in the same SNR as the undithered ADC. However, peak dynamic range is still reduced by the amount of noise added.

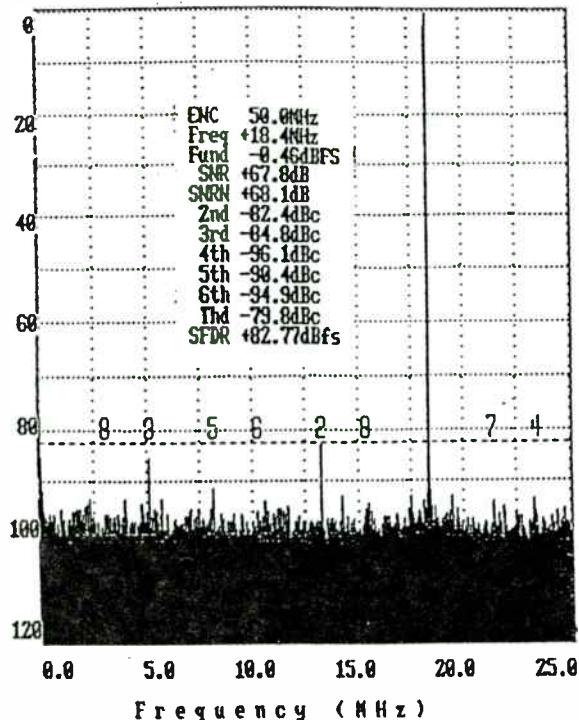


Figure 7. AD9042, 12-bit ADC Clocked at 50 MSPS

Wideband DACs

The "universal" base station of Figure 5 also requires wideband digital-to-analog converters. Because the base station designer has more control over the signals being transmitted, the dynamic range requirements on the DAC tend to be lower than for the ADC. Still, DAC non-linearities will degrade the purity of the wideband spectrum to be transmitted, and DAC selection criteria must be established.

The DAC output spectrum contains images of the fundamental frequencies about integer multiples of the sample clock, f_c . To visualize this, consider a synthesizer clocked at 51 MHz, generating a signal centered at 19 MHz. A look at this spectrum reveals components at 19 MHz (f_0), 32 MHz ($f_c - f_0$), 70 MHz ($f_c + f_0$), 83 MHz ($2f_c - f_0$)... The amplitudes of these components are weighted by the $\sin(\pi f/f_c)/(\pi f/f_c)$ function. A few observations can be made about the DAC output spectrum. First, lowpass filtering at one half of the clock rate, $f_c/2$, will attenuate the higher order images. Frequencies close to $f_c/2$ generate images, $f_c - f_0$, that are difficult to filter. For this reason, most system designers elect to limit operation to less than 40 percent of the clock rate. Second, even the "in-band" frequencies, those less than $f_c/2$, will be attenuated by the $\sin x/x$ function. Filters with an inverse $\sin x/x$ response can be used to "re-weight" the spectrum thus achieving constant amplitude channels over the nyquist band. This $\sin x/x$ correction may be accomplished in the digital domain prior to sending data to the DAC, or an analog filter may be implemented after the DAC.

Now that an ideal DAC output spectrum has been discussed, how should a designer select a DAC suitable for multi-channel transceiver applications? First, start by examining the DAC's static specifications such as differential and integral nonlinearity (DNL and INL). DNL errors affect noise; INL errors affect distortion. Most N-bit converters are specified to have less than 1 LSB of static error (1 LSB = Fullscale* 2^{-N}). A 10-bit DAC has a theoretical signal-to-noise ratio (SNR) of 62 dB (SNR is the ratio of RMS signal to RMS noise). DNL errors greater than 0.5 LSB will further degrade SNR. Since quantization noise is typically distributed over the entire nyquist band, however, SNR is not the most pertinent specification. Once again, spurious-free dynamic range (SFDR), sometimes called "spectral cleanliness" is actually the most common figure of merit. Whereas SNR compares the signal to the *total noise* in a given bandwidth, SFDR compares the signal to the *next highest frequency component* in a given bandwidth. This component might be a direct harmonic of the fundamental signal, an aliased harmonic, intermodulation products, or some other non-harmonically related spurious signal. A 10-bit DAC can achieve a SFDR of 85 dB if the preceding DDS chip preserves 15-bits of phase accuracy.

Static INL errors affect converter harmonic distortion. Ideally, the transfer function of a DAC is a straight line. Real transfer functions are bowed, S-shaped, have sharp discontinuities at midscale, etc. Fourier analysis can predict the effect of non-ideal transfer functions on harmonics. A large bow will result in a stronger 2nd harmonic; an S-shaped transfer will result in a stronger 3rd harmonic. In any event, realize that the worst-case static INL specified in the manufacturer's datasheet conveys little information in and of itself. A DAC specified at 0.25 LSB INL(max), whose transfer function is a nice smooth bow, may have a worse affect on SFDR than a DAC whose transfer function is jagged, yet is specified at 0.5 LSB INL(max).

Time domain parameters such as settling time, output slew rate, and glitch impulse have traditionally been relied on to predict DAC performance. The ideal DAC has infinite slew, settles in 0 ns, and has no glitch. The AD9721 slews at 1000 V/ μ s, settles to .5 LSB in 4.5 ns, and has a typical glitch impulse of 1.5 pV-s when driving 50 Ω to ground. While good time domain specifications do not guarantee good frequency domain performance, some correlation does exist. First of all, unequal output rise and fall times contribute to 2nd harmonic distortion. Secondly, more important than a worst-case glitch specification is the code-dependent nature of the glitch. Midscale glitches and other code-dependent transient errors will show up as harmonically-related spurs in the frequency domain. DACs which use a segmented architecture generally have less code-dependent glitch compared to traditional R-2R DACs.

DAC manufacturers who characterize and specify their parts for frequency domain performance make the converter selection process a lot easier. Higher order harmonics will be aliased "in-band" by the sampling process. The location of these harmonically-related spurs *can* be predicted. An image of the 3rd harmonic is aliased near the fundamental carrier when f_{out} approaches 1/4 of the clock. At $f_{out} = f_{clock}/4$ the 3rd will actually alias on top of the fundamental. The 2nd harmonic will be aliased close to the fundamental carrier when f_{out} approaches 1/3 of the clock. At $f_{out} = f_{clock}/3$, the aliased 2nd will fall on top of the fundamental.

Looking Ahead

ADC sample rates will continue to increase as evidenced by the AD9042, 12-Bit 41 MSPS ADC from Analog Devices; ADCs designed for communications will extend the usable input bandwidth to common intermediate frequencies. Digital-to-analog converters will soon provide the 75-80 dBc needed for wideband transmitters. BiCMOS and Complimentary Bipolar technologies open the way for both ADCs and DACs to preserve good performance at lower power and cost. By working closely with communications systems designers, component manufacturers can make sure that new technologies such as these, are applied correctly, paving the way for small, low cost, and flexible base stations.

References

Richard G. Lyons, "How Fast Must You Sample?", Test and Measurement World, November, 1988, pp.47-57.

Richard C. Webb, "IF Signal Sampling Improves Receiver Detection Accuracy", Microwaves and RF, March, 1989, pp.99-103.

Joseph F. Garvey and Daniel Babitch, "An Exact Spectral Analysis of a Number Controlled Oscillator Based Synthesizer", IEEE 44th Annual Frequency Control Symposium Digest of Papers, 1990, pp. 511-521, IEEE Publication No. CH2818-3/90/0000-511.

Scott Behrhorst, "Design DDS Systems and Digitize IFs with DACs/ADCs", Microwaves and RF, August, 1993, pp. 111-119.

Chuck Jones, "Is There Really Room for PCS?", Telephony, November 8, 1993, pp. 30-36.

David Duff, "Signal Processing Requirements for Direct IF Sampling Receivers", Proceedings of Wireless Symposium, February, 1994.

A 1.5 Volts / 25 μ A CMOS Microcontroller with Pager Decoder for Alphanumeric and Numeric applications

Rémy PACHE, François BAUDUIN

CSEM, Jaquet-Droz 1, CH-2007 Neuchâtel, Switzerland

ABSTRACT

This paper presents a CMOS low power integrated circuit, which includes a 2400/1200/512 bits/s POCSAG decoder and a 8-bits 6k instructions RISC microcontroller.

The circuit has been designed for highly integrated paging receivers. Along with a RF front-end and a small serial EEPROM it can be used to build a numeric pager. It can store 1K characters, can drive a 12 digits 7-segments LCD display and an external buzzer. It has a bus serial interface, a crystal oscillator and multipurpose inputs/outputs. It can also drive an external display driver for alphanumeric applications.

This device has an operating current consumption of 25 μ A working at 2.7 Volts, thereby facilitating the use of a single and small battery.

It has been designed in a 0.7 μ m CMOS process. The die size is 33 sq. mm.

I. INTRODUCTION

Wide area radio paging, one of the earliest form of one-way mobile data communications, is still a growing market, with a CAGR of 15% over the 1990 - 1996 period for the U.S. market [1]. It is an efficient communication system to alert and to pass on messages to users away from a base. The paging receiver or pager is a radio receiver able to alert

the bearer of an incoming message. In addition to an audible signal, products usually have a numeric or an alphanumeric display. While most of the pagers were 5 x 4 x 1.5 cm in size or larger an important trend appeared with smaller pagers. Among these, the wristwatch pagers which combine an electronic watch and a pager working on a small button-like cell [2] have been successful. They require a small size electronic module, a good radio performance and a low power consumption. In addition they should be low cost since they are targeted towards consumer market.

The most critical part of a pager (Fig. 1) in term of complexity and power consumption is the Radio Frequency (RF) front-end which deliver the data bitstream.

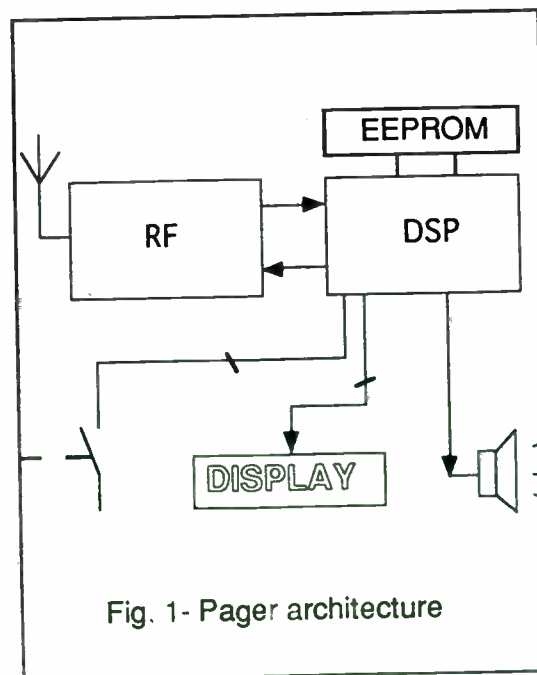


Fig. 1- Pager architecture

The Digital Signal Processing (DSP) unit which converts this data stream into messages and perform the user interface is of great importance too. One of the reasons for this is that most of the time a pager do not receive message, but instead it has to monitor the incoming bit-stream to detect a new message. In the well-known POCSAG paging system [3], a message for a given Radio Identification Code (RIC) can only begin in 2 out of the 17 codewords which form a batch. So the DSP unit can optimise the average power consumption of the RF front-end by turning on and off this unit. A second reason to have a clever design of the DSP unit is that the pager function can be turned off during the night, so the power consumption of the DSP will also influence the battery lifetime.

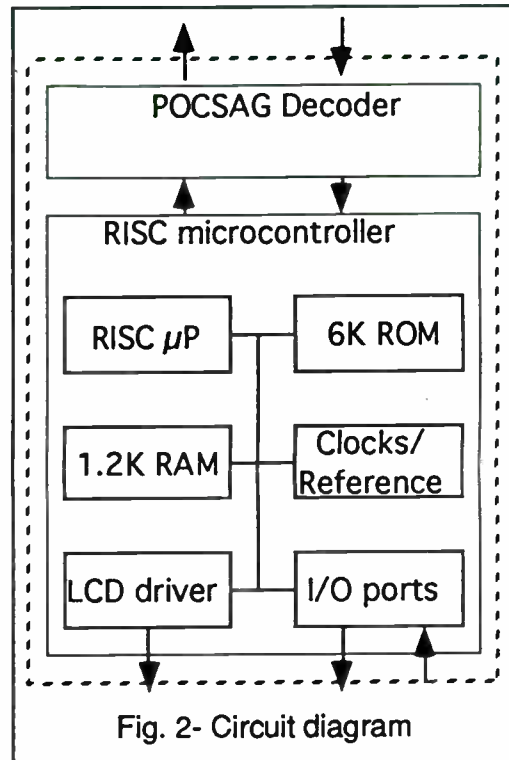
This paper will describe a single chip CMOS low power DSP unit , which has been designed for a wristwatch POCSAG pager. Along with a RF front-end and a small serial EEPROM it can be used to build a numeric pager. It can also drive an external display driver for alphanumeric (text) pagers.

II. CIRCUIT DESCRIPTION

The circuit diagram is described in Fig. 2. It includes a 2400/1200/512 bits/s POCSAG decoder and a 8-bits 6k instructions RISC microcontroller.

The decoder is the first main building block. It performs various functions to process the incoming bitstream and extract messages. Firstly a digital PLL does the bit synchronisation to correctly lock on the 2400-, 1200-, or 512 bits/s data stream. Then the possible transmission errors are detected and corrected with a ROM-based lock-up table. Frame synchronisation is then performed by a specific circuit which has 2 modes of operation. It can either compare

the 32 bits of the received synchronisation word (SCW) [3] with a reference and allow 1 or 2 errors, or compare only a shorter portion of the SCW. The first mode is used when the pager is not frame synchronised, while the second mode is used to verify the status of frame synchronisation and this allow to save power since the RF front-end is turned on for a shorter period of time [4].



Once it is frame-synchronised the decoder wake up periodically the RF front-end to verify if a message is sent to the pager. This is performed by a serial comparator which verify that the address word [3] is equal to the pager RIC, the RIC being stored in the EEPROM circuit of the pager. Finally a serial in - parallel out register send the received characters to the microcontroller part. The decoder can handle 2 RIC, with 4 extension per RIC. In turn, the extension define the type of call - Tone Only, Numeric, or Alphanumeric.

The microcontroller is the second main building block of the circuit. It includes a RISC microprocessor core, a 6k instructions ROM, 1280 bytes of RAM to store messages, a 12 digits 7-segments LCD display driver, a 76.8 kHz crystal oscillator, a voltage reference, and multipurpose input/output ports. These I/O ports are a buzzer driver, a serial bus interface, 2 step motor drivers, 4 bidirectional ports, and 6 inputs for mechanical contacts. The circuit can also drive an external display driver for alphanumeric applications.

The micropower microprocessor has been designed for battery operated devices such as watches, pager receivers or other man-machine interface [5]. A minimum power consumption has to be reached while maintaining a reasonable speed. A characteristic of these applications is that functions are, in general, not continuously executed. Therefore the processor is event driven, i. e. a task is started by an external event. Upon completion of the task, the processor goes in sleep-mode and awaits for the next task. The implemented microprocessor is a multi-task architecture, i.e. up to four separate tasks can be handled by a hardware scheduler in a pseudo-parallel way [6]. Context switching does not need additional instructions. The basic architecture is a 8-bit RISC processor executing a one word instruction per cycle of 4 clock periods. Due to the reduced number of clock periods that are necessary to execute a task, one contributes to a power consumption reduction.

The circuit can be supplied between 1.5 and 3.6 Volts. To minimise the total power consumption the logic part is supplied at a reduced voltage. The maximum operating current consumption of the circuit, which is the consumption when the pager is turned on and the microprocessor is

continuously running, is 30 μ A working at 2.7 Volts. This value is rather pessimistic since the activity of the microcontroller is rarely 100 percent. In normal condition we expect the average current consumption to vary between 15 and 25 μ A, thereby facilitating the use of a single and small battery.

The circuit has 84 I/O pads and requires only 12 external components: a 78.6 kHz crystal, 7 capacitors, a resistor, a NPN transistor, a coil and a buzzer in addition to an LCD display. It has been designed in a 0.7 μ m CMOS process and has 134'000 transistors excluding 150'000 bits of ROM. The die size is 30 sq. mm.

III. CELL LIBRARY

In order to minimise the power consumption at the cell level, the logic style of the standard cell library which has been used for this design is the static branch-based style [7, 8, 9]. This library is characterized by the following features :

- branch-based schematics. The logic cells are designed exclusively with branches. In such cells, branches are made of transistors in series (limited to 3 MOS) connected between a power line and a gate output.

- complex gate decomposition. The number of MOS in series in a branch is limited to 3. For higher number of inputs gates are decomposed into several simple gates. It can be shown that the delay, for instance, of a 2N-input gate is larger than the total delay of two N-input gates and one inverter in series. In the latter case, less parasitic capacitances are switched from the input to the output.

- layout regularity. As branch-based logic is very regular, the layout design is also regular, resulting in the

minimization of the source/drain parasitic capacitances.

- no transmission gate. An inverter followed by a transmission gate can be replaced advantageously by a tristate gate.

- race-free and delay independent flip-flops. Critical races are due to badly controlled delays that may bring the circuit into a different stable state than desired [10]. Race-free flip-flops have therefore been designed to obtain delay-independent library cells. The method [10] provides sequential cell structures in which each input or internal variable can produce the transition of at most one next internal variable (minimal activity). Such cells are therefore race-free and delay-independent structures and very suitable for a low voltage cell library.

IV. CONCLUSIONS

In addition to state-of-the-art RF front-end and small EEPROM circuit, the development of small size wristwatch pagers requires a low power, high integration digital signal processing unit.

With only 12 external components the circuit which has been presented perform all the necessary baseband signal processing and user interface functions for a POCSAG pager. Its maximum operating current consumption is 30 μ A @ 2.7 Volts and its specific decoder allows a low average current consumption of the RF front-end.

References

[1] T.H. Murtha, *MobileCom 92*, Frost & Sullivan, New York, NY, 1992, pp. 91-103.

[2] P.A. Meister, "Swatch Pager", *Proceedings of the "4ème Congrès*

Européen de Chronométrie", 1992, pp. 155-158

[3] CCIR, *The Book of the CCIR Radiopaging Code Nr. 1 - CCIR 584*, Radiopaging Code Standard Group, 1986.

[4] R. Pache, "Récepteur d'appel local à faible consommation d'énergie", patent application CH 01 718/92-7, 1992.

[5] J.F. Perotto et al, "A 8-bits Multitask Micropower RISC Core", *IEE JSSC*, Vol.29, no. 8, August 1994, pp. 986-991

[6] J.F. Perotto et al, "Multitask Micropower CMOS Microprocessor", *ESSCIRC '93*, September 21-23, 1993, Sevilla, Spain

[7] J-M. Masgonty et al, "Technology- and Power-Supply-Independent Cell Library", *IEEE CICC'91*, May 12-15, 1991, San Diego, CA, USA, Conf. 25.5

[8] J-M. Masgonty et al, "Branch-Based Digital Cell Libraries", *EURO-ASIC'91*, 27-30 Mai 1991, Paris.

[9] C. Pigué et al, "Low Power Low Voltage Digital CMOS Cell Design", *Proceeding of PATMOS '94*, Barcelona, Spain, October 1994, pp. 132-139

[10] C. Pigué, "Logic Synthesis of Race-Free Asynchronous CMOS Circuits", *IEEE JSSC-26*, No 3, March 1991, pp. 271-380

Designing the Virtual Battery

Raymond W. Waugh
Hewlett-Packard Company
Communications Components Division
39201 Cherry Street
Newark, California 94560
510-505-5773
ray_waugh@hp0100.desk.hp.com

Abstract -- Many of today's portable RF products, such as RF/ID tags used in automotive electronic toll tag applications, are too small to contain a battery sufficient to power them over their expected lifetime. Where such devices operate in the presence of a RF field, a simple and inexpensive circuit consisting of an antenna, one or more Schottky diodes, and a few passive components can be designed to convert part of the illuminating RF field into DC power. This paper will present design techniques and illustrate them with data obtained on prototype circuits.

I. INTRODUCTION

The term "virtual battery" [1] has been coined to describe a simple, compact and low cost replacement for a battery in RF tags and other portable applications where three design considerations apply:

The RF application to be powered is very small and portable.

The design lifetime of the application is long.

The application does not require primary power in the absence of an illuminating RF field.

A good example of such an application is the modulated backscatter type of RF/ID tag [2], which operates only when passing through a highway toll booth and which is expected to last five years or more without service. The interrogator in the toll booth includes a 915 MHz transmitter which illuminates the tag with a relatively robust RF field, providing a source of energy to be converted by the virtual battery. As shown in the section below, such virtual batteries consist of an antenna, one or two Schottky diodes and one or more inexpensive passive components.

Such a circuit is a variation on the ordinary video detector [3],[4]. Design considerations are presented and test data are provided for a practical circuit.

II. SCHOTTKY DETECTOR CIRCUITS

The Schottky diode can be represented by a linear equivalent circuit, as shown in Figure 1.

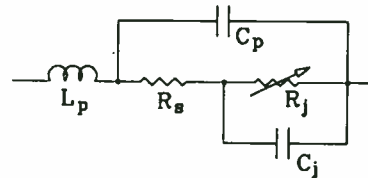


Figure 1: Equivalent circuit of a Schottky diode

C_j is the parasitic junction capacitance of the Schottky chip and R_s is parasitic series resistance of the chip. L_p and C_p are package parasitics. R_j is the junction resistance of the diode, where RF power is converted into DC output voltage. For maximum output, all the incoming RF voltage should ideally appear across R_j , with nothing lost in R_s . The equation for junction resistance is:

$$R_j = 0.026 / I_T \quad (1)$$

where

$I_T = I_s + I_b + I_o$, in amperes

I_s = the diode's saturation current, a function of Schottky barrier height

I_b = circulating current generated by the rectification of RF power

I_o = External bias current (if any)

Such a diode can be used to convert RF power to DC with a simple detector circuit, as shown in Figure 2.

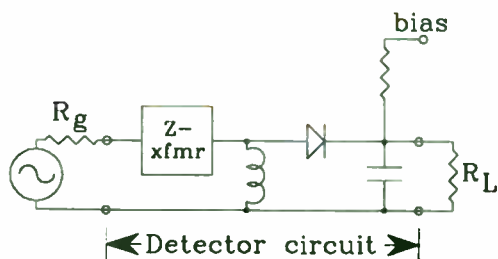


Figure 2: Schottky detector circuit

The behavior of Schottky detector circuits has been well studied in an operating region defined by two conditions; low input power (square law operation) and high load resistance. These two conditions, however, are not consistent with the use of a Schottky diode to generate reasonable levels of DC voltage and current.

A recent analysis [5] provides a single equation which describes the operation of a Schottky diode over the entire practical range of input power and load resistance.

$$I_0 \left(\frac{\Lambda}{n} \sqrt{8R_g P_{inc}} \right) = \left(1 + \frac{I_0}{I_s} + \frac{V_o}{R_L I_s} \right) \cdot \exp \left\{ \left[1 + \frac{R_g + R_s}{R_L} \right] \frac{\Lambda}{n} V_o + \frac{\Lambda}{n} R_s I_0 \right\} \quad (2)$$

where

- I_0 = zero order Bessel function
- P_{inc} = incident RF power
- R_g = generator or source impedance
- n = diode ideality factor (emission coefficient)
- $\Lambda = q/(kT)$
- q = electronic charge
- k = Boltzmann's constant
- T = temperature in degrees Kelvin
- R_L = output load resistance
- V_o = output voltage

This equation neglects the effects of diode package parasitics (which can easily be absorbed into the input matching network), junction capacitance C_j , and (therefore) frequency. However, as shall be seen later, these necessary simplifications are quite reasonable in the analysis of virtual batteries operating at RF frequencies. The equation also neglects the effect of RF impedance matching at the input to the diode, a matter which will be treated in a later section.

Equation (2) presents the *input* (P_{inc}) as a function of *output* (V_o), as is often the case when obtaining the solution of a nonlinear problem. To solve (2), it is necessary to obtain the inverse of the Bessel function. Such an equation is easily analyzed by a program such as Mathcad⁽¹⁾, where the output voltage can be iterated to obtain a series of values for P_{inc} , after which a plot of V_o vs. P_{inc} can be made. Appendix A is a printout of the Mathcad file used to obtain the plots shown in this paper.

It should be noted that equation (2) is useful only if accurate values of the diode parameters I_s , n , and R_s are used. These are generally provided by the diode manufacturer, or they can be determined from measurements as described in Appendix B.

Schottky diodes have evolved into many designs, which can be reduced to two basic categories. The first, those formed on n-type silicon, are characterized by relatively high barrier heights and low values of series resistance - these are ideal for mixer applications and detectors where DC bias is available. The second type are formed on p-type silicon, and are distinguished by low barrier height (high I_s) and high R_s . These diodes were developed for square law detector applications where load resistance is high and DC bias is not available. Both types were evaluated for virtual battery applications. Table 1 lists the characteristics of two microwave diodes, both having $C_j \approx 0.25$ pF, which were analyzed and measured.

Table 1: Diode parameters

	n-type	p-type
Part	HSMS-8201	HSMS-2850
n	1.12	1.17
I_s (A)	55×10^{-9}	2×10^{-6}
R_s (Ω)	7	25

Using equation (2), the calculated transfer curve for these two diodes was obtained as shown in Figure 3.

(1) Product of MathSoft, Inc., 201 Broadway, Cambridge, Massachusetts.

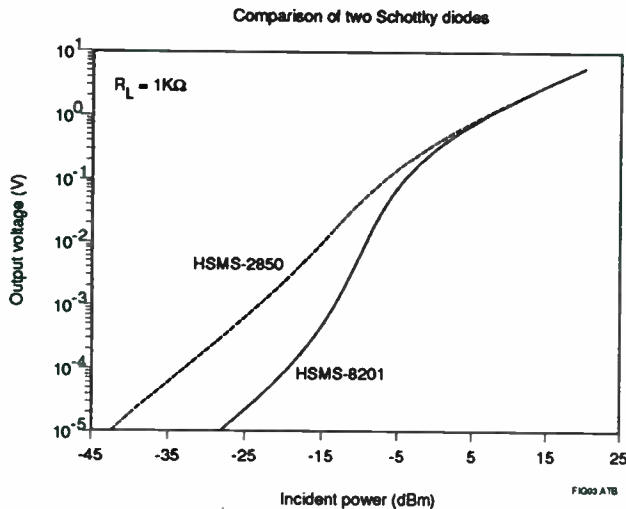


Figure 3: Calculated transfer curves

As can be seen, the higher saturation current of the p-type diode results in a substantially higher output voltage at low power levels where square law detectors typically operate. However, at output voltage levels of interest for this paper, the differences between the two types of diodes appears to disappear.

Two sample diodes, having the characteristics given in Table 1, were mounted on the end of a 50Ω transmission line with no matching network and transfer curves were measured, as shown in Figure 4.

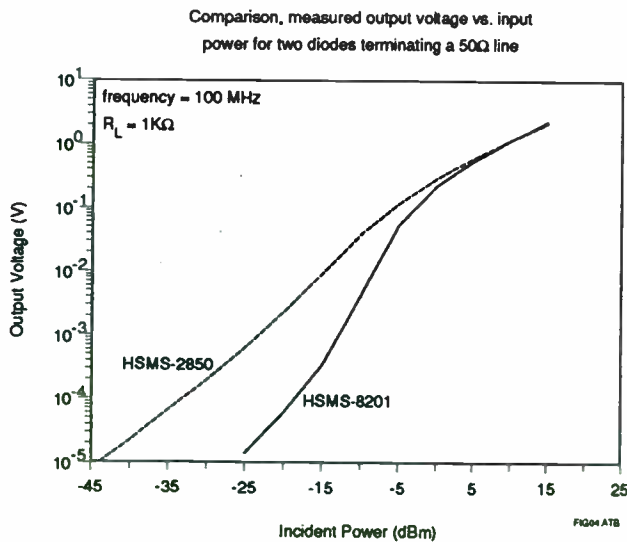


Figure 4: Measured transfer curves

The agreement between these data and the calculations shown in Figure 3 is very good.

III. VOLTAGE DOUBLERS

The primary goal of a virtual battery circuit is maximum voltage at a given power level. The voltage doubler [6] provides a higher output than the single diode shown in Figure 2. It is illustrated in Figure 5 (zero bias or virtual battery configuration).

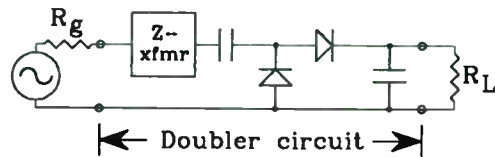


Figure 5: The voltage doubler

The doubler puts the Schottky diodes in parallel with respect to the input RF signal, which lowers the input impedance and reduces the difficulty of the impedance matching network. However, the diodes appear in series with respect to the output load, which (approximately) doubles the voltage. If the two diodes are contained in a single SOT-23 package, the cost impact associated with the second diode is very small, making the doubler an interesting circuit for virtual battery applications.

In Figure 6, an equivalent circuit is evolved for the doubler, by means of which it can be analyzed using equation (2).

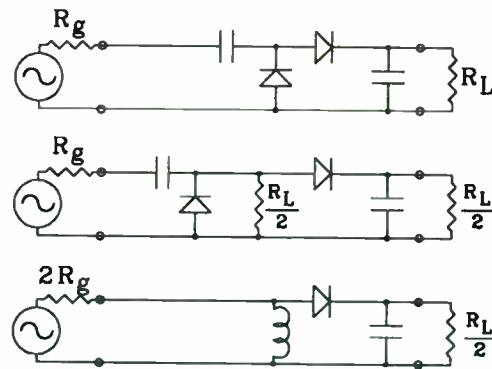


Figure 6: Doubler equivalent circuit

It can be seen that the transfer curve for a doubler can be predicted using equation (2) by doubling the value of R_g , halving the value of R_L and doubling the calculated values of V_o .

Calculations were made for a doubler using the p-type diode described in Table 1, and such a

diode pair (the HSMS-2852) was placed on the end of a 50Ω transmission line with no RF matching network. Both calculated and measured data for this doubler, as well as for the single diode shown in Figures 3 and 4, are given in Figure 7.

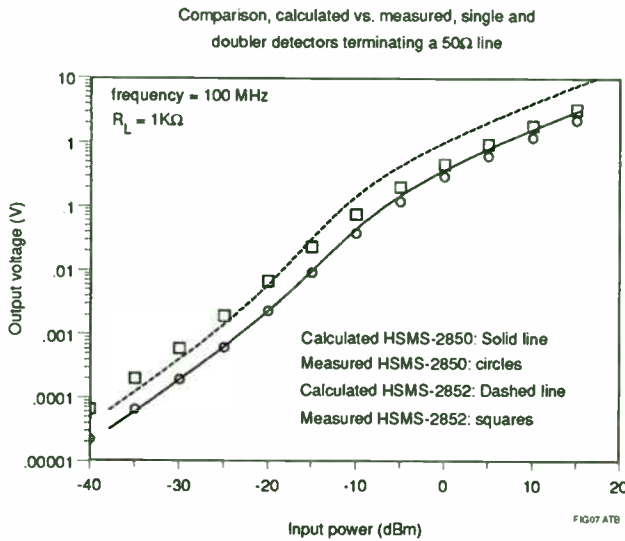


Figure 7: Data for an unmatched doubler

Agreement between calculated and measured data is not as good as it was for the single diode case, but is adequate nonetheless. Both calculated and measured curves predict a substantial improvement in output voltage for the doubler, when compared to a single diode circuit.

IV. JUNCTION CAPACITANCE

The effect of the diode's junction capacitance is to short out the junction resistance, diverting incoming RF energy into the parasitic series resistance where it does no useful work. At high frequencies and high values of R_j , as are typical of square law detectors, junction capacitance has a large effect upon output voltage.

The effect of capacitance on output voltage is given by [7]:

$$M = \frac{1}{1 + \omega^2 C_j^2 R_s R_j} \quad (3)$$

where

- $\omega = 2\pi$ times frequency
- M = a multiplier for V_o

While this equation is an approximation, its accuracy is quite good for our purposes.

If M is plotted against junction resistance, the curve of Figure 8 is the result.

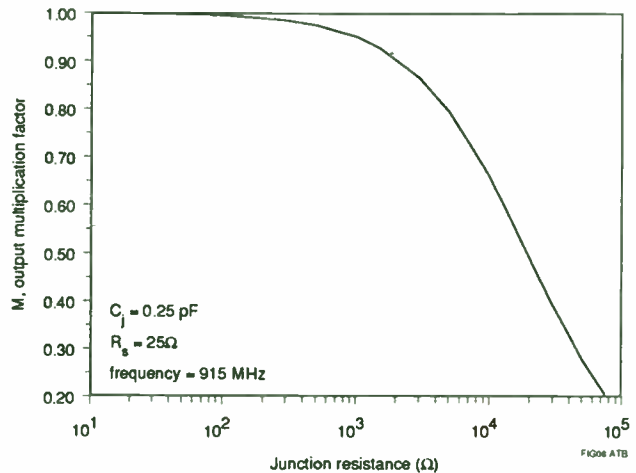


Figure 8: The effect of C_j

At the input power levels of interest to this analysis, output voltages will be in excess of 1V and circulating current I_b will be on the order of 0.1 mA or more. At these levels of current R_j is less than 250Ω, and junction capacitance has no significant effect.

V. RF IMPEDANCE MATCHING

When the input impedance of the virtual battery or detector circuit is other than the complex conjugate of the source, some incident RF power is reflected back to the source and lost. In the case of the square law (small signal) detector, R_j is fixed by the diode's saturation current or the circuit's bias current. This value is inserted into the linear equivalent circuit of Figure 1 and a RF matching circuit can be derived. Of course, since $R_j \gg 50\Omega$, losses in the matching network [4] will reduce the gain in output voltage from a lossless-case value of 50 times to a more realistic value of 10 times.

However, the impedance matching case for the virtual battery is much different. First, the impedance of the diode is much lower owing to the high value of circulating current which

depresses R_j . The situation is made even easier when the voltage doubler circuit is used. However, R_j is not a constant for the virtual battery. As input power is increased or load resistance is decreased, the value of circulating current will go up and junction resistance will be reduced. In the virtual battery, R_j is not a constant -- it spans a significant range.

As part of the design of a 915 MHz voltage doubler, the impedance of a HSMS-2852 Schottky pair was measured as a function of external bias. The data are shown in Figure 9.

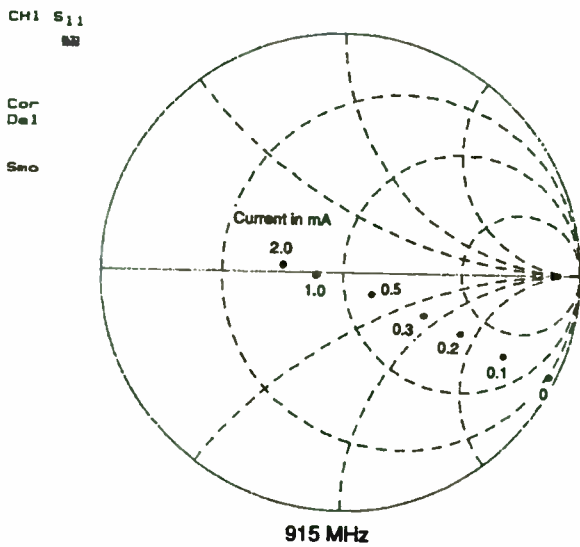


Figure 9: Impedance of a HSMS-2852

0.3 to 0.5 mA was selected as a probable operating range for the doubler, and the value of R_j was estimated to be 250Ω for each diode in the pair. The model of Figure 2 was set up for each diode of the pair in a linear analysis program (MMICAD²) and a 3-element low pass filter matching section was optimized at the input to the diode pair. The final matching network consisted of a series microstrip transmission line (on 0.032" thick FR4) of length = 1.07" and width = 0.015", with a small capacitive flag at each end. The flags constituted the shunt capacitors and the high impedance line the series inductor of the low pass filter. The predicted impedance of this matched diode pair, over the frequency range of 865 to 965 MHz, is shown in Figure 10.

(2) Product of Optotek Limited, 62 Steacie Drive, Kanata, Ontario, Canada K2K 2A9

HSMS-2852 Schottky Pair, as virtual bat

MMICAD -- Fri Nov 18 14:59:21 1994

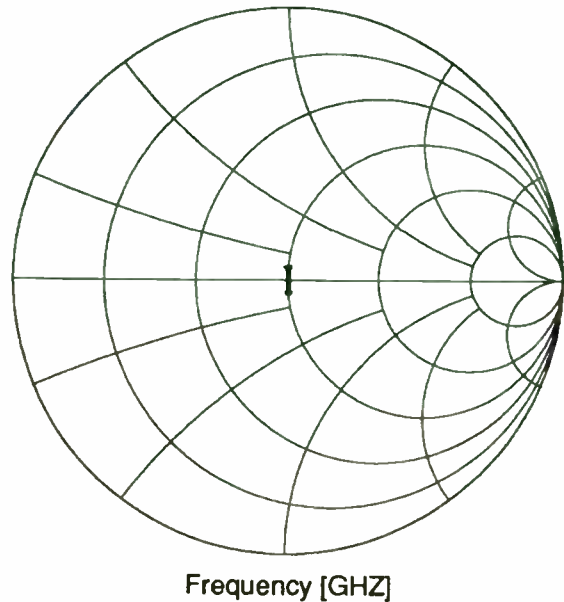


Figure 10: Predicted input impedance match

Note that this analysis assumes that the diode is to be matched to a source impedance of $50 + j0$, since measurements were to be made using conventional test equipment. In the virtual battery, the antenna is the source, and its impedance is probably something very different from 50Ω . This may make the design of the actual matching network somewhat more challenging.

VI. MEASURED RESULTS

The two doubler circuits of the type described above were fabricated on 0.032" thick FR4 microstrip. The first used the HSMS-2852 low barrier diode pair and the second used the HSMS-8202 low R_s diode pair. They were tested, and their performance compared to a small signal (square law) detector created for an earlier work [4]. All three were designed to operate from a source of $50 + j0\Omega$ at a frequency of 915 MHz.

The two virtual battery circuits were tested for input return loss vs. input power and empirically optimized for minimum VSWR at 0 dBm. In both cases, this optimization resulted in the elimination of the capacitive flags on the input matching net-

work, which was then reduced to a single high impedance (inductive) line. The square law detector, on the other hand, had been designed for optimum match at very small signal levels. Plots of return loss vs. input power for all three circuits are shown in Figure 11.

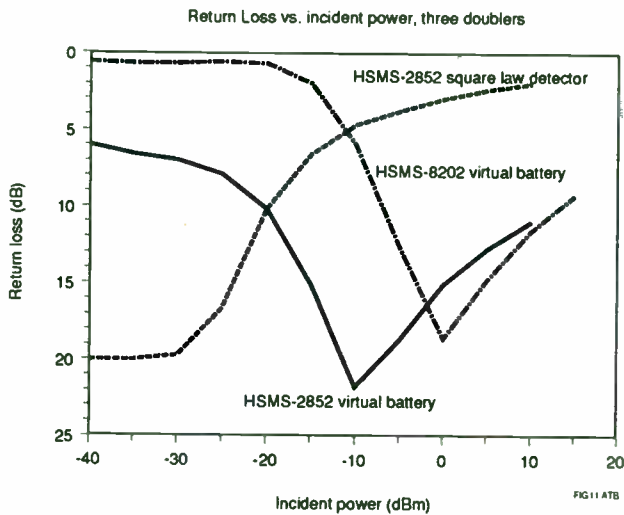


Figure 11: Return loss vs. input power

All three circuits were characterized for their transfer characteristic with load resistances of 100K Ω , 1K Ω and 100 Ω . The curves for $R_L = 1K\Omega$ are shown in Figures 12.

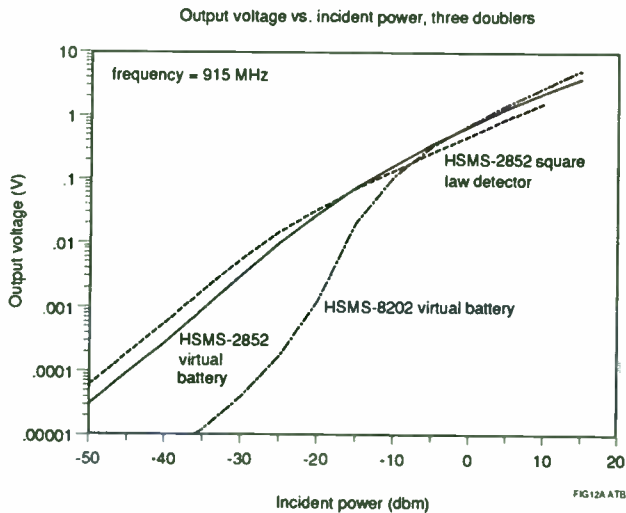


Figure 12A: Transfer curves for three doublers

It is interesting to note that the square law detector, using the self-biasing low barrier diodes, produces the largest voltage output at very small signal levels. However, at the large signal levels

of interest to this analysis, its poor impedance match results in a lower output voltage than the virtual battery which uses the same HSMS-2852 diode pair.

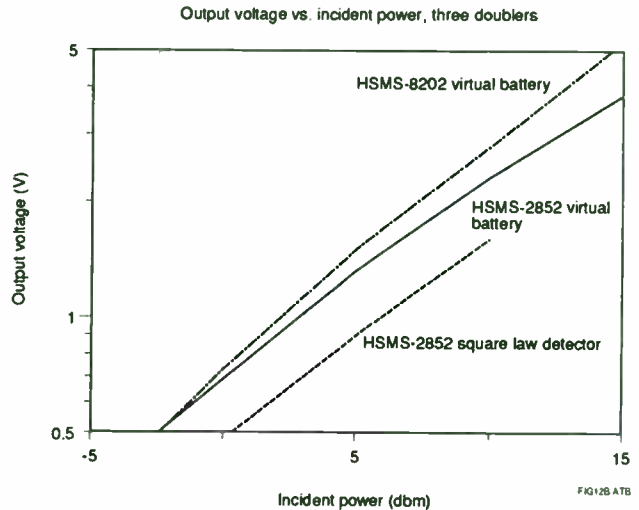


Figure 12B: Transfer curve, expanded scale

These data lead to a more significant observation. At input power levels below 0 dBm, the HSMS-2852 low barrier pair produces a higher output voltage than the HSMS-8202 low R_S pair. This difference in performance was predicted by equation (2), as illustrated in Figure 3. What was not predicted by equation (2), however, is the significantly higher output voltage produced by the HSMS-8202 at incident power levels greater than 0 dBm. When an impedance matching network is placed before the diode, designed for low values of R_i , the importance of R_S is increased. For example, when the value of total current I_T is increased until $R_i = R_S$, the output voltage of the virtual battery will be half the value it would have been for $R_S = 0$. While this point can be reached at some input power level for any diode type, it is achieved at a much lower value of input power when an impedance matching network is used.

The efficiency (output power/input power) of the two virtual batteries was measured, at an incident power level of +10 dBm, as a function of load resistance. These data are presented in Figure 13.

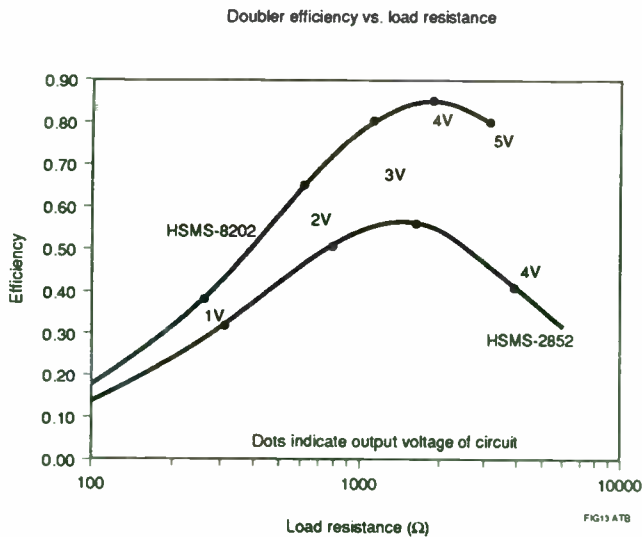


Figure 13: efficiency vs. load resistance

These data illustrate the significant effect that parasitic series resistance can have on the efficiency of a virtual battery. Peak efficiency was achieved at a load resistance of approximately $2K\Omega$, a practical value for virtual battery applications.

VII. CONCLUSION

Design considerations for a virtual battery have been presented, and measured data from practical circuits have been presented. It has been shown that a Schottky diode voltage doubler, with an impedance matching network optimized for high values of incident power, can be a efficient substitute for a larger and more expensive battery in certain applications.

REFERENCES

- [1] Private communication with Robert Myers of Hewlett-Packard Company.
- [2] Lawrence Livermore Labs, *An Automatic Vehicle ID System for Toll Collecting*, Lawrence Livermore National Laboratory LLNL Transportation Program, L-644
- [3] Hewlett-Packard Application Note 923, *Schottky Barrier Diode Video Detectors*.
- [4] Raymond W. Waugh, "Designing Detectors for RF/ID Tags," *Proceedings of RF Expo West*, 1995
- [5] Robert G. Harrison & Xavier Le Polozec, "Nonsquarelaw Behavior of Diode Detectors Analyzed by the Ritz-Galérkin Method," *IEEE Transactions on Microwave Theory and Techniques*, Vol. 42, No. 5, May 1994, pp. 840 - 845.
- [6] Hewlett-Packard Application Note 956-4, *Schottky Diode Voltage Doubler*.
- [7] Hewlett-Packard Application Note 969, *The Zero Bias Schottky Detector Diode* (revised 8/94).

APPENDIX A - MATHCAD FILE

Vo vs. Pin calculator, based upon Harrison & Polozec, "Nonsquarelaw Behavior of Diode Detectors Analyzed by the Ritz-Galerkin Method," IEEE Trans MTT, Vol. 42, No. 5, May, 1994. This Mathcad file was developed with the assistance of Bob Gauthier of Mathsoft, Inc.



t := 25 in °C

$\Lambda := 38.5 \cdot \frac{300}{275 + t}$

I_o := 0 external bias, A

n := 1.12 Ideality factor

I_s := 54 · 10⁻⁹ saturation current, A

R_g := 50 Generator impedance, in Ω

R_s := 7 in Ω

R_L := 500 in Ω

Values shown above are for the HSMS-8201 Schottky diode.

m := 18, 19 .. 43 Note that you might have to reduce the high end of this range from 43 to something less for certain sets of input values. If adjustment of guess values z does not result in a solution for a_{kn}, reduce the maximum value of the range for m. For small signal analysis, equations A3 through A8 may be deleted.

V_{o_m} := 10^{k_m} Output voltage is stepped. (A1)

$B_m := \left(1 + \frac{I_o}{I_s} + \frac{V_{o_m}}{R_L \cdot I_s}\right) \cdot e^{\left[\left(1 + \frac{R_g + R_s}{R_L}\right) \cdot \frac{\Lambda}{n} \cdot V_{o_m} + \frac{\Lambda}{n} \cdot R_s \cdot I_o\right]}$ (A2)

k1 := 18 .. 35 z := 13 a_{k1} := root $\left(\frac{B_{k1}}{B_{k1}} - \frac{10(z)}{B_{k1}}, z\right)$ (A3)

k2 := 36 .. 39 z := 40 a_{k2} := root $\left(\frac{B_{k2}}{B_{k2}} - \frac{10(z)}{B_{k2}}, z\right)$ (A4)

k3 := 40 z := 50 a_{k3} := root $\left(\frac{B_{k3}}{B_{k3}} - \frac{10(z)}{B_{k3}}, z\right)$ (A5)

k4 := 41 z := 1.85 · a_{k3} a_{k4} := root $\left(\frac{B_{k4}}{B_{k4}} - \frac{10(z)}{B_{k4}}, z\right)$ (A6)

k5 := 42 z := 1.85 · a_{k4} a_{k5} := root $\left(\frac{B_{k5}}{B_{k5}} - \frac{10(z)}{B_{k5}}, z\right)$ (A7)

k6 := 43 z := 1.85 · a_{k5} a_{k6} := root $\left(\frac{B_{k6}}{B_{k6}} - \frac{10(z)}{B_{k6}}, z\right)$ (A8)

P_{inc_m} := $\frac{1}{8 \cdot R_g} \cdot \left(\frac{n \cdot a_m}{\Lambda}\right)^2$ Watts

dBm_m := 10 · log(P_{inc_m} · 1000)

dBm _m
-30.13
-27.74
-25.40

P _{inc_m} W
9.71 · 10 ⁻⁷
1.68 · 10 ⁻⁶
2.88 · 10 ⁻⁶
4.95 · 10 ⁻⁶

a _m
6.8 · 10 ⁻¹
8.9 · 10 ⁻¹
1.2
1.5

a _{k1}
0.68
0.89
1.17
1.51
1.93
2.42
2.96
3.54
4.15
4.78
5.41
6.07
6.75
7.47
8.26
9.19
10.35
11.94

a_{k3} = 52
a_{k4} = 82
a_{k5} = 136
a_{k6} = 231

B _m
1.117
1.209
1.371
1.660
2.174
3.089
4.722
7.638
1.287 · 10
2.230 · 10
3.952 · 10
7.157 · 10
1.333 · 10 ²
2.596 · 10 ²
5.446 · 10 ²
1.303 · 10 ³
3.935 · 10 ³
1.795 · 10 ⁴
1.705 · 10 ⁵
5.972 · 10 ⁶
2.127 · 10 ⁹
4.686 · 10 ¹³
1.583 · 10 ²¹
2.471 · 10 ³⁴

V_{o_m} Volts

3.2 · 10 ⁻⁶
5.6 · 10 ⁻⁶
1.0 · 10 ⁻⁵
1.8 · 10 ⁻⁵
3.2 · 10 ⁻⁵
5.6 · 10 ⁻⁵
1.0 · 10 ⁻⁴
1.8 · 10 ⁻⁴
3.2 · 10 ⁻⁴
5.6 · 10 ⁻⁴
1.0 · 10 ⁻³
1.8 · 10 ⁻³
3.2 · 10 ⁻³
5.6 · 10 ⁻³
1.0 · 10 ⁻²
1.8 · 10 ⁻²
3.2 · 10 ⁻²
5.6 · 10 ⁻²
1.0 · 10 ⁻¹
1.8 · 10 ⁻¹
3.2 · 10 ⁻¹
5.6 · 10 ⁻¹
1.0
1.8

APPENDIX B - DIODE PARAMETERS

To obtain diode characteristics I_S , n and R_S from laboratory measurements, take the following steps.

1. Measure forward voltage V_1 at $I_f = 0.010$ mA and V_2 at $I_f = 0.100$ mA. For most Schottky diodes, these two points fall on that part of the curve which corresponds to an ideal diode characteristic (ie, the effect of R_S is not seen).
2. Measure V_3 and V_4 at $I_f = 4.80$ mA and 5.20 mA respectively. Note that accurate voltmeters and ammeters, with good resolution, must be used for the measurements in steps 1 and 2.
3. Compute $n = (V_2 - V_1)/0.0586$

4. Compute $I_S = \frac{0.010}{e^{(V_1/0.025n)}} \text{ mA}$

5. Compute $R_S = \frac{V_4 - V_3}{0.0004} \Omega$

Monolithic Gain Blocks in Mini-Packages for DC to 4000 MHz Wireless Hand-Held Communication

Henrik Morkner , N.M. Nguyen, Gary Carr
Hewlett-Packard Communication Components Division
39201 Cherry Street, Newark, California 95014

ABSTRACT

Engineers face many challenges designing wireless hand-held systems. These systems not only need to meet stringent RF and DC performance specifications, they must fit into tight space requirements. This paper describes how to design high performance amplifiers that reduce the printed circuit board area required 25% to 75% compared to traditional methods. Discussed are discrete vs. MMIC (Monolithic Microwave Integrated Circuits) designs and SO-8 package MMIC vs. SOT-363 MMIC designs. The paper shows several application examples with descriptions for popular 1575 MHz and 2400 MHz wireless applications.

I. INTRODUCTION

Increasingly, the challenge for the wireless designer is to develop and deliver smaller systems for cellular and cordless systems. Weight and size have become major considerations by the consumers of this rapidly-growing market. The components manufacturers have addressed this problem by designing more of the receiver into VLSI silicon solutions. However, the receiver amplification and downconversion conditions exceed the available performance of VLSI silicon integrated circuits.

Consequently, many wireless systems operating in the widely used 900 MHz to 2400 MHz bands still use discrete surface mount transistors with support resistors and capacitors. Present discrete designs fulfill price and performance specification demands. However, they are now being challenged as MMIC solutions provide the same function with less space requirements. This paper will compare discrete and MMIC designs for performance and space parameters. Several application examples will be shown demonstrating how Hewlett-Packard's new line of miniature SOT-363 (SC70, 6 lead, 2 mm length) MMICs that can propel system designers to new levels of space efficiency.

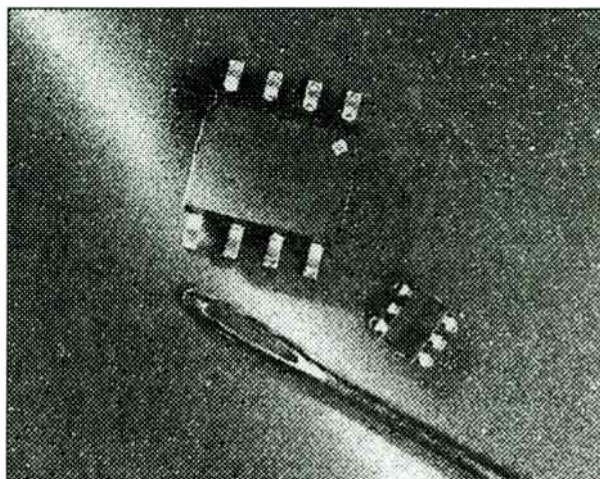


Figure 1. Photographic comparison of a standard SO-8 MMIC versus a SOT-363 (SC70) MMIC

II. A SMALLER PACKAGE

There is a vast array of package options available to the wireless system designer today. For simplicity this paper confines itself to surface mount package types typically used for front end wireless 900 MHz to 2400 MHz receiver systems. For convention this paper refers to package types by the EIA/IEC standard designation followed by the EIAJ designation in parentheses.

Discrete transistors are traditionally used in SOT-23 (SC59), SOT-143 (SC61), and SOT-323 (SC73) style packages. Low cost MMICs are available in traditional SO-8 and SOT-143 (SC61) packages. Hewlett-Packard offers MMICs now in the miniature SOT-363 (SC70) package. Figure 1 compares a SO-8 MMIC to a SOT-363 MMIC. Figure 2 details various MMIC package styles.

The SOT-363 (SC70) package is a natural progression from the SOT-23/143 style packages (the world's first surface mount miniature transistor packages). It is manufactured using the same technology as the older SOT packages and the new outline (though very small) is well within the capabilities of modern pick-and-place assembly equipment.

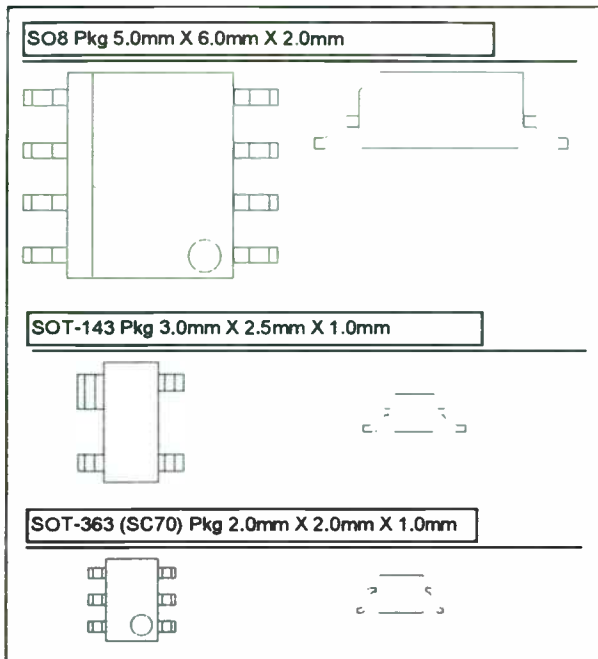


Figure 2. Scaled comparison of size of various standard surface mount plastic packages.

The SOT-363 package offers many benefits to the modern wireless system designer. The smaller size of the SOT-363 package (vs. the SOT-23/143 or SO-8) provide the obvious advantage of smaller system board real estate. A less apparent advantage is that the package has lower RF parasitics. The result is that both noise figure, gain, and frequency bandwidth are improved (primarily due to lower lead inductance and capacitance). Repeatability is also improved due to tighter mechanical tolerances and smaller interconnections.

An obvious problem with a miniature package is that the MMIC die must be small enough to be assembled reliably. This has assuredly hindered many manufacturers from offering MMICs in miniature packages. Hewlett-Packard engineers have taken great care in designing ultra small silicon and GaAs MMICs that can take advantage of today's high performance miniature packages. Figure 3 demonstrates a GaAs MMIC in the SOT-363 (SC70) package with a comfortable margin for assembly and reliability. Another problem with miniature packages is power dissipation. Copper lead frames and paddle mounted center leads allow the SOT-363 (SC70) to dissipate heat more efficiently than its predecessors.

The result is a new line of surface mount silicon and GaAs MMICs that are smaller than any other known part on the market. The SOT-

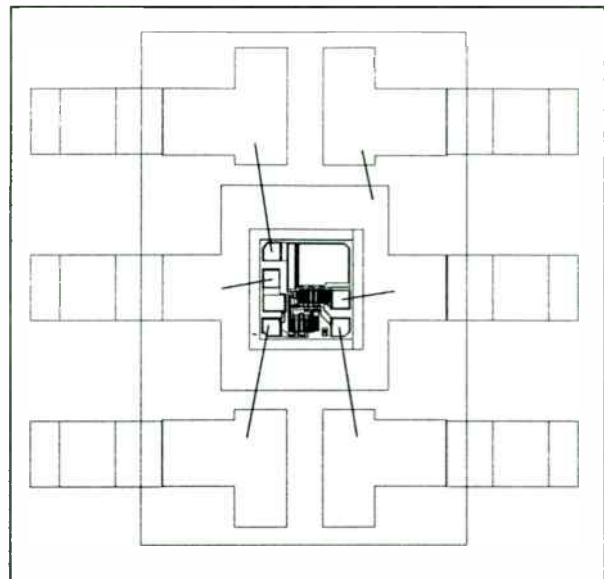


Figure 3. Example of a GaAs PHEMT MMIC bonded into a SOT-363 (SC70) package

363 (SC70) designs are 47% smaller than SOT-23/143 designs and an incredible 87% smaller than SO-8 designs.

II. Discrete or MMIC ?

In most wireless applications discrete transistors have held an advantage in price, performance, flexibility, and component size. The major drawback with utilizing discrete components in space-constricted system is that a large number of support components (resistors, capacitors, inductors) are required. The support components are required for RF matching and DC biasing the transistor. They typically occupy 10 to 20 times the area of the transistor they support.

Modern MMICs simplify component usage by incorporating most bias and matching elements into an integrated circuit. MMICs take advantage of their small size to also incorporate topology advantages (such as feedback) that are otherwise not available to the discrete design. The results are components that offer similar electrical performance to discrete designs but with dramatic board space improvements. As with any integrated circuit, system design is simplified. The matching, biasing, and placement are improved, thus reducing system design time and improving productivity.

As an example, Figure 4. demonstrates a GPS LNA(Low Noise Amplifier) designed using discrete transistors [1]. The design required a detailed analysis of the input matching characteristics of the transistor in order to provide

the maximum gain with lowest noise figure. The design is further complicated by the need to stabilize a potentially unstable transistor. The result is a low noise amplifier design that requires a 3 element input match and 3 element output match. An additional 5 components are required to bias the transistor properly. The layout occupies 0.25 square inches on a 0.5" by 0.5" board. The LNA matching network uses transmission lines (no cost, repeatable) as opposed to SMT inductors (high cost, high Q) which would consume much less real estate. The final electrical result is a conditionally stable LNA with a 1.9 dB noise figure and 10.5 dB gain at 1575 MHz. The LNA requires 3 volts, 3 mA and would cost approximately \$0.45 to build in volume.

Figure 5. demonstrates a GPS low noise amplifier designed at Hewlett-Packard with similar electrical specifications to that shown in Figure 4. The primary difference is that the design utilizes a HP MGA-87563 GaAs PHEMT MMIC LNA to reduce board size. The implementation of the matching network requires 1 element for the input

and 2 elements for the output. Obtaining the noise match is simplified and the magnitude of the match (overall mis-match) is less severe for the MMIC compared to the discrete transistor. Again, transmission lines were used to minimize cost (with a small real estate penalty). The LNA layout occupies a 0.0875 square inch board area (0.35" X 0.25") that is almost 3 times smaller than the discrete design. Electrical results show an unconditionally stable low noise amplifier that has a 1.8 dB noise figure with 14.5 dB gain. The MMIC based LNA requires 3 volts, 4.5 mA and costs approximately \$0.95 to build in volume.

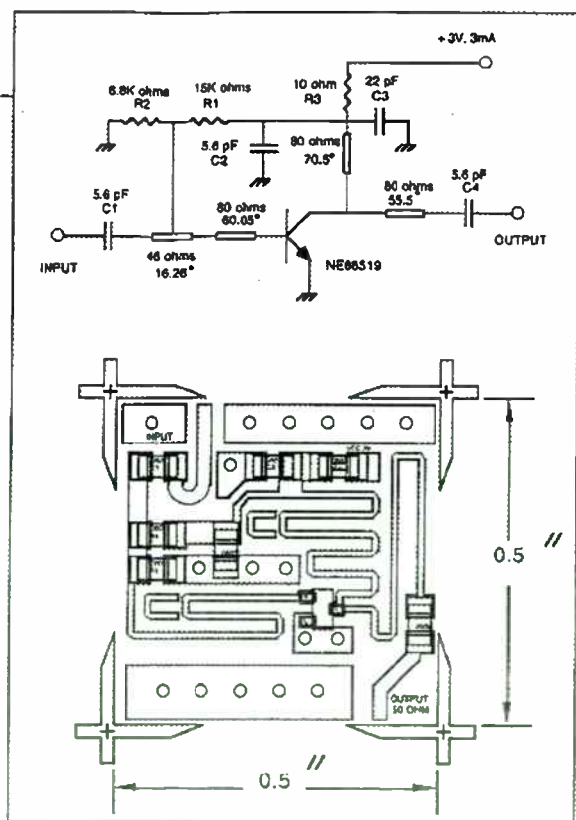


Figure 4. A GPS (1570 MHz) LNA design built with a discrete transistor [1]. Area is 0.25 in.sq.

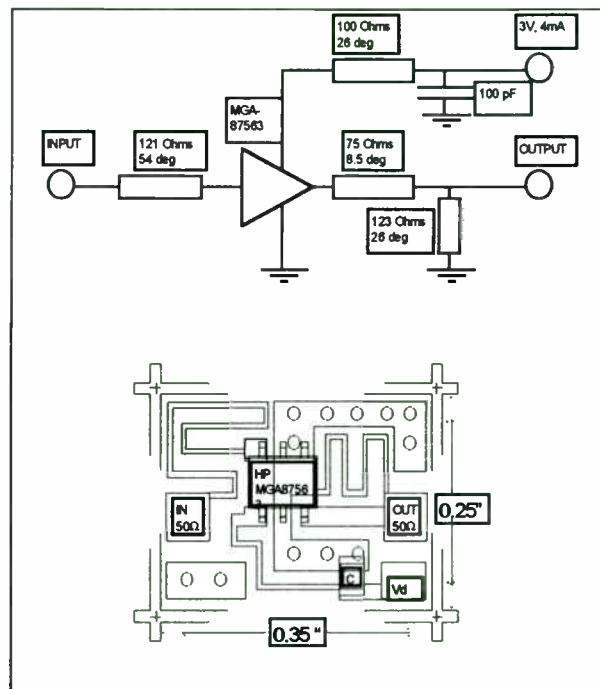


Figure 5. A GPS (1570 MHz) LNA design built using a GaAs MMIC. Area is 0.0875 in. sq.

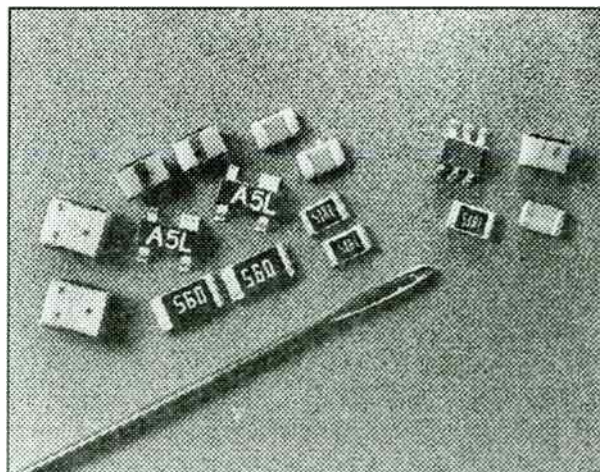


Figure 6. Surface mount parts required to build a discrete based 2 stage LNA versus a MMIC.

III. Which MMIC to use ?

GaAs and Silicon MMICs are now being used in almost every sector of the commercial RF industry, from personal communication to direct broadcast satellite. Component manufacturers are offering new MMICs constantly to meet changing performance and cost requirements. The question now facing the system designer is "How do I select the right MMIC ?". Manufacturers offer a wide range of package styles and performance levels.

The first step in selection of a MMIC is not whether to use GaAs or silicon. A recent study by Venture Development Corp. (Natick, MA) said it expects the market for GaAs RF/MMICs to account for about \$302 million, or 61 %, of total projected market for integrated circuits for mobile wireless communications products in 1997 [2]. The split between GaAs and silicon will be where there's the best performance to price ratio. Silicon has advantages in price and more highly integrated functions such as synthesizers, modulators, and mixers. GaAs has advantages in power efficiency and noise figure for amplifiers and switches. The system designer should pick the best MMIC for the function, and ignore the technology. Major manufacturers offer MMICs in both technologies.

When designing systems that are sensitive to available board space, the system designer should obviously select the smallest packaged MMIC that fulfills the application requirement. To demonstrate the advantage of MMICs in miniature packages, an example design was done for a 2400 MHz low noise amplifier using a SO-8 and SOT-363 (SC70) packages.

Figure 7. demonstrates a low noise amplifier designed using a SO-8 MMIC per manufacturers recommendations [3]. This LNA would typically be used for applications in the unlicensed 2400 MHz to 2480 MHz Industrial-Scientific-Medical (ISM) band. The LNA requires the MMIC and four support elements. A capacitor is used for a DC block on the output and another for DC supply de-coupling. For minimum noise a shunt-series inductive network is used to provide optimum noise match (Γ_{opt} , Gamma Optimum) over the narrow band of use. The board layout uses 0.141 square inches (0.47" X 0.30"). The result is a 1.6 dB noise figure LNA with 20 dB of gain. Output power (P-1dB) is -11 dBm. The LNA uses a +5 volt, 18 mA supply. The cost would be around \$2 to \$3 in volume.

Figure 8. demonstrates a Hewlett-Packard MGA-86563 MMIC based LNA design for the same 2400 - 2480 MHz ISM band. The MMIC requires five support elements. The HP design

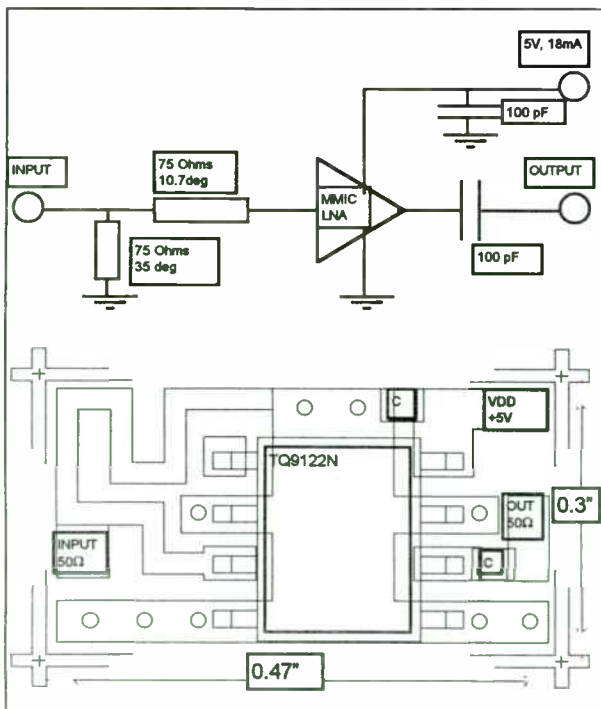


Figure 7. A 2.4 GHz LNA using a S08 packaged MMIC.

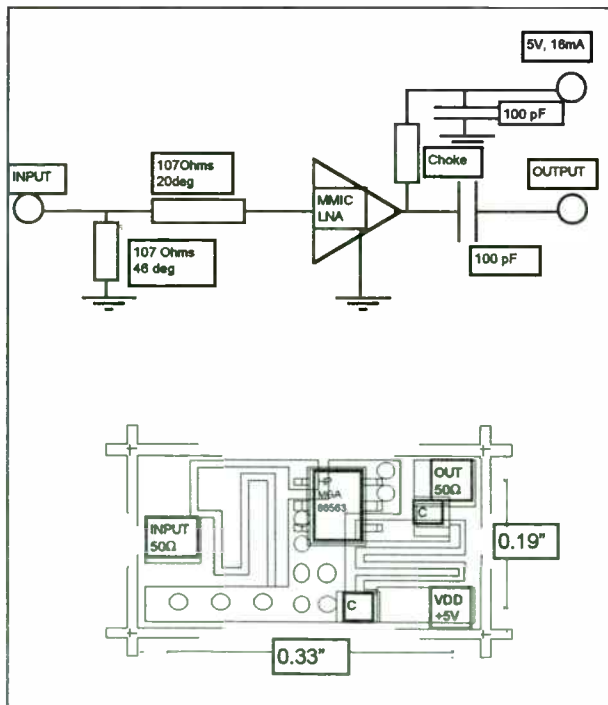


Figure 8. A 2.4 GHz LNA designed using a SOT-363 packaged MMIC.

requires an output RF choke and de-coupling capacitor since the bias is brought into the amplifier MMIC through the output pin. As in the previous example, a shunt-series inductive network is also used in the HP MMIC to provide Γ_{opt} to the MMIC for minimum noise figure. Board size is 0.0627 square inches (0.33"X 0.19") or 66% smaller than the SO-8 design. The HP LNA provides a 1.7 dB noise figure and 20.5 dB of gain. The output power (P-1dB) is +5 dBm with a +5 volt, 14 mA supply. Typical cost is \$ 2 in volume. The clear advantage to this HP design is the space savings and linearity.

A basic question may arise in the system designers mind as to why MMIC manufactures do not provide the full low noise match at the input. The answer is that although the match could be done monolithically within the MMIC (some MMICs are available this way), it is best to leave the narrow band match of a wide band part to the MMIC user. This allows manufactures to produce fewer custom ASICs and lower MMIC costs. With such a variety of frequency standards it would be cost prohibitive to offer a MMIC for each. Also, the real estate hungry input match is cheaper and better on the PC board.

IV. WHAT HP HAS TO OFFER

Hewlett-Packard now offers four new MMICs in the SOT-363 (SC70) package available in early 1995. These devices offer range and flexibility that can be applied to most wireless applications in the 50 MHz to 6 GHz bands. All of the designs take to heart the Hewlett-Packard tradition of offering reliable, easy to use, cost effective components for RF and microwave applications.

Specification	HP INA-51	HP INA-52
Technology	Silicon Isosat	Silicon Isosat
Voltage	5.0 V	5.0 V
Current	12 mA typical	30 mA typical
Frequency range	DC-2500 MHz	DC-1500 MHz
Test Frequency	900 MHz	900 MHz
Input match	50 Ω	50 Ω
Output match	50 Ω	50 Ω
Typ Noise Figure	3.0 dB	3.5 dB
Typical Gain	19 dB	20 dB
P-1 dB comp.	0 dBm	9 dBm
Package	SOT-363	SOT-363
Typical price	\$ 0.50	\$ 0.50

Table 1. Specification summary for HP silicon SOT-363 (SC70) miniature surface mount MMICs.

Both the INA-51 and INA-52 are implemented in the Hewlett-Packard ISOSAT-II silicon bipolar IC technology. This process features a typical F_T of 15 GHz and uses submicron lithography and trench isolation. The fabrication utilizes a thick field oxide and gold metalization that allow high-Q capacitors and spiral inductors. The MMICs utilize a multi-feedback approach for broadband frequency performance. A combination of a shunt series and a shunt-shunt feedback between the input and output stages make the MMICs highly tolerant to semiconductor processing as well as variation in power supply voltage and temperature. The circuit is matched internally to 50 Ω at the input and output. Well suited for IF applications (up to 500 MHz), the circuits can also provide satisfactory performance through 2300 MHz. See Table 1 for information on the INA performance.

The MGA-87563 and MGA-86563 are fabricated using a GaAs PHEMT (Pseudomorphic High Electron Mobility Transistor) process. The base material is MBE (Molecular Beam Epitaxy) grown and the 0.2 micron FET gates are written using electron-beam lithography. The remaining layers are placed on the 3-inch wafers using precision steppers. The result is a process with typical F_T of 60 GHz and able to operate under very low voltage and current conditions. Each design incorporates feedback to provide stability and reduce mis-match. Current is regulated internally with the use of current sources. This results in designs that are tolerant of fabrication and voltage supply variations. Costs are kept low on these GaAs PHEMT MMICs (traditionally expensive) through the use of a high yield fabrication, small die size, and automated test.

Specification	HP MGA-86563	HP MGA-87563
Technology	GaAs PHEMT	GaAs PHEMT
Voltage	5.0 V	3.0 V
Current	14 mA typical	4.5 mA typical
Frequency range	0.5 - 6.0 GHz	0.5 - 4.0 GHz
Test Frequency	2.0 GHz	2.0 GHz
Input match	External to Γ_{opt}	External to Γ_{opt}
Output match	50 Ω	50 Ω above 2 GHz
Typ Noise Figure	1.7 dB	1.6 dB
Typical Gain	20 dB	14 dB
P-1 dB comp.	5 dBm	-2.0 dBm
Package	SOT-363	SOT-363
Typical price	\$ 2.00	\$ 1.00

Table 2. Specification summary for HP GaAs SOT-363 (SC70) miniature surface mount MMICs.

V. CONCLUSION

System designers are being pushed to develop smaller, cheaper, and better wireless receivers for rapidly-growing personal communications market. This is a daunting task considering all the cellular and cordless system standards worldwide.

To build the next generation systems, traditional discrete designs will be hard pressed to meet space requirements. Modern MMICs will slowly fill these switching, amplification, and downconversion RF signal processing tasks. CMOS and bipolar technology will continue to integrate IF and digital signal processing. The result will be phones and receivers that have fewer parts, cost less, and are smaller.

This paper has described the benefits of miniature packages for MMICs. It has demonstrated the space savings possible by using a MMIC to replace discrete components. Also shown was the design advantages of a miniature MMIC versus a traditional SO-8 based MMIC. Last, Hewlett-Packard's new line of miniature SOT-363 (SC70) silicon and GaAs MMICs were described.

The authors wish to thank Tsong Kao, Ruben Reyes, Patrick Chye, Ding Day for die fabrication; John Coward, Joe Stephens, Tony Niedzwiecki for their test work; Bob Myers and Al Ward for application expertise. Finally, Mike Frank, Kevin Negus and Craig Snapp for management support.

Any application help, application notes, and data sheets for the products mentioned are available from your Hewlett-Packard sales office or distributor.

VI. REFERENCES

1. T. Cummings, "Designing a Low Cost GPS LNA Using the NE68519", *RF Design*, June, 1994, pp 36-45.
2. R. Schneiderman, "Silicon or GaAs?"; *Microwaves & RF*, October 1994, pp 31-37.
3. Triquint Semiconductor, TQ9122N Low Noise Amplifier Data Sheet, Revision B, 1993
4. M. Williams, F. Bonn, C. Gong, T. Quach, "GaAs RF ICs Target 2.4-GHz Frequency Band"; *Microwaves and RF*, July 1994, pp 111-118.
5. H. Morkner, M. Frank, D. Millicker, "A High Performance 1.5 dB Low Noise PHEMT MMIC Amplifier for low cost 1.5 - 8 GHz Commercial Applications"; *1993 Microwave and Millimeter-Wave Monolithic Circuits Symposium*, pp 13 - 16.
6. Stephen A. Maas, "Microwave Mixers"; Artech House, INC., Dedham, MA, 1986
7. H. Morkner, M. Frank, R. Kishimura, "A Novel MMIC PHEMT Low Noise Amplifier for GPS Applications"; *1992 Microwave and Millimeter-Wave Monolithic Circuits Symposium*, pp 13-16.
8. P.M. Smith, P.C. Chao, K.H.G Duh, L.F. Lester, B.R.Lee, and J.M. Ballingall, "Advances in HEMT Technology and Applications"; *1987 IEEE MTT-S International Symposium*, p. 749.
9. M. Frank, "The Current Source as a Microwave Biasing Element", US Patent # 4,912,430.
10. M. Frank, "The 2 to 6 GHz Block GaAs MMIC Amplifier"; *Microwave Journal*, Aug. 1990, pp 83-92.
11. C. Yuen, et al., "Application of HEMT Devices to MMICs"; *Microwave Journal*, August 1988, vol 31, No 8., pp 87-104.

Measurement Solutions

Session Chairperson: Ben Zarlingo,
Hewlett-Packard Co. (Everett, WA)

Adjacent-channel power measurements and troubleshooting. **Bob Cutler,** Hewlett-Packard Co. (Everett, WA).....176

Cost-effective frequency calibration in field environments. **Stuart Jensen,** Fluke Manufacturing Co. (Everett, WA).....183

Testing data-communications systems. **David W. Tarver,** Telecom Analysis Systems, Inc. (Eatontown, NJ).....193

Evaluating communications systems and components under multiple-signal conditions, **Tim Carey,** Hewlett-Packard Co., Video Communications Division (Santa Clara, CA).....194

Wafer-probe technology for high-speed digital and RF IC testing. **Ken Smith, Reed Gleason, and Eric Strid,** Cascade Microtech (Beaverton, OR).....200

Fast phase-noise measurements for high-volume design and manufacturing. **Darryl Schick,** RDL, Inc. (Conshohocken, PA).....210

Quantifying the benefits of improved antenna performance in terms of microwave point-to-point link density. **Gary Heane,** Flann Microwave Instruments Ltd. (Bodmin, Cornwall, England).....215

Adjacent Channel Power Measurements and Troubleshooting

Bob Cutler

Hewlett-Packard Company
8600 Soper Hill Road
Everett, WA 98205
bobc@labrtc.lsid.hp.com

Abstract

The explosion in the number of digitally modulated carriers has generated a great deal of interest in power measurements, especially measurements relating to spectral occupancy. In this paper we will review the basic theory of spectrum measurements, including measurements on pulsed signals such as those found in TDMA systems. In particular, we will consider the implications of measurements that are both time and frequency selective. For example, we will discuss how to interpret a spectrum based measurement of adjacent channel power (ACP) given a finite, if not short, observation interval. Then, using new measurement techniques, we will identify the sources of excess ACP in two different systems: a continuous 32QAM system, and a pulsed PI/4 DQPSK system.

Introduction

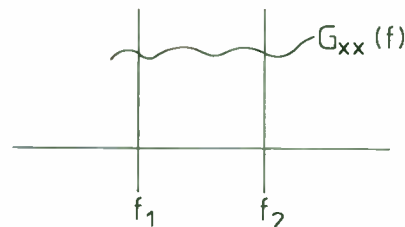
There are almost as many ways to define adjacent channel power (ACP), as there are types of radio systems. Rather than try and describe each, this paper will take a more general approach to ACP measurements with the goal being a better understanding of how to use time-selective ACP measurements to isolate and identify transmitter problems.

The term *adjacent channel power* might lead one to believe that the goal of ACP measurements is to determine the amount of power that a transmitter puts into an adjacent (or alternate) frequency channel. The real goal is to quantify a transmitter's potential for interference. For this reason, the definition of "power" is somewhat variable from system to system. In one system, ACP might be defined as *the peak power at the output of a specified 30 kHz filter centered on the adjacent channel*. In another system ACP may

have exactly the same definition except that instead of peak power, it might use the average power over some specified time interval. Both of these definitions incorporate the concept of time selectivity. In the first example, the signal is observed over a period of time and the peak power level recorded. In the second example, the measurement interval is specified exactly.

Frequency Selective Measurements

Before getting into measurements that are time selective, it's useful to review measurements that are frequency selective only. In these measurements, ACP is typically defined as the power in a channel obtained by integrating the power spectral density function $G_{xx}(f)$ over the bandwidth of the channel. As its name implies, power spectral density is a frequency domain



The PSD function $G_{xx}(f)$ is defined as:

$$G_{xx}(f) = \lim_{T \rightarrow \infty} \frac{2}{T} E[X(f, T)]^2 \quad (1)$$

where:

$$X(f, T) = \int_{-\frac{T}{2}}^{\frac{T}{2}} x(t) e^{-j2\pi ft} dt \quad (2)$$

The power in the channel defined by f_1, f_2 is:

$$P = \int_{f_1}^{f_2} G_{xx}(f) df \quad (3)$$

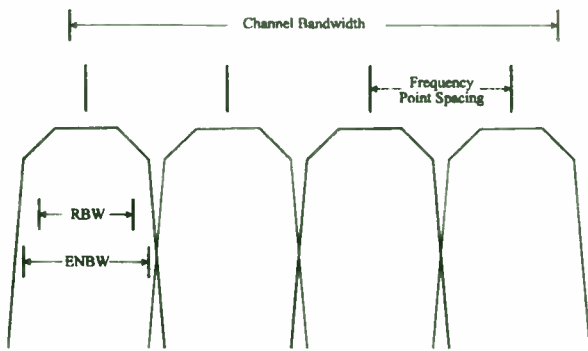


Figure 1. Relationship between frequency point spacing, RBW, ENBW and channel bandwidth.

measure of a signal's power density. It's usually expressed in units of Watts/Hz or dBm/Hz.

The PSD function is defined as the Fourier transform of the autocorrelation function. In practice it's measured using narrow filters – usually the RBW filters of a spectrum or vector signal analyzer. Figure 1 shows how these filters are used to sample the power spectrum. As the filters are usually wider than 1 Hz, the PSD must be computed by dividing the power in the filter by the filter's equivalent noise bandwidth (ENBW). For example, if the power in a 30 kHz RBW filter with an ENBW of 33.84 kHz is -20 dBm, then the PSD at the center frequency of the filter is $-20 - 10\log(33840) = -65.3$ dBm/Hz. This calculation is based on the assumption that the PSD is constant over the bandwidth of the filter. Usually this is true. However, if a signal is periodic, or contains periodic components (as shown in figure 2), then the spectrum will contain discrete spectral lines and the assumption will be invalid.

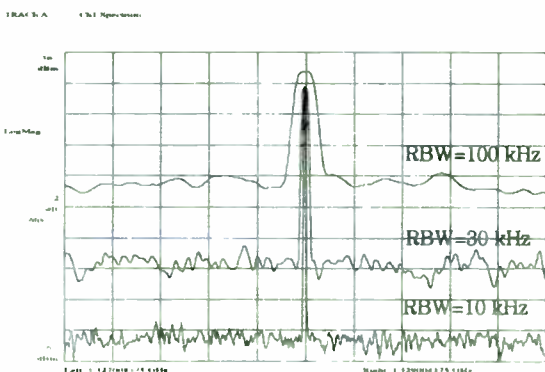


Figure 2. Spectrum measurements of a sine wave plus noise at three different RBW settings. The amplitude of the periodic component is constant.

Figure 1 illustrates several important points. First, the ENBW of a filter describes the bandwidth of a rectangular filter that has the same power response. So, unless a filter is rectangular, its RBW and its ENBW are likely to be different. Second, the frequency point spacing is independent of the filter width. In other words, the filters may be heavily overlapped, or they may not overlap at all. Third, the start and stop frequencies for the channel may not line up with the edges of the filters. When this occurs, the first and last PSD estimates can be affected by energy outside of the channel bandwidth. Obviously, this is more likely to occur with wider filters, or filters with poor shape factors.

Since the PSD is a continuous function and we've measured the function at discrete points, we must use integration techniques designed to work with sampled data, e.g. trapezoidal integration. However, if we assume that the PSD is more or less constant between samples, then we can approximate the integral and compute the total power by summing the powers at each frequency point divided by the ENBW and then multiplied by the span over which that value applies. The span over which each value applies is usually the frequency point spacing (except for the points at the upper and lower edges of the band).

Time Selective ACP Measurements

In theory, it's necessary to observe a signal over an infinite amount of time to determine its power spectral density function. Since infinitely long observation intervals aren't practical, signals are usually observed over shorter periods of time with a corresponding loss in frequency resolution. In general, shortening the observation interval does not degrade the estimate of the PSD provided the signal appears to be stationary (in a statistical sense) within the period of observation. For pulsed signals, this would imply an observation interval that includes many pulses (i.e. many frames of a TDMA signal). If the observation interval is decreased further, beyond the point where the signal no longer appears stationary within the observation interval, then the measurement is said to be time-selective.

For continuous signals, that is signals that aren't pulsed, ACP measurements may provide a good indication of a transmitter's potential for causing interference even if the measurements aren't time selective. However, most receivers have finite memories. In other words, they respond to how energy is distributed in time as well as frequency. For example, if a transmitter that is interfering with a receiver on an adjacent channel is turned off, then the receiver will no longer suffer from the effects of the interference. While this is an extreme example, it does lead us to consider definitions of PSD that incorporate finite, if not short observation intervals. In fact we might conclude that the length of observation should be based, not on the characteristics of the transmitter, but on the characteristics of the receiver.

To gain further insight into time-selective measurements let's use a Fourier transform to look at several signals and their spectrums as computed over different observation intervals.

Consider an unmodulated carrier. It's spectrum contains a pair of impulse functions, one at the carrier frequency, and one at the negative of the carrier frequency (which we'll ignore). If the previously unmodulated carrier is modulated with a single pulse, then the spectrum takes the shape of a sinc function ($\sin(x)/x$) centered at the carrier frequency (as shown in figure 3). We can easily predict this spectrum by observing that the multiplication of the sine wave by a RECT function

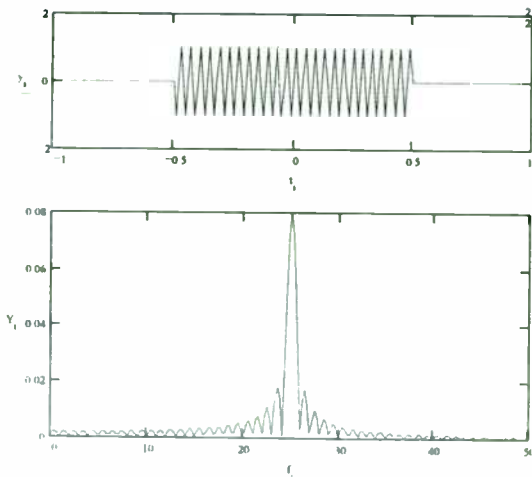


Figure 3. A sine wave multiplied by a RECT function has a spectrum that is a sinc function convolved with a dirac delta

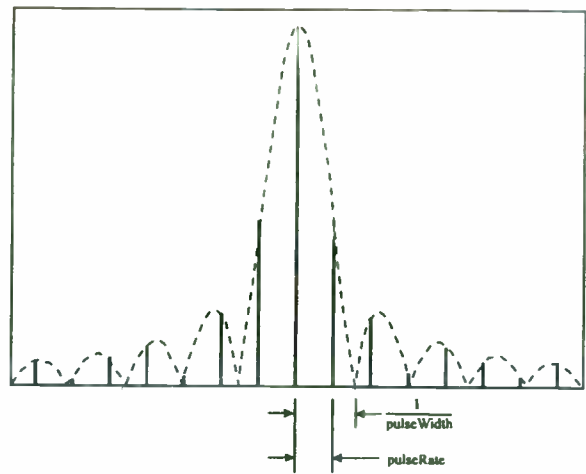


Figure 4. Spectrum sine wave multiplied by a train of RECT functions

in the time domain corresponds to the convolution of an impulse (at the carrier frequency) and a sinc function in the frequency domain.

If instead of a single pulse, the carrier is modulated with a pulse train, then the spectrum will be comprised of impulse functions. The overall shape of the spectrum will remain unchanged provided the pulse width remains unchanged. The spacing of the impulses, or spectral lines, is determined by the pulse repetition rate.

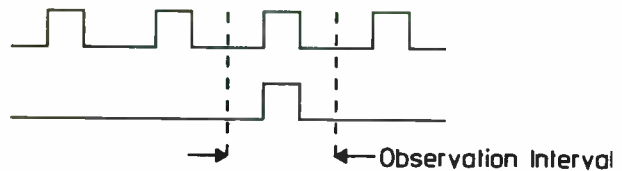


Figure 5. With a short observation interval, the PSD for the pulse train and single pulse can be identical.

The single pulse and pulse train examples illustrate two important concepts. First, the single pulse example can be thought of as a time-selective measurement of the pulse train. In other words, by limiting the observation interval to a single pulse in the pulse train, we get a different spectrum than would be obtained by observing the signal over hundreds of pulses. Second, the pulse train has a spectrum with discrete spectral lines because the signal is periodic. Digitally modulated carriers normally transmit data that is random, however if

the data contains a synchronization word that repeats periodically, then the spectrum will contain discrete spectral lines.

This last signal is designed to show how dramatically different the spectrum can appear when the observation interval used to compute the PSD is changed. In figure 6, the spectrum computed using the entire burst has a null at the carrier frequency. If we limit the observation interval to either the first half or the last half of the burst, we will compute a spectrum that has a shape similar to that shown in figure 3. So, for the same signal, we can make two different measurements – one that shows energy at the carrier frequency, and one that doesn't.

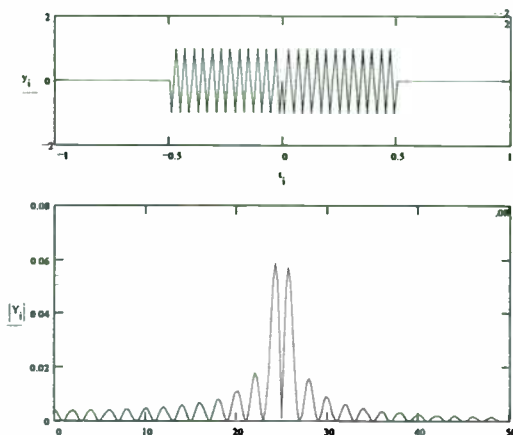


Figure 6. Sine wave multiplied by a RECT function that changes polarity at $t=0$

Practical Time-Selective ACP Measurements

One of the most common time-selective measurements uses a technique called gating. Gated measurements provide a way of limiting the observation interval to specific portions of the time waveform. This technique can be used with both spectrum analyzers and vector signal analyzers. Figure 7 illustrates how gating is used to isolate the spectrum due to the digital modulation from the spectrum that includes the effects of both the digital modulation and the pulse modulation. In this example the on-off transitions of the pulse modulation clearly increase the amount of energy in the adjacent channels.

While this measurement suggests that the on-off transitions are a problem, it's not clear if the

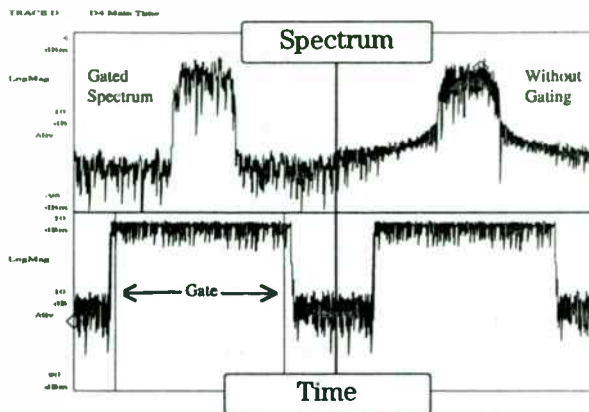


Figure 7. Gating is used to observe the spectrum without the effects of the on-off transitions.

problem is with the rising edge, the falling edge, or both. This information can be easily obtained by simply changing the position of the gate, and perhaps its length, so that gate includes only one of the edges.

Not all ACP measurements are based on measuring, and then integrating, the power spectral density function. An alternative approach defines ACP in terms of the power at the output of a filter that has approximately the same bandwidth as the channel. Three of these filters are shown operating in parallel in figure 8. One filter is centered on the assigned channel and two filters are centered on the upper and lower adjacent channels. The input waveform is a pulse modulated carrier. The output of the detectors give an indication of the instantaneous power in each of their respective channels. Obviously, the results obtained are going to depend heavily on the impulse response of each filter.

Normally, a spectrum analyzer is used to make this type of ACP measurement. The analyzer is configured for zero-span operation with the RBW

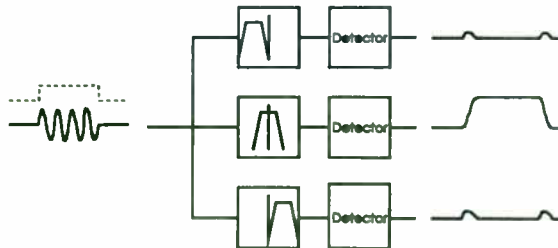


Figure 8. Filters and detectors are used to determine the instantaneous power in the assigned and adjacent channels.

filter acting as the channel filter. Since the spectrum analyzer can only measure a single frequency at a time, each channel must be measured separately. For certain types of ACP problems this may be an acceptable limitation. However, there are many instances where it's desirable to observe the behavior of the assigned channel and the adjacent channels simultaneously. For example, a modulation error may cause the instantaneous power to exceed its designed limits for certain combinations of transmitted symbols. This type of problem will be transitory so it's unlikely that it will appear in both the assigned channel and adjacent channel measurements.

A vector signal analyzer (VSA) can be used to simultaneously view the outputs of hundreds or thousands of parallel filters. By adjusting the bandwidths of the filters, tradeoffs can be made between frequency resolution and time resolution. For example, better frequency resolution may show that excess ACP is due to a spurious signal that couldn't be resolved using the wider channel filter.

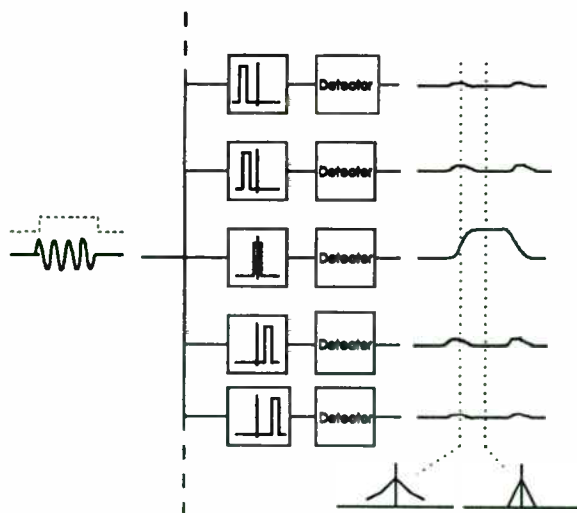


Figure 9. Narrower filters provide better frequency resolution at the expense of time resolution. Spectrums can be constructed from the parallel detector outputs.

The parallel filter, demodulation and display capabilities of the HP 89400 Vector Signal Analyzer will be now used to characterize ACP problems in two digitally modulated signals.

Troubleshooting a 32 QAM Continuous Carrier Signal

Figure 10 contains two spectrum measurements which have been overlaid, one on top of the other. Band power markers have been used to compute the power between the markers for the assigned channel and the upper adjacent channel. The adjacent channel power ratio (ACPR) has been computed for both spectrums. In both cases the measurements were not time selective.

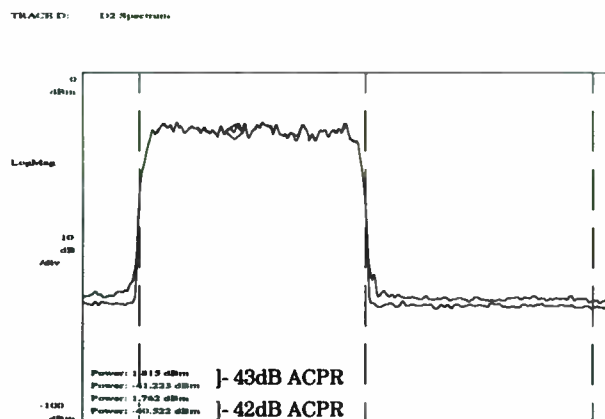


Figure 10. A problem introduces a 1 dB degradation in the ACPR for a 32 QAM signal. This measurement provides little insight into the nature, or seriousness of the problem.

Without time selectivity, this ACP measurement gives little insight into the nature of problem, and may even understate the potential for interference from the impaired signal. We don't know if the problem's due to distortion in the power amplifier, improper filtering of the baseband signals, a defective component, or a coding error in the modulator software. In fact, with only 1 dB of degradation, we might conclude that there isn't a problem.

In figure 9 we showed how spectrums could be constructed from the outputs of the detectors. Although two spectrums are shown, it should be obvious that more spectrums, representing more points in time, can be easily computed. The VSA can display hundreds of spectrums on a single

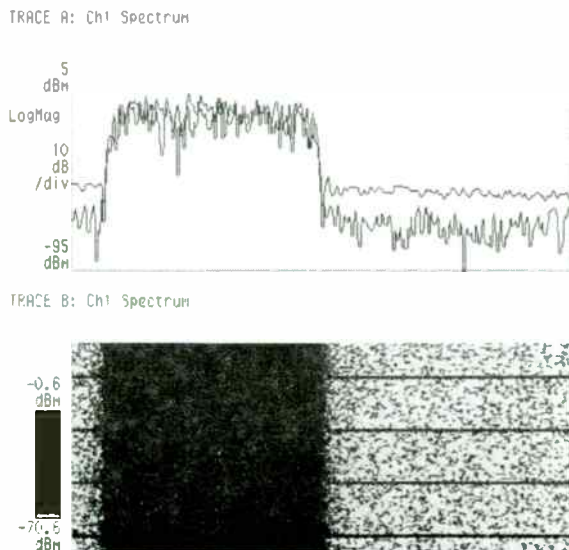


Figure 11. Two time selective measurements in the upper trace show a higher level of ACP than previously observed. The lower trace contains more than 100 spectrum measurements in a spectrogram. It shows that the excess ACP is periodic.

display using a display type called a spectrogram. In a spectrogram, the amplitude of the spectrum is encoded into color or intensity so that each spectrum can be displayed in a single row of pixels. The spectrogram in the lower trace of figure 11 has an x-axis of frequency and a y-axis corresponding to time. As the legend on the left indicates, the amplitude scaling is from -0.6 dBm (dark) to -70.6 dBm (light).

Two separate time-selective measurements of the continuous 32 QAM signal, shown in the upper trace in figure 11, indicate that the excess ACP can be much worse than indicated by the measurement that wasn't time selective. The spectrogram clearly shows that the excess ACP occurs periodically. This rules out several distortion mechanisms, and problems such as improper filtering, and points to an algorithmic problem in the modulator. To isolate the problem further, the VSA's digital demodulator was used to check the quality of the modulation. The error vector magnitude (EVM), which is an indicator of overall quality looks good at 1.6%. However, the peak in the error vector plot in the lower left trace of figure 12 indicates that one symbol is slightly misplaced.

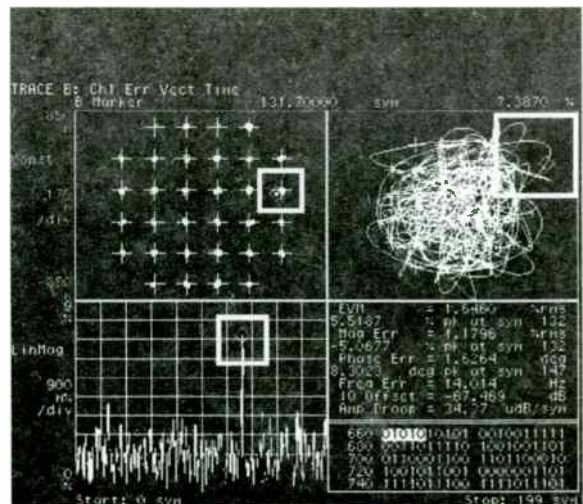


Figure 12. Digital demodulation of the 32 QAM signal uncovers a misplaced symbol in an otherwise clean signal.

From the vector diagram in the upper right trace we see that the symbol with the largest error is associated with a large amplitude excursion. In fact, the error in this system caused the data going to the DAC to be improperly scaled. This resulted in distortion on signals with large amplitudes. In the particular test pattern used, it happened that only one combination of symbols caused amplitudes large enough to exceed the maximum count on the DAC. The periodicity of the ACP was caused by the repetition of the binary test pattern.

Troubleshooting a Pulsed PI/4 DQPSK Signal

In the gated measurement mentioned earlier in this paper, it was determined that the pulse modulation contributed to the signal's excessive ACP. It was also mentioned that the gate could be moved, and possibly shortened, so that only the rising or the falling edge appeared within the observation interval. This would be done to determine which transitions contributed to the ACP problem.

Using the Vector Signal Analyzer it's possible to incrementally move the gate through the pulse and observe the resulting spectrums. Because the gate is moved incrementally, each observation interval is heavily overlapped with the previous observation interval. Although described differently, this is the

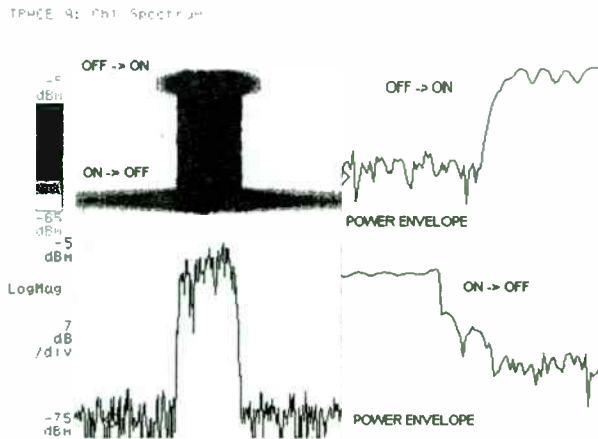


Figure 13. The spectrogram clearly shows how the faster ON to OFF transition affects ACP. The spectrogram and the lower left trace also show that the data modulation portion of the burst is clean.

same *parallel filter* measurement technique that was used to evaluate the 32 QAM signal. The VSA's spectrogram capability will again be used to simultaneously view all of the results.

The measurement results shown in figure 13 clearly show what most power amp designers already know – fast power transitions cause splatter. In this example, there was no attempt to control the on-to-off transition. The result is obvious. What may not be obvious is that the system could have had controlled transitions and still produced a spectrogram similar to the one shown. For example, a phase instability in the carrier caused by the power-on transition coupling into one of the local oscillators could have also caused excessive ACP.

Summary

There are many ways of making adjacent channel power measurements. While specific measurement techniques may be required for compliance testing, other techniques such as those presented here, can and should be used. These techniques are useful in the design lab and on the manufacturing floor. Not only do they provide better visibility into the nature of an ACP problem, but in many cases the measurements requires less time to perform.

The goal of ACP measurements is not to make a *textbook* power measurement, but rather to identify and prevent sources of interference in communication systems. For this reason, the

definitions of *power* and *power spectral density* may vary from the norm. Even terms like *peak power* may not have the usual meaning.

All of the measurements in this paper were made using an HP 89440A Vector Signal Analyzer.

References

1. C. Rhodes, "Measuring Peak and Average Power of Digitally Modulated Advanced Televisions Systems", IEEE Transactions on Broadcasting, Vol. 38, No. 4, December 1992
2. "Frequency and Time Selective Power Measurements with the HP 89410A and 89440A", HP Product Note 89440A-1
3. H. Chen, "Time Selective Spectrum Analysis: A powerful tool for analyzing TDMA communication signals", Hewlett-Packard RF & Microwave Measurement Symposium, 1992
4. J. Gorin, "Make Adjacent Channel Power Measurements", Microwaves and RF, May 1992
5. "Innovations in Spectrum Analyzer Noise Measurements", Hewlett Packard, PN 5091-2316E
6. K. Johnson, "Use spectrum analyzers' selectivity to precisely measure random noise", EDN, March 2, 1992
7. B. Cutler, "Power Measurements on Digitally Modulated Signals", Hewlett-Packard Wireless Communications Symposium 1994

Cost-Effective Frequency Calibration in Field Environments

by
Stuart Jensen
Product Specialist, Diagnostic Tools Division
Fluke Corporation

An increasing need is arising throughout the electronics industry for equipment calibration at locations other than the traditional Cal Lab. This need can be attributed to two main factors. First, requirements for traceable, high-precision calibration result from the need to comply with quality standard demands such as those of ISO 9000. Second, advanced electronic equipment is increasingly being installed in the field, as is the case with the continually growing communications networks, many of which require regular local maintenance and calibration.

These demands create the need for calibration equipment that meets a number of stringent requirements. The equipment must be portable and convenient to use in field environments. Also, the equipment must meet specified standards of accuracy and stability with adequate margins relative to the primary equipment specifications to ensure reliable calibration test accuracy ratios. The equipment must also be relatively immune to a wide range of adverse environmental conditions such as temperature and power instabilities.

In addition, to minimize the cost of ownership, suitable equipment for field calibration must have low maintenance requirements and be able to operate for long periods of time without itself needing to be calibrated.

Frequency Calibration of Clock Systems

Formerly, clock inaccuracies of the order of 1 part per million (ppm) were regarded as acceptable for many installed systems. This meant measuring instruments such as frequency counters with typical errors of 0.1 ppm were considered adequate for "calibration" of these systems; however, increases in the density of activity in allocated bandwidths have tightened the performance requirements on communication systems. Today's higher precision demands require more stringent calibration standards. Clear examples are evident when looking at the strict measurement requirements for TDMA architecture digital communication networks.

Potential Frequency References

Today's frequency counters, equipped with ovenized high-stability timebase oscillators, typically reach an overall accuracy of a few parts in 10^8 ; however, this generally requires they themselves be calibrated at regular two-month intervals. In comparison, the global System for Mobile Communications (GSM) specification requires that Base Station transmitter system clocks maintain an accuracy of $\pm 5 \times 10^{-8}$. To meet these more stringent calibration requirements, even these high-performance ovenized crystal oscillators are not sufficiently accurate.

To obtain this stability requirement, a number of available external frequency references, used in combination with a high-resolution counter, can be considered.

- *Radio-transmitted reference frequency sources*

Radio-transmitted frequency references employ receivers tuned to a broadcast clock reference such as WWVB, GPS, LORAN or others. These receivers then use the broadcast signal as a reference for the instrumentation at the site. The broadcast signal may contain more information than simply a clock reference, such as time of day information. Radio-transmitted frequency signals can be influenced by propagation delay variation and other forms of radio interference. This can cause short-term instability, which makes this form of frequency inadequate as a direct source for external reference. The short-term influences will be of different kinds, depending on

the frequency. Long and medium-wave frequencies will be strongly influenced by the changes in the reflection layer during sunset and sunrise. High-frequency signals will suffer from dispersions and other short-term influences; however, over a long integration period, the stability will be high.

Radio-transmitted reference sources can in many cases provide accuracy better than 10^{-11} . These systems require the reference signal to be acquired and averaged over a period of many hours. These sources can be quite practical in stationary field calibration systems, but are hardly usable in mobile applications.

- *External stand-alone atomic reference oscillators*

A stand-alone atomic reference oscillator is sometimes used the same way as a radio reference signal. Instead of receiving a broadcast standard, the local stand-alone frequency source provides an adequate reference oscillator for the local test equipment. In this manner, the accuracy of the atomic standard is "transferred" to the test equipment used. Both rubidium and cesium-based atomic reference oscillators are available. Cesium standards are generally larger and more expensive, but have truly negligible aging. Rubidium oscillators are less costly and show little aging. Both solutions have limited portability because they require a separate box of significant size and weight.

- *Frequency counter with self-contained standard*

A viable and widely used alternative is provided by the new PM 6685R frequency counter by Fluke. The PM 6685R employs a built-in rubidium timebase that provides high accuracy, quick warm-up and stability in a compact and easily portable form factor. When compared to a crystal oscillator, the rubidium reference is much less susceptible to temperature, mechanical shock, power instability, and physical orientation. Like the stand-alone reference, the aging of the rubidium element is minimal. In addition, the PM 6685R's high-performance, accuracy and stability are reached without long warm-up times (six minutes versus 24 to 48 hours for ovenized

crystals) or battery stand-by support, and does not require frequent recalibration. With an aging of only 0.0002 ppm per year and calibration intervals as long as two years, the built-in reference meets most field calibration requirements within a wide margin.

The actual rubidium timebase oscillator is an atomic frequency standard which behaves differently than conventional crystal oscillators. The frequency determining element is based on intrinsic atomic properties, which results in low sensitivities to temperature, shock, vibration and other environmental influences. Furthermore, the atomic properties are basically time-independent, resulting in excellent long-term aging performance.

Example: GSM Base Station Calibration

A typical example of today's field calibration requirements is the on-site frequency calibration of Global System for Mobile (GSM) communications base stations (BS). Key criteria for these calibrations have been formulated by the European Telecommunications Standards Institute (ETSI) in the GSM 05.10 recommendation. The "Radio sub-system synchronization" guideline reads as follows:

The BS shall use a single frequency source of absolute accuracy better than 0.05 ppm for both RF frequency generation and clocking the timebase. The same source shall be used for all carriers at the BS.

The base station system clock is typically a 13 MHz high-precision oscillator, and is often synchronized to the Central Office master clock system. The base station's own system clock must still be fairly close to the central clock to obtain and maintain network synchronization.

The 0.05 ppm limit results in the following:

- Maximum permissible deviation of ± 0.65 Hz (0.05 ppm in 13 MHz);

- Maximum error at the moment of calibration of the base station approximately 0.26 Hz or 2×10^{-8} (allows for drift between calibrations);
- Calibrating counter to have a maximum error of 0.05 Hz or 4×10^{-9} (as defined by metrology rules, to give a test accuracy ratio of four times between the measured object and the measuring instrument).

Although it is doubtful whether they actually meet the accuracy requirements for this application, quartz crystal oscillator-referenced counters are often used to calibrate GSM base station clocks. However, to come close to the minimum requirements, even a super-high-stability crystal oscillator needs frequent recalibration and battery back-up to maintain the oven temperatures. Furthermore, the strains placed upon the oven/crystal elements due to the practical requirements of actually visiting the BST and setting up the equipment will significantly affect its performance.

High-resolution counters are ideal for performing accurate measurements of frequency and time-related parameters in most high-precision applications, provided the instruments can be equipped with the right timebase option. The latest frequency counters have measuring resolutions of 10 to 12 digits. Such resolutions are not matched by even the best available timebase crystal oscillators.

Choice of Time Base -- The Error Budget

Most high-performance counters have a range of timebase options, from plain crystal oscillators and those which use correction tables based on testing the crystal across its thermal range of operation (temperature-compensated crystal oscillators), to highly sophisticated and expensive oven-enclosed crystal oscillators. To meet the high precision requirements, Fluke and just a few other suppliers offer a rubidium atomic-referenced timebase option for their counters.

The choice of the preferred option must be based on the actual calibration situation. A survey of possible timebase frequencies, features and benefits for high-precision frequency calibration with counters is given in Table 1.

Table 1. High-Frequency Calibration with Counter Comparison

Parameter	Reference Built Into Counter		External Reference Used With Counter		
	High-precision crystal oscillator	Rubidium atomic reference (PM 6685R)	GPS, radio transmitted reference	Cesium atomic reference	Rubidium atomic reference
Short-term stability (1s)	Very Good	Good	Poor	Good	Good
Aging/24h	Good	Very Good	Very Good	Excellent	Very Good
Aging/year	Good	Very Good	Excellent	Excellent	Very Good
Need for cont. operation	Yes	No	Yes**/No	Yes	No
Stability against vibration	Moderate	Very Good	Very Good	Moderate	Very Good
Stability against temp. variations	Moderate	Very Good	Excellent	Excellent	Very Good
Retrace*	Moderate	Excellent	Excellent	Excellent	Excellent
Warm-up time	Long	Very Short	Moderate	Moderate	Very Short
Fundamental wear-out devices	None	Lamp Life (15 years)	None	C ₅ contamination of electron mult. (5 years)	Lamp Life (15 years)

*Relative frequency deviation from a stabilized value before switch-off to the stabilized value after power-on, with a power-off period of e.g. 24 h.

**Continuous operation preferred for maximum accuracy. In case of loss of power and satellite information, a new start-up and acquisition period must elapse before full stability is reached. The time needed for this acquisition depends on the system used.

A timebase can best be selected by developing an error budget, in which all the relevant error elements are incorporated, including the accepted calibration intervals. To meet the specific requirements for the GSM base station frequency calibration, the significance of these elements can be considered. Error elements for the PM 6685R are discussed below.

Sources of errors for a counter's timebase:

The three major sources of error in counters are:

1. ϵ_1 Uncertainty directly after calibration including retracing. Retrace, is the relative frequency deviation after stabilization, compared to the previous value, before a switch-off period of, for instance, 24 h.
2. ϵ_a Timebase uncertainty due to aging.
3. ϵ_t Timebase uncertainty due to ambient temperature uncertainty.

Other sources of error in a counter

1. ϵ_q Counter resolution uncertainty (quantization error).
2. ϵ_n Counter trigger uncertainty due to noise.

Total uncertainty (U) using a Fluke PM 6685R frequency counter

Calculations are based on "Guidelines for Expressions of Uncertainty of Measurements in Calibration" from the Western European Calibration Cooperation (WECC).

Notice the trigger error due to noise, ϵ_n has been left out of the formula since we normally can neglect this error for frequencies above 1 MHz and for measuring times (MT) >1 s.

Under these three error conditions, we can calculate the total uncertainty (2σ) using the following formula*:

$$U_{2\sigma} = 2x\sqrt{\frac{(e_i)^2 + (e_a)^2 + (e_t)^2}{3}} + (e_q)^2$$

*Due to rounding, the LSD displayed may limit the actual readout resolution. For measuring times > 1 s, the overflow or nulling mode will increase resolution beyond the basic 10 digits up to 12 digits.

Table 2. Major Factors Influencing Various Types of Time Base Options

Source of Error		PM 6685R Incl. Osc. Option		
		/04 (TCXO)	/05 (OCXO)	/07 (Rb-osc)
ϵ_i		$\approx 1 \times 10^{-8}$	$\approx 0.5 \times 10^{-8}$	$\approx 5 \times 10^{-11}$
ϵ_a per/	10 days	1×10^{-8}	3×10^{-9}	$< 5 \times 10^{-11}$
	1 month	2×10^{-8}	1×10^{-8}	5×10^{-11}
	3 month	4×10^{-8}	2×10^{-8}	1×10^{-10}
	12 month	1×10^{-7}	7.5×10^{-8}	5×10^{-10}
	24 month	2×10^{-7}	1.5×10^{-7}	7×10^{-10}
ϵ_t	23±3°C	$\approx 2 \times 10^{-9}$	$\approx 0.6 \times 10^{-9}$	$\approx 4 \times 10^{-11}$

Using the figures the previous formula, we can summarize the calculated total uncertainty to a 2 sigma confidence level. The Table 3 lists the results of calibration intervals from 10 days to two years, versus timebase options available for the PM 6685R.

Table 3. Results of Calibration Intervals Versus Time Base Options for the PM 6685R

Total Uncertainty U_2 for:	Oscillator Versions			
	TCXO /04	OCXO /05	Rb-osc /07	
Measuring Time	1/10 s	1/10 s	1 s	10 s
10 days cal. interval	1.7×10^{-8}	0.7×10^{-8}	5×10^{-10}	1×10^{-10}
1 month cal. int.	2.6×10^{-8}	1.3×10^{-8}	5×10^{-10}	1×10^{-10}
3 month cal. int.	5×10^{-8}	2.4×10^{-8}	5×10^{-10}	1.5×10^{-10}
12 month cal. int.	1.2×10^{-7}	9×10^{-8}	8×10^{-10}	6×10^{-10}
24 month cal. int.	2.3×10^{-7}	1.7×10^{-7}	1×10^{-9}	8×10^{-10}

Calculation of requirement for the counter's time base accuracy:

- Maximum allowed GSM base station clock deviation according to ETSI:

$$0.05 \text{ ppm } (5 \times 10^{-8})$$

- To allow for aging and other environmental influences, equipment is often calibrated to a margin of three times its operational requirement. The final maximum adjustment deviation after calibration will then be:

$$5 \times 10^{-8} / 3 = 1.5 \times 10^{-8}$$

- It is common metrology practice that a 4 to 1 margin between the measured elements performance requirement and the measurement equipment's performance is maintained. This means the frequency counter's maximum error should be:

$$1.5 \times 10^{-8} / 4 = 4 \times 10^{-9}$$

Built-In and External Timebase References for High-Precision Frequency Calibration by Counters

The error budget calculation shows the defined inaccuracy requirement of 4×10^{-9} is close to impossible to achieve with a normal crystal oscillator and with instrument calibration intervals of two months or longer. Formerly, when alternatives were limited, users had to simply accept the fact that normal crystal oscillators were not capable of fully meeting industry requirements. They had to analyze the error sources and try to minimize the errors that could be influenced. Aging, for example, could only be minimized by frequent calibration of the counter.

The initial error due to setting accuracy and retracting, a dominant element, can be reduced through careful alignment and continuous operation using built-in batteries. In this way, it would theoretically be possible to reach a total error of $<4 \times 10^{-9}$, but it would only be achievable by re-calibrating every 10 days.

The required performance can easily be reached with the rubidium oscillator version available in the PM 6685R frequency counter.

Significant benefits of the PM 6685R for field calibration purposes include the following:

- Meets and exceeds the required accuracy after only six minutes of warming-up time;
- Meets the required specifications with a wide margin, providing ample room for environmental influences and adjustment tolerances;
- Itself, has low calibration costs, due to long calibration intervals;
- Requires less maintenance and has easier handling than a battery-equipped counter with a normal high-stability crystal oscillator;
- Is virtually insensitive to environmental influences such as vibration, shocks and temperature variations.

For GSM base station frequency calibration and maintenance, the rubidium timebase-equipped PM 6685R offers an excellent fitness for purpose. Thanks to its high overall performance, the PM 6685R is also ideal for other highly demanding field frequency calibrations. In spite of a higher initial cost, the PM 6685R will in the long run give an overall low cost of ownership with extended calibration intervals of up to two years.

Testing data communications systems

W. David Tarver
Telecom Analysis Systems, Inc.
34 Industrial Way East
Eatontown, NJ 07724
Phone: (908) 544-8700
FAX: (908) 544-8347

Data communications via wireless media are becoming a more and more important factor. Wireless communications are subject to the unique characteristics of the RF channel, including attenuation, fading, and multipath distortion. Successful communication requires properly designed radios and proper baseband signal processing.

At TAS, a system has been developed for evaluating the performance of wireless data communications devices. This system includes a new device for emulating the RF channels, and a new performance measurement means for measuring bit error rate and throughput. Using these devices, it is possible to take performance measurements on some commercially available communications products.

Results will show significant variation in the performance of commercial wireless communications devices. These differences are due to both radio design and baseband signal processing issues.

Evaluating Communications Systems and Components Under Multiple Signal Conditions

**Tim Carey
Hewlett-Packard Co.
PO Box 58059
Santa Clara, Ca. 95052**

Abstract

All communications systems operate in multiple signal environments containing desired and unwanted signals. Understanding how a system, sub-system or component will perform when exposed to this harsh environment is vital to insuring successful operation and customer satisfaction. To date, system designers have used computer simulations and time-consuming field trials to evaluate the actual operating conditions found in real use. Due to the difficulties and high costs associated with generating realistic multiple signal environments, limited hardware testing has been employed in the laboratory. A new signal simulation system is available that can generate the multiple, high-precision adjacent-channel, co-channel and out-of-band signals required for fast hardware testing at a cost that places this capability in the hands of almost any development team. This paper describes several measurement applications including carrier sensing, receiver blocking, dynamic range and distortion testing which require a multiple signal stimulus.

1. Introduction

Frequently the testing of wireless communications devices and systems requires the generation of multiple RF test signals. Examples include pre-compliance testing in

R&D prior to sending units to a standards lab for type approval and full compliance testing. Performance verification prior to releasing a design to production usually involves field trials since this is an accurate method of determining real operational performance. Of all the signals used in wireless device and system development, multi-signal stimuli are the most difficult to set up; and multi-signal tests are the most expensive and time-consuming to run. The following paragraphs highlight some of the more common multi-signal tests as well as describe how advances in digital signal synthesis can make these tests easier and more cost effective.

2. Intermodulation Tests

Because most wireless appliances operate in dense signal environments, intermodulation (IM) distortion is a critical performance specification. IM distortion is caused by third-order and higher non-linearities in the signal path, usually in amplifier stages, especially receiver RF and IF amplifiers, transmitter output power amplifiers and semiconductor T/R circuits. Signals entering these circuits are linearly processed but are also subject to unintentional mixing action due to the non-linearities. The results are signals that occupy one or more channels that the same or another device is to receive. These signals limit the receiver's sensitivity to desired signals on the channels. Signals producing the interfering intermodulation products may be in-band (other channels in the same system) or out-of-band

(other services in other frequency allocations). If these signals are not sufficiently attenuated by a receiver's early selectivity, they can enter the first amplifier stage and generate intermodulation products. In the case of base station power amplifiers, the signals of several channels can mix causing new signals to be radiated on occupied or unoccupied channels. Since in-band signals are usually not attenuated in either system receivers or the base station power amplifiers, these signals are primary candidates for examination. In addition, the signal density in heavily-used systems means that there are many combinations of signals than can generate IM distortion.

All cellular systems (GSM, DECT, NADC etc) have specifications governing intermodulation performance in their system standards. These specifications also describe the test methodology including the channel allocations to be used in the testing. For example, the DECT standard has two separate IM tests. The first describes intermodulation generated in base station power amplifiers (transmit side) and the second in personal receivers. The DECT receiver IM test is described graphically in Figure 1. A communications link is established between a base station simulator and the device-under-test (DUT). Two potential interfering signals are generated, one with DECT modulation and the other as an unmodulated, continuous-wave (CW) signal. The signal level of the interferers is raised until the the measurement performance parameter is degraded below specification. Note that in digital transmission systems the performance parameter is Bit Error Rate (BER).

Traditionally engineers have relied on two-tone or three-tone IM tests. These stimuli were easier to generate and control than multi-channel signals. The utility of these signals was enhanced by their fit in theoretical

models to estimate the IM performance of a design. Their drawback is that in multi-channel systems these models tend to under-estimate the IM that would be generated. The advent of powerful circuit and system analysis software has enabled the calculation of device and system IM performance in environments containing multiple signals ($N > 3$). Until recently the actual hardware testing of such devices has depended on using a limited number of signals in the lab combined with time-consuming and costly field testing. However, new technology allows multiple signal testing in the laboratory that simulates the actual multiple signal environments encountered in field trials.

The best example of the movement toward multi-signal testing is IM testing in base station transmitter power amplifiers. As the design of base stations has evolved from separate amplifiers for each channel to multi-channel amplifier architectures, multi-tone (multiple CW carriers) testing has become the standard for channelized systems. [1]

3. Receiver Blocking and Dynamic Range

Another multiple-signal measurement application is receiver dynamic range. Sensitivity can be degraded by strong adjacent or alternate channel signals that overload linear stages in the RF or IF sections of the receiver. Bias conditions can be altered by extremely strong signals. Instantaneous dynamic range is the difference between the minimum discernable signal (MDS) a receiver can process in a single signal mode and the level of one or more additional strong signals that causes the MDS to degrade.

Receiver dynamic range is measured by establishing a traffic link between a base station simulator and the DUT at a level slightly higher than the MDS. One or more strong signals are

also generated on selected channels and their levels are varied to determine the receiver dynamic range. Dynamic range measurements are usually performed with static signals from which estimates are made to determine performance under the time-varying power levels encountered in actual operation. Figure 2 depicts a typical receiver dynamic range test scenario.

4. Channel Access

Many wireless systems have standards governing how a user may access a channel. Traffic collisions are minimized by frequency multiplexing and time multiplexing techniques. Nonetheless, some systems have adopted protocols where a base station or user appliance must listen before transmitting on any potentially open channel. These protocols are included in the system standard along with compliance tests to ensure that all devices meet the performance specified. For example, the Japanese Personal Handy-Phone System (PHS) specifies a carrier-sense test that evaluates a device's ability to sense other carriers on each of the system's 77 channels. Signal level thresholds are specified that determine if a channel is to be considered busy or open. The station seeking system access must locate an open channel prior to initiating a transmission. Figure 3 demonstrates the three possible test states for this multi-signal environment. All devices submitted for compliance with the PHS standard must prove that they can differentiate between open and occupied channels correctly.

Generating a 77 channel spectrum is not easy and generating one that acts dynamically is even more difficult. The thought of systems with 77 oscillators or signal generators may be a instrument manufacturer's dream but is a test engineer's nightmare! How are PHS test engineers measuring compliance with system standards?

The unlicensed Personal Communications System (UPCS) standard being developed in the U.S. also has a listen-before-transmit specification. Rather than using separate carriers to load busy channels, the UPCS standard will require the generation of broadband noise interspersed with CW carriers. Several notches are generated in the noise spectrum to establish "windows" for the CW carriers. The CW carrier levels must be precisely controlled as they determine the test threshold. Figure 4 depicts the UPCS test. Generating precisely flat broadband noise power levels and multiple simultaneous carriers poses significant challenges regarding accuracy, repeatability and distortion. How do the authors of the UPCS standard envision generating this complex signal?

5. Dynamic Signal Environments

One key advantage of field testing is that the signal environments to which a DUT is exposed are dynamic; i.e they vary with time and with the position of the DUT relative to their sources. While dynamic environments can be generated with modern computer simulators, laboratory hardware testing has had to be content with static signal environments or dynamic signals on only a few channels. Laboratory testing has sacrificed the realism and stress of the field trial for ease of test generation.

Signal sources with the capability of generating dynamic signal environments are feasible using modern digital signal synthesis technology. An example is the HP E2507A Multi-format Communications Signal Simulator (MCSS). Most modern digitally modulated signal sources generate only the in-phase and quadrature baseband signals using digital techniques. In the MCSS, the entire complex-modulated RF signal is generated

digitally. This technique delivers unprecedented signal fidelity and accuracy and provides the capability to generate multiple signal environments. The system firmware calculates the data sequence to be used, the filtering to be applied and performs the FFT and IFFT operations needed to generate single complex-modulated signals or multiple complex-modulated signal environments. Dynamic environments are generated by storing several variations of each channel and sequencing through the variations on all channels in a pre-determined manner. Systems like the MCSS can generate multiple independent channels with a single user-interface and a single RF output port.

Since the entire multiple-channel signal is calculated and generated at RF in one step, the sources of IM and other signal degradations are minimized. The performance of the output digital-to-analog converter (DAC) is critical to the quality of all digital signal generators. Dynamic range, spurious signal levels, IM performance and signal fidelity and accuracy are directly affected by DAC non-linearities, quantization errors and monotonicity. In the HP MCSS special "de-glitching" circuits at the DAC output enable generation of 32 simultaneous carriers with IM levels typically below -70 dBc.

The limitations of such architectures include finite memory length which impacts the length of the modulation data sequence, the scenario length in dynamic mode and the maximum number of channels generated. Long scenarios or the need for formatted and pre-ambled data sequences on the channel of interest may necessitate the use of a separate on-channel signal source. Instruments like the MCSS would be used to generate the "background" or adjacent channel signals in a multi-signal environment.

Another limitation is the finite bandwidth of the digital synthesis which depends on the speed of the system clock. This "instantaneous bandwidth" determines the frequency range over which multiple simultaneous signals can be generated as well as the maximum symbol rate which can be accommodated. As digital signal synthesis hardware evolves we should see many of these limitations disappear or be greatly reduced.

The power of systems like the MCSS is that the realism and stress of actual operation can now be duplicated in the laboratory at a fraction of the time and cost of field testing. In addition, these systems offer almost perfect repeatability ensuring that tests and test results can be duplicated in different locations or at different times. Real improvements are easily determined because the stimulus can be repeated accurately and easily as often as required. Lastly, these systems add powerful capability to existing test equipment and test facilities without necessitating the replacement of existing investments.

6. Summary

Several multiple signal tests included in almost every wireless system standard were described. The nature of these tests necessitates that multiple signals be available to stimulate the device-under-test. Recent advances in digital signal synthesis technology now allow easy generation of these multi-signal test environments. The advantages and limitations of these new stimuli were described. More products of this type and capability will appear as the capability and value of these instruments is recognized. The primary value of these instruments is that they can bring the realism and stress of actual operation into the laboratory at significant savings of time and cost compared to field testing or traditional multiple generator systems

[1] David R. Koberstein, "Evaluating Communications System Performance in Multiple Signal Environments", *Hewlett-Packard Wireless Communications Symposium*, 1994.

Figure 1. DECT Receiver IM Test

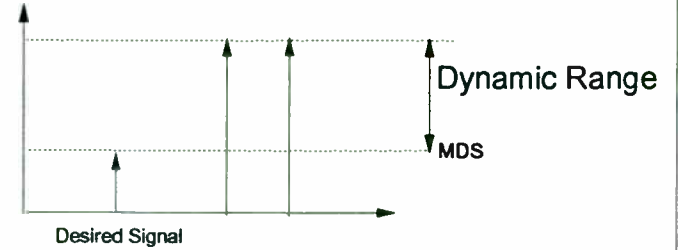
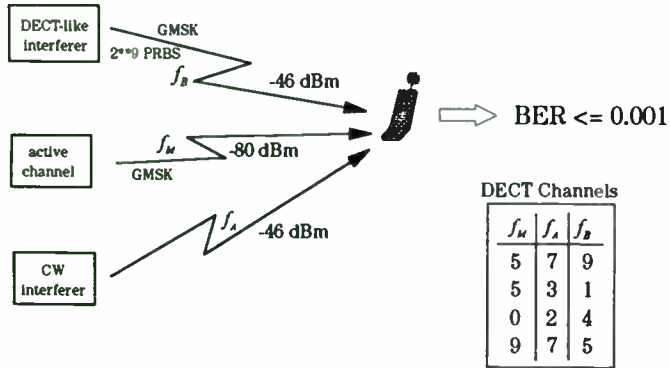


Figure 2. Instantaneous Dynamic Range (Desense) Test

Figure 3. PHS Carrier Sense Test

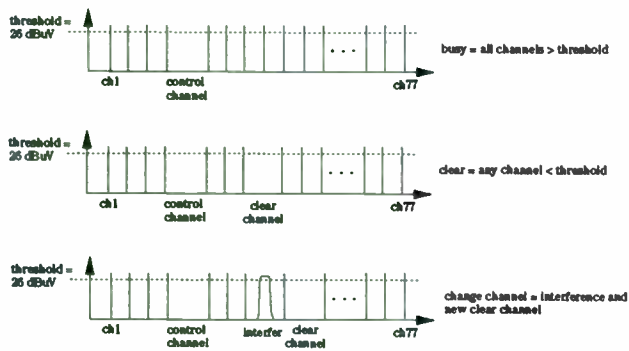
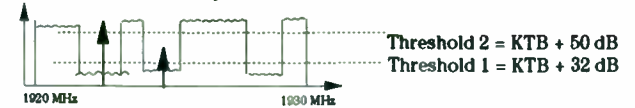


Figure 4. UPCS (Unlicensed PCS) Channel Access Test

Sub-band 1: Asynchronous Systems



Sub-band 2: Isochronous Systems



if $P_{ch} < \text{threshold 1}$ then clear, $P_{ch} > \text{threshold 1}$ then busy
 if busy, find channel with smallest $P_{ch} < \text{threshold 2}$

New Wafer Probing Technology for High-Speed Digital and RFIC Testing

By Ken Smith, Reed Gleason, and Eric Strid
Cascade Microtech, 14255 S.W. Brigadoon Ct., Beaverton, Ore. 97005

Future cost reductions in wireless hardware require ever-increasing IC integration. Conventional needle-probe technology cannot keep up with the development of large, fast ICs and MCMs. Using thin-film technology, Cascade Microtech has developed a new cost-efficient wafer probe with 108 signal lines, 20 GHz bandwidth, and power and ground lines with much lower impedance than needle probes. The probe includes a user-replaceable core, custom designed for a particular IC's pad layout. The probe can provide a clean 50-ohm die interface, or can emulate package parasitics and impedance-matching networks. This paper discusses test results from three different applications of this new wafer-probing technology.

This paper presents test results from three applications: a TriQuint telecommunications demultiplexer, a Rockwell 3 GB/s analog-to-digital converter, and a cellular phone switch application. These three companies have used the membrane probe's 20 GHz bandwidth, oscillation-free power supplies, and production friendliness to improve quality, cost, and accuracy of their test strategies.

I. TRIQUINT DEMULTIPLEXER

"Cascade's membrane probe technology gives us the ability to do wafer-level, at-speed testing of our high data rate devices in a production environment. This will help significantly reduce overall manufacturing costs of very high performance digital devices," says Dr. Gordon Roper, chief engineer for TriQuint Semiconductor.

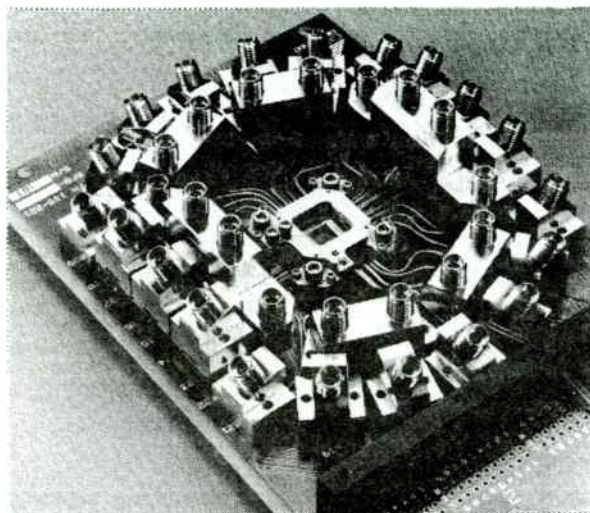


Figure 1. Cascade membrane probe and probe card

Dr. Roper first used Cascade's membrane probe to test one of TriQuint's established products, a telecommunications demultiplexer designed to operate at a data rate of 1.244 Gbit/sec. His goal was to establish a "known-good-die" (KGD) test strategy which could be applied to other telecommunications products operating at 2.4 Gbit and beyond. Using Cascade's membrane probe, Dr. Roper was able to fully test demultiplexer die in wafer form at the rated speed of the device. Being able to guarantee KGD is a strategic value TriQuint plans to deliver to its MCM customers. This test capability will also significantly reduce scrap costs for devices fabricated in more conventional high performance packages.

A. Design Criteria

To test his design, Dr. Roper needed 19 signal lines with rise times as fast as 70 ps and excellent power bypassing for the 10 single ended output drivers. Cascade's membrane probe supplies 108 signal lines, and allows up to 36 lines with a 20 GHz bandwidth. Low-impedance power planes with on-board bypassing provide state-of-the-art power supplies. Figure 1 shows the membrane-probe card Cascade built for TriQuint's application.

The major criteria for qualifying Cascade's membrane probe are listed below along with the relevant probe information:

1. **Input/output signal integrity goal:** Clean monotonic edges with less than 5% preshoot and overshoot at the IC pad with a source rise time of 100 ps.

Membrane probe specified bandwidth: 20 GHz with less than 80 mrho reflections with a 35 ps TDR

2. **Rise/fall time preservation:** Clock and data edges delivered to the IC with less than 200 ps rise and fall times.

Membrane probe specified rise time: Less than 30 ps (shown in Figure 2)

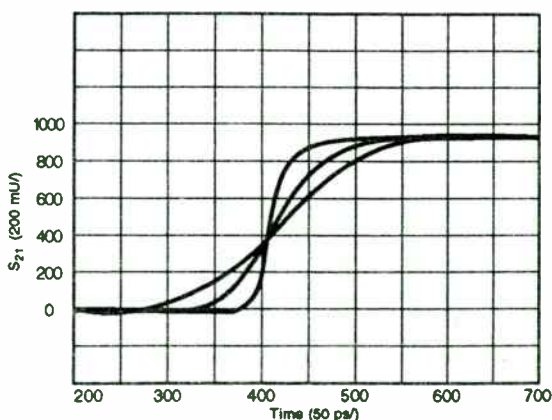


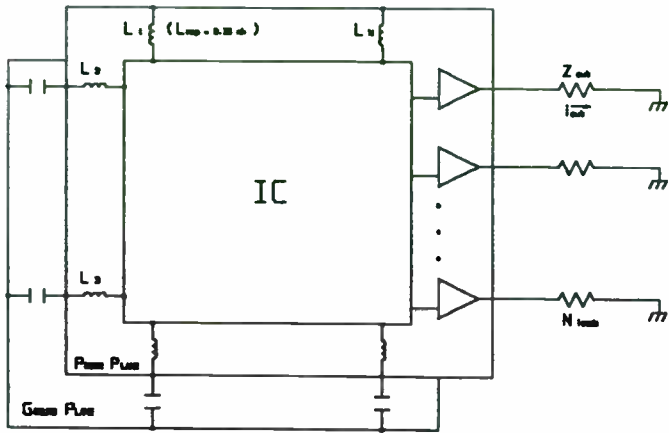
Figure 2. Transmitted pulses (TDT) with 30, 100, and 200 ps rise-time input step

3. **Compatible with wire-OR multiplexing strategy.** This requires fly-by or loop-thru termination routing, with the stub from the loop to the IC not degrading signal integrity.

Probe capability: Unlike traditional wire/needle probe cards, the lithographic microstrip construction of the membrane probe allows TriQuint to create a loop-thru on the membrane itself. This loop can pass directly over the IC, or even out the opposite side. SPICE simulations indicate that a stub less than one-sixth the rise time creates minimal aberrations. The stub length on this design is one sixth of the expected 100 ps rise time, or about 17 ps.

4. **Output driver signal integrity goal:** Ten 50-ohm output signals with less than 5% aberrations. The output drivers are single ended outputs with 175 to 250 ps rise and fall times. They are all driving 50 ohms so the bypass circuitry required is very demanding.

Probe power-supply bypassing capability: The interconnect to the bypass capacitor can be modeled either as a lumped power-supply inductance (Figure 3) or as a distributed transmission line (Figure 4). Either method is sufficiently accurate for most applications. The distributed transmission line model is more accurate above a few gigahertz, especially for analog or broad band applications. The transmission line model has been evaluated with SPICE simulation, but the lumped model can be readily calculated as shown.



$$L_{\text{power}} = \frac{L_{\text{cap}}}{N_{\text{caps}}} = \frac{0.35 \text{ nh}}{8} = 0.044 \text{ nh}$$

$$di_{\text{out}} = \frac{dV_{\text{out}}}{Z_{\text{out}}} = \frac{1 \text{ volt}}{50 \text{ ohms}} = 0.02 \text{ amps}$$

$$di_{\text{load}} = N_{\text{loads}} \times di_{\text{out}} = 0.2 \text{ amps}$$

$$V_{\text{bounce}} = \frac{L_{\text{power}} \times di_{\text{load}}}{dt} = \frac{0.044 \text{ nh} \times 0.2 \text{ amps}}{250 \text{ ps}} = 3.5\%$$

Figure 3. Lumped power supply model

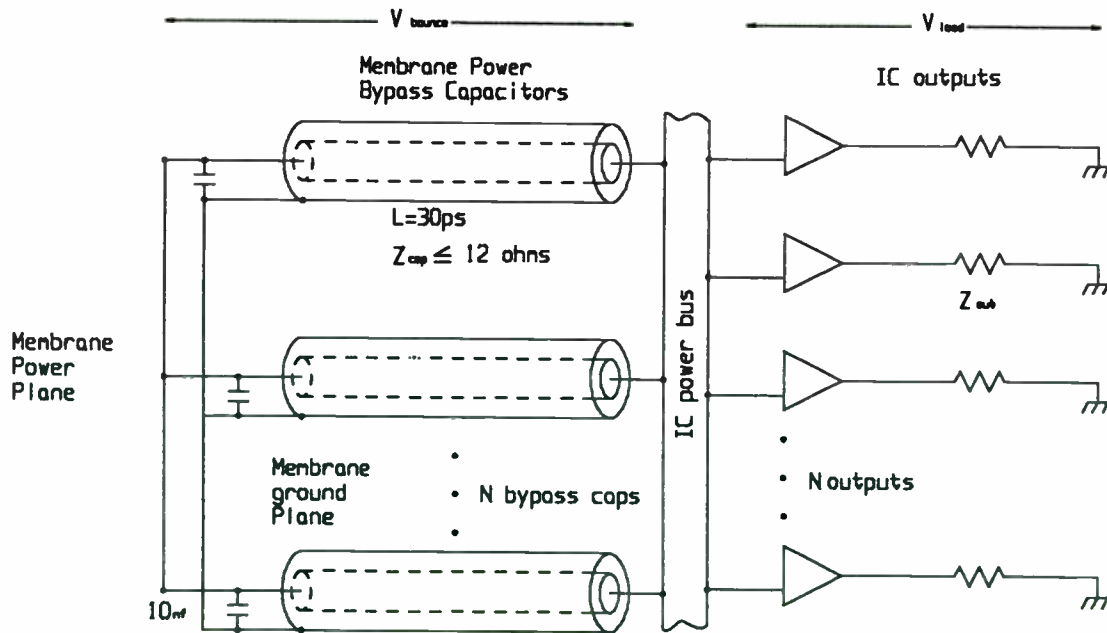


Figure 4. Distributed transmission line model

With 10 drivers being driven, clean resonance-free power to the IC is essential. Each of the 8 bypass structures in the lumped model measure less than 0.35 nH. Since they are in parallel, the effective inductance is less than 0.06 nH. Due to the patented ground and power planes and the 8 on-board power bypass capacitors (see Figure 5), the measured power supply bounce is less than 5%.

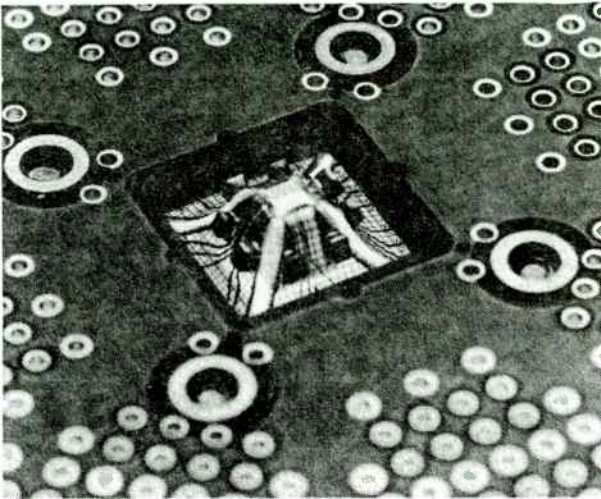


Figure 5. Bypass capacitors within 30 ps of IC bond pads provide the required ground and power bounce performance

B. Probe Evaluation

1. Test System. The target test system is the HP 83000, which clocks the DEMUX at 1 GHz by using a fly-by or loop-thru termination strategy that maximizes the clock speed deliverable to the IC under test. Two drivers are run at 500 MHz and wire-OR multiplexed together with 25% duty cycles to provide a 1 GHz clock. The drivers terminate each other in 50 ohms. An HP 80000 high speed pattern generator was used for signal integrity measurements in qualifying the membrane probe because of its ability to clock at 1 GHz, 50 ps rise time, and its ease of set up.

2. DEMUX Layout. Eight bypass capacitors are each within 30 ps of the IC bond pads and are connected by low-impedance triangular structures that have a typical impedance of 12 ohms. The ceramic capacitors are available in values from 25 pf to 10 nf. The 10 nf capacitors demonstrate the best performance for most applications in both SPICE model studies and in measurements, and are used for all 8 nodes in this design.

Each RF line is designed as a Ground-Signal-Ground contact at the interface between the membrane and the circuit board. They are routed as microstrip from the circuit board transition down to the IC. The electrical length of the stubs on the loop-thrus is 17 ps, about one-sixth of the expected 100 ps edge rates of the HP 83000 target test system. Figure 6 shows the membrane probe layout with the loop-thrus on the bottom.

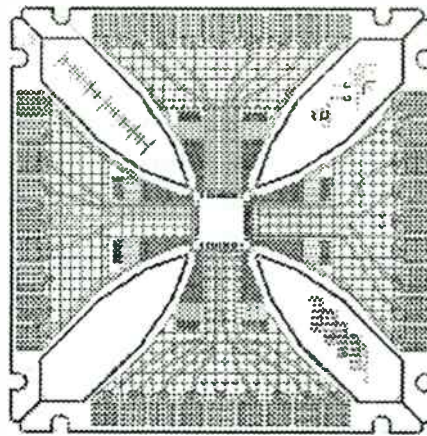


Figure 6. TriQuint membrane probe layout

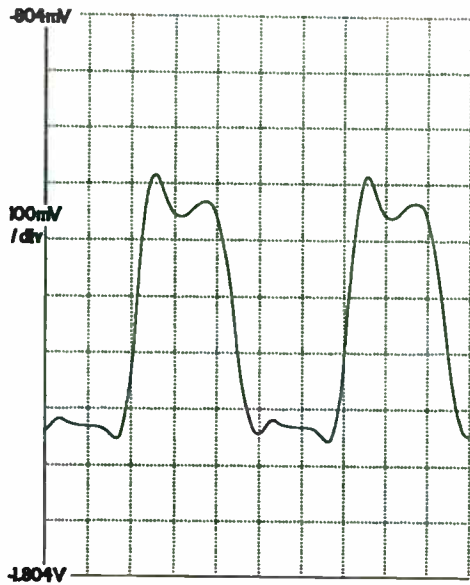


Figure 7. Source signal (200 ps/div.)

3. **Electrical Data.** Figure 7 shows the source signal with 1 meter of cable connected from the HP 80000 data generator system to an oscilloscope. The critical parameters are: rise time of 53 ps, fall time of 80 ps, and clock frequency of 1.0 GHz.

In Figure 8, the first trace shows the clock signal fed back to the oscilloscope from the loop thru on the probe card. Skin effects with the total cable length of 4 meters cause most of rise and fall time degradation to 72 and 100 ps. The second trace shows the same loop thru when in contact with the IC. The IC load slows rise and fall times by an additional 6 ps. The signal is monotonic and has less preshoot and overshoot than the input signal. This demonstrates no measurable reflections with the 72 ps edges.

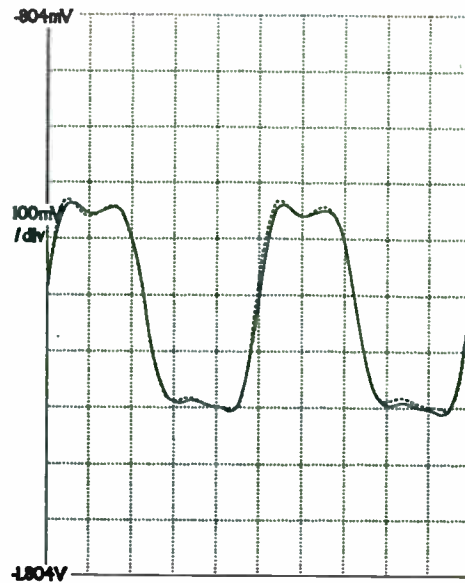


Figure 8. Clock signal from probe-card loop thru (200 ps/div)

Figure 9 shows that the critical signal path on the divide-by-4 clock output matches the expected rise and fall times of the output drivers in the 200 ps range. The trace shows no preshoot, ringing or other signal integrity problems.

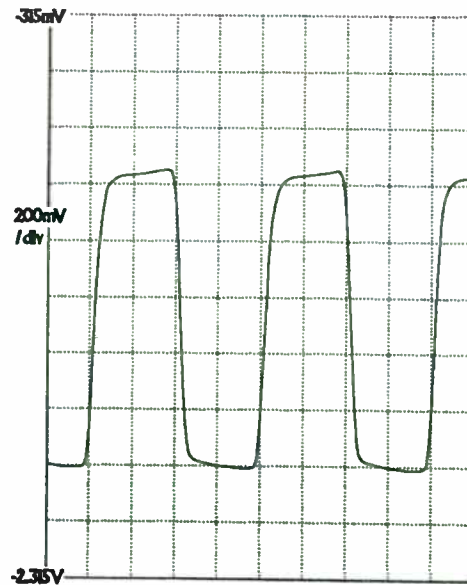


Figure 9. Divide-by-4 clock output signal (1 ns/div)

In Figure 10, the D6 data line shows near-ideal signal integrity, no crosstalk or power/ground bounce effects. This was the typical performance of the parity and other data lines.

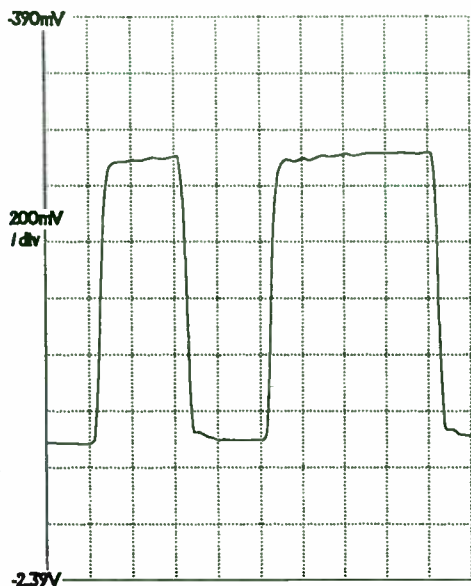


Figure 10. Typical data line (2 ns/div)

C. Future Test Plans

Cascade Microtech's Membrane probe met all the evaluation criteria, and TriQuint has included the membrane probe in their next generation test plans.

Dr. Roper is currently working on TriQuint's next generation of MUX and DEMUX ICs. The next design has 17 RF lines clocking at 2.5 GB/s and uses the same bypassing structures as the probe qualified in this study. Using the high-density standard probe card with 36 RF contacts allows the probe card to be upgraded to new designs simply by dropping in a new membrane core, as shown in Figure 11.

II. ROCKWELL 3 GS/S 8 BIT ANALOG-TO-DIGITAL CONVERTER

A-to-D converter designer Kevin Nary's biggest test challenge was to keep ground and power supplies noise free for 8-bit accuracy with 3 gigasamples per second (GS/s) data output rates. Multiple bypass capacitors on each power supply were needed, along with chip-crossing power buses on the membrane internal to the bond pads (see Figure 12). To improve power-supply noise rejection, analog supplies were kept separate from the digital supplies and bypassed to each other rather than ground. SPICE models of the entire power structure allowed circuit optimization resulting in successful on-wafer test to the full specification of 3 GS/s. Temperature tests

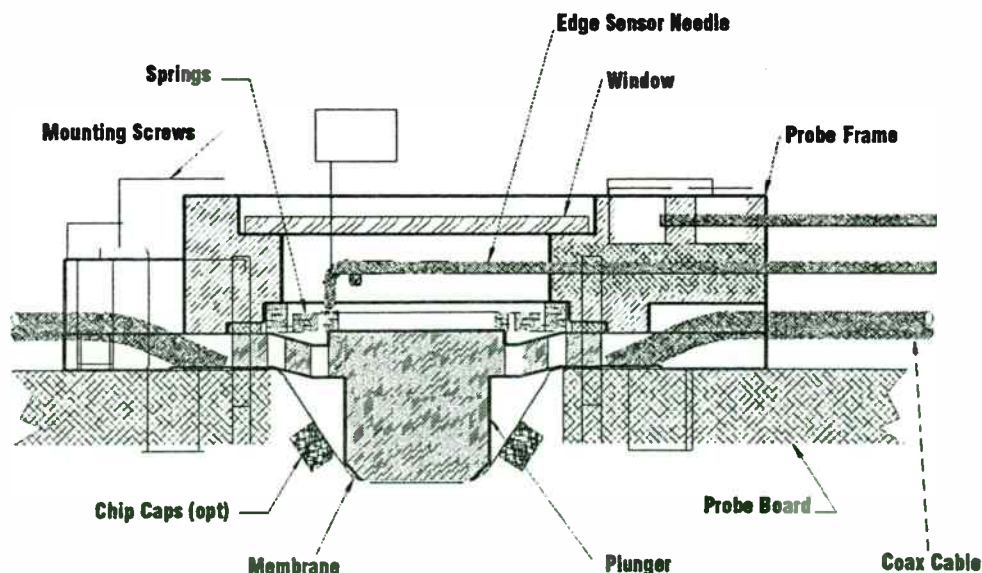


Figure 11. Replaceable membrane core

indicate less than 0.2 bits of accuracy loss at 100°C and half a bit through 125°C. Nary's current work focuses on a demultiplexer to interface the ADC to slower data-rate circuits. For more information on these products contact Lori Budnick at (805) 375-1256.

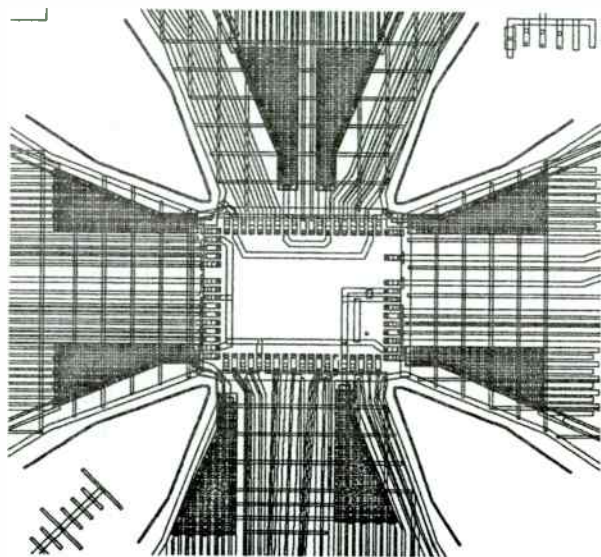


Figure 12. Membrane probe for Rockwell

III. CELLULAR PHONE TRANSMIT/RECEIVE SWITCH

Isolation when the switch is turned off and loss through the switch when it is turned on are the two most critical operating parameters for cellular phone switches. Figures 13 and 14 show that this switch has nearly double its rated performance when measured on wafer as it has in package measurements. The package reduces isolation from 35 dB to 20 dB at the 900 MHz operating point, and loss deteriorates from only 0.3 dB on wafer to 0.5 dB in the package. Improved packages or integration into an MCM are two possibilities to take full advantage of the semiconductor technology. Attempts are underway at many fabrication facilities to relate RF performance and DC parameters to reduce test cost, but correlation is elusive so far.

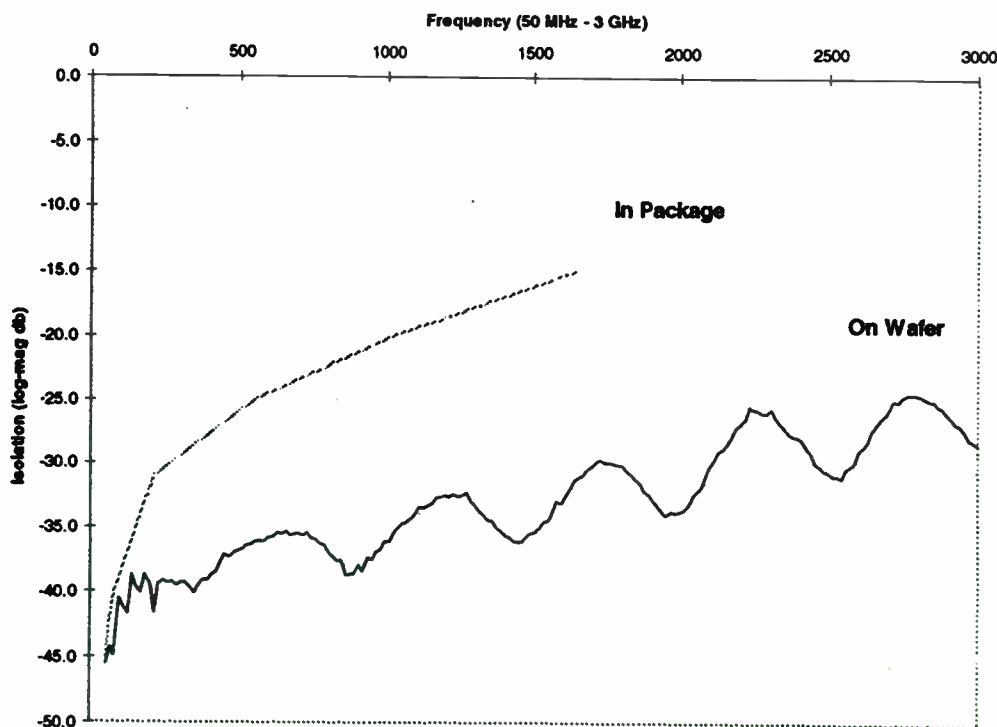


Figure 13. RF switch isolation on-wafer vs. in-package

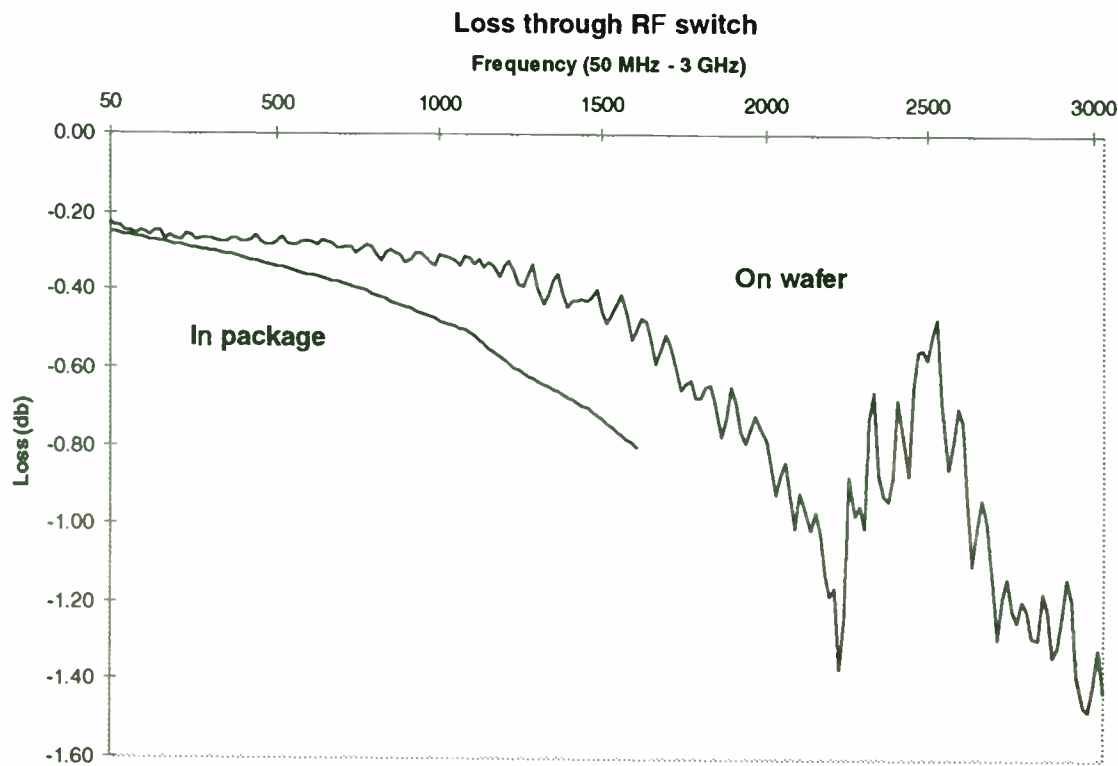


Figure 14. RF switch loss on-wafer vs. in-package

IV. DESIGNED FOR PRODUCTION

Over 1 million contact cycle reliability on gold pads has been demonstrated with no planarizing or alignment required. User replaceable probe cores combined with robustness and self-planarization save time and money in production environments. Cost per test for replacing the core ranges from three-tenths to one-half cents per contact. Figure 15 shows the nickel alloy bumps after one million test cycles. No wear is seen, but a few microns of gold accumulate on the contact surface. Figure 16 shows typical resistance on nine lines for 1000 consecutive contacts after one million cycle life test. The probe demonstrates like-new performance with only 0.002 to 0.005 ohms of contact resistance variation.

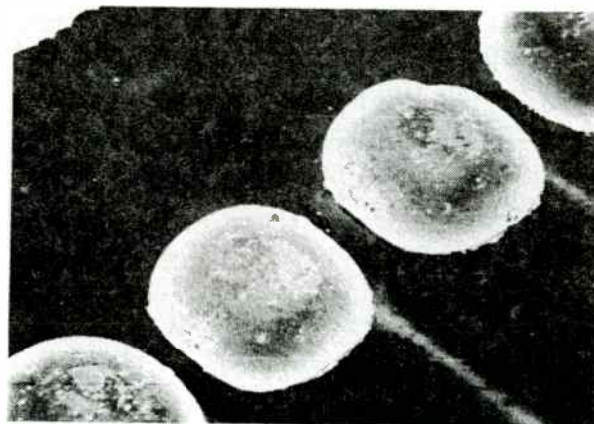


Figure 15. Wear on probe contact bumps after 1 million test cycles

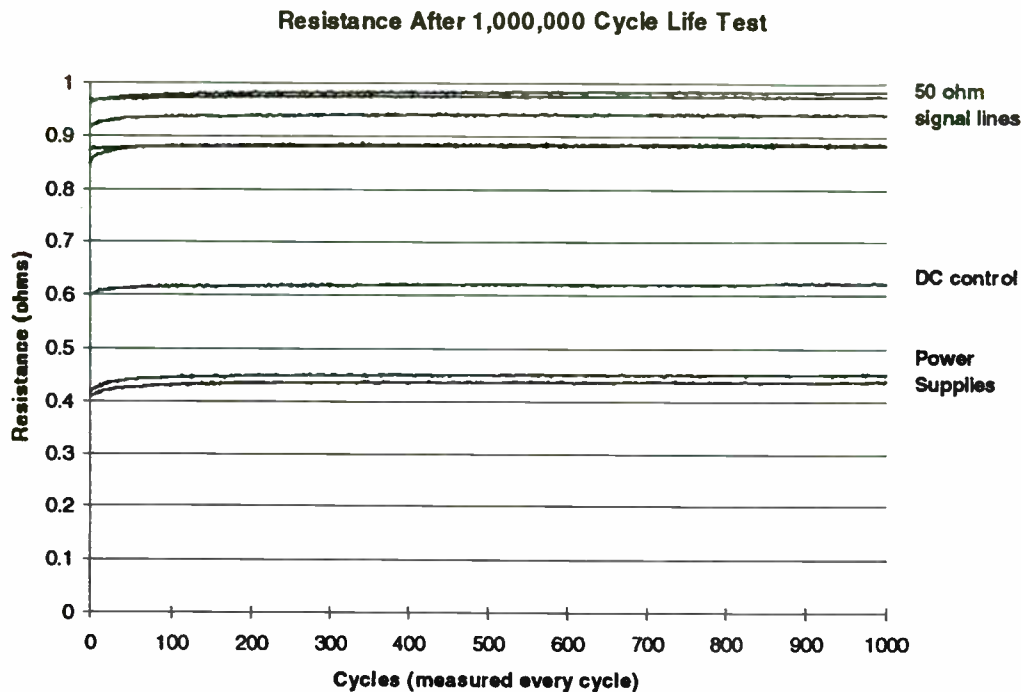


Figure 16. Line resistance after 1 million test cycles

V. CALIBRATION

Complex ICs tend to be pad-limited so it is not feasible to place ground pads on both sides of all high frequency lines. They also have three, five, or more high-speed channels that require calibration. Bond pads for these channels may be located on opposite or adjacent sides of the IC. Designing calibration structures to provide good "thru" standards requires an IC-specific approach. The thin film microstrip used for the membrane probe has been used to create these custom "thrus" with excellent results up to 20 GHz. Using microstrip instead of coplanar-waveguide (CPW) allows all ground paths to be contacted and avoids moding problems caused by the CPW corners and unbalanced ground paths. A general purpose calibration substrate is also available.

VI. PROBE LAYOUT

Since the probe card is a lithographic structure, rather than hand-crafted, membrane

probe layout can be facilitated from electronic data transfer, such as a GDSII data file. All cores for a given design are identical, so probe parasitics are well controlled and repeatable. Some designers have optimized performance by building SPICE models for power supplies and even on-board matching elements.

VII. PROBE STATION COMPATIBILITY

The membrane probe card is compatible with all industry-standard probe stations and mounts neatly into Cascade's patented MicroChamber chuck enclosure. This allows tests to be performed in an EMI shielded and light tight environment. With the addition of thermal equipment, the MicroChamber also becomes a temperature-controlled test environment. Figure 17 shows the membrane probe card mounted in a Cascade Summit 12000-series probe station. For applications down to -60°C, the probe card is sealed to provide an air-tight environment, which prevents moisture from reaching the cold wafer.

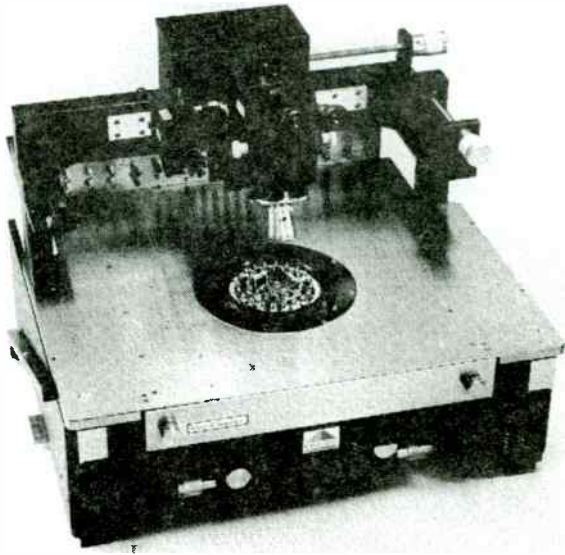


Figure 17. Cascade probe station with membrane probe card

VIII. FUTURE WORK

The membrane probe product family will be extended in frequency range, pin count, and pad metallurgy compatibility. The current structures are extendible to about 40 GHz bandwidth, or 10 ps rise times. Array pad probing has been demonstrated, but the current minimum pad pitch of 125 microns will need to shrink to 100 microns or less to allow pin counts up to 1,000. Proprietary methods which allow long life time for probing aluminum pads are in alpha test. Preliminary results indicate standard deviations of less than one-tenth of an ohm over 15,000 cycles without cleaning the bumps.

Authors:

Ken Smith, Vice President of the Membrane Probe Business Unit; Eric Strid, CEO; and Reed Gleason, Vice President of Advanced Research, Cascade Microtech, Inc., 14255 SW Brigadoon Ct., Beaverton, Oregon 97005; (503) 626-8245, FAX: (503) 626-6023

Fast Phase Noise Measurements

for High-Volume Design and Manufacturing

Darryl Schick

**RDL
West 7th Avenue
Conshohocken, PA 19428
(610) 825-3750**

Introduction

Low phase noise design, and the measurement thereof, had once been the exclusive domain of designers of high performance military-oriented frequency generation circuits. Military electronics designers have long been accustomed to the complicated measurement setups, long measurement times, and extraordinary equipment cost associated with phase noise measurements.

Phase noise performance is now becoming a critical design parameter in commercial communications systems. High volume manufacturing, low cost, and fast time-to-market requirements define a need for fast, accurate, and inexpensive phase noise measurement equipment.

This presentation compares several methods of phase noise measurement. The tradeoffs of each method are discussed relative to measurement speed, measurement accuracy, sensitivity, complexity, and cost. A new phase noise analyzer is described that provides fast, accurate phase noise measurement capability with no external setup requirements.

Fast, Accurate Phase Noise Measurements: Overview

- Phase noise measurements in as little as one second.
- Accuracy of ± 2 dB.
- Easy to set up and operate
- 19" rack compatible equipment format.
- UHF through X-band frequency range.

RDL INC

Frequency Generation and Noise Measurement Systems

7th Avenue and Freedley Street, Conshohocken, PA 19428 Phone: (610) 825-3750 FAX: (610) 825-3530

Phase noise measurement techniques: Overview

- **Phase-Locked Loop technique**
 - Requires an expensive low-noise reference source
 - Requires establishment of phase lock
 - Requires time-consuming PLL calibration
 - Accuracy questionable inside the PLL bandwidth
- **Delay-line discriminator technique**
 - Complicated setup
 - Must be vibration-hardened
 - Standard calibration techniques require external spectrum analyzer and modulation source, and limit accuracy to ± 4 dB

RDL INC

Frequency Generation and Noise Measurement Systems

7th Avenue and Freedley Street, Conshohocken, PA 19428 Phone: (610) 825-3750 FAX: (610) 825-3530

Fast Phase Noise Measurement: Essentials for speed

- **Direct FM demodulation of noise sidebands**
- **Direct calibration of the RF signal under test**
- **Digital (DSP) spectral analysis using FFT processing algorithms**

RDL

INC

Frequency Generation and Noise Measurement Systems

7th Avenue and Freedley Street, Conshohocken, PA 19428

Phone: (610) 825-3750

FAX: (610) 825-3530

Fast Phase Noise Measurement: Essentials for accuracy

- **FM demodulator linearity and frequency response**
- **Calibration performed prior to every measurement**
- **Digital spectral analysis provides precise correction for "resolution bandwidth"**

RDL

INC

Frequency Generation and Noise Measurement Systems

7th Avenue and Freedley Street, Conshohocken, PA 19428

Phone: (610) 825-3750

FAX: (610) 825-3530

Fast Phase Noise Measurement: Easy measurement setup

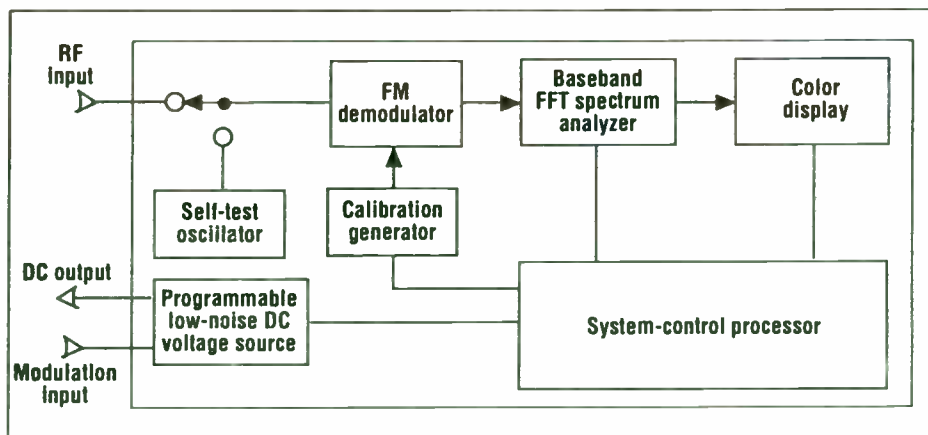
- Phase noise measurements need not require any measurement setup
- External measurement setups suffer from RF and acoustic noise pickup, are non-repeatable, and application-specific
- Phase noise analyzer (NTS-1000) provides "plug-in and measure" capability with no external test setup.

RDL

Frequency Generation and Noise Measurement Systems

7th Avenue and Freedley Street, Conshohocken, PA 19428 Phone: (610) 825-3750 FAX: (610) 825-3530

Phase Noise Analyzer: the NTS-1000

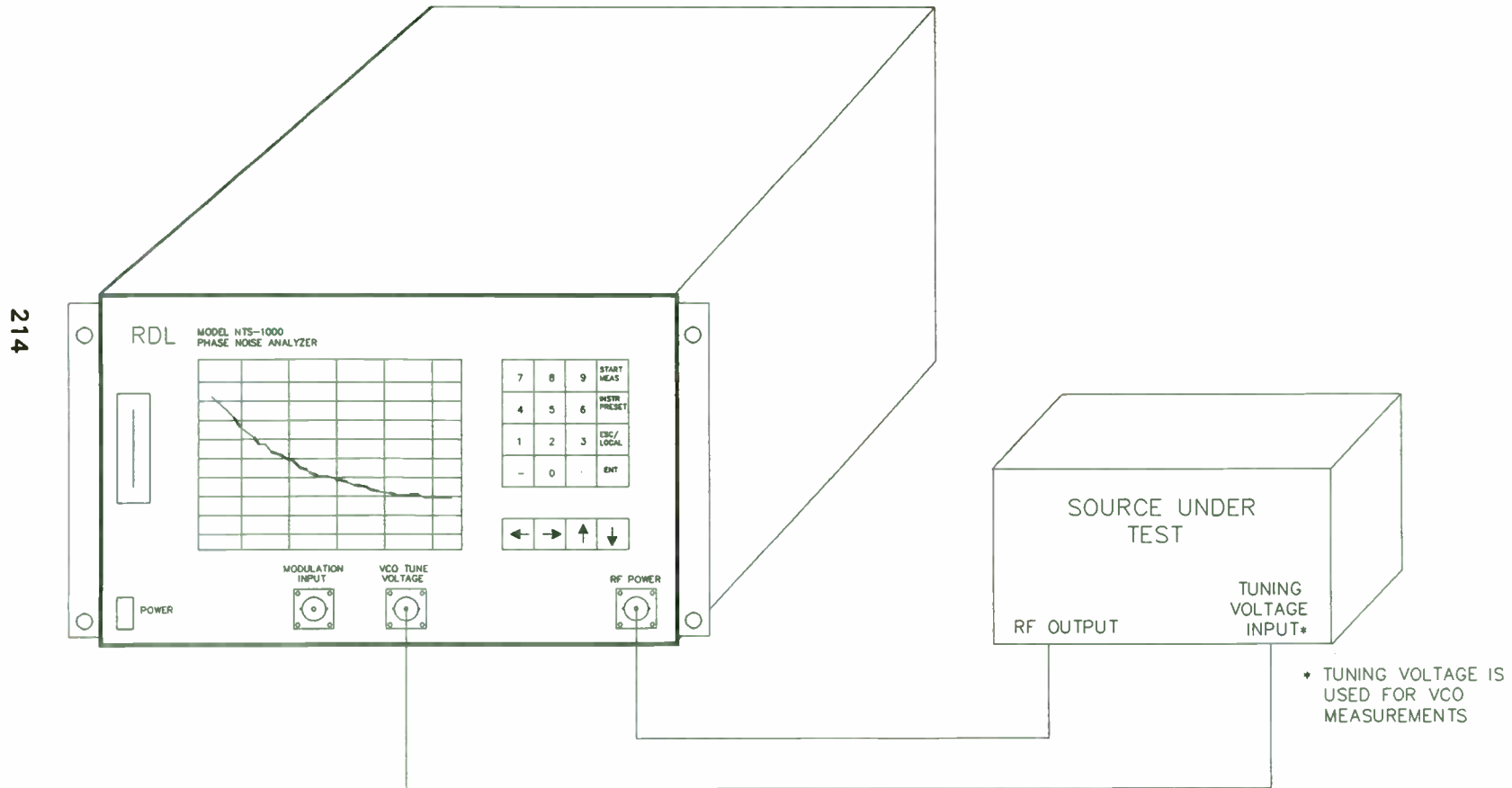


RDL

Frequency Generation and Noise Measurement Systems

7th Avenue and Freedley Street, Conshohocken, PA 19428 Phone: (610) 825-3750 FAX: (610) 825-3530

NTS-1000 Measurement Setup



RDL INC

Frequency Generation and Noise Measurement Systems

7th Avenue and Freedley Street, Conshohocken, PA 19428 Phone: (610) 825-3750 FAX: (610) 825-3530

QUANTIFYING THE BENEFITS OF IMPROVED ANTENNA PERFORMANCE IN TERMS OF MICROWAVE POINT TO POINT LINK DENSITY

Gary Heane

FLANN MICROWAVE INSTRUMENTS LTD.
Dunmere Rd., Bodmin, Cornwall,
PL31 2QL, U.K.
Tel: 01208 77777
Fax: 01208 75426

ABSTRACT

There has been a large and steady increase in the number of microwave point to point links over recent years, and this trend looks set to continue as the technology becomes cheaper and finds applications in new areas. Whilst microwave links are often seen as a 'temporary' solution in many situations, i.e. as a means of establishing communications relatively quickly before cabling can be installed, in many cases the cost of cabling can be prohibitive and the microwave link becomes the only viable option. With the increasing demand for radio communications services it is becoming more important to utilise the allocated frequency bands efficiently. The directional properties of both the transmit and the receive antenna contribute equally to the determination of the re-use of available frequencies in a line of sight region. For point to point applications the ideal antenna would have a small aperture, high gain, very low sidelobes and a beamwidth wide enough to facilitate and maintain alignment in

adverse conditions. Unfortunately, these are conflicting factors. Maximising the antenna gain differential between the wanted and unwanted directions will directly reduce co-channel interference, and this can be achieved in a number of ways. This paper aims to identify the ways in which antenna performance can be improved and to quantify the benefits in terms of the impact on link density. The results of various methods of analysis are presented.

INTRODUCTION

Almost all of the radio regulatory authorities employ some kind of Antenna Radiation Pattern Envelope (RPE) for the planning of microwave link layout. The RPE and the output power of the radio are used to calculate the likely amounts of power in the off axis directions, which is then assessed to determine whether or not the link may be assigned the particular channel frequency. If it is found that there is a high likelihood that interference will

occur then the regulatory authority may suggest the use of an alternative antenna so as to reduce the amount of off-axis signal.

The objective, then, was to explore the relationship between antenna gain / sidelobe performance and likely interference potential, measured in terms of link density. In theory, higher performance antennas would allow greater link densities, but to what extent? Also, were certain parts of the antenna RPE more critical than others in the reduction of interference potential? Answers to these questions would allow the regulatory authorities to restrict the use of certain types of antenna in areas which were likely to become congested, and antenna manufacturers to focus design effort and produce better link antennas.

IMPROVED PERFORMANCE

Two methods commonly used when difficulty in assigning a link to a particular frequency channel is experienced are a) to increase the gain of the antennas used and, b) reduce the sidelobe levels. Let us first examine why both of these options reduce the potential for interference.

Increasing the antenna gain, which in practice usually means using a larger antenna, allows the transmitter output power to be reduced. Where an antenna RPE is used in the planning process, employing a higher gain antenna and reducing the power output *appears* to reduce the amount of off-axis signal. In practice the reduction will depend entirely on the difference between the two antenna patterns. Moreover, use of a

higher gain antenna will not reduce the potential to *receive* interference. The use of larger antennas creates other problems, e.g. the resulting narrower beamwidth creates difficulties in alignment, both at the time of installation and in subsequent adverse conditions where wind pressure leads to antenna deflection. Larger antennas also require stronger support structures to accommodate the increased weight and wind loading.

Decreasing antenna sidelobes directly affects the amount of signal in the off-axis direction and is achieved by designing a more efficient antenna - i.e. less power in the sidelobes *should* mean more power in the main beam. An antenna with low sidelobe characteristics will not only transmit less power in the unwanted direction, but will also *receive* less interfering signal. However, the benefits of lower sidelobe antennas will not be apparent to the link planners unless antenna RPEs are adjusted to match the increased performance.

Arriving at a suitable antenna RPE for a particular frequency band is a problem. Firstly, one has to try and estimate the likely link density in the most congested areas. Add to this other variables such as link length, power output, atmospheric and environmental effects and it is easy to see why most antenna RPEs have tended to have been designed around existing antennas.

LINK LAYOUTS

Consideration to possible link arrangements for the purposes of evaluating interference potential identifies two groups. Firstly, consideration is given to interference

between links occupying the same site, which is a fairly straightforward exercise. Interference between links occupying different sites is a more complex task which is tackled by analysis of actual link layouts.

INTERFERENCE BETWEEN LINKS OCCUPYING THE SAME SITE

It is common for a number of links to occupy the same site and it is likely that some of these links will be required to operate in the same channel. In order to assess the interference potential it is necessary to determine the following :

- a) minimum angular separation
- b) minimum distance separation

Minimum distances between antennas is a function of the near field coupling and can be easily determined by measurement and applied when siting the antennas on the tower. It is therefore reasonable to assume that interference from adjacent antennas can be ignored.

The minimum angular separation will depend on the antenna radiation pattern, the required carrier to interference ratio, and the receiver input / transmitter output power level. Once determined, the maximum number of links for a given site can be calculated. The value will, of course, be a theoretical maximum as it assumes that all links are equally spaced in angle and that antennas are all of the same type. This assumption will not be valid in practice where the direction and antenna type is determined by the position of the other end of the link, but it suggests that perhaps the minimum angular separation should be used as a factor in link assignments criteria. Table 1 shows the effect of antenna

performance on minimum angular separation for a range of antenna types.

Table 1

Antenna Performance Grade	Minimum Angular Separation	Maximum Number of Links
Standard	36	10
High	11	32
Super High	9	40

The above analysis was based on an antenna gain of 36dBi and for typical RPEs, aiming for a minimum angular separation at a nodal site to satisfy a given co-channel carrier / interference ratio of 24dB.

The analysis of links occupying the same site is simple because one only has to consider the effects of the performance on the antenna at one end of the link, i.e. the antenna that is at the common point. The other link ends will all be directed towards the common point and so the effects of the sidelobe performance of these antennas can be ignored. In this case a reduction in sidelobe level has the same effect as reducing the carrier to interference ratio, i.e. the number of links possible increases. Increasing the gain produces a greater number of possible links *only* if the absolute RPE level (dBi) at a given angle does not increase.

INTERFERENCE BETWEEN LINKS OCCUPYING DIFFERENT SITES

Where links occupy different sites, the interference potential will again be dependent on the angle and distance between the interferer and receiver, but in this case the radiation pattern of the interfering antenna will also enter the equation because the main beam will be

directed at some other site. So for every 1dB improvement in main beam to sidelobe discrimination, a 2dB benefit will be realised between links. The angle between interferer and receiver will be dependent on their relative positions and the coupling between them will be a function of their relative directions. Clearly there is an infinite number of possible combinations of positions and directions which makes a simple analysis impracticable and of little value since it would dictate that the ideal link antenna would possess a main beam and no sidelobes !

In order to obtain a realistic assessment of how antenna performance affects link density, a method which utilised actual link layouts was adopted. Three locations were selected, Coventry, Leeds and Inner London, representing low,

medium and high link density areas respectively. These locations were then modelled using four antenna RPEs, chosen to allow comparisons between :

- i) standard and high performance
- ii) high performance and manufacturer's RPE
- iii) 34dBi and 38dBi gain.

The interference signal level was computed at 38GHz for each site individually, based on a carrier to interference limit of 21dB, a receiver input threshold of -105dBm and rainfall attenuation of 2dB/Km.

Ultimately, a measure of the total number of possible links per RPE type per location was obtained. The result was a direct comparison between the RPEs for each of the three locations. The results are presented in table 2 below.

Table 2 :

Coventry	Antenna Gain	Interference count	% of total	Ratio to 34dBi std performance
MPT1414 std	34dBi	74	0.76%	1
MPT1414 high	34dBi	43	0.44%	0.58
MPT1414 high	38dBi	25	0.26%	0.34
2288TXCP	38dBi	17	0.17%	0.23

Leeds	Antenna Gain	Interference count	% of total	Ratio to 34dBi std performance
MPT1414 std	34dBi	510	6.03%	1
MPT1414 high	34dBi	261	3.08%	0.51
MPT1414 high	38dBi	170	2.00%	0.33
2288TXCP	38dBi	96	1.13%	0.19

London	Antenna Gain	Interference count	% of total	Ratio to 34dBi std performance
MPT1414 std	34dBi	2086	21.3%	1
MPT1414 high	34dBi	1439	14.7%	0.69
MPT1414 high	38dBi	991	10.1%	0.48
2288TXCP	38dBi	655	6.8%	0.31

RESULTS

The results of the interference analysis for the four antenna RPEs are presented in table 2. The number of interference paths is expressed as a percentage of the total number of potential interference problems in the samples analysed. As was expected, the potential for interference can be significantly reduced by using antennas with lower sidelobe levels as is illustrated by the comparisons between '34dBi std' and '34dBi high', and between '38dBi high' and '2288TXCP'. Interference potential can also be reduced by increasing antenna gain, as is shown by the comparison between '34dBi high' and '38dBi high'. Looking further into the results it is seen that, even though the number of potential interference problems was much smaller for the Coventry sample than for the Leeds sample, the ratio of improvements between RPEs was similar. This was not the case for the London sample where improvement ratios were not quite as good. One may assume that the extremely high link densities encountered here became a limiting factor, i.e. antennas with *even better* performance are required in such areas. A study of the link layout maps confirms that, far from being randomly situated, it is very common for links to occupy the same site, i.e. nodal points, even in the less densely populated areas. A measure of the extent of nodal point grouping can be obtained if one compares the number of links to the number of sites. This ratio is found to be highest in the most densely populated areas. The nodal point arrangement contributes the largest proportion of possible interference paths, particularly when two or more nodal

points are situated close to one another as is the case in the London sample

CONCLUSION

This paper has attempted to assess the impact of improved antenna performance on microwave point to point link density. The results of a simple nodal point analysis are presented, together with the results for three actual link layouts. Significant reductions in interference potential can be obtained if antenna performance requirements are increased. A prime contributor to interference has been identified in the form of the nodal point. The nodal point analysis shows that in order to effectively minimise interference in this situation it is important to minimise the angular separation between adjacent links. This translates to a requirement to reduce RPE levels to below the carrier to interference limit for all points outside the main beam. In the move towards higher link densities, antenna design effort should be concentrated on the reduction of the higher (close in) sidelobe levels and the maximisation of antenna gain through aperture efficiency.

ACKNOWLEDGEMENTS

The author would like to thank colleagues at Flann Microwave Instruments for useful contributions and discussions.

Monolithic Solutions

Session Chairperson: David Sprague,
INMARK—Independent Marketing Corp. (Walnut Creek, CA)

Study of the feasibility of 20-GHz multistage amplifiers with monolithic technology. **Angelo Angelucci, P. Audagnotto, R. Comitangelo, P. Corda, and B. Piovano,** Centro Studi e Laboratorio Telecomunications (Torino, Italy); **E. Marazzi,** M.C. & S.S.R.L. (Milan, Italy).....**221**

A MMIC-compatible impedance transformer. **Mark W. Ingalls and Eric D. Arnold,** Dielectric Laboratories, Inc. (Cazenovia, NY); **L. Christopher Henning,** Motorola (Fort Lauderdale, FL).....**225**

GaAs MMIC LNAs for commercial applications: A new product platform. **Michael T. Murphy, Holly Laferrara, S. Smith, and S. Mitchell,** M/A-COM, Microelectronics Division (Lowell, MA).....**229**

Optimizing the performance of monolithic spread-spectrum receivers in low-power commercial applications. **Alex Nadler and Victor Steel,** RF Micro-Devices (Greensboro, NC).....**234**

Half-rate GSM speech codec: True silicon complexity versus ETSI complexity evaluation. **Chris Cavigioli,** Analog Devices, Inc. (Wilmington, MA).....**249**

Performance evaluation of a low-voltage monolithic FM/IF system for GMSK/GFSK applications. **Yanpeng Guo and Alvin Wong,** Philips Semiconductors (Sunnyvale, CA).....**264**

STUDY OF FEASIBILITY OF 20 GHz MULTISTAGE AMPLIFIERS WITH MONOLITHIC TECHNOLOGY

A. Angelucci⁽¹⁾, P. Audagnotto⁽¹⁾, R. Comitangelo⁽¹⁾,
P. Corda⁽¹⁾, E. Marazzi⁽²⁾, B. Piovano⁽¹⁾

(1) CSELT - CENTRO STUDI E LABORATORI TELECOMUNICAZIONI
VIA G. REISS ROMOLI, 274 - 10148 - TORINO - ITALY

(2) M.C. & S. S.R.L.
PIAZZA NOVELLI, 10 - 20129 - MILANO - ITALY
Phone: 39 - 2 - 55187602 - Fax: 39 - 2 - 5450906

ABSTRACT - In this work a study of feasibility of a multistage amplifier operating over the 20 GHz band (frequencies used in radio-links applications) using monolithic technology is presented. Prototypes of a three-stage amplifier, designed using Libra software by Eesof, were fabricated on a GaAs substrate employing 0.5 micron MESFETs. Measured and computed results are in close agreement.

INTRODUCTION

The aim of this study was to verify the possibility of performing an accurate design of monolithic multistage amplifiers at 20 GHz entirely at computer level using a standard CAD package, with a reduction of fabrication costs and fabrication time, in view of a large scale production.

The monolithic amplifier presented here consists of three stages, with the goal of obtaining an optimum compromise among gain, noise and circuit complexity.

The design was carried out using the standard software package Libra and manufactured on a GaAs substrate.

DESIGN

Each stage consists of an active element, a 0.5 micron MESFET, along with its bias networks and was designed so as to minimize the noise figure. This was necessary because the low gain of the first stage makes the contribution of the subsequent stages to the overall noise figure be considerable, as can be seen from the general equation

$$F_{tot} = F_1 + \frac{F_2 - 1}{G_1} + \frac{F_3 - 1}{G_1 G_2} \quad (1)$$

where F_{tot} represents the overall noise figure, F_i 's are the noise figures of the various stages, and G_1 and G_2 the gains of the first and second stage respectively.

In order to guarantee a good stability, resistors were introduced between the gate of each MESFET and the ground [1]. Furthermore, each stage is biased separately in order to have the possibility of DC testing each active element and of avoiding unwanted couplings among the bias networks.

The design was based on the nominal values, provided by the foundry [2], of the parameters of the various components constituting the amplifier.

In practice, in order to keep into account the dispersion introduced in the parameters by the technological process, the dispersion bands of the overall parameters (gain, noise figure and return loss) of the amplifier were computed as shown in Figs. 1-3.

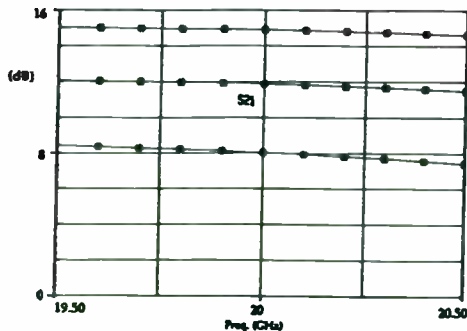


Fig. 1 - Computed dispersion band of gain values

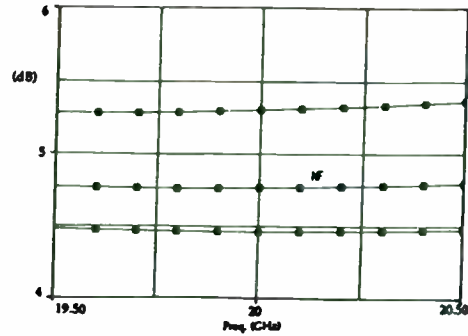


Fig. 2 - Computed dispersion band of noise figure values

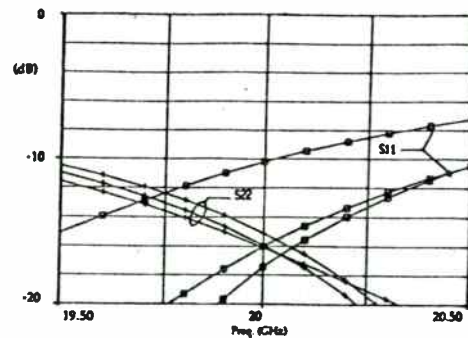


Fig. 3 - Computed dispersion band of return loss values

Furthermore, the yield analysis provided a probability of 45.6 % that the global electrical performance stays within the following limits

$$\begin{aligned} 10dB < |S_{21}| < 14dB \\ N_f < 5.4dB \\ |S_{11}| < -9dB, |S_{22}| < -9dB \end{aligned} \quad (2)$$

The computed electrical performance over the frequency band 19.5-20.5 GHz exhibits a total gain of about 12 dB, a flat noise figure better than 4.8 dB and a return loss of at least 12 dB.

RESULTS

The final layout of the three-stage amplifier is shown in Fig. 4.

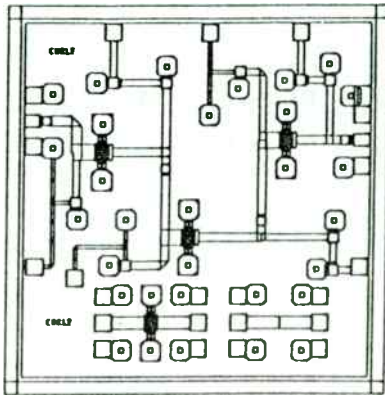


Fig. 4 - Layout of the three stage MMIC amplifier

On this chip, the total area of which is 90 x 90 mils, a further transistor of the same type was added in order to measure its scattering parameters and to check the validity of the design.

A prototype was measured using a Cascade Probestation connected with a HP 8510-C Network Analyzer and a HP 8971 Noise Figure Meter.

Results are presented in Figs. 5-7, in which also a comparison between measurements and theory is performed.

The noise figure closely agrees with computations (see Fig. 6), while the gain and the return loss remain within the dispersion bands stated by the above equations.

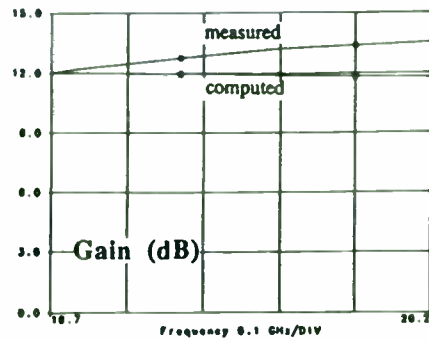


Fig. 5 - Comparison between measured and computed gain

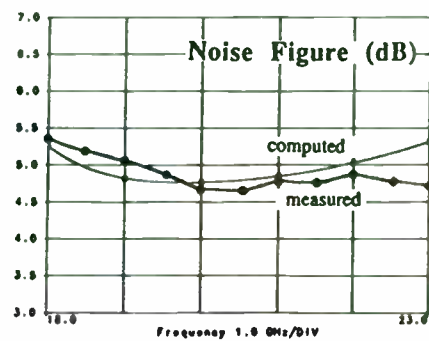


Fig. 6 - Comparison between measured and computed noise figure

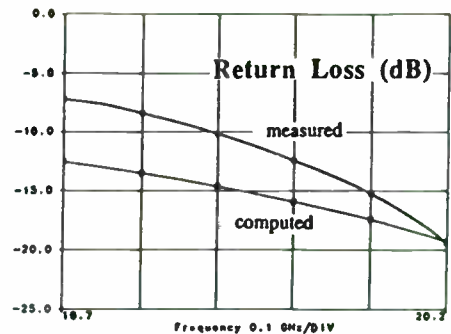


Fig. 7 - Comparison between measured and computed return loss (S_{22})

CONCLUSIONS

In this work an accurate design procedure of monolithic multistage amplifiers at 20 GHz was presented.

A three stage prototype built on a GaAs substrate showed a good elec-

trical performance with measured values. Main parameters (noise figure, gain and return loss) always within the computed dispersion bands.

This prototype does not represent the state of the art of the MMIC amplifiers because the MESFETs used in this design do not present, among the commercially available transistors, the best electrical performance, especially in terms of noise figure [3]. In fact, the aim of this study was to span the possibility, in view of a production on a large scale, of performing the design of a monolithic amplifier entirely at computer, with remarkable reduction of manufacturing costs and realization time.

ACKNOWLEDGEMENT

The authors greatly acknowledge the support by Dr. E. M. Bastida in MMIC technology development.

REFERENCES

- [1] R. Soares "GaAs MESFET Circuit Design", chap.3, Artech House, 1988.
- [2] TriQuint "Gallium Arsenide IC Design Manual", May 1992.
- [3] P. H. Ladbrooke "MMIC Design GaAs FETs and HEMTs", chaps. 9 and 10, Artech House, 1989.

A MMIC Compatible Impedance Transformer

Mark W. Ingalls, Eric D. Arnold
Dielectric Laboratories
2777 Rt 20E, Cazenovia, NY 13035
(315) 655-8710

L. Christopher Henning
Motorola
800 W Sunrise Blvd, Ft Lauderdale, FL 33322
(305) 475-6184

Background

The invention of the transistor was an important step in the electronic age but the realization of the transistor's potential required smaller passive and reactive devices for supporting circuitry. Today, the maturation of MMIC technology creates the same need. MMIC chips, to achieve full potential, require miniaturized ancillary circuitry. The realization of miniaturized circuitry requires new thinking. For instance, parasitic behavior of closely spaced elements cannot be ignored. By acknowledging stray capacitance and inductance (and moreover making use of it) miniaturized passive and reactive networks can be engineered.

The problem of matching a 6 Ω source impedance to a 50 Ω load at 900 MHz is presented from three viewpoints: matching with lumped elements, matching with transmission line elements, and matching with a combination of the two.

Design Goals

The impedance transformer had these design goals: Operating frequency: 880 – 925 MHz, maximum insertion loss - 0.35 dB, maximum return loss -20 dB.

Two further requirements restricted the design: The transformer had to block DC and its allowable maximum

dimensions were 0.8 mm wide and 2.6 mm long.

Matching with Lumped Elements

The electrical design goals can be achieved by using the discrete network shown in fig. 1. However, the size of this circuit would be at least four times that of the MMIC. In addition, the cost of assembling the network is comparatively high.

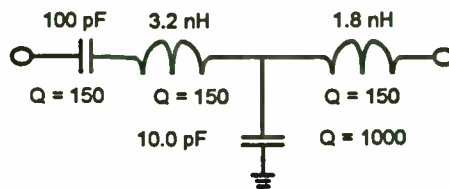


Fig. 1. Lumped element matching network for 6 to 50 Ω at 900 MHz.

The size and cost may be reduced by printing the inductors and shunt capacitor on a substrate and mounting the blocking capacitor. Inductors made this way evidently contribute too much

loss – a modeled printed circuit of this design predicted $S_{21} = -2$ dB at the center frequency. The modeled insertion loss was halved by eliminating one of the inductors from the model, but the resulting bandwidth was too narrow.

Matching by Quarter-wave Transformer

Another way to match the source and load impedances is to use a quarter-wave section of transmission line with the appropriate Z_c (in this case, 17.3 Ω). The circuit shown in fig. 2 would give good electrical performance at a lower cost than the lumped element solution. The size may be reduced somewhat by increasing the relative dielectric constant (ϵ_r) of the material, but not enough to meet the design goal of 0.8 x 2.6

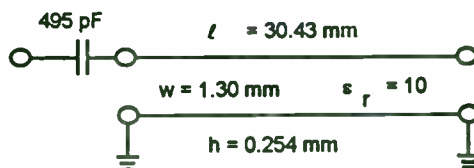


Fig. 2. Quarter-wave matching network for 6 to 50 Ω at 900 MHz. Substrate is alumina.

Integrating Parasitics

A third technique for constructing the matching transformer is to make use of lumped and distributed elements. Fig. 3 shows the resulting schematic.

The network is approximately one third the size of the specified MMIC amplifier, fig. 4, allowing it to be placed inside the MMIC package.

The design philosophy is to use parasitic effects to good advantage, rather than to eliminate them. To mount the blocking capacitor to the circuit in fig. 2 a pad must be included. By loading the transmission line with the shunt capacitance of this pad, the resonant frequency of the line can be lowered.

Folding the transmission line makes its geometry more compatible with a circuit package, and decreases the chance of breakage during circuit assembly. Folding the line can be accomplished two ways. If the line is meandered, or folded back on itself, the parasitic coupling of the folds tends to cancel some of the line's electrical length. If the line is coiled, as in fig. 4, the self-coupling effect enhances the circuit performance by increasing the line's characteristic impedance and electrical length.

The reactance of the blocking capacitor in fig. 2 is intended to be nearly zero, forcing the quarter wave transmission line to accomplish the entire job of transformation. In fig. 3 the blocking capacitor contributes to the matching circuit.

The initial study of the circuit indicated that not all of the design goals could be met. In particular, given the dimensional constraints, either $S_{11} < -20$ dB or $S_{22} < -20$ dB could be achieved but not both. The decision was made to optimize for S_{11} and let S_{22} go to -15 dB. Analysis of S_{21} indicated that -0.25 dB was possible.

The circuit was designed with the program

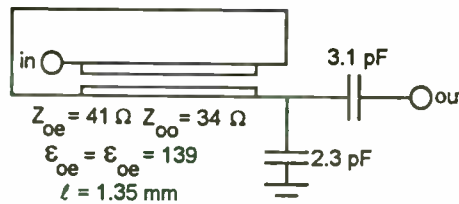


Fig. 3. Electrical schematic of integrated matching network for 6 to 50 Ω at 900 MHz.

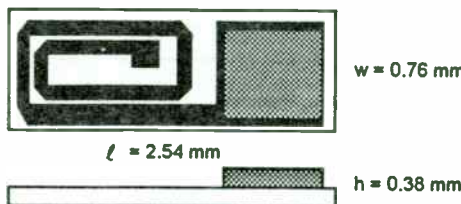


Fig. 4. Realized matching network for 6 to 50 Ω at 900 MHz.

=Superstar= Professional from Eagleware Corporation. The effective dielectric constant (ϵ_{eff}) at 900 MHz and the proper choice of 1 MHz capacitance value to give the correct capacitance at 900 MHz were calculated using the program CAPCAD from Dielectric Laboratories. Note that the accuracy of the coupled transmission line model contained in =Superstar= Professional is unspecified for $\epsilon_r > 18$. Because of this, an iterative design process was expected.

Circuit Fabrication

The first prototypes of the transformer were fabricated using ceramic substrates with a relative dielectric constant (ϵ_r) of 150 and a loss tangent ($\tan \delta$) of 0.0027. The ϵ_r was measured using the Kent method [3] at 6 GHz.

The substrates were machined to a thickness of 0.25 mm. Metalization was applied by sputtering a 300 \AA Ti/W adhesion layer, followed by a 1.4 μ Ni/V barrier layer and a 2.8 μ layer of Au.

The circuit was subtractively patterned to ± 2.5 μ tolerance. Positive photoresist was spin applied and contact printed, followed by a non-proprietary wet chemical etch. The pattern geometry was verified optically. Metal thicknesses were verified with a Dektak-3 profilometer.

A 3.1 pF series capacitor was silver epoxied to a pad which doubled as a 2.3 pF shunt element.

First Prototype Electrical Measurements

Initial electrical measurements, shown in fig. 5, were made by terminating the transformer with a thin film 6 Ω resistor and making a one port scalar swept measurement. As such, it was a measurement of S_{22} . The result was $S_{22} = -19.3$ dB at 1.02 GHz.

A second set of measurements were made by connecting two transformers at their 6 Ω ports with a pair of 25 μ bond wires and making a two

port scalar sweep of the combination, fig 6. The bond wire lengths were increased ~ 0.5 mm for each pair of transformers, from ~ 1.3 mm for the first pair to ~ 2.8 mm for the fourth pair. Note the shift in frequency and the corresponding change in performance of the four pairs. These changes are attributable to increasing the bond wire lengths between the 6Ω ports. The frequency shift between data sets 1 and 2 is about 60 MHz, which represents the practical limit for Δf without degrading performance, as shown by data sets 3 and 4. The measured performance of the first transformer pair was $S_{11} = -17.7$ dB, $S_{21} = -1.6$ dB, $f_0 = 1.02$ GHz.

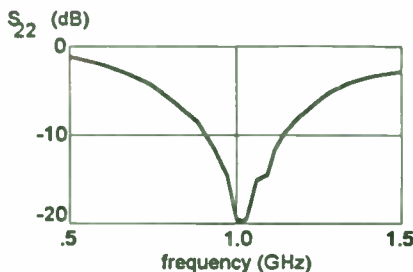


Fig. 5. Measured S_{22} of transformer terminated with a 6Ω resistor.

frequency and return loss of all three measurements are in good agreement, as shown by the following calculation.

Assume S_{11} of the first transformer in the first pair in fig. 6 is equal to S_{22} of the transformer depicted in fig. 5, -19.3 dB (magnitude, 0.0170). To make S_{11} for the pair -17.7 dB (magnitude, 0.0117) S_{11} assignable to the second transformer must be -22.8 dB (magnitude, 0.0052) which compares well with the result shown in fig. 7. By applying these results to the insertion loss of the transformer pair in fig. 6, it can be shown that for one transformer, $S_{21} = -0.7$ dB, of which 97% is attributable to dissipated power.

A third measurement was made by connecting one transformer prototype in series with two ground – signal – ground contacts and making a two port vector sweep with a pair of CPW probes. The results were then transformed to a 6Ω input, 50Ω output system, fig. 7. The transformed results were $S_{11} = -21.6$ dB, $S_{21} = -1.12$ dB, $f_0 = 1.01$ GHz.

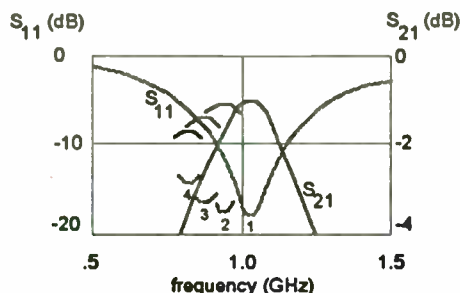


Fig. 6. Measured S parameters of four different pairs of transformers connected at their 6Ω ports.

The vector results show that the input impedance of the transformer prototype was in fact 7.28Ω , approximately 20% in excess of the design goal. All results show the center frequency is 13% in excess of the design goal. The calculated S_{21} was twice as high as the design goal.

These results indicate that the coupled transmission line was not correctly modeled

and that the metal thickness was too low.

Analysis of First Prototype

The measured results depicted in figs. 6 and 7 are in conflict because the insertion loss of the single transformer in fig. 7 is as large as a pair of transformers in fig. 6. This difference could be attributed to either a difference in individual samples of the prototype, or to a difference in measurement. Because the matched condition of the transformer pairs to themselves and to the 50Ω test ports should give less measurement error than the unmatched condition of measuring one transformer in a 50Ω system, the S_{21} data in fig. 6 will be used in this analysis. The center

Second Prototype

A second prototype of the transformer was fabricated with the following changes. The Au layer was increased to 12μ and the length of the coupled transmission line was increased by 0.41 mm. The line length increase was intended to shift the resonant frequency to 900 MHz. The increase in conductor thickness was intended to accomplish two purposes, 1) to decrease the insertion loss, 2) to increase the coupling of the coiled transmission line, thus lowering its impedance.

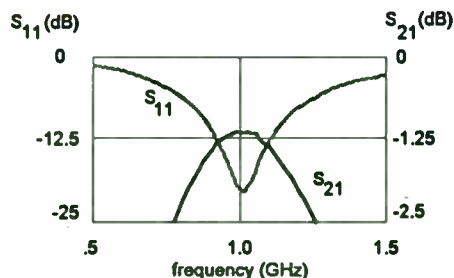


Fig. 7. Measured S parameters of series connected transformer, transformed to 6Ω source and 50Ω load.

Scalar measurements of the second prototypes were performed by wire bonding a pair at their $6\ \Omega$ ports and wire bonding the combination to two sections of $50\ \Omega$ microstrip transmission line. The losses of the bond wires were extracted by wire bonding two microstrip lines in series and treating the resulting circuit as a through line in the calibration of the SNA.

Fig. 8 shows the results of the scalar measurements of a pair of second prototype transformers connected at their $6\ \Omega$ ports. Evidently, the changes corrected some of the problems of the first prototypes: $f_0 = 895\ \text{MHz}$, $S_{11} = -20.6\ \text{dB}$, $S_{21} = -0.6\ \text{dB}$ for the pair.

Vector measurements were again made on a single transformer in a $50\ \Omega$ system and transformed to $6\ \Omega$ input, $50\ \Omega$ output. These measurements were performed with SMA launchers and $50\ \Omega$ microstrip transmission lines wire-bonded to the ports of the transformer, instead of the ground – signal – ground contacts and CPW probes used on the first prototypes. A section of $50\ \Omega$ transmission line terminated with a short circuit and two sections of line connected by wire bonds were used to de-embed the transformer from the test circuit.

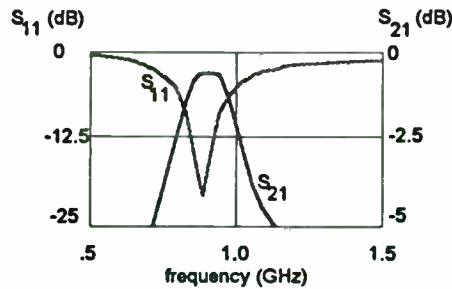


Fig. 8. Measured scalar S parameters of one pair of transformers (2nd prototype) connected at their $6\ \Omega$ ports.

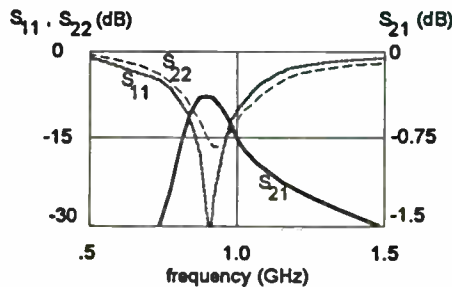


Fig. 9. Measured vector S parameters of one series connected transformer (2nd prototype) transformed to $6\ \Omega$ source and $50\ \Omega$ load.

The results, shown in fig. 9, also show improved performance: $f_0 = 900\ \text{MHz}$, minimum $S_{11} = -31.2\ \text{dB}$, minimum $S_{21} = -0.235\ \text{dB}$, minimum $S_{22} = -16.25\ \text{dB}$. Note, however that the minima in S_{11} , S_{21} , and S_{22} do not occur at the same frequency. The upward shift in S_{11} caused the second prototype to miss the design goal by 1 dB at 880 MHz. The S_{22} design goal was not achieved for any configuration at any frequency. The S_{21} results were good. The design goal of $-0.35\ \text{dB}$ was achieved from 865 to 945 MHz.

Conclusions

An impedance transformer which is physically small enough to be inserted inside a MMIC package has been designed, built and characterized. The transformer shows good performance, with less than $-0.35\ \text{dB}$ insertion loss over the frequency range, 865 – 945 MHz. The design is compatible with die and wire assembly techniques.

Although the first and second design prototypes did not meet all the design goals, the validity of fabricating a useful miniature circuit on very high ϵ_r substrate has been established. Further study to establish design requirements and limitations are indicated.

References

- [1] Eagleware Corporation, 1750 Mountain Glen, Stone Mt., GA, 30087, TEL (404) 939-0156, FAX (404) 939-0157.
- [2] Dielectric Laboratories Inc., 2777 Rt 20E, Cazenovia, NY, 13035, TEL (315) 655-8710, FAX (315) 655-8179.
- [3] G. Kent, "Non-destructive permittivity measurements of substrates," Digest of the 1994 Conference on Precision Electromagnetic Measurements, IEEE Catalog Number 94CH3449-6.

GaAs MMIC LNAs for Commercial Applications: A New Product Platform

M. Murphy, H. LaFerrara, S. Smith, S. Mitchell

M/A-COM, MED, IC Product Development

Abstract

A GaAs MMIC LNA product platform that was developed to address multiple commercial applications is introduced. The platform concept and its impact on the development of this product family is presented. The LNAs are encapsulated in 8-lead SOIC plastic packages and automatically tested in M/A-COM's high-volume IC manufacturing facility to achieve a low sell price. The price of each of these products is less than \$2.00 in 100,000 piece quantities. The electrical performance to price ratio of these LNAs is unsurpassed in the marketplace.

Introduction

Early in 1994 M/A-COM began offering a family of low cost, high performance GaAs MMIC low noise amplifiers (LNAs) intended for commercial applications. These amplifiers are ideally suited for use where low noise figure, high dynamic range, and low power consumption are required. The initial product family contains five LNAs that offer a wide range of solutions for applications such as Global Positioning (GPS), Japanese Digital Cellular (JDC), Personal Communication Systems and Networks (PCS, PCN), Japanese Personal Handy Phone (PHP), Private Branch Exchange (PBX) and Wireless Local Area Networks (WLAN).

The entire product development cycle from inception to preliminary release of the initial product family took six months. All of the products were released after a single design and fabrication cycle. This can be attributed to accurate modeling of the ICs and the plastic package, as well as strict adherence to a proven design methodology. The quick introduction of this product family illustrates the effectiveness of

applying a "product platform" philosophy to product development. By developing platforms rather than individual products, the productivity of a development team can be dramatically improved. Once a platform is established, derivative products that adhere to it are quick-turn; three month development cycles have been demonstrated.

The commercial MMIC LNA platform is based on M/A-COM's .5 um low-noise GaAs MESFET process. The IC chips are encapsulated in a low-cost 8-lead SOIC plastic package. They are fully monolithic, which eliminates the need for external tuning networks and ensures excellent uniformity. The LNAs can be biased using 3 or 5 volt supplies and include an option for biasing at higher current to increase dynamic range. Consistent with the platform concept, all products share a common manufacturing and test methodology.

Part #	Function	Intended Markets
MAAM12021	1.5 - 1.6 GHz (HG)	GPS, JDC
MAAM12022	1.5 - 1.6 GHz (LG)	GPS, JDC
MAAM12031	1.7 - 2.0 GHz (HG)	PCN, PHP, PBX
MAAM12032	1.7 - 2.0 GHz (LG)	PCN, PHP, PBX
MAAM22010	2.4 - 2.5 GHz (LG)	WLAN

Table 1, Commercial LNA products

(LG) Low Gain Version	(HG) High Gain Version
Gain = 14 dB	Gain = 21 dB
NF = 1.7 dB	NF = 1.6 dB
VSWR = 1.5 : 1	VSWR = 1.5 : 1
IP3 in = 0 dBm	IP3 in = 0 dBm
Vdd = 3 - 5 V	Vdd = 3 - 5 V
Idd = 5 mA	Idd = 8 mA
Price (@10K) = \$3.65	Price (@10K) = \$3.83

Table 2, Typical LNA performance

The Commercial LNA Platform

The LNAs that comprise the initial product offering are shown with their respective target markets in table 1. As indicated in the table, the amplifiers can be classified into either a high-gain (HG) or low-gain (LG) category. Table 2 shows the typical electrical performance and sell price for the HG and LG amplifiers. The performance level at the accompanying price make these products very attractive for use in the targeted commercial markets. The development and introduction of these products establishes a new "product platform". A "platform" is a proven product concept and manufacturing methodology that translates core competencies into product families which fill the needs of strategic markets. All the commercial LNAs share a common design, manufacturing and test methodology. The primary advantage of the platform approach is that derivative products can be developed and introduced quickly, usually with a single design cycle.

The commercial MMIC LNA platform is based on M/A-COM's mature .5 μm low-noise GaAs MESFET process. The active layer of the GaAs substrate is formed using ion-implantation for high through-put and low cost. A "buried-p" doping layer combined with .5 μm T-gates result in high performance MESFETs. At a bias of 3 volts and .5 Idss, the FETs exhibit an Ftau of 30 GHz and a Gmax and Fmin at 12 GHz of 13 and 1.3 dB, respectively.

The LG designs employ a cascode configuration with series inductive feedback added to achieve noise and conjugate match conditions simultaneously. The HG designs use two cascaded stages biased in series for high gain and low current dissipation. To reduce cost the chip sizes were kept to a minimum. The MMIC chip used in the MAAM12021 product is shown in figure 1. The chip size is 1 mm². Being of the HG variety, this represents the largest chip size of the product family. The ICs are encapsulated in a low-cost 8-lead SOIC plastic package. The amplifiers employ a special split-paddle lead-frame design to ensure unconditional stability. The LNAs are self-biased using a single polarity 3 to 5 volt supply.

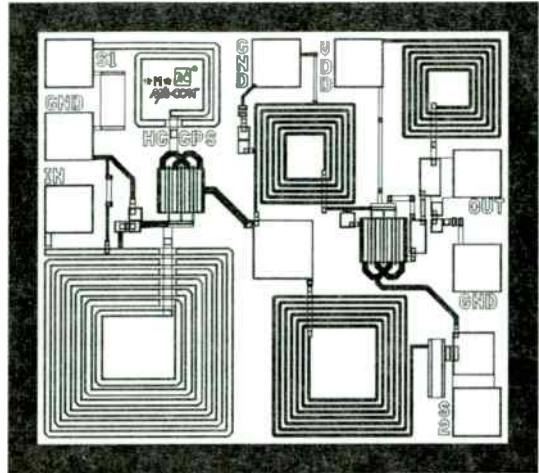


Figure 1. MAAM12021 GaAs MMIC Chip

The self-bias resistor is by-passed internal to the package with an MNS single-layer capacitor supplied by M/A-COM's Burlington Semiconductor Operation. Figure 2 shows the assembly diagram of the MAAM12021. The current can be increased to achieve higher dynamic range by adding a surface-mount chip resistor external to the package. Figure 3 shows a functional block diagram that applies to each amplifier in this platform.

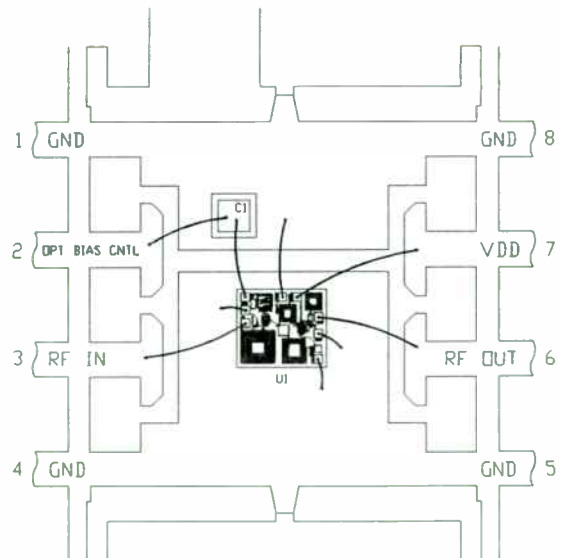


Figure 2. MAAM12021 Assembly drawing

The most challenging aspects involved in the design of these products were deriving an equivalent circuit model of the plastic package and

quantifying the effects of the plastic encapsulant on the MMIC die. A model for the package including the self and mutual inductance of the leads, bond-wires and the lead-frame paddle was obtained using a combination of multiple coupled line analysis and empirical data. By encapsulating inductor and FET library elements in plastic, the impact on circuit parasitics was assessed. These effects were mostly reactive and were incorporated into the design by adding correction terms to the internode capacitance of these circuit elements.

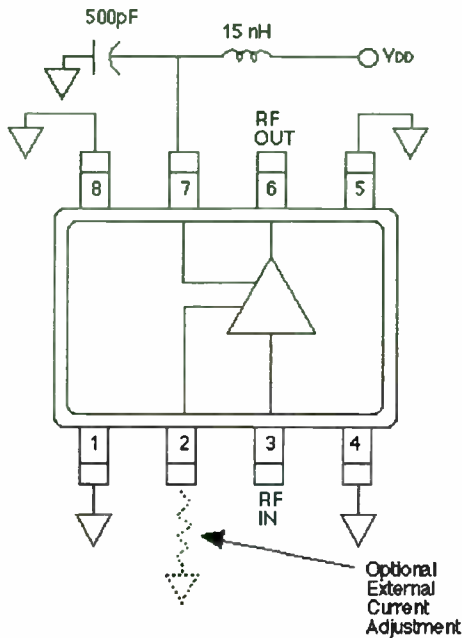


Figure 3. Commercial LNA Functional Diagram

Experimental results

The layout of the printed circuit board (PCB) used in the commercial LNA evaluation fixture is shown in figure 4. This layout is also recommended to customers who use these products in their systems. The PCB material is 20 mil thick FR-4. The figure also shows the location of the packaged amplifier, optional bias control resistor and external bias decoupling circuitry. A 500 pF bypass capacitor shunting the supply bias line is necessary. For optimum performance, an inductor that serves as an RF choke is also shown in series with the bias line. Because the pin assignment for each of the amplifiers is identical, one test board is used to evaluate all products.

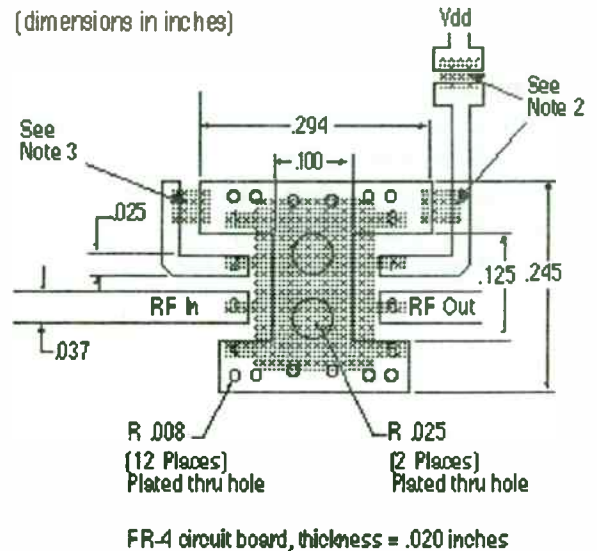


Figure 4. Recommended PC Board Layout

In order to demonstrate some performance data, the MAAM12021 LNA will be highlighted here. The MAAM12021 is a high-gain (HG) LNA intended to fill requirements in GPS applications. The amplifiers were characterized at bias points of 5 volts at nominal current (~ 8 mA for the MAAM12021), 3 volts at nominal current and 5 volts at 20 mA. The 20 mA bias is achieved by attaching a 35 ohm surface mount chip resistor from pin 2 to ground. Because of the larger voltage drop across the self-bias resistor at the higher current, a 3 volt and 20 mA bias was shown to offer no dynamic range improvement over the 3 volt and nominal current bias.

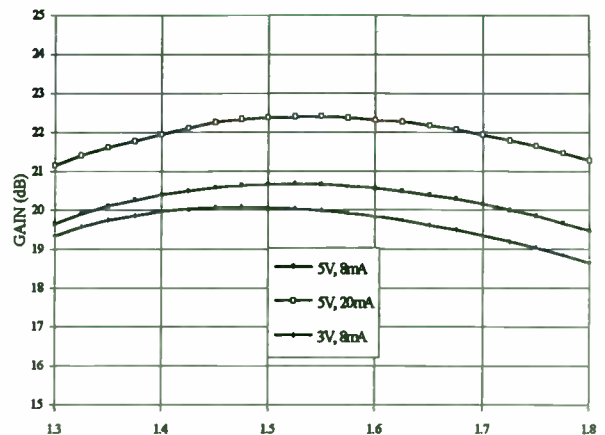


Figure 5. MAAM12021 Gain vs. Frequency (GHz)

Figure 5 shows the gain of a typical MAAM12021 device at the three bias points described above. At the nominal bias, the gain of this part is greater than 20 dB over the 1.5 to 1.6 GHz bandwidth. The gain degrades less than 1 dB at the 3 volt bias. The noise figure of the same MAAM12021 device is shown at each bias level in figure 6.

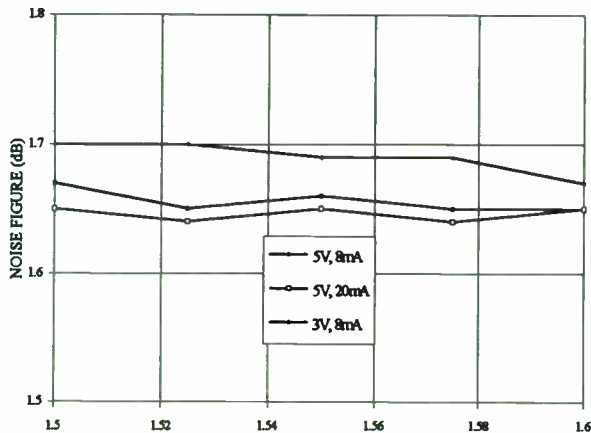


Figure 6. MAAM12021 Noise Figure vs. Frequency (GHz)

As shown, the noise figure is nominally 1.65 dB across the band and degrades to 1.7 dB at the 3 volt bias. Noise figure is actually improved slightly at the higher current bias because the FETs are operating closer to an optimum bias for minimum noise figure (~ 25 % Idss). As expected, the third-order-intercept and output power at 1 dB compression is largely dependent on bias level.

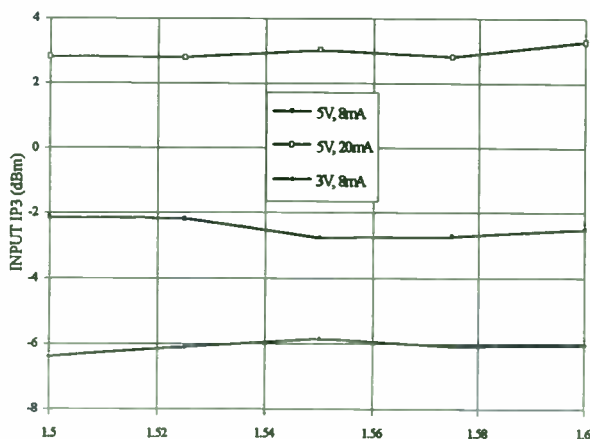


Figure 7. MAAM12021 Input IP3 vs. Frequency (GHz)

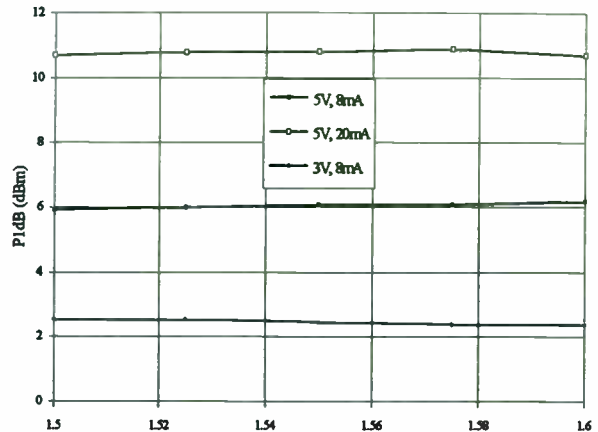


Figure 8. MAAM12021 Pout (@-1dB) vs. Frequency (GHz)

Figures 7 and 8 show the IP3, referenced to the device input, and the Pout (@-1 dB) of the MAAM12021 as a function of bias, respectively. For this device at the nominal bias of 5 volts and 8 mA, the input IP3 is -2 dBm and the Pout (@-1 dB) is 6 dBm. Of course, these performance levels are significantly improved at the higher current bias which increases the amplifier's dynamic range.

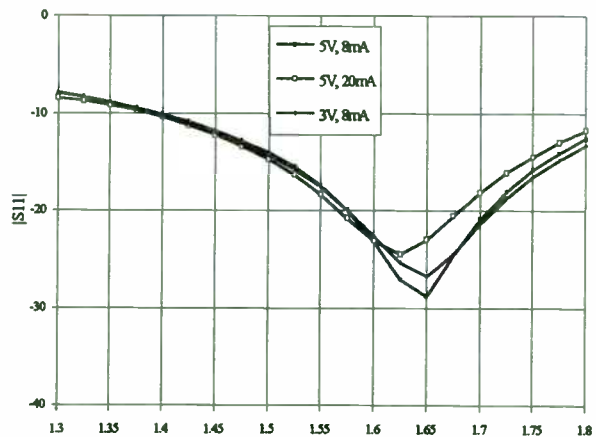


Figure 9. MAAM12021 Input Return Loss vs. Frequency (GHz)

As shown in figures 9 and 10 respectively, the input and output return loss of the MAAM12021 at each of the three bias points is substantially better than 10 dB over the full band of interest.

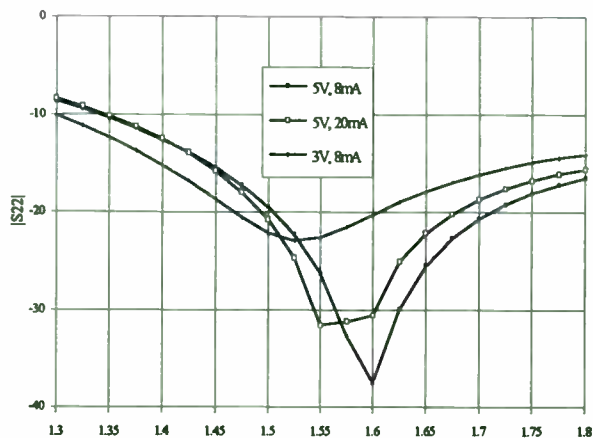


Figure 10. MAAM12021 Output Return Loss vs. Frequency (GHz)

Production testing of these products is done in M/A-COM's IC manufacturing operation using an auto-handler test system. One handler test board is used to production test all LNAs from this platform. In production, the current draw, S-parameters, and noise figure are tested on 100 % of the amplifiers at the frequency band edges. Only minimum gain, noise figure and maximum current are guaranteed for these standard products. The test time is 9 seconds per unit, adding very little to the product cost. Total yields of the commercial LNA products have been in the 80 to 85 % range. This is largely due to having sufficient design margin relative to the electrical performance specifications.

Conclusion

A new product platform has been established in M/A-COM's IC business unit which addresses the high volume LNA requirements of wireless communication systems. The platform concept was rigidly adhered to which made the design and development of these products essentially a batch process. The initial family of five LNAs were developed in parallel. Consistent with the platform concept, all products share a common design, manufacturing and test methodology. Additional products are being developed on this platform to address other commercial markets. Because the platform is mature, the development cycle for these new derivatives is anticipated to take 3 months and involve a single design and development phase.

Optimizing the Performance of Monolithic Spread-Spectrum Receivers in Low-Power Commercial Applications

Alex J. Nadler and Victor Steel
RF Micro Devices, Inc.
7341-D West Friendly Ave.
Greensboro, NC 27410
(910) 855-8085

ABSTRACT

As digital spread-spectrum (SS) modulation techniques become increasingly more common in commercial cellular, PCS, and ISM-band battery-powered communications systems, monolithic solutions to RF front-ends, IF/AGC amplifier chains, and despreaders/demodulators must be developed to provide the highest electrical performance at low DC power levels. In addition to low-powered operation, IC solutions applicable to commercial digital spread-spectrum systems must also provide the lowest overall manufactured cost and smallest physical size. To simultaneously achieve all of these design goals, careful consideration and selection of the appropriate IC technology at the intended operating frequency is essential. Furthermore, RF system and circuit design techniques must be applied in the design of the IC's that optimize system performance in the potentially harsh signal environments of the commercial bands. This paper focuses on Optimum Technology Matching™ using high-Ft silicon bipolar, GaAs MESFET, and GaAs Heterojunction Bipolar Transistor (HBT) IC technologies in commercial spread-spectrum receiver design to maximize system performance and provide the most economical technical solution in applications through 6 GHz. RF system/circuit issues related to SS receiver noise figure, third-order intercept point (IP3), and filtering are discussed. Standard products developed using all three technologies are also discussed that are applicable to commercial SS systems.

I. SPREAD SPECTRUM SYSTEMS

The allocation of frequency bands for unlicensed use by the FCC offers an opportunity for many wireless systems to provide functions which only a few years ago were unimaginable. These unlicensed bands are termed ISM (Industrial, Scientific, and Medical), to indicate the intended commercial use. Many systems operate in these bands today, including the new generation of 900 MHz cordless telephones, wireless data modems, wireless meter reading equipment, wireless security systems, and so on. These systems generally use spread-spectrum modulation to enhance security, increase range, improve interference rejection, etc. Also gaining much momentum are the 2.5 GHz ISM systems, both high data rate like Wireless Local Area Network (WLAN) and lower data rate applications such as Point-of-Sale terminals and bar-code readers. This frequency is accepted in Europe and Japan as well, allowing much wider distribution for commercial products using 2.5 GHz spread-spectrum modulation. The FCC also provides frequencies for systems operating at 5.8 GHz. These have yet to see widespread use in the commercial market, primarily due to the prevalence of low-cost RFICs and discrete components operating at the lower frequencies. More bandwidth is available at 5.8 GHz, however, so it is expected that the market will eventually move to that band to obtain higher data rates.

Many systems use a technique called "Direct Sequence spread-spectrum", or DSSS. This involves directly combining the pseudo-noise code with the data signal, forming a wideband data stream of encoded data. These

data are then modulated onto an RF carrier, using BPSK, QPSK, FM(FSK), or any of several other techniques. Direct sequence systems tend to be relatively simple to construct, and maintain synchronization upon receive. Other systems use "Frequency Hopping spread-spectrum", or FHSS. As the name implies, the carrier is shifted in frequency by the pseudo-noise code in order to spread out the energy. Essentially, the average power of the two systems is equivalent, but the method of operation is quite different. Frequency hoppers tend to have better immunity to CW interferers, as they can hop to an open channel to avoid the jammer. As is often the case, many systems use a combination of both, whereby the signal is spread using direct sequence over a limited bandwidth, then that entire band is frequency hopped within the available ISM band. An example is a cordless phone with <10 kHz data rate, using a 100 kHz to 500 kHz direct sequence data rate, hopping in 1MHz steps within the 26 MHz available in the 902-928 MHz band.

Both types of spread-spectrum systems are specified under the FCC Part 15.247 rules, which effectively allow up to 1-W transmitted power. This provides extremely good range, albeit at the expense of battery life in a typical consumer item such as a cordless phone. For this reason, most systems actually transmit less than 1-W, typically 100-250 mW. The 6-10 dB reduction in output power only slightly affects the range of the system, but significantly improves the battery life due to current consumption.

Not only are unlicensed users such as the ISM band applications using spread-spectrum for their digital communication systems, but also licensed users are finding advantages as well. Of recent interest is the Qualcomm-sponsored CDMA standard which was recently approved by the FCC under Interim Standard 95 (IS-95) for digital cellular communications in the US. Korea, China, and other countries are adopting the CDMA standard for cellular as well. Likewise, several companies developing hardware for the new Personal Communication System (PCS) are basing the architecture on spread-spectrum modulation.

The primary performance advantages of spread-spectrum modulation are security and processing gain. Security is intrinsic due to the coded nature of the transmitted signal. The receiver must have the exact code, and be constantly scanning for the matching code in order to properly receive the signal. If another spread-spectrum signal is present at the input, it will look like low-level noise. A CW interferer will be handled in different ways, depending on how the receiver is designed. This will be discussed later in this paper. Processing gain occurs due to the correlation of the coded signals, and basically converts bandwidth into signal strength. For example, a spread-spectrum signal in which the code has 10 times greater bandwidth than the data, will give ~10dB of processing gain upon de-spreading. This is very useful for low-level input signals which can be buried in noise, yet still be detectable by a spread-spectrum receiver.

II. SPREAD SPECTRUM (SS) RECEIVER SYSTEM AND CIRCUIT CONSIDERATIONS

THE IDEAL RECEIVER

The ultimate goal of any receiver is to maintain a reliable communication link under all conditions. In order to accomplish this, the receiver must receive only the desired transmission from all signals at its input and reject all others. The ability of a SS receiver to accomplish this goal can be quantified by similar performance measures historically applied in the characterization of narrowband receivers. Specifically, measures of receiver frequency selectivity and spurious-free dynamic range are technical parameters that are meaningful measures of a SS receiver's ability to meet the objectives of a given communication problem. With respect to frequency selectivity, or simply selectivity, an ideal receiver would exhibit a "brick wall" frequency response with the center frequency equal to the carrier frequency and the width of the filter equal to the modulation bandwidth in narrowband systems, or equal to the spread bandwidth prior to despreading followed by the modulation bandwidth after despreading in SS systems. Generally speaking, the selectivity of a receiver is established by the filters and their location in the receiver design. Secondly, an ideal receiver

would maintain acceptable reception under all possible input signal levels within this bandwidth and also in the presence of any in-band and/or adjacent channel interference. Obviously, none of the attributes of the ideal receiver can be realized in the practical world. For battery powered commercial applications, the trade-offs of technical performance versus DC power consumption and cost in SS receiver design become a tangled web indeed. Nevertheless, the attributes of the ideal receiver are what all designers seek, albeit, in vain. Having defined the goal, it is now possible to consider how battery powered commercial SS receivers might best be architected to approach the ideal case.

DIRECT SEQUENCE SPREAD SPECTRUM (DSSS) RECEIVER ARCHITECTURES

Unlike narrowband receivers, SS receivers operate on signals that have bandwidths much wider than the modulated baseband signal. In order to consider how the frequency selectivity and linearity issues effect spread spectrum receiver performance, Figures 1-3 present three DSSS superhetrodyne receiver architectures that are applicable to commercial spread spectrum communications. In these three examples, we have elected to consider receiver architectures for QPSK modulation. Similar topologies can be developed for other modulation schemes, such as, BPSK, FSK, and many others. In Figure 1, the wideband signal is filtered, amplified, and then despread at the RF or carrier frequency. In Figure 2, the wideband RF signal is filtered, amplified, down-converted to a lower IF frequency, and then despread at the IF frequency. Correlation, bit synchronization, and data demodulation are performed by a digital ASIC or a microprocessor. The dual-conversion architecture of Figure 3 is much like that of Figure 2, but the signal despreding is performed at a second IF. In the case of Figure 3, despreding, correlation, and demodulation/bit synchronization are digitally by sampling and digitizing the second IF. For systems using chip rates in the MHz range, digitizing the IF prior to despreding (as in Figure 3) can be a significant drain on the battery. Analog methods of despreding (as

shown in Figure 2) typically consume less DC power than digital approaches that require digital processing at high data rates.

FREQUENCY SELECTIVITY

In DSSS receivers, the RF front-end and/or antenna must have a bandwidth that is at least as wide as the SS signal and a detection bandwidth that supports the modulated baseband signal. Large out-of-band interferers when allowed to pass through the various stages of the receiver have several deleterious effects on receiver performance including receiver desense, in-band intermodulation distortion, and capture of the AGC circuits. Improving the selectivity of the receiver mitigates the degradation associated with all of these effects. In general, the selectivity of any receiver is enhanced by reducing the receiver bandwidth to the detection bandwidth as close to the receiver front-end as possible. Of the architectures presented in Figures 1-3, Figure 1 provides the most selective receiver. In this case, the wideband signal is despread in the front-end of the receiver prior to IF amplification. The jamming margin of the receiver is applied against interference prior to it entering the high gain stages in the IF electronics and the receiver bandwidth is reduced to the detection bandwidth as close to the front-end as possible. This avoids, or at least reduces, the detrimental effects mentioned previously. Unfortunately, this architecture has other drawbacks when compared against the other two in commercial battery powered applications. Specifically, the local SS signal used to despread must be centered at the RF carrier and the balanced mixer(s) used for despreding must operate at RF. This requirement imposes significant performance requirements on IC's designed to operate in the commercial cellular, PCS, or ISM bands. Specifically, carrier suppression, phase/amplitude balance, and other design parameters associated with the modulator(s) and mixer(s) in the receiver electronics must be maintained at RF. Today's IC technologies are capable of providing these high levels of performance at commercial RF, but RF despreding is not prevalent due to the increase in DC power consumption and the increase in complexity in the IF electronics.

SPURIOUS-FREE DYNAMIC RANGE

The spurious-free dynamic range (SFDR) of a receiver is defined as the difference in dB between the receiver noise floor (usually the noise power in the detection bandwidth) and the level of two equal signals that produce an intermodulation product equal to the noise power in the detection bandwidth. The SFDR can be related mathematically to the n-order input intercept point, thermal noise in the detection bandwidth, and receiver noise figure. The two-tone third order intercept point relation is used most often because third order distortion products are generally most likely to fall inside the receiver detection bandwidth. It can be derived that the SFDR of a receiver is related to the two-tone third order input intercept point (IIP3) by the following Equation 1

$$\text{Eq 1. } \text{SFDR} = 2/3[\text{IIP3} + 174 - \text{NF} - 10\log(\text{BW})] \text{ dB}$$

IIP3 = Two-tone third order intercept point referred to the receiver input

NF = Receiver Noise Figure

BW = Detection BW

The SFDR is a useful quantity for receiver designers because it provides a figure of merit indicative of the receiver's ability to receive signals near or at the minimum detectable level in the presence of interference (usually from adjacent channels). SFDR also can be computed from technical parameters that are familiar to RF designers. Parameters such as noise figure, third-order intercept point, and receiver detection bandwidth are also easy to measure. Obviously, in the case of SFDR more is better.

THIRD-ORDER INTERCEPT POINT (IP3)

In their never ending quest to approach the attributes of the ideal receiver, wireless SS receiver designers seek to achieve the highest possible input IP3 (IIP3) in their receivers. The desire for the wireless system designer to achieve the highest possible IIP3 in his receiver

is often tempered by his willingness to provide additional DC power to the circuit designer to meet this objective. IC process technologies available to RF IC designers, such as, GaAs HBT, achieve device gain-bandwidth products of nearly 20 GHz for as little as 2mW of DC power. As an example, Figure 4 shows a plot of device Ft for a GaAs HBT device operating from 2V and 1mA collector current. The point here of course is that today's IC active devices do not require large amounts of DC current to achieve high frequency, wideband small signal gain in commercial applications through 2.4 GHz. RF IC's applicable to commercial wireless SS receivers commonly have their DC power consumption dictated by the IIP3 and filter impedances that the part is required to provide. The IP3/impedance/DC current issue is really no more than providing a linear RF output power into a specified load. Recalling the familiar relation ,

$$\text{Eq 2. } \text{OIP3} = \text{Po}_{1\text{dB}} + 10\text{dB}$$

Where $\text{Po}_{1\text{dB}}$ = Output 1dB Compression Point
= Power level at which the power gain is reduced by 1dB from the small signal gain

From Eq.2 , we observe that we have indirectly specified a linear power level that a circuit must provide to the load in order to meet the OIP3 specification. In the design process, this really boils down to managing the DC-RF efficiency of every functional element in the receiver. Unlike RF power amplifiers, active devices predominately operate Class A in receivers. Theoretically, Class A amplifiers with tuning can achieve a DC-RF efficiency of fifty (50) percent [1]. In certain applications, for instance in the RF portion of a SS receiver, narrow band tuning methods are the best way to optimize DC-RF efficiency.

In the IF portion of a SS receiver prior to despreading, it is particularly desirable to optimize load impedance levels to simultaneously conserve DC power and increase IP3. The signal power levels are highest in the IF section and the receiver must remain linear in this section if there is any hope of recovering the transmission. By maintaining a relatively constant IF signal level, the linearity

performance of the receiver can be optimized under low DC bias conditions. Automatic gain control (AGC) and impedance optimization are two methods the RF designer can utilize to achieve the desired intercept point performance.

AGC is generally employed to maintain a near constant IF output level to the digital portion (or A/D converter) without limiting. Although some form of PSK modulation is often used in many commercial applications, limiting can reduce receiver jamming margin by as much as 6 dB[2]. Although signal strength variations due to multipath are mitigated by the natural frequency diversity of the SS signal, input signal strengths can easily vary by more than 100 dB depending on the proximity of the receiver to the transmitter or base station. In addition, background noise levels can vary significantly, or the presence of other users in the channel can dictate a gain adjustment. Given these considerations and others, it is not uncommon to encounter AGC circuits providing more than 80 dB of AGC range in commercial SS receivers.

Maintaining a constant IF level in the receiver also affords the receiver designer the ability to select impedance levels in IF that avoid unnecessary DC power dissipation. Load impedance design issues at IF might best be handled by careful consideration of the dynamic load line[3]. In battery powered receiver design, the terminal or supply voltage is most often predefined (by the person who designed or selected the battery). As a system designer, the one way to conserve DC power is through considering the load line. The general idea is to maximize the DC-RF efficiency of every active device in receiver remembering that there exists an optimum slope (load) to achieve a given RF output power for a fixed supply voltage and minimum amount of DC current. Figure 5 is an example using the dynamic load line concept for a silicon bipolar device operating from a 3V supply and at a 3mA collector current level. Illustrated in this graph are three AC load lines associated with a 50, 1K and 5K ohm loads for this device. The area of triangular regions shaded in the Figure 5 are representative of the power delivered to each load. Clearly, the device delivers the maximum average power to the 1K ohm load. Unfortunately, practical impedance issues in the IF section are often more involved than simply investigating various

load lines. Available filter impedance levels or practical component quality factors often drive selection of IF impedance levels.

As an additional consideration, the most inefficient method (at least from a DC power management perspective) to provide a conjugate match for filters, or to provide an impedance on a given port, is through the use of series or shunt resistance on the port input or output. In SS receivers, this seems desirable due to the wideband impedance match provided by a resistor. For those desiring a 50 ohm impedance, the penalty can be a major increase in current consumption in the LO drive circuitry. This design practice is probably most often encountered on the LO-ports of active mixers. For bipolar, Gilbert-cell type mixers, the LO-port requires a little more than 100mV_{peak} to operate effectively in most applications. Depending on the technology selected, the inherent LO port input impedance can be as high as several hundred ohms (or even Kohms). As an illustration, if the LO input impedance to the Gilbert Cell mixer is 500 ohms, then the designer will have to expend 10x the DC current (without tuning or transformers) to drive this port to create the same 100mV_{peak} level when a 50 ohm shunt terminating resistor is used at the port input.

NOISE FIGURE

The noise figure achieved in a receiver is predominately influenced by the noise performance of the RF front-end components used in the design. Of the receiver technical parameters discussed in this paper, noise figure is probably the most dependent on IC process selection. Although a great deal could be written on how to achieve the lowest noise figure in a given IC design, this is well beyond the scope of this paper. Some general comments are possible. The noise performance of LNA's designed using bipolar devices is dominated by the device base spreading resistance, R_b . Advanced silicon bipolar devices generally suffer from an increase in R_b as device geometries are made smaller to achieve high gain-bandwidth products at low collector current levels. For applications near 900 Mhz, silicon bipolar LNA/Mixers are adequate in certain applications where a 3-4 dB noise figures in the LNA/Mixer is required. GaAs MESFET

LNA/Mixers devices generally provide equivalent or better noise figure than their silicon counterparts at lower DC bias levels in 900 Mhz applications. In PCS and 2.4 Ghz ISM applications, the GaAs MESFET devices begin to widen the performance gap between equivalently biased silicon bipolar devices. In PCS and ISM applications where ultimate low noise performance is required, GaAs HBT technology out perform both silicon bipolar and GaAs MESFET devices in low power applications. Unlike silicon bipolar devices, HBT devices simultaneously achieve low device Rb and high gain bandwidth products at low DC bias levels. For instance, using GaAs HBT technology it is possible to achieve a 50 ohm noise figure of 1.5 dB and 15 dB power gain for as little as 10 mW of DC power in a 1900 Mhz LNA for PCS.

GaAs IC's are slightly more expensive to process than silicon IC's on a cost per wafer basis. This does not necessarily mean that a GaAs part will always be more expensive than a silicon part for an equivalent functional device. Higher performance levels are possible using GaAs technologies using devices that are physically smaller than their silicon counterparts. This often yields more devices per wafer. In low noise, RF applications, designers must be careful to consider all competing technologies to simultaneously achieve the required performance at the lowest cost.

III. RF COMPONENTS FOR LOW-COST SPREAD SPECTRUM RECEIVERS

Having addressed SS receiver architecture and circuit considerations, the issue of how to best meet the demands of today's cost-conscious consumer wireless customer remains unanswered. Clearly, given the multitude of applications for SS, the answer to this question is not any one answer. Of the block diagrams presented previously in Figures 1-3, the later two architectures of Figures 2 & 3 are most likely to find application in commercial applications. It is possible to implement the active RF/analog portions of both of these SS receivers using low cost, low power, off-the-shelf components. Shown in Figure 6 is a single chip, low cost solution to a DSSS heterodyne receiver suitable for 800 or 900 Mhz communications in the cellular or ISM

frequency bands. The RF2903 is the single chip solution that provides an RF amplifier, RF mixer, 90 dB AGC with RSSI, and an I/Q demodulator suitable for data rates through 50MHz. The RF2903 is packaged in a 28-lead plastic SSOP and was developed using low cost bipolar silicon IC technology. The RF2903 single chip receiver operates from a 3-5 V supply and typically draws 11 mA of DC current. An overall the RF2903 exhibits an 8 dB cascaded noise figure and over 100 dB of RF-Baseband conversion gain.

For SS applications in the 700-1000 Mhz frequency range requiring a more sensitive receiver, the RF2418, can be used, as shown in Figure 7, as the RF front-end with the RF2903 providing the IF AGC/Demodulator functions. The RF2418 was developed using a GaAs MESFET IC technology. The RF2418 provides and RF-IF conversion gain of 24 dB with a 3.5 dB associated noise figure at 900 Mhz. The RF2418 require only 6 external components to apply and achieves an IIP3 of -10dBm. In applications requiring higher performance levels selection of GaAs components, such as, the RF2418, often provide the highest performance level at the lowest cost. In this example, we have elected to not employ the RF amplifier and RF mixer functions associated with the RF2903. Alternatively, we could have elected to use these functions for a dual-conversion superhetrodyne receiver architecture. The RF2418 operates from a 3-6V supply and typically consumes 6.5 mA of DC current. For the case of Figure 7, the receiver noise figure* has improved to 3.6 dB and RF-baseband conversion gain has increased to 114 dB.

For applications in the 1800-2400 Mhz frequency range, chip rates are generally higher to take advantage of the increased bandwidth allocation. WLAN applications at 2.4 Ghz also generally involve higher data rates. For these applications, the RF2431 LNA-Mixer, RF2604 AGC amplifier, and RF2703 Quadrature Demodulator provide yet another highly integrated solution to DSSS reception. Figure 8 provides a block diagram of the 2.4 Ghz chip-set. Also, included in this block diagram is the optional RF2703 configured as a quadrature modulator. In applications where the spreading is performed using QPSK digital modulation at

higher chip rates (>10 Mbs), DC power consumption can be reduced by generating the local SS reference using an analog quadrature modulator, such as, the RF2703. This avoids having to sample and digitize the IF at twice the chip rate. The RF2703 is a quadrature modulator/demodulator that is capable of handling data rates in excess of 50 Mhz at IF's up to 250 MHz. The entire chip-set supports DSSS applications with chip rates in excess of 400 Mbs and data rates of up to 100 Mbs and draws 45 mA from a 3-5V supply. The overall receiver noise figure* is 3.8 dB over the 1800 Mhz -2400 Mhz band.

* Overall noise figure calculations do not include filter losses.

SUMMARY

In this paper we have addressed only some of the applications and circuit and system design issues that face the SS receiver designer. As solutions to commercial applications of SS technology have become more highly integrated to achieve the lowest manufactured cost and highest performance, it has become increasingly clear that RF system design issues play a major role in the development of IC's. Similarly, to meet the demands of a given commercial cellular, PCS, or ISM application it is essential that the Optimum Technology Matching™ is employed in the design process to provide wireless customers with economical products that really work.

REFERENCES

- [1] H.L. Krauss, C.W. Bostian, F.H. Raab *Solid State Radio Engineering*, John Wiley & Sons, Inc., New York, New York, 1980, pp 354-355.
- [2] R.C. Dixon, *Spread Spectrum Communications with Commercial Applications*, John Wiley & Sons, Inc., New York, New York, 1990, pg. 273
- [3] P.R. Gray, R.C. Meyer, *Analysis and Design of Analog Integrated Circuits*, John Wiley & Sons, Inc., New York, New York, 1993, pp 359-361.

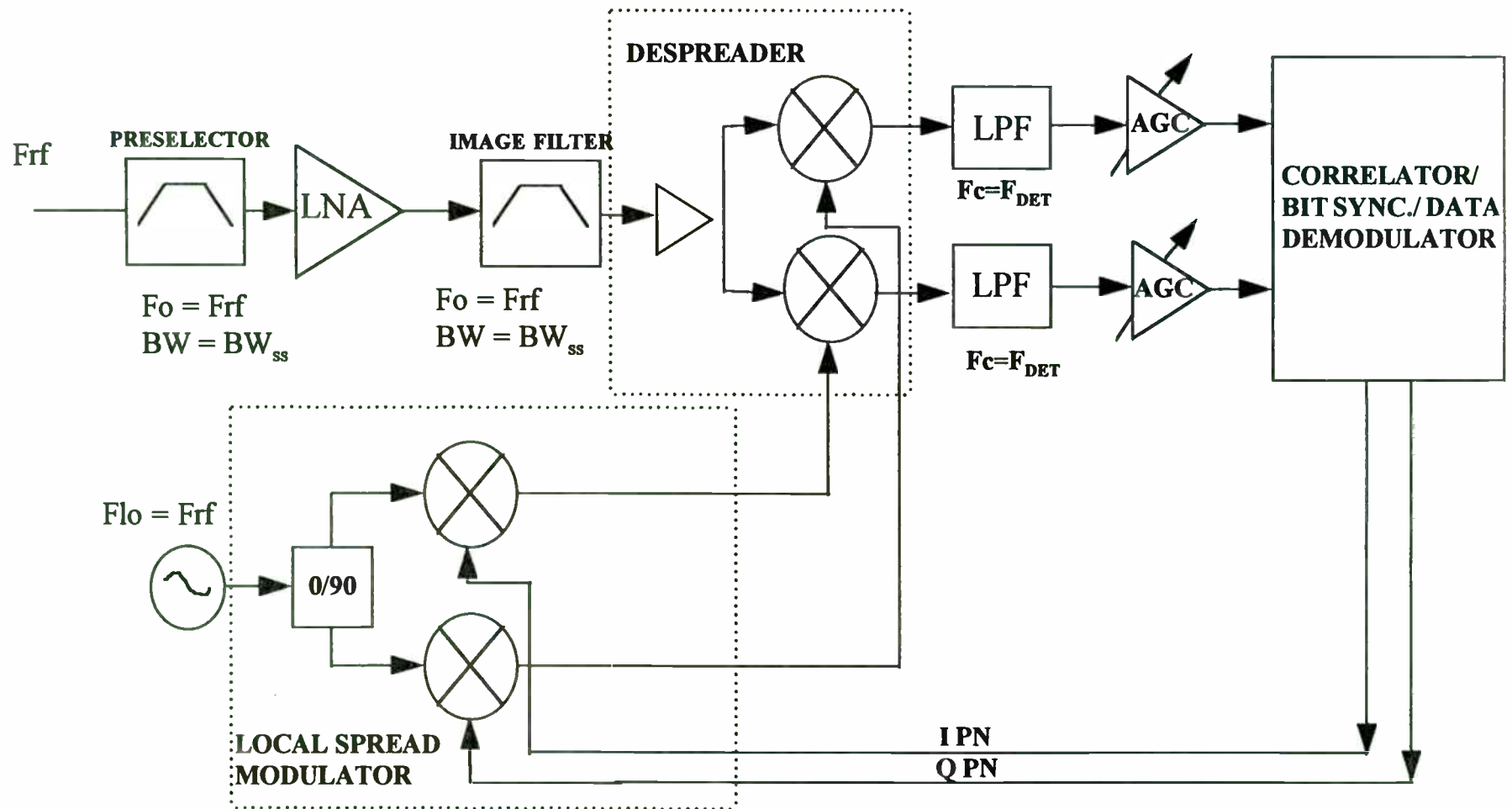
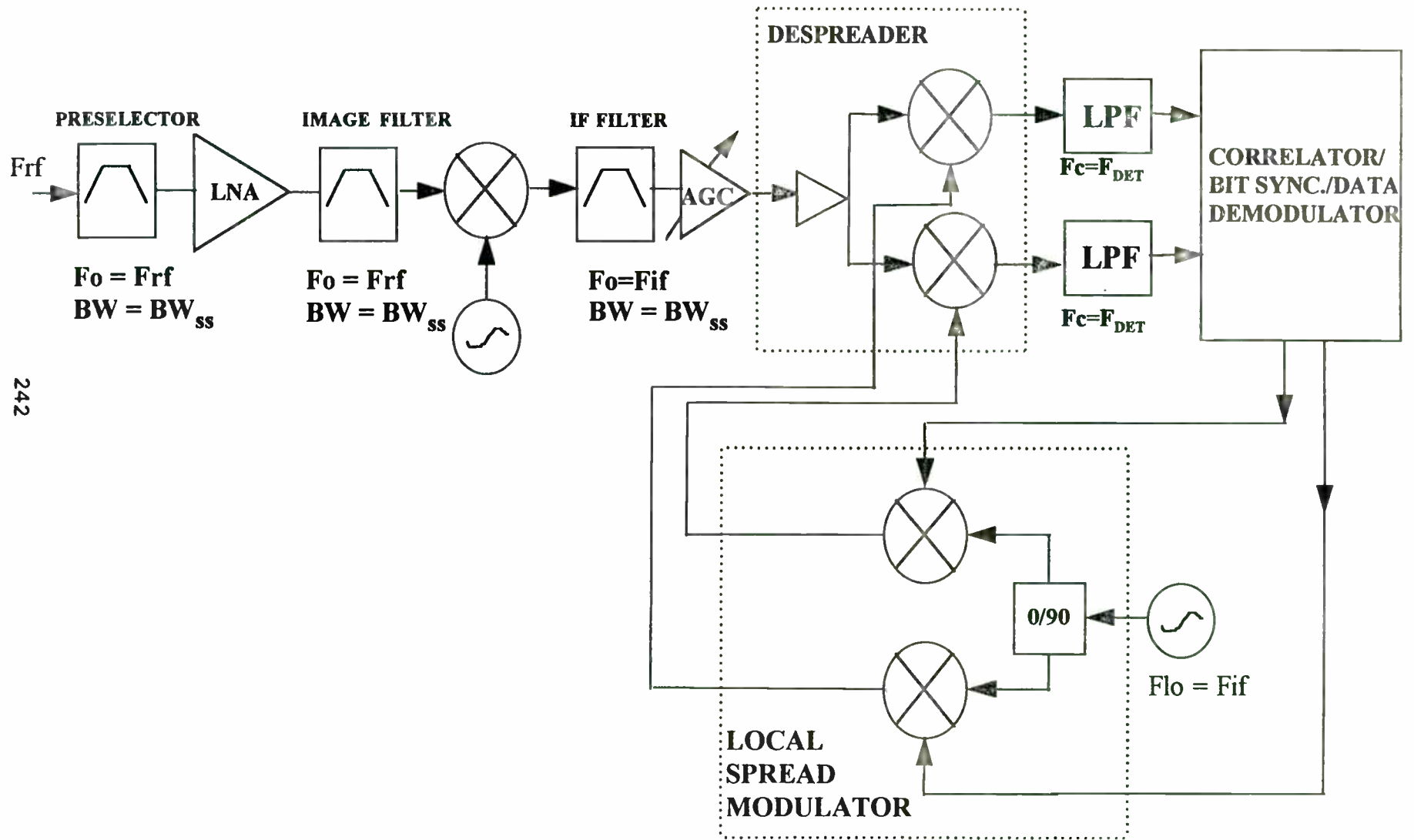
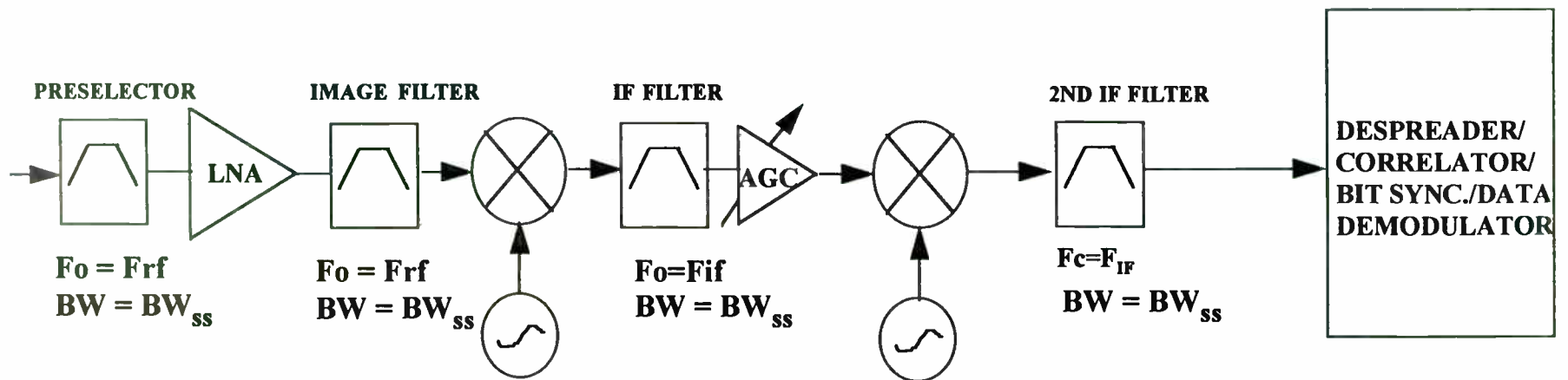


FIGURE 1- DSSS RECEIVER WITH RF DESPREAD



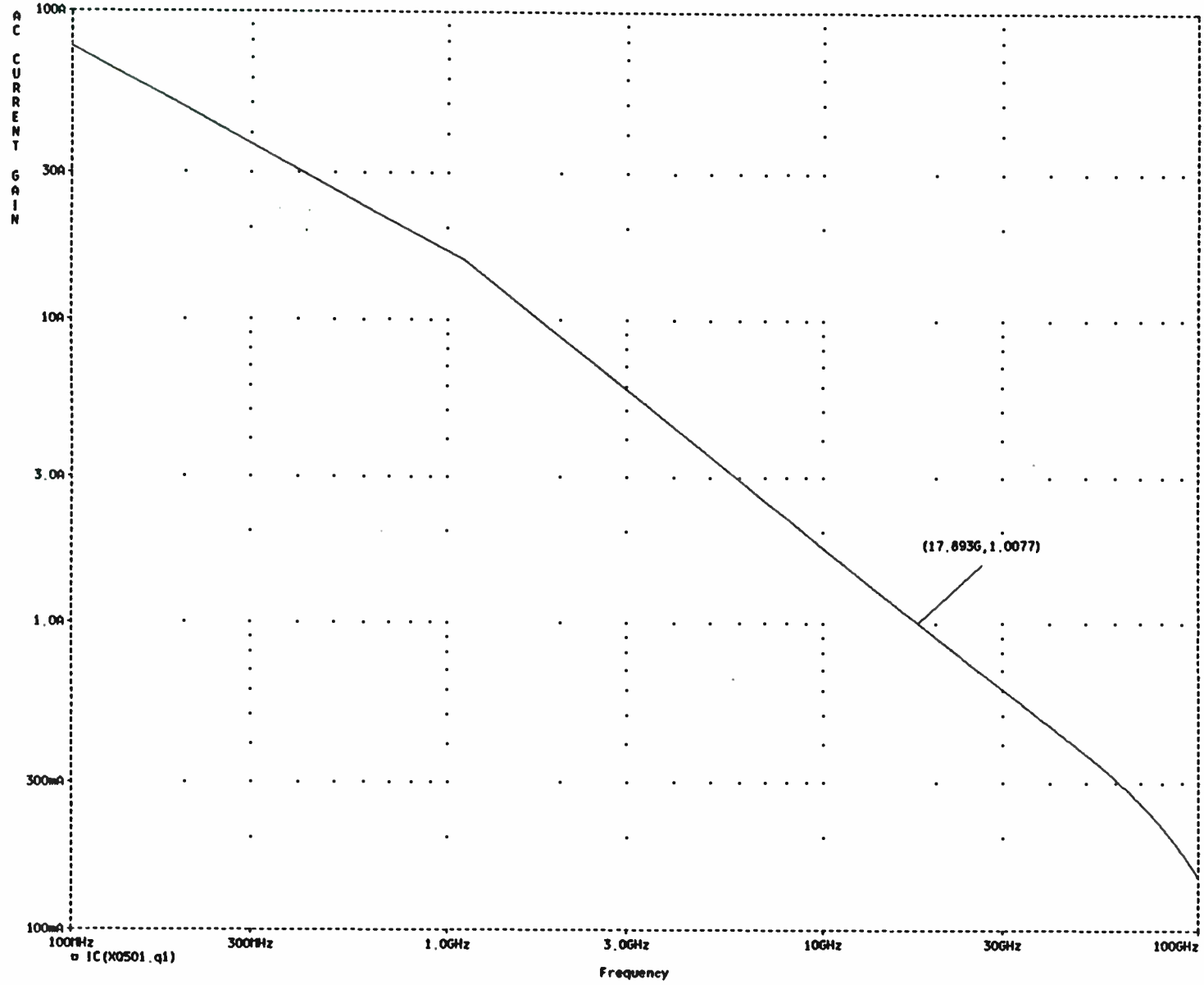
242

FIGURE 2 -DSSS RECEIVER WITH IF DESPREAD



243

FIGURE 3- DSSS RECEIVER WITH WIDEBAND DIGITAL DESPREADER/DEMODULATOR



244

FIGURE 4- CURRENT GAIN OF HBT DEVICE VS FREQUENCY AT $I_c=1\text{mA}$, $V_{CE}=2\text{V}$

245

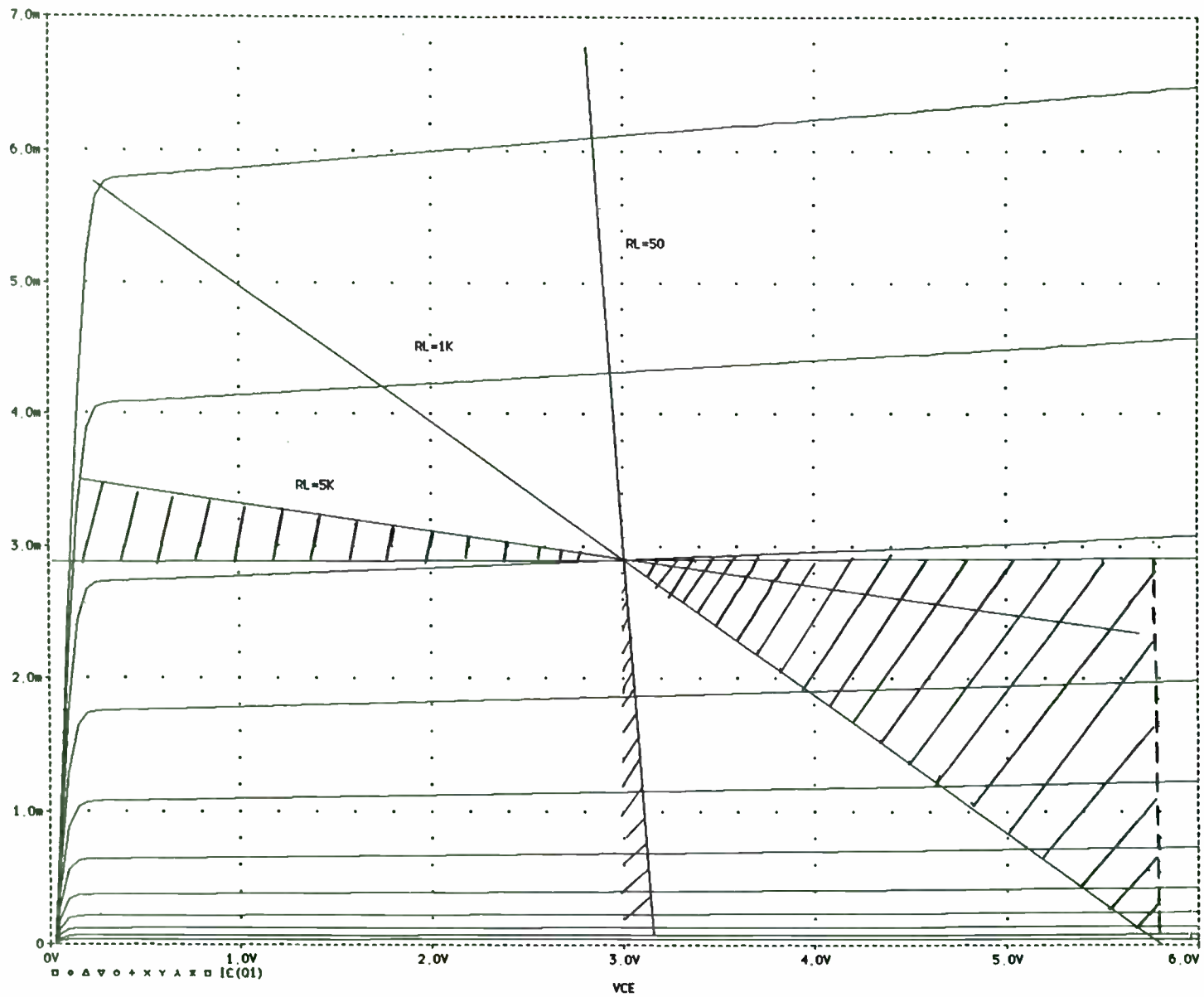
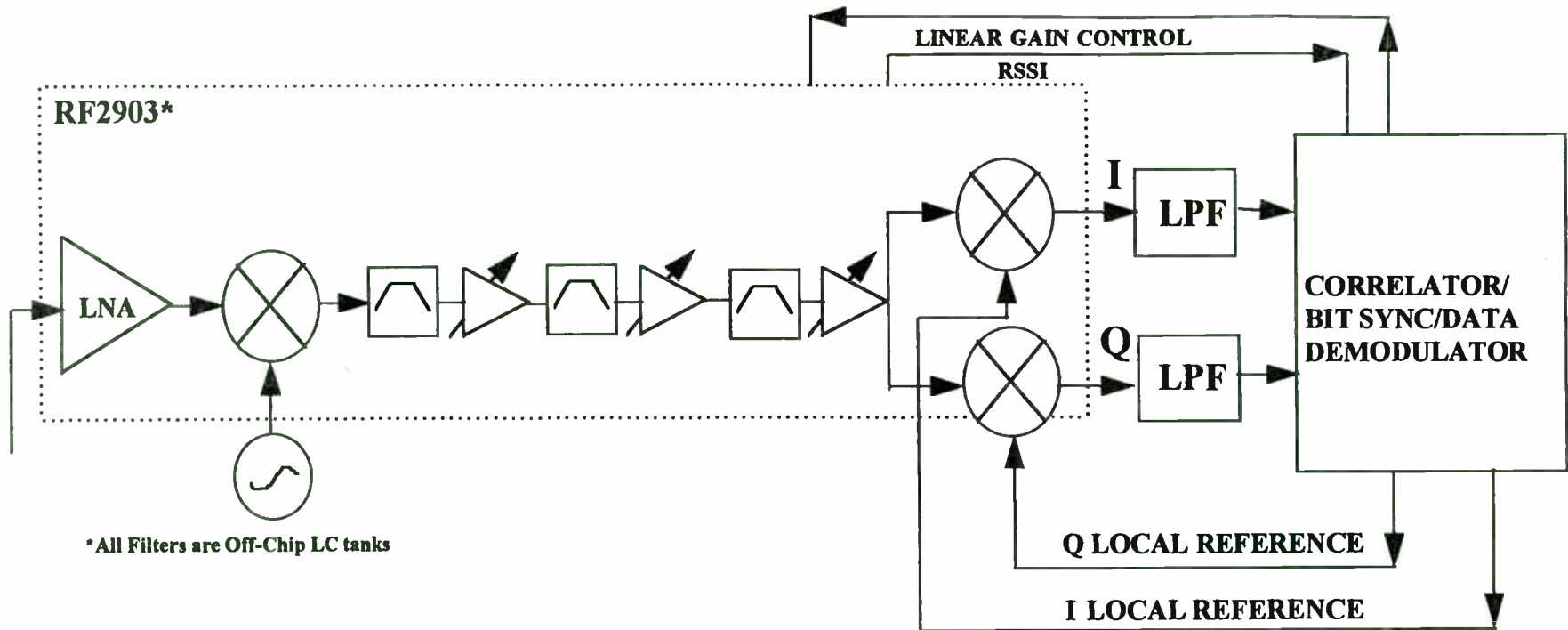


FIGURE 5- OPTIMUM LOAD CONSIDERATION VS DC BIAS POINT TO MAXIMIZE EFFICIENCY



246

CHIP PERFORMANCE SUMMARY	
RF FREQ. RANGE	150-930MHz
IF FREQUENCY RANGE	10-200 MHz
DEMOD OUTPUT FREQ. RANGE	DC-50MHZ
CONVERSION GAIN	100 dB
IIP3	TBD
NF	8dB
DC POWER	11 mA @ 3V

FIGURE 6 -LOW-COST, SINGLE CHIP UHF DSSS RECEIVER WITH IF DESPREAD

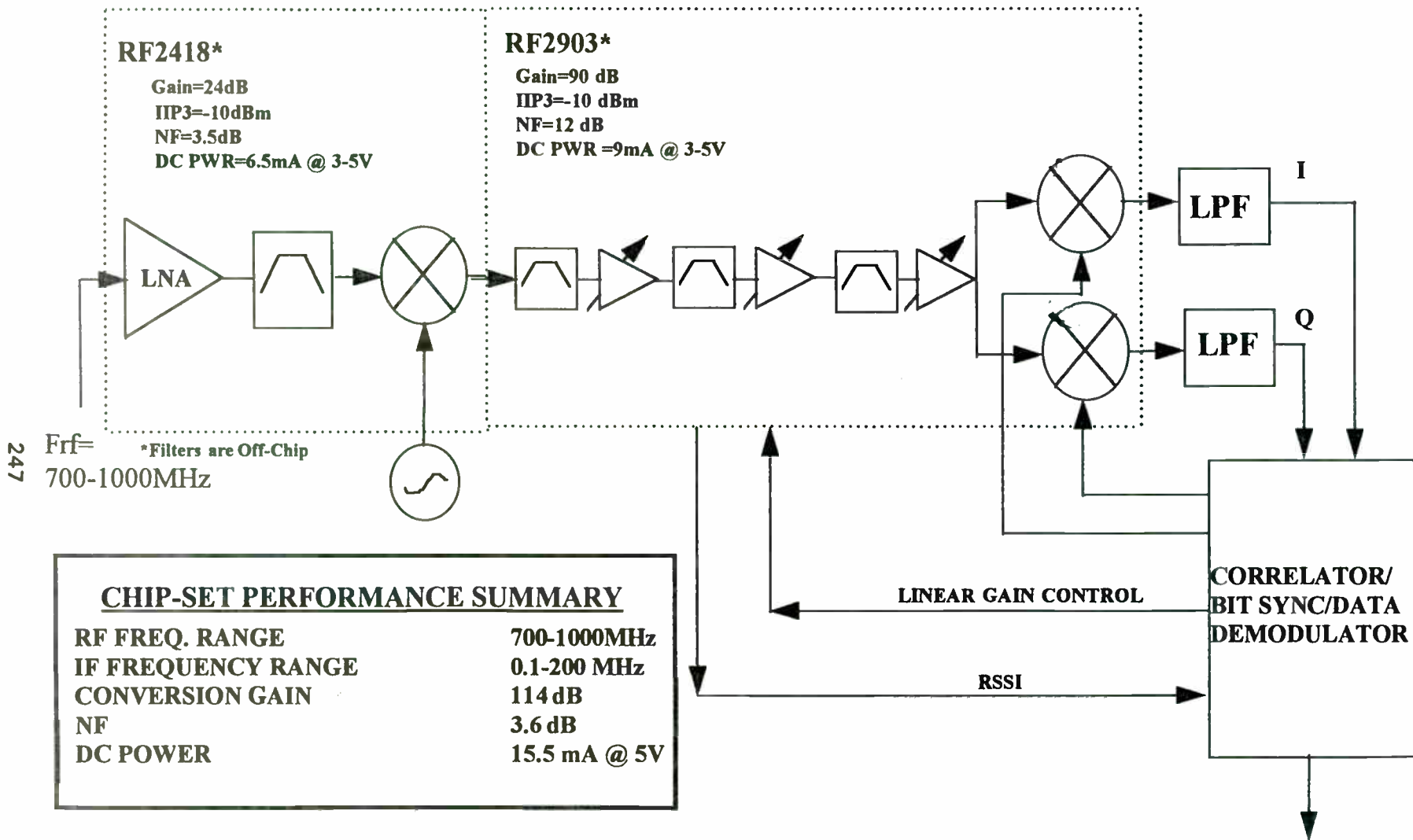


FIGURE 7 -HIGH PERFORMANCE, LOW COST UHF DSSS RECEIVER WITH IF DESPREAD

Half-Rate GSM Speech Codec: True Silicon Complexity vs. ETSI Complexity Evaluation

Author: Chris Cavigioli, Analog Devices

chris.cavigioli@analog.com
+1 (617) 461-3058

Significant Contributors:

Emmanuel Rousseau	Chris Cavigioli	Fausto Giovanni Andreotti	Kari Jarvinen
Michel Galligo	Gordon Sterling	Mario Giani	Olli Ali-Yrkko
	Jerry Lenaz		Pekka Kapanen
	<i>Analog Devices</i>		Tero Honkanen
<i>Alcatel Radiotelephone</i>	Munich, Germany	<i>Italtel-SIT</i>	<i>Nokia</i>
Colombes, France	Norwood, MA, USA	Settimo-Milan, Italy	Tampere, Finland

Abstract

This paper reviews the methodology used to evaluate the complexity of several candidate algorithms for the GSM speech and channel codec based solely on bit-exact ANSI-C programs provided by the respective candidate proponent organizations. This methodology was devised by a special, dedicated sub-group within ETSI TCH-HS, the committee responsible for proposing the GSM Half-Rate coding standard. After presentation of the ETSI method, a real-time, silicon implementation is presented and the true MIPS and memory benchmarks are compared to the original ETSI estimate. The paper roughly breaks down as follows:

- Introduction and Background of the ETSI Complexity Evaluation Method
- ETSI Theoretical Worst-Case
- ETSI Average
- Real, Silicon Implementation
- Conclusions

Introduction and Background of the ETSI Complexity Evaluation Method

Within the framework of the European Telecommunications Standards Institute (ETSI), the TCH-HS committee (Traffic Channel Half-rate Speech) has been chartered to select, on a technical basis, the Half-Rate codec (total speech + channel: 11.4 kbit/s) for the GSM digital cellular standard. During the course of this selection procedure, several candidate codecs have been evaluated in terms of various criteria, including the computational and memory complexity relative to the current standard GSM Full-Rate codec (speech: 13 kbit/s, total speech + channel: 22.8 kbit/s). In December 1993, two candidate codecs remained in the competition: one from ANT Bosch Nachrichtentechnik (Backnang, Germany) and one from Motorola, Inc. (Schaumburg, IL, USA). In order to best compare the complexity of these candidates relative to each other and to the current Full-Rate standard, a complexity evaluation subgroup was formed within TCH-HS to specifically study this matter based on typical DSPs available and ANSI-C simulation programs supplied by the candidate proponents.

Previous work (1), (2), describe in greater detail the exact methodology used in the ETSI complexity evaluation for the theoretical worst-case (1), and the measured average (2). This paper summarizes these results and additionally compares also a true, real-time, DSP silicon implementation and its complexity.

Note that whenever “speech codec” is mentioned, this does NOT include the voice activity detection (VAD) nor the discontinuous transmission (DTX) algorithms.

ETSI Theoretical Worst-Case --- ETSI Mandate

Within ETSI, TCH-HS has been mandated by SMG to perform a technical selection of the two remaining speech and channel codec candidates (ANT and Motorola) for GSM Half-Rate speech traffic. Part of this technical selection involves estimating the complexity of the codecs such that they can be compared to each other and to the standard GSM Full-Rate codec (GSM recommendation 06 series and 05.03) in use today.

Previous complexity evaluation cases within ETSI or CCITT have resulted in incorrect or misleading information due to various interpretations of generic rules applied to differing DSP implementations and reported by the non-impartial candidates themselves. Lack of specific, detailed, supporting documentation allowing cross-checking of the complexity number themselves has also cast previous such cases into doubt. Examples of such cases have been witnessed within ETSI during previous preselections of the GSM Half-Rate candidates and also in other similar ETSI activities such as the TETRA codec selection.

Consequently a subgroup dedicated to complexity evaluation was formed with the following mandate:

- show theoretical worst case figures in weighted Million Operations per second (wMOPs)
- show data memory figures in Kbytes (ROM, RAM)
- compute figures of merit using a formula ultimately agreed in Colombes (TCH-HS TD 91/98)
$$C(\text{codec}) = \text{wMOPs} + \text{RAM}/5 + \text{ROM}/20$$
- compute the ratios vs. Full-Rate:
$$C(\text{ANT}) / C(\text{Full-Rate})$$
$$C(\text{Motorola}) / C(\text{Full-Rate})$$

ETSI Theoretical Worst-Case --- Rules and Methodology

The work of the subgroup was divided in three steps: (1) definition of the complexity evaluation rules, (2) calculation of the complexity figures for the three codecs (Full-Rate, ANT, Motorola), and (3) reaching an agreement for the final figures and publishing the results. The first step was open to any volunteer organization within TCH-HS, including especially both candidates (ANT and Motorola). During the second and third steps, the subgroup worked alone, considering that both candidates were not to participate, in order to reach an impartial agreement for the final figures in due time.

ETSI Theoretical Worst-Case --- Agreeing on Rules for Complexity Estimation

Much thought and discussion was devoted to creating common rules to be used for complexity evaluation, including: (1) memory evaluation rules, (2) allowed operators to be used and their

associated weightings. These weightings are intended to normalize the differences between various DSP architectures and instruction sets and are used to compute the wMOPs figures.

ETSI Theoretical Worst-Case --- Memory Evaluation Rules

The amount of memory will be evaluated separately for each of the four modules (speech encoder, channel encoder, channel decoder, speech decoder). For each module two figures must be given: static RAM and scratch RAM. Scratch memory which can be shared or re-used by different routines will be counted only once. The final RAM figure to be used for complexity evaluation will be computed by summing up the four values of static RAM and adding to that sum the maximum value among the four values of scratch RAM.

The data ROM figure will likewise be separately evaluated for each the four modules described above. The total data ROM figure will be computed by counting all the different tables only once. The C program will be written only using 16-bit words or 32-bit words. The amount of memory will be counted in 16-bit words.

ETSI Theoretical Worst-Case --- Operators to be Used and Associated Weightings

A list of operators was defined with their associated weightings and can be found in document TCH-HS TD 93/141. It is based on the Full-Rate operators published in the GSM 06.10 recommendation plus three additional operators allowed for the Half-Rate codec. Note that only 16-bit and 32-bit arithmetic operations are allowed, specifically also limiting intermediate "accumulator" values to 32-bits only.

An example of these basic operator definitions and weights appears in excerpt form thus:

<code>add(var1, var2)</code>	<code>wgt=1</code>	performs the addition (<code>var1 + var2</code>) with overflow control and saturation; the 16-bit result is set at +32767 when overflow occurs or at -32768 when underflow occurs
<code>shr(var1, var2)</code>	<code>wgt=1</code>	Arithmetically shift the 16-bit input <code>var1</code> right <code>var2</code> positions with sign extension. If <code>var2</code> is negative, arithmetically shift <code>var1</code> left by <code>-var2</code> and zero fill the <code>-var2</code> LSB of the result: <code>shr(var1, var2) = shl(var1, -var2)</code> . Saturate the result in case of underflows or overflows.
<code>L_add(L_var1, L_var2)</code>	<code>wgt=2</code>	32-bit addition of the two 32-bit variables (<code>L_var1 + L_var2</code>) with overflow control and saturation; the result is set at +2147483647 when overflow occurs or at -2147483648 when underflow occurs
<code>L_abs(L_var1)</code>	<code>wgt=3</code>	absolute value of <code>L_var1</code> ; <code>L_abs(-2147483648) = 2147483647</code>
<code>div_s(var1, var2)</code>	<code>wgt=18</code>	produces a result which is the fractional integer division of <code>var1</code> by <code>var2</code> ; <code>var1</code> and <code>var2</code> must be positive, and <code>var2</code> must be greater or equal to <code>var1</code> ; the result is positive (leading bit equal to 0) and truncated to 16 bits; if <code>var1 = var2</code> , then <code>div_s(var1, var2) = 32767</code>
...etc...		

ETSI Theoretical Worst-Case --- Methodology for Theoretical Worst Case Evaluation

Determination of the Theoretical Worst Case (TWC) complexity of the program was carried out for the three programs (Full-Rate, ANT, Motorola) considering each program is subdivided into two parts: (1) speech encoder and channel encoder, and (2) channel decoder and speech decoder. The TWC is obtained by summing the TWC of all encoding modules and decoding modules.

This calculation of the TWC of the complexity of the encoding and decoding parts is done in two steps: (1) preselection of the most complex flow paths of the program, and (2) calculation and selection of the program flow-path with the TWC complexity

ETSI Theoretical Worst-Case --- Preselecting the Most Complex Flow Paths of the Program

Preselecting the most complex flow paths of the program is done by traveling through the listing of the program from its beginning until its end, in order to represent the program flow structures in a tree format thus:

ROOT	beginning of the program
NODE	encounter of a choice ("if", "while", ...)
BRANCH	list of the consecutively executed functions associated with their calling parameter values, where no choice (i.e. node) has been encountered.
LEAF	end of a possible flow-path of the program
TREE	complete program flow structure diagram

The tree structure is constructed using the following **tree-building rules**:

- The first single branch following the root will correspond to the list of the first consecutive functions invoked before a "choice" has been encountered.
- Each function will be associated with calling parameters values leading to the TWC complexity of that function. These passed parameters are determined considering **the coherence rule** described below.
- If the complexity of the function is independent of its calling parameter values, these parameters have only to be chosen considering previous choices of functions calling parameter values.
- If the complexity of the function is dependent of its calling parameter values, these parameters will then correspond to the ones that give the function its maximum complexity, with respect to the previous choices of previous functions calling parameter values.
- Next, when a choice is encountered in the program flow, it will be shown as a node in the tree.
- Each branch following this node will be evaluated and, like the first branch, each one will correspond to the list of the consecutive functions associated to their respective TWC calling parameter values (determined like above), until the next function encountered introduces a choice (creation of a new node with multiple branches) or the end of the program (creation of a leaf).
- Continue in this manner until the complete program has been evaluated.

Each possible flow path of the program is then represented by a specific path from the root to one leaf, and each such path corresponds to a list of functions with their associated TWC calling parameter values.

ETSI Theoretical Worst-Case --- Calculation and Selection of the TWC Flow-Path

The calculation of the complexity of the different possible flow paths and the overall TWC of the complexity of the program is achieved by traveling through the program backwards (backtracing), using the program listing, from a leaf back to the root, with respect to the following **branch selection rules**:

- The calculation begins with the identification of the first "competitor" sub-paths group, consisting of the sub-paths from different leaves leading to the closest common node.
- Each sub-path of this group is then evaluated in wMOPs from the leaf to the common node. Each one corresponds to a list of function associated with its respective calling parameter TWC values. The number of wMOPs of a sub-path is equal to the sum of all its function wMOPs.

--- The number of wMOPs of each function is calculated by the decomposition of the function into basic operators (already done in the C program), with their associated occurrences. Each of these basic operators are associated with a particular weighting, as defined in the document TCH-HS TD 93/141. The number of wMOPs of a function corresponds to the summation of each basic operator weighting multiplied by its TWC occurrence in the function. This TWC occurrence is calculated from the TWC function calling parameter values with the same coherency rule as the one explained in the preselection above.

--- Once all sub-paths leading to the same node are evaluated, their final number of wMOPs are compared, and the path with the maximum number of wMOPs is chosen and the other ones are eliminated. Now, there is only one surviving sub-path so far.

--- Then, the next "competitor" sub-paths leading to the closest new common node is identified, this group contains the sub-path made from the surviving sub-path to the new common node and the other sub-path(s) from different leaves to this new common node.

--- The selection of the surviving path of this "competitor" group is then done like the previous one, by calculation of the maximum wMOPs between the different sub-paths, and so on until only one path is left surviving.

The final surviving path from the root to this leaf defines a listing of consecutive functions with their associated TWC values of calling parameters, and corresponds to the worst case possible path of the program flow. The associated total number of wMOPs corresponds to the TWC of the complexity of the program.

An example of flow-paths is shown by taking an excerpt of the Motorola speech encoder thus:

<i>FUNCTION</i>	<i>NUMBER OF CALLS</i>
SPEECHENCODER()	1
FILTA_2ND(NPTS=160)	1
IIR_D(NPTS=160)	1 X 2
AFLAT()	1
FLAT()	1 X 1
COV16()	1 X 1 X 1
SQROOT()	1 X 1 X 1
ROQUANT()	1 X 1 X 1
ATOCORDPL()	1 X 1
L_MPY_LS()	1 X 1 X 45
L_MPY_LL()	1 X 1 X 55
INITPBARFULLVBARFULLL()	1 X 1
...etc...	...etc...

The TWC complexity results of each function in these TWC paths is given by tables, containing for each function, the TWC occurrence of each basic operators within the C functions. Here is an excerpt from ANT, although weights are not shown due to space constraints of this paper:

<i>operation occurrences</i>	<i>SpeechDecode()</i>	<i>lspdec()</i>	<i>lsp_lpc()</i>	<i>lspsyn()</i>	<i>ff_calc()</i>	<i>...etc...</i>
SDM (16-bit move)	371	26	88	48	660	
LDM (32-bit move)	1			33		
abs						
shr, shl	160			6		
add, sub, neg		14	60	51	84	
mult						
mult_r	160		90		408	
mac_r, msu_r		5			168	
L_shr, L_shl				30		
L_add, L_sub, L_neg				63		
L_abs				30		
L_mult						

L_mac,L_msu	160	10		105	336	
extract				30		
L_deposit					168	
Atest		4		36	168	
SLog	160					
LLog						
norm_s						
norm_l				3		
div_s						
weighted TOTAL 20 ms	1175	68	328	744	2904	...etc...

The complete justification of each element of the TWC tables of the codecs is given by the annotated listings of the C program. Here is a short excerpt from the annotated Motorola listing:

```

/* Decorrelate vectors */
/*-----*/

for (iLoopCnt = 0; iLoopCnt < iNumVects; iLoopCnt++) {

    swCShift = g_corr2_(pswGivenCopy, &pswVects[iLoopCnt*S_LEN], &L_temp1);
    // 9 g_corr2_()
    // 9 g_DM
    L_Temp2 = L_Temp1;
    // 9 L_DM
    L_Temp1 = L_abs(L_Temp1);
    // 9 L_abs
    swCShift = sub(swCShift, 1);
    // 9 sub
    swShiftSum = sub(swCShift, swEShift);
    // 9 sub
    L_Temp1 = L_shr(L_Temp1, 1);
    // 9 L_shr
    if ( swNorm_energy == 0 ) {
    // 9 A_test
    //$$NWC ..not worst case..
        return;
    }
    swTemp = divide_s( round(L_Temp1), swNorm_energy);
    // 9 div_s
    // 9 round
...etc...

```

ETSI Theoretical Worst-Case --- Methodology for Data Memory Determination

The determination of the memory contribution has been made for the three programs (Full-Rate, ANT, Motorola) considering the following procedure. Each codec program is subdivided into four parts: (1) speech encoder, (2) speech decoder, (3) channel encoder, and (4) channel decoder.

As it was decided that the total figure for the ROM and the static RAM memory will be the sum of the four respective ROM and static RAM contributions, and the figure of the scratch RAM will be the maximum of the four scratch RAM contributions.

ROM identification: The ROM memory corresponds to all the variables which have constant values, even if these variables are not specifically defined using the C preprocessor directives. The constant values used by different parts of the program are only counted once and are indicated as shared ROM memory.

Static RAM identification: Differentiating data memory between static and scratch RAM takes into account its C declaration characteristics, without taking into account various possible DSP implementations. It has been considered that all the variables declared in C using the "static" keyword,

and only these variables, are to be considered as static RAM, with the exception of the static RAM arrays that are used like constant tables (counted as ROM).

Scratch RAM identification: All other variables that are not static RAM, according to the above static RAM definition, are considered as scratch RAM. This is also true for the variables passed as parameters to the procedures `speech_encoder`, `speech_decoder`, `channel_encoder`, `channel_decoder`. These are considered as scratch RAM without any consideration regarding their use or their declaration.

The final figure of scratch RAM is calculated using the following scratch RAM tally procedure:

--- For each function, the value of the scratch RAM is the sum of the value of the scratch RAM of the calling procedure and of its own local scratch RAM variables. No optimizations due to possible DSP implementations is taken into account.

--- If a function is called by another function, a value of the scratch RAM is evaluated in each case.

--- For each of the four parts of the program, the final value of the scratch RAM is the maximum value of the scratch RAM on all these subprocedures.

ETSI Theoretical Worst-Case --- Estimation of the Program Memory Instruction Storage

An estimation of the program memory instruction storage was requested "for consideration", since this figure is absent in the "figure of merit" formula.

Considering that the amount of program memory words is very dependent on the DSP where the code is implemented, the figures obtained can only be considered as a rough estimation. This is the reason why the results are given as an interval instead of a fixed figure.

The estimation of the program memory storage, for the three codecs (Full-Rate, ANT, Motorola) was made based on some existing real-world DSP implementations of the Full-Rate codec, and then extrapolation using the approximate ratio between the Full-Rate reference and the Half-Rate candidates.

The ratio between the Full-Rate and the Half-Rate candidate codecs has been calculated from the number of "pure instruction" C lines of the source. This "pure instruction" C lines number has been computed from the C lines number of the three source programs where all the C lines for comments, preprocessor directives and data memory declaration have been removed.

ETSI Theoretical Worst-Case --- Results

The table below represents a summary of the result of the ETSI theoretical worst-case complexity evaluation for the GSM Half-Rate codec candidates:

<i>algorithm module</i>	<i>weighted operations per 20 ms frame</i>	<i>wMOPs (worst case)</i>	<i>16-bit scratch data RAM</i>	<i>16-bit static data RAM</i>	<i>16-bit data ROM</i>	<i>estimated program instruction storage</i>
sp enc	45575	2.2788	694	140	80	
ch enc	4272	0.2136	1499	0	824	
ch dec	30097	1.5049	1689	1	*824	
sp dec	13536	0.6768	838	223	*39	
Full-Rate total	93480	4.6740	**1689	364	904	2000-3000
sp enc	281507	14.0754	1301	1387	*694+853	
ch enc	3617	0.1809	620	228	*363	

ch dec	75092	3.7546	1643	486	160	
sp dec	27661	1.3831	469	601	95	
ANT total	387877	19.3939	**1643	2702	2165	4000-8000
sp enc	328994	16.4497	1903	1132	*6556+1105	
ch enc	1656	0.0828	714	114	*452+192	
ch dec	57359	2.8680	2876	164	*452+256	
sp dec	42628	2.1314	679	582	*6556+125	
Motorola total	430637	21.5319	**2876	1992	8686	8000-12000

* = shared ROM counted only once

** = total scratch RAM is maximum among the four modules

sp = speech, ch = channel, enc = encoder, dec = decoder

ETSI Average --- Methodology Used for the Average Complexity Evaluation

As opposed to the fairly complicated and labor-intensive method of determining the theoretical worst case complexity using the tree structure decomposition and checking for coherency, computing the average complexity is much more straightforward, especially since functional, bit-exact, ANSI-C programs are available.

The methodology used for average complexity evaluation is based on adding complexity counters directly in the three C programs (Full-Rate, ANT and Motorola).

In addition to the standard output data from the codec program, complexity statistics are reported by the program. These statistics are directly related to the input sequence used. In some cases, the reported complexity could approach the theoretical worst case, and in other cases, the instantaneous complexity could be much lower. One 20 ms speech frame is considered to be the smallest measuring period for this complexity figure. By processing many speech frames and averaging the reported statistics of all the frames, an overall "average complexity" can be obtained as well as also selecting the "worst observed frame". It could also be interesting to investigate how often and how close individual frame statistics approach the theoretical worst case and as well as the standard deviation of the observed frame reports over time.

Of course, it is mandatory that the standard output of this modified codec program exhibits "bit-exactness" with its respective original program. This has been verified at each step of the code modification development using the test files supplied by the candidates: ANT and Motorola and with the test files from Alcatel SEL for the Full-Rate codec.

The additional output created by these modified codec programs report the complexity average of the given input sequence in wMOPs and indicates also the worst observed frame of the input sequence. (wMOPs have been defined previously(1) as weighted million operations per second ... where weights have been agreed upon and assigned).

The average complexity figures were requested during the 16th TCH-HS meeting in order to have an estimate of the average power consumption of a real hardware VLSI implementation. This power consumption is directly proportional to the average complexity.

The worst observed frame information can be compared to the evaluated theoretical worst case complexity figures and can be expected to be the lower boundary of the those figures.

ETSI Average --- Adding Complexity Counters to the Codec Programs

The three resulting programs have been realized by adding local complexity counters, and an overall complexity counter tallying routine.

The local complexity counters have been added inside the code parts where the basic-operators are defined as C-functions. These counters increment by its associated weight every time the basic operator is invoked in the program.

But this is not complete, because the following basic operations do not appear in the C program as C-callable functions: SDM = short (16-bit) data move, LDM = long (32-bit) data move, the IF-THEN operation and logical operations. It was then decided to create a special incrementation macro for each of these four operators and to add this where the operation appears.

The following macros were defined:

- IncSDM(n): increment SDM tally by n
- IncLDM(n): increment LDM tally by n
- IncLog(n): increment logical tally by n
- Incif(n): increment IF tally by n

While the codec program processes the input sequence file provided, the overall complexity tallying routine reads all the local counters and reports the final results in a table presenting:

- The average complexity tally for each basic operator of each function
- A detailed complexity table for the Worst Observed Frame of this input sequence.

The three modified codec programs and example input sequences were supplied to interested TCH-HS members on floppy diskette so that anyone could re-create the results themselves at home.

In order to be fair with the three codecs, the same input sequence representing 8198 frames of speech at 20 ms per frame was used. This input test sequence concatenates the three different speech frames groups that were corresponding to the worst observed frames for each of the programs. These groups were selected from the speech test files that were used for the quality evaluation of the Half-Rate candidates.

Results of three candidate codecs (Full-Rate, ANT, Motorola) for same specific input test sequence are presented together with the theoretical worst case and memory usage evaluations in the following table.

ETSI Average --- Results

The table below represents a summary of the result of the ETSI measured average complexity evaluation for the GSM Half-Rate codec candidates based on given 8198 input speech frames:

algorithm module	wMOPs (theoretical worst case)	wMOPs (average measured over 8198 frames)	wMOPs (singular worst observed frame within 8198 frames)
speech encoder		2.2788	

channel encoder	0.2136		
channel decoder	1.5049		
speech decoder	0.6768		
Full-Rate total	4.6740	4.5423	4.5698
speech encoder	14.0754		
channel encoder	0.1809		
channel decoder	3.7546		
speech decoder	1.3831		
ANT total	19.3939	17.0989	17.5971
speech encoder	16.4497		
channel encoder	0.0828		
channel decoder	2.8680		
speech decoder	2.1314		
Motorola total	21.5319	17.1471	19.3064

Real, Silicon Implementation --- Introduction

The reason for performing a complexity analysis is to get an estimate in advance with the highest degree of certainty of the true MIPS and memory requirements of future real silicon implementations before they become available. With this in mind, it is very interesting to review these evaluations after true silicon implementations have become available and compare them to judge the accuracy of the original complexity evaluation predictions. This section discusses a true silicon implementation of the GSM Half-Rate speech codec. Note that this does not include the DTX system (and the ETSI evaluation doesn't either), and it does not include the channel codec (which the ETSI evaluation does, but the ETSI evaluation shows the channel and speech codec numbers separately, allowing convenient comparisons). Contact the author for additional information on DTX and channel coding implementations on Analog Devices DSP silicon.

Real, Silicon Implementation --- Implementation of Version 3.1 Motorola Speech Codec

This section presents a brief summary of the worst case timing (MIPS) analysis of the ADSP-21062 implementation of the GSM Half-Rate speech codec. More details are available from the author. No special analysis for memory usage has been carried out, however, the DSP software development tools for the target DSP chip provide a linker program which also outputs a file detailing the actual memory usage which is sufficient to draw some memory benchmark conclusions. The assembly language version of the codec implementation is based on version 3.1 (December 1993) of the Motorola GSM Half-Rate speech codec candidate. This version is practically identical as version 3.0.2 used in the ETSI analysis.

The assembly language implementation has been tested using the 'short.spd' input and output files that is contained in the version 3.1 software release. The assembly language implementation produces exactly the same the same outputs (bit-exact coefficients and bit-exact output speech) as the C-language version.

The worst case execution paths are discussed in Annex 12 of the ETSI analysis (3). Annex 12 lists the major subroutines of the codec with the critical parameters (which cause the worst case path to be followed) and the number of calls to that function. Annex 12 is based on version 3.0.2 of the Motorola speech transcoder. There are no significant differences in worst case path between version 3.0.2, and version 3.1 used in this analysis.

Real, Silicon Implementation --- Selecting a Suitable DSP

Analog Devices manufactures both a 16-bit DSP processor product line (ADSP-2100 family) and a 32-bit DSP processor product line (ADSP-21000 family). Both product families (7) are based on internal DSP cores with various permutations of on-chip memory and peripherals.

Although the GSM speech coding algorithm recommendation implies using 16-bit arithmetic, this does not preclude an implementation on a processor which uses a 32-bit native data type. Although there is a performance overhead associated with performing bit-exact 16-bit arithmetic on a 32-bit machine, there are also significant performance enhancements due to the ADSP-21000 family core architecture and instruction set. The end result is that due to additional requirements imposed by GSM base station needs, and due to a possible changes in the Half-Rate coding algorithm during code development, it was decided that a highly reliable implementation would be developed using a DSP with more performance than is required. The ADSP-21062 processor was selected. Upon closer inspection of the actual benchmarks observed, this choice allows not only the GSM speech codec software to run successfully bit-exact, but it also allows an additional channel to be processed fully. Furthermore, on-chip memory integration allows an ADSP-21062 to fully process the two independent channels without requiring any external SRAM (static RAM) memories whatsoever. This offers significant cost savings even when compared to cheaper 16-bit DSPs which require fast, expensive external SRAMs and only allow one channel of processing per DSP.

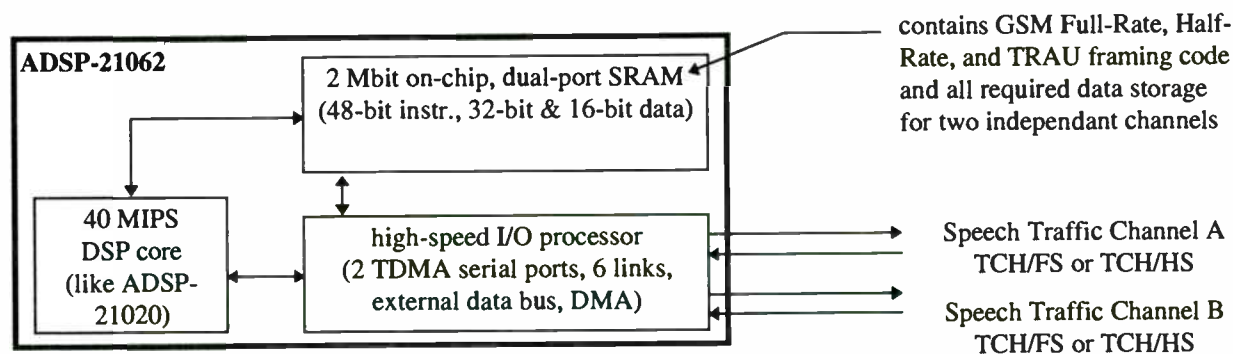


Figure 1: experimental set-up processing two GSM speech traffic channels with one chip (ADSP-21062) only

Real, Silicon Implementation --- Assembly Code Implementation and Simulation

The assembly language implementation is currently written for the ADSP-21020 Digital Signal Processor (DSP), because the ADSP-21062 chip and its hardware development tools were not yet readily available during the bulk of the code development process in early 1994. This is fully compatible with the ADSP-21062 which is a superset of the ADSP-21020. The real-time hardware was realized using "Gamma 20/25" PC-compatible ISA bus plug-in development boards commercially available from Bittware (8) for ADSP-21020 development.

The numbers reported here are the exact numbers taken from a simulation of the assembly language implementation using the bit-level assembly simulator called 'sim21k.exe' contained within the Analog Devices software development tools, ADDS-210XX-SW-PC, version 3.1.

The code will be ported to the ADSP-21062 processor in the final stages of development. Porting to the ADSP-21062 will reduce the overall MIPS requirements slightly due to the enhanced instruction set of the ADSP-21062. This reduction in MIPS was *not* considered when performing this analysis.

This analysis uses the worst case path as shown in Annex 12 of the ETSI complexity evaluation (3).

Real, Silicon Implementation --- Goals of Benchmark Study

This analysis answers the following questions (of both academic and commercial interest) for utilizing a single chip ADSP-21062 running at 40 MHz (i.e. 40 MIPS) without requiring external memory chips in a GSM base station to:

- transcode two full duplex GSM speech traffic channels (either Full-Rate or Half-Rate)
- support all the TRAU framing (14,15) for communications between the MSC and the BTS

Not reported here, but also available from the author is additional information demonstrating that:

- delay requirements are met for both channels in all modes (Full-Rate, Half-Rate, mixed mode)
- component costs using this scheme are about half the cost of equivalent 16-bit DSP implementations using external SRAM memory storage and two DSPs, one for each channel.

For understanding the GSM architecture and the many acronyms which are used in the GSM system, and the reader is encouraged to find more informative definitions of such items such as TRAU (transcoder and rate adapter), MSC (mobile switching center), BTS (base station transceiver system) and so forth within the GSM recommendations themselves (16).

Real, Silicon Implementation --- True MIPS Benchmarks

This discussion of the Half-Rate benchmarks (13) does not cover the GSM Full Rate software in detail (also available from Analog Devices for the ADSP-21020 target, bit-exact with the ETSI digital test sequences). The Full Rate software requires significantly fewer MIPS (about 10% of the MIPS required for Half Rate). Further analysis is available which discusses the exact time slicing of the various algorithms.

The TRAU framing software is estimated to require about 50 μ s every 2.5 ms per channel in the worst case. The worst case for TRAU framing is the three windows that the TRAU framing software is attempting to find the TRAU header. This works out to about 1 MIPS (50 microseconds = 2000 instructions at 40 MHz, multiplied by 400 times per second). This number can be tripled to 3 MIPS per channel for a highly reliable estimate.

The TRAU framing is estimated to require 3 MIPS per channel or 6 MIPS for two channels running on the ADSP-21062. This leaves 34 MIPS available for processing the two channels of GSM transcoded speech.

The GSM Half Rate speech encoder requires a conservative 281,000 cycles per invocation. This corresponds to about 14 MIPS per channel to encode a 20 ms frame of speech traffic.

The GSM Half Rate speech decoder requires a conservative 31,000 cycles per invocation. This corresponds to about 1.6 MIPS per channel to decode a 20 ms frame of speech traffic.

The GSM Half Rate speech transcoder requires less than 16 MIPS per channel to transcode (encode and decode) a 20 ms frame of speech traffic. A two channel system would require 32 MIPS to transcode two full-duplex, Half Rate speech channels. This is well within the 34 MIPS available, even with the conservative estimate for TRAU framing.

Real, Silicon Implementation --- True Memory Benchmarks

After successful assembly of each of the ADSP-21020 code modules, the linker is invoked (9). By invoking the linker with a special command line switch, a memory map file (identified by .MAP file extension) reports the exact usage of data and program memory segments (12).

Upon inspection of this memory map file for a case where only one channel of GSM Half-Rate (only) speech is implemented without DTX functions, the following results were reported:

- 5377 words + 256 words program memory instructions in program memory (PM) space. The 256 words represents the default allocation for the interrupt vector table space on the ADSP-21020.
- 1428 total words of RAM and ROM storage mapped in program memory (PM) space
- 7079 words + 7064 words total RAM and ROM storage mapped in data memory (DM) space.

Note also that much data storage does not need to be duplicated to handle the second channel. Likewise, most of the program instructions could be re-used for processing of the second channel in dual-channel implementations.

Note that the difference between RAM and ROM storage is not reported. This is due to the fact that all the ROM storage on the ADSP-21062 might as well be stored as RAM since there is more than adequate RAM available on-chip already anyhow.

Analog Devices Conclusion: A 40 MHz ADSP-21062 can reliably support two full-duplex channels of GSM transcoded speech on one ADSP-21062 chip without using external memory components.

Real, Silicon Implementation --- Comparing with ETSI Evaluation

The table below summarizes the ETSI complexity evaluation results for the Motorola version 3.0.2 speech codec using the bit-exact ANSI-C programs and compares these results to a true, real-time implementation of the Motorola version 3.1 speech codec on an ADSP-21020 chip in assembly code.

speech codec (single-channel)	wMOPS (ETSI eval.) vs. MIPS (DSP simul.) (cycles per 20 ms frame)	Program Code Instructions (words)	Total Data Storage (RAM + ROM in both PM + DM in bytes)
Mot ver.3.0.2 (ETSI eval.)	328,994 encode 42,628 decode	8000 to 12000	12082
Mot ver.3.1 (AD DSP impl.)	281,000 encode 31,000 decode	5377 + 256	31142
Full-Rate (ETSI eval.)	45,575 encode 13,536 decode	2000 to 3000	1975
Full-Rate (AD DSP impl.)	37,000 encode 16,000 decode	1719 + 256	3760

Conclusions

For the first time in ETSI, a dedicated subgroup has defined a very rigorous, scientific, well documented and reproducible methodology in order to evaluate the complexity of different digital signal processing algorithms written in ANSI-C using agreed formats and basic operations. This methodology proved to be very valuable and accurate in comparing algorithms in terms of their complexities. Subsequently, one of the GSM Half-Rate candidate algorithms was implemented on a true, real-time, commercially available, single-chip DSP. MIPS and memory usage benchmarks were likewise recorded and then compared to the original ETSI evaluations. It can be seen that the ETSI evaluations were quite accurate. Slightly better results are reported on the real-time implementation, but this is likely attributable to the choice of DSP. The implementation was performed on a 32-bit architecture whereas the ETSI evaluation assumes average, commercially available 16-bit architectures. Furthermore, it is shown that this 32-bit chip is capable of completely transcoding two independent, full-duplex, GSM speech traffic channels (Full-Rate, Half-Rate, or mixed) without requiring any external memory components, thereby significantly saving the expenses of alternative solutions based on dual 16-bit DSPs and external memory.

Bibliography

1. Complexity Evaluation Subgroup of ETSI TCH-HS, "Complexity Evaluation of the Full-Rate, ANT and Motorola Codecs for the Selection of the GSM Half-Rate Codec", Proceedings of: The 1994 DSPx Exposition & Symposium, June 13-15, 1994, San Francisco, Reed Exhibition Companies, Stamford, CT, 1994.
2. Complexity Evaluation Subgroup of ETSI TCH-HS, "Average Complexity: GSM Full-Rate versus Candidate Half-Rate Codecs", Proceedings of: ICSPAT '94, October 18-21, 1994, Dallas, Texas, DSP Associates, Waltham, MA, 1994.
3. ETSI/TM/TM5/TCH-HS Temporary Document TD 93/95 (including confidential annexes), "Complexity Evaluation of the Full-Rate, ANT and MOTOROLA CODECS for the Phase III Selection of the Half-Rate Codec", TCH-HS Complexity Evaluation Subgroup, Issy les Moulineaux, France, December 1993.
4. ETSI/TM/TM5/TCH-HS Temporary Document TD 93/141, "Reference Document of GSM Full- and Half-Rate Complexity Evaluation Rules for the Half-Rate Selection", TCH-HS Complexity Evaluation Subgroup, Issy les Moulineaux, France, December 1993.
5. ETSI/TM/TM5/TCH-HS Temporary Document TD 93/146, "Tables added to TD 93/95", TCH-HS Complexity Evaluation Subgroup, Issy les Moulineaux, France, December 1993.
6. ETSI/TM/TM5/TCH-HS Temporary Document TD 91/98, "Report of the 9th Meeting of TCH-HS", Chairman of TCH-HS, Colombes, France, November 1991.

7. Analog Devices, Inc., "Digital Signal Processing" (a product overview brochure), Document Stocking Number: G1633a-50-9/95, Norwood, MA, USA, September 1994.
8. Bittware Product Brochure, Bittware, Inc., New Hampshire, USA, 1994.
9. Analog Devices, Inc., "ADSP-21000 Family Hardware and Software Development Tools", Document Stocking Number: C1855-16-10/93, Norwood, MA, USA, October 1993.
10. Analog Devices, Inc., "ADSP-21060/62 SHARC Super Harvard Architecture Computer", Document Stocking Number: P1841b-6-11/94, Norwood, MA, USA, November 1994.
11. Analog Devices, Inc., "32/40-Bit IEEE Floating-Point DSP Microprocessor", Document Stocking Number: C1601c-5-8/94, Norwood, MA, USA, August 1994.
12. e-mail communication: To: Chris Cavigioli, From: Gordon Sterling, Date: 23-Dec-94, Subject: Gordon: .MAP file ?
13. e-mail communication: To: Chris Cavigioli, From: Gordon Sterling, Date: 23-Dec-94, Subject: Worst Case Timing Analysis (WCTA)
14. European Telecommunications Standards Institute (ETSI), "GSM 08.60, Inband Control of Remote Transcoders and Rate Adaptors", Sophia Antipolis, France, July 1993.
15. ETSI/SMG/SMG3/WPA/08.61adhoc, "Draft #6 of GSM 08.61", November 1994.
16. European Telecommunications Standards Institute (ETSI), "GSM 01.04, Vocabulary in a GSM PLMN", Sophia Antipolis, France, February 1991.

For additional information or comments, you may kindly contact: chris.cavigioli@analog.com

Performance Evaluation of a Low-voltage Monolithic FM/IF System for GMSK/GFSK Applications

Yanpeng Guo and Alvin Wong, Philips Semiconductors

Abstract — Experimental performance evaluation of the Philips Semiconductors' low-voltage high performance monolithic FM/IF system is presented in this paper for GMSK/GFSK applications. Bit error rate (BER) and sensitivity to frequency off-set and FM deviation variation are investigated in the CT-2 environment. Results indicate that superior performance can be achieved with the Philips' FM/IF systems.

I. INTRODUCTION

In digital cellular and wireless mobile communications, power efficiency is one of the most important issues to be considered for modulation techniques. Especially for the emerging PCS, a wide range of services including voice and data transmission has to be provided whenever and wherever it is needed with a small size, long talk time, high voice quality, and low cost handset. This makes high power efficiency become an essential factor to any modulation techniques being considered for PCS. The following most important features have made GMSK/GFSK modulation techniques become the most popular modulation format for worldwide digital cellular and PCS applications as illustrated in Table 1.

- (i) Constant envelope nature: this allows GMSK/GFSK modulated signal to be operated with class-C power amplifier without introducing spectrum regeneration. Therefore lower power consumption and higher power efficiency can be achieved.
- (ii) Narrow power spectrum: narrow mainlobe and low spectral tails keep the adjacent channel interference to low levels and achieve higher spectral efficiency.
- (iii) Non-coherent detection: GMSK/GFSK modulated signal can be demodulated by the limiter/FM discriminator receiver. This simple structure leads to low cost GMSK/GFSK receivers.

In this paper, a low-voltage monolithic FM/IF system based GMSK/GFSK receiver is presented. A GMSK/GFSK modem evaluation board has been developed for the experimental investigation. BER and sensitivity to frequency off-set and FM deviation variation of this system are evaluated in the CT-2 environment. Results indicate that superior performance can be achieved with the Philips' FM/IF systems.

Table 1. A Summary of Digital Cellular and Cordless Standards

Standard	Access	Modulation	Bit Rate	Channel Spacing
IS-54	TDMA	$\pi/4$ -DQPSK	48(kb/s)	30kHz
GSM	TDMA	GMSK	270(kb/s)	200kHz
CT-2	TDMA	GFSK	72(kb/s)	100kHz
DECT	TDMA	GFSK	1.152Mb/s	1.728MHz

This paper is organized as follows: After the introduction, GMSK and GFSK modulation techniques are briefly reviewed. An overview of the evaluation board is presented in Section III, which includes the general block diagram and detailed description of each part. In Section IV BER measurement procedures and measured results are presented. Section V is the conclusion.

II. REVIEW OF GMSK/GFSK MODULATION

GMSK (Gaussian Minimum Shift Keying) is a premodulation Gaussian filtered binary digital frequency modulation scheme with modulation index of 0.5. GMSK modulation can be implemented by two ways. The most straight forward way is to transmit the data stream through a Gaussian low pass filter and apply the resultant wave form to a voltage controlled oscillator (VCO) as shown in Figure 1. The output of the VCO is then a frequency modulated signal with a Gaussian response. The advantage of this scheme is the simplicity, but it is difficult to keep an exact modulation index of 0.5 with this scheme. Therefore VCO implemented GMSK is usually used in non-coherent detection systems such as DECT and CT2.

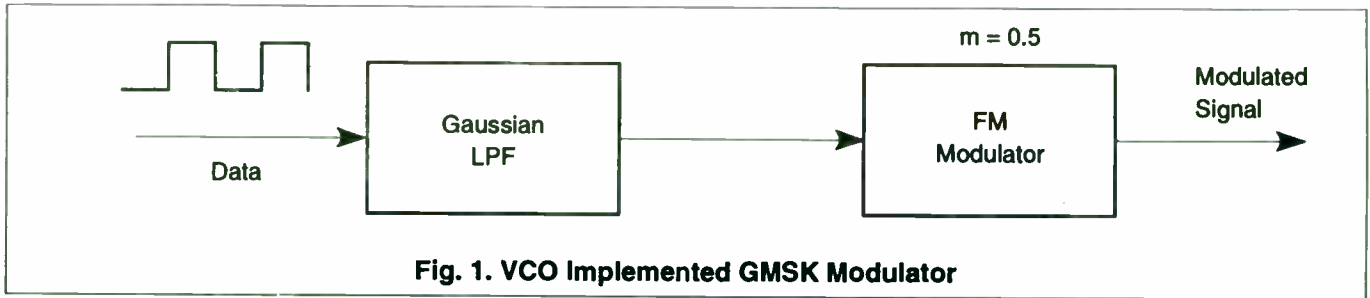


Fig. 1. VCO Implemented GMSK Modulator

GMSK signal can also be generated using quadrature modulation structure. Consider the phase modulated signal given by:

$$s(t) = \cos[\omega_c t + \phi(t)] \tag{EQ. 1}$$

This can be expanded into its in-phase and quadrature components,

$$s(t) = \cos[\phi(t)] \cos(\omega_c t) - \sin[\phi(t)] \sin(\omega_c t) \tag{EQ. 2}$$

The quadrature modulator is based on Equation (2). The implementation of such a GMSK modulator is shown in Figure 2. The incoming data is used to address two separated ROM's which contain the sampled versions of all possible phase trajectories within a given interval. After D/A conversion, the output of each ROM is applied to the I/Q modulator. The output is the GMSK modulated signal. This implementation scheme provides an exact modulation index of 0.5, which allows coherent detection.

GFSK(Gaussian Frequency Shift Keying) is also a premodulation Gaussian filtered digital FM scheme, but without the restriction of modulation index to be 0.5. The block diagram of GFSK modulator is the same as shown in Figure 1, but the modulation index can be specified according to different applications.

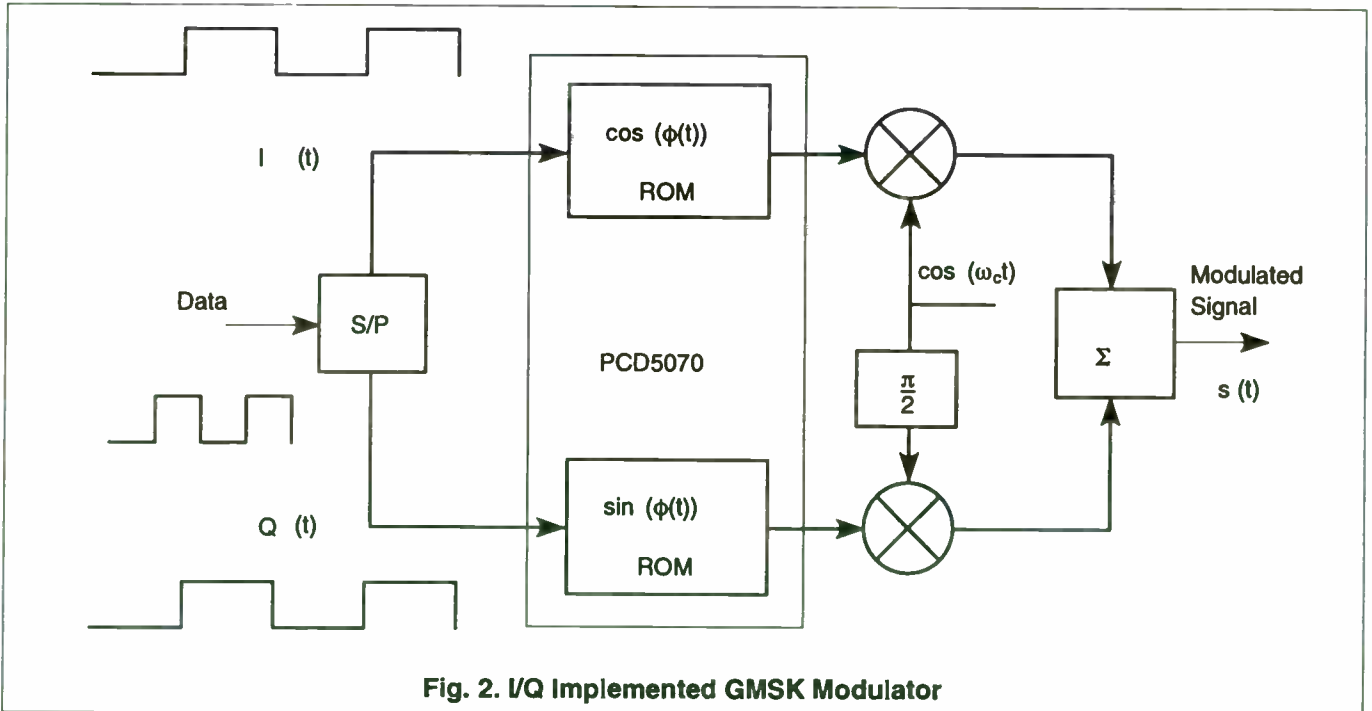
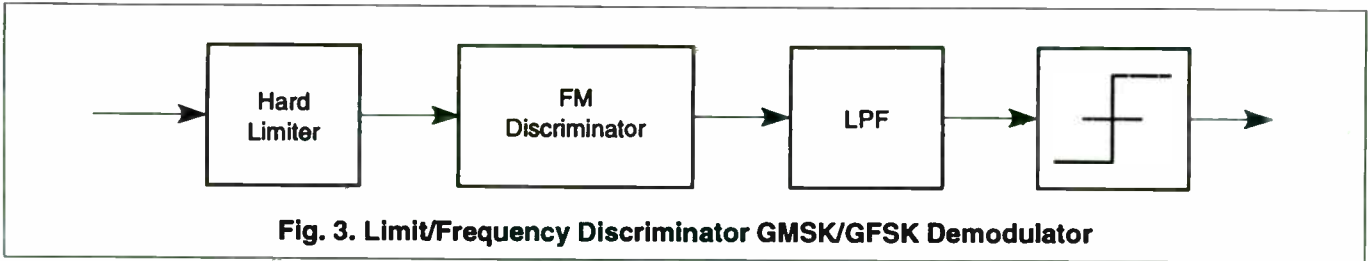


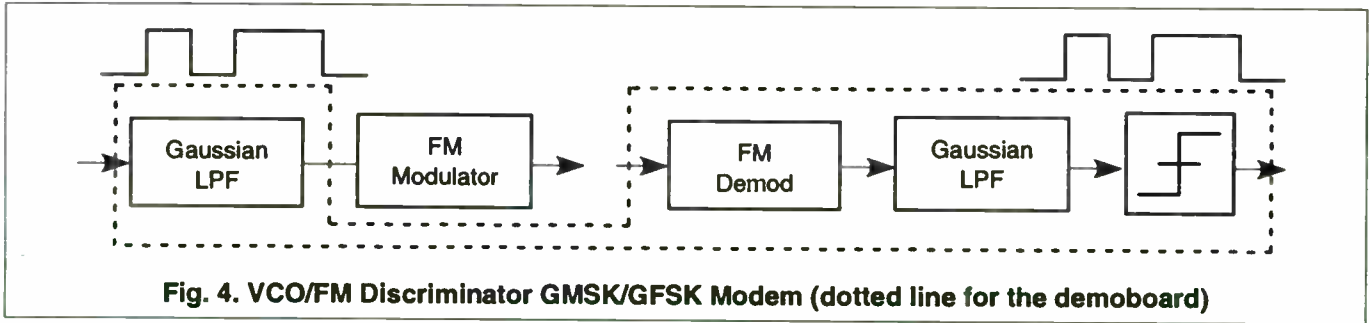
Fig. 2. I/Q Implemented GMSK Modulator

GMSK signal can be demodulated by three methods: FM discriminator detection, differential detection, and coherent detection. Coherent detection scheme has the best BER performance, but only suitable for I/Q structure based GMSK systems [Ref. 6]. Differential detection method has BER degradation even with complex implementation [Ref. 7]. The limit/discriminator structure is the simplest scheme suitable for both GMSK and GFSK applications. Therefore, the FM discriminator technique is widely used for GMSK/GFSK demodulation in digital cellular/PCS applications. Figure 3 presents the block diagram of a FM discriminator GMSK/GFSK demodulator.



III. OVERVIEW OF THE GSMK/GFSK EVALUATION BOARD

Figure 4 is the block diagram of a VCO/FM discriminator based GSMK/GFSK modem (modulator/demodulator), which also illustrates the structure of the GSMK/GFSK evaluation board. The demo board contains the entire demodulator as well as the Gaussian low-pass filter (LPF) for the modulator. The input data stream is first premodulation filtered by the Gaussian LPF, then the filtered base band wave form is applied to a FM signal generator with specific modulation index. The output is then the GSMK/GFSK modulated signal. After the limit/frequency discriminator detection, a Gaussian LPF is employed to eliminate noise. The output of the threshold detector is the regenerated binary data, which can be send to a data error analyzer to evaluate the BER performance.



Gaussian LPF:

On the demo board, a 4th order Gaussian LPF is implemented for both premodulation filtering and post demodulation filtering. The response function of this 4th order filter can be expressed as [Ref. 4]:

$$H(s) = \frac{\omega_1^2}{S^2 + 2\zeta_1\omega_1S + \omega_1^2} \cdot \frac{\omega_2^2}{S^2 + 2\zeta_2\omega_2S + \omega_2^2} \quad (\text{EQ. 3})$$

This 4th order Gaussian LPF is implemented with switched capacitor filters [Ref. 5]. The reason for using this scheme is that the LPF's 3dB bandwidth can be controlled by an external clock which allows generating GSMK signals with different BTb. Figure 5 presents the circuits diagram of this 4th order Gaussian LPF. Baseband eye-diagram at the output of the Gaussian LPF is presented in Figure 6, and the spectrum of the GSMK modulated signal is illustrated in Figure 7.

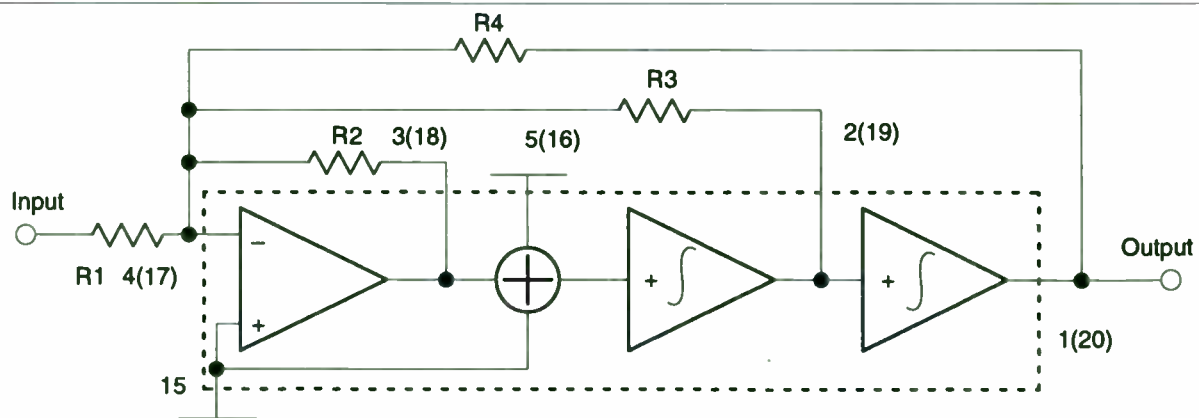


Fig. 5. Circuit Diagram of LPF with LMF100 at Mode-3

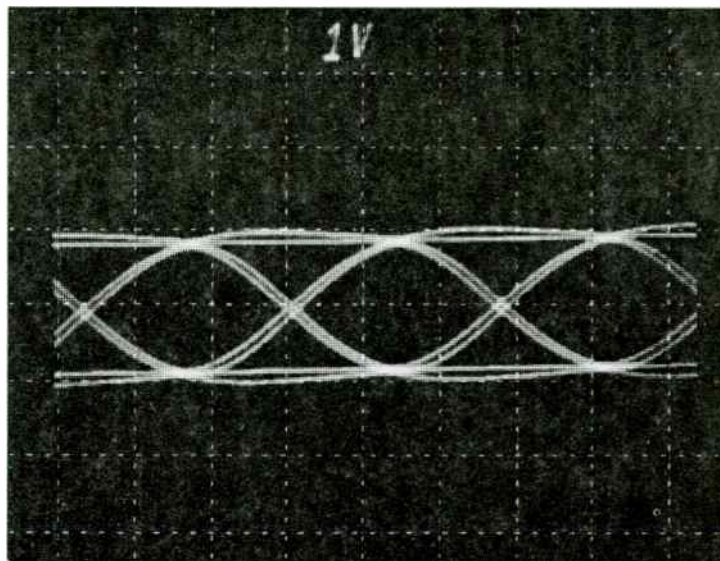


Fig. 6. Baseband Eye-Diagram at the Output of Tx Gaussian LPF

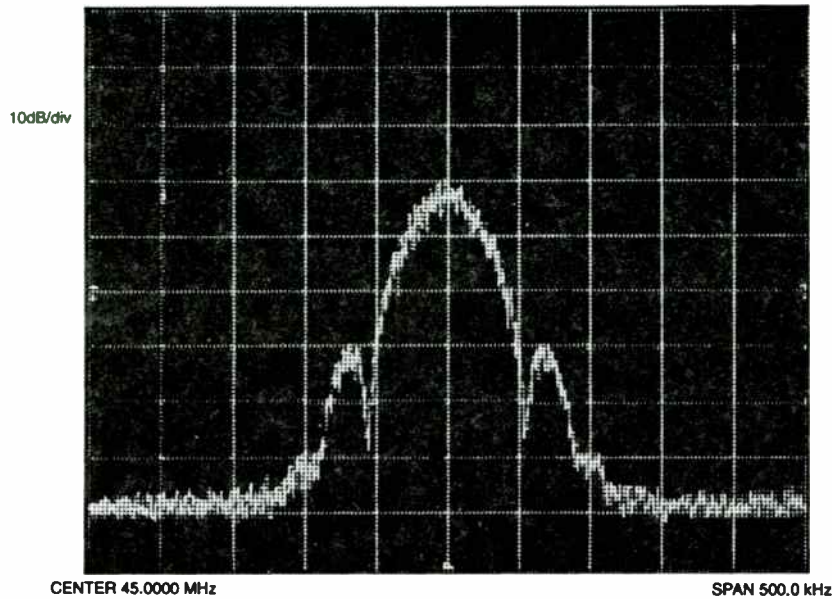


Fig. 7. Spectrum of GMSK Modulated Signal ($BT_b = 0.5$)

FM/IF System:

The Philips' low-voltage high performance monolithic FM/IF system, SA626, is employed for demodulation on the GMSK/GFSK demo board. The SA626 was designed specially for high bandwidth portable communications applications, incorporating with a mixer/oscillator, two limiting intermediate frequency amplifiers, quadrature detector, and audio and RSSI op amps. The RF section is similar to the famous SA605. The audio and RSSI outputs have amplifiers. With power down mode, SA626 will function down to 2.7 V. Figure 8 is the block diagram of SA626. Detailed information can be found in the data book and applications note [1, 2, 3].

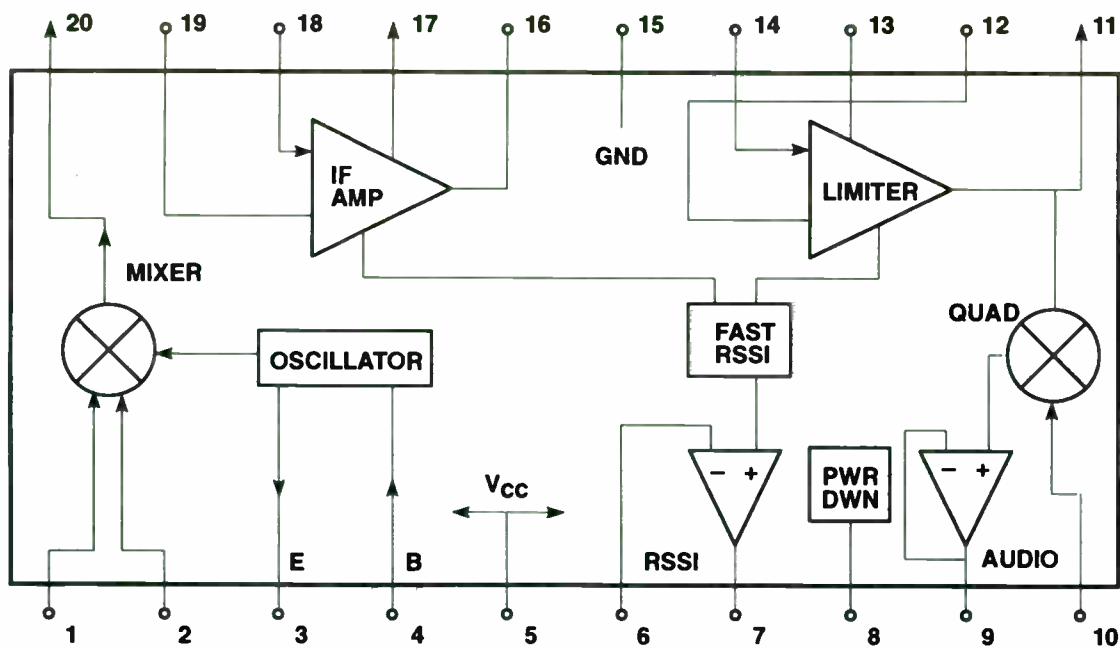


Fig. 8. Block Diagram of the FM/IF System SA626

The GMSK/GFSK demo board is designed at RF frequency of 45 MHz, LO frequency of 55.7 MHz, and intermediate frequency of 10.7 MHz. For different RF frequency applications, the step-by-step matching circuits design procedure is presented in [Ref. 1].

Although this demo board is designed with SA626 based on CT-2 specifications, Philips also provides FM/IF solutions for many other GMSK/GFSK systems. The SA626 is specially designed for wide bandwidth applications. For lower data rate applications such as CDPD (19.2 kb/s), the SA605/625 family is recommended. For DECT and other high data rate applications, SA636 and SA639 are the recommended solutions. Table 2 presents a summary of the major characteristics of Philips FM/IF systems. The suggested maximum data rate for each part is an approximation based on the baseband eye pattern. Higher data rate could be operated with some modifications or if more BER degradation is allowed.

Table 2. Major Characteristics of the FM/IF Systems

	NE602/604	NE605	NE625	NE626	NE636	NE639*
V _{cc}	4.5 - 8V	4.5 - 8V	4.5 - 8V	2.7 - 5.5V	2.7 - 5.5V	2.7 - 5.5V
I _{cc}	2.4/3.3mA @ 6V	5.7mA @ 6V	5.7mA @ 6V	6.5mA @ 3V	6.5mA @ 3V	8.3mA @ 3V
SINAD	-120dBm/.22μV (RF: 45MHz, IF: 455kHz, 1kHz tone, 8kHz Dev.)	-120dBm/.22μV (RF: 45MHz, IF: 455kHz, 1kHz tone, 8kHz Dev.)	-120dBm/.22μV (RF: 45MHz, IF: 455kHz, 1kHz tone, 8kHz Dev.)	-112dBm/.54μV (RF: 240MHz, IF: 10.7kHz, 1kHz tone, 70kHz Dev.)	-111dBm/.54μV (RF: 240MHz, IF: 10.7kHz, 1kHz tone, 125kHz Dev.)	-111dBm/.54μV (RF: 240MHz, IF: 10.7kHz, 576kHz tone, 288kHz Dev.)
Features	Audio & Data pins IF BW of 25MHz Matching for standard 455kHz IF filters	Audio & Data pins IF BW of 25MHz Matching for 455kHz IF filters	Pin compatible with NE605 Fast RSSI IF BW of 25MHz Matching for 455kHz IF filters	Power down mode Low voltage Fast RSSI IF BW of 25MHz Int. RSSI & Audio op amp Matching for 10.7MHz IF filters	Power down mode Low voltage Fast RSSI IF BW of 25MHz Int. RSSI op amp Wideband data out Matching for 10.7MHz IF filters	Power down mode Low voltage Fast RSSI IF BW of 25MHz Int. RSSI op amp Wideband data out Post detection amp Matching for 10.7MHz IF filters
Data Rate**	100kb/s	100kb/s	100kb/s	300kb/s	1.5Mb/s	2Mb/s
NOTES	* Objective specifications. ** Approximated maximum data rate. With some modifications, higher data rate might be operated.					

Threshold Detector & Data Regeneration:

A 2-level threshold detector with sampling timing adjustment circuits is implemented for data regeneration. The output base band signal (eye diagrams) from SA626 is first fed into a comparator (LM311) to generate a TTL logic signal, this signal then is sampled with data clock at the transmitting bit rate. The phase of data clock can be adjusted manually through a monostable multivibrator (74HC123) to achieve the optimal sampling timing. The demo board is initially adjusted for a bit rate of 72 kb/s. If different data rate is used, the sampling timing has to be re-adjusted.

The symbol timing recovery (STR) circuit is not implemented on this demo board. Transmitting data clock either hard-wire connected from the transmitter or from a separated STR circuit is required for the operation. Measured performance presented in this paper is conducted with hard-wire connected data clock. However BER degradation caused by STR should not be more than 1 dB [Ref. 8].

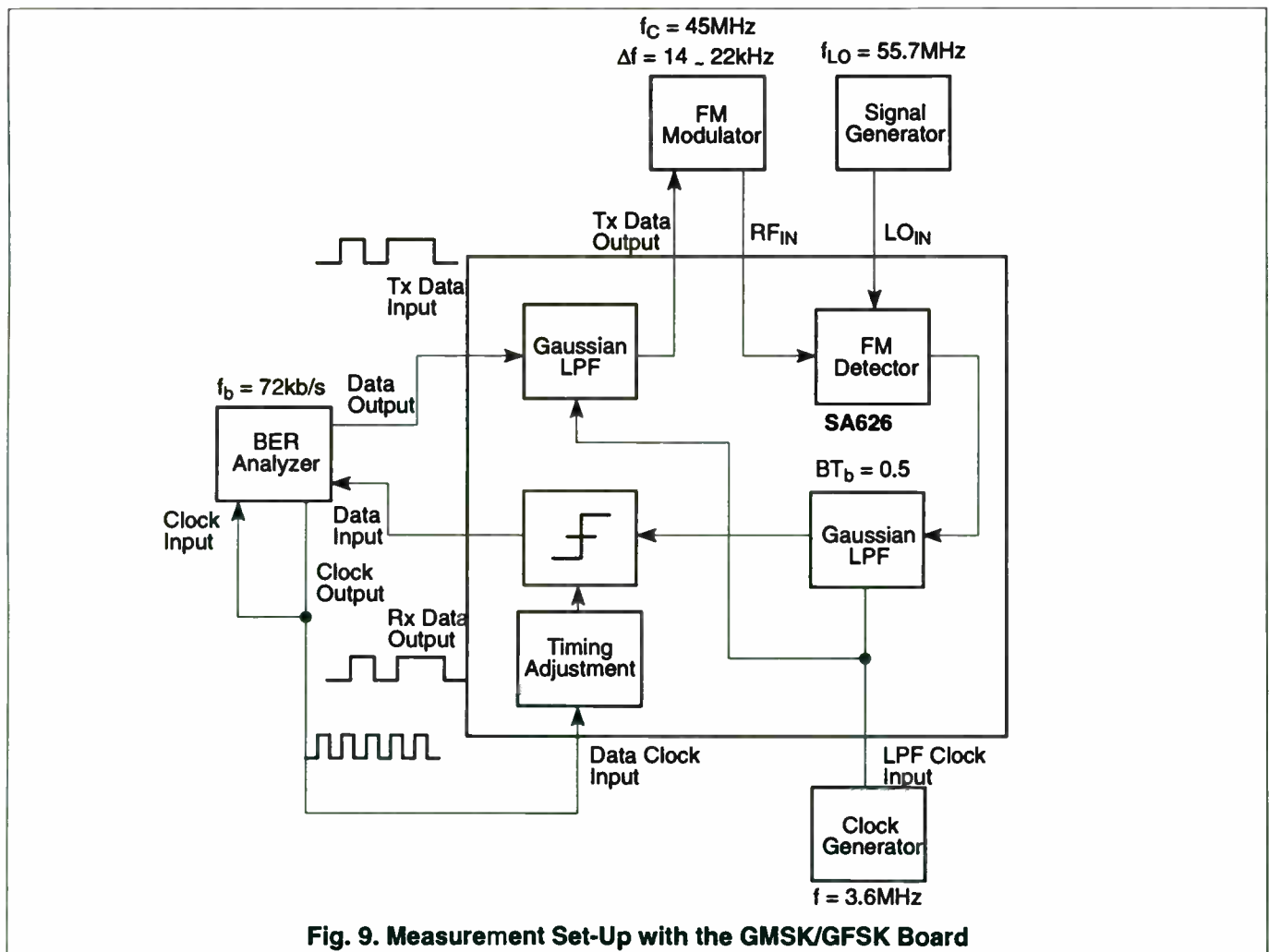
IV. EXPERIMENTAL PERFORMANCE EVALUATION

Performance of this GMSK/GFSK system including BER and sensitivity to frequency off-set and FM deviation variation is experimentally evaluated based on CT-2 specifications. Measurement procedures and the measured results are presented in this section.

Measurement Set-up:

Figure 9 illustrates the measurement set-up with the GMSK/GFSK demo board. A data error analyzer is employed to generate a pseudo random binary sequence (PRBS) with length of 10^9-1 at a data rate of 72 kb/s. This data sequence is sent to the Gaussian LPF on the board for premodulation filtering. The output Gaussian filtered base band signal is then applied to a FM signal generator as modulating signal. To generate a GMSK modulated signal (modulations index = 0.5) at a bit rate of 72 kb/s, frequency deviation of the FM signal generator needs to be set at 18 kHz. The output from the generator is then a GMSK modulated signal (at 45 MHz). Another signal generator is employed to provide an LO signal at 55.7 MHz for the FM/IF system detection.

After FM discriminator detection, the output base band signal is fed into another Gaussian LPF on the board to eliminate noise. The 3 dB bandwidth of both Gaussian LPF's is controlled by an external clock. This clock should be a square wave signal with TTL level. By controlling the frequency of this clock, different BT_b can be achieved for certain bit rate. To have BT_b equal 0.5 with bit rate of 72 kb/s, the clock signal is set at 3.6 MHz (100 times the required 3 dB bandwidth). The output from the LPF is then sent to the threshold detector for data regeneration. Data clock signal is directly from the data error analyzer. The sampling time can be controlled by adjusting the phase of the clock signal. Recovered data sequence is fed back to the Data Error Analyzer for BER measurement.



Measured Results:

The recovered baseband eye-diagram is shown in Figure 10. and the measured BER vs. RF input level is presented in Figure 11. To achieve $P_e = 10^{-3}$, only about -98.5 dBm RF power is needed. RF input level can be converted into E_b/N_0 by the following calculation.

E_b/N_o can be expressed as:

$$\frac{E_b}{N_o} = \frac{(C \cdot T_b)}{N_o} = \frac{C}{(f_b \cdot N_o)} \quad (\text{EQ. 4})$$

where C is the carrier power (signal power), T_b is the bit duration, and f_b is the bit rate. N_o is noise density, which equals,

$$N_o = k T_o F_n \quad (\text{EQ. 5})$$

where k is the Boltzmann constant (1.38×10^{-23} K/J), T_o is the standard temperature, (290 k), and F_n is the noise factor. By inserting these values to equation (5), we obtain:

$$\begin{aligned} \left(\frac{E_b}{N_o}\right)_{\text{dB}} &= C_{\text{dBm}} - F_n - 10 \log (f_b k T_o) \\ &= C_{\text{dBm}} - F_n - (-125.4)_{\text{dB}} \end{aligned} \quad (\text{EQ. 6})$$

The first stage mixer noise figure of SA626 is 14dB [3], therefore,

$$\begin{aligned} \left(\frac{E_b}{N_o}\right)_{\text{dB}} &= C_{\text{dBm}} - 14_n + 125.4_{\text{dB}} \\ &= C_{\text{dBm}} + 111.4_{\text{dB}} \end{aligned} \quad (\text{EQ. 7})$$

Since -98.5 dBm RF signal power is needed to achieve $P_e = 10^{-3}$, 12.9 dB E_b/N_o ratio (based on equation 7) is enough for this BER. The performance degradation caused by frequency off-set and the sensitivity to FM deviation variation of this system are also evaluated. Figure 12 presents the measured BER vs. frequency off-set. With 10 kHz off-set, only minor degradation can be observed. The sensitivity of this system to FM deviation variation is illustrated in Figure 11. Even with the smallest deviation (14kHz), less than -96 dBm RF signal is needed to achieve the BER of 10^{-3} . These results indicate that the Philips' FM/IF systems can provide superior performance for GMSK/GFSK applications.

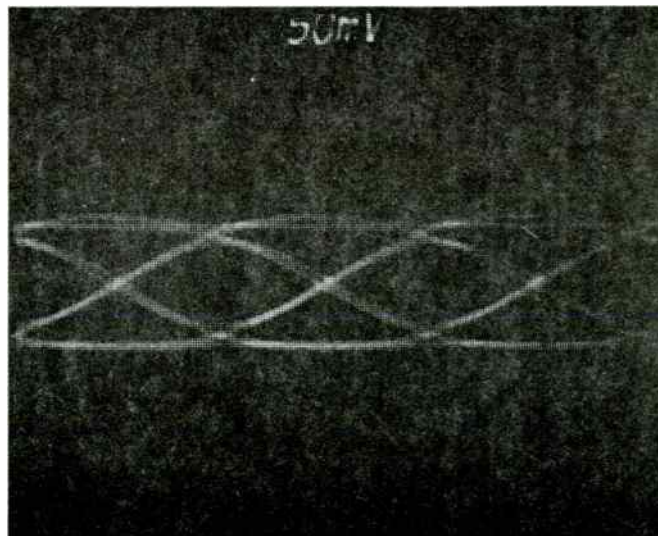
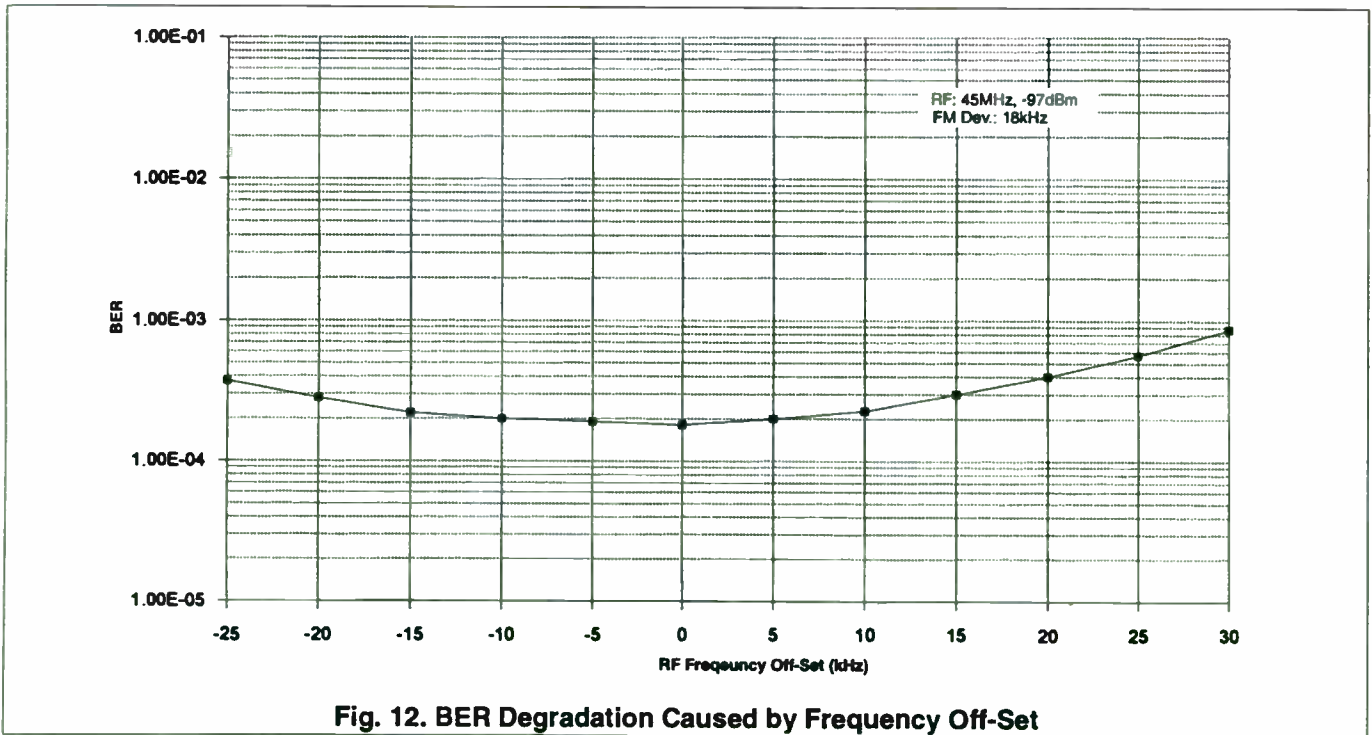
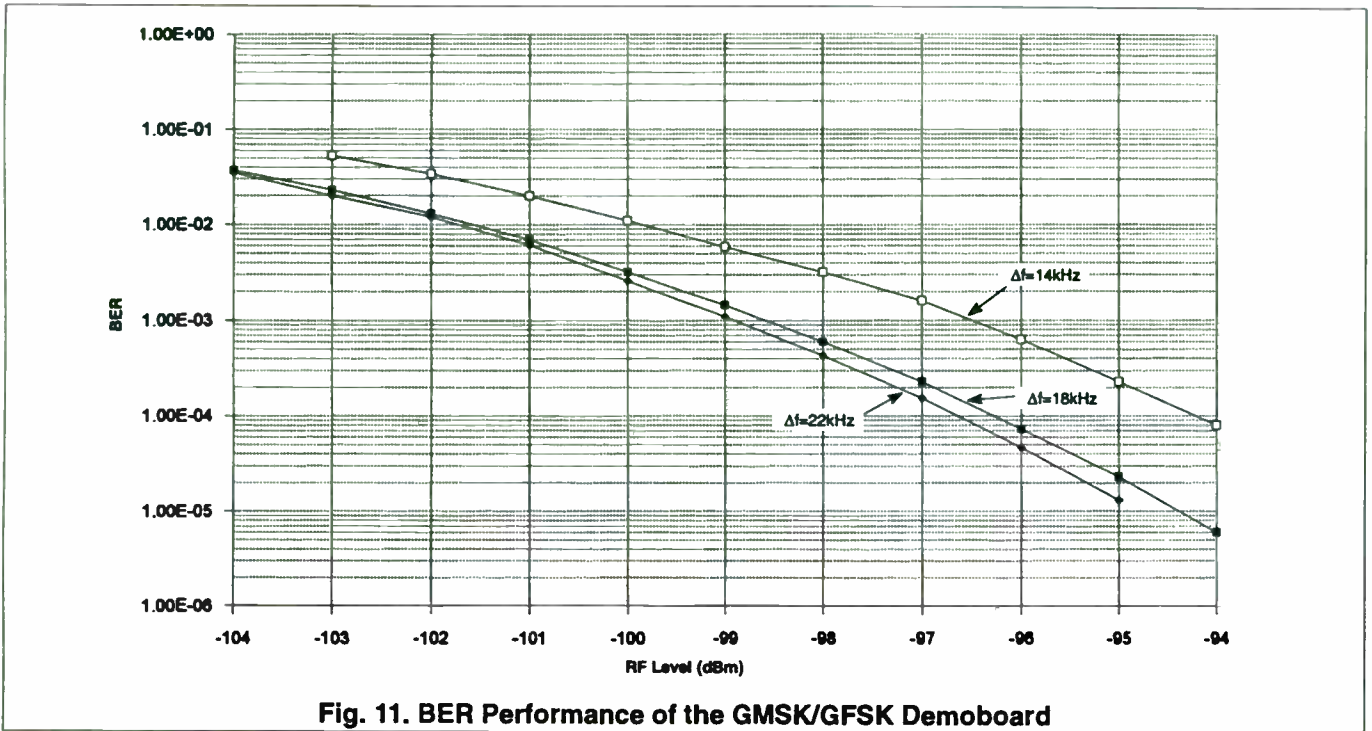


Fig. 10. Baseband Eye-Diagram at the Output of Rx Gaussian LPF



V. CONCLUSION

A Philips' FM/IF family based GMSK/GFSK modem evaluation system is presented. Experimental performance evaluation including bit error rate (BER) and sensitivity to frequency off-set and FM deviation variation of this system are conducted in the CT-2 environment. Results indicate that superior performance can be achieved with the Philips' FM/IF systems for GMSK/GFSK applications.

VI. REFERENCES

1. "AN1994: Reviewing key areas when designing with the NE605," *RF/Wireless Communications Data Handbook*, Philips Semiconductors, 1994.
2. "AN1996: Demodulation at 10.7 MHz IF with NE/SA605/625," *RF/Wireless Communications Data Handbook*, Philips Semiconductors, 1994.
3. "Low voltage high performance mixer FM IF system with high speed RSSI," (SA626 data sheet), *RF/Wireless Communications Data Handbook*, Philips Semiconductors, 1994.
4. C. S. Lindquist, *Active Network Design with Signal Filtering Applications*, Steward & Sons, 1977.
5. *Linear Data Book*, National Semiconductor.
6. K. Murota and K. Hirade, "GMSK modulation for digital mobile radio telephony," *IEEE Transactions on Communications*, July 1981.
7. S. Grath and C. J. Burkley, "Low complexity GMSK modulator for integrated circuit implementation," *Proceedings of IEEE VTC'90*.
8. K. Feher, *Digital Communications, Satellite/Earth Station Engineering*, Prentice Hall, 1983.

Cellular/RFID Applications

Session Chairperson: Victor Perrote,
Microwaves & RF (Hasbrouck Heights, NJ)

- Advantages of mobile cellular-packet-data services for in-car navigation systems. **Bernd Eschke**, Robert Bosch GmbH (Hildesheim, Germany); **Michael Mayer and Wolfgang Schulz**, Department of Communications Engineering, University of Paderborn (Paderborn, Germany).....275
- Correlative channel estimation in DS-CDMA systems. **Volker Kuhn and Michael Meyer**, Department of Communications Engineering, University of Paderborn (Paderborn, Germany).....279
- Improving the reading distance of omnidirectional transponder-based systems. **Boni Angelo and Massimo Montecchi**, MED s.p.A. (Reggio Emilia, Italy).....285
- Fundamental constraints on RFID tagging systems. **Peter H. Cole and David M. Hall**, Department of Electrical and Electronic Engineering, The University of Adelaide (Adelaide, Australia); **Michael Y. Loukine and Clayton D. Werner**, Integrated Silicon Design Pty (Adelaide, Australia).....294
- Field-strength monitor receiver for remote-control applications. **Rainer Perthold, Albert Heuberger, and Ludwig Wallrapp**, Fraunhofer-Institut für Integrierte Schaltungen (Erlangen, Germany).....304
- Integrated SAW oscillator in bipolar technology. **Albert Heuberger and Eberhard Gamm**, Fraunhofer-Institut für Integrierte Schaltungen (Erlangen, Germany).....305

ADVANTAGES OF MOBILE CELLULAR PACKET DATA SERVICES FOR IN-CAR NAVIGATION SYSTEMS

B. Eschke¹, M. Meyer², W. Schulz²

¹ Robert Bosch GmbH, K7/EFI,
P.O. Box 777777, 31132 Hildesheim, Germany

² University of Paderborn, Dept. of Communications Engineering,
33095 Paderborn, Germany

Abstract: Autonomous vehicle navigation systems offer route guidance to the driver. The major weak point of autonomous systems is that only static information are used to calculate the best route. The application of some existing communication systems has been considered to provide current traffic information to the navigation system to allow dynamic route guidance. For example, radio broadcast (RDS/TMC) and data services of the GSM cellular mobile radio network have been investigated. At the moment, a packet-oriented data service for GSM is under discussion for standardisation which is called GPRS (General Packet Radio Service). This paper gives an overview on the development of dynamic data concepts for route guidance systems and highlights the advantages of GPRS for this application.

I. INTRODUCTION

In the recent years the increase of street traffic has caused a significant deterioration of the traffic situation in Europe. Not only the longer driving times for individuals but also the economical and ecological effects are a serious burden.

Besides collective traffic management concepts, the use of autonomous in-car navigation systems is a step forward to influence the traffic flow positively. Another step ahead is the application of communication systems to transmit actual traffic information which allows dynamic route guidance. This fact has lead to many proposals to exchange traffic information to improve route guidance.

This paper describes concepts to transmit traffic related information to mobiles and is organized as follows. The next section introduces the basic autonomous navigation system. Then,

RDS/TMC, data services of the current GSM-standard, and the future service GPRS of GSM are considered for transmission of traffic information to improve route guidance.

II. AUTONOMOUS IN-CAR NAVIGATION SYSTEMS

Autonomous in-car navigation systems guide the driver of an equipped vehicle by acoustic and optical instructions to the desired destination. Such systems consist of a navigation computer, wheel sensors, compass, GPS-receiver, and CD-player (s. Fig. 1). The information (road-map with street attributes) required to calculate the route is stored on a CD-ROM.

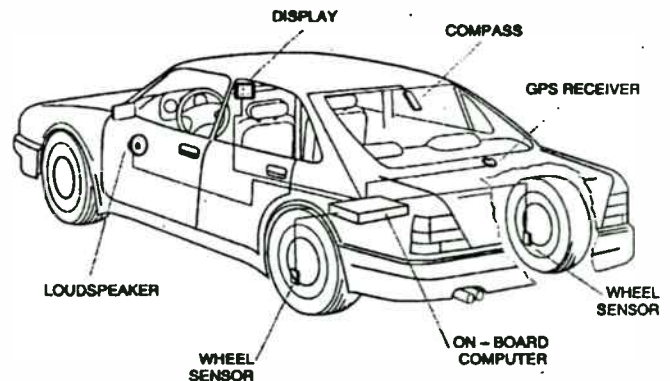


Fig. 1: Components of an autonomous in-car navigation system

At the beginning of a journey the driver inputs his destination. Based on the knowledge of the current location provided by the GPS-receiver and the digital map on CD-ROM, the navigation



Fig. 2: Display of the navigation system

computer calculates the best route. According to the instructions given by the system the driver starts to drive. During the trip the computer keeps track by correlating the information gathered by the wheel sensors, the compass, and the GPS-receiver with the calculated route based on the digital map. Early enough it gives acoustic instructions, for example, to turn left or right or to use another lane. Additionally, a display (s. Fig. 2) provides assistance which is useful for example at of complex crossings.

Should the driver have missed to turn or has turned because of a traffic incident ahead, the navigation computer would recognize the deviation and starts immediately to estimate the new route.

Autonomous in-car navigation systems have reached marketability. They are able to perform static route guidance for drivers. Unfortunately, these systems are not able to include the current traffic situation for route calculation. They do not have knowledge of congestions, accidents, and street closings.

This short-coming has been identified and many proposals have been made to provide actual traffic information to the navigation system to enable dynamic route guidance. Two different concepts shall be discussed in the following sections.

III. RDS/TMC

One possibility to transmit traffic information to in-car navigation systems was identified to be the Radio-Data-System (RDS). In addition to a radio broadcast signal, a subcarrier modulated by digital data is transmitted. Mainly, RDS provides information concerning the program (e.g. name of the program, alternative frequencies, ...). An additionally defined data services is the Traffic Message Channel (RDS/TMC) [1,2]. Due to the capacity of RDS, it is possible to transmit approximately one traffic message per second.

RDS/TMC is an efficient method to transmit traffic information to vehicles and will replace spoken traffic messages in future. Since the data is broadcast, a good information level can be achieved. Nevertheless, concerning the route guidance application there are some disadvantages of RDS/TMC:

- The data capacity is restricted.
- The data are often not relevant because the information is broadcast in large areas.
- Since radio broadcast is a one-directional communication, the driver cannot ask for individual information.

Consequently, the need of a two-way communication system arises. Furthermore, it is desirable to be able to send traffic messages only to areas they are relevant to.

IV. GSM

The Global System for Mobile Communications (GSM) [3] is the pan-European mobile cellular radio network. GSM provides two-way communication links between mobile stations and base stations. Various voice and data services are implemented for communications within the mobile network or between mobile stations and the public telephone network.

GSM seems to overcome the disadvantages outlined above for RDS/TMC. The cells are significantly smaller compared with the coverage area of radio broadcast. The transmitted traffic information can be restricted to relevant data for each cell which allows to report on more traffic incidents.

The DRIVE-project (Dedicated Road Infrastructure for Vehicle Safety in Europe) SOCRATES (System of Cellular Radio for Traffic Efficiency and Safety) [4, 5, 6] investigates the application of cellular radio to improve Road

Traffic Informatics (RTI). Beside the main aspect, support of navigation systems, this project covers some other applications:

- automatic emergency call
- fleet management
- automatic vehicle location (AVL)
- park & ride information
- yellow pages
- tourist information

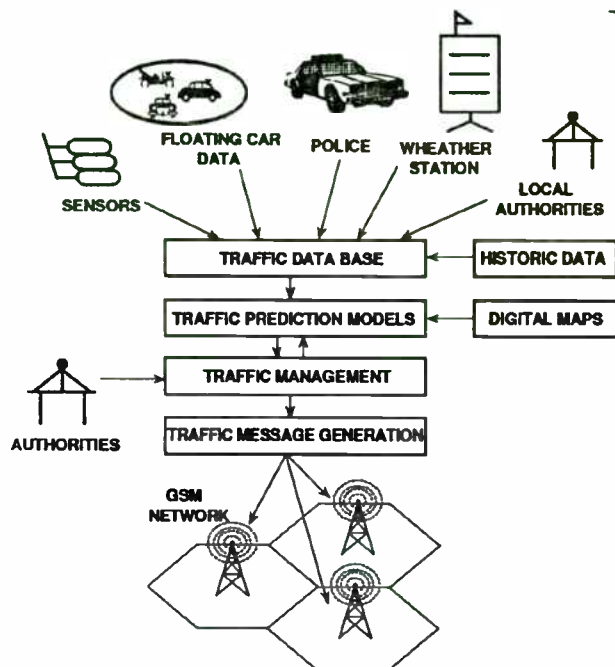


Fig. 3: Topology of the SOCRATES infrastructure

The principle of SOCRATES for transmitting traffic messages to enable dynamic route guidance is shown in Fig. 3.

To be able to transmit accurate traffic messages a huge amount of information gathered from many sources has to be processed.

- Sensors provide information on the traffic density and the speed at important street segments.
- Vehicles with SOCRATES equipment do not only receive information, moreover they serve also as information sources. They report in regular intervals on the traveltimes for street segments they passed (floating car data). Therefore, accurate information can be collected without the need to install street sensors.

- Additional input is gained by the police, weather stations and local authorities.

All information is processed in a regional traffic information centre. Together with historic data the gathered data are used for traffic modelling. The traffic is predicted for the next few hours. Based on the prediction, suitable messages are generated to inform the in-car navigation system of traffic incidents and to control the traffic to avoid the development of congestion.

The application of the two-way communication system GSM enables better traffic modelling because vehicles can act as information sources. This improved traffic model allows more accurate traffic messages which results in superior route guidance.

Although this proposal achieves that each individual driver receives the relevant data he needs, there exists one disadvantage, i.e., the SOCRATES system leads to a significantly increased load of the cellular network.

To overcome this weak point of the SOCRATES architecture, it was proposed to extend GSM by an additional data service, which is described in the next section.

V. GENERAL PURPOSE RADIO SERVICE

The General Purpose Radio Service (GPRS) is a packet-oriented data service for GSM and currently under definition. This service should accomplish the following requirements [7]:

- data rate up to 9.6 kbit/s
- flexible packet sizes
- various qualities of service
- fast access
- flexible addressing schemes for the downlink:
 - singlecast (point-to-point)
 - multicast (point-to-multipoint), group-addressing
 - broadcast (point-to-multipoint)
 - geographical routing

What makes GPRS interesting for the route guidance application? To answer this question, the main two types of messages have to be considered. Firstly, the traffic information sent by the traffic information centre and, secondly, the mobile originated traffic data (s. Fig. 3).

For the first message type the multicast mode is highly desirable because all service subscribers in the cell are updated simultaneously. Since the load of the communications network can be essentially reduced, GPRS would be the basis for a low cost service. Additionally, the feature geographical routing enables to inform all subscribers in a certain area which is normally covered by more than one cell. This is very convenient and efficient to address all subscribers affected by a traffic incident.

Since acknowledgement of multicast or broadcast messages is not useful, only the downlink of the communications link is used. The free capacity on the uplink can be occupied by other applications. For the application it is not a serious problem when a message is not received because of the high repetition rate of traffic messages.

The second type of message is sent on the uplink of the communications network where only singlecast messages are possible. The equipped vehicles sent their reports on the road status to the traffic information centre at regular intervals. These messages are relatively short, which would not justify the normal access procedure of GSM which loads the network for several seconds. It is much more efficient to transmit this information via a packet-oriented service. Therefore, GPRS has advantages compared with the existing data services of GSM also for relatively short uplink messages.

VI. CONCLUSIONS

The argumentation of this paper about the considered communication systems is summarised in the following table.

Table 1: Comparison of the three considered systems

	RDS/TMC	existing GSM data services	GSM/GPRS
data rate	low	high	high
mode	broadcast one-way-comm.	singlecast two-way-comm.	singlecast, broadcast, two-way-comm.
addressable area	broadcast area	individual	individual, cell
equipment	radio	GSM-transceiver	GSM-transceiver
costs	low	high	medium

RDS/TMC is certainly the cheapest solution to provide dynamic data to a navigation computer.

But because of its restricted capacity, it is necessary to concentrate on the most important traffic messages. The more flexible existing data services of the GSM-system seem to be more appropriate to exchange traffic information. Additionally, according to the SOCRATES principle, they permit gathering road status reports of equipped vehicles which further improves the traffic modelling. On the other hand, they are expected to be too expensive for a mass-market. The most promising concept for a future implementation of an information system supporting dynamic route guidance (e.g. SOCRATES) seems to be the General Packet Radio Service of GSM because it covers best the requirements compared with the other solutions.

REFERENCES

- [1] Pamall, S.J, Riley, J.L.: "RDS developments", International Broadcasting Convention, 21-25 Sept. 1990, Brighton, UK, pp. 234-240, 1990.
- [2] Ely, S.R.: "RDS-ALERT: A DRIVE project to develop a proposed standard for the Traffic Message Channel feature of the radio data system RDS", *Colloquium on the Car and its Environment: What DRIVE and PROMETHEUS have to offer*, IEE Colloquium, pp 8/1-8/6, 1990.
- [3] Mouly, M., Pautet, M.B.: *The GSM System for Mobile Communications*, Published by the authors, 1992.
- [4] Deuper, H., Pfeiffer, G., Schulz, W.: "Improvement of Safety in Traffic using Autonomous Navigation Systems and Duplex Data Communication between Mobiles and Traffic Centres", *EUROSAFE Conference*, London, July 1992.
- [5] Catling, I., Zijderhand, F.: "SOCRATES - What Now?", *VNIS '92 Conference*, Oslo, Norway, September 1992.
- [6] Gilchrist, P. et al.: "The Path From The SOCRATES/RHAPIT Pilot To A Commercial System", *Proceedings Vehicular Technology Conference '94*, Stockholm, Sweden, pp. 420-424, 1994.
- [7] Tdoc SMG4 299/93rev1: "Requirements of General Packet Radio Service", *ETSI STC SMG1/SMG4*, Vienna, 7.-8. 12. 1993.

Correlative Channel Estimation in DS-CDMA Systems

Volker Kühn and Michael Meyer
 Department of Communications Engineering
 University of Paderborn, 33095 Paderborn, Germany

Abstract: The determination of the propagation conditions of time-variant mobile radio channels is a main task in mobile communication systems. For systems based on CDMA, it is essentially that the receiver knows the corresponding spreading sequence. Therefore, this sequence can be used for correlative channel estimation. This paper considers several concepts for the channel estimation in direct-sequence code division multiple access systems and compares their performances by simulation results.

I. INTRODUCTION

The recent discussion (e.g. [1]) about the standardization of third generation mobile communication systems shows that systems based on code division multiple access (CDMA) seem to have advantages over conventional systems using time or frequency division multiple access (TDMA respectively FDMA). Particularly, a higher capacity of users is expected [2].

Due to the specific behaviour of these systems such as the inherent diversity when transmitting over mobile radio channels and the low spectral density of the data signal, it is necessary to investigate efficient possible realizations.

This paper examines concepts for correlative channel estimation using code sequences utilized for spreading the data signal. Systems based on the GSM-standard [3] realize the estimation with training sequences occupying a significant part of the transmission. Therefore, the net data rate is reduced. In contrast to this, receivers in a DS-CDMA (*direct-sequence code division multiple access*) system need to know their corresponding spreading codes so that they can be used instead of training sequences [4]. However, there are some effects rendering the estimation. The signals possess a significant lower spectral power density than their GSM counterparts resulting in less accurate estimates due to additive noise.

The structure of this paper is as follows. In the next section the assumed communication system model is presented. Section III and IV describe the

correlative channel estimation in DS-CDMA systems and several realization concepts. Finally, simulation results illustrate the performance of these different methods.

II. SYSTEM MODEL

Figure 1 shows the equivalent baseband system model used in this article.

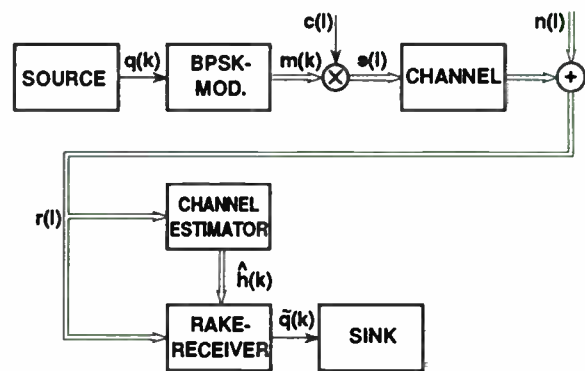


Figure 1: Model of a CDMA-communication system

A binary information source provides an information sequence $q(k)$. This sequence is BPSK-modulated. The symbol duration is denoted by T_s and k indicates the symbol interval. The modulated signal $m(k)$ is spread with a suitable code $c(l)$, where the chip duration T_c is indicated by l . After expanding the bandwidth, the signal $s(l)$ is transmitted over a mobile radio channel with the time-variant impulse response

$$h(l) = \sum_{p=0}^L h^{(p)}(l)\delta(l-p), \quad (1)$$

where $L+1$ propagation paths are taken into account. Furthermore, $h^{(p)}(l)$ denotes the channel coefficient of the p -th propagation path. Additional disturbances are caused by additive white Gaussian noise $n(l)$. The interference of users transmitting at the same time in the same frequency band is treated as white noise according to the Gaussian approximation [5] and is contained in the noise signal $n(l)$.

By using the Rake receiver, the sampled signal $r(l)$ is despread and the signal components delayed by the channel are constructively superposed so that the distortion can be nearly compensated. The quality of this compensation depends on the accuracy of the estimated channel impulse response. Here, it is assumed that the channel estimator provides an estimate once in a symbol interval T_s . Finally, the Rake receiver performs a quantization and feeds the sink with the detected values $\tilde{q}(k)$.

III. CORRELATIVE CHANNEL ESTIMATION

The correlative channel estimation has been successfully applied in GSM-systems for determining the channel impulse response [8], where training sequences known at the receiver are used. A similar procedure is applied to the system discussed in this paper. Principally, DS-SS receiver have knowledge of the respective spreading sequence; this can be used for the correlative channel estimation.

First of all, to estimate the time-variant coefficients $h^{(p)}(l)$ of the channel impulse response, the received signal

$$r(l) = \sum_{p=0}^L s(l-p) \cdot h^{(p)}(l) + n(l) \quad (2)$$

with

$$s(l-p) = m(l-p) \cdot c(l-p) \quad (3)$$

has to be investigated.

The estimate $\hat{h}^{(i)}(k)$ of the coefficient of the i -th propagation path can be expressed by the correlation of the spreading sequence $c(l)$ and the received signal, with

$$\hat{h}^{(i)}(k) = \frac{1}{G_p} \sum_{l=kG_p+1}^{(k+1)G_p} r(l) \cdot c(l-i). \quad (4)$$

In equation (4) G_p denotes the number of chips per symbol, called the processing gain. Incorporating equation (2) in equation (4) yields

$$\hat{h}^{(i)}(k) = \frac{1}{G_p} \sum_{l=kG_p+1}^{(k+1)G_p} \sum_{p=0}^L [m(l-p) \cdot c(l-p) \cdot h^{(p)}(l) + n(l)] c(l-i). \quad (5)$$

By recognizing that the information symbols change only once in a symbol interval T_s and assuming that intersymbol interference can be neglected, it is possible to extract $m(l-p)$ in equation (5) in front of the

summation. If the noise term is replaced by $n'(k)$, equation (5) can be expressed as

$$\hat{h}^{(i)}(k) = n'(k) + \frac{m(k)}{G_p} \sum_{l=kG_p+1}^{(k+1)G_p} \sum_{p=0}^L c(l-p) h^{(p)}(l) c(l-i). \quad (6)$$

Supposing ideal autocorrelation properties of the spreading codes

$$\frac{1}{G_p} \sum_{l=1}^{G_p} c(l-p) c(l-i) = \begin{cases} 1 & p=i \\ 0 & p \neq i \end{cases}, \quad (7)$$

equation (6) can be simplified as

$$\hat{h}^{(i)}(k) = m(k) h^{(i)}(k) + n'(k), \quad (8)$$

assuming that the channel coefficients remain nearly unchanged during a symbol interval. Equation (8) shows that the channel coefficients can be estimated in each symbol interval if the value $m(k)$ is known and the disturbance caused by $n'(k)$ is sufficiently small. If $m(k)$ is unknown, only the absolute value of the coefficients can be determined because there is an ambiguity in the sign of $\hat{h}^{(i)}(k)$.

IV. CHANNEL ESTIMATION CONCEPTS

A. Overview

In reality, the channel impulse response is generally not known and has to be estimated. Therefore, two concepts for estimating the channel impulse response are presented. Additionally, a technique which does not depend on the knowledge of the channel state is discussed.

The results discussed in this paper are based on the following conditions. The data rate is 9.6 kbit/s and the processing gain takes the value $G_p=127$ so that there is a symbol duration of $T_s=104 \mu s$, a chip duration of $T_c=0.82 \mu s$, and a bandwidth of 1.22 MHz. For spreading m-sequences with a period equal to the symbol duration are applied.

Simulations have been carried out with two channel models, the frequency selective channel *Hilly Terrain* and the model *Rural Area* [9] which does not possess this property. The applied channels are modelled as tapped delay lines and consist of 8 paths in case of *Hilly Terrain* and 2 paths for *Rural Area*. Both channels are simulated with a maximum doppler frequency shift of $f_{dmax}=200$ Hz. Due to the maximum delay of $\tau_{max}=20 \mu s$, it seems to be expedient to build

up a rake receiver with 26 paths, each of which is delayed with T_c .

Figure 2 illustrates the bit error rates P_b in dependence of the signal-to-noise ratio in the case of exactly known channel coefficients at the receiver. These results are used for performance classification of the different channel estimation techniques. Furthermore, the theoretical bit error rates of a BPSK-modulated signal transmitted over an AWGN (*Additive White Gaussian Noise*)-channel are shown.

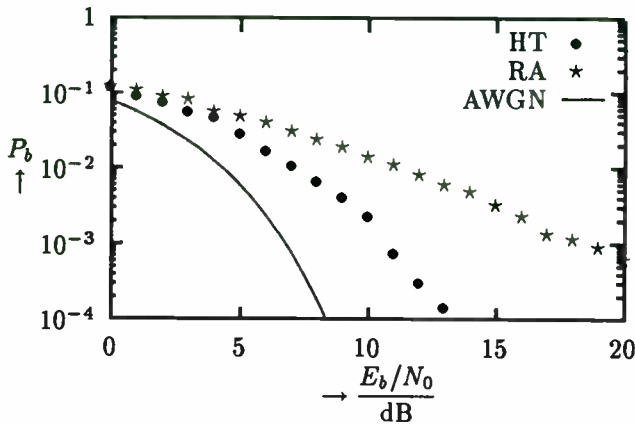


Figure 2: Bit error rates for ideally known channel coefficients for the AWGN-channel and the models *Rural Area* (RA) and *Hilly Terrain* (HT)

The results indicate the advantage of multipath diversity exploited by the rake receiver for the channel model *Hilly Terrain*. For a bit error rate of $P_b = 10^{-3}$ there is only 3.5 dB performance loss compared with the AWGN-channel. In contrast to this, a loss of more than 10 dB arises in the case of *Rural Area*, where the difference increases for lower bit error rates. The obvious poorer behaviour of the channel *Rural Area* results from the inferior multipath diversity compared with the model *Hilly Terrain*.

B. Channel Estimation with Training Sequences

In analogy to the GSM system, it is possible to determine the channel impulse response by using training sequences. As shown in Figure 3, training and information sequences, each consisting of m symbols, are transmitted alternately. Therefore, the net data rate is reduced.

The channel coefficients are detected during the training phase and are used in the next interval by the Rake receiver for equalizing the data signal. Because the estimated values can be averaged during the training interval, their variances can be reduced.

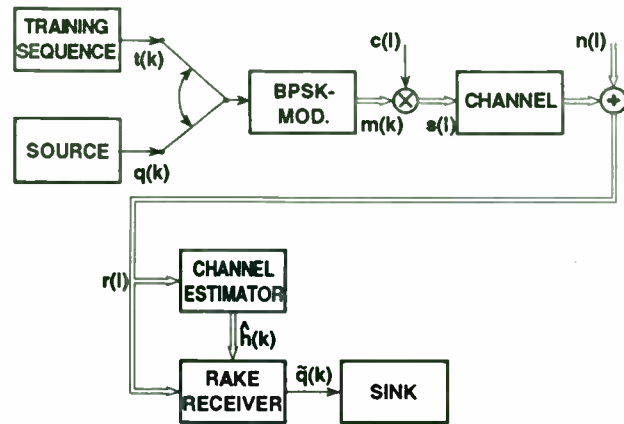


Figure 3: CDMA system with channel estimation based on training sequences

If the training phase lasts too long, the bit error rate deteriorates because the channel is time-variant.

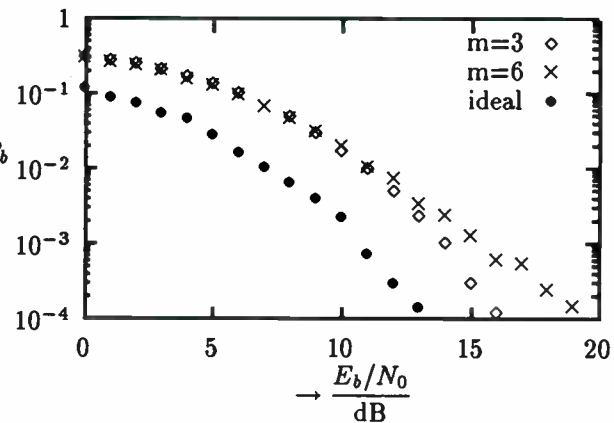


Figure 4: Bit error rates for the channel model *Hilly Terrain* with an impulse response estimated by the use of training sequences

Figure 4 illustrates the good performance of this method for an interval length of $m=3$. Averaging the calculated channel coefficients during 3 symbol intervals yields accurate estimates so that a loss of only 3.5 dB for a bit error rate of $P_b = 10^{-3}$ is achieved. Due to the high maximum doppler frequency shift of $f_{dmax} = 200$ Hz, which is equivalent to a mobile velocity of 240 km/h assuming the 900 MHz-band, the performance decreases for $m=6$. In this case, the channel coefficients change so quickly that the assumption of nearly constant coefficients during the training phase is violated. Perhaps an iterative adaptation can be used to improve the performance.

Similar results for the channel model *Rural Area* are shown in Figure 5. However, the deterioration

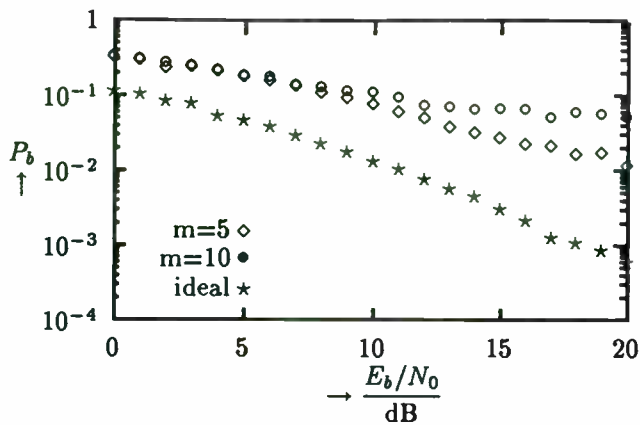


Figure 5: Bit error rates for the channel model *Rural Area* with an impulse response estimated by the use of training sequences

compared with the case of ideally known coefficients is much more significant.

C. Pilot Channel Assisted Estimation

Concerning the synchronization in CDMA mobile radio systems it seems to be advantageous to use a pilot channel in the downlink [1]. This signal is transmitted with a higher power than the data channels in order to secure the connection between base station and mobiles. Thus, the signal-to-noise ratio is higher compared with data channels. As the propagation conditions are the same for the data signal and the pilot signal, the latter can be used to determine the channel impulse response. Furthermore, there is no necessity to add more redundancy to the system in order to estimate the channel, because the pilot channel already exists on the downlink.

Figure 6 illustrates the corresponding system model. For simplicity, it is assumed that the pilot channel does not transmit any information, which means the signal is perfectly known by the receiver. For channel estimation the code signal $c(l)$ and the data signal $m(k)$ in the equations of section III have to be replaced by $c_p(l)$ and $m_p(k)$, respectively. Figures 7 and 8 show the received bit error rates for different power ratios g between pilot and data channel for the channel models *Hilly Terrain* and *Rural Area*.

As expected, the inexact knowledge of the channel impulse response yields a performance degradation. Furthermore, the bit error rates decrease for both channel models if the power ratio between pilot channel and data channel is increased.

Unfortunately, the channel estimation based on a pilot signal cannot be applied in the uplink due to the enormous interferences. Thus, other techniques

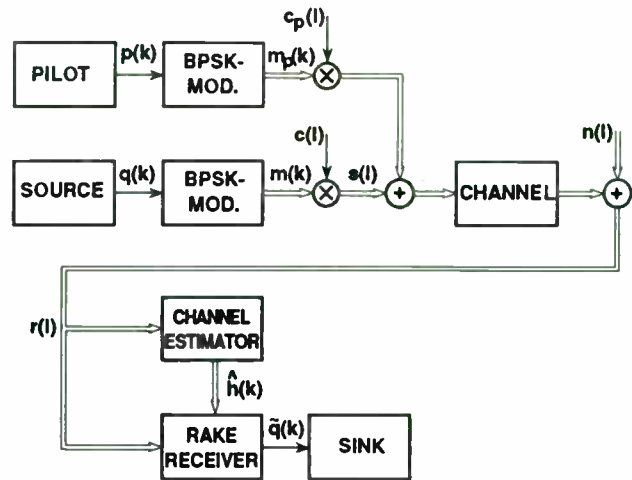


Figure 6: CDMA system with pilot channel assisted channel estimation

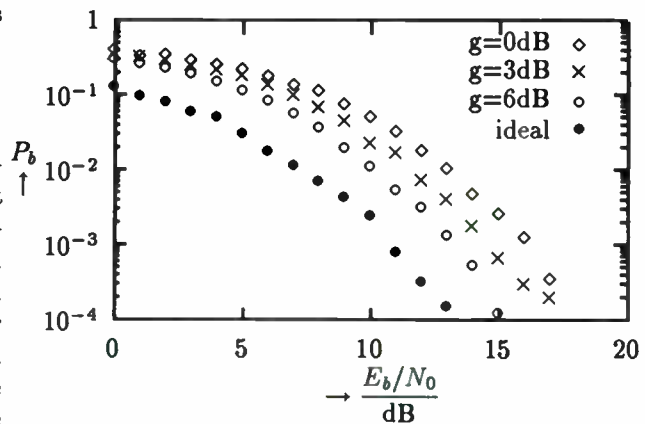


Figure 7: Bit error rates for the model *Hilly Terrain* with pilot channel assisted estimation

have to be considered there. Consequently, a third possibility is investigated in the next section.

D. Differential Modulation

The transmission of differential encoded signals makes it possible to avoid the channel estimation as shown in Figure 9. Therefore, it is necessary to assume that the channel impulse response remains nearly unchanged during two consecutive symbol intervals, which is valid for the considered simulation parameters. Here, the transmission of DPSK-modulated signals is investigated. Accordingly, the Rake-receiver has to be replaced by a Rake-receiver for DPSK-signals (s. [7]).

Figures 10 and 11 illustrate the results for both channel models. Additionally, they contain the reference curves for ideally known coefficients using a

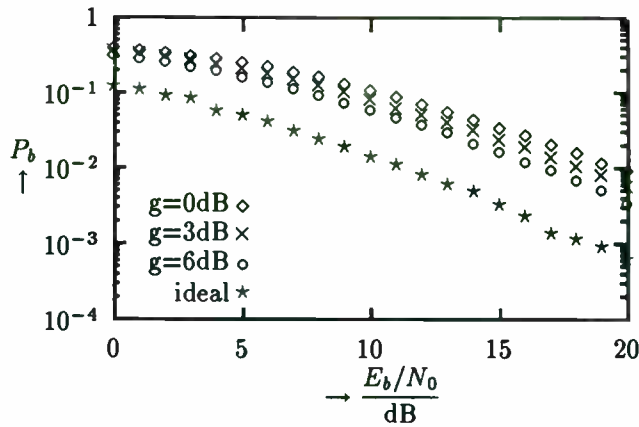


Figure 8: Bit error rates for the channel model *Rural Area* with pilot channel assisted estimation

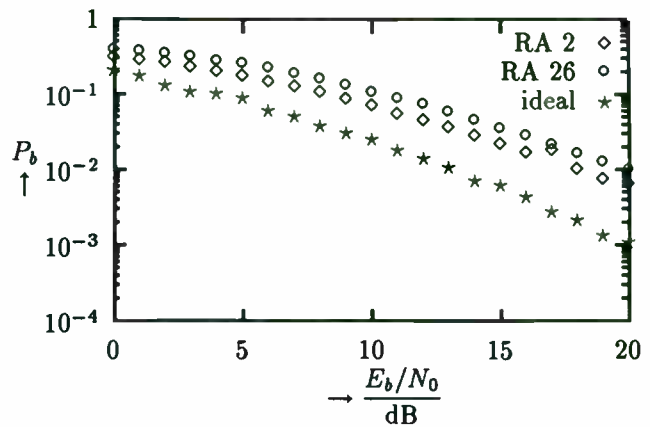


Figure 11: Bit error rates for DPSK-modulation for the channel model *Rural Area* (RA)

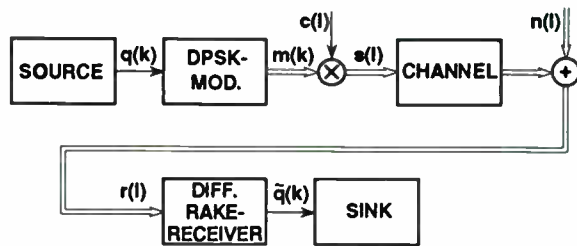


Figure 9: CDMA system with DPSK-modulation

DPSK-modulation. For those systems an approximately doubled bit error rate is achieved compared with the system described in section II, because an error event results in bit errors over two consecutive symbols [7].

The curves marked by HT 26 and RA 26 show the bit error rate for the full Rake receiver with 26 paths. Additionally, the bit error rates are given for a Rake

receiver with the number of paths restricted to the paths of the channel (HT 8 and RA 2) contributing to the received signal. The results in Figure 10 and 11 indicate that branches of the Rake receiver having no counterpart in the channel model do not contribute any information and are reducing therefore the signal-to-noise ratio. Thus, the bit error rates for Rake receivers with 26 paths are worse compared to the cases of HT 8 and RA 2. Although not explicitly examined here, the influence of Rake paths contributing only noise is also valid for the other considered techniques.

V. CONCLUSIONS

This article considers different methods to estimate the channel impulse response in CDMA-systems and compares their performances for a specific system configuration.

Comparing the different concepts, it must be mentioned that the parameter sets are not optimized with regard to a low bit error rate. Therefore, an exact comparison is hardly possible. Nevertheless, differences can be recognized in tendency. The poorest performance is yielded in the system with differential modulation, where the inherent disadvantage of occurring double faults has to be noticed. A major advantage of this technique is the low realization effort compared with the other methods.

The use of a pilot channel seems to provide the best performance. However, this techniques is only practicable in the downlink. To employ training sequences represents also a possible concept but the net data rate is reduced.

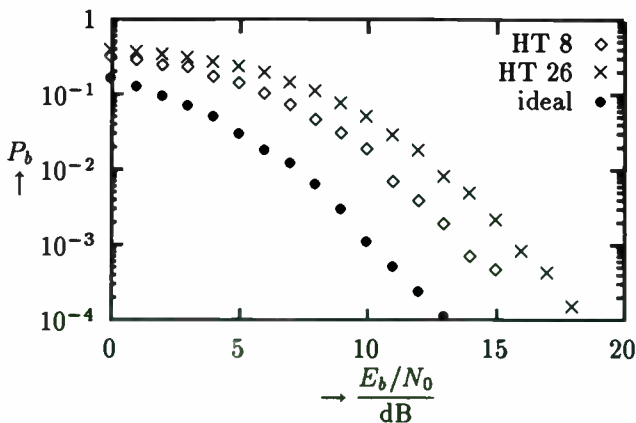


Figure 10: Bit error rates for DPSK-modulation for the channel model *Hilly Terrain* (HT)

References

- [1] Salmasi, A., Gilhousen, K.S., "On the System Design Aspects of Code Division Multiple Access (CDMA) Applied to Digital Cellular and Personal Communications Networks", *41st IEEE Conference on Vehicular Technology*, pp. 57-62, May 1991.
- [2] Lee, W.C.Y., "Overview of Cellular CDMA", *IEEE Transactions on Vehicular Technology*, Vol. 40, No. 2, pp. 291-302, May 1991.
- [3] Mouly, M., Pautet, M.B., *The GSM-System for Mobile Communications*, Published by the authors, 1992.
- [4] Steiner, B., Naßhan, M., Jung, P., Baier, P.W., "Ein Konzept der Kanalschätzung, Interferenzeliminierung und Leistungsregelung für CDMA-Mobilfunksysteme", *ITG Fachbericht, 'Mobile Kommunikation'*, VDE-Verlag, Vol. 124, pp. 77-88, 1993.
- [5] Pursley, M.B., "Performance Evaluation for Phase-Coded Spread-Spectrum Multiple-Access Communication—Part I: System Analysis", *IEEE Transactions on Communications*, Vol. 25, No. 8, pp. 795-799, August 1977.
- [6] Turin, G.L., "The Effects of Multipath and Fading on the Performance of Direct-Sequence CDMA Systems", *IEEE Journal on Selected Areas in Communications*, Vol. 2, No. 4, pp. 597-603, July 1984.
- [7] Proakis, J.G., *Digital Communications*, McGraw-Hill, 2. Ed., 1989.
- [8] Baier A., "Correlative and Iterative Channel Estimation in Adaptive Viterbi Equalizers for TDMA Mobile Radio Systems", *ITG-Fachbericht 'Stochastische Modelle und Methoden der Informationstechnik'*, VDE-Verlag, Vol. 107, pp. 363-368, 1989.
- [9] GSM Recommendation 05.05, *Radio Transmission and Reception*, 1990, Version 3.11.0.

"IMPROVING THE READING DISTANCE OF OMNIDIRECTIONAL TRANSPONDER-BASED SYSTEMS".

BONI ANGELO

is electronic design responsible at MED S.p.A., a company involved in the design of high technology security access systems and anti-theft devices, especially for cars and trucks. He holds 15 patents in the electronic field.

MASSIMO MONTECCHI

is R&D engineer at MED S.p.A. He holds 2 patents in the electronic field.

**MED S.p.A.
R&D lab.
v. TITO, 11
42100 Reggio Emilia, ITALY
Tel. 0039-522-302852
Fax. 0039-522-302834**

Abstract

Low frequency transponder-based systems (≈ 125 KHz) use the electromagnetic field generated by a transmitting coil to energise (via a small receiving coil) the I.C. contained in the transponder. That I.C. modulates the field by absorption, sending back an identification code. The system is very simple and useful, because the transponder don't need any battery to operate. Unfortunately, when the distance increase, the field modulation index is very low, on the order of $1 \cdot 10^{-5}$ at the maximum distance, and hence difficult to detect. The authors describe the problems encountered in designing a "maximum distance" transponder reader system, and their practical solutions. Another problem with transponder-based systems is the omnidirectionality: since the antennas are coils, they exhibit strong directionality, with null points and null planes.

BASIC APPLICATIONS AND OPERATING PRINCIPLES

Transponder based systems are used to transmit wireless informations between a fixed module (usually) and a portable one. Reading distance can range from few millimetres to several metres, depending on applications and technologies (Fig.1).

Applications spans from contactless credit card, animal identification, parking access control, security access and personnel identification, anti-theft for cars and trucks, industrial process tracing,

container identification, luggage and goods management, merchandise protection, etc.

Transponder's dimensions range from glass tube type, with a diameter of 2 mm and a length of 16 mm, typically for animal implantation, to credit-card size for people access control, and to 10x10x5 cm or more for long range types, mainly for cars access control or industrial processes tracing.

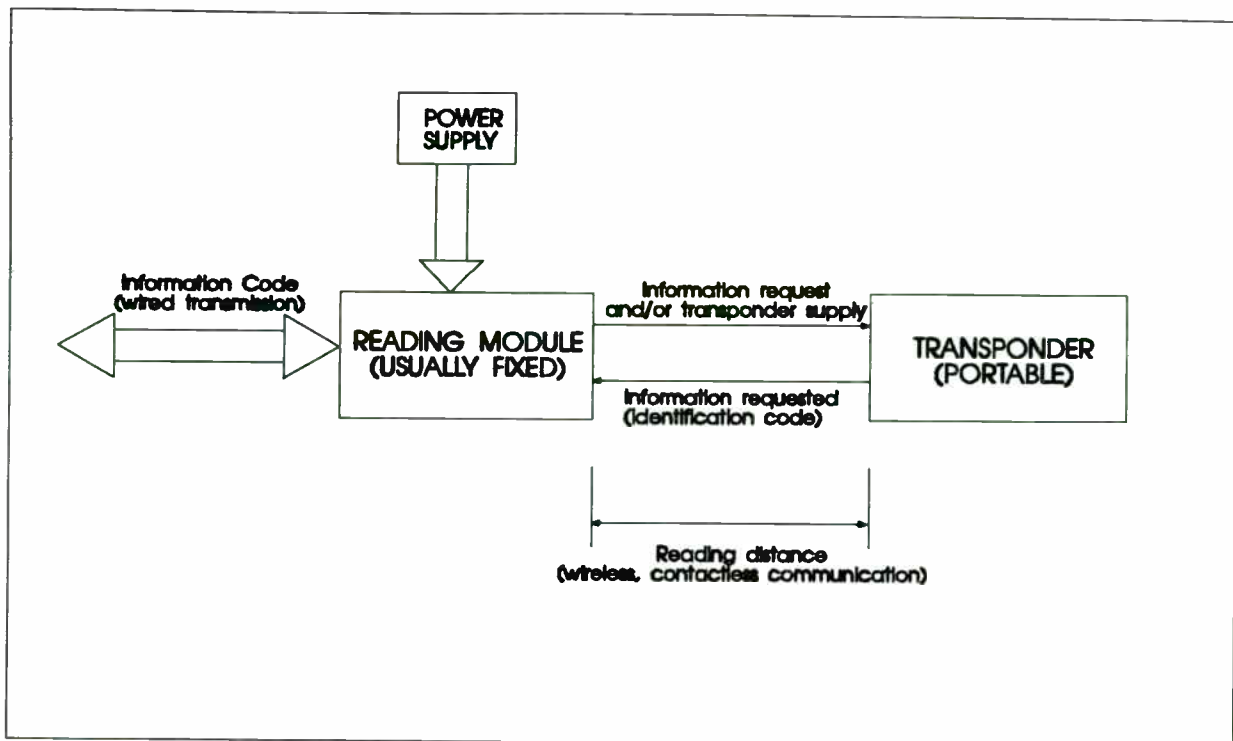


Fig.1

Several intermediate dimensions are available, such as bigger glass tubes or disc types, ranging from 1 cm diameter and 2 mm thickness to 10 or more cm diameter. Different technologies are used to cover the broad spectrum of applications in which transponders are employed: for example luggage identification requires a very low cost transponder (\$1 or less), in high run production, with a reading distance in the order of 20-50 cm. Vehicle identification and parking access control, instead, require a reading distance of at least 1 or 2 metres,

and transponder's cost can be in the \$10 to \$100 range. Transponder reading units can range widely in price and dimensions, depending on reading distance and number of users. Intelligence capability of the reading units can also range widely, from a simple gateway function between transponder and the rest of the system, or, especially for small systems, to a stand alone access control unit.

Automotive security, for example, demand a small, low cost central unit (\$5 to \$20) which is able to handle 2 to 4 transponders.

BRIEF SURVEY ON TRANSPONDER TECHNOLOGIES

LOW FREQUENCY TRANSPONDERS

They operate typically in the 125 KHz frequency band and use magnetic antennas to transmit and receive data. They can be self powered by the 125 KHz carrier or battery powered, and can be very small and very low-priced. This technology is the most diffused at the moment.

MICROWAVE TRANSPONDERS

They operate in the GHz range of the R.F. spectrum and are usually bigger than their low frequency counterparts, although they exhibit a longer reading distance. At the moment this

technology is more expensive (especially from the central unit side) and is not very diffused.

ACTIVE TRANSPONDERS

Active transponders are biased by an internal battery to supply power to an internal microprocessor (or to a special purpose control I.C.). The central unit sends a (usually coded) interrogation request. The transponder answers, sinking power from the battery, for example by activation of an internal R.F. transmitter. They generally exhibit a very good reading distance that does not change in dependence of transponder operation (reading or writing data). They are

however bigger and more expensive than their passive counterparts. Reliability is strongly related to battery life and hence to low power circuitry and immunity to parasitic activation by electromagnetic noise. Commercial transponders, with battery life in excess of 10 years, are common.

PASSIVE TRANSPONDERS

The electromagnetic energy associated with the carrier wave transmitted by the central unit is extracted by the transponder and used as a power source. Three different principles are used to answer to the central unit:

1. Amplitude modulation of the transmitted carrier by magnetic field absorption.
2. Bidirectional communication using different frequencies for transmission and answer.
3. Transponder temporary storing of the received energy into a capacitor. Coded data are sent back, at the end of an interrogation request, using the energy previously stored.

In Fig 2 a brief table of transponder's performance vs. technology is given.

TRANSPONDER TYPE	DIMENSIONS	COST	READING DISTANCE	READING RELIABILITY	REMARKS
Low frequency, passive, read only	Very small: from \varnothing 1.6 x 16 mm, to several cm	Very low	Short / Medium short	Excellent	<ul style="list-style-type: none"> • Very good, very diffused. • Can be fully integrated in a single chip.
Low frequency, passive, read/write	Very small: from \varnothing 2.3 x 16 mm, to several cm	Low	Short	Excellent	<ul style="list-style-type: none"> • The writing distance is lower than the reading distance.
Low frequency, active, read/write	Medium: in the few cm range	Medium	Medium / Long (few meters)	Good to poor (depending on electronic circuitry)	<ul style="list-style-type: none"> • The writing distance is equal to the reading distance. • Intelligence and large memory capabilities
Microwaves, passive, read-only	Medium and Large	<ul style="list-style-type: none"> • Transponder: medium • Central unit: high 	Medium / Long (few meters)	Good	<ul style="list-style-type: none"> • Microwaves power need can be excessive.
Microwaves, passive, read/write	Medium and Large	High	Medium / Long (few meters)	Good	<ul style="list-style-type: none"> • Microwaves power need can be excessive
Microwaves, active, read/write	Medium and Large	High	Long	Good to poor (depending on electronic circuitry)	<ul style="list-style-type: none"> • Very complex system

Fig. 2

THE ABSORPTION BASED SELF FEEDED TRANSPONDER

The design goals were to obtain a transponder access system to be used in MED's anti theft devices with the following characteristics:

- reading distance: at least 20 cm, omnidirectional

- receiving antenna: ferrite coil \varnothing 6x30 mm max.
- transmitting antenna: 70x50x15 mm
- operating temperature: -40°C to +85°C
- stand by current: less than 5 mA.

Two different technologies were tried: the low frequency passive, and the low frequency active.

The second approach gave us, of course, a great advantage in terms of reading distance improvement, but on the other hand there are higher costs, greater dimensions and poor reliability (due to battery dependence). In any case, the MED's low frequency active transponder system generated good results, since the system operated at a distance of over 1 meter with very small receiving and transmitting coils, and a stand by current in the μA range (assuring a battery life more than 10 years long). Furthermore, a MED patented circuit configuration provided to the system a reduced operation capability in case of battery failure, assuring a distance range from 5 to 10 cm.

Even if the active transponder system was a good starting point it was decided to proceed with the passive transponder approach, in order to decrease size and costs.

Two were the main problems to overcome for obtaining a good, omnidirectional reading distance:

1. Since both the reading and the transmitting coils are very small it was necessary to dramatically improve the signal-to-noise ratio.
2. The antennas radiation pattern was characterised by null points and also null planes, which in fact tend to decrease the overall system sensitivity more than one order of magnitude (Fig.3).

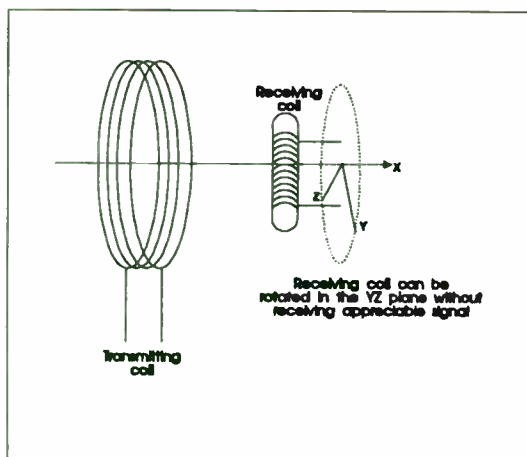


Fig.3

Before the description of the methods adopted to improve the reading distance, a brief explanation of the basic principles related to the absorption-type self fed transponder is given (Fig.4).

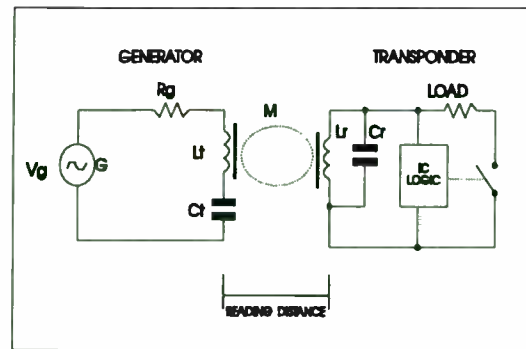


Fig.4

The sinusoidal generator G feed the resonant circuit C_t, L_t , with a signal:

$$A = \sin \omega t \quad (1)$$

with $\omega = 2\pi f$, f typically 125KHz

The maximum current flowing into the resonant circuit, considering ideal (lossless) components, is given by:

$$I = \frac{V_g}{R_g} \quad (2)$$

being R_g the source resistance. From equation (2) it can be seen that the main limiting factor for the current flowing is R_g .

L_t is an open magnetic circuit inductor and hence it radiates a magnetic field in the space.

A small part of that field is picked up by the L_r coil, which also resonates with its C_r capacitor at the generator's frequency. If the voltage amplitude induced across L_r is in the order of 3 to 4 volts, the logic I.C. will start to operate, controlling an internal switch that open and close at the code rate. The net result is to connect and disconnect a load to the parallel resonant L_r, C_r circuit so that the magnetic field is modulated accordingly (scope waveforms plot of Fig.5).

This modulated field is seen, by the transmitting L_t coil, as a difference in energy absorption, and hence in an amplitude modulation superimposed to the generator's sinusoidal wave. The modulation index is very small because the mutual inductance "M" between the two magnetic circuits is barely measurable: at the maximum reading distance M can be estimated in the 10^{-5} to 10^{-6} range.

Two factors are crucial in determining the maximum reading distance (provided that

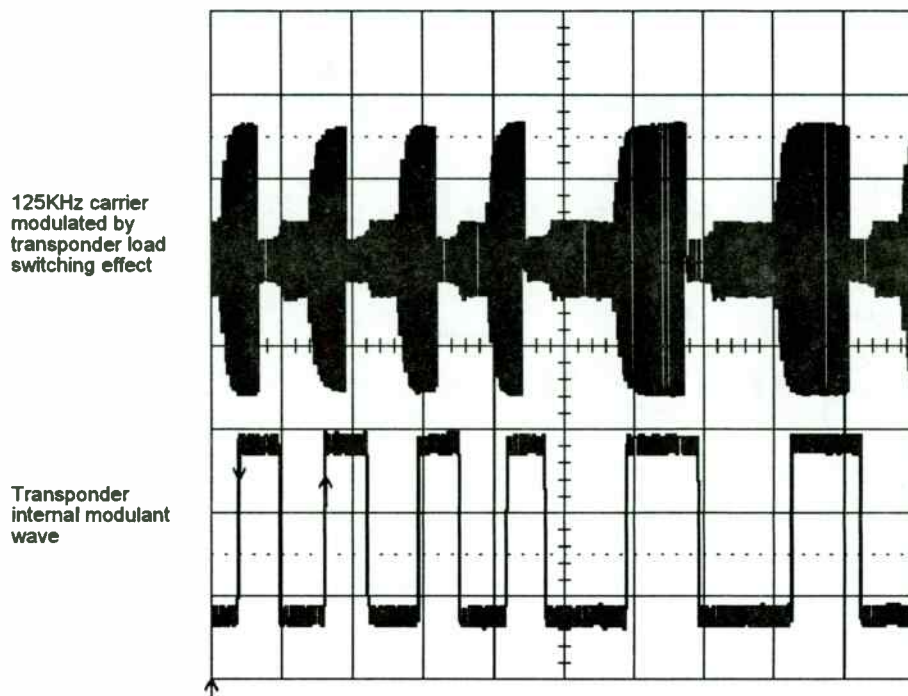


Fig.5

geometries of transmitting and receiving coils are kept constants):

- 1) The maximum distance at which the transmitting coil L_t is able to generate a field strong enough to activate the logic I.C. in the transponder.
- 2) The maximum distance at which the modulated field received by L_t is detected with a suitable signal to noise ratio.

Point 1) may be a limiting factor in certain countries, where those systems must meet more stringent regulations in terms of maximum radiated energy, thus limiting the maximum emitted power.

Point 2) is a function of the system's capability of being low noise in the emitter and in the detector circuitry. In Fig.6 is showed a block diagram of the system as implemented in the MED's product.

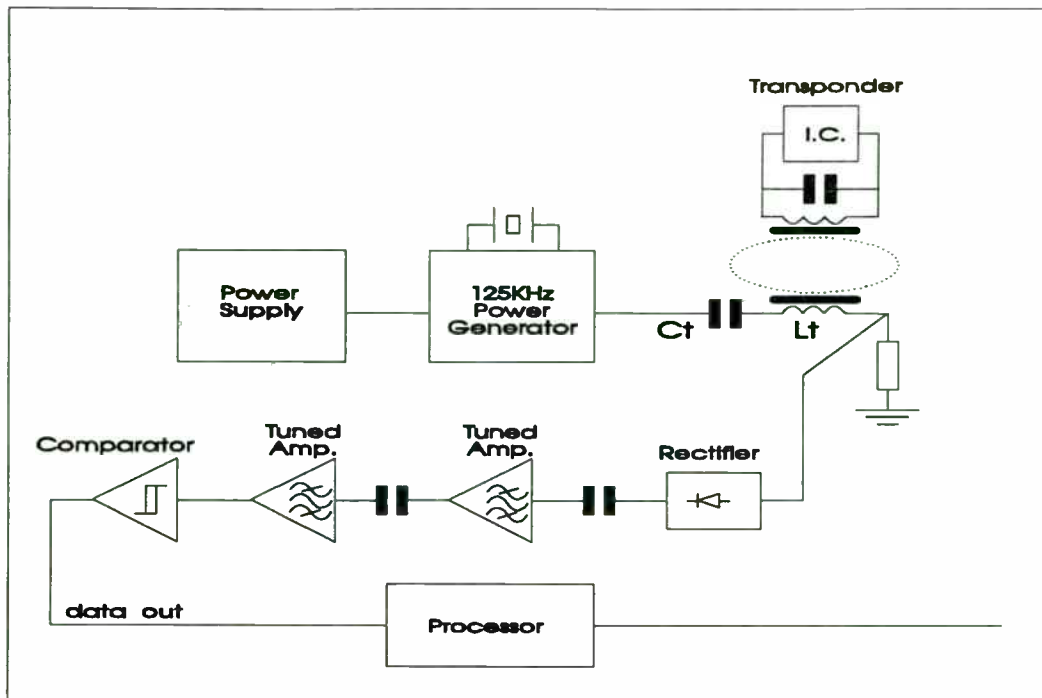


Fig.6

Following, a brief description of each block and its contribute to the overall noise is given.

- A) **POWER SUPPLY:** the 125KHz sinusoidal wave power generator is fed by that stabilized supply circuit, and hence its internal noise is fully superimposed to the transmitted signal, thus generating AM noise. Since the detected signal is also an AM modulation (being the modulation index in the order of 10^{-5} to 10^{-6}), the power supply's internal noise should be at least three times less, almost in the frequency band of the transmitted data code. As an example, for a 10Vdc power supply, this translates to a noise not greater than 3 to 30 μ V!
- B) **125KHz POWER GENERATOR:** the emitted carrier signal must be kept clean and with a low residual FM noise. In fact FM noise is translated, by the Lt,Ct series tuned circuit, into AM noise, as can be understood looking at Fig.7.
- C) The resonant circuit Lt,Ct should exhibit a good electrical and mechanical stability, to avoid any related mechanical vibration noise.
- D) **Tuned circuits:** the first stage is very similar to a standard receiver's first stage: it should be characterised by low noise figure and high gain.

The bandwidth of the whole circuit is related to the bandwidth of the transmitted data.

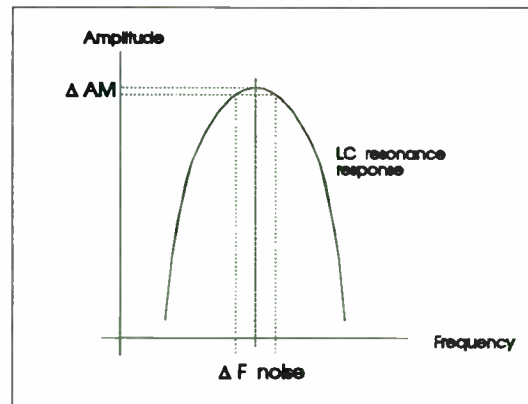


Fig.7

- E) **Rectifier:** noise contribution is negligible: at least one block that isn't critical!
- F) **Microprocessor:** clever software algorithms can help, at the maximum reading distance, to regenerate the correct transponder's data code, and hence help to increase the system reliability.

Thanks to the optimisation process applied to each block we have been able to improve the reading

distance from the initial 20cm to 32cm, as shown in Fig.8. Considering that the magnetic field decreases with the square of the distance, the real improvement factor must be calculated as:

$$1: (32/20)^2 = 1 : 2.54 . \quad (3)$$

ANTENNAS DIRECTIVITY

The maximum reading distance of a transponder-based system, as shown in Fig.8, represent of course a best case if both the coil's magnetic axis are coplanar and oriented for maximum flux transfer.

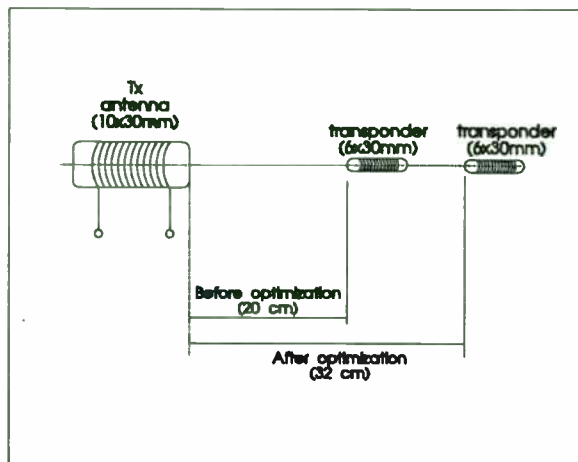


Fig.8

Nevertheless practical applications are far different from the ideal one. In the most general case the transponder axial direction can assume any angle to respect to the transmitter coil. A set of measurements were carried out to plot a sort of polar directivity diagram of the system in real conditions. Results are reported in Fig.9, which points out the reference orientation angles, and in Graphs 1 to 12 added in the next page.

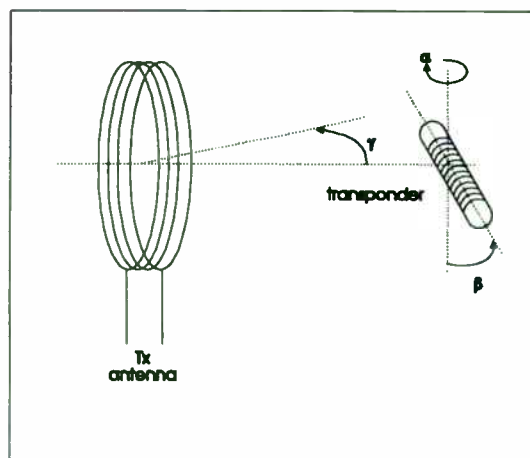


Fig.9

It can be seen that the system exhibit some null points and null planes which cannot be accepted, especially in a MED product.

The null cancellation possibilities are essentially two:

- A) Cancellation obtained by coil motion.
- B) Cancellation by means of tridimensional geometry.

CANCELLATION BY MOTION

Cancellation by motion is the more natural way to avoid null points in receiving coded data from a transponder. For example, in people access control systems the person carrying the transponder is walking parallel to the antenna coil.

The null point (see Fig.10) occurs only when the transponder is at the centre of the transmitting coil axis. Unfortunately in MED's applications there is no motion between the transponder and the transmitting coil.

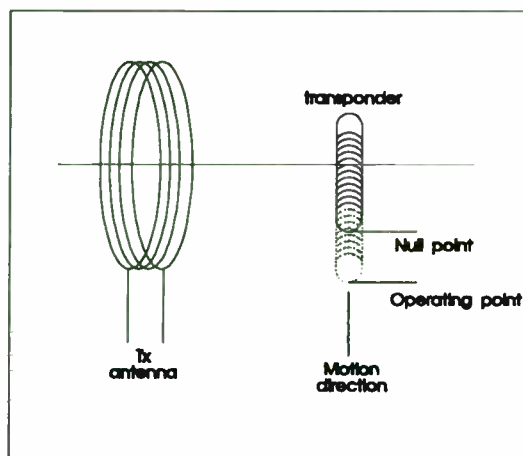
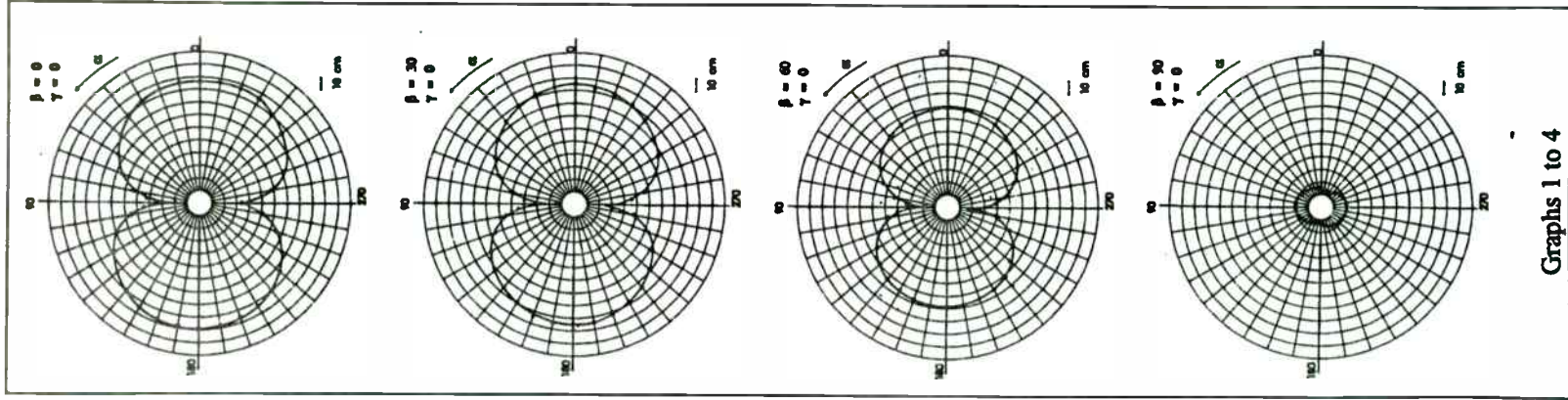


Fig.10

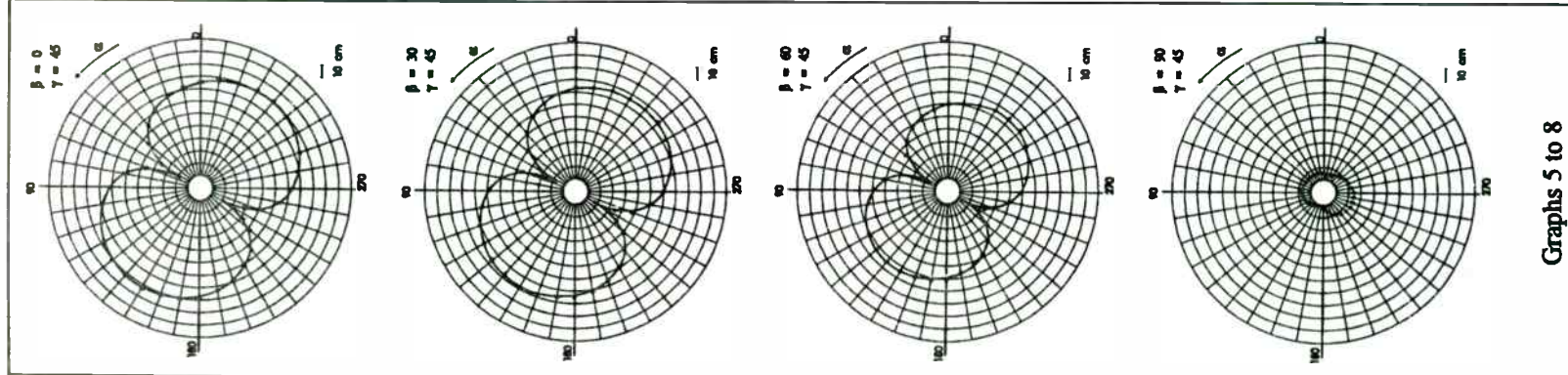
CANCELLATION BY GEOMETRY

Tridimensional geometry give the most reliable solution to the null points problem. Using three transmitting coils, oriented on the three axis X,Y,Z of the space, there is no virtually a null point. It must be pointed out that the coils can't be operated simultaneously, otherwise destructive interference can occur, being the magnetic field a vectorial entity.

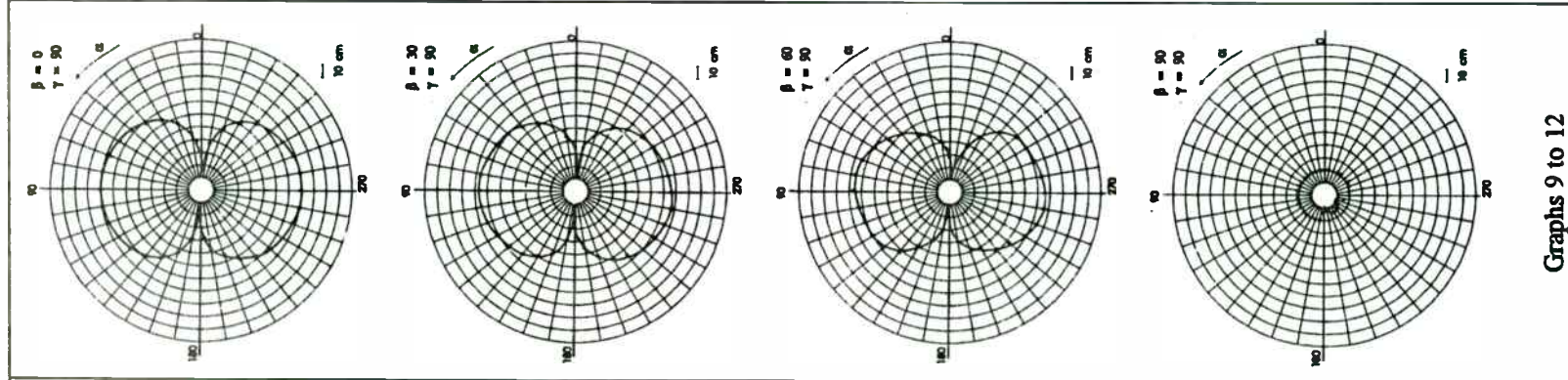
The main problem, adopting a three coils antenna, is to realise a clever circuitry to be able to switch the magnetic energy from one coil to the other as quick as possible, and without an excessive cost and



Graphs 1 to 4



Graphs 5 to 8



Graphs 9 to 12

dimension increase. About the dimensions the right idea was to use two ferrite coils and one air wounded coil (Fig.11). This disposition does not increase excessively the antenna dimensions, in

particular under a thickness point of view, and permitted very good performances. The system has been patented.

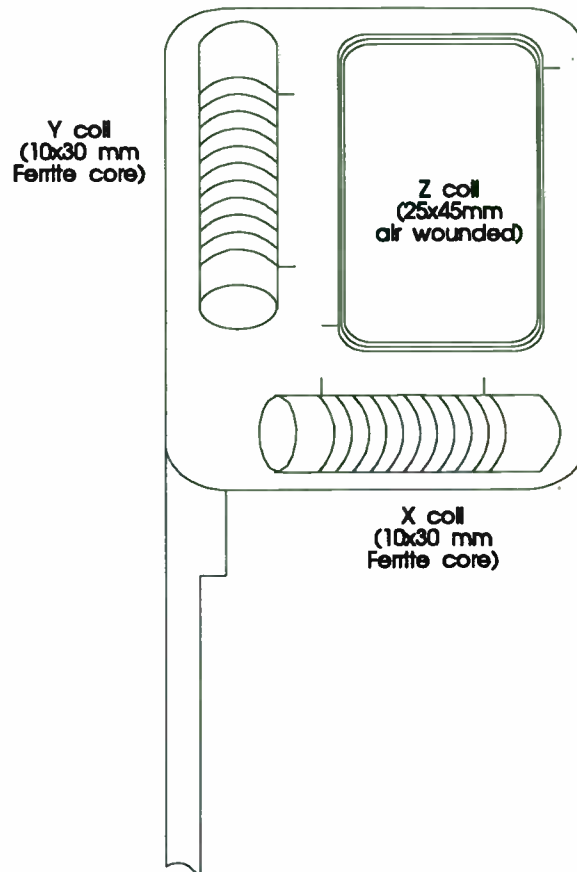


Fig.11

RESULTS

Clever design of the transponder-based system permitted reliable operation. A transponder based access system made in MED, named "PRO30", is part of an immobilizer system for cars and trucks, and is able of doing sure identification of a transponder at a distance in excess of 20 cm, aside from receiving and transmitting coil orientation. Since the PRO30 system is designed for after-market installation, the omnidirectionality is mandatory. In fact, if the transponder must be added to the customer's key holder, the transmitting to receiving

coils position is not known (it depends on antenna installation, transponder placement, and ignition key lock position in the car).

The three-coils approach used on the antenna, oriented along the X,Y,Z axis and feeded not simultaneously, allows a compact solution of null point problems. Optimisation of each circuit's block for low noise operation permitted to further increase the reading range while keeping the antenna dimensions unaltered.

FUNDAMENTAL CONSTRAINTS ON RFID TAGGING SYSTEMS

Peter H. Cole and David M. Hall

Department of Electrical and Electronic Engineering
The University of Adelaide
Adelaide SA 5005
Australia.

Michael Y. Loukine and Clayton D. Werner

Integrated Silicon Design Pty. Ltd.
99 Frome St.
Adelaide SA 5000
Australia.

ABSTRACT

The paper considers some fundamental constraints limiting the performance of microwave, high frequency and low frequency near and far field passive electronic labels for remote object identification.

Electromagnetic compatibility constraints imposed by various countries upon energising field creation for microwave, high frequency and low frequency tags are examined, their influence on shaping design of interrogator to tag coupling systems is investigated, and several theorems leading to the optimisation of antenna structures are presented.

The influence of various noise sources in the detection of passive electronic tags is considered. The dominant sources of noise being found to be environmental noise and noise deriving from the interrogator transmitter itself.

A description of the Company's successful systems for highway toll collection, vehicle theft detection, automated navigation and high temperature object identification for manufacturing automation in hostile environments is included.

1. INTRODUCTION

Radio frequency interrogatable electronic coded labels more commonly known as rf id tags, are in use in such diverse applications as access control, highway toll collection, personnel identification, warehouse navigation, refuse container identification, vehicle theft detection, manufacturing control. The technologies employed include surface electroacoustics [1,10], subharmonic generation via cmos circuits [2], self powered or battery assisted radio frequency backscatter [3], or tags with generally battery driven transmitters triggered by but otherwise independent of the interrogation signal, all implemented using a very wide range of operating frequencies for both the interrogation signal and the reply.

The performance of such systems is limited by a variety of factors resembling in their diversity the multiplicity of operating principles. It is our aim in this paper to review principally constraints on the performance of passive tags, to provide an assessment of their influence in the variety of tagging systems, and to give an indication of the future of rf id tagging.

In the following Section an brief overview of the different systems and their operating principles is provided. In Section 3 the influence of electromagnetic compatibility regulations in both local and overseas jurisdictions on system performance is explored, the interaction between electromagnetic compatibility

measurement instruments and the signals used by rf id tagging equipment is considered, some regulatory inconsistencies are pointed out and some suggestions for greater recognition of the needs of rf id systems are made. In Section 4 the process of electromagnetic coupling to small electronic labels is analysed, and methodologies appropriate to different frequency ranges identified. In Section 5 the sources of noise which limit the performance of almost all systems are reviewed, and an analysis of the influence of this noise in systems of current interest is provided. In Section 6, conclusion are drawn and the present status and possibilities for the future of rf id systems are reviewed.

2. OVERVIEW OF SYSTEMS

2.1 Classification of systems: In its most basic form, an rf id system has components as illustrated in Fig. 1. Although the diagram shows separate antennas for the transmitter and receiver, in practice a single antenna is often used, with separation of transmitter and receiver signals being performed by a circulator or directional coupler, most frequently the latter.

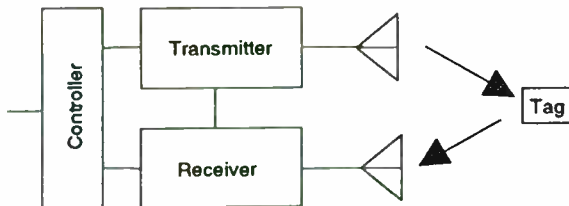


Fig. 1 Electromagnetic Labelling System.

The richness of variety of rf id systems [18] and their operating principles presents challenge when attempts to classify them are made. Classification must be made along several independent dimensions, firstly whether the labels are *passive*, deriving all of their operating power from the interrogation signal, or whether they are *active* in that they contain a battery, which is of assistance in either generating a reply which is independent of the interrogation signal, or a reply in which either the information or the power provided by the interrogation signal plays a part.

In the major classification of passive tags, it is clear that the reply signals are inevitably weak when compared with the interrogation signal.

This fact requires that more attention be given to separation of the reply signal from the interrogation signal, which given the fact that the transmitter and receiver of the interrogator scan the same region of space, is likely to be coupled into the receiver at a level which competes seriously with that reply.

The fact that separation may be effected in either the time or frequency domain leads to a second major classification, the *reply-now* tags, almost always involving microelectronic circuits and in which the tags reply at a different frequency to that of the interrogation signal, and the *reply-later* tags, in which the reply arrives after the interrogation signal has ceased, at least temporarily.

Thirdly there is the classification of *one-bit* tags, generally used for theft detection in stores, in which only the single bit of information signifying the tag's presence is obtained, and the *many-bit* tags, in which some information about the item labelled is encoded.

Fourthly in the many-bit tags there are the classifications of *read-only* tags, in which the information is permanently encoded at time of manufacture, and the *read-write* tags, in which some of the information may be changed in use.

Among the read-write tags, there are *battery-supported* memories, with fast write times but limited although sometimes long life, and the *non-volatile* memories, of virtually indefinite life but burdened by longer write times.

A major classification dimension is that of *operating frequency*, in which it will be convenient to recognise the *microwave and uhf* tags, operating from 300 MHz upwards, the *low frequency* tags, operating in the near field of the interrogator antenna in the frequency range 10 kHz to 400 kHz, and *medium frequency* tags operating generally in the hf region from 3 to 30 MHz.

Tags can also be distinguished according to the manner of generation of the reply, and of its relation to the interrogation signal. In this scheme there are: the *harmonic tags*, [4] in which the reply is superimposed as a modulation upon an harmonic (generally the second) of the interrogation signal; the *sub-harmonic tags* [2,8,9], in which a generally cmos circuit divides the interrogation signal down to a sub-harmonic frequency before superimposing the reply by modulation; the *anharmonic* tags, in which the interrogation signal energy is used to

generate a signal unrelated in frequency to that of the interrogation signal; the *saw* tags [1,10], a unique variety of reply-later tag in which fixed coded reply signals, distinguishable from the interrogation signal, are generated through the efficient storage, for times long enough for environmental transients to die away, in the form of surface acoustic waves; the *actively transmitting* tags, which produce their own code-modulated radio frequency carrier transmission in response to interrogation; and finally the very significant group of *backscatter* tags, which do not contain components which generate radio frequency energy, but act as field disturbance devices by reflecting in a coded manner the incident rf signal.

The popularity of this last class of tags can be traced to the fact that only very low power is

required to operate the low frequency modulating circuits within them, while the rf signal responsible for energising and reply can be positioned at places in the electromagnetic spectrum convenient from the point of view of allowed radiation and environmental noise.

This low operating power can come from the interrogation signal or from a battery. When a battery is used, it is common to incorporate a *turn-on circuit*, which senses when the tag is being interrogated, and supplies battery power for a limited time after each such event.

2.2 Illustration of practical systems:

The variety of rf id systems and achievable performance characteristics is further illustrated by the listing in Table 1 of systems developed by the Company.

TABLE 1.
ISD rf id systems

Interrogation Frequency MHz	Tag Size description or mm	Tag type Active or Passive	Range m	Tag antenna type E or H	Multi-read capability Y or N	Installed application (see text)
2,450	192 by 54	A	8	H	N	1
2,450	80 by 59	P	1	H	N	1
915	credit card	A	40	E&H	N	7
915	credit card	P	7	E&H	Y	1,2,3,4,5,6,7,8
915	25mmØ	P	5	H	N	1,4,7
433/458	credit card	A	40	E&H	N	7
433/458	credit card	P	3	E&H	N	2
27	40 by 68	P	0.4	H	Y	2,7
13.5	credit card	P	1	H	Y	2,5

In the above Table the applications are identified according to the key: 1. Factory Automation, 2. Waste Management, 3. Toll Collection, 4. Vehicle Anti-Theft, 5. Personnel Tracking, 6. Vehicle tracking, 7. Access Control, 8. Warehouse Management.

2.3 Factors limiting performance: From the above discussion we could deduce that despite the multiplicity of operating principles and frequencies the performance will be limited by the following factors.

- For passive microcircuit based tags, obtaining at useful distances enough power to energise the circuits within the tag.

- Performing the latter function at frequencies and power levels which are in accord with electromagnetic compatibility regulations over the jurisdictions in which sales are sought.
- For all types of tags achieving satisfactory signal to noise ratio for the reply signal at the receiver.
- For battery operated tags, minimising the battery drain so as to increase lifetime.

3. ELECTROMAGNETIC COMPATIBILITY

3.1 The General Arrangement of Components: Fig. 2 shows a general picture of the interrogator and tag antennas in relation to

the measurement position. In the LF band the near field boundary is 398 m (for 120 kHz) thus both the tag and measurement position are in the near field. In the HF band the near field boundary is 3.5 m (for 13.5 MHz) or 1.8 m (for 27 MHz). For these frequency bands a tag is usually in the near field and the measurement position (typically 10 m or 30 m) is in the far field. For a UHF or microwave tag (near field boundary 53 mm for 915 MHz) the measurement position (typically 3 m) is closer to the interrogator than the tag (6 m typical of ISD passive systems) both being in the far field.

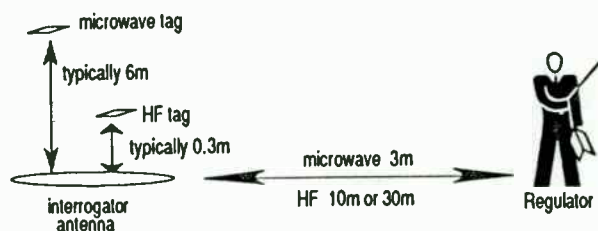


Fig. 2 Relative positions of interrogator and tag antennas and position of limit measurement

The regulation measurement distance from the interrogator antenna is dependent on the frequency of interrogation and the country in which the system is operated.

3.2 Generic regulations: Electromagnetic compatibility regulations around the world are very varied and in a state of flux, but one can identify firstly *generic* emc regulations, and then *exceptions* to the regulations made for specific purposes or in specific bands. In the USA, generic regulations [5] tend to cover frequency bands and be purpose independent, with exceptions being confined to particular bands, with particular purposes sometimes stated and sometimes not. In Europe, in contrast, regulations are very much organised around product categories, with generic regulations [6,7] being confined to devices not yet classified.

Operation under generic regulations is possible for very short range devices. For longer ranges, much higher operating powers are available for rfid systems in specific bands. Frequently such bands are within ISM bands, but powers in some jurisdictions are still limited, in some they are undetermined, and in some they are informally tolerated. There is however the contrast that some classes of ISM equipment are allowed unlimited radiation in

such bands. In the opinion of the authors this difference in treatment is unsatisfactory.

3.3 Regulation variation: Considerable variability in regulations is encountered in power levels and methods of measurement although convergence between jurisdictions is occurring.

Such variability seems most pronounced in relation to low frequency near-field measurements, and in treatment of pulse operated systems.

Taking as an example the problem of near field measurements, the draft European regulations [11] are explicit in stating when magnetic field sensitive antennas are to be used in measurements and the field limits are specified in terms of magnetic fields. Further, the regulations vary in logically discernible ways in respect of the different limits which apply to antennas which generate predominantly magnetic fields and those which are designed to generate predominantly electric fields, even though magnetic field is what is measured. US regulations [5] on the other hand seem almost invariably couched in terms of electric field, even when it is magnetic field which will predominantly be generated, and in most cases measured.

Taking as a second example the question of measurements in relation to pulsed systems, one may find in regulations of both the European and USA jurisdictions, in some bands no allowance for pulsed operation is made, in some nearby bands an allowance for pulsed operation which amounts to requiring that average signal *amplitude* (not average power) be measured (up to a 20 dB peak to average ratio) while in some other bands it is specifically average signal *power* which is measured.

There is also variation in the type of detector used for measurements. Invariably the CISPR receiver defined in [12] is specified in Europe, but is accepted in the USA in only some bands as an appropriate measurement instrument. Moreover, the effect of specifying that instrument for measurements of different levels both in and outside of the ISM bands results in a situation in which spectrally pure systems operating at the allowed power level within an ISM band will, because of the quite broad frequency response of the CISPR receiver, be seen as producing spurious signals of unacceptable amplitude at regions outside the ISM band, whereas such signals are not in fact being produced. It is the view of the authors that

much work needs still to be done in harmonising worlds regulations, and it is the hope that as this work is done the legitimate but modest needs of rf id systems will be recognised.

3.4 Short range devices: Of interest are the draft European regulations for rf id systems contained in [11] Those regulations specify measurement of magnetic field, and give for very low frequency devices a large magnetic field limit, progressively decreasing to a lower limit at the upper edge of the specified band. At the low end of the band, a duty cycle dependent allowance equivalent to 10 dB per decade of duty cycle is available, but this concession does not exist above 135 kHz. At three frequencies corresponding to ISM bands, viz 6.78, 13.56 MHz and 27.12 MHz, elevated values of magnetic field strength are allowed in small bands.

To assess the impact of these regulations on rf id systems over the band, we make use of results to be obtained in Section 4, which indicate that the effective driving power of a tag is the reactive power density $\mu\omega H^2$ established at the tag position by the interrogator. Assuming a dipolar field configuration and an interrogation distance of one metre, making allowance for scaling factors in the near and far field as appropriate for the different frequencies [14], and taking advantage of pulsed operation where this helps, it is possible to construct Table 2 showing the allowed magnetic field strengths at 10 m and their relative effectiveness as energisers of passive tags.

TABLE 2.
Available reactive power densities at one metre for various frequencies

Operating Frequency Hz	Field Limit dB μ A/m	Reactive Power Density dB(μ A/m)/Hz
120k	55	118.79
6.78M	42	104.22
13.56M	42	95.18
27.12M	42	86.14

Clearly these regulations favour low frequency operation.

4. INTERROGATOR TO TAG COUPLING

4.1 Antenna Optimisation: The ratio of the field at the tag position to the field at the

regulation measurement position is one which needs to be maximised for the benefit of maximum system range whilst complying with the regulations.

In the near field coupling situation, it may be shown, perhaps unexpectedly, that the ratio of field at the tag position to field at the regulation measurement position can be maximised by using a *very small* interrogator antenna. This maximisation of ratio is, however, accomplished at the expense of requiring a large input power. An alternative and more practical criterion for optimisation of interrogator antenna size is discussed below.

4.2 The Radian Sphere: The concept of the radian sphere [13], which has a value for its radius of $\lambda/(2\pi)$, aids in the visualisation of whether the tag coupling is in the near or far field. If the tag is inside this sphere, the energy storage fields (dipolar field terms) dominate and coupling volume theory [15] is used, and if outside the propagating fields dominate and the familiar concepts of gain, effective area and eirp are used.

4.3 Coupling and Dispersal Volumes: The concept of coupling and dispersal volumes [15] is used for the optimisation of antenna sizes when the tag antenna couples to the magnetic field of the interrogator antenna, in the near field. In this weak coupling situation the magnetic field at the tag position can be regarded as uniform over the comparatively small volume of the tag, and is determined only by the parameters interrogator antenna and is not affected by the small amount of power in the tag. Also the real power delivered to tag can be approximated to be proportional to the reactive power density, of the interrogator antenna's energy storage field, at the tag position.

The relationship between received power in the tag and transmitted power from the interrogator antenna is given by:

$$\frac{P_{tag}}{P_{int}} = \frac{Q_{tag} Q_{int} V_c}{V_d} \quad (1)$$

Here it is seen that for efficient coupling for a given interrogator output power and quality factors of both tag and interrogator antennas, the coupling volume should be made as large as possible and the dispersal volume as small as possible.

The coupling volume, which is defined in (2), is a figure of merit for the tag antennas ability to

couple to a field at the position of the tag and is determined only by the tag antenna characteristics.

$$V_c = \frac{\left(\begin{array}{c} \text{peak stored magnetic energy} \\ \text{in tag self inductance} \\ \text{when shorted} \end{array} \right)}{\left(\begin{array}{c} \text{peak magnetic energy density} \\ \text{at tag position produced} \\ \text{from interrogator} \end{array} \right)} \quad (2)$$

Increasing the largest dimension of the antenna increases the coupling volume. The dispersal volume, which is defined in (3), is determined by the dimensions of the antenna and on the position of the tag.

$$V_d = \frac{\left(\begin{array}{c} \text{peak stored magnetic} \\ \text{energy in interrogator} \\ \text{antenna} \end{array} \right)}{\left(\begin{array}{c} \text{peak magnetic energy} \\ \text{density at tag position} \\ \text{produced by interrogator} \end{array} \right)} \quad (3)$$

It is though the field at the tag position is uniformly spread over a volume equal to the dispersal volume. There is an optimum size for an antenna such that the field does not cover more volume than necessary. As examples of the sizes required for the interrogator antenna, a loop requires a radius equal to the interrogation distance, and a solenoid (length greater than diameter) requires a length equal to the interrogation distance. Comparing these two antennas, the loop is the better performer.

The use of ferrite in the core of a solenoid increases the coupling volume or decreases the dispersal volume by a factor equal to the effective permeability, which depends on the size, shape and grade of ferrite used.

4.4 Field Selective Antennas: The cost and ease of manufacture usually determine the choice of antenna for the tag and interrogator. However, certain applications dictate the use of one particular type of antenna over another. For example if one antenna is required to be used against a metallic object or surface, magnetic field coupling would be chosen and the antenna would be a ferrite cored solenoid.

Quadrupole antennas give the advantage of allowing a strong field to be set up in the near field for tag coupling, while the close separation

($\ll \lambda/2$) of the two constituent dipoles give a far field cancellation factor.

4.5 Small Antennas: As the tags are usually required to be unobtrusive, the antennas used are usually small, not only physically but electrically as compared to a wavelength. A small antenna has a high Q (given by the radiation resistance and its reactance) due to a small radiation resistance. Efficient transfer of power is more difficult to achieve as the losses in the antenna can be of the same magnitude as the radiation resistance.

Rather than treat the antenna as having an effective area, gain, a small radiation resistance and a large mismatch factor relating to the loss resistance, coupling volume theory may be used. Here the quality factor of the antenna includes the losses and ignores the small radiation resistance.

4.6 Comparative Examples of Planar and Ferrite Tag Antennas: As an illustration of the effectiveness of planar antennas relative to solenoidal antennas, even when ferrite cores are used, a comparison is made of the measured coupling volumes [15] of three antennas, viz. a 6 turn printed planar rectangular spiral coil of credit card size, a 13 turn solenoid on a rod of F25 grade material, and a 22 turn solenoid on a rod, also of F25 grade material (dimensions as in Table 3.).

The coupling volumes for each antenna were calculated, as in [15], and appear in Table 2.

TABLE 3.
Summary of antenna comparison

Antenna	Planar 83mm x 51.5mm	6mmØ 75mm long	10.5mØ 140mm long
V_c ($\times 10^{-6} \text{m}^3$)	101	62	371

From experimental results, the relative performance of these antennas gave close agreement with the relative performance indicated by the coupling volumes in Table 3.

5. NOISE IN ELECTRONIC LABELLING

5.1 Thermal noise: From a perspective established by familiarity with ordinary radio

communications, it might be expected that the important sources of noise in rf id tagging are thermal noise (well known as $kT = -204$ dBW per Hz for room temperature of 300K in the receiver section of an interrogator, man-made environmental noise, and signals from other users of the electromagnetic spectrum.

It cannot be denied that thermal noise in a receiver is significant in that it provides, unless heroic attempts to minimise it are made, an irreducible minimum noise level against which tag reply signals compete. It is also significant in that it provides, in some favoured sections of the wide spectrum within which electromagnetic tagging operations are conducted, the principal noise source among the three mentioned above.

5.2 Environmental noise: It is difficult to generalise about man made noise, as the effects vary greatly with environment, and with position in the spectrum. Experience indicates, however, that in industrial environments at the low frequency end of the spectrum, (10 kHz to 400 kHz), machinery has proven to be a prolific source of in practice unregulated interference of such strength that many low frequency tagging systems become inoperable in those environments, whereas hf or uhf based systems are substantially unaffected.

5.3 Backscatter systems: A large number of systems make use of the *modulated backscatter principle*, and employ for detection of the reply signal homodyne receivers [16] and antenna and signal separation systems such as are shown in Fig. 3. In contrast with the situation in a normal communication link where the transmitter is at a distant point from the receiver, the transmitter in an rf id system is immediately adjacent to the receiver, and scans the same region of space. In a system employing passive tags, any noise generated by the transmitter itself is likely to enter the receiver with relative ease, and there competes directly with the reply which, in a system employing small and passive tags, will have suffered from a two way propagation loss and whatever conversion loss is involved in generating a reply from the energy which can be extracted from the interrogation beam, and will therefore be a weak one.

Important sources of noise and other interfering signals in the transmitter of such an interrogator are (a) phase noise in its master oscillator, (b) shot noise in the collector currents

of transistors, (c) modulation noise which may be introduced in transmitter pulse shaping, and (d) spreading of the transmitter pulse spectrum into the reply band as a result of unduly fast pulse modulation of the transmitter output. To analyse the effect of such signals we must first derive in the next section some basic results.

5.4 Some general principles: In passive backscatter systems in which interrogation takes place at a frequency f_0 and the reply code is produced by the generation first within the tag a *reply sub-carrier* at frequency f_s and then modulating that sub-carrier with the reply code, the modulated signal being used then control the backscatter by the tag of the interrogation frequency f_0 , and that frequency is in the low or medium frequency range.

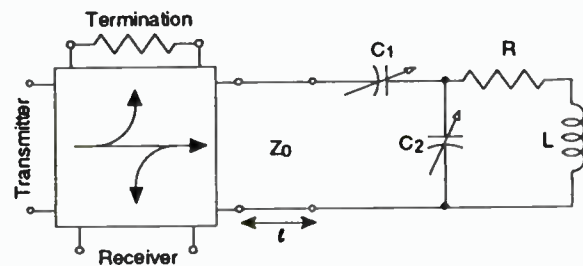


Fig. 3 Typical Low and Medium Frequency Antenna System.

Generally in such systems excitation is via a resonant loop antenna with deliberately controlled quality factor, connected to the interrogator via a transmission line, and separation between interrogation and reply signals is via a directional coupler or equivalent network. A matching network to achieve a convenient impedance is often incorporated into the tuned circuit. Fig. 3, in which L is the self inductance of the loop, R provides necessary damping, C_1 and C_2 provide combination of tuning and matching, Z_0 and l are the characteristic impedance and length of the transmission line, and the four port network at the left is a directional coupler, shows all these features.

For the analysis there is defined for the antenna circuit, firstly a "field creation quality factor" Q_f given by

$$Q_f = 2\pi \frac{\left(\text{peak magnetic energy stored in inductor } L \right)}{\left(\text{energy dissipated per cycle} \right)} \quad (4)$$

and secondly a "noise rejection quality factor" Q_n given by

$$Q_n = \frac{f_0}{2} \frac{\partial X}{\partial f_0} \quad (5)$$

where f_0 is the resonant frequency and X is the reactance of the antenna circuit, normalised with respect to the characteristic impedance of the transmission line and directional coupler.

In a system of this type, it is convenient to define the sub-carrier to carrier ratio α as

$$\alpha = \frac{f_s}{f_0} \quad (6)$$

The extent to which the transmitter signal is reflected by the load is of interest. When the load had been matched at resonance to the transmission line, a suitable approximation to the tuned circuit impedance Z is

$$Z = Z_0 \left[1 + j2Q_n \frac{(f - f_0)}{f_0} \right] \quad (7)$$

From which the reflection factor of the load in the system of characteristic impedance Z_0 is seen to be

$$\Gamma_v = jQ_n \frac{(f - f_0)}{f_0} \quad (8)$$

As the reply takes place at sidebands distant from the interrogation frequency by an amount equal to the sub-carrier frequency, the reflection factor in the reply band is approximately

$$\Gamma_v = \pm jQ_n \frac{f_s}{f_0} = \pm jQ_n \alpha \quad (9)$$

the positive sign applying to the upper sideband and the negative sign applying to the lower sideband.

5.5 Effects of transmitter noise: As transmitter powers are increased in an effort to obtain increased interrogation range, the influence of such noise in receivers becomes severe. Minimisation of the effect of that noise in the receiver is important, and is usually effected by ensuring the antenna is a good match to the transmission line, and the directional coupler is of high directivity, or more correctly that the resultant signal arising from the combination of residual mismatch from the

antenna and the imperfect directivity of the coupler is minimised by an adjustment.

Analysis of noise effects in the receiver must take into account the effects of the phase relation between local oscillator (which derives from the transmitter) and the phase relation between the transmitter signal directly reaching the receiver. The following conclusions can be drawn: (a) in each receiver channel the local oscillator phase for maximum detection of transmitter am noise is in quadrature with the local oscillator phase for maximum detection of fm noise. (b) both the shot noise effects and the local oscillator phase noise are potentially significant. (c) in homodyne systems in which the frequency responses of the transmitter leakage signal and local oscillator paths are equal there is a tendency for transmitter phase noise to be reduced from its potentially worst case value (d) the tuned load of Fig. 3 may have a low reflection of transmitter signal at the interrogation frequency but will have a significant reflection of transmitter noise at the reply sidebands, and the reflection factors will have opposite signs at the upper and lower sidebands, so that incident fm noise will be apparently reflected as am noise. (e) minimisation of the local oscillator phase noise is very important through the use of high quality low phase noise oscillators. (f) there is a practical upper limit, deriving from these phenomena, to the transmitter output power which can be employed before transmitter noise becomes the limiting factor in system performance.

5.6 Example: As an example of such noise effects, the practical example of a system operating at 13.56 MHz with a reply superimposed on a sub-carrier frequency of 200 kHz, is considered. The sub-carrier to carrier ratio is thus 0.15. If the noise rejection quality factor Q_n is 10, the reflection factor $|\Gamma_v| = Q_n \alpha$ of the transmitter antenna at the reply frequency has the value 0.15, ie. -16.5 dB. This figure represents the amount of transmitter noise which reaches the receiver.

The amount of noise in the transmitter may be estimated in various ways. The single sideband phase noise to carrier ratio in a 1 Hz bandwidth for a state of the art fixed frequency oscillator operating at this frequency has been given [17] as -165 dBc. Alternatively, a calculation based on shot noise in low level bipolar transistor amplifiers gives a value of

-155 dBc. Taking the lower noise estimate, and assuming a 10 W output for the transmitter, and assuming also a coupling factor of 10 dB in the directional coupler of Fig. 3, gives a transmitter noise level reaching the receiver of -181.5 dBW. This may be compared with a thermal noise level of -204 dBW. Clearly the system with these parameters is transmitter noise rather than receiver noise limited.

5.7 Transmitter modulation: Noise is not the only signal which originates in the transmitter and is capable of providing significant competition to the received signals from passive tags. Various modulation processes, both deliberate and accidental, at work in the transmitter can produce significant sidebands at the reply frequency of a backscatter tag. This phenomenon is particularly important when the interrogation signal has been pulse modulated, perhaps for the purpose of power saving or emc compliance. For a transmitter signal with a rectangular envelope of pulse length τ seconds, repeated every T seconds, the amplitude of transmitter sidebands at a frequency distant from the interrogation carrier by an amount equal to the reply sub-carrier frequency f_s is $1/(\pi f_s \tau)$.

5.8 Practical example: The importance of the effect can be assessed by adopting the practical system parameters $f_s = 200$ kHz, $\tau = 3$ ms, giving a sideband to carrier amplitude ratio of 5.305×10^{-4} ie. -65.5 dB. Allowing as in the case of the noise signals, for a reflection factor of -16.5 dB from the transmitter antenna and a further 10 dB in a directional coupler, and for a 10 W peak output from the transmitter, the level of signal reaching the receiver is -82 dBW. Despite the conversion of am to fm by the particular characteristics of the antenna reflection, this is an unacceptably large amplitude which must be controlled by transmitter pulse shaping to a significantly more rounded envelope.

6. CONCLUSIONS

In the area of passive rf id the factors limiting achievable range are largely electromagnetic compatibility regulations and transmitter noise. The greatest ranges are available when that part of the uhf band from 400 MHz to 1000 MHz is employed, with pulse operation, and in a

jurisdiction which provides a healthy ratio of peak to average power for the application.

At low frequencies, tag performance is frequently limited by environmental noise. At medium frequencies, where the greatest amount of circuit integration is possible, performance is limited by electromagnetic compatibility regulations, which are in a state of change and for which a case for revision in favour of rf id can be made. In almost all passive labelling systems transmitter noise plays a very significant role.

The optimisation of low frequency and medium frequency antennas with respect to electromagnetic compatibility constraints and with respect to interrogation power places conflicting requirements on antenna geometries, and compromise is needed.

As rf id tagging grows in popularity and customer demands increase, various forms of battery operated tags are expected to become increasingly popular, but limited lifetimes will have to be accepted by customers.

References

- [1] Cole P.H., Burgess A.S., and Vaughan R. "Article sorting using acoustic surface wave passive one port labels", IREE 17th International Electronics Convention Digest, pp. 277-280, Aug 1979.
- [2] Eshraghian K., Cole P.H., "A new class of passive subharmonic transponder", IEEE Proc. Vol. 130 Pt.G, pp. 45-52, Apr 1983.
- [3] Koelle A.R., Depp S.W., Freyman R., "Short range telemetry for electronic identification using modulated rf backscatter", IEEE Proc., Vol. 63, Aug 1975, pp. 1260-1261.
- [4] Razban T., Lemaitre R., Bouthinon M., Coumes A., "Passive transponder card system", Microwave Journal, pp.135-146, Oct 1987.
- [5] FCC 47 part 15, "Radio Frequency Devices", Federal Communications Commission, pp.536-583, Oct 1, 1993.

[6] BS EN 50081-1:1992, "Electromagnetic compatibility. Generic emission standard. Part 1. Residential, commercial and light industry", General Electrotechnical Standards Policy Committee to Technical Committee GEL/110, 15 Jan, 1994.

[7] BS EN 50081-2:1992, "Electromagnetic compatibility. Generic emission standard. Part 2. Industrial environment", General Electrotechnical Standards Policy Committee to Technical Committee GEL/110, 15 Jan, 1994.

[8] Cole P.H., Eshraghian K. and Roy A.K. "Efficient object identification system", US Patent 4,364,043 (1982).

[9] Ryley J.E., "Improvements in or relating to vehicle identification systems", British Patent 1,187,130 (1970).

[10] Nysen P.A., "RFID systems SAW vs CMOS", Proc. 2nd Annual WIRELESS Symposium Santa Clara, Feb, 1994, pp.412-422.

[11] Draft ETS-300 330 "Short range devices: Technical characteristic and test methods for radio equipment in the frequency range 9 kHz to 25 MHz and inductive loop systems in the frequency range 9 kHz to 30 MHz.", Aug, 1993.

[12] IEC/CISPR 16:1987, "C.I.S.P.R. specification for radio interference measuring apparatus and measurement methods", International Special Committee on Radio Interference, Sub-Committee A., 1987.

[13] Wheeler H.A., "The Radiansphere around a Small Antenna", IRE proc., vol. 47, August 1959, pp. 1325-1331.

[14] Ramo S., Whinnery J. R., and Van Duzer T., "Fields and Waves in Communication Electronics", 2nd Edition, Wiley, 1984.

[15] Eshraghian K., Cole P.H., and Roy A.K., "Electromagnetic Coupling in Subharmonic Transponders", Journal of Electrical and Electronic Engineering Australia, 2, pp. 28-35, March 1982.

[16] King R.J., "Microwave homodyne systems", IEE 1978, Peter Peregrinus Ltd.

[17] Widman D., "Generation of Low Phase Noise Microwave Signals", Hewlett-Packard RF and Microwave Measurement Symposium, Feb.-Mar. 1983.

[18] Turner L., "An Overview of Technologies for Remote Object Identification using Electromagnetic Energy", Journal of the Ngee Ann Polytechnic Institute, vol.10, pp.32-41, Oct 1993.

Field Strength Monitor Receiver For Remote Control Applications

Rainer Perthold, Albert Heuberger, Ludwig Wallrapp

Fraunhofer-Institut für Integrierte Schaltungen
Am Weichselgarten 3
D-91058 Erlangen, Germany

Abstract

A typical industrial remote control system is a narrow band FM FDMA system. A reverse channel from the controlled machine back to the operator is usually not provided.

The transmitter therefore has no feedback whether the frequency it operates on has already been occupied by another user and interference is caused. This problem can only be solved by adding a field strength monitor to the transmitter. The cost for this should be significantly lower than for a full duplex system.

This article describes the concept of such a field strength monitor which can be easily added to an existing transmitter at lower cost than a conventional superhet receiver. No changes in the transmitter itself are necessary.

The concept is based on a zero IF receiver using the transmitter as local oscillator. Modulating the transmitter (local oscillator) with a special waveform overcomes the specific disadvantages of zero IF when no IQ demodulator is available.

The paper will discuss the concept and its advantages. It will also describe a demonstration system which has been built.

Integrated SAW Oscillator in Bipolar Technology

Albert Heuberger, Eberhard Gamm

Fraunhofer-Institut für Integrierte Schaltungen
Am Weichselgarten 3
D-91058 Erlangen, Germany

Abstract

For the use in wireless control systems an integrated circuit SAW oscillator at 433 MHz has been designed. It comprises an active feedback amplifier with amplitude control and a power amplifier with symmetric output to drive a loop antenna. The output power can be modulated by an external voltage.

It should be noted, that in the off state the oscillator is still running, thus providing higher bit rates than with conventional designs. The oscillator IC is mounted together with the SAW resonator in a surface mount ceramic package. Only the loop antenna including tuning elements is necessary.

The circuit has been fabricated in 5 V UHF bipolar technology. The paper presents the concepts of the loop amplifier and the output stage. Measurement results also show the performance of the circuit.

Personal Communications

Session Chairperson: Thomas Brinkoetter,
Tektronix, Inc. (Beaverton, OR)

Unlicensed PCS market acts as springboard into emerging mobile communications field. **Henk Koopmans**, Symbionics Communications Ltd. (Cambridge, England).....**307**

Design of direct digital frequency synthesizers for wireless personal communications systems. **Sang-Gon Lee, Eun-Taek Jeong, Yong-Ro Kim, and Heung-Gyoon Ryu**, Department of Electrical Engineering, Chungbuk National University (Chungbuk, Republic of Korea).....**311**

PCS designers turn to component manufacturers with systems engineering and integration experience. **Kim Goryance**, Allen Telecom Group, Allen Telecom Systems Division (Cleveland, OH).....**318**

High-speed subcarrier data system (HSDS). **Gary Gaskill and Ken Gray**, SEIKO Telecommunication Systems, Inc. (Beaverton, OR).....**322**

Multimedia support in personal communications networks. **Kamran Ghane**, Neda Communications, Inc. (Bellevue, WA).....**341**

Unlicensed PCS Market Acts as Springboard into Emerging Mobile Communications Field

by Henk Koopmans, sales and marketing manager
Symbionics Communications Ltd.
St. John's Innovation Park
Cowley Road, Cambridge, CB4 4WS, UK

ABSTRACT

As the much ballyhooed licensed personal communications services spectrum (PCS) becomes available, the equally available unlicensed personal communications services spectrum remains largely overlooked by most in the communications industry. Licenses for PCS spectrum sells for millions of dollars and will be followed by a similarly expensive infrastructure. However, unlicensed PCS spectrum carries a relatively low price tag and will serve as a cost-effective entrance into this emerging communications field. With the right technology, those companies with unlicensed PCS products, such as wireless PBXs and handsets, will be able to migrate easily into the PCS market when it becomes widely available.

The wireless customer premises equipment (WCPE) standard is the right technology to set the pace for this emerging market. WCPE combines true mobility with standard PBX features. Because WCPE provides a micro cell environment, users can move freely about an office complex while conducting normal phone communications from an untethered device. Users benefit from wireless PBXs with a substantial increase in employee productivity and improved customer service.

Koopmans will discuss the characteristics and advantages of unlicensed PCS and its relationship to PCS. He also will explore the impact the WCPE standard will have on the unlicensed PCS spectrum.

I. UNLICENSED PCS vs. LICENSED PCS

The Federal Communications Commission has approved the release of 140 megahertz of spectrum at 2 gigahertz for the use of wireless public and private personal communications devices. This action paves the way for everyday digital communications for the masses. The spectrum allocated for these personal communications services is split into two divisions, one for licensed use and another for unlicensed use. The majority of these frequencies will be auctioned off by geographic regions to commercial operators who will offer consumers a variety of services for a fee. These kinds of services can range from voice communications and paging to fax capabilities and data communications. Of that 140 MHz, 20 MHz is set aside for private, unlicensed communications purposes for anyone willing to purchase the appropriate equipment.

A. PCS

The licensed PCS spectrum, 120 megahertz wide, is sold by the FCC to the highest bidder in public auctions. The price tags for the geographical licenses sold so far have reached into the hundreds of millions of dollars. Services offered to the public across this spectrum will rival the commonplace cellular infrastructure. Because of the hefty costs in obtaining the licenses, communications companies that implement PCS applications will recover from consumers the cost of the spectrum, equipment development and deployment. In order to offset the consumer expense and to make PCS acceptable to the mass market, its equipment must meet a high degree of interoperability and standardization, and five technologies are under consideration

for adoption in the licensed band. Although equipment based on different standards exists, interoperability at the air interface must be achieved. Despite substantial progress to converge standards, consumers remain confused about the products and services PCS can provide. Because of this confusion, manufacturers and operators are reluctant to commit to any one standard, potentially risking large investment losses.

B. Unlicensed PCS

In September 1993, the FCC allocated 20 MHz of spectrum — from 1910 to 1930 MHz — for unlicensed personal communications services. This space is divided equally for voice and data services, one 10 MHz band assigned to isochronous transmission in time division multiple access (TDMA) frame structures and one 10 MHz band assigned to asynchronous transmission for packet data protocols. The unlicensed PCS band is subject to minimal restrictions that are designed to avoid interference with other users and to ensure efficient use of the radio spectrum. Users are free to determine which applications and technology they adopt for this spectrum. Even though consumers tailor unlicensed PCS applications and technology to individual needs, interoperability still is desirable for the unlicensed band, and a number of standards are in development. Despite its higher cost, digital technologies may be used in the residential marketplace through offering features such as security and conference calling. However, digital systems will find their first uses in business and industry. Wireless PBXs are the most immediate applications for digital technology.

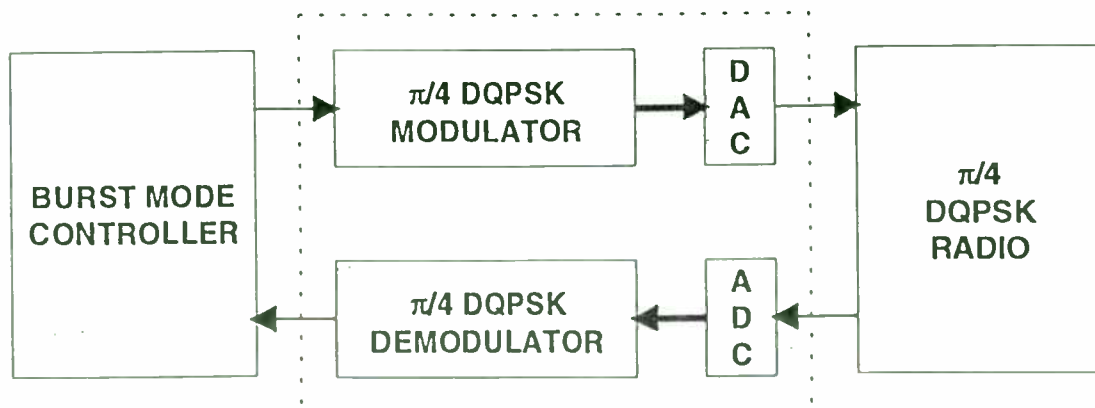
II. THE WCPE STANDARD

Developed by the Telecommunications Industry Association and supported by telecommunications powerhouses, the wireless customer premise equipment (WCPE) standard is emerging as the front runner for the first unlicensed PCS applications. The WCPE standard is derived from the Digital European Cordless Telecommunications standard, already incorporated in wireless equipment for the European market. WCPE technology is suitable for unlicensed PCS applications because its enabling features are designed for the wireless PBX environment. Those features include capabilities for seamless signal hand over, mobility management and a high handset to base station ratio. The capability of WCPE systems to hand over a link seamlessly from one call to the next allowing users to roam throughout an office without dropping calls. The identity structures and associated procedures mean that WCPE technology comes equipped with the mobility management facilities required in a micro cellular environment. WCPE is a time division multiple access/time division duplex system; therefore, the system can handle a 12-1 handset-to-base station ratio. The handset-to-base station ratio is an important feature because of the heavy call load a wireless PBX must handle in an office environment. WCPE also provides larger cells through class II features for campus systems. A modular design

approach to radio, baseband and software means manufacturers can adapt the technology to their specific needs, yet maintain interoperability among different applications. Micro cellular features designed for wireless voice and data systems allow large networks of contiguous coverage to be built in unlicensed PCS office systems. Wireless capability can be added to existing PBX systems to offer mobility to office staff. The technology components already available include the $\pi/4$ differential quadrature phase shift keying radio (QPSK), the differential QPSK modem and the WCPE-customer premises access profile software.

A. The $\pi/4$ differential QPSK radio

The $\pi/4$ differential QPSK radio is the basis for PCS handset radios operating in the unlicensed and licensed 1.9 GHz PCS bands. By employing this pre-characterized radio module, equipment manufacturers can gain a head start in product development, creating faster entry into the market. The radio architecture offers a high performance radio for a comparatively low cost. Though optimized for WCPE operation, the core of the radio design contains the necessary features for other standards employing $\pi/4$ differential QPSK such as the personal handy phone system and the personal activity center.



B. The $\pi/4$ differential QPSK modem

The $\pi/4$ differential QPSK modem provides the link between bit-serial baseband data and analog internal protocol. The $\pi/4$ differential QPSK modem can be integrated with any digital burst mode controller design or implemented as a stand-alone integrated circuit or application specific integrated circuit. The $\pi/4$ differential QPSK modem blocks can be combined with commercially available DECT burst mode controller and a suitable radio design to complete a unlicensed PCS product that complies with Part 15 with FCC regulations. The modem operates over a wide range of clock frequencies and bit rates. With voltage ranges of 2.7 to 5.5 V,

the modem blocks can be targeted to any suitable integrated circuit technology.

C. Wireless customer premise equipment/ customer premises access profile

To enhance interoperability, the customer premises access profile (CPAP) software for both handsets and base stations incorporate all the required protocol features to support speech operation at home, at the office or on the street. The CPAP protocol, which defines the procedures required to make voice calls, ensures interoperability in all voice equipment. For manufacturers and users, the CPAP protocol means a single handset will function in all environments.

III. THE LONG RUN

Even in the long run, licensed PCS will be expensive until the infrastructure is in place and communications across that spectrum become as routine and widespread as those across today's ordinary cellular networks. Until use of the PCS spectrum is affordable enough for the masses, manufacturers and users, seeking quick entrance into this market should consider communications products for the unlicensed PCS spectrum.

Pre-designed modules or building blocks based on the existing WCPE standard will give manufacturers and users quick, inexpensive access to the unlicensed PCS spectrum. Manufacturers and consumers can secure their investments for the long run and even accelerate access to the licensed PCS spectrum with dual mode communications products that are capable of functioning in both licensed and unlicensed PCS bands.

Design of Direct Digital Frequency Synthesizers for Wireless Personal Communications Systems

Sang-Gon Lee*, Eun-Taek Jeong*, Yong-Ro Kim*, Heung-Gyoon Ryu*

*Department of Electronic Engineering, Graduate School,
Chungbuk National University, CheongJu, ChungBuk, Korea*

Abstract

In this paper, the phase accumulator that limits the maximum synthesized frequency of DDFS (direct digital frequency synthesizer) is improved with a pipeline adder and dynamic D-F/F.

Using the proposed two methods of coarse/fine ROM and sine amplitude-difference algorithm, the data compression ratio is approximately 6.4:1 (2048 bits to 320 bits), where the address and data are set to 8 bits.

The operating frequency of the dynamic D-F/F is about 1.25GHz, and 1-bit full adder run at 925MHz. The maximum operating frequency of phase accumulator in DDFS is estimated to be 526.6MHz in the consideration of the propagation delay times of D-F/F and 1-bit full adder.

I. Introduction

Direct frequency synthesizer produces various frequencies applicable to such digital communication systems CDMA digital cellular telephone, spread spectrum equipment and wireless LAN. Resolution, bandwidth, and frequency switching speed of the synthesizer are especially important in modern mobile communication. The phase information of the synthesizer used in those systems is needed for the precise calculation converting to amplitude of sine function.

In this paper, the DDFS is designed using the pipeline method, coarse/fine ROM, and sine amplitude-difference algorithm. Adopting pipeline algorithm, time delay of a phase accumulator is the same as that of a 1 bit full adder, regardless of the number of accumulator bits.

The ROM data compression ratio by coarse/fine and sine amplitude-phase difference algorithm is compared with that of conventional ROM. The speed of the phase accumulator is estimated by simulating adder and the dynamic D-F/F.

II. Pipeline phase accumulator

A conventional structure of a phase accumulator is not fit for getting UHF frequencies. An addition of one digit can be performed only after the carry of the previous digit occurs. In the case of the N-bit adder of which delay time is t_d , the total delay time of the adder is $N \times t_d$. The problem can be solved by rearranging delivery path of each carry.

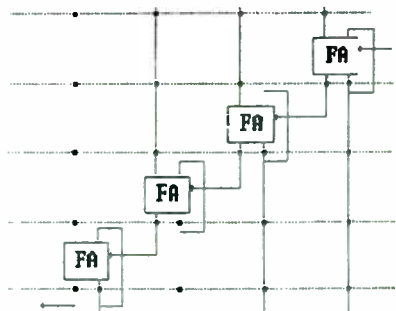


Fig. 1 Pipeline phase accumulator

In non-pipeline phase accumulator, a high speed phase accumulator as a carry-lookahead method, requires so many logic

gates and long critical path. Consequently, total delay time of carry-lookahead method is more than that of 1-bit full adder.

In case that delay time of a pipelined N-bit adder is t_d , the total delay time is just t_d . Because, irrelevant to the number of bits, the pipelined phase accumulator has just a delay time (t_d), the phase accumulator can run faster N times than conventional phase accumulator.

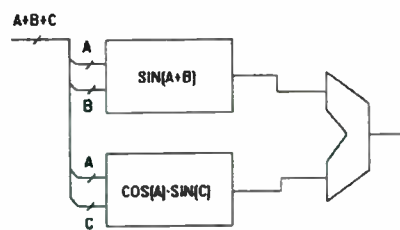


Fig. 2 Coarse/Fine ROM block diagram

III. ROM data compressions

The data number of sine function can be reduced by coarse ROM and fine ROM. The assignment of look-up table samples in this architecture is based upon several trigonometric approximations. First, the bits representing the phase argument, θ , of one quarter period of the sine function are decomposed into the sum of three functions;

$a < \frac{\pi}{2}$, $b < \frac{\pi}{2}(2^{-A})$, and $c < \frac{\pi}{2}(2^{-(A+B)})$ such that $\theta = a+b+c$.

$$\sin(A+B+C) \cong \sin(A+B)\cos C + \cos A \cos B \sin C - \sin A \sin B \sin C \quad (1)$$

$$\sin(A+B+C) \cong \sin(A+B) + \cos A \sin C \quad (2)$$

Using trigonometric identity, eq. (1), and its approximation, eq. (2), the function is given by

$$\sin(A+B+C) \cong \sin(A+B) + \cos A \sin C.$$

For example, lower 9-bit of phase accumulator except higher 2 bits are assigned to A, B, and C each 3 bits respectively. When data are 10 bits, equation (1) requires 5120 ($=10 \times 2^{3+3+3} = 10 \times 2^9$) bits. On the other hand, equation (2) needs just 960 ($=10 \times 2^{3+3} + 5 \times 2^{3+3} = 10 \times 64 + 5 \times 64$) bits. Therefore, ROM area of equation (2) is less 5.1 times than that of equation (1).

A quarter period of a sine function can be represented by $f(\theta) = \sin(\theta) - 2\theta/\pi$ to improve the compression ratio. The maximum value of $[\sin(\theta) - 2\theta/\pi]$ is less quarter than that of a sine function. Using this method, 2 bits of ROM address is able to be saved. $f(\theta)$ is shown by Fig. 3.

IV. D-F/F design

In conventional CMOS circuit both static and dynamic CMOS logic is used. For the purpose of system timing a clocking strategy is always involved except for a self-timed system. The most popular clocking strategy is clocked CMOS logic (C²MOS), which uses a nonoverlapping pseudo two phase clock. Clock skew in the system will cause serious problems and result in difficulties in increasing circuit speed. New clocking method, known as TSPC[5], which fits not only dynamic but also static CMOS circuits and in most cases can replace the NORA CMOS technique, doesn't require more than one clock phase.

This flipflop has a hazardous discharge when its output should remain stable.

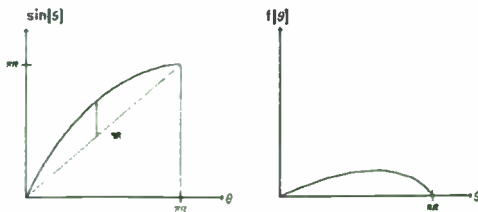


Fig. 3 amplitude-phase difference algorithm

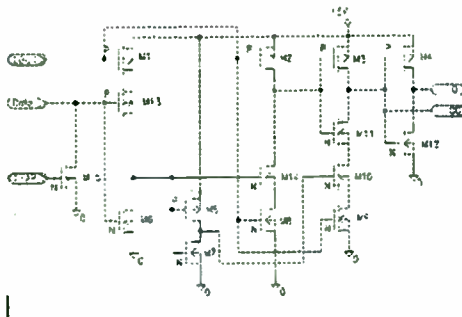


Fig. 4 final version of dynamic D-F/F with CLEAR

The structure[6], which is inserted another transistor, prevents the output QB from discharging when it should be remain stable. However, this circuit which has unnecessary transistors is modified as above figure. Also CLEAR of D-F/F is added.

V. DDFS implementation and logic simulation

Frequency controller consists of 16-bit D-Flip/Flop and phase accumulator is composed of pipeline adder which uses 272 D-F/Fs. Total 16 bits of pipeline phase accumulator consist of 8-bit address of sine ROM, 2 bits of phase control, and the other bits are not used.

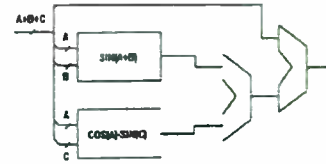


Fig. 5 Sine ROM block diagram with coarse/fine and amplitude-phase difference algorithm

In a 12-bit address of phase accumulator, 2 bits are used for phase control, 8 bits for address of coarse/fine ROM, and the other bits are truncated. When an address consists of $a=2$, $b=3$, $c=3$, respectively, and 8 data bits, it is possible to design fine ROM with 5 bits. Two generation equation of coarse/fine ROM data is given by

$$F_c(a, b) = \sin\left(\frac{\pi}{2} \times \frac{a \times 2^{B+b}}{2^{(A+B)}}\right) \quad (3)$$

$$F_f(a, c) = \sin\left(\frac{\pi}{2} \times \frac{a \times 2^{(B-C)} - b \times 2^c + c}{2^{(A+B+C)}}\right) - F_c(a, b) \quad (4)$$

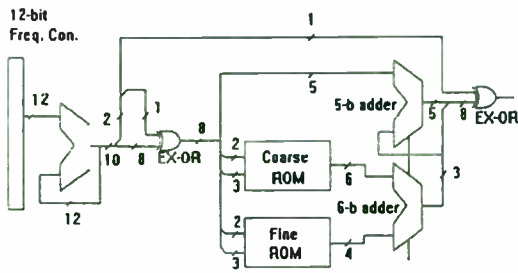


Fig. 6 Overall direct frequency synthesizer block diagram

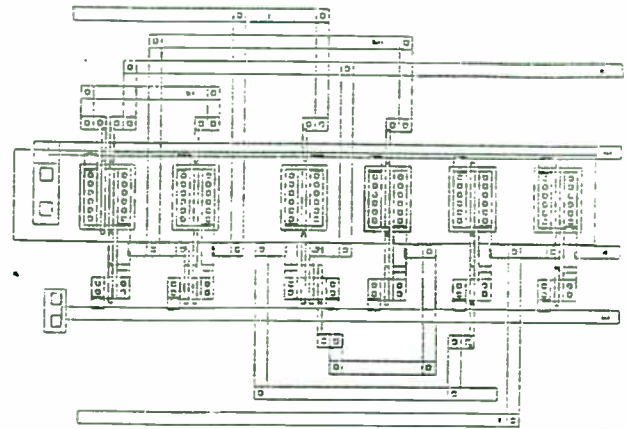


Fig. 7 Layout of D-F/F

Table 1. Table of D-F/F simulation results

Symbol	Parameter	Time
CLOCK	Period of clock	0.8ns
t _{HL} or t _{LH}	Rise Time Or Fall Time	0.1ns
t _{PLH1}	Propagation Delay time	0.305ns
t _{PLH2}	Propagation Delay time	0.549ns
t _{SETUP}	Setup Time	0.3ns
f _{TOG}	Toggle Frequency	1.25GHz
P _d	Total Power Dissipation	0.687mW

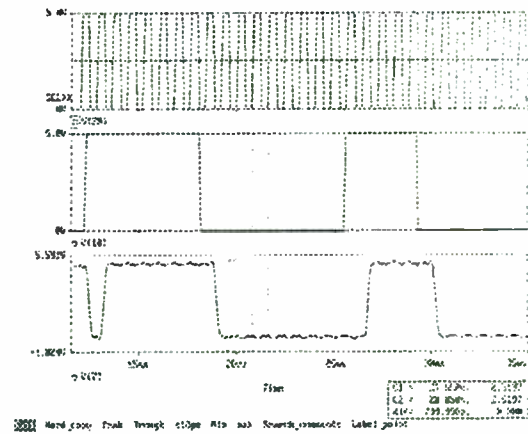


Fig. 8 Simulation results of D-F/F

Fig. 8 shows the simulation results. Simulation conditions are $0.8\mu\text{m}$ of gate length of MOSFET, $V_{cc} = 5\text{v}$, the rising time and falling time of input stage of 0.1ns respectively, and clock 0.1ns.

For SPICE simulation, the rising and falling time in the clock part, is 0.1ns respectively, the period 0.8ns, the duty cycle 50 %, and the rising and falling time of input data which has nonperiodic property 0.1ns respectively.

Table 2. Table of 1-bit full adder simulation results

Symbol	Parameter	Time
t_{HL} OR t_{LH}	Rise Time Or Fall Time	0.1ns
t_{DMAX}	Maximum Propagation Delay	1.05ns
f_{DN}	Input Data Frequency	952MHz
P_d	Total Power Dissipation	$3.5 \times 10^{-10}W$

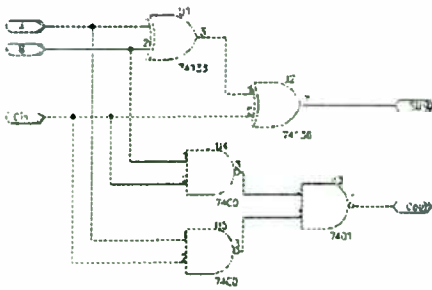


Fig. 9 Circuit of 1-bit full adder

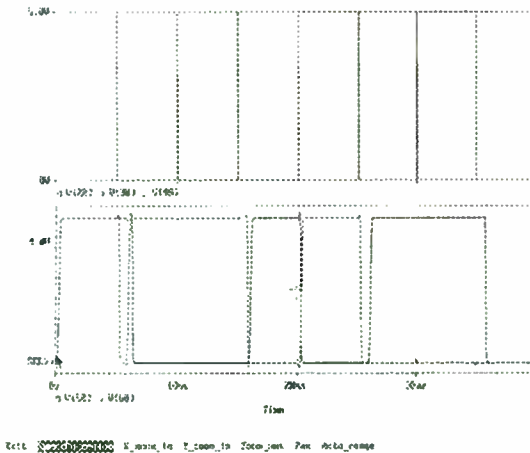


Fig. 10 simulation results of 1-bit full adder

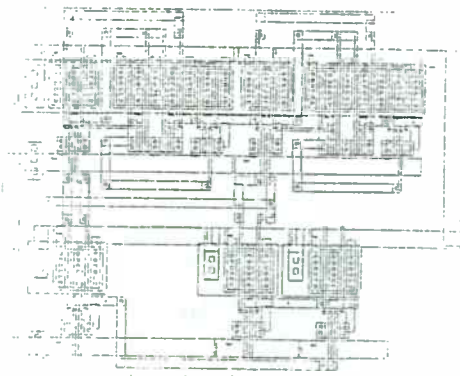


Fig. 11 Layout of 1-bit full adder

On the table 2, in the case of $L=0.8\mu m$ of gate length of MOSFET, $V_{cc}=5V$, simulation results show the maximum operating frequency of 952MHz and power consumption of 3.5×10^{10} . In the simulation waveform, the outputs of adder indicate long delay time which may be caused by parasitic capacitance.

On the above condition, the simulation results show that the maximum propagation delay time of a pipeline phase accumulator having the maximum delay time 0.849ns of D-F/F and 1.05ns of 1-bit full adder is 1.899ns. In other words, the maximum operating frequency of it is 526.6MHz

V. Conclusions

In this paper, the DDFS is designed using the pipeline method, coarse/fine ROM, and sine amplitude-difference algorithm. Adopting pipeline algorithm, the time delay of a phase accumulator is the

same as that of a 1 bit full adder, regardless of the number of accumulator bits. If address and data bits are set to 8-bits with existing ROM table, the used bits are 2048, but using the data compression algorithm the used bits are reduced to 320 bits.

It shows that the data compression ratio of novelly presented frequency synthesizer is roughly 1:6.4 in contrast with existing products. We also design the phase accumulator deciding the maximum frequency of the digital frequency synthesizer, and simulate it. As design tools, after drawing up the GEX layout, we extract SPICE files and make simulations.

The operating frequency of D-F/F is accurately 1.25GHz, and that of 1-bit full adder 925MHz.

The maximum operating frequency of phase accumulator in DDFS is estimated to be 526.6MHz in the consideration of the propagation delay times of D-F/F and 1-bit full adder.

Henceforth, when designing layouts, it will be considered parasitic capacitance to minimize the maximum delay time, and the design process having the phase accumulator of n-bit pipeline accumulator and ROM table.

- REFERENCE -

- [1] Henry T. Nicholas III, "The optimization of direct digital frequency synthesizer performance in the presence of finite word length effects," in *Proc. 42nd Annual Frequency Control Symp. USERCOM*, pp. 357-363, May, 1988.
- [2] J. Tierney, "A digital Frequency Synthesizer," *IEEE Trans. Audio Electroacoust.*, vol. AU-19, pp. 48-57, March. 1971.
- [3] Fang Lu, "A 700-MHz 24-b pipelined accumulator in 1.2 μ m CMOS for application as a numerically controlled oscillator," *IEEE Journal of Solid-State Circuits*, vol. 28, No. 8, pp. 878-886, August. 1993.
- [4] P.O'leary, F.Maloderti, "A Direct Digital Synthesizer with Improved spectral performance," *IEEE Comm.*, vol. 39, No. 7, July, 1991.
- [5] Jieren Yuan et al, "High-speed CMOS Circuit Technique", *IEEE Journal of Solid-State Cir.*, Vol. 24, No. 1, pp.62-70, February, 1989.
- [6] R. Rogenmoser et al, "1.57MHz Asynchronous and 1.4GHz Dual-Modulus 1.2 μ m CMOS Prescaler," *IEEE CICC*, pp.387-390, 1994.

PCS Designers Turn to Component Manufacturers with Systems Engineering and Integration Experience

Kim Goryance, director of marketing
Allen Telecom Group
30500 Bruce Industrial Parkway
Cleveland, Ohio 44139

ABSTRACT

Personal communications services (PCS) is an emerging technology market that wireless communications providers are pursuing feverishly. As the networks develop, systems engineers and designers will be looking for assistance in infrastructure configuration in addition to components that can carry the new service to fruition.

Because of the nature of PCS technology — a concentrated layout of low-power base stations with more precise radio frequency patterns — systems engineers have a smaller

margin of error than allowable in cellular transmission technology. Configuration plans must be more strategic than ever before. Radio frequency (RF) patterns must be more pervasive. Network coverage must be ubiquitous.

To achieve this high level of technical sophistication successfully, systems engineers charged with designing and implementing PCS networks should seek out components manufacturers who can do more than make sales, hand out boxes and cash checks.

I. PCS ADDS SPECIFIC REQUIREMENTS

As personal communications services (PCS) becomes a widespread technology, the nature and function of cell sites will undergo significant changes in the near future. Coverage areas are shrinking in order to provide more precise, higher quality service. Service is expanding beyond traditional metropolitan areas and along major thoroughfares into specialized locations such as amusement parks and convention centers where site components must be invisible to the casual observer.

PCS will become ingrained into our society. As the service rolls out, more people will rely on the link it provides, and subscribers will assume and demand ubiquitous coverage. To meet these elevated demands, carriers and equipment manufacturers must develop hardware and components that are better, faster, lighter, smaller and more aesthetically pleasing.

More stringent zoning regulations nationwide are limiting options in deploying cell sites or installing repeaters and microcells to expand coverage. However, these regulations don't affect structures already in place.

Because advancements in technology have made components smaller and more efficient, zoning restrictions can be circumvented by using existing structures such as billboards, building roof tops, lamp posts and telephone poles as equipment installation sites.

Building new cell sites can involve a lengthy approval process by the Federal Communications Commission, Federal Aviation Administration and municipal zoning committees. Employing an existing structure rather than building a new site can eliminate bureaucratic delays and expedite PCS availability.

II. SHIFTING REQUIREMENTS

As population centers shift and grow, and users become micro-mobile – phones moving out of automobiles and into brief cases and pockets – the need for farther ranging services becomes paramount to the wireless industry. If radio frequency (RF) coverage cannot be provided in areas traditionally posing barriers to cellular service (e.g., tunnels, convention centers, sports arenas, amusement parks, suburban and rural areas) the service provider will be at a competitive disadvantage when implementing PCS.

With the cellular infrastructure established, carriers have turned their attention to fine-tuning the networks to provide high-quality PCS coverage when and where users want it. The question is not whether to expand and enhance service coverage, but rather where to expand and how to enhance the coverage in the most cost-effective manner? In some cases a new cell site is the proper answer, but building before all the research and development (R&D) is complete could mean moving in the wrong direction. Building too late can put the carrier behind the competitive curve.

When the time comes to consider expanding for PCS, whether out to the suburbs and beyond or into an airport concourse, the service provider faces a number of questions. Will an additional cell site be compatible with the area's topography and its relation to any existing service systems? From a coverage and financial standpoint, is there an alternative to a

cell site? How will the components – if they are of multivendor origin – of the other cell sites in the service system interface with the new components?

Specific coverage environments require specific answers. Establishing coverage in a downtown metropolitan area is a different challenge from a rural service area (RSA). For example, diverse coverage areas require specialized types of base station antennas.

A small panel sector antenna covered with a radome may best suit the zoning restrictions and concentration of subscribers in Beverly Hills, Calif. An adjustable downtilt antenna could be the best fit for Rapid City, S.D., located at the foot of the Black Hills.

An antenna with a high front-to-back ratio would be necessary for a cell site located in a relatively flat geographical area and covering the expanse between two metropolitan areas such as along Interstate-30 in Dallas-Fort Worth. A high front-to-back ratio also is necessary to avoid co-channel interference with another cell site located toward the rear of the antenna.

Deciding on which RF pattern and base station antenna will provide the best coverage radiation for an application can be made more carefully when working with an experienced manufacturer. Regardless of the type of PCS implementation being undertaken, integrators can gain a great measure of confidence by working with a vendor that offers a complete range of products and technical support.

III. WORKING WITH AN EXPERT

PCS quality can be described as call clarity within the coverage area and subscriber satisfaction. By working in partnership with a vendor possessing years of experience designing system components and a successful history of systems engineering, integration and lay out consulting, a service provider can focus on fine-tuning its system to serve its customers better. Additionally, manufacturing components for every facet of successful site operation give the systems engineers a thorough working knowledge of each component and how it will interact with the other equipment in the system.

suburban and rural areas or filling coverage holes in airports and subway tunnels – partnering with a manufacturer capable of supplying more than cell site components can prove to be cost-effective. PCS applications can be economically implemented by a strategically configured series of low-power broadband boosters or high-power narrow-band repeaters performing in conjunction with existing cell sites.

Simply stated, a booster or repeater is a dual-path RF amplifier. It receives signals from an existing donor cell site and amplifies them. Then, depending on coverage needs, the booster or repeater transmits the amplified signals into the area designated for PCS. Simultaneously, it receives the signals from subscribers in the enhanced coverage areas, amplifies those signals as well, and transmits them back the donor cell site.

Microcells are best deployed in applications where the RF signals of traditional sites are impeded such as inside office buildings and transit tunnels. The microcell system receives RF signals from the cell site via

The prevailing opinion among cellular systems engineers is they would rather deal directly with manufacturers because the company that makes the product will have an inherent in-depth knowledge of the components it markets. Everyone from the technical sales staff through the systems support engineers is generally well versed in the capabilities and capacities of the product line. Supporting technical manuals and installation documents also will be more readily available through the manufacturer than a distributor.

When a carrier needs to provide coverage to areas previously mentioned – an exterior antenna and blankets the interior of the structure with a boosted signal.

Microcells offer the additional benefit of concentrating radio frequencies into smaller areas, which allows the system to reuse channels within shorter distances than the channel reuse plans of traditional cell sites. Typically, each cell site carries between 60 and 90 channels. This translates into a capacity of 60 to 90 calls per cell at any given moment. Microcell systems, in addition to providing coverage where conventional cell site signals alone can't reach, significantly increase the system's capacity. By reducing the geographical coverage of all cells within the system and deploying microcells, channels can be reused more often for PCS. Depending on the system's design and its frequency reuse plan, a significant increase in the system's total capacity can be achieved.

By working with a manufacturer experienced in system lay out and integration, the service provider is assured of the most efficient, cost-effective means of providing the complete PCS coverage subscribers demand.

IV. KEEP THE CUSTOMER SATISFIED

This challenge to keeping satisfied subscribers can be met by installing a call traffic manager (CTM) in overlapping coverage areas. A CTM combines the functions of a cell site and repeater, and adds call monitoring to create a three-way service enhancement in these areas. By generating its own control signal, the CTM strengthens the home carrier's service signal and keeps users in the service system to which they subscribe.

Quality, service, support and stability should be the main attributes a carrier looks for in a components manufacturer. The hardware necessary in building PCS to enhance service coverage is basically the same with advanced technological quality being the separating factor between the components.

To gain a competitive edge, service

providers have relatively few options. One option readily available and perhaps most beneficial is to establish a long-term working relationship with a manufacturer capable of providing virtually every component required in bringing quality PCS to subscribers. The benefits are compounded when that same manufacturer can provide systems engineering expertise to assist in service layout to ensure technically advanced PCS coverage in the most cost-effective manner possible.

Beyond supplying components, a manufacturer is most beneficial when it supplies service coverage answers with no third- and fourth-party involvement to increase any potential margin of error. Bringing the highest quality service to the subscriber will further the benefits derived by service providers.

V. THE ROLLOUT OF PCS

The advent of PCS will raise the service expectations of subscribers and push the capabilities of service providers. With PCS on the horizon, carriers are looking for methods of providing more concentrated service in smaller, more precise patterns. Because PCS will encompass areas where there are large numbers of users close to the equipment, the components must be unobtrusive to the point of being invisible to the casual pedestrian.

Advancing technology has and will continue to produce the more sophisticated components necessary to successful PCS capabilities. By nature of the system's design, components will have to be more efficient to provide the type of ubiquitous coverage PCS applications will demand. Cell sites and the associated components must evolve not only to

deliver more demanding service, but in a smaller and more innocuous way.

Utilizing existing structures such as billboards and roof tops for antennas and microcells will play an integral role in deploying PCS. Common cell sites among carriers also provide an alternative to municipal zoning boards' reluctance to permit a mushroom effect of sites.

As providers push the coverage boundaries to bring PCS to their subscribers, the search is on for every competitive advantage they can attain. Partnering with a complete connection vendor can tip the scales of competition.

PCS is turning heads. By developing superior systems, carriers can ensure that customers don't turn their backs.

HIGH SPEED SUBCARRIER DATA SYSTEM (HSDS)

Gary Gaskill and Ken Gray
SEIKO Telecommunication Systems Inc.
Beaverton, Oregon USA

Abstract

This paper summarizes some of the key features of a High Speed FM Subcarrier Data System (HSDS); with emphasis on the subcarrier data channel. The modulation and demodulation techniques used by HSDS are described. HSDS receiver sensitivity and its relationship to coverage are discussed, along with compatibility of the subcarrier with the main channel audio and RDS. The packet and frame structures and multi-station methods are defined and the reliability techniques are explained. In addition, general specifications the modulator and available receiver and demodulator integrated circuits are described. Results from lab and field tests are provided including error correcting effectiveness. Results of the Portland, Oregon coverage tests are shown. Finally, the services currently provided in the Northwest USA are described.

INTRODUCTION

Wireless personal communication is becoming an increasingly important aspect of the communications industry. One facet of this rapidly evolving technology is the development of one-way systems providing messaging and information services including: personal messaging, traffic information, time of day, news, sports, weather, business and emergency information.

SEIKO Telecommunication Systems Inc. (STS) has developed such a system. It is a flexible High Speed FM Broadcasting Subcarrier Data System (known as HSDS) with capability for world wide operation. HSDS is fully developed and has been deployed by STS under the RECEPTOR trademark in a number of cities around the world. Its commercial introduction was in Portland, Oregon in July of 1990. Seattle - Tacoma, Washington began commercial operation in October of 1992. Currently marketed applications include paging and information services to numeric display wrist-watch

receivers (SEIKO® Receptor™ MessageWatches™) and pocket pagers.

Two highly integrated circuits -- a receiver and demodulator, operating with 3 volt lithium cells, are available for small, inexpensive low power designs. These ICs are the basis for the wrist-watch receiver. Queuer/encoders and modulators are also available for the system. Utilization of existing FM radio broadcast infrastructure, currently available integrated circuits and transmission equipment make this system very inexpensive to deploy.

SUMMARY OF HSDS SYSTEM

The HSDS protocol is a very flexible, one-way, communications protocol. The system design permits very small receivers. Receivers, with duty cycles varying from continuously on to duty cycles of less than 0.01%, provide flexibility to select message delay, data throughput and battery life. HSDS can operate as a stand alone single station (channel) system, or as multiple systems operating independently in a geographical area with each system including multiple stations. Multiple stations are accommodated by frequency agile receivers, time offset message transmission on each station, and transmitted lists of stations surrounding each station. Reliability can be enhanced via multiple transmissions of messages. Duplicate messages are rejected via comparison with the transmitted message number.

The system is time division multiplexed. Time is subdivided into a system of master frames, subframes and time slots. Each slot contains a packet of information. In multiple station systems, each station's transmissions are synchronized to UTC ensuring synchronization between stations. Each receiver is assigned a subset of slots as times for monitoring transmissions. Multiple receivers may share time slots, due to the random nature of expected communications. Each slot is numbered and

each packet contains the slot number that permits rapid location of assigned time slots.

The error correction scheme is very flexible. The methods used vary with the applications. The method used in the watches is designed to correct a short burst of errors associated with random noise or automotive ignition noise. The standard CCITT 16 bit CRC is typically added as a component of each packet and minimizes the chance of false messages.

HSDS modulation and encoding provide a high data rate, a narrow bandwidth with high spectral efficiency and negligible impact on the main channel. HSDS modulation is AM-PSK with duobinary encoding. The HSDS data rate is 19,000 bits per second in a bandwidth of 19kHz, centered at 66.5kHz. The HSDS signal is modulated as a subcarrier ranging from 5% to 20% injection but typically at 10% on a commercial FM radio station's carriers in the frequency range of 87.5 to 108Mhz. Sharp transmission filter skirts cause extremely little impact on the main channel in no multipath situations; and generation of a pseudo-randomized data stream reduces impact on the audio even in multipath situations. The narrow bandwidth of HSDS allows for compatibility with RDS operation world wide. HSDS allows for use of subcarriers above 76kHz in the USA and compatibility with European spectrum allocation.

PHYSICAL LAYER

This section describes the characteristics of the subcarrier data channel for the HSDS messaging system. Included in this discussion are the modulation and demodulation techniques used to achieve communications through the subcarrier channel at an acceptable bit-error-rate (BER), and the performance of the subcarrier channel in the FM broadcast channel. The ultimate performance or reliability of the HSDS messaging system is determined not only by the physical layer but also by the characteristics of the messaging protocol described in later sections. Additional considerations of the physical layer included in this section are the issues of subcarrier interference with the main channel audio, and the compatibility of the HSDS subcarrier signal with an RDS signal.

Modulation and Demodulation

The HSDS modulation / demodulation scheme was chosen to satisfy the following criteria:

- Non interference with commercial FM radio receivers.
- Compatibility with world wide broadcast FM regulations.
- Simplicity in IC implementation of the demodulator.
- Low-cost mobile receiver with a small form factor.
- Adequate BER performance in the presence of noise.
- Commercially satisfactory coverage area.
- High data rate.

Modulation

The HSDS subcarrier channel is centered at 66.5kHz. The choice of 66.5kHz as a subcarrier frequency is compatible with international (CCIR) standards of 53 to 75kHz and the US standard of 53 to 99kHz. The 66.5kHz center frequency was also chosen because it is 3.5 times the 19 kHz pilot which allows phase locking to the pilot. Additional advantages include: reduced receiver parabolic noise in relation to higher frequency subcarriers and better audio performance than other subcarrier frequencies because 67kHz subcarriers have been common for many years and receivers typically have 67kHz reject filters.

For ease of receiver implementation the subcarrier frequency and transmitted data are phase-locked to the main channel 19kHz stereo pilot. The subcarrier data to pilot phase relationship is approximately 63 degrees. The raw data rate of the system is 19kbps. The 66.5kHz subcarrier is a double-sideband suppressed-carrier amplitude modulated signal using the duobinary technique described by Lender (1963). The duobinary technique uses controlled intersymbol interference to achieve 1bits/sec/Hz efficiency with realizable filters while 2-level DSB PAM system cannot achieve this efficiency. The duobinary encoding technique achieves this result by using a filter to create intersymbol interference that combines the current and previous data bit, creating a three level output signal in the demodulator. Normally intersymbol interference degrades the performance of a demodulator; but for duobinary, the use of a cosine filter allows the receiver to decode the current bit in the presence of the intersymbol interference using a simple symbol by symbol decoding scheme. In addition to the improved spectral efficiency obtained by the duobinary modulation technique, the cosine filter required for optimum performance is simple to implement.

The transfer function $H(\omega)$ of the duobinary filter is given by

$$H(\omega) = \cos(\omega T / 2), \quad |\omega| \leq \pi / T$$

= 0, elsewhere, where T is the symbol period = 1/19kHz.

In the usual situation where the channel symbol power is limited, the optimum filtering required to maximize the signal-noise ratio at the receiver would involve equally splitting the filtering between the transmitter and the receiver as $\sqrt{H(\omega)}$. However, the FM subcarrier situation is different in that the limiting factor for the channel is not symbol power but the frequency deviation of the carrier caused by the modulation. This frequency deviation constraint implies a voltage-limiting constraint for this modulation rather than a power-limiting constraint. As a result the usual matched-filter theorem for maximizing signal-noise ratio does not apply. An improved filtering split between transmitter and receiver when a voltage constraint is applied has been found through simulation to be:

$$3/4 \sqrt{H(\omega)} \quad \text{at the transmitter, and}$$

$$1/4 \sqrt{H(\omega)} \quad \text{at the receiver}$$

Demodulation

Synchronous demodulation with sub-Nyquist sampling is achieved by phase locking the sampling clock to the 19kHz pilot. The receiver filter is implemented as an FIR with symmetrical coefficients. The time domain waveform of the modulated subcarrier is shown in Figure 1.

HSDS Subcarrier Receiver Performance

It is of particular interest to determine the signal-to-noise ratio in the subcarrier channel SNR_{sc} , since this determines BER performance for a given modulation technique. For an FM receiver system in the absence of multipath effects, SNR_{sc} depends primarily on the following parameters:

- Carrier power C in dBm in the main FM channel receiver IF.
- Percentage of power available to the subcarrier, typically specified as an injection percentage.
- Effective subcarrier channel bandwidth B_{sc} in Hz.
- Receiver noise figure NF_{rcvr} .

The relationship that contains all the above factors then becomes a key system design equation for coverage

tradeoff studies. Assuming narrowband FM and an ideal FM demodulator, the general relationship for the SNR in any subcarrier channel is given by:

$$SNR_{sc} = C * \beta^2 / (F_{rcvr} k T B_{sc}),$$

where

β = ratio of peak frequency deviation of the subcarrier to the subcarrier modulating frequency

$k = 1.38 * 10^{-23}$ Joules/K Boltzmann's constant,

$T = 290^\circ$ K Thermal noise temperature.

Expressed in logarithmic units the result becomes:

$$SNR_{sc} = C + 20 * \text{Log}(\beta) - 10 * \text{Log}(kT) - 10 * \text{Log}(B_{sc}) - 10 * \text{Log}(F_{rcvr})$$

As an example of the use of the above formula we will consider the HSDS case:

$$kT = -174 \text{ dBm/Hz}$$

$$NF_{rcvr} = 5 \text{ dB (worst case for current receiver IC)}$$

$$B_{sc} = 25 \text{ kHz (} 10 \text{Log}(B_{sc}) = 44 \text{ dB)}$$

$$SNR_{sc} = 12 \text{ dB,}$$

$$20 \text{Log}(\beta) = -19 \text{ dB (10\% injection),}$$

where an SNR_{sc} of 12dB is assumed to be the minimum required for an acceptable BER performance, and B_{sc} , the noise bandwidth at RF is twice the effective receive filter bandwidth at baseband.

Under the above conditions with a subcarrier injection of 10%, the weakest signal at the receiver input that can be demodulated to give an adequate BER performance can be calculated as receiver sensitivity:

$$\begin{aligned} C_{min} &= SNR_{sc} - 20 * \text{Log}(\beta) + 10 * \text{Log}(kT) \\ &\quad + 10 * \text{Log}(B_{sc}) + NF_{rcvr} \\ &= 12 + 19 - 174 + 44 + 5 \\ &= -94 \text{ dBm} \end{aligned}$$

The above result can now be used to consider coverage. To this end a relationship is needed connecting receiver sensitivity with an electromagnetic field strength value. This is obtained using the standard free-space half-wave

dipole equation relating field strength E (volts/m) to power P_{dipole} (watts) developed at the dipole terminals.

$$P_{\text{dipole}} = (E^2 / 120\pi) * (\lambda^2 / 4\pi) * 1.64$$

λ = wavelength of the radiation and is assumed = 3 meters (f = 100Mhz) for illustration purposes.

For a given antenna gain, relative to a dipole, the receiver sensitivity computed above can be related to the required field strength E. Two cases are considered:

1. An automobile whip antenna with a gain of 0 dBd with an appropriate receiver results in a field strength requirement of 23.5 dBuV/m.
2. A wrist sized loop antenna with a gain of -29dBd and the current HSDS MessageWatch™ module results in a sensitivity of 52.5 dBuV/m.

The nominal sensitivity of the HSDS MessageWatch™ receiver and a HSDS automobile receiver sensitivity as computed above can then be related back to the standard coverage charts for any given FM station.

FM Broadcast Environment

The FM radio base band signal is discussed in this section. HSDS is described and shown with a typical stereo station's base band signal. Compatibility of HSDS with the audio and RDS is discussed.

HSDS in the FM Broadcast Channel

The HSDS subcarrier is summed onto the FM station's baseband signal before being FM modulated onto the RF carrier. The spectrum of an audio stereo baseband signal with HSDS signal is pictured in Figure 2.

Compatibility with main channel audio

In subcarrier applications it is critical that the subcarrier not interfere with the audio channel in a way that would affect a listener's perception of audio quality. There are two principal considerations in this regard: the first relates to the transmission filter and the out of band filter attenuation. HSDS filtering at the transmitter is implemented digitally with a finite impulse response filter. The subcarrier is more than 60dB below the pilot at the band edges.

The second interference source is potential nonlinear mixing of the subcarrier with the audio due to multipath. As a countermeasure to interference from multipath, the

HSDS protocol (described in later sections) uses data randomization to 'whiten' the signal and in particular avoid the generation of tones in the audio portion of the band. Extensive field and laboratory testing, along with significant operational experience in Seattle and Portland have demonstrated HSDS has no noticeable interference with the main channel audio.

Compatibility with the RDS subcarrier

RDS is a subcarrier standard first available in Europe and now gaining acceptance in the USA. The standard occupies the band of 54.6kHz to 59.4kHz and provides a data rate of 1187.5 bps. Lab tests were performed to evaluate the effects of the HSDS signal on RDS reception. A highly compressed audio was used for these tests. Seven commercial RDS automobile radios were tested. RDS receiver sensitivity was defined as .01 BER using 2.66% injection. Results from a representative receiver are summarized in Table 1.

RDS receiver sensitivity	No Audio	With L-R Audio
No HSDS	-93.5 dBm	-92.5 dBm
With HSDS	-93.0 dBm	-91.75 dBm

Table 1

As can be seen from the table, impact of HSDS signal is less than .75 dB with or without audio. The impact of L-R audio on RDS sensitivity is 1 dB or more. Considering L-R audio has a greater impact on RDS than HSDS, the impact of HSDS on RDS is entirely acceptable.

Link Layer

This section describes the link layer. The layer includes features required to make a reliable single station data link. The link layer includes the frame structure and packet structure (size, word synchronization, error detection and correction).

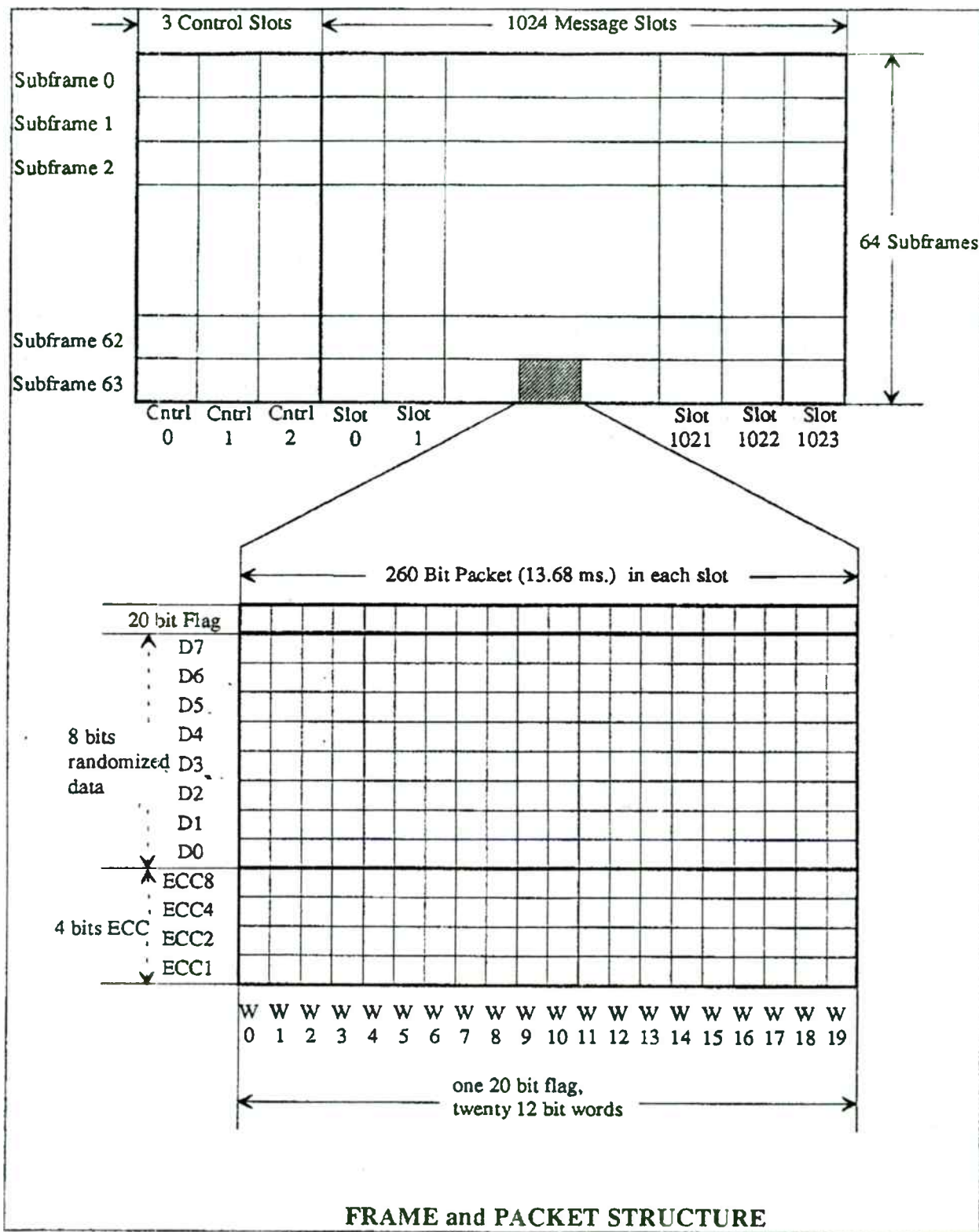


Figure 3

Packet Structure

HSDS Data is transmitted in fixed length packets. The bottom part of Figure 3 illustrates the packet structure used in the HSDS Protocol. Each packet is 260 bits long. Packet format bits in each packet control the packet's structure. A typical packet format consists of a word synchronization flag, error correction code (ECC), information bits and error detection code (CRC). The following description assumes the packet format used in currently operating HSDS systems.

The information bits from higher layers consist of 18 octets (8 bits per octet) per packet. A two octet CCITT standard 16 bit CRC is generated from the 18 octets and appended thus creating a 20 octet link data unit. The first octet (the incrementing slot number) of the 20 octet data unit is XOR'd with each of the following 19 octets that results in pseudo-randomized data. (In the event of multipath or other distortions to the signal during reception data randomization tend to 'whiten' the sounds in the audio channel.) Appended to each octet of randomized data are 4 bits of Hamming ECC, the resulting 20 - twelve bit words are referred to as ECC'd data. This error correction method provides single bit error detection and correction in 12 bits, or 8.3% correction capability. This method is quite easy to decode and reasonably efficient.

To increase burst error correction capability, the ECC'd data is interleaved on transmission providing immunity to 20 bit error bursts. Word synchronization is established by a 20 bit flag sequence that is added at the beginning of the CRC'd, randomized, ECC'd, interleaved data. Table 2 shows the steps in the link layer transmitter encoder and the reverse steps performed by the receiver decoder.

A double error correction on a stream of packets is being planned for applications with less severe power constraints, and requirements for higher data reliability.

Step	Transmit Encoder	Receive Decoder
1	Compute and add CRC	Find flag
2	Randomize data	Deinterleave data
3	Add error correction	Apply error correction
4	Interleave data	Derandomize data
5	Add flag	Compute and compare CRC

Packet Structure Encode and Decode steps
Table 2

Frame Structure

The HSDS Protocol is based on a packet oriented time division multiplexed (TDM) scheme. The top section of Figure 2 illustrates the frame structure used in the HSDS Protocol. The largest structure used by the protocol is a master frame. Each master frame contains 64 subframes. Each subframe is divided into 1027 units called time slots. Each slot contains a packet. The first three times slots in each subframe are control slots, and the remaining 1024 are regular message time slots. Control slot packets include time of day & date and lists of surrounding stations using the HSDS Protocol. Regular message time slot packets typically include a slot number, receiver address, data format, packet format and the message data.

The 19khz stereo pilot signal is used as the clock for the data. Since the stereo pilot may not be exactly 19khz, at the time of transmission, a single bit may be added (pad bit) between packets as required to maintain exactly 19,000 bits per second data rate. This occasional addition of a pad bit maintains proper synchronization with UTC.

Network Layer

This section describes the network layer. The network layer includes features required to make a number of individual stations act as a single system. The network layer includes receiver addresses, multiple application multiplexing, multiple station concepts such as local station lists, station time offsets and synchronization between stations via UTC, and network reliability concepts.

Multiple Station Systems

When multiple station systems are required, master frames are synchronized to UTC and begin at the start of each quarter hour (plus an individual transmitter's time offset). The synchronized and time offset stations provide an opportunity to change the tuned frequency and make subsequent attempts on other frequencies to receive packets.

System Reliability

Robust wireless systems require methods to address multipath and shadowing issues. The effects of multipath, which are not included in the analysis of

receiver performance earlier, play a significant role in determining system performance. Multipath can be viewed as a time-varying nonlinearity that can distort or reduce the received signal to a point that reliable reception is no longer possible. Shadows behind hills and mountains or due to man made obstacles to radio frequencies can reduce signal strengths below sensitivity levels.

Some systems attempt to address these issues with extensive error correction schemes. While these techniques are useful for the moving receiver, they become ineffective when the receiver is stopped in an extremely low signal strength area or moving very slowly through multipath nulls. A car stopped at a traffic light or a person at a desk wearing a receiver are two examples of the breakdown of even the most robust error correction methods. Diversity techniques are frequently used to combat multipath effects. HSDS addresses multipath and barrier issues with a combination of frequency, space and time diversity and message numbering.

Diversity Techniques possible with HSDS

Frequency diversity can be achieved through the capability to tune any frequency in the range from 87.5 to 108Mhz. By transmitting on multiple frequencies a receiver in a multipath null at one frequency is not likely to be in a multipath null on another frequency. In the event a receiver is behind a hill or other such obstacle to reception, space diversity can be used as required by the application.

Space diversity (transmitters at different locations) provides paths from two or more directions reducing the size of shadowed areas, and reduce the possibility of missed messages.

Time diversity can be provided in two ways -- multiple transmission on the same station and delayed transmission between stations. Multiple transmissions of information several minutes apart is utilized for wrist mobile applications where a receiver may be passing through a radio frequency shielded area, such as a tunnel or deep basement. The second method for time diversity includes a time offset for data transmission. This time offset between stations provides an opportunity to change the tuned frequency and make subsequent attempts to receive a packet for low data rate receivers. When much greater throughput is required, receivers operate on the best station selected from the stations available.

Message Numbers

In addition to diversity techniques, each transmission includes a transmitted message number that eliminates duplicate messages and permits detection of missed messages. When there are multiple transmissions of a message, it is possible to receive the same message several times. By rejecting duplicated message numbers, multiple transmissions do not appear as duplicate messages. A receiver can keep track of the received message numbers, and if there is a skip in the message number sequence, it can be concluded that a message was missed. The input system can log each message by message number and permit retrieval of missed messages by the owner of the receiver.

Implementation

Receiver Integrated Circuit

The receiver integrated circuit's primary function is an FM receiver that takes the RF signal from the antenna and generates the base band signal from 0 to 100kHz. General Specifications for the IC are as follows:

- sensitivity < -91.5 dBm at 10% subcarrier injection
- 12 dB subcarrier to noise ratio output at sensitivity
- frequency range from 87.4 to 108Mhz
- power required 2.1 to 3.3 Volts, 18 mA maximum
- operating temperature 0 - 50° C
- number of external components - about 29
- number of adjustments required - none

Demodulator Integrated Circuit

The demodulator integrated circuit's primary function is to demodulate the base band signal into a 19 kbs synchronous binary data stream. Other functions include a synthesizer for the receiver IC (providing 100kHz steps over the FM band) and loop antenna tuner control, and a 256 bit EE-PROM. General specifications for the IC are as follows:

- Demodulator
 - data filter - 32 point FIR square root cosine filter, 66.5kHz center
 - variable level data detection from 5% to 20% injection levels
 - clock - 19kHz digital phase locked loop
- power required - 2.1 to 3.3 Volts
3.5 mA maximum - data demodulator
1.5 mA maximum - synthesizer
- operating temperature 0 - 50° C
- number of external components - 10
- number of adjustments required - none

Complete Receiver / Demodulator Module

The above integrated circuits have been combined into a complete receiver / demodulator module. This module, when attached to an external antenna, provides a 19,000 bit per second synchronous data to external decoder chips and processors. Its approximate size is 30 x 27 x 6 mm.

Subcarrier Generator

An HSDS subcarrier generator using DSP technology is available. Features include:

- Data is phase locked to 19kHz pilot with adjustable phase angle.
- Full redundant operation including automatic switch over to secondary subcarrier generator with separate power supply.
- Out of band energy detection and auto shut down for fail-safe operation of audio.

- Internal watch dog timer for automatic reset
- Remote control operation

Protocol Queuer / Encoder

An HSDS Protocol queuer and encoder is also available.

Lab Tests

HSDS with a 10% injection and the described integrated circuits provide a receiver with a -91.5 dBm sensitivity, 12 dB subcarrier to noise ratio, 2×10^{-2} BER, a 0.55 packet completion rate (PCR) and, with 3 transmissions on a single station, a 0.91 message completion rate (MCR). This is illustrated graphically with Figure 4, which shows the various components and their sensitivity specifications

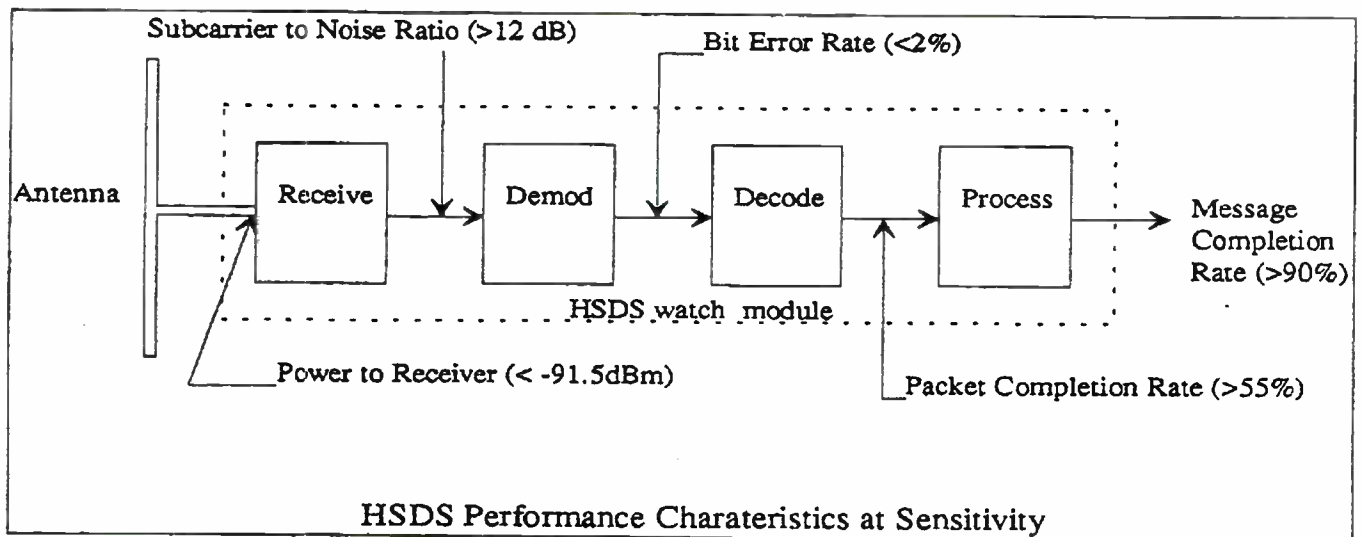


Figure 4

A plot of a current MessageWatch™ module's performance PCR versus input power in the lab is shown in Figure 5.

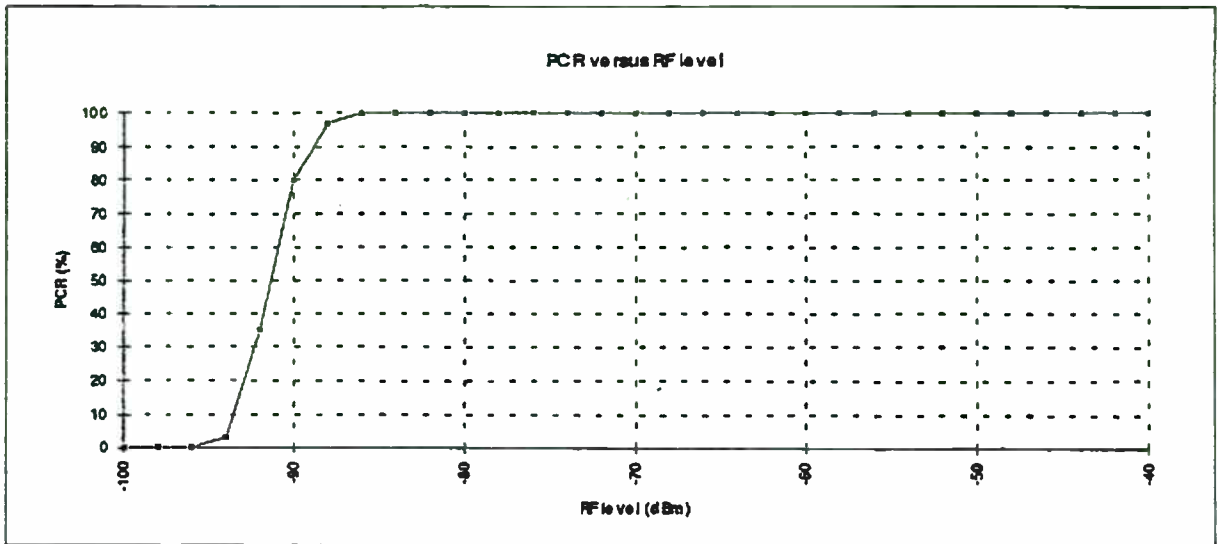


Figure 5

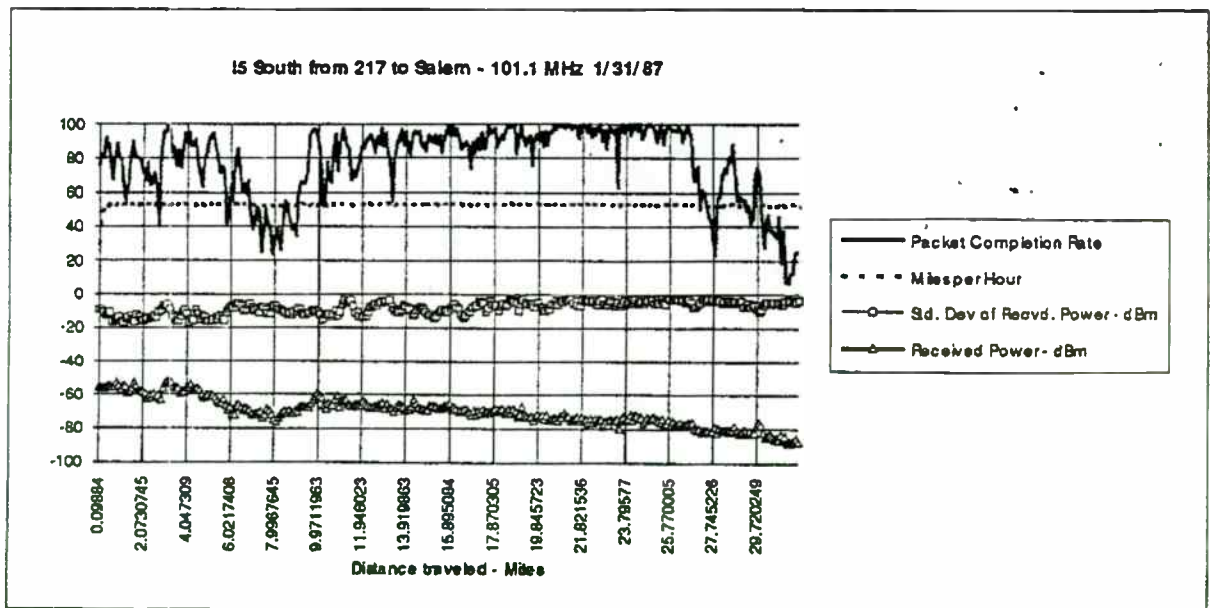


Figure 6

Field Tests

Results from two field tests in Portland, Oregon are shown. The first tests, in 1987, were used for initial range and performance evaluation including error correction techniques. The second tests, in 1989, were used to determine coverage of the then planned commercial system.

1987 Field Test -- Error Correction

Results shown are from field tests in Portland, Oregon in 1987 on a single station. The transmitter is 100 kW ERP on a tower 830 feet above average terrain on frequency 101.1Mhz located 45-30-55 N and 122-43-50 W.

A sample from a single run from the intersection of Oregon Highway 217 and Interstate 5 (7 miles from the tower) going South toward Salem on I5 (41.5 miles from the tower) is used for all the following analysis. This data is referred to as the I5 to Salem run.

Figure 6 shows basic results from the I5 to Salem run -- the packet completion rate (PCR), mean received power in dBm, standard deviation of the power in dBm, and travel speeds in miles per hour are plotted versus the distance traveled. The signal to the receiver was reduced to reflect a -30 dBd wrist band antenna. Each plotted point represents a distance of about 500 feet and the average of 250 samples of PCR and received power. The standard deviation is plotted as a negative value to help distinguish it from PCR data. Standard deviation of the received power reflects the degree of multipath -- the larger the deviation, the greater the multipath. Travel speed was maintained at about 55 miles per hour. Received power level is clearly declining as one moves away from the tower. The highest PCR appears to be in areas with adequate signal and minimal multipath as would be expected.

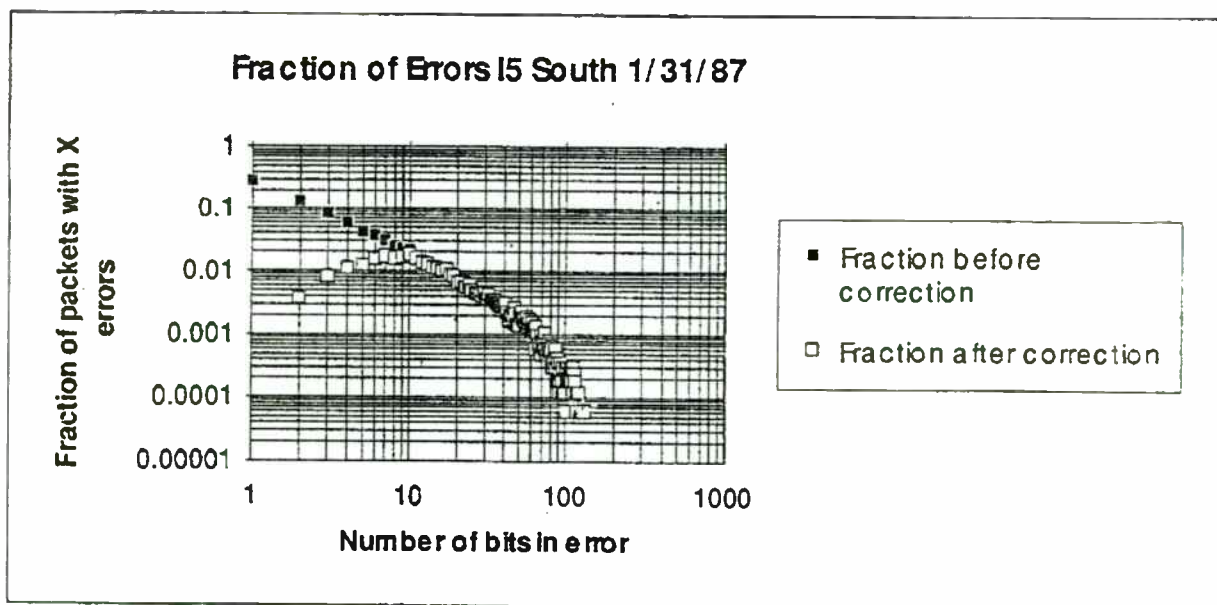


Figure 7

A study of bit errors and the effectiveness of the Error Correction method was performed. An analysis of the I5 to Salem run shows the packets sorted into four categories -- error free packets requiring no error correction, packets that could be corrected, packets that could not be corrected, and packets missed entirely due to failure to obtain word synchronization. Fully 64.1% were error free prior to error correction, 11.9 % were correctable, 7.2% were in error after error correction and 16.7% were missed due to lack of synchronization flag. (A later modification of the system decreased the

percentage of packets with missed word synchronization by looking for either the leading flag of the packet of interest or the flag of the following packet.)

Figure 7 shows the correctable and not correctable packets sorted for the number of bits initially in error. This shows a nearly log log linear decline in the percentage and the number of the errors in the packets. All packets with 1 bit in error were corrected while the majority of packets with less than 10 bits in error were corrected. Again from figure 7, the correction scheme

performed poorly with greater than 10 bits in error but there are few packets with such errors.

No error correction method can be 100% successful. Of the packets needing error correction, more than 62% of the packets were correctable, while 38% were not correctable. These results lead to the conclusion that repeating packets is necessary to provide satisfactory completion rates for receivers with very small mobile antennas and the error correction scheme should not be too extensive.

commercial operation: 95.5Mhz, 98.5Mhz, and 101.1Mhz. The recorded signal strength was taken from a quarter wave vertical monopole mounted on a vehicle's roof with its center height 2 meters above ground through a splitter to a spectrum analyzer measuring the power. The recorded Packet Completion Rate results were obtained using the same antenna used for signal strength and a -90 dBm receiver padded down to simulate a -30 dBd_{vertical} antenna at a center height of 1 meter. Current MessageWatch™ receiver sensitivity of -91.5 dBm and antenna gain of -29 dBd_{vertical} specifications

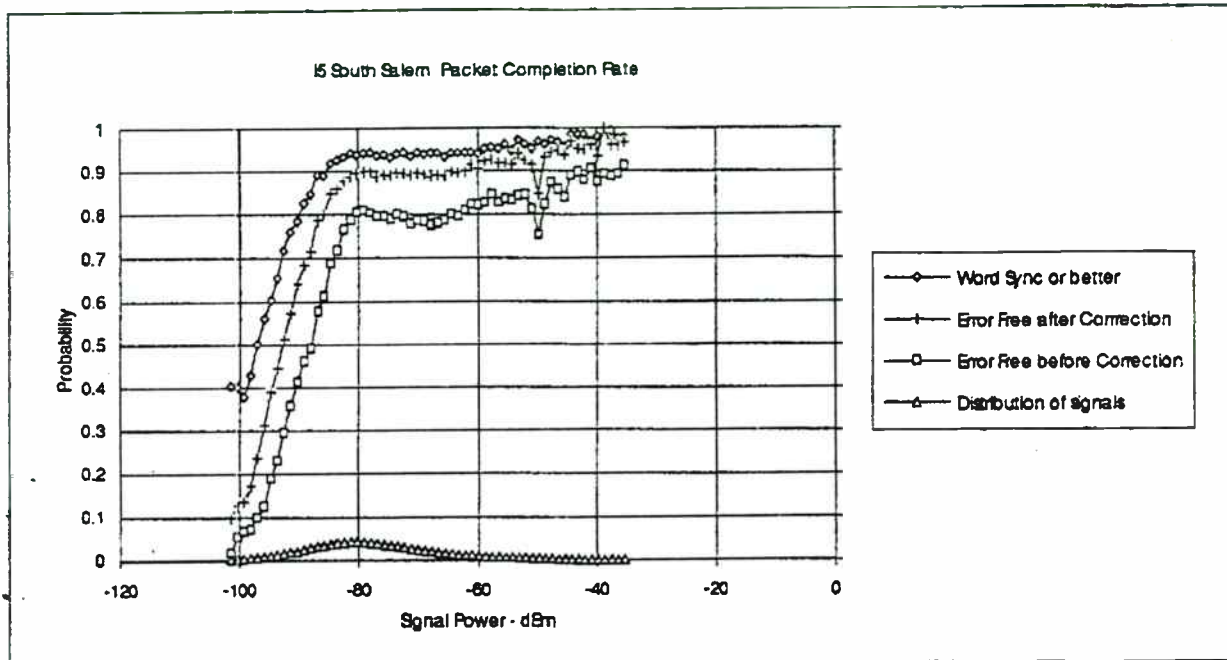


Figure 8

The same data was then sorted based on received signal power and is plotted in Figure 8.

The distribution of samples from that run are also included. The effectiveness of error correction is clearly significant and is even very helpful at relatively high RF power levels. More extensive error correction schemes cannot improve these results significantly and the capacity of the system used by extensive correction schemes is better used for repeating transmissions.

1989 Field Tests -- Portland Range / Coverage

The following set up was used for 1989 Portland range / coverage testing. Three stations were selected for

are 2.5 dB better than simulated in this testing.

A map of the Portland Area is provided as Figure 9 showing major towns. Thin lines or dots on the chart show the data points taken in the testing. Figure 10 shows signal strength contours of 60dBuV/m and 80dBuV/m for station 101.1Mhz. Portland is in a valley surrounded by mountains to the East and West that limit coverage in those directions. The Packet Completion Rate Maps - Figures 11, 12, 13 & 14 show areas of >90%, >69%, >55%, >44% PCR respectively for station 101.1 Mhz . These maps represent 90% or better Message Completion Rate areas for 1, 2, 3 and 4 transmissions respectively. The dramatic increase in coverage associated with multiple transmissions is clear.

Commercial Operations

Currently commercial service under the Receptor trademark is offered in two metropolitan areas: Portland, Oregon, and Seattle/Tacoma, Washington. Portland utilizes three FM radio stations to provide a coverage footprint with approximately 1.2 million people living within its boundaries. In Seattle and Tacoma, seven FM radio stations are used to provide a coverage area with 2.6 million people.

Beside numeric and standardized messages (such as Call Home, Call Office, etc.), more than 10,000 customers receive various combinations of the following informational services:

- Professional and collegiate football, basketball, and baseball scores
- Daily weather forecasts
- Local ski reports during winter months
- Daily Dow Jones Industrial Average closing information
- Winning daily and weekly lottery numbers

Summary

A high speed data system (HSDS) delivered over commercial FM radio subcarriers has been shown. It is a flexible system, providing inexpensive one-way wireless data communications that will be used in many applications.

References

Lender, A.(1963), "The Duobinary Technique for High Speed Data Transmission," AIEE Trans. Commun. Electronics, vol. 82, pp. 214-218.

Portland Data Points 4/28/89

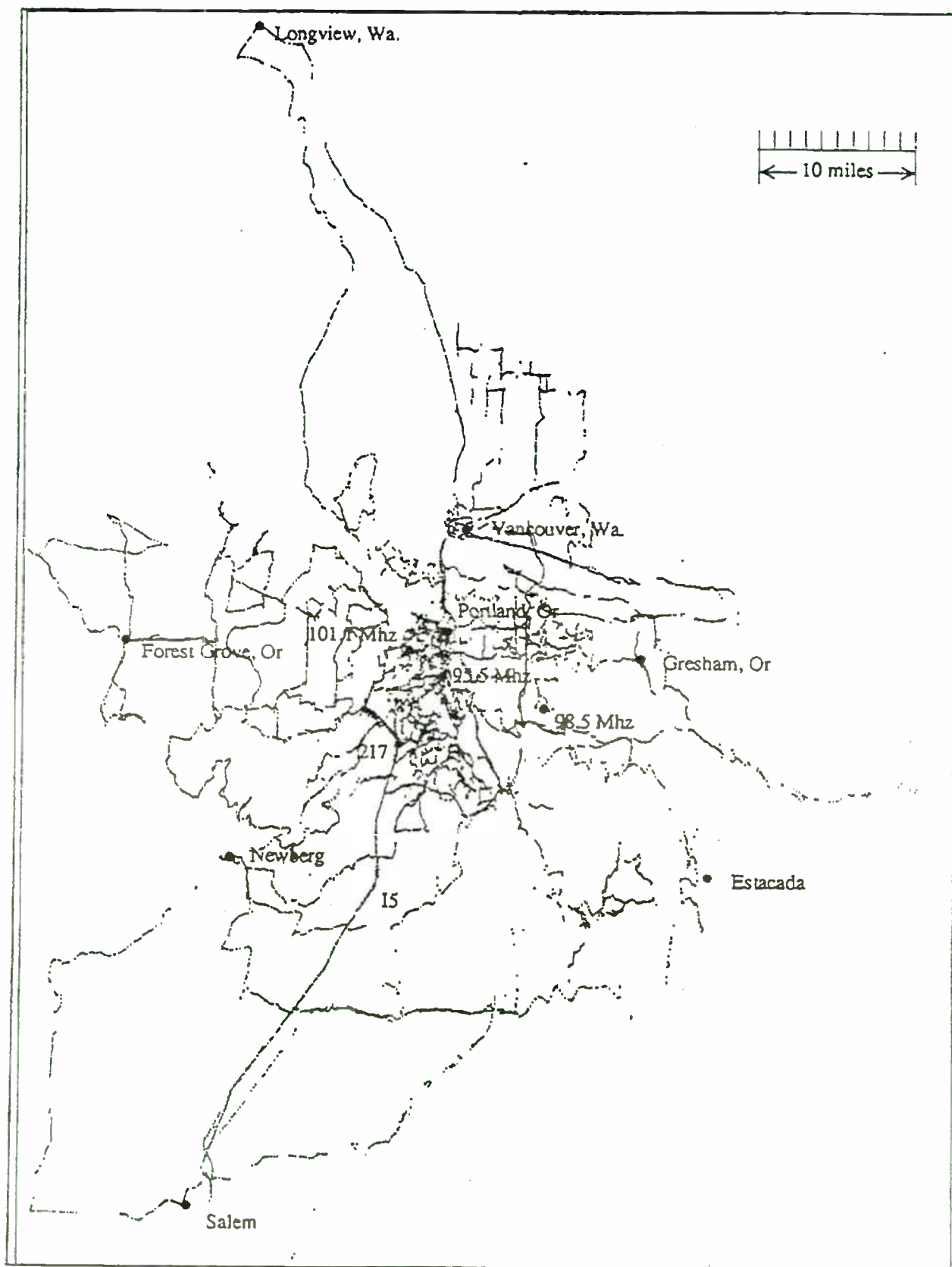


Figure 9

Portland Field Strength 101.1 Mhz 4/28/89

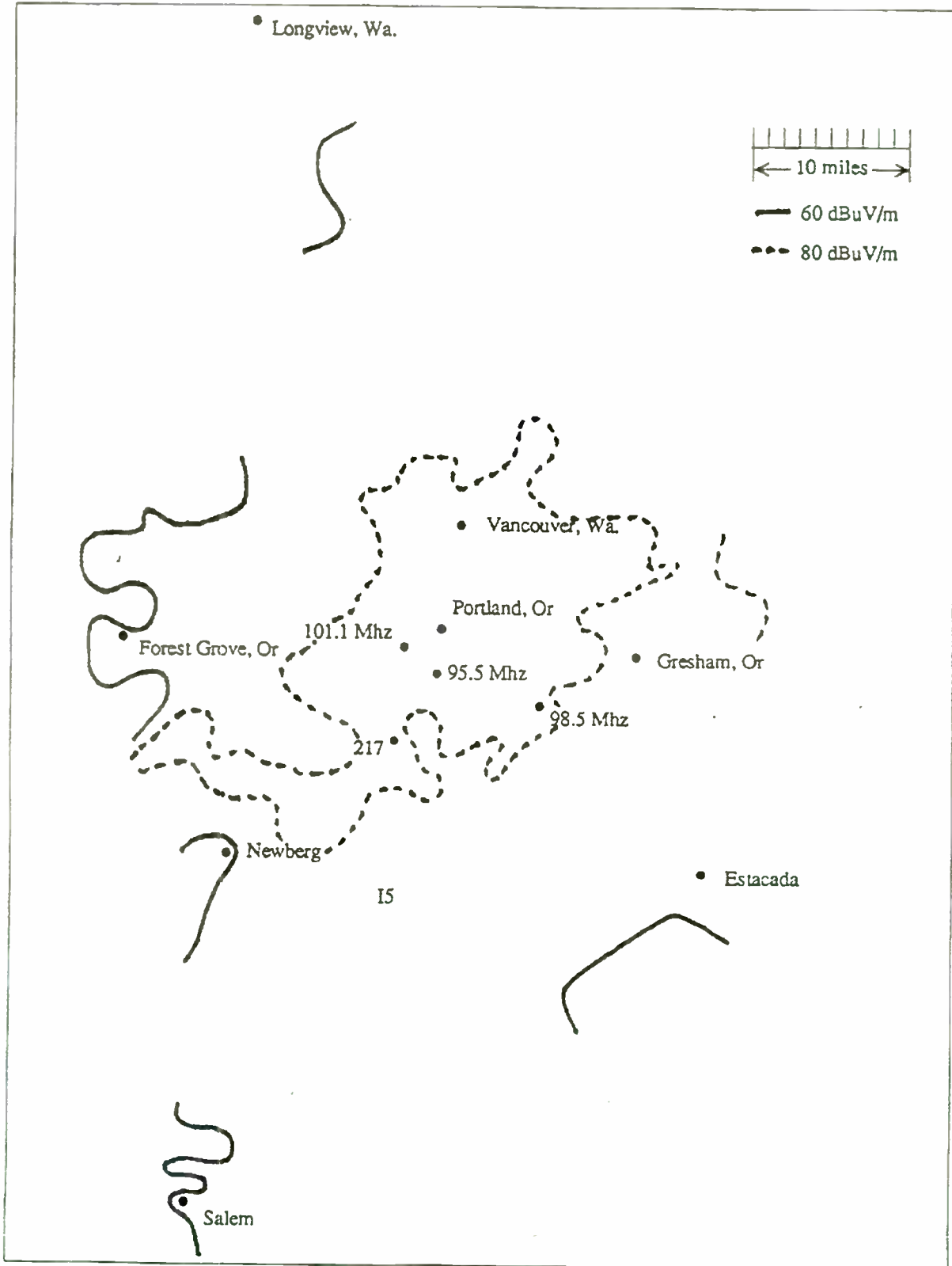
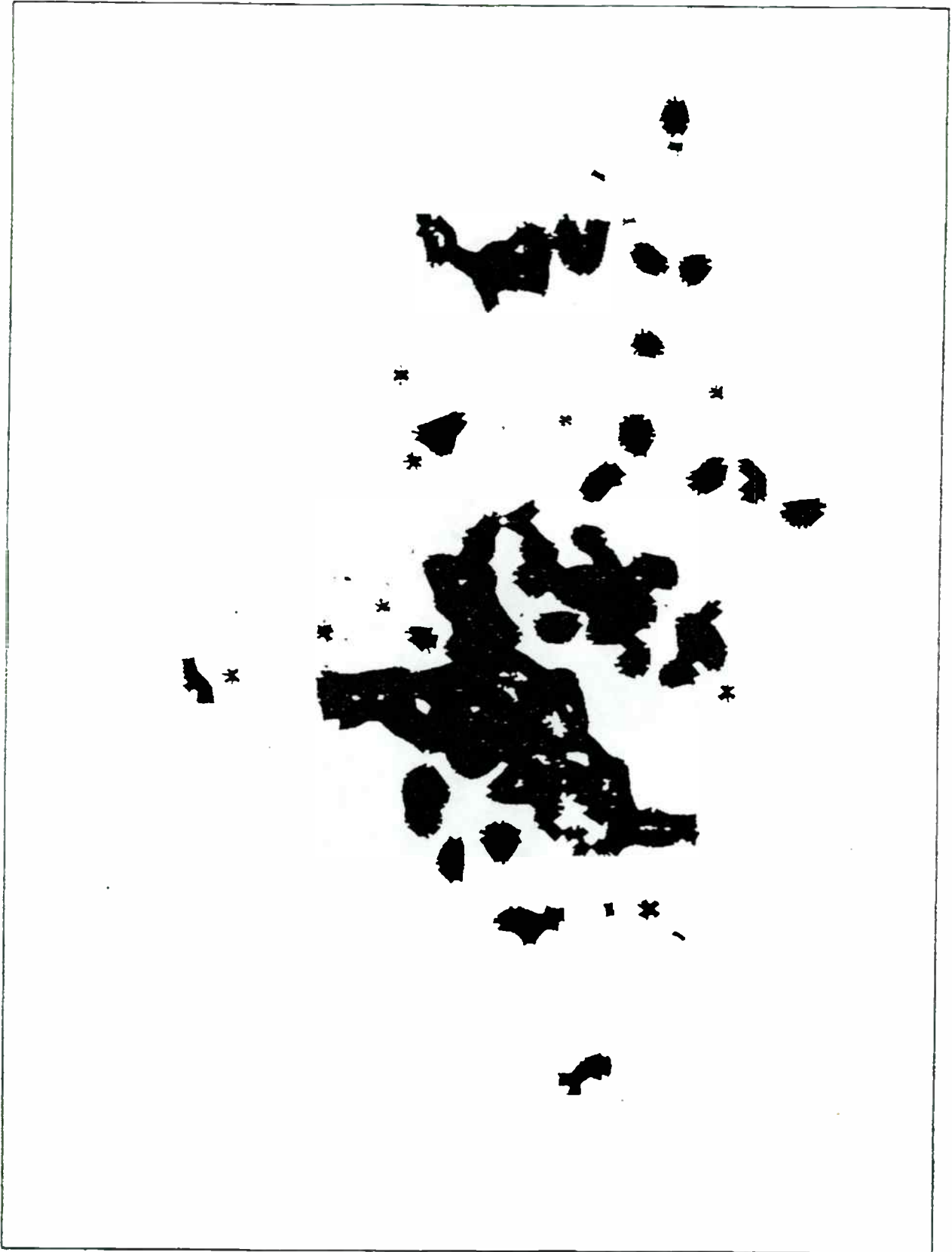


Figure 10

Figure 11



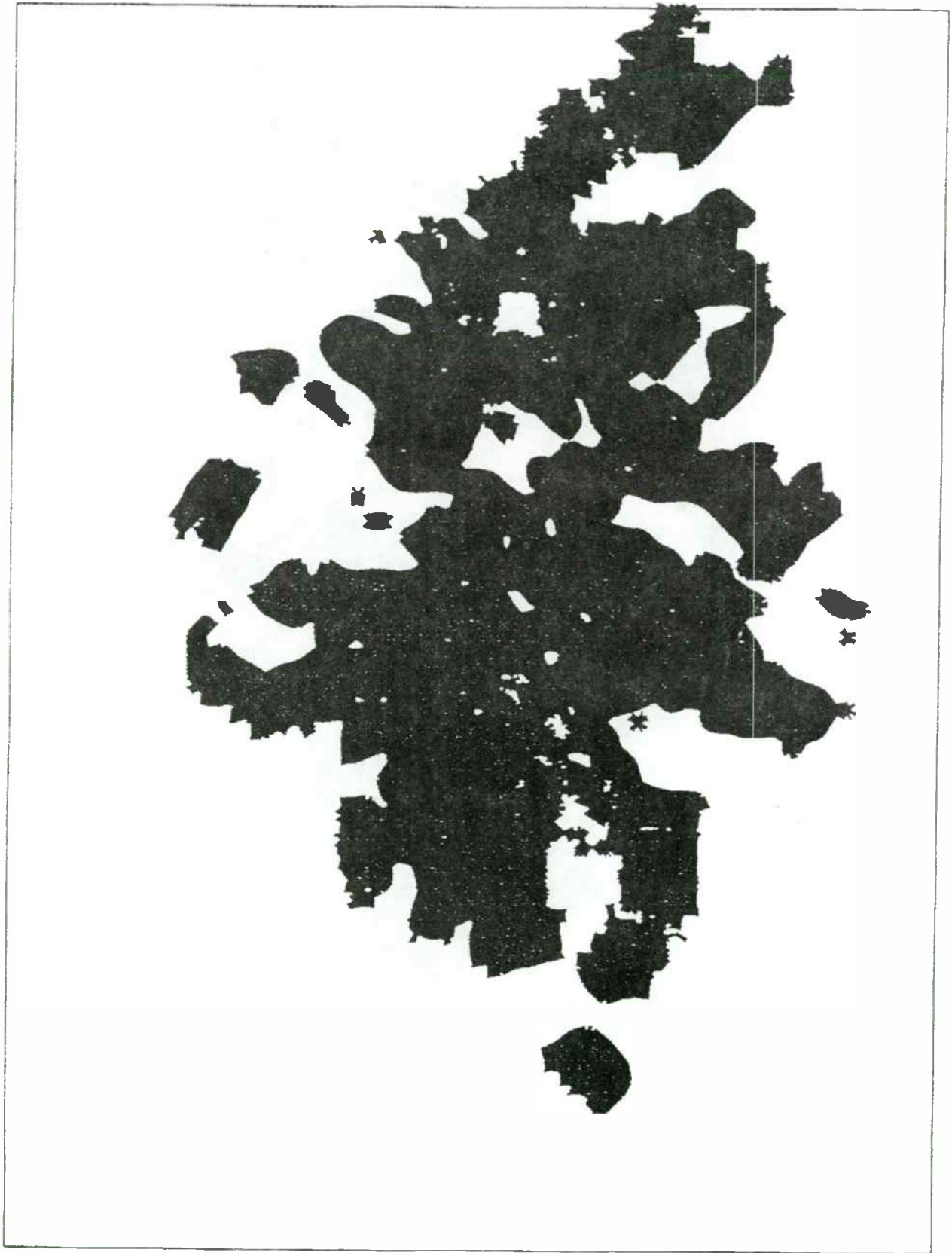
Portland > 90% PCR 101.1 Mhz 4/28/89

Portland >69% PCR 101.1 Mhz 4/28/89



Figure 12

Figure 13



Portland > 55% PCR 101.1 Mhz 4/28/89

Portland >44% PCR 101.1 Mhz 4/28/89

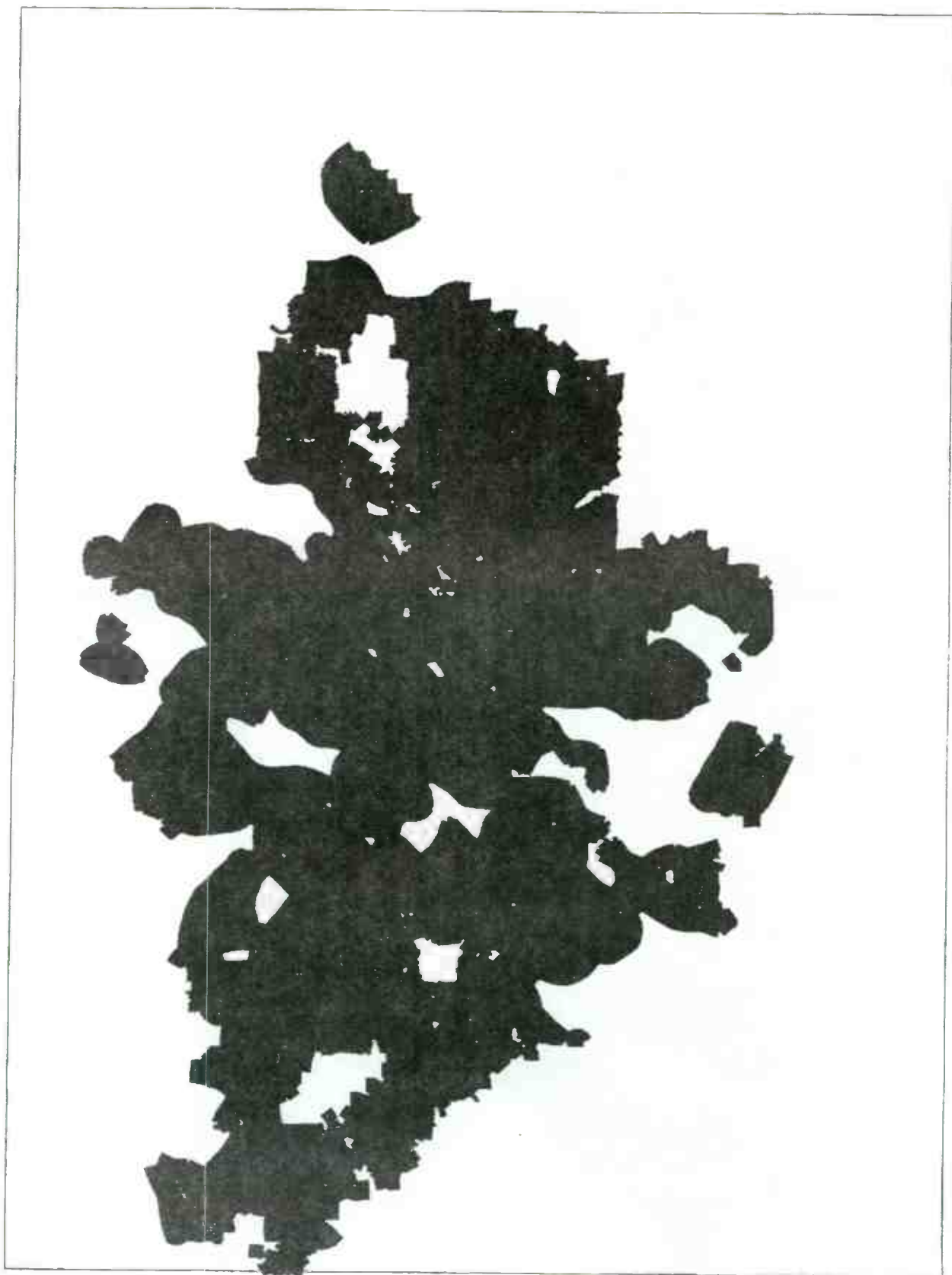


Figure 14

340

Multimedia support in Personal Communications Networks

Kamran Ghane
Neda Communications, Inc.

ABSTRACT

The demand for multimedia applications is growing day by day and ATM addresses this issue in wired networks. The growing market of wireless communication demands the same services and a multimedia PCN will have a high market demand in near future. Several issues are involved in the design of a PCN with multimedia support. Traffic control is one of the issues in multimedia and real time applications. The packet switching approach for such services is preferred. To become able to decide about the technology for such services, a good understanding of the implementation approach, cost of the network and cost of the end terminals is a necessity.

Since the major characteristic of multimedia applications is their high demand for bandwidth, the channel sharing and optimal use of available channels is a key issue here. The other issues are throughput and effective use of the bandwidth, power level and cost of the end user terminals. The ATM concepts can be well used in the design of multimedia PCN and by doing so the compatibility between ATM and multimedia PCN is achieved, which would be of great value for internetworking.

While CDMA and TDMA have their own cons and pros for PCN, media access control can be realized in different ways like circuit or packet mode CDMA, multi-code and multi-level CDMA, fixed chip rate and variable forward error control, dynamic TDMA with both CBR and VBR modes, or a CBR mode TDMA.

1. Introduction

The fast growing multimedia services in wired networks such as B-ISDN and ATM and also advances in digital wireless technologies and Personal Communication Networks (PCN) means that there will be a need for an integrated voice, data, and video wireless service in near future. The PCN which is a subset of Personal Communication Services (PCS) and sometimes used with the same meaning is getting more and more attention. After the recent FCC spectrum auctions for PCS, the PCN networks will have a widespread market very soon. PCN operating in a microcell network is planned to provide services like voice, data, e-mail, and facsimile to individual mobile users. The user gets a portable terminal which is light, small and low-power. The fast progress of multimedia services in wired networks and also growing advances in PCN technologies leads us to the conclusion that there will be a demand for multimedia support in the PCN systems very soon and by the end of this decade. It's reasonable to plan for a PCN with flexible support for different types of transport services for voice,

data, and video, which are compatible with BISDN/ATM and with an architecture close to these technologies that are the major platforms of wired multimedia services.

It is predictable that the analog/digital cordless phone will be replaced by PCN. While by considering the difference between the high power and large cell sites of cellular mobile voice and data networks, and the low power microcellular PCN, it's unlikely that these two can merge in future. On the other hand the fast growing ATM networks make us think about ATM as the wired backbone of wireless PCN with multimedia support and design of a PCN with multimedia support that is compatible with ATM.

2. Integrated multimedia services in PCN

2.1 General issues

The integrated services can be categorized in two groups of applications: sensitive to bandwidth and delay and insensitive to bandwidth and delay. Data services on PCN like email, one way paging, acknowledged paging, facsimile, and phone pictures are relatively insensitive to variations in bandwidth and delay. Bandwidth and delay sensitive applications like video conferencing, multimedia voice/data/video applications for lightweight portable terminals, digital audio, high definition TV, multimedia information distribution and data retrieval services are future services of PCN. The real time applications, which interact with human beings like multimedia applications, are sensitive to bandwidth and delay. Applications using sound, video, and computer graphics like teleconferencing, viewphone, interactive video services, telepresence or virtual reality demand a higher quality of service from the network. Video applications, either moving or still, are the most sensitive applications. Commercial compression algorithms can reduce the data with a factor of 30 to 1 or better. About 30 frames a second or more is needed to give a nonflickering video. In a circuit switching network, the video is transmitted over a fixed bandwidth but in a packet switching network, Variable Bit Rate (VBR) video is a necessity. The Moving Pictures Experts Group (MPEG) and H.261 encoding schemes are the efforts in this line by ISO and CCITT. Considering the limitations of PCN, the higher degree of compression can be used because the lossy compression is well acceptable for lots of video applications. Those applications that demand precise and lossless videos are not in the context of PCN or mobile users. On the other hand, more compression means more delay for decompression but considering the fast progress of IC technology and DSP, it won't be a problem. It's not necessary to have a strict performance guarantee for PCN multimedia. But adaptive applications ask for large receiving buffers for optimum operation which directly affects the playback point. The ongoing progress in memory sizes and costs, and implementation of dynamic playback point can result in a light and cheap terminal for PCS.

2.2 Packet switching vs. circuit switching

Packet switching is the choice for multimedia PCN because of the restrictions of the media used. Circuit switching is not flexible enough to support the variety of multimedia services with different bandwidth/response time requirements. Regarding the channel utilization, circuit switching has poor resource sharing. Considering the nature of wireless networks, which have a less reliable media compared to wired networks, the packet switching is a better choice that can tolerate errors with ARQ retransmission at the data link layer. As it is experienced with wired networks, the PCN wireless network demands a packet switching switch-based network like ATM. ATM will be widespread wired network for multimedia and using the ATM infrastructure as the backbone for PCN will be the way to go in future networks. By the time the multimedia PCN is implemented, the availability of ATM and its cost won't be a barrier to this approach. Since the multimedia PCN will have a large number of microcells, the interconnection of microcells and the connection to the backbone can be directly or through intermediate networks that will operate based on ATM switching approach. To make the interfacing easier, an ATM compatible approach is a good solution for PCN design. As a result a 48 byte ATM cell will be the packet (cell) unit of PCN networks. The PCN wireless channel specific protocol data will be added to PCN data unit while the data is in the PCN network and as soon as the data enters the wired ATM backbone, the cell will have the ATM headers.

2.3 Media access

There are two major access methods for multimedia PCN, which are TDMA and CDMA. The FDMA and random access methods are other solutions that are not suitable for this case. The same discussions that resulted to the failure of FDMA as a media access for digital cellular networks, can be applied here too. On the other hand in the FDMA scheme, the variable bit rates of different data services and the efficient use of media means different size FDMA channels, which makes the channel allocation and channel reuse complicated. With identical small FDMA channels, several RF units are required or a multi-tone unit are required, which makes the PCN terminal complicated and expensive.

In the case of TDMA, the data rate can be easily set by changing the number of allocated slots in the time domain. It's possible to use the transmission media more efficiently by implementing the modified versions of the TDMA scheme, i.e. by combining the TDMA with a random packet access like Slotted Aloha. In such a scheme the data source reserves slots when it needs them and makes them free when it has no data to send them. Therefore, the slot allocation becomes dynamic and the inefficiency problem of TDMA with static slot allocation for bursty traffic is solved and the channel utilization is optimized. CDMA has good channel utilization. When a data source is silent, it doesn't cause any interference, which means it makes room for other sources to access the spectrum while the interference level remains in an acceptable level. With good power control, CDMA can have high capacity in terms of

users/Hz/unit area. Direct Sequence (DS) CDMA and Frequency Hopping (FH) can be used for multimedia PCN. Various combinations of chip rate, processing gain and Forward Error Control (FEC) can be chosen. In the case of variable chip rate with fixed processing gain, variable bandwidths are used by variable chip rate transmissions. So, the RF units and frequency planning are complicated because of variable bandwidths. The conclusion is that the fixed chip rate approach is preferred. In the case of variable processing gain with fixed chip rate, this problem doesn't exist and the RF unit is simplified. The variable processing gain is used to implement variable bit rate. So higher data rates have more power and generate more interference, which results in less high data rate user for a given interference. This scheme needs good pseudo random codes with different lengths. In the case of variable FEC code rate with fixed chip rate the different data rates are implemented by variable FEC code rate. Combinations of convolutional codes and pseudo random codes can be used which can give a higher coding gain. The decoding is more complicated when the decoder works at the chip rate and not at the bit rate. Variable FEC rate can be combined with variable spreading ratio too. Combining the spread spectrum and TDMA access methods can be a good solution too. Another approach is having a basic data rate and implement the higher data rates by using multi codes for a data source. This means that the data are splitted into several streams with basic rates and then combined at the receiver. Multi level CDMA is another possible scheme and higher order fields have better pseudo random codes.

2.4 Data rate

The different access methods mentioned above result in different data rates. Thanks to the advancement in DSP and programmable filters, support for a wide range of data rates in modems has become simple and affordable. However, the data rate is limited by coherence bandwidth but this restriction can be overcome by concatenating time slots in TDMA. In mobile systems, the multipath effect which results in Inter Symbol Interference (ISI) restricts the data rate. In a multimedia PCN network with small microcells, the line of sight components of the multipath signals is stronger than the others and high data rates in the order of Mbps are possible. However, the equalizers make it possible to have symbol rates that are several orders more than the coherence bandwidth of the channel in TDMA. In CDMA, multipath signals can be combined and receivers can be improved to give bit rates much higher than the channel coherence bandwidth.

2.5 Bandwidth and delay control

Multimedia and real time services ask for a guaranteed bandwidth and delay. Traffic management is translated to queue management and controls in the network and the device. PCN multimedia services doesn't need a deterministic guarantee and statistical guarantee is good enough for the target applications in PCN. The guarantee for loss rate, bandwidth, and queuing delay in PCN services is less complicated than the requirements of applications in

wired networks. There are several approaches to this issue, like leaky bucket with priority (Makreki) or weighted fair queuing, which can give good guarantee (Parekh).

3. Design issues

3.1 Cost and complexity

The multimedia terminal should provide the user with voice communication, data services, fix and motion video and should be small and lightweight. Other than the issues of complex modulation and compression, the power consumption is the major concern in such a terminal. The RF unit with receiver/transmitter, mixer, oscillators, amplifiers, and filters, a color LCD display, speech codec, and video decompression module are the major power consumers. One of the sources of power dissipation is chip I/O because chip boundaries have higher capacitances than the inside of the chip. Multichip module (MCM) and similar technologies can reduce the power dissipation. In addition to this, the power dissipation resulted from switching, direct path and linkage currents in DSP circuits should be improved by advances in design, technology, architecture and algorithms. Reducing the power results in a degrade in performance, which should be compensated by reducing the size and implementing parallel/pipeline algorithms and time shared structures that can give higher performance. There are also issues in circuit design that affect the power consumption like static/dynamic logic design, passgate/conventional gate, and the voltage threshold adjustment.

3.2 Network architecture

As mentioned before, the PCN architecture will be an ATM compatible packet switching scheme. The PCN data unit is an ATM cell containing 48 byte data and the network header. Various quality of services (QOS) are supported for real time applications of the network through constant bit rate (CBR) and variable bit rate (VBR). The media access will be either CDMA or TDMA with dynamic slot allocation. Mobility is supported by using the intelligent ATM encapsulators and the existing mobility unaware ATM backbone is used. Since the number of microcells in such a PCN network will be large, the cell base stations can be grouped and connected to each other based on the density of the cells in an area. The grouped microcells are connected to each other via an optical network in the form of a tree and branch and then connected to an ATM switching node. Each of these microcell group networks will have an ATM address and each base station will have a connection identification number. When a cell arrives in a microcell network, it's broadcasted to all the attached base stations and each base stations checks the connection identification number in the cell to see if the cell is destined to it. The ATM's Virtual Path Identifier (VPI) and Virtual Channel Identifier (VCI) is used to route cells. Signaling information for connection establishment is carried through reserved bandwidth with high priority. VPI multiplexing lets such reserved signaling bandwidth be used by other sources when there is no signaling. Each mobile terminal has a home and can go away from its home and visit other group microcells. When a mobile terminal,

which has established a connection moves from one group microcell to another, all base stations in the same group microcell store information about the mobile's current address, the destination address of its connection, connection identification and the reference controller. Whenever a mobile terminal moves from one microcell to another, all these information are updated for both ends of the connection. Whenever mobile visits a group microcell network, a new connection identification is assigned to it and each group microcell has some free IDs to assign to visitor mobiles. Each established connection has a reference controller, which keeps track of charging and performs other necessary controls.

Conclusion

This paper discussed the issues of multimedia support in future PCN systems. Considering the advances in multimedia services in ATM networks and also the rapid growth of voice and data services in PCN systems, integrated services of voice/data/video will play an important role in the future PCN systems. Compatibility with ATM and using ATM as the backbone of such an integrated voice/data/video PCN is proposed, which will lead to success of multimedia PCN. CDMA with fixed chip rate or TDMA with dynamic slot allocation can be the media access scheme. Quality of service for real time applications and traffic control are important issues. Fortunately these are not unique to this system and lots of work is in progress in this area. It's also possible to plan for statistical guarantee for PCN services. Terminal cost won't be a barrier because of the advances in IC design, DSP and LCD technologies. There is room for a great deal of design and prototyping work before the technology cost and market is ready for such services.

References

- [1] Bakoglu H.B., "Circuits, Interconnections, and Packaging for VLSI, Addison-Wesley, 1990.
- [2] Cox D.C., "Personal Communications A Viewpoint", IEEE Communications Magazine, Nov 1990, p. 8-20
- [3] Gilhousen K.S., "On the Capacity of a Cellular CDMA System", IEEE Transactions on Vehicular Technology, May 1991.
- [4] Goodman D.J., "Cellular Packet Communications", IEEE Transactions on Communications, Aug 1990, p. 1272-1280.
- [5] Goodman D.J., "Trends in Cellular and Cordless Communications", IEEE Communications Magazine, June 1991, p. 31-40
- [6] Goodman D.J. et. al., "Packet Reservation Multiple Access for Local Wireless Communications", IEEE Transactions Communications, Vol. 37, No. 8, 1989.

- [7] Joseph K. and Raychaudhuri D., "Stability Analysis of Asynchronous Random Access CDMA Systems", Proc. IEEE GlobCom Conference, Dec 1986.
- [8] Lim J.S., "Two-Dimensional signal and Image Processing", Prentice Hall, 1990.
- [9] Pursley M.B. et al., "Error probability for direct-sequence spread-spectrum multiple access communications", IEEE Trans. Communications, May 1982
- [10] Pursley M.B. and Taipale D.J., "Error probabilities for spread spectrum packet radio with convolutional codes", IEEE Trans. Comm., 1987.
- [11] Schilling D.L. et al., "Spread spectrum goes commercial", IEEE Spectrum, Aug 1990, p. 40-45.
- [12] Schilling D.L. et al., "Spread Spectrum for Commercial Communications", IEEE Communications Magazine, April 1991
- [13] Steele R., "The cellular environment of lightweight hand-held portables", IEEE Communications Magazine, July 1989, p. 20-20
- [14] Steele R., "Deploying Personal Communication Networks", IEEE Communications Magazine, Sept. 1990, p. 12-15
- [15] Viterbi A.J., "Wireless digital communications: a view based on three lessons learned", IEEE Communications Magazine, Sept. 1991, p. 33-36
- [16] Woerner B.D. and Stark W. E., "Packet error probability of DS/SSMA Communications with convolutional codes", Proceedings 1991 MILCOM, Nov. 1991

Mobile Communications/ Wireless Design

Session Chairperson: Victor Perrote,
Microwaves & RF (Hasbrouck Heights, NJ)

The AC power line as a wireless medium. **Michael Propp,** Adaptive Networks, Inc. (Cambridge, MA).....**349**

Wireless options abound. **Wayne Stargardt,** Pinpoint Communications, Inc. (Dallas, TX).....**358**

An integrated power-amplifier/switch solution for 1.9-GHz personal communicators. **Tom Schiltz, Bill Backwith, and Anju Kapur,** Motorola Communications, Semiconductor Products Division (Tempe, AZ); **Jean-Baptiste Verdier,** Motorola Semiconducteurs S.A. (Toulouse, France).....**363**

Mobile communications: High-frequency parts for GSM, PCN, DECT, and other systems, with special focus on GaAs MMICs and small-signal semiconductors. **Ludwig Scharf and Jorg Lutzner,** Siemens AG, Semiconductor Group (Munich, Germany).....**370**

An improved PLL design method without ω_0 and ζ . **Morris Smith,** Motorola, Inc., MOS Digital/Analog IC Division (Austin, TX).....**381**

Phase-prediction digital synthesizer for mobile communications. **Young J. Jung and Young O. Park,** Mobile Communications Technology Division, Electronics and Telecommunications Research Institute (Daejeon, Republic of Korea).....**400**

The AC Powerline as a Wireless Medium

Michael Propp
Adaptive Networks, Inc.
P.O. Box 1020, Kendall Square Branch
Cambridge, MA 02142, USA
Tel: (617) 497-5150

Abstract

The AC Powerline has long been recognized as a wireless medium potentially offering communications connectivity within a building, but in the past its use has been precluded by the seemingly insurmountable difficulties of receiving data corrupted by powerline noise and attenuation. By understanding these obstacles, reliable powerline communications becomes possible, providing simple, low-cost, easily installable connections to a medium already used for AC power.

Advances in the technology have enabled highly-integrated chip set implementations and applications with substantial information transfer, for example, point-of-sale or telephony.

In-Building Wireless Communications

The proliferation of intelligent devices has increased the demand for cost-effective means of communication among these devices, distributed throughout a building and dependent upon shared information for proper operation. Examples of applications include energy management, material handling, building automation, point-of-sale transaction processing, automated meter reading, lighting controls, and security and access control.

The common key requirement of these systems is the need for data communications connectivity within buildings, requiring the frequent transfer of short messages at data rates between 10 and 100 kilobits per second (kbps), rather than the transfer of large files at megabit per second data rates.

The installation of networked systems has been hindered by the costs, delays, inconvenience, and complexities of installing communications wiring and cabling, particularly in existing buildings. These installation problems include scheduling delays, dislocations during installation, asbestos regulations, preserving building appearances, and the logistics of allocating installation personnel. Installing communications wiring can account for up to 60% of the total cost of installing a network. Furthermore, with installed cabling, the network is neither flexible, reconfigurable, nor easily expandable.

Wireless communications, including both radio-frequency (RF) and powerline communications, is an alternative. In building-wide wireless communications where the communications environment suffers from interference and signal attenuation, even if a system is successfully installed, the changing characteristics of these impairments can render the system inoperative. The baffled user knows only one fact: the system does not work. Clearly the underlying technology must be robust and reliable enough to handle its intended environment.

RF communications, while offering a measure of convenience, can be expensive and, in an indoor environment, can be subject to interference and signal fadeout that limit range and achievable error rates. An alternative existing medium which is present in all buildings is the AC electrical wiring. Buildings and building complexes already have comprehensive, flexible, and accessible networks in place in the form of existing AC powerlines and most, if not all, electronic devices are already plugged into the AC grid. Clearly, given a technology for reliable network communications over powerlines, one would have a solution for such environments offering universal access and minimal installation time and cost.

The AC powerline has long been recognized as a possible wireless alternative, but in the past its use has been precluded by the seemingly insurmountable difficulties of receiving data corrupted by powerline noise and attenuation. By understanding these obstacles, new approaches make reliable powerline communications possible, providing simple, low-cost, easily-installable connections to a medium already used for AC power.

The Powerline Communications Architecture

A hierarchical design is central to a robust and reliable powerline communications technology. Each level of the design is optimized specifically to overcome the inhospitable characteristics of the powerline environment.

Both substantial noise and frequency-dependent signal attenuation are found on almost every powerline. Unlike dedicated wiring, without well-designed error control coding, bit errors will occur at unacceptably high rates. Actual error-free data throughput is always a fraction of the raw data rate.

The key features necessary to provide immunity from powerline attenuation and noise are spread spectrum wideband modulation, fast synchronization, adaptive equalization, error control coding, and powerline-optimized network protocols.

Chip sets developed by Adaptive Networks incorporate these essential features to provide reliable powerline communications at a 10^{-9} error rate, an error rate that is equivalent to that of dedicated wire. The AN192 Chip Set, with a raw data rate of 134.4 kbps and a 19.2 kbps throughput, consists of the PLC192 Powerline Physical Layer Controller and the DLP Datalink Layer and Application Processor. A high level of integration allows the design of a powerline communications subsystem into products on a small section of a printed circuit board with minimal external components (Figure 1).

The chip set implements the Physical and Data Link layers of the ISO Open Systems Interconnection (OSI) Reference Model. Often, the OSI Reference Model is implemented as an abbreviated three-layer communications architecture which is easily implemented using the chip set (Figure 2). The PLC192 implements the physical layer and the DLP implements the data link and higher layers.

A Powerline Physical Layer

In the past, efforts to use powerlines for communication utilized modems to modulate a carrier frequency of between 50 and 500 kHz using frequency shift keying (FSK) or amplitude shift keying (ASK). Experience has shown that such powerline communication modems require constant tuning or become inoperable when electrical devices are plugged into or unplugged from the electrical network.

In general, a spread spectrum system will exhibit improved noise immunity over narrowband systems on the powerline. However, using the traditional spread spectrum approaches (direct sequence, frequency hopping, chirp) does not solve the difficulty of signal synchronization on the powerline in the presence of constantly-changing noise and frequency-dependent attenuation.

Adaptive Networks' approach is based upon a unique physical layer spread spectrum technology that provides very rapid synchronization. Rapid synchronization is an important component of a fast, practical, and reliable powerline communications system and is achieved in an adaptive detection process. In the protocol, data is transmitted in short frames. The PLC192 Powerline Physical Layer Controller quickly detects the start of a frame followed by a fast verification process which eliminates the possibility of a false detection. The high raw data rate of the physical layer is sufficient to implement protocol messages in single frames.

Another important component of a reliable and robust spread spectrum powerline communications system is a method of rapid equalization of the received signal even in the presence of frequency-dependent noise and attenuation.

The PLC192 is a digitally-controlled analog chip which implements the powerline transceiver functions using both analog and digital signal processing to provide patented adaptive spread spectrum synchronization, equalization, and modulation/demodulation functions. The chip can transmit and receive on two independent powerline paths.

The Powerline Reliable Low Level Link Protocol

Several key features of a data link layer are required for reliable operation of large, multi-node networks on the powerline:

- decomposition of larger packets to powerline frames to create reliable communications
- rigorous error correction and detection
- effective adaptive equalization
- reliable transfer of control

Only a certain amount of contiguous information can be sent before it is almost a certainty that a transmission will be corrupted. This suggests a requirement for transmissions of short frames on the powerline. To further ensure the integrity of any frame of data, it is necessary to use both error correcting and detecting codes, forward error correction to minimize the number of retransmissions, and error detection to know if there is a need for a retransmission on a frame basis. Each frame should be acknowledged by the receiver before the transmission proceeds to the next frame. To implement this low-level link protocol, the higher level packet is broken up into such short frames.

Another benefit of the low-level link protocol is the effectiveness of adaptive equalization. Powerline conditions can change on the order of a few milliseconds, and the receiver must be able to adapt to these changing conditions. Using a low-

level link protocol built upon short frames, the receiver can adapt on a frame basis and, because acknowledgments are required, no information is lost.

Using forward error correction (FEC) and automatic repeat request (ARQ) developed specifically for the powerline environment, the AN192CS transfers data with an effective throughput of 19.2 kbps at an error rate of 10^{-9} , using a raw data rate of 134.4 kbps. This provides both the required reliability and bandwidth.

Powerline Token Passing Media Access Control Sublayer

To provide reliable multi-access network communications, Adaptive Networks developed a noise-immune token passing protocol. For example, transfer of the token between nodes is done via a three-way handshake ensuring a transfer of control without loss of the token.

Different media access algorithms have been demonstrated on dedicated wire. The algorithms are generally based on either a carrier sense technique or token passing. However, results for other media are not transferable to the powerline.

Token passing is uniquely suited to the powerline medium for the following reasons:

- (1) There is only one token holder at any point in time. A reliable three-way handshake is used to transfer the token between nodes. This ensures an orderly transfer of control without loss of the token.
- (2) In token passing schemes, nodes cannot transmit unless they hold the token. Therefore there is no possibility of nodes starting to transmit in the midst of another node's transmission.
- (3) Token passing allows for deterministic access to the network under heavy loads. In fact, one can predict the maximum time required to access the network from the maximum number of nodes in the logical ring. Similarly, one can predict the maximum time required for a response to an interrogation.
- (4) Each node on the logical ring, and, when applicable, each subnetwork, receives a fair share of the network bandwidth.
- (5) The failure of a node on the logical ring can be easily detected without additional overhead.
- (6) The architecture allows arbitrary mixes of intelligent and dumb nodes. A token passing logical ring can be formed only of the intelligent nodes, with the dumb nodes granted access to the network by the nodes on the logical ring. This provides for a simple and straightforward implementation of request-response interaction.
- (7) The transmitting node can determine if the destination node is on the network, without resorting to detection at a higher layer in the protocol stack.

The DLP Data Link Layer and Applications Processor is a network processor and microcontroller that provides the powerline-optimized low level link protocol and media access control sublayer, with serial and parallel interfaces to standard application protocols.

Network Architectures

A communications architecture specific to control and monitoring and transaction processing networks best fits the user's requirements. The wrong network standard, such as one for a high-speed computer-to-computer file transfer network, can be a Procrustean bed, for which the user must alter existing protocols already successfully in use. However, there are well-suited standard communications protocols. These protocols fall into three communications architectures which meet most requirements, as described below and shown in Figure 3.

Transparent Multiple Serial Links

A distributed system often simply consists of dedicated RS-232 serial connections between devices. Such configurations of multiple serial connections are best handled transparently to the network user, such that each attached device "thinks" it is attached to an RS-232 serial cable.

Single Master, Multiple Slaves

Many control and monitoring systems consist of a number of sensors, scanners and actuators controlled by a single intelligent node. In such single-master, multiple-slave networks a simple software driver usually resides on the host computer. The monitoring and control devices support either a minimal driver or require a transparent serial interface to the communications hardware. We have found such a communications architecture can be implemented with a command-response master-slave network. In a command-response network, the master node initiates all communications and the slave nodes respond to the master over a transparent serial interface.

General Command Set

There is no single user network architecture which is suitable for all applications. Sometimes the user may need to configure the network from the host devices, at the link level.

In the most general configuration, a network can consist of a token-passing loop of master nodes that each control associated groups of slave nodes. Control of the medium access functions can be left to the host without creating a communications bottleneck. Furthermore, the network can then be dynamically configured to handle changing loads and uses.

Applications of Powerline Communications

Powerline communications technology, as implemented by Adaptive Networks, has been proven in the field in a broad group of applications worldwide. It is the high data rate standard for communications aboard refrigerated container ships as selected by the International Standards Organization (ISO) and has been designed to comply with international standards such as IEC TC57 Distribution Automation using Distribution Line Carrier Systems. The AN192 technology has similarly found acceptance in applications such as point-of-sale (POS) networks, vending machine monitoring, utility telemetering, automated storage and retrieval, security access control, public transit vehicles, residential LANs, and factory automation.

In the point-of-sale retail market - particularly in department stores and discount houses - there is a need for mobile "plug and play" registers and terminals. Powerline communications allow terminals to access the network anywhere in the store where there is an AC wall or floor outlet rather than being limited to a fixed cable position.

Powerline communications enable companies that service vending machines to track the flow of products sold in the machines and to monitor the operational status of those machines on a real-time basis throughout the local area of a building or campus. By connecting each local area powerline network to a wide area radio or telephone network, status can be monitored throughout a region. Machines can be efficiently supplied and usage evaluated in real-time.

In a future application, the powerline can be used as an alternative medium to allow access to homes and businesses for providers of "information highway" services, such as telephony.

Summary

A powerline communications chip set provides a cable-free alternative to dedicated wiring for distributed systems communications in both control and monitoring and general data transfer applications. Using innovative spread spectrum technology and networking protocols, the AN192 Chip Set can reliably network digital devices over electrical powerlines, eliminating the high cost and inconvenience of wire installation, and enabling easy relocation of devices connected to the network.

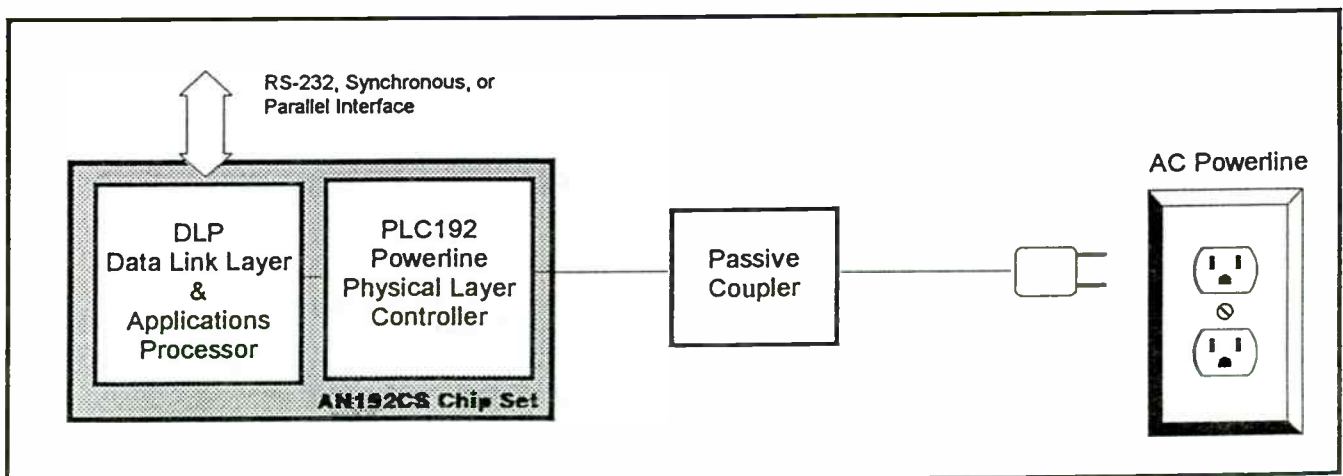


Figure 1 AN192 Powerline Communications Node Block Diagram

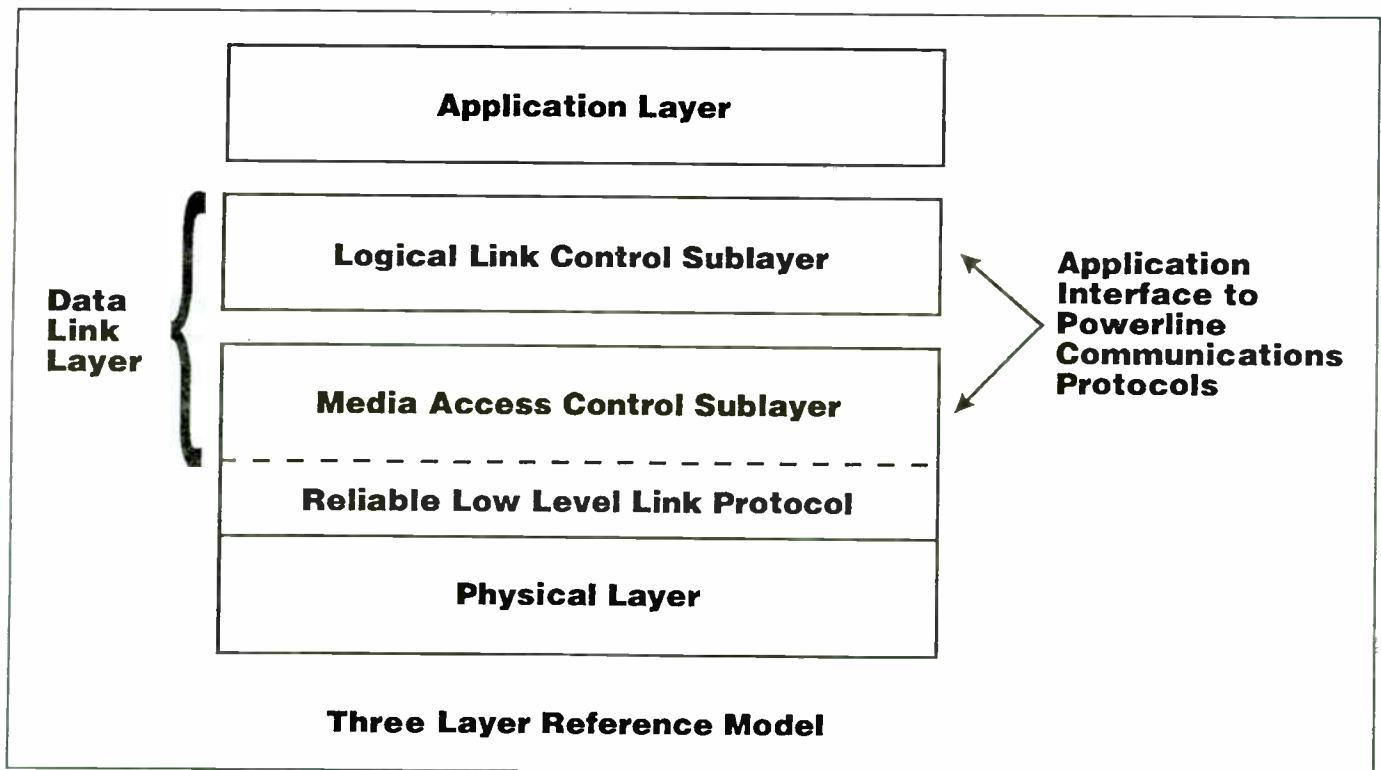


Figure 2 Three Layer Powerline Communications Architecture

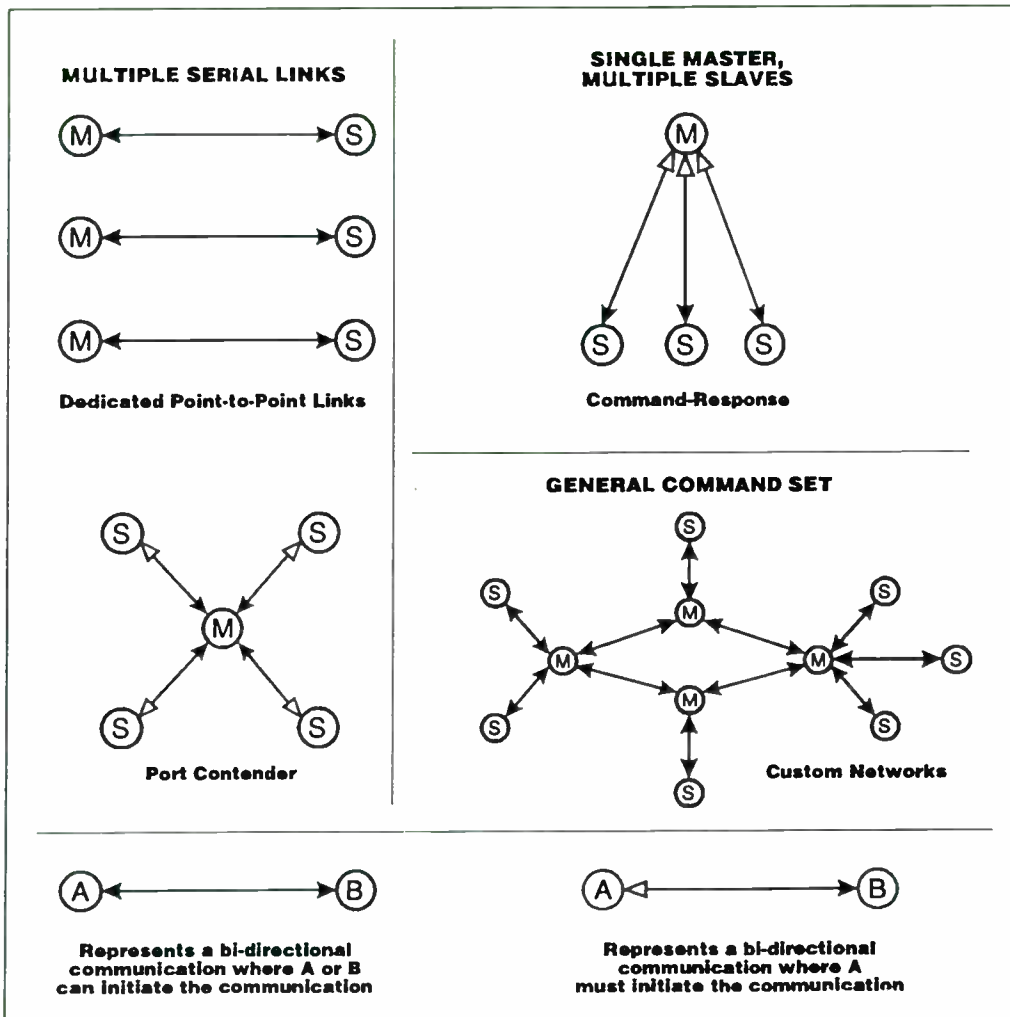


Figure 3 Network Architectures of the AN192

Wireless Options Abound

by Wayne Stargardt, vice president, marketing
Pinpoint Communications, Inc.

Park Central VII
12750 Merit Drive, Suite 800, LB 20
Dallas, TX 75251

One of the attractive emerging technologies is wireless data communications. Wireless data offers the potential to extend the corporate enterprise, bring mobile workers into the network fold and ostensibly change the way business is done.

However, incorporating wireless data communications into a corporate information infrastructure may be more complex than most think. Potential users will first need to select the wireless communications technology appropriate for their application. Then they will need to select the specific network service provider. Finally, they will need to adapt their application to make it cost effective and appropriate to the wireless environment. What early adopters of this technology should consider is that wireless data is categorized into three network types: wide area networks (WANs), metropolitan area networks (MANs) and local area networks (LANs.)

The coverage of a wide area network is generally ubiquitous and far-reaching, over land and water. A WAN is based on infrastructure that is extraterrestrial in nature, and may use geosynchronous earth orbit (GEO) satellites, for example. Metropolitan area networks are concentrated in regions of high population or usage and are based on a terrestrial infrastructure, such as cellular telephone or private land mobile radio. LANs usually involve no infrastructure and use some form of radio, such as microwave, to communicate directly from one device to another within a building or a campus environment.

Wireless MANs have become the area of strong interest and activity because they serve a large number of people and applications, they offer good price/performance, and the technology and associated services are improving rapidly.

Application Requirements

Potential applications for wireless data communications vary broadly and place vastly different requirements on the wireless network. To

compound complexity, most potential users underestimate how many different wireless technologies exist and how much they differ in functionality, performance and price. There is no one single wireless data network that is the best for all applications. So users will have to choose a wireless network carefully, and that choice must be driven by the requirements of a company's specific application.

When exploring wireless MANs, an application-driven needs assessment should include asking questions such as: Which information is worth getting quickly? With which locations do we wish to communicate and under what conditions? Which mobile devices should be connected into the network? Which applications, data bases and networks do mobile users need to access?

Application v. Adoption

With the potential for so many applications and wide-spread benefits, what's preventing broader adoption of wireless MANs today? According to Deloitte & Touche, barriers in the minds of potential adopters include, in order of significance: expense of service, lack of coverage, expense of equipment and transmission quality. Less frequently mentioned reasons for not implementing wireless communications are technology obsolescence, battery limitations and network capacity.

Coverage is a concern that is only addressed over time as terrestrial networks are deployed. But corporations looking for a national wireless MAN service face a paradoxical challenge. Wireless communications technologies are changing rapidly, but deployment of a wireless network can take years. During those years, technology races ahead and by the time a network has been built out nationally, the technology it is based on is being eclipsed by newer, emerging technologies.

An example of technology racing ahead of deployment in cellular telephone is the migration from analog cellular to digital and later to PCS. The

largest public packet data network, ARDIS™, is receiving competition from RAM Mobile Data, and the future cellular digital packet data (CDPD) technology threatens both. Paging is moving toward two-way capability and specialized mobile radio is going digital. So where does one begin in evaluating Wireless MANs?

What's real?

Again, the wireless data technology selection should be appropriate for the application. This means forcing service providers to present their technology as it relates to your application. Selecting the best service provider for your application will mean evaluating alternatives in five areas: equipment cost, operating cost, coverage, functionality and communications interfaces.

Available Wireless Data Technologies

From LANs, to MANs to WANs, there a number of options for wireless data service. In the area of metropolitan area network technologies, there are five basic categories: land mobile radio, cellular telephone, paging, Part 15 and PCS. Each category operates with an allocated amount of spectrum, which directly correlates to capacity. Some technologies, such as paging, operate with a limited amount of spectrum, making large-scale data communications applications difficult to broadly deploy due to capacity constraints.

Land Mobile Radio

It's important to look at how land mobile radio is defined. It generally is divided into two categories: voice radio and packet data radio. Voice radio can be subdivided as channel oriented or trunked. Trunked radio is further categorized private or Specialized Mobile Radio (SMR). Land mobile radio, with about 17 million subscribers, is gaining about 10 percent in subscriber growth annually, which includes voice. It is allocated 85 MHz of spectrum.

The high-growth arena is packet data radio. Packet data radio currently has 60,000 subscribers and is growing 30 percent annually. Packet data radio is allocated only slightly more than 1 MHz of bandwidth, implying that it may be capacity constrained in the future. And while many companies are vying for position in this market, to date only

narrow band options have been available — either channel-oriented or SMR. A broadband network would increase the capacity of private land mobile radio technology.

A promising variation of private land mobile radio technology is a broadband radio-location network with inherent wireless data communications capabilities, such as that which Pinpoint Communications, Inc. is deploying.

Cellular Telephone

Cellular telephone is growing at a rate of 45 percent annually, with about 14 million subscribers today. It is allocated 50 MHz of spectrum. Cellular employs several concurrent methods to increase overall network capacity by permitting subscribers to share spectrum. These spectrum sharing technologies include frequency division, spatial division, time division and code division. Frequency division assigns a separate channel (frequency pair) for each call, which is also the primary approach of land mobile radio. Spatial division is a significant innovation of cellular. It re-uses channels by limiting cell propagation areas. Further, cells are subdivided with sector antennas and hand-offs occur between cells or sectors. The third means of spectrum sharing is time division, in which calls are assigned to different time slots in the channel. An alternative third method of spectrum sharing is code division, which digitally encodes/decodes speech and, with a unique code, converts it to a spread spectrum signal. Calls with different codes share a broadband channel.

Even with multiple ways to use spectrum more effectively, cellular has significant difficulty achieving the data communications efficiencies of a packet data network because it is a circuit switched architecture. Except when transmitting very large volumes of data, the cost and delay in setting up the circuit connection and synchronizing the modems makes cellular's expense and performance inappropriate for many applications. Many cellular service providers hope to solve this problem by overlaying a packet data technology, such as CDPD, on their networks.

Paging

Paging is a growing market, with a subscriber base of more than 15 million, increasing

about 25 percent annually. Paging companies operate with 3 MHz of allocated spectrum. It is a public network using digital signaling, its connection is packet-switched and it time shares spectrum. Paging provides no interconnect for the public switched telephone network (PSTN) and today is only one-way. Paging, however, is undergoing tremendous change in moving from one-way communication to two-way. It will be an interesting option for data only, however capacity constraints and the fact that there is no added value, such as radio-location, will limit its ability to serve broader markets.

Part 15

Part 15 networks operate as low-priority users in the industrial/scientific/medical (ISM) bands and are subject to interference from other operators in the band without recourse. They are private, digital packet-oriented networks with two-way directionality. Some networks do offer interconnectivity to the PSTN and Part 15's technique for spectrum sharing is the code division multiple access (CDMA) technique of spread spectrum radio.

PCS

Much is left to be defined about PCS. It will have many network operators and has been allocated 120 MHz of spectrum. It will be a two-way public, circuit-switched network with digital signaling. It will be linked with the PSTN, yet much is to be determined about spectrum sharing.

Functionality considerations

While the way a technology uses spectrum is important, those selecting wireless MAN networks still must consider the core set of evaluation criteria: equipment cost, operating cost, coverage, functionality and interfaces.

When evaluating network functionality, the specific considerations will vary for each application. In some applications, the network needs to be suitable for portable computers. Also the form factor and weight of the radio modem must be considered. Further, what is its power consumption, and what connections to the portable computer are supported?

Also, it may be important to consider whether the chosen wireless communications operate inside buildings because the application may require communicating with people who are frequently

inside. Does the application require integral or combined voice and data and does the application require this in one device? Does the application require store and forward or roaming capabilities? What is the network transmission latency or delay and is that response time important to the application? (Latency and delay can be significant with some wireless communications.) Does the application need to know the location of the mobile user, as is often the case in fleet management applications?

Statistics to Ignore

Many times numbers and statistics on wireless data can be meaningless, particularly in light of the most common applications. For example, many companies publish a price per megabyte transmitted. But on every network, the cost of sending a megabyte of data varies significantly depending on whether that data is sent all at once or sent 10 bytes at a time. In fact, the cost can vary by 10 or 100 times over such a range.

Because transaction size has such a significant impact on operating cost, companies need to evaluate the most common character-size message that their applications may place over a wireless data network. Companies with specialized or vertical applications will find the most common transaction is 100 characters or less, while companies with mobile office or other horizontal applications will find that average transaction sizes are generally thousands of characters.

Equipment and usage pricing

The mobile unit in a wireless data network has been the source of traditionally high equipment prices, ranging upwards of \$1,000 for many networks. For widespread adoption to occur, the entry price of a mobile radio should probably be well under \$500.

Further, usage charges can range from about 10 cents per packet or 25 to 40 cents a minute with cellular. In addition, there is often a monthly charge associated ranging from \$15 to \$45. Many potential users have determined that network usage costs at this level are still too high to be able to justify their application. Newer technologies offer the promise of lower equipment and usage costs, but they are not generally available today.

However, most of the more expensive, traditional service providers have widely deployed networks in place, albeit with older technology. If the selection of a wireless MAN platform is urgent, then information managers have little choice. However, if the decision rests more on a long-term return on investment, then several new, more efficient and cost effective networks will be coming on line over the next few years.

Decide Interfaces Today

In the meantime, potential wireless data network adopters should be aware that most wireless communications networks support only a limited set of communications interfaces for connecting to enterprise networks and applications. The network needs to interface to both the enterprise network and the mobile computer system. For many existing wireless networks the native interfaces are proprietary, but some standard interfaces are supported. Common enterprise network host interfaces include SNA, X.25, HDLC, TCP/IP, and others. Standard interfaces for mobile computers range from the AT command set to IEEE 802.2 to IP and others. The difficulty required to interface to the wireless network is another factor that companies must evaluate when considering a wireless data service provider.

Implications for Applications

No matter the wireless MAN technology or service provider, most information managers are strongly considering implementing wireless data communications in some form into the enterprise network. The benefits of wireless applications include having connectivity any time, any where. Mobile workers become a part of the enterprise network with access to corporate databases and on-line transaction processing capability. Further, mobility allows for source data capture and information transfer. Wireless provides for real-time access to data with the ability to broadcast data at a very low cost. The more mobility is enhanced with connectivity, the more corporate productivity increases.

The most common types of wireless applications being evaluated to make workers more productive include interactive, terminal to host communication, as with transaction processing or database queries. Mobile electronic mail is another commonly considered function that is enabled by

wireless. Wireless communications is desired to serve as a LAN extension, for example, to remote, mobile users. Uploading and downloading file transfers are another wireless application, which is often discussed. Also information broadcasts, such as news, stocks, traffic, weather or sports, are enabled by wireless.

Wireless data communications technology is being sought to enhance a broad range of specialized or vertically oriented applications. For example, a field sales force can benefit from wireless automation of facsimile or document transfer, quotation and order entry, order status or other database queries. A low-cost wireless connection also enables remote customer, product or pricing file updates.

Field service personnel can rely on wireless applications for computer-aided dispatch, service order processing, database queries for service history, parts availability, etc.

Bringing wireless into the enterprise

Extending existing enterprise applications to mobile users will be difficult. It also can be expensive due to the large volumes of data transmission that existing applications generally involve, because they were designed for much less expensive communications environments. Existing applications drive up wireless usage costs by sending unnecessary data in many ways, both large ways and small ways, such as with full English text, display formats and forms, or keystroke echoes. There will be topology difference, likely poor performance and gateway limitations. Gateways prevent transparent extension of the enterprise network and its functionality, performance and manageability are limited.

There are several alternatives that can make existing applications more compatible with wireless networks. The alternatives with the most impact are also usually the most difficult to implement. Alternatives include compression, radio-aware conversion, application modification (such as using pre-formatted data, coded communications, tables and vectors and local user display management), rewriting the application and converting to the client/server architecture.

The client/server architecture has grown to take advantage of powerful, low-cost workstations, distributed networks and graphical user interfaces.

Wireless applications benefit uniquely well from many of the properties of the client/server architectures, including the naturally limited flow of data between a mobile and host, its message-oriented architecture, and the fact that data format and user input management reside entirely within the client/mobile and the fact that poor wireless network response times can be somewhat hidden.

Wireless Data — A New Frontier

If one walks away with only one realization after exploring wireless data communications, it will be that wireless data is more complex than first imagined. The definition of the enterprise network will have to be re-examined and existing applications likely will not transition into a wireless domain.

What decision makers today need to start doing is reviewing applications and the areas in which wireless communications will give business that cutting competitive edge. Start now to transition to a client/server architecture and begin to write mobile or wireless applications based on that architecture. This will help make the transition to wireless data much smoother.

Finally, potential users should remember that wireless data will remain expensive relative to wire media networks because the market is embryonic, spectrum is scarce, new networks are expensive and the technology is still not widely used. But wireless applications are coming, as are developments in a number of supporting technologies such as portable computing hardware, off-the-shelf mobile application software, and mobile information service providers and databases all are making wireless applications more feasible and cost effective. The wireless data industry will continue to see tumultuous change as significant evolution takes place with new technologies and architectures. If a wireless MAN is not imperative today, take a deep breath, plan, prepare and delay a major decision until better price/performance technology is available.

An Integrated Power Amplifier / Switch Solution for 1.9 GHz Personal Communicators

Tom Schiltz, Bill Beckwith and Anju Kapur
Motorola Communications Semiconductor Products Division
Tempe, AZ

Jean-Baptiste Verdier
Motorola Semiconducteurs S.A.
Toulouse, France

ABSTRACT

A 3V GaAs RFIC power amplifier/antenna switch solution for 1.9 GHz cordless telephones has been developed by Motorola Semiconductor's RFIC group. The functions have been partitioned into two SOIC-16 packages for maximum performance and flexibility and minimum cost. The first IC includes a two-stage Class-AB driver with CMOS-compatible ramp circuit. The second IC integrates a class-AB power amplifier and antenna switch with CMOS-compatible control. In the transmit mode, the two-chip solution produces 26 dBm output power at the antenna port of the switch with 0 dBm input power. Typical efficiency of the three-stage PA is 55%. In the receive mode, the switch has 1 dB typical insertion loss. Application of the IC's to the European DECT and Japan PHS cordless telephones are discussed as well as measured performance under dynamic operating conditions.

I. INTRODUCTION

Manufacturers of digital cordless telephones demand highly integrated RF circuits to simplify manufacturing and improve yields. They also demand low prices to satisfy the consumer market. To the RFIC semiconductor supplier, these two requirements (high integration and low cost) present a significant challenge. The difficulty is primarily due to limitations in package technology, price, and testability.

Motorola Semiconductor's RFIC group has created an integrated power amplifier and antenna switch solution for the 1.9 GHz DECT and PHS markets that satisfies customer requirements for integration and price. The devices are implemented in Motorola's 0.7 μ m GaAs IC process [1]. The process offers enhancement, depletion, and power implant

FETs as well as MIM capacitors, spiral inductors and resistors.

II. REQUIREMENTS AND PARTITIONING

The primary goals included low-cost surface-mount packaging compatible with existing high-volume RF test handlers. The functionality was to include a 3.5V, +27 dBm power amplifier, with bias circuits, transmit burst shaping to meet the DECT requirements, and a transmit/receive (T/R) antenna switch. In addition, for ease of use and interfacing, digital control pins should be compatible with 3V CMOS logic levels.

After studying various partitioning schemes and associated cost models, the partitioning shown in Fig. 1 was selected. This partitioning, places a two-stage driver amplifier and ramp circuit in one IC. The final PA stage and antenna switch are packaged in a second IC. This scheme was determined to be most economical because it minimized total die area and utilized the low cost SOIC-16 package. Furthermore, amplifier stability was simplified because there is no more than 23 dB gain in one IC. Finally, because the PA and switch are integrated, system performance variation due to impedance variation at the PA output is minimized.

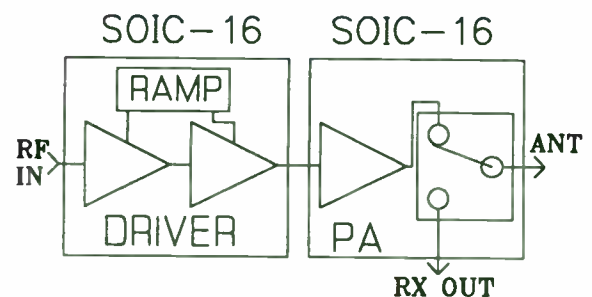


Fig. 1. Power amplifier / switch partitioning.

III. MRFIC1806 CIRCUIT DESIGN AND MEASURED PERFORMANCE

A. Description

The MRFIC1806 (1806) Driver/Ramp IC integrates a two-stage exciter amp, bias circuit, and a ramp circuit in a SOIC-16 package. A block diagram of the IC with external components for a DECT application is shown in Fig. 2. The RF input match is completed externally with a series high-impedance transmission line and a shunt 1.5 pF capacitor. The transmission line can be replaced with a 4.7 nH inductor. Drain bias for the first stage is brought in through pin 14. A shunt 22 pF capacitor at pin 14 completes the interstage match. The RF output is partially matched on the IC. The output load line is completed with a shunt 1.5 pF capacitor at pin 11. Drain bias for the second stage is applied to the RF out pin through a printed 100Ω quarter-wave choke. Capacitor C5 at the RF output is a dc block.

A positive voltage is applied to PCNTRL (pin 8) to set bias current for both stages. A typical voltage of 1.4 V sets the 1st stage at 24 mA and the second stage at 96 mA for 120 mA total. This voltage can be decreased for higher efficiency or increased for higher linearity.

The ramp circuit consists of a low-current logic translator, a power-implant FET ($V_{to} = -1.5$ V) for drain voltage ramping, two resistors and two capacitors [2]. The topology is a variation of a television horizontal sweep circuit and is discussed in the Motorola MC33128 Power Management Controller data sheet [3]. Positive bias voltage for the two-stage RF amplifier is applied to the drain of the ramp FET at VDR (pin 16). The ramp FET operates as a source follower, with the source terminal supplying drain voltage to the first and second stages of the RF amplifier at VDR (pin 16). The logic translator converts 0V / 3V CMOS logic levels at TXRAMP (pin 2) to -2.5 V / 3 V levels to operate the gate of the ramp FET. The ramp rate of the drain supply voltage at pin 16 is controlled by the value of external components C1, C2, R1 and the internal 20 kΩ resistor. The external feedback resistor, R1, controls the symmetry of the waveshape. The values for C1, C2 and R1 shown in Fig. 2 create a rise/fall time of 10 μs or slightly less to satisfy the DECT requirement. Dynamic range is typically 45 dB.

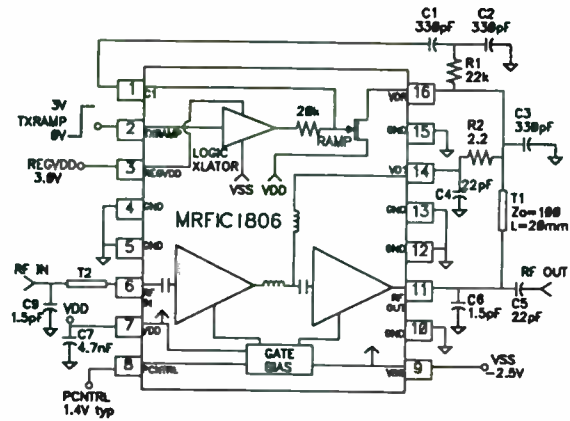


Fig. 2. MRFIC1806 Driver/Ramp IC with external components (DECT application).

B. Measured Performance

Burst-mode output power versus input power using the integrated logic translator and ramp circuit is shown in Fig. 3. As shown, an output power of 19 dBm is achieved for an input power of -3 dBm.

It is possible to get higher output power from the 1806 by disabling the internal logic translator and applying a level translated control signal to pin 1 of the IC. The level-translated signal could be derived from an external pnp transistor or an op-amp. Details of this modification are discussed in the device data sheet [4]. Burst-mode output power versus input power for this alternate configuration is also shown in Fig. 3. The saturated output power is 23 dBm and power-added efficiency is 40%.

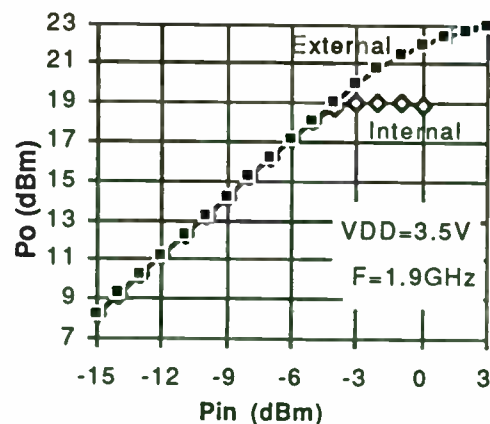


Fig. 3. MRFIC1806 burst-mode RF output power versus input power.

IV. MRFIC1807 CIRCUIT DESIGN AND MEASURED PERFORMANCE

A. Description

The MRFIC1807 (1807) combines a single-stage power amplifier and a T/R switch in a low cost SOIC-16 package. A block diagram of the IC with external components is shown in Fig. 4.

The PA, which employs a 9 mm power-implant MESFET, constitutes the third stage of the transmit lineup. The circuit has been designed to be driven by the 1806 Driver/Ramp IC. A significant part of the RF matching is accomplished by using the package inductances and integrated MIM capacitors. A special lead frame has been developed to minimize package parasitics, which are considerable at 1.9 GHz, and to decrease the thermal resistance of the package. The increased power dissipation capability permits the PA to be used in applications with duty cycles as high as 100 percent.

The input match to the PA is completed with an external shunt 2.2 pF capacitor (C1) on the RF IN pin. The VDD supply is applied to the output of the PA (open drain) through a high impedance printed quarter-wave choke (T1). The shunt 2.2 pF capacitor on the output, combined with the lead and bond-wire inductances, forms a low-pass matching network which presents the optimum load line to the device. Under nominal conditions, the PA delivers more than 27 dBm to the switch with 20 dBm input power.

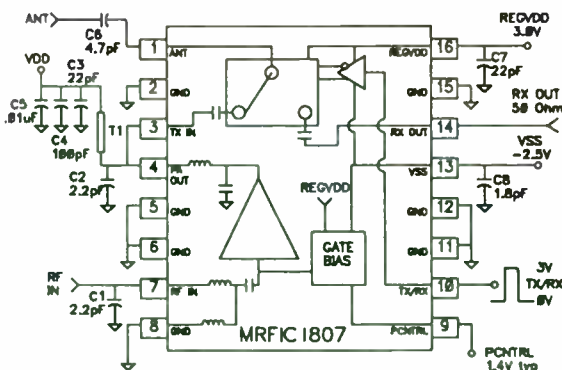


Fig. 4. MRFIC1807 PA/Switch IC with external components.

As with the 1806 Driver/Ramp, a regulated -2.5 V supply (VSS) is required for the PA bias circuit and the switch control circuits. The DC current is typically 0.5 mA in transmit mode and less than 100 μ A in receive mode. The bias circuit allows the use of a positive control voltage to set the DC current of the PA. A bias

control voltage close to 1 V results in class-AB operation, which is ideal for most DECT applications. Increasing the voltage to 2 volts sets the PA near class A, resulting in higher linearity, as required in PHS.

The functional implementation of the T/R switch is also shown in Fig. 4. The switch is a single-pole-double-throw topology. Each RF signal path is comprised of a series-shunt pair of FETs, the sizes of which have been optimized for best overall performance in the SOIC package.

Internal control circuitry facilitates the use of a single CMOS-compatible signal to select RX or TX mode of operation. Internal control circuitry makes use of the negative supply to increase the power handling capability of the switch. In TX mode, the switch is capable of handling RF power levels greater than 28 dBm.

On-chip MIM capacitors in the TX and RX paths provide DC blocking and RF matching. These capacitors are small, and their inclusion has no impact on the die size. DC blocking of the ANT port is realized with a 4.7 pF capacitor (C6).

B. Measured Performance (PA+Switch)

The TX-mode performance is illustrated in Fig. 5. The RF power level, measured at the switch antenna port (ANT), is plotted as a function of the RF power applied to the PA input (RF IN). Also shown is the DC current. For these measurements, VDD = 3.5 V, VSS = -2.5 V, REGVDD = 3 V and TXRX = 3 V. The test frequency is 1.9 GHz. PCNTL is set at 2 V. As shown, the small-signal gain is 8.2 dB. At $P_{IN} = 22$ dBm, output power is 27.2 dBm and current is 289 mA. Considering the 0.7 dB switch insertion loss (Tx-path), drain efficiency for the PA is 61% at this operating level.

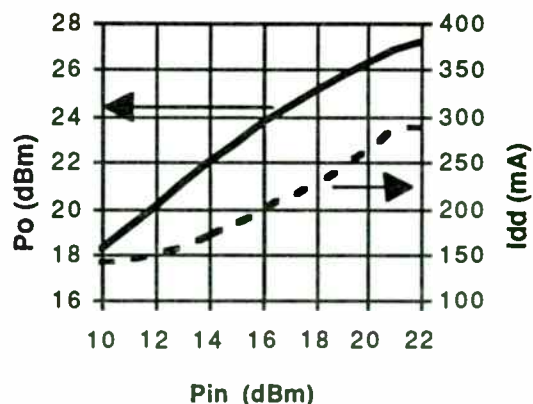


Fig. 5. MRFIC1807 TX-mode output power and supply current versus input power.

In the RX-mode, the PA supply is turned off ($V_{DD} = 0$ V) by an external battery switch and the RX path of the switch is enabled by setting $TXRX = 0$ V. Small signal behavior of the RX path is demonstrated in Fig. 6 where measured s-parameters of the switch, are plotted versus frequency. As shown in the graph, the RX insertion loss is 1 dB at 1.9 GHz. The switch is well matched, with return losses of better than 17 dB on both the RX and ANT ports.

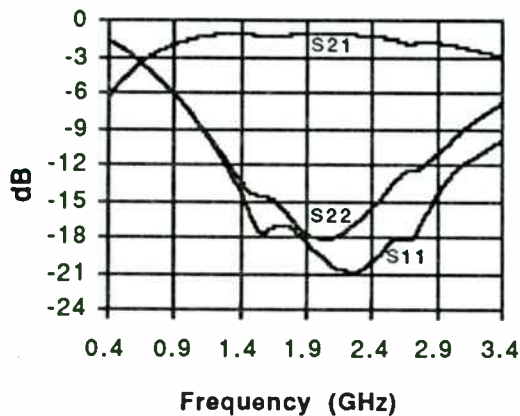


Fig. 6. Measured s-parameters of the MRFIC1807 RX path.

V. CHIP-SET APPLICATION TO DECT

A. Evaluation Board Description

A circuit board to evaluate the cascaded performance of the 1806 and 1807 for a DECT application has been developed. A complete schematic is shown in Fig. 7. In addition to the three-stage PA and T/R switch created by the 1806 and 1807, the board also includes a 900 MHz trap at the RF IN port, a low-pass filter at the ANT port, and a MOSFET battery switch. The 900 MHz trap attenuates fundamental feedthrough from a VCO and may not be required depending on the system configuration. The low-pass filter at the ANT port attenuates harmonics to satisfy the DECT specification (-30 dBm max).

In the transmit mode, the board allows evaluation of DECT system level transmitter performance specifications including:

- transmit power versus time response,
- adjacent channel interference,
- out of band emissions,
- emissions between bursts,
- supply current.

In the receive mode, T/R switch performance can be evaluated.

Two digital control lines are shown in the schematic, $TXRX$ and $TXRAMP$. $TXRX$, when high, enables the MOSFET switch which applies battery voltage to the 1806 (pin 7) and the PA in the 1807 (pin 4). $TXRX$ also places the T/R switch of the 1807 in the transmit mode. $TXRAMP$ controls the ramp circuit in the 1806. The $PCNTL$ lines for both ICs are tied together for single-point bias control.

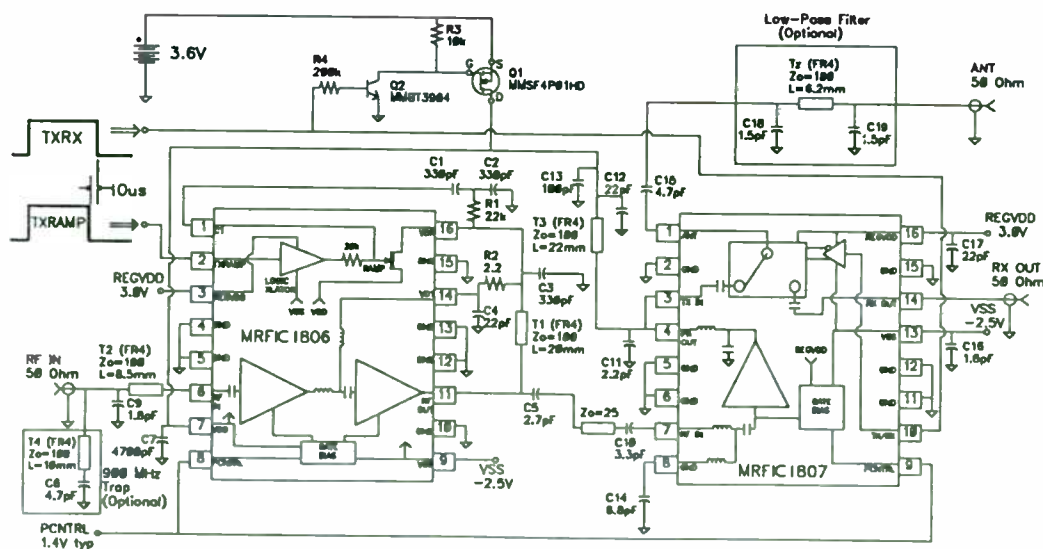


Fig. 7. 1806/1807 DECT evaluation board schematic.

B. Evaluation Board Performance

Measured small-signal performance of the DECT evaluation board in TX-mode is shown in Fig. 8. PCNTRL was set for a supply current of 300 mA. The roll-off above 2 GHz is primarily due to the low-pass filter on the board. The notch at 900 MHz is due to the 900 MHz trap at the RF IN port on the board.

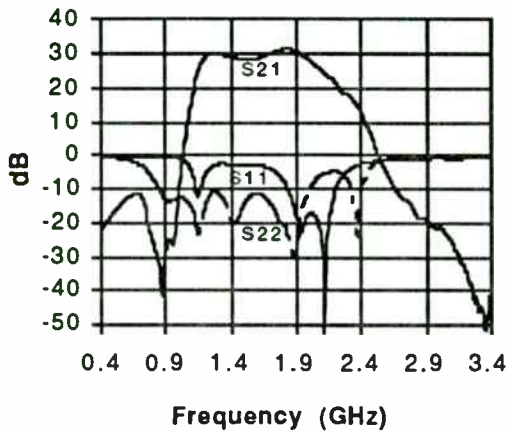


Fig. 8. DECT evaluation board TX-mode small-signal performance versus frequency.

To approximate performance in a DECT application, the evaluation board was tested with the following conditions:

- VBATT = 3.6 V,
- Freq. = 1.9 GHz,
- PIN = -3 dBm,
- TXRAMP: 10 ms period / 405 μ s pulse width,
- TXRX: 10 ms period / 415 μ s pulse width
(Duty Cycle = 1/24).

The rising edges of TXRX and TXRAMP are coincident as shown in Fig. 9. The falling edge of TXRAMP precedes the falling edge of TXRX by 10 μ s to keep the T/R switch in the transmit mode until the PA ramps down. PCNTRL was adjusted for a burst output power of 24 dBm at the ANT connector.

Output power versus time at the ANT connector is traced in Fig. 9 with the DECT specification. A spectrum analyzer set for zero-span was used for the measurement. The TXRAMP signal was used to externally trigger the spectrum analyzer sweep. As shown, the transmit power versus time response satisfies the DECT requirement.

DC supply current from VBATT was 9.5 mA. Correcting for the 1/24 duty cycle, supply current during the burst would be 228 mA. From this, "system efficiency" for the evaluation board is 30% based on 250 mW at the ANT connector and 3.6 V VBATT. Between the PA output (1807 pin 4) and the ANT connector, there is 1.4 dB of loss (switch loss + low-pass filter loss + microstrip loss). Therefore, efficiency of the three-stage PA is 42% at this operating level.

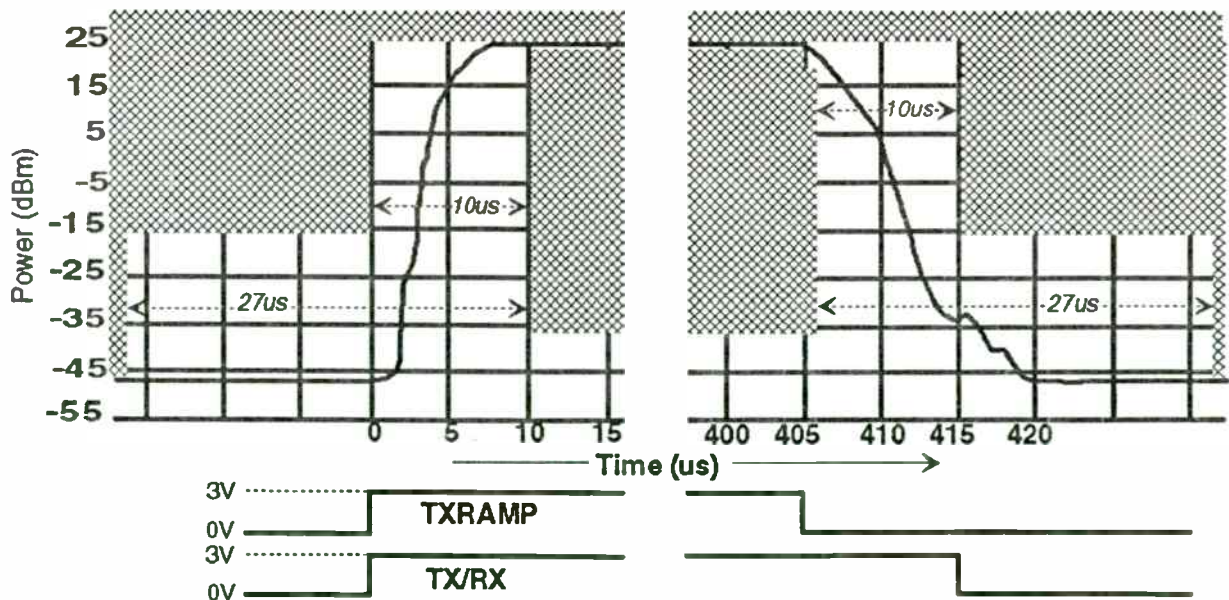


Fig. 9. 1806/1807 DECT evaluation board burst response.

VI. APPLICATION TO HIGHER POWER DECT

The burst-mode performance discussed in the previous section is a good solution for DECT applications that require up to 25.5 dBm from the 1807 output (pin 1). Some system configurations may require more power from the PA to overcome additional loss between the T/R switch and antenna connector. Such losses could be due to a band-pass filter or a diversity switch. The 1806 and 1807 are easily adapted to these systems by disabling the internal logic translator in the 1806 as described in Motorola Application Note AN1532 [5]. The simple modification which requires one resistor and a level-translated control signal for TXRAMP will allow higher RF input drive to the 1806 as shown in Fig. 3, producing 1.5 dB higher output power from the 1807 and higher efficiency.

Output power and supply current versus input power is shown in Fig. 10. As shown, saturated output power from the 1807 ANT pin is 27 dBm for 0 dBm into the 1806. Supply current is 297 mA for the three stages. Considering the 0.7 dB insertion loss of the T/R switch, PA output power is 590 mW and efficiency of the three-stage PA is 55%.

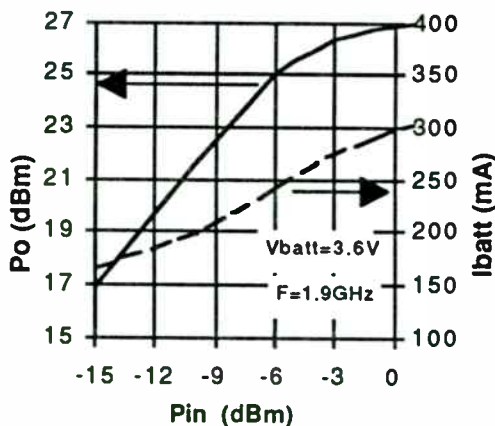


Fig. 10. 1806/1807 Output power and supply current versus input power with logic translator disabled.

VII. APPLICATION TO JAPAN PHS

For Japan PHS, transmit burst ramping is specified as two symbol periods before and after the burst. This ramping, however, is most likely implemented before the PA in the IF or baseband section to preserve linearity and limit adjacent channel power (ACP). In this application, the internal logic translator on the

1806 is disabled as discussed in the previous section. The TXRAMP signal is not required. The 1807 PA should be biased to a higher quiescent current for linearity. Therefore, two PCNTRL voltages are required: one for the 1806 and one for the 1807.

Output power and ACP versus input power for a PHS application is plotted in Fig. 11. Modulation is $\pi/4$ DQPSK with root-raised cosine filtering. The 1806 was biased to 120 mA (PCNTRL=1.4 V) and the 1807 was biased to 180 mA (PCNTRL=1.9 V) for 300 mA total. For an output power level of 21 dBm from the antenna switch, ACP at a 600 kHz offset was -61 dBc and 900 kHz ACP was -69 dBc. This provides considerable margin over the PHS system specifications of -50 dBc and -55 dBc respectively.

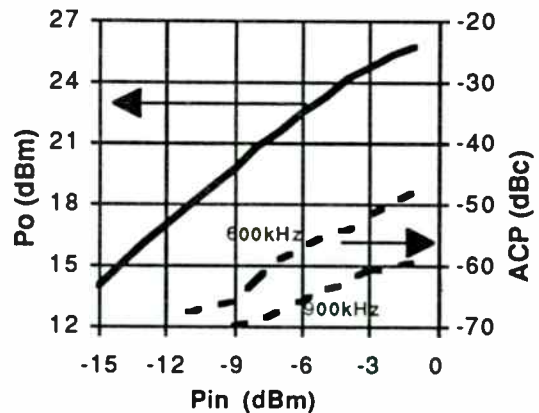


Fig. 11. 1806/1807 modulated output power and ACP versus input power - PHS application.

VIII. CONCLUSION

A low-cost two-chip solution for the DECT/PHS power amplifier switch function has been presented. The ICs have been designed for ease of use by integrating the ramping function, CMOS-compatible control, and positive voltage bias control. Compliance to the DECT and PHS system requirements has also been demonstrated.

IX. ACKNOWLEDGMENT

The authors are grateful to Andrew Schlaiss for his laboratory expertise, circuit board layouts, and constant help.

REFERENCES

- [1] P. O'Neil et al, "GaAs Integrated Circuit Fabrication at Motorola", *IEEE 1993 GaAs IC Symposium*, pp. 123 - 126.

- [2] T. Schiltz and B. Beckwith, "Integrated Logic Translator and Ramp Circuit for GaAs Power Amp," *Motorola Inc. Technical Developments*, Vol. 23, October 1994, pp. 13 - 14.

- [3] Motorola Semiconductor MC33128 Power Management Controller Data Sheet, 1994, page 6.

- [4] Motorola Semiconductor MRFIC1806 1.8GHz PA Driver/Ramp Data Sheet, 1994, pp. 3 - 5.

- [5] T. Schiltz, A. Kapur, S. Zavion, and J. Verdier, "Using the Motorola MRFIC1806/1807 Dual Demonstration Board," *Motorola Semiconductor Application Note AN1532/D*, December 1994.

Mobile Communication

High frequency parts for GSM, PCN, DECT
and other systems with special focus on
GaAs MMICs and Small Signal
Semiconductors

Jörg Lützner and Ludwig Scharf
Siemens AG Munich, Germany

Small Signal Semiconductors

HL EH

29.12.1994
WS27MBA.PPT Folie 1 / LB-A



Mobile Communication System

System	Description	Market	Region	Frequency
CT 1	Cordless Telephone	Private home	Europe (Worldwide)	900 MHz
CT 2	Cordless Telephone	Private home, telepoint	USA/HK	900 MHz
DECT	Digital European Cordless Telephone	Office building Private home Wireless LAN	Europe	1900 MHz
GSM	Global System for Mobile Communication	Business, private Handheld and carphone with international roaming	Europe (Worldwide)	900 MHz
PCN	Personal Communication Network	Private, business Handheld with international roaming	Europe	1800 MHz
D-AMPS	Digital Advanced Mobile Phone System	Private, business Handheld and carphone North America	USA	900 MHz

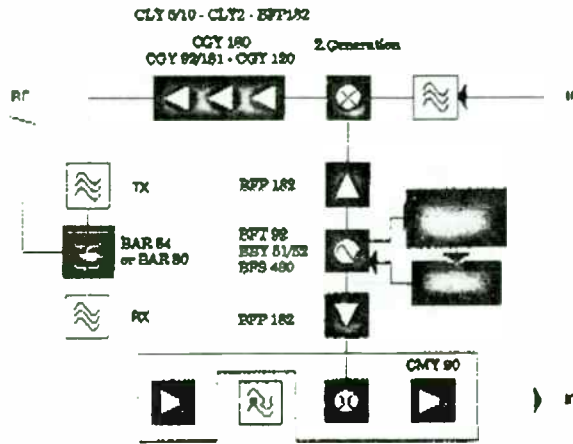
Small Signal Semiconductors

HL EH

29.12.1994
WS27MBA.PPT Folie 1 / LB-A



Principal Mobile Communication Circuitry



Small Signal Semiconductors

HL EH
28.12.1994
WERTHOLD/PTT Feb 2 / LG-2

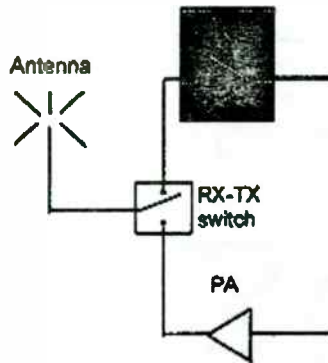
List of Priorities

- 1 COST !!
- 2 COST !!
- 3 COST !!
- 4 Performance
- 5 Power consumption
- 6 Design simplicity

Small Signal Semiconductors

HL EH
28.12.1994
WERTHOLD/PTT Feb 2 / LG-2

Low Noise Amplifier



Requirements for low noise amplifier

- Very low noise figure
- Very high gain
- Capable of high performance at or below 3V supply
- Good intermodulation performance
- Easy matching
- Low current consumption

Small Signal Semiconductors

HL EH 
25.12.1994
WESTWELPPT Folio: 9 / L8-A

LNA : Silicon or GaAs, MMIC or Discrete

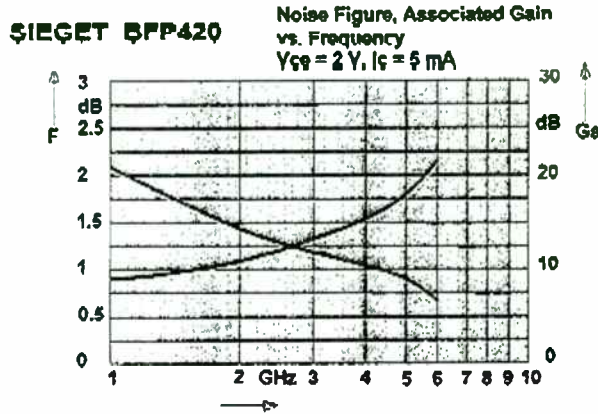
	Silicon	GaAs
Discrete	Low cost High performance Low current Easy matching	High cost High performance Low current Difficult matching
MMIC	Medium cost Medium performance High current No 3V capability Easy matching	High cost Medium performance High current Easy matching

... possible noise figure and highest possible gain are the ideal solution for cost effective, high performance LNA's.

Small Signal Semiconductors

HL EH 
25.12.1994
WESTWELPPT Folio: 9 / L8-A

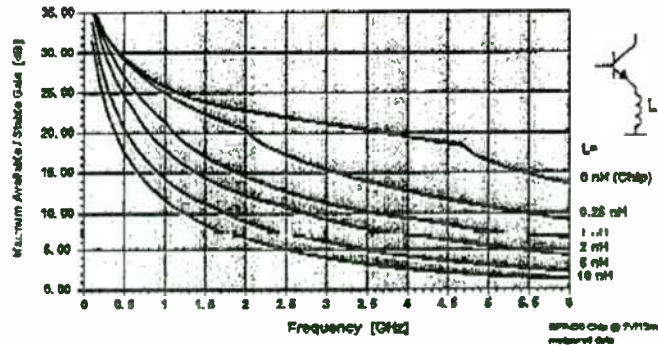
State of the Art Silicon LNA Performance



Small Signal Semiconductors



LNA : Influence of Emitter Inductance on Gain



Small Signal Semiconductors



Influence of LNA Performance on Overall System Sensitivity

Noise and gain performance of LNA is decisive for overall system sensitivity!

Approximation for fixed backend:

SENSITIVITY proportional to LNA GAIN

SENSITIVITY inversely proportional to LNA NOISE FIGURE

Performance sacrificed in the front end, cost a multiple of front end to recover in the back end.

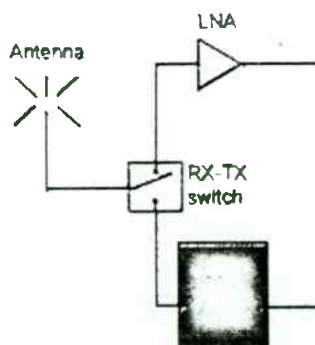
Small Signal Semiconductors

HL EH



30.01.1994
WESTINGHOUSE Corp. 9 / L6-A

Power Amplifier



- High efficiency
- Low distortion/high linearity
- High dynamic range
- Small footprint
- 3V capability
- Low consumption in switch-off mode
- Easy design
- Good back isolation

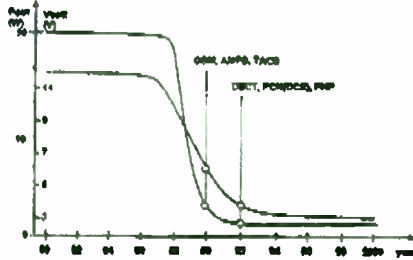
Small Signal Semiconductors

HL EH



30.01.1994
WESTINGHOUSE Corp. 9 / L6-A

Output Power and Supply Voltage -Evolution



Today state of the art is output power of 1 - 2 Watts and 3V design!

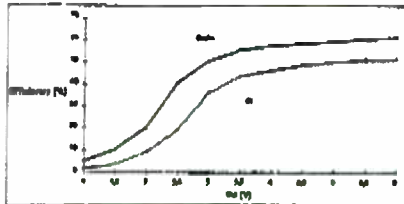
- Due to decreasing cell sizes the output power of the devices also decrease
- Smaller terminals i.e. "handies" ask for smaller battery packs leading to 3 cell designs

Small Signal Semiconductors

HL EH 

29.12.1994
WS95SYM00PPT Folio: 11 / 18-04

Efficiency...



Efficiency of GaAs vs Silicon for a mixed A/B mode

- System PAE is not equal to components PAE!
- One stage amplifiers have theoretically:
 - 77% efficiency for class C
 - 75% efficiency for class A/B
 - 50% efficiency for class A

Class C amplifiers need additional filtering at the power port, class A/B amplifiers perhaps don't!

In practice, one, two or three stage amplifiers will always have lower efficiencies than stated above.

Small Signal Semiconductors

HL EH 

29.12.1994
WS95SYM00PPT Folio: 12 / 18-04

GaAs versus Silicon for Power Amplifiers

- Is GaAs really more expensive?
 - right for the single component
 - wrong for the whole system
- Silicon is easier to match
- GaAs needs negative voltage
- Do GaAs and Silicon have comparable efficiencies?
 - No! GaAs is better if you compare correctly

There is no way to beat GaAs at 3V!

Small Signal Semiconductors

HL EH

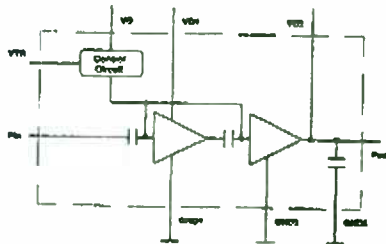


28, 02, 1994
W887288L (PPT) Pwr: 12 / Lb-A, L

SIEMENS

Wireless Symposium Feb 1995

CGY 92: GSM Power Amplifier



- 3V Data
 - Power Gain 22 dB
 - Output Power 31.5 dBm
 - PAE 42 %
- 5V Data
 - Power Gain 23 dB
 - Output Power 34.5 dBm
 - PAE 36 %
- Input matched to 50 Ohm
- Simple output match

Small Signal Semiconductors

HL EH



28, 02, 1994
W887288L (PPT) Pwr: 14 / Lb-A, L

Power Amplifier Generations and Specification @ 3V

Application	Test Results					Device Selection			Device Gen/Ref
	P ₁ dBm	P ₀ dBm	PAE %	VGA	F MHz	1. Stage	2. Stage	3. Stage	
1 GSM ADC JDC	-11	32	40	Yes	890-915	BFP 183 -	CLY 2 OGY 120	CLY 10 OGY 92	SiBip; P-MESFE P-MMICs
2 DECT	-3	27	35	No	1800-1900	CLY 2 -	CLY 5 OGY 180	- -	P-MESFETs P-MMIC
3 PCN	-18	32	38	Yes	1710-1785	CP 739 -	CLY 2 OGY 120	CLY 5 OGY 181	DGFET; P-MESF P-MMICs
4 w-LAN	0	20	> 20	Yes	2400-2500	CLY 2	CLY 5 OGY 250	-	P-MESFETs P-MMIC

Small Signal Semiconductors

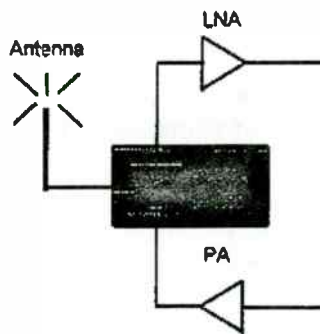
HL EH 

28.02.1994
W89786LPPD Fabr: 18 / L8-A

SIEMENS

Wireless Symposium Feb 1995

Transmit / Receive Switch



- Requirements for transmit/receive switch
- Low insertion loss between PA and antenna in transmit mode
- High isolation between PA and LNA in transmit mode
- Low insertion loss between antenna and LNA in receive mode
- High isolation between antenna and PA in receive mode
- No distortion of transmit or receive signal

Small Signal Semiconductors

HL EH 

28.02.1994
W89786LPPD Fabr: 18 / L8-A

GaAs SPDT or PIN Diode Switch for TDMA Systems ?

PIN Diode Switch

Advantages

- Low cost solution
- Very good performance
- Good design flexibility
- No negative voltage required

Disadvantage

- Requires somewhat more space than SPDT switch.

SPDT Switch

Advantages

- Little pcb space required
- Consumes no current in receive or transmit mode

Disadvantage

- Very expensive
- Negative voltage required

Conclusion: PIN diode switches offer the ideal compromise between cost and performance and thus are ideal for use as antenna switches in TDMA systems.

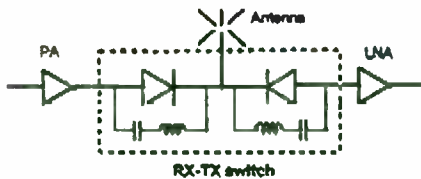
Small Signal Semiconductors

HL EH



30.11.1994
V202Y100.PPT Folio: 17 / 18-A

Series Antenna Switch



Advantages

- Requires very little space
- Simple implementation of diversity switch

Disadvantage

- Requires switching voltage at the nodes
- Consumes current in transmit and receive mode
- Tight tolerance of coils required
- Spurious can be a problem in transmit mode

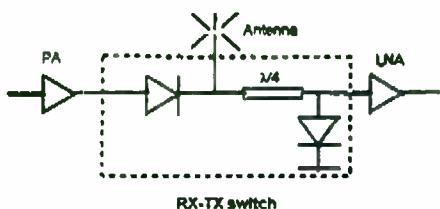
Small Signal Semiconductors

HL EH



30.11.1994
V202Y100.PPT Folio: 18 / 18-A

Series-Shunt Antenna Switch



Advantages

- Consumes no current in receive mode
- $\lambda/4$ stripline gives large flexibility in circuit design
- Requires switching voltage at only one node
- Less problems with spurious in transmit mode

Disadvantage

- $\lambda/4$ stripline can be space consuming at lower frequencies

Small Signal Semiconductors

HL EH

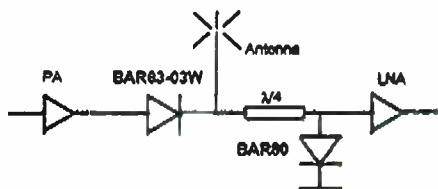


25.02.1994
W89Y186L.PPT Folio: 39 / 50-A

SIEMENS

Wireless Symposium Feb 1995

State of the Art PIN Switch Performance



Transmit mode

- TX insertion loss 0.4dB
- RX isolation 24dB

Receive mode

- RX insertion loss 0.45dB
- TX isolation 19dB

All data at 1.8GHz

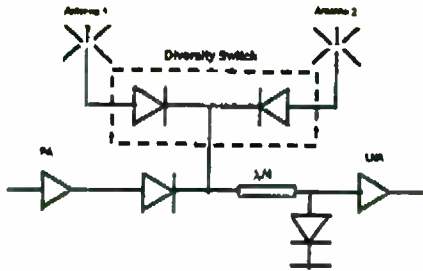
Small Signal Semiconductors

HL EH



25.02.1994
W89Y186L.PPT Folio: 39 / 50-A

Diversity Switch with PIN Diodes



Application

- Useful for decreasing multipath distortion in building environment (important for DECT)

Requirements

- Low insertion loss
- Very low signal distortion

Small Signal Semiconductors

HL EH



28.12.1994
WSP/1994, PPT/1994, P/1994

SIEMENS

Wireless Symposium Feb 1995

Summary

State of the art today:

- Receive stage with silicon LNA
- Transmit stage with GaAs power transistors or MMICs
- Diode switch systems offer best compromise between cost and performance
- Different concepts give comparable performance with different components

Market tendency - low price at acceptable performance

- System price and not part price is the key to successful and competitive design
- Customers only pay for benefits they see and need

Small Signal Semiconductors

HL EH



28.12.1994
WSP/1994, PPT/1994, P/1994

An Improved PLL Design Method Without ω_n and ζ

Morris Smith, Motorola,
Mos Digital Analog IC Division
MD F8, 3501 Ed Bluestein Blvd.
Austin, Texas 78721

Introduction

This paper is a design guide for PLL synthesizers used in wireless products. It focuses on compact, low current and low cost synthesizers. Natural frequency and damping are not used in the calculations. The topics covered are:

- a) PLL related limitations on receiver and transmitter performance.
- b) A simple measurement of charge pump spurious current at the reference frequency has been developed. It will be included on future data sheets. Formulas have been developed relating the spurious current at one reference frequency to other frequencies.
- c) Optimal loop filter component values and PLL performance where design criteria include reference modulation bandwidth, VCO modulation bandwidth, switching time, overshoot after switching time period, reference sideband level and noise within loop bandwidth.
- d) Circuit and charge pump design compromises. Also design tolerance to changes in loop gain can be determined.

Topics are divided into three sections. Section A covers system limitations and spurious current measurement. Section B is formulas and related tradeoffs. Section C is a worked out and tested example.

System Limitations and Current Measurement

Third Order Intermodulation

This is mixing in a receiver front end which causes two adjacent strong undesired signals to mix on to a weak desired signal. Intermod dynamic range is defined as the difference between noise floor and undesired signal level that causes third order products to be mixed at the noise floor level. Third order products are shown below:

Example: f = desired signal, f_1, f_2 = undesired signal
 $f_1 = f + \Delta$
 $f_2 = f + 2\Delta$
 Δ = channel spacing

3rd order product falling on f:

$$\begin{aligned}
 &= 2f_1 - f_2 \\
 &= 2(f + \Delta) - (f + 2\Delta) \\
 &= 2f + 2\Delta - f - 2\Delta \\
 &= f
 \end{aligned}$$

Phase Noise

VCO phase noise can mix with strong adjacent channel signals to cover up a weak desired signal. The level of translated noise would depend on IF filter bandwidth and VCO noise density at a one channel offset from center frequency. Phase noise dynamic range is defined as the difference between noise floor and input signal level that causes phase noise to be mixed at the noise floor level. The formula is:

$$DR_{\emptyset} = I_{\emptyset} - 10 \log B$$

- DR_{\emptyset} - Phase noise dynamic range (in dB)
- \emptyset - Phase noise power density at adjacent channel offset (in dBc/Hz)
- B - IF Bandwidth (in Hz)

Reference Sidebands

Sidebands cause the same effects as phase noise. They are however represented as a power level rather than power density. Also the product on the desired channel can be demodulated. Reference sideband dynamic range is the dB ratio between VCO carrier level and first sideband level.

Optimal Design

Optimal receiver design requires that 3rd order intermod dynamic range be equal to both the phase noise dynamic range and reference sideband dynamic range.

Signal to Noise Ratio

Signal to noise ratio in an FM or AM system can be estimated from the phase noise at the lowest offset frequency that contains information and the IF filter bandwidth.

$$SNR = I_{\emptyset} - 10 \log B, \text{ where } I_{\emptyset} = \text{phase noise at lowest offset frequency}$$

Actual signal to noise is better due to the noise decrease as offset frequency is increased. In a FM system preemphasis and deemphasis provides additional SNR improvement. A good telephone line has a SNR of 40 dB and a cassette tape is 60 dB. Digital communications need better phase noise closer in.

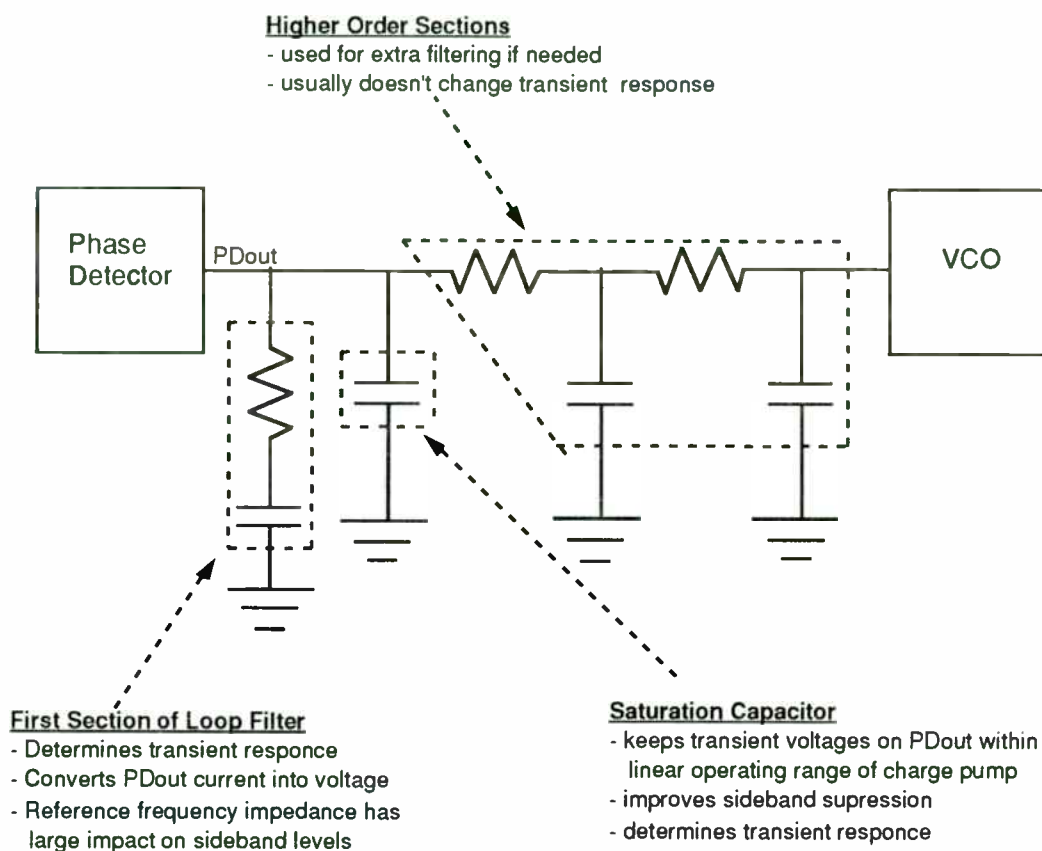
Why use a Current Source Charge Pump?

The current source charge pump has advantages over both the switching (pull up/pull down) and sample and hold types. Switching types have nonlinear gain over their output voltage range which also depends on the direction the VCO is being pulled. The output FET's have a fixed on resistance. As a supply rail is approached, current the FET supplies when turned on decreases. This effect could mean a 10:1 variation of loop gain. The current source has a constant output current over it's operating range. Sample and Hold types have a transient output pulse present when state changes from sample to hold. This moves the VCO off frequency.

Charge Pump Linearity

Pull up and pull down current must be equal for loop linearity. Current must be constant over the operating voltage range and from unit to unit over temperature. Loop gain changes proportionate to changes in charge pump current. As an example of what can happen, a 25 mS switching loop was analyzed with a reduction in loop gain of 40 %. Switching time increased to 41 mS, an increase of 64%. Transmitters which modulate the VCO or reference rely on constant current to maintain desired modulation rolloff frequencies. To reduce current consumption and noise the following filter has been widely adopted:

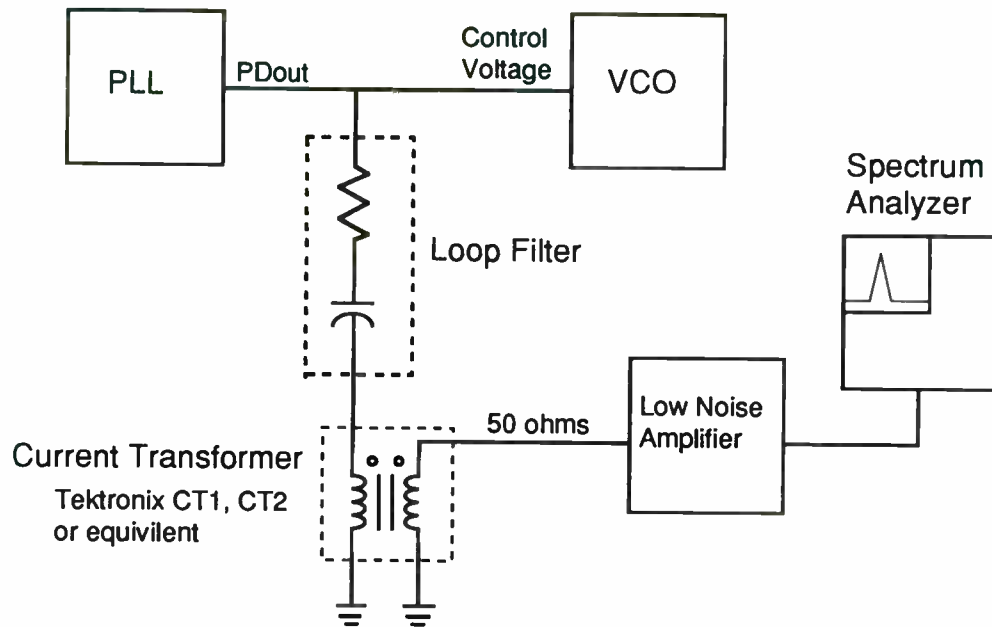
Standard Loop Filter



Spurious Current Measurement

The spurious current measured is the RMS current component at the reference frequency passing through a two element filter. The PLL must be phase locked. Current source charge pumps produce current components at least up to the 30th harmonic of reference frequency. Levels do not decline rapidly from harmonic to harmonic. Through a current probe with 50 ohm output and possibly a low noise amplifier, the Spectrum Analyzer can make a direct measurement. Many modern analyzers can convert the units of measure and add a correction factor. Try to use the current transformer with one turn through the core and increase the signal with the LNA. This will reduce the inductance in series with the loop filter. Inductance has not been a problem as long as the hole in the core isn't filled with wire. The test setup is shown on the following page:

Spurious Current Measurement



Sample measurements for the Motorola MC145190 PLL

Reference Frequency (KHz)	Current (nA)
10	1.95
20	4.5
25	11.0
50	28.4
100	141

Formula Summary for Second Order PLL

Definition of Variables

When r and c are referred to, it is the first section resistor and capacitor of the loop filter.. The loop analyzed has a second order response. Also described is a way to add additional higher order sections. All variables use base units. Bandwidth relations assume the use of optimal component values for maximum reference suppression. Log[x] is natural Log of x. Log[10,x] is base 10 Log of x. '190 and '191 are the Motorola MC145190 and MC145191 devices.

kv = VCO Gain (Radians/Second)/Volt
 kp = Phase Detector gain (Amps/Radian)
 a = kp*kv
 n = Feedback divide ratio from VCO
 t = time variable or switching time depending on formula (Seconds)
 w = frequency variable or 3dB cutoff frequency depending on formula (Radians/Second)
 r = resistor value (Ohms)
 c = capacitor value (Farads)

$$b = \text{Log}\left[\frac{\text{deviation}}{\text{tune_range}}\right]$$

deviation = Allowed frequency deviation (absolute value) from final frequency after switching time has elapsed (Hz)
 tune_range = Output Frequency Range of VCO (Hz)

Closed loop gain in S plane is:

$$\text{CG} = \frac{\text{VCO_Phase}}{\text{Reference_Phase}} = \frac{a}{n c} \frac{a r s + \frac{a}{c}}{a^2 + \frac{a r s}{n} + s^2}$$

To satisfy switching time, overshoot requirements, provide best reference suppression and lowest thermal noise, resistance r and capacitance c are:

$$r = -\left(\frac{2 n b}{a t}\right)$$

$$c = \frac{a^2}{n (b^2 + \text{Pi}^2)}$$

Normalized phase or frequency step response as a function of time (t) is:

$$nsr = 1 - \frac{\cos\left[\frac{a^{1/2} (4n - acr)^{2 1/2} t}{2 c^{1/2} n}\right]}{E \frac{(art)/(2n)}{(4n - acr)^{2 1/2}}} + \frac{a^{1/2} c^{1/2} r \sin\left[\frac{a^{1/2} (4n - acr)^{2 1/2} t}{2 c^{1/2} n}\right]}{E \frac{(art)/(2n)}{(4n - acr)^{2 1/2}}}$$

The step response gives a final value of 1 and can be scaled for any frequency step.

Impedance of the optimal loop filter as a function of radian frequency (w) is:

$$z = \frac{n \left(\frac{b^4 + 2 b^2 \pi^2 + \pi^4 + 4 b^2 t w^2}{4 t w^2} \right)^{1/2}}{a}$$

VCO Modulation Voltage

- l = RMS leakage current component at reference frequency
- lx = RMS leakage current component at highest frequency
- f = Reference Frequency
- fx = Highest reference frequency
- Vrms = RMS modulation voltage

Over at least a 10 KHz to 100 KHz reference frequency range, leakage current can be predicted from a measurement at the highest frequency. Accuracy is better than 3 dB in sideband level.

Charge pump leakage current (lx) is measured using a Tektronix CT-1 or CT-2 probe and Spectrum Analyzer. The probe is placed in the ground leg of loop filter. The Spectrum Analyzer measures RMS voltage into 50 ohms at the reference frequency. Using the probe calibration factor, current is computed. It's important that during measurement the ground lead of loop filter be connected at the point where it ordinarily

VCO Modulation Voltage con't

would be attached. Currents are in the nano-amp range and can be affected by digital circuit ground currents in other parts of the board. Leakage current is:

$$I = \left(\frac{f}{f_x} \right)^2 I_x$$

VCO modulation voltage is: $V_{rms} = I \cdot Z$

Sideband Suppression in dB's

where V_{rms} = RMS volts modulating voltage on VCO tune line
 P_{sb} = Reference sideband suppression in dB (stated as positive number)
 k_v = VCO tuning sensitivity in (radians/second)/volt
 f = Modulation (reference) frequency in Hz

$$P_{sb} = 3.01 + 20 \text{ Log}[10, f] - 20 \text{ Log}\left[10, \frac{k_v}{2 \text{ Pi}}\right] - 20 \text{ Log}[10, V_{rms}]$$

To increase sideband suppression, without changing other performance traits, an extra resistor capacitor section can be added. The corner frequency should be at 10x the closed loop gain -3 dB frequency and the resistor value should be 10x the loop filter resistor. A high resistor value helps isolate the two filter sections. On a functioning PLL it may be possible to lower both the corner frequency and resistor value. The extra section will add 20 dB/decade reference suppression above it's corner frequency.

Closed loop gain as a function of radian frequency (ω) is:

$$\text{Closed loop gain} = \frac{\text{VCO frequency deviation}}{\text{Reference frequency deviation}}$$

$$cgw = \left(\frac{n \left(b^2 + 2 b^2 \text{ Pi} + \text{Pi}^2 + 4 b^2 t^2 w^2 \right)^{1/2}}{b^4 + 2 b^2 \text{ Pi}^2 + \text{Pi}^4 + 2 b^2 t^2 w^2 - 2 \text{ Pi}^2 t^2 w^2 + t^4 w^4} \right)^{1/2}$$

DC gain is n. At Infinite frequency it is 0. For cgw in Hz make the substitution for ω ($\omega = 2 \text{ Pi} f$). When stated in dB's closed loop gain is the phase detector noise multiplication factor. In dB's:

$$cgw_{dB} = 20 * \text{Log}[10, cgw]$$

The following 3 formulas relate switching time, overshoot and the -3dB frequency of closed loop gain using an optimal filter.

The -3 dB (relative to DC) frequency is:

$$\omega = \frac{(3b^2 + \pi^2 + 2)^{1/2} (5b^4 + 4b^2\pi^2 + \pi^4)^{1/2}}{t}$$

Overshoot is:

$$b = -\frac{(-\pi^2 - 3t^2\omega^2 + 2)^{1/2}}{t\omega(2\pi^2 + 5t^2\omega^2)^{1/2}}$$

Switching time is:

$$t = \frac{(3b^2 + \pi^2 + 2)^{1/2} (5b^4 + 4b^2\pi^2 + \pi^4)^{1/2}}{\omega}$$

Modulation response as function of radian frequency (ω) is:

If modulation response is needed in Hz use $K_v/(2\pi)$ to replace K_v and ($\omega = 2\pi f$) to replace ω .

$$\text{Modulation Response} = \frac{\text{VCO frequency Change}}{\text{Control voltage change}}$$

$$mr = \frac{k_v t^2 \omega^2}{(b^4 + 2b^2\pi^2 + \pi^4 + 2b^2 t^2 \omega^2 - 2\pi^2 t^2 \omega^2 + t^4 \omega^4)^{1/2}}$$

In dB's: $mr_{dB} = 20 \cdot \text{Log}[10, mr]$

At infinite frequency $mr = k_v$ and at DC $mr = 0$

The following 3 formulas relate switching time, overshoot and the -3dB frequency of VCO modulation response using optimal filter.

The -3dB frequency is:

$$\omega = \frac{(b^2 - \pi^2 + 2)^{1/2} (b^4 + \pi^4)^{1/2}}{t}$$

Overshoot is:

$$b = -\frac{(-\pi^2 - t^2\omega^2 + 2)^{1/2}}{t\omega(2\pi^2 + t^2\omega^2)^{1/2}}$$

Switching time is:

$$t = \frac{(b^2 - \pi^2 + 2)^{1/2} (b^4 + \pi^4)^{1/2}}{\omega}$$

Charge Pump Dynamic Range

The charge pump output voltage range must cover VCO tune range, twice the overshoot and twice the voltage spikes caused by correction pulses. When switching from low to high channel or high to low channel there will be a point where correction pulses ride on top of peak overshoot. The voltage spike magnitude is given by ohms law where (i) is charge pump current and (r) is loop filter resistor. For a maximum value of r in a given circuit there is a minimum switching time.

Charge Pump Current

Increasing charge pump current will reduce thermal noise from the loop filter resistor but it won't change the minimum switching time. It will also increase the capacitor value proportionately.

Reduce Switching Time by Increasing VCO Sensitivity

The 25 mS loop given as an example, was the minimum switching time for the tuning range and VCO used with the '190 and a 8.5 volt charge pump supply. Increasing VCO sensitivity reduces switching time somewhat more than proportionately. Sideband levels would remain the same for the same switching time. This is because increasing K_v decreases loop filter resistor to exactly compensate. Noise within loop bandwidth will stay the same but thermal noise from the loop filter resistor gets worse. Thermal noise modulation voltage is proportional to Square root of r . For a 10x increase in K_v , r drops by a factor of 10 and thermal noise level increases by 10 dB. It's possible to have spurious pickup problems outside loop bandwidth with high K_v . Also maintaining Q in the VCO while increasing coupling between varicap diodes and tuned circuit and obtaining high value high tolerance loop filter capacitors can be difficult. Thermal noise will probably not be a problem in common high volume applications of PLL's.

Source Sink current match changes Switching Time

Lack of source sink match makes it difficult to achieve design values of switching time. For some value of mismatch and switching in one direction, the design value should be in between the source and sink, and closer to the one which is on for the most time. The position of the design value relative to source and sink should be inversely proportionate to the relative on times during the switching period. In the example circuit, for a low to high channel jump, the design value was 2mA, optimal source current was 1.97 mA, and sink was 2.14 mA. Measured switching time was 27.4 mS. Switching in the opposite direction took 34.3 mS. The 8.5% source sink mismatch caused worst case switching time to be 37% slower than the design value.

Effects of using step size which is submultiple of channel spacing

The same sideband suppression can be obtained with the same switching time at any submultiple step size of the channel spacing. This assumes the loop is linear. Since r is proportionate to the feedback divider ratio, the loop will only be linear for longer switching times. Thermal noise gets worse proportionate to square root of r . Noise in loop bandwidth gets a little worse over a wide range of step sizes. The '190 phase detector at 10Hz offset with 10 KHz step size had noise of -156 dB/Hz and at 100 KHz step size, it was -141 dBc/Hz. Because of noise multiplication there would be a 5 dB benefit to using the 100 KHz step size.

VCO Sensitivity change as Modulation Frequency varies

Above the -3 dB frequency of modulation response, the output frequency will deviate the same amount for the same modulation voltage regardless of modulation frequency. However the sidebands created will be greatest in magnitude at the lowest frequency. Sidebands will decline in value at a 20 dB /decade rate as modulation frequency increases. Due to the sideband slope, thermal noise if it is a problem will appear as a bump at the -3 dB frequency of modulation response.

Higher Charge Pump Supply Voltages Reduce Switching time and noise

Using a higher supply voltage on the charge pump allows correction pulses to be larger with the loop remaining linear. The loop filter resistor can increase in value. Minimum switching time can decrease. Also VCO gain (kv) could be reduced. Lower VCO gain results in less thermal noise, less tendency to pick up noise outside loop bandwidth, higher oscillator Q and smaller value tighter tolerance capacitors in loop filter.

Production Sensitivity

$$r = -\left(\frac{2nb}{at}\right)$$

$$c = \frac{at^2}{n(b^2 + \pi^2)}$$

There are two extrema of performance variation with component change. Only one need be calculated. One is:

$$n = n_{\max}; \quad a = a_{\min}; \quad r = r_{\min}; \quad c = c_{\max};$$

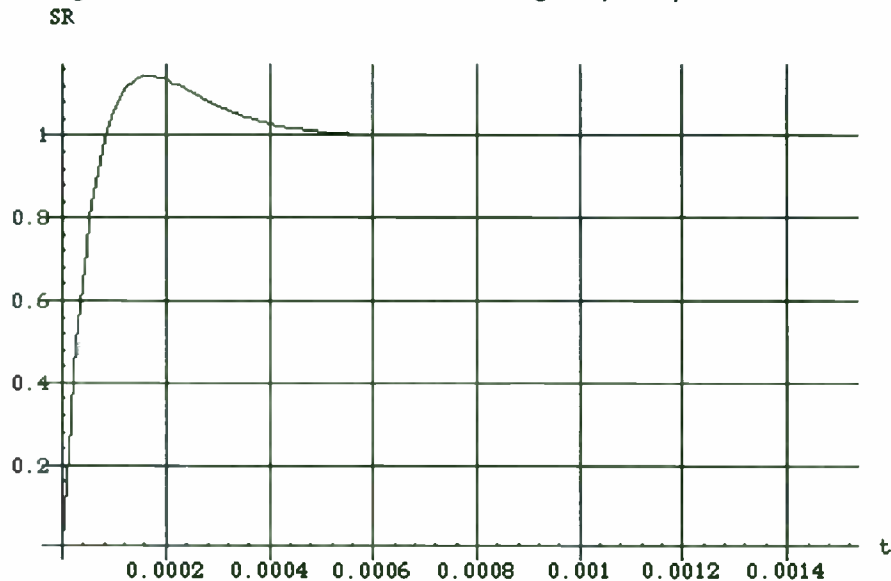
n in most applications varies by up to +/- 10 %. It isn't a problem if charge pump current can be ramped up and down (in software) to compensate (although the '190 and '191 devices presently do it in 10% steps). (a/n) ratio must be kept constant for all output frequencies. (a=kp*kv) is the major production problem. kv for a Motorola 'V17 VCO varies +/-5%. kp of the 14519X PLL's varies +/-40%. Total variation of (a) could be +/-47% using the above. A second order loop designed with a 40% tolerance of (a) had a 64% tolerance of switching time.

r can have up to 1% tolerance with 5% being standard. c can be 1% tolerance up to 5,000 pF (COG dielectric) with 5% standard. Above 5,000 pF dielectric changes to X7R which has 5% or 10% tolerance. X7R dielectric is available up to about 0.5 uF in 5% tolerance. Above 0.5 uF tantalum, polystyrene or polypropylene can be used. Polypropylene and polystyrene are too large for compact wireless circuits. The only choice left, tantalum is available only in 10% tolerance. Charge pump current should be set to keep capacitor in high tolerance range.

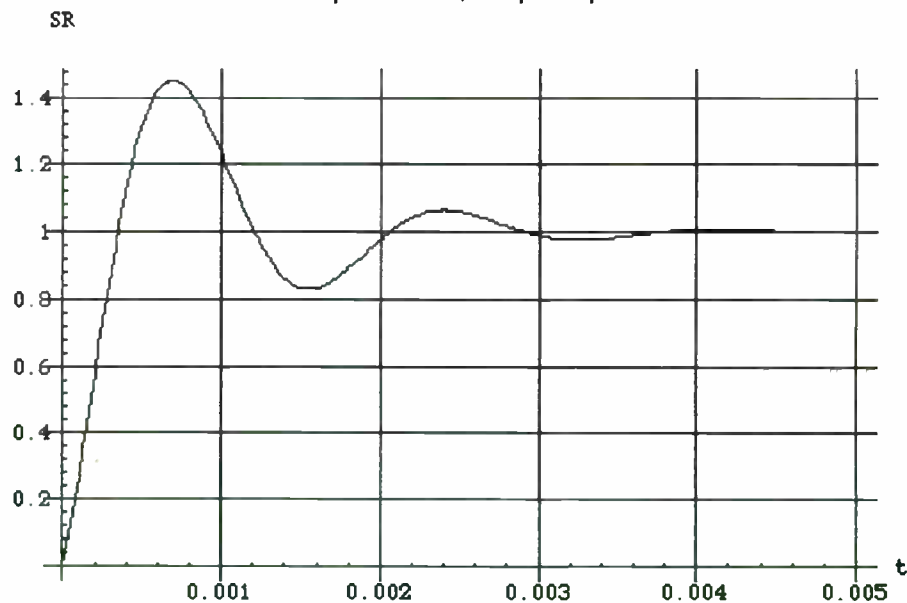
Conclusion: To build an optimal loop, high tolerance of kv and kp is needed.

Can (a) be reduced to lower sideband levels after loop lock?

A GSM loop designed for $a=6300$ has the following step response:



With all parameters the same except $a=630$, step response is:



Note that time scales for the two graphs are different!

In most instances reducing (a) upsets loop dynamics too much. Even when locked the VCO experiences disturbances ie. vibration. Overshoot can pull the PLL off frequency. Natural frequency is also much lower so response is slow.

Saturation Capacitor and extra filter sections

The values for r and c have appeared experimentally to be optimum when the saturation capacitor is added. To design the loop filter, r and c should first be selected. It is allright for the resistor to cause loop non-linearity. The saturation capacitor is added and adjusted for minimum switching time. A good initial value is 5-25% of c. Loop linearity is checked by making both small and large frequency jumps. If the loop isn't linear then the filter must be designed for a longer switching time. Extra filter sections are added to rolloff sidebands and PLL device noise but shouldn't modify transient response.

Example: PLL that switches in 25mS

The PLL uses a MC145190 chip with 2 mA of charge pump current. Thus:

$$k_p = \frac{0.002}{2 \text{ Pi}}$$

The V17 VCO we use has a sensitivity of 3.0-3.3 MHz/Volt. So converting to (radians / second) / volt:

$$k_v = 2 \text{ Pi } 3.15 \cdot 10^6 ;$$

The design constant a is: $a = k_p k_v = 6300$

The VCO operates 739.3 - 749.3 MHz. Channel spacing is 100 KHz. The median feedback divide ratio (n) is:

$$n = \frac{744.3}{0.1} = 7443 .$$

Switching time t given by system specification is 25 mS. Thus:

$$t = \frac{25}{10^3} ;$$

Frequency deviation tolerance is set at 1 KHz. Tune range is 10 MHz. b is:

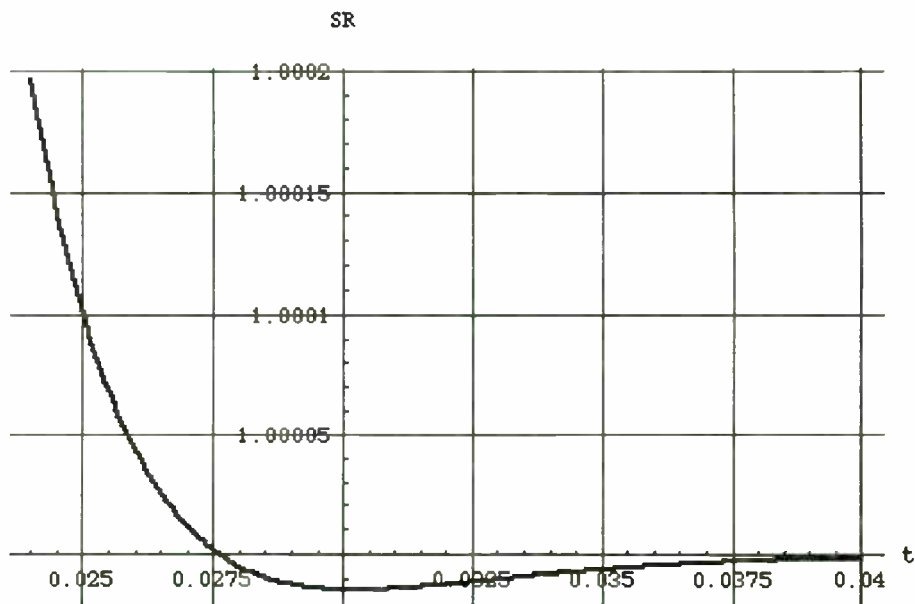
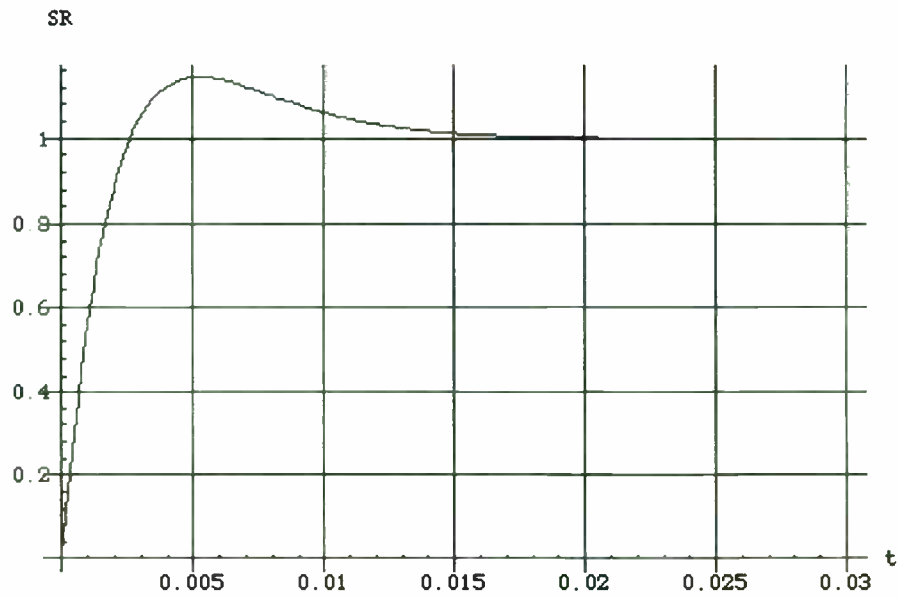
$$b = \text{Log} \left[\frac{0.001}{10} \right] = -9.21034$$

Resistor and capacitor values are:

$$r = - \left(\frac{2 n b}{a t} \right) = 870.509$$

$$c = \frac{2}{n (b^2 + \text{Pi}^2)} = 5.58628 \cdot 10^{-6}$$

Normalized step response is:



Loop filter Impedance at 100 KHz is:

$$w = 2 \text{ Pi } 10^5 ; t = \frac{25}{3 \cdot 10^3}$$

Loop filter Impedance at 100 KHz is: (con't)

$$z = \frac{n \left(\frac{b^4 + 2 b^2 \pi^2 + \pi^4 + 4 b^2 t^2 + w^2}{t^4} \right)^{1/2}}{a} = 870.509$$

VCO Modulation Voltage

l = RMS leakage current component at reference frequency

l_x = RMS leakage current component at highest frequency

f = Reference Frequency

f_x = Highest reference frequency

V_{rms} = RMS modulation voltage

Over at least a 10 KHz to 100 KHz reference frequency range, leakage current can be predicted from a measurement at the highest frequency. Accuracy is better than 3 dB in sideband level.

$$f = 100 \cdot 10^3 ; f_x = 200 \cdot 10^3 ; l_x = \frac{564}{9 \cdot 10^9}$$

$$l = \left(\frac{f}{f_x} \right)^2 l_x = 1.41 \cdot 10^{-7}$$

VCO modulation voltage is: $V_{rms} = l z = 0.000122742$

Sideband Suppression in dB's

where V_{rms} = RMS volts modulating voltage on VCO tune line

P_{sb} = Reference sideband suppression in dB (stated as positive number)

K_v = VCO tuning sensitivity in (Radians/Second)/volt

f = Modulating frequency in Hz

$$P_{sb} = 3.01 + 20 \text{ Log}[10, f] - 20 \text{ Log}\left[10, \frac{K_v}{2 \pi}\right] - 20 \text{ Log}[10, V_{rms}];$$

$$= 51.2639$$

Closed loop gain as a function of frequency

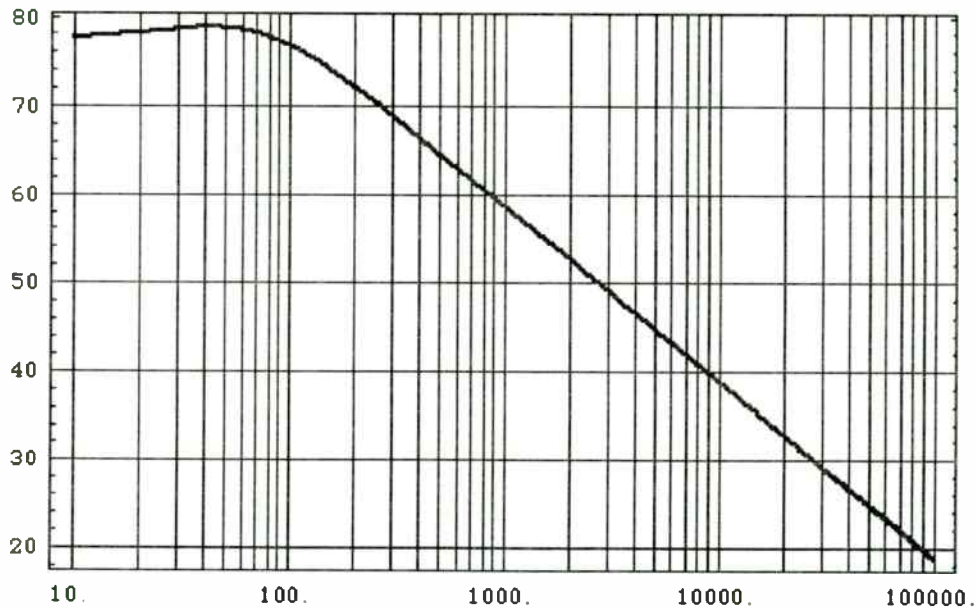
This also gives phase detector noise multiplication when stated in dB's. For ω in Hz make the substitution for ω ($\omega = 2 \pi f$).

$$\text{Closed loop gain} = \frac{\text{VCO frequency deviation}}{\text{Reference frequency deviation}}$$

$$\text{cgw} = \left(\frac{n^2 (b^2 + 2 b^2 \pi^2 + \pi^4 + 4 b^2 t^2 \omega^2)}{b^4 + 2 b^2 \pi^2 + \pi^4 + 2 b^2 t^2 \omega^2 - 2 \pi^2 t^2 \omega^2 + t^4 \omega^4} \right)^{1/2}$$

$$\text{cgw}_{\text{dB}} = 20 * \text{Log}[10, \text{cgw}];$$

Closed Loop Gain
(in dB's and Hz)



The -3dB frequency of closed loop gain is:

$$\omega = \frac{(3 b^2 + \pi^2 + 2^{1/2} (5 b^2 + 4 b^2 \pi^2 + \pi^4)^{1/2})^{1/2}}{t} = 933.956$$

$$f = \frac{\omega}{2 \pi} = 148.644$$

Modulation Response is:

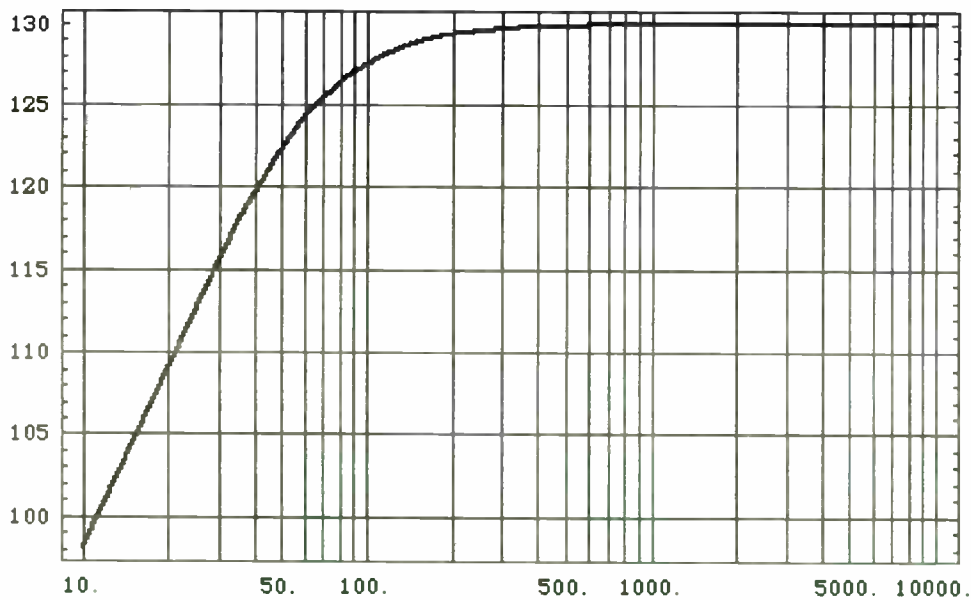
If modulation response is needed in Hz use $K_v/(2 \text{ Pi})$ to replace K_v and $(w = 2 \text{ Pi } f)$ to replace w .

$$k_v = \frac{k_v}{(2 * \text{Pi})} = 3.15 \cdot 10^6$$

$$mr = \frac{k_v^2 t^2 w^2}{(b^4 + 2 b^2 \text{Pi}^2 + \text{Pi}^4 + 2 b^2 t^2 w^2 - 2 \text{Pi}^2 t^2 w^2 + t^4 w^4)}$$

$$mr_{dB} = 20 * \text{Log}[10, mr];$$

Modulation Response
(in dB's and Hz)



The -3 dB frequency of modulation response is:

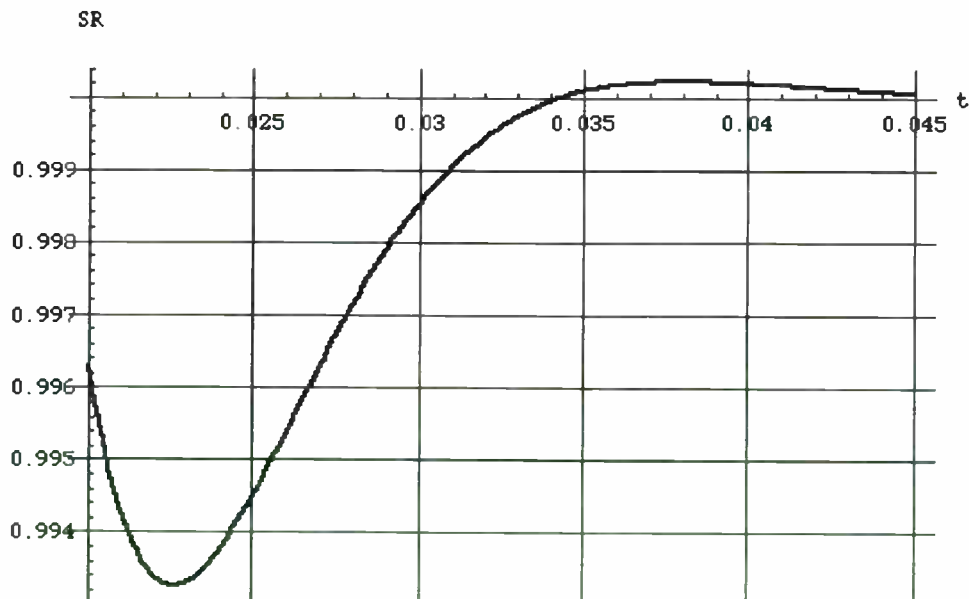
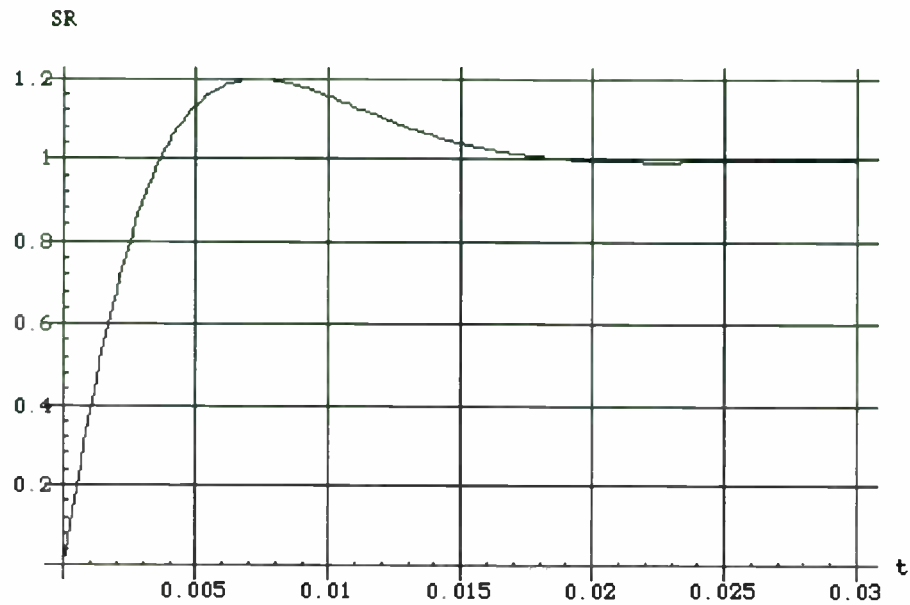
$$w = \frac{(b^2 - \text{Pi}^2 + 2 \text{Pi}^2)^{1/2} (b^4 + \text{Pi}^4)^{1/2}}{t}; \text{ where } f = \frac{w}{2 \text{ Pi}}$$

$$f = 89.0672 \text{ Hz}$$

Production Sensitivity - a tolerance only

$a = k_p \cdot k_v$ is decreased by 40% to account for charge pump current tolerance in the '190 or '191 PLL. Thus $a = 0.6 \cdot a = 3780$.

Normalized Step Response
($a = 3780$)



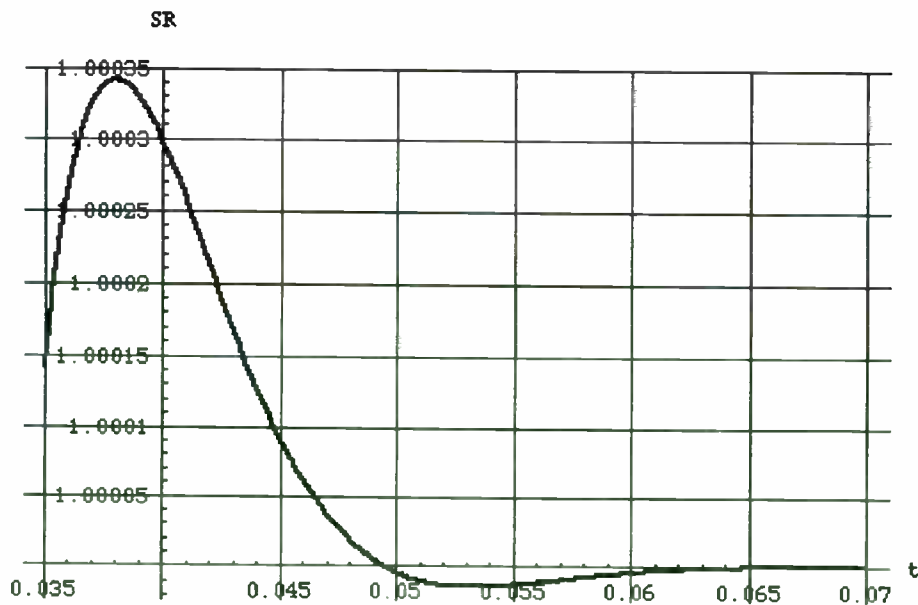
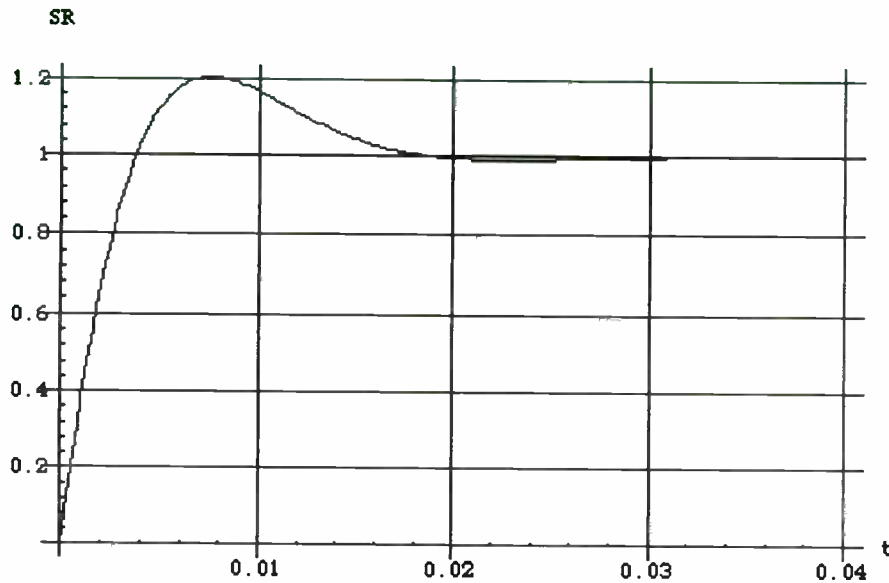
The reduction in (a) of 40% has caused switching time to change from 25 mS to 41 mS. This is an increase of 64%.

Production Sensitivity - Cumulative tolerance

a was decreased previously by 40% to account for tolerance. r and c 5% tolerances are assumed. Therefore:

$$c = 1.05 * c = 5.86559 \cdot 10^{-6}, \quad r = 0.95 * r = 826.983$$

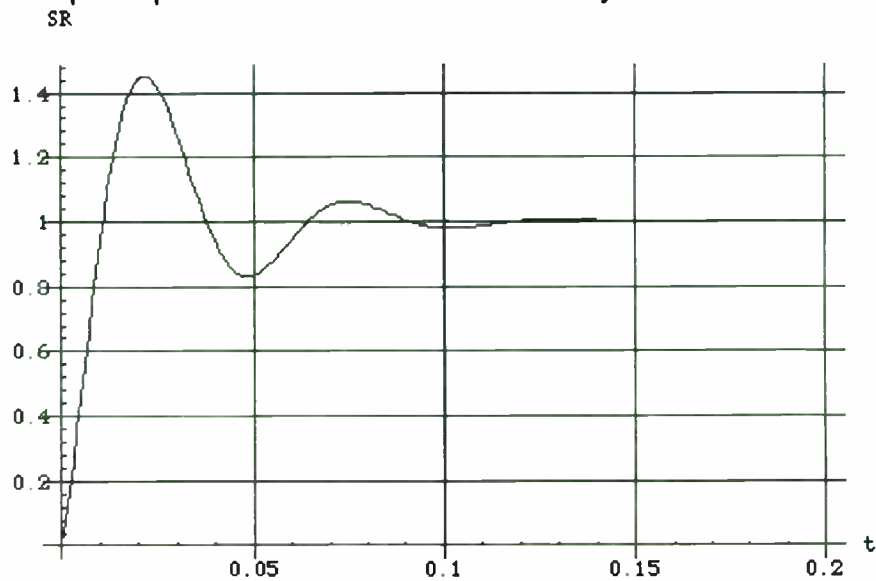
Normalized step response



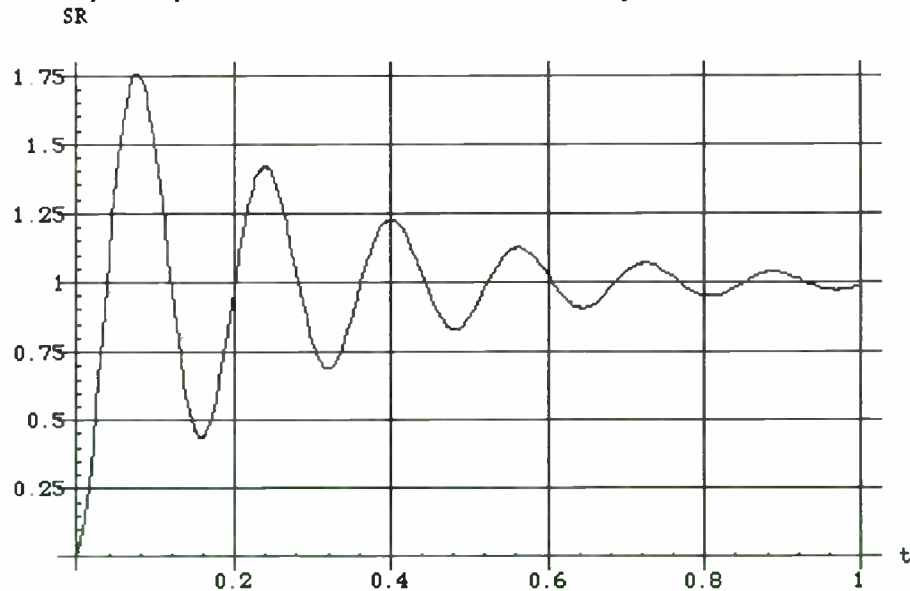
Switching time is 45 mS with resistor capacitor and charge pump variation. Original design value was 25 mS. Switching time is 80% worse.

Can (a) be reduced to lower sideband levels after loop lock?

Normalized step response when a is reduced by factor of 10 is:



Normalized step response when a is reduced by factor of 100 is:



References

- [1] Mathematica Enhanced version 2.2, Wolfram Research, Champaign IL, 1993.
- [2] Discussions with Jim Irwin of Motorola, Semiconductor Products Sector.

All products or brand names appearing herein are registered trademarks or trademarks of their respective holders.

© Motorola 1994, all rights reserved.

Phase Prediction Digital Synthesizer for Mobile Communications

Young J. Jung and Young O. Park

Mobile Communications Technology Division
Electronics and Telecommunications Research Institute
P.O. Box 106, Yusung Post Office
Daejeon, 305-606
Korea
Phone : (42) 860 - 5302
Fax : (42) 861 - 1033

Abstract

A frequency synthesizer which provides good spectral purity, fast settling, high resolution, and accuracy is required for the fast channel scanning and handoffs in the mobile communications systems. In order to meet this requirements hybrid synthesizers of direct and indirect methods have been currently studied for most advanced systems.

This paper proposes a new frequency synthesizer named phase prediction digital synthesizer (PDS) to improve the periodic amplitude fluctuations and drift problems for the conventional direct digital synthesizers. PDS eliminates the residual phase component in the phase accumulator by predicting the maximum accumulated phase point (2π) and initializing the phase accumulator at that instance. Added new building blocks are 2nd phase accumulator, 2π estimation function, and initializer. An experimental model has been developed using PLD design tool, and the performances have been tested for the accuracy and spectral purity of the synthesized output frequency. It has been confirmed from the experimental results that the residual phase components in the phase accumulator are effectively eliminated, and therefore there are no amplitude fluctuations and periodic drifts on the output waveform. Spurious level about -70dBc is obtained through the entire output frequency band.

The PDS is expected to be well suited to the hybrid synthesizer for mobile communications systems.

Satellite Communications

Session Chairperson: Mark A. Sturza,
Teledesic Corporation (Encino, CA)

The Teledesic satellite system: Overview and design trades. **Mark A. Sturza,** Teledesic Corporation (Encino, CA).....**402**

MCPC-VSATs for rural communications. **M.L. Sharma,** ITI Limited (Bangalore, India).....**410**

Automatic frequency control for VSAT networks. **Cheol Sig Pyo, Jae Ick Choi, and Choon Sik Yim,** Satcom Technology Division, Electronics and Telecom Research Institute (Yusong Gu, Daejeon, Korea).....**419**

Performance of a PM HEMT-based LNA vs. temperature for VSAT applications. **A. Caddemi, P. Livreri, and M. Sannino,** Dipartimento di Ingegneria Elettrica, Universita degli Studi Palermo (Palermo, Italy).....**425**

Direct digital synthesis of FM (chirp) waveforms. **D. Cioppi,** Micrel S.p.A. (Florence, Italy); **P. Tortoli and E. Guidi,** University of Florence (Florence, Italy).....**430**

THE TELEDESIC SATELLITE SYSTEM: OVERVIEW AND DESIGN TRADES

Mark A. Sturza

Teledesic Corporation

2300 Carillon Point
Kirkland, Washington 98033

(818) 907-1302 fax (818) 907-1357

ABSTRACT

There is a significant worldwide demand for broadband communications capacity. Teledesic plans to meet this demand using a constellation of 924 low-Earth orbit (LEO) satellites operating in Ka-band (30/20 GHz). The Teledesic network will provide "fiber-like" service quality, including low transmission delay, high data rates, and low bit error rates, to almost 100% of the world's population starting in 2001.

I. INTRODUCTION

Teledesic was founded in June 1990. Its principle shareholders are Craig McCaw, founder of McCaw Cellular Communications, the world's largest wireless communications company, and Bill Gates, founder of Microsoft, the world's largest computer software company.

"Teledesic seeks to organize a broad, cooperative effort to bring affordable access to advanced information services to rural and remote parts of the world that would not be economic to serve through traditional wireline means." [1]

The economics of wireline access are such that rural and remote areas may never get wireline access to broadband networks. As advanced information services become increasingly essential to economic development, education, health care, and public services, the gap between urban and rural areas will widen.

The solution is a satellite-based broadband network whose service cost in rural, remote areas is comparable to that of wireline networks in advanced urban areas. Such a network can

provide a variety of services including multimedia conferencing, video conferencing, videotelephony, distance learning, and voice. It will allow people to live and work in areas based on family, community, and quality of life.

The global scope of the Teledesic network embraces a wide range of service needs. Local partners will determine products and prices and provide sales and service in host countries. Teledesic will not market service directly to users. Rather, it will provide an open network for service providers in host countries. Teledesic will not manufacture satellites or terminals. Its goal is to provide the highest quality communications services at the lowest cost.

Wireline broadband (fiber) networks in advanced urban areas will drive demand for global access to broadband applications. Advanced information services are increasingly essential to education, health care, government, and economic development. Continued decrease in the price/performance ratio of microprocessors and computer memory will increase the demand for transmission of information. Video and high-resolution graphics require high data rates.

Most of the world's population will never get access to advanced digital applications through terrestrial means. The majority of the world does not even have access to basic voice service. Most areas that are not now wired never will be wired. Increasingly, wireless cellular will be the access technology of first choice in rural and remote areas. Cellular is limited to narrowband applications and most existing wireline networks will not support advanced digital applications.

Teledesic will provide seamless compatibility with terrestrial broadband (fiber) networks. Future broadband applications and data protocols will not be designed to accommodate the delays of geostationary

satellites. Users will want one network for all applications.

The Teledesic network will be complementary to terrestrial wireless networks. It will be a broadband overlay for narrowband cellular systems, backbone infrastructure for cell site interconnect, and backhaul for long distance and international connections. The aggregation of voice channels requires low-delay broadband capability.

Teledesic will provide a global wide-area network, a seamless, advanced, digital broadband network. It will fill in missing and problematic links everywhere, facilitating economic and social development in rural and remote areas.

Teledesic will supply instant infrastructure, providing rapid availability of advanced "fiber-like" services to almost 100% of the world's population. System capacity is not rigidly dedicated to particular end users or locations.

The cost of the Teledesic network will be \$9 billion. This is a fraction of what will be spent on installing fiber in just the United States. It is less than the \$15 billion that will be spent just to lay fiber for interactive TV in California [2]. Teledesic plans to initiate service in 2001.

II. DESIGN CONSIDERATIONS

Some of the key design drivers of the Teledesic Network are:

- High data rate (broadband) service
- Continuous global coverage
- Fiber-like delay
- Bit error rates less than 10^{-10}
- Mitigate effects of rain attenuation and blockage
- Rapid network repair
- Geodesic (mesh) network interconnect

The broadband service requirement drives Ka-band operation. No lower frequency bands are available to support a broadband satellite-based network. The Teledesic satellite uplinks operate in the 30 GHz band and the downlinks operate in the 20 GHz band.

Fiber-like delay requires a low-Earth orbit (LEO) constellation. Geostationary (GEO) satellites introduce a minimum 500 msec round-trip transmission delay. Medium-Earth orbit (MEO) constellations introduce a minimum 133 msec round-trip transmission delay. The round

trip transmission delay for a LEO constellation is typically less than 20 msec.

The practical altitude range for LEO constellations is 500 km to 1400 km. Below 500 km, atmospheric drag significantly shortens the satellites lifetime in orbit. Above 1400 km, the Van Allen radiation belt makes radiation hardening of the satellite prohibitively expensive.

Continuous global coverage requires a constellation with a near-polar inclination angle. Rapid network repair requires that the satellites in each orbital plane are decoupled from those in other orbital planes. This allows for the inclusion of active spare satellites in each plane. When a satellite fails, the remaining satellites in the plane spread out to close the resulting gap.

Ka-band communications links are subject to severe rain fading (Fig. 1). This effect is reduced as the Earth terminal to satellite elevation angle is increased. The Teledesic constellation is designed to operate with an Earth terminal elevation mask angle of 40° to provide rain availability of 99.9% over most of the United States.

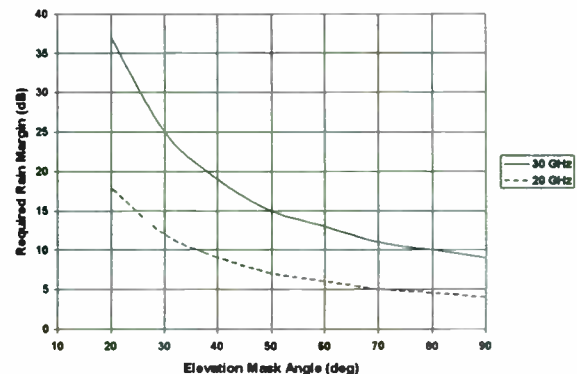


Fig. 1. Required Rain Margin (Region D2, 99.9% Availability)

The Teledesic constellation [3] is organized into 21 circular orbit planes that are staggered in altitude between 695 and 705 km. Each plane contains a minimum of 40 operational satellites plus up to four on-orbit spares spaced evenly around the orbit. The orbit planes are at a sun-synchronous inclination (approximately 98.16°), which keeps them at a constant angle relative to the sun. The ascending nodes of adjacent orbit planes are spaced at 9.5° around the Equator (Fig. 2).

Satellites in adjacent planes travel in the same direction except at the constellation "seams", where ascending and descending

portions of the orbits overlap. The orbital parameters are shown in Table 1.

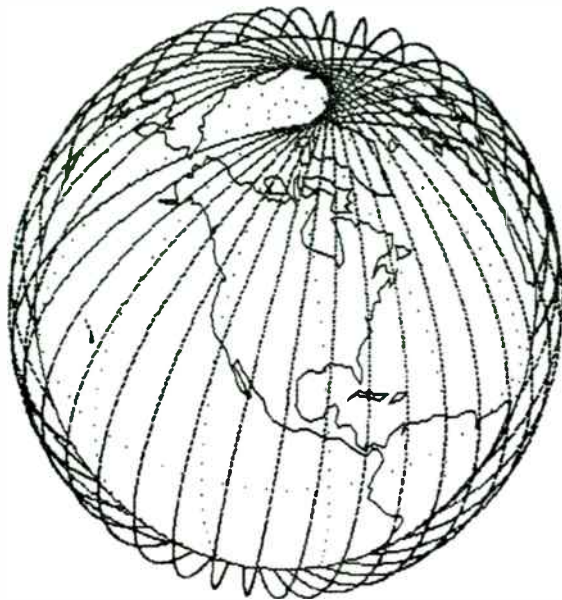


Fig. 2. Teledesic Orbits

Table 1. Constellation Parameters

Total Number of Satellites	840
Number of Planes	21
Number of Satellites Per Plane	40
Satellite Altitude	695 to 705 km
Eccentricity	0.00118
Inclination Angle	98.142° to 98.182°
Inter-Plane Spacing	9.5°
Intra-Plane Satellite Spacing	9°
Inter-Plane Satellite Phasing	Random
Earth Terminal Elevation Mask Angle	40°

III. SYSTEM DESIGN

The system design is described in Teledesic's FCC application [2]. The network (Fig. 3) uses fast packet switching technology based on Asynchronous Transfer Mode (ATM) developments. Each satellite in the constellation is a node in the fast packet switch network, and has intersatellite communication links with eight neighboring satellites. This interconnection arrangement forms a non-hierarchical geodesic

network that is tolerant to faults and local congestion.

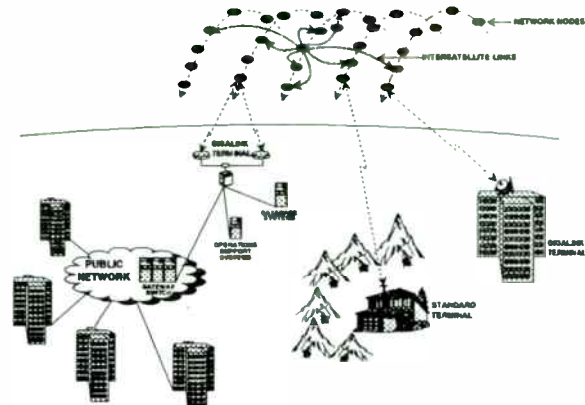


Fig. 3. The Teledesic Network

All communication is treated identically within the network as streams of short fixed-length packets. Each packet contains a header that includes address and sequence information, an error-control section used to verify the integrity of the header, and a payload section that carries the digitally-encoded video, voice, or data. Conversion to and from the packet format takes place in the terminals. Fast packet switching technology is ideally suited for the dynamic nature of a LEO network.

The network uses a "connectionless" protocol. Packets of the same connection may follow different paths through the network. Each node independently routes the packet along the path that currently offers the least expected delay to its destination, see Fig. 4. The required packets are buffered, and if necessary resequenced, at the destination terminal to eliminate the effect of timing variations. Teledesic has performed extensive and detailed simulation of the network and adaptive routing algorithm to verify that they meet Teledesic's network delay and delay variability requirements.

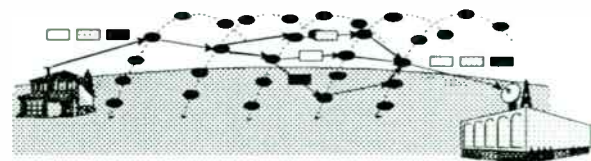


Fig. 4. Distributed Adaptive Routing Algorithm

A. Earth Fixed Cells

The Teledesic Network uses an Earth-fixed cell design to minimize hand-offs. The Earth's surface is mapped into a fixed grid of

approximately 20,000 "supercells". Each supercell is a square 160 Km on each side and is divided into 9 cells as shown in Figure 5.

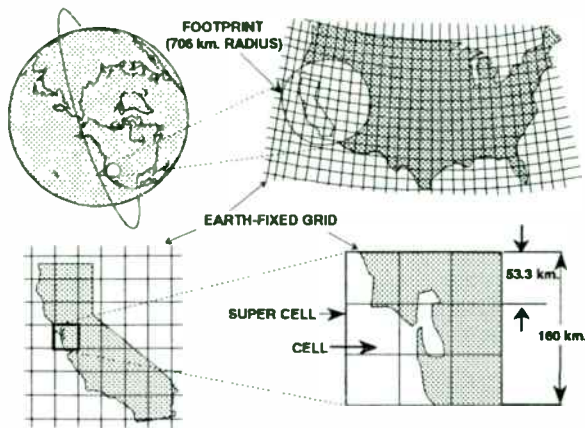


Fig. 5. Earth-Fixed Cells

Supercells are arranged in bands parallel to the Equator. There are approximately 250 supercells in the band at the Equator, and the number per band decreases with increasing latitude. Since the number of supercells per band is not constant, the "north-south" supercell borders in adjacent bands are not aligned.

A satellite footprint encompasses a maximum of 64 supercells, or 576 cells. The actual number of cells for which a satellite is responsible varies by satellite with its orbital position and its distance from adjacent satellites. In general, the satellite closest to the center of a supercell has coverage responsibility. As a satellite passes over, it steers its antenna beams to the fixed cell locations within its footprint. This beam steering compensates for the satellite's motion as well as the Earth's rotation. This concept is illustrated in Fig. 6.

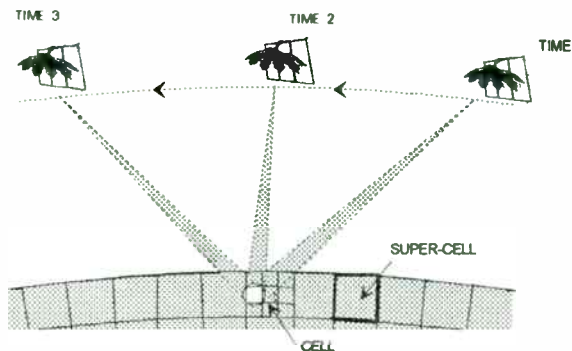


Fig. 6. Beam Steering

Channel resources (frequencies and time slots) are associated with each cell and are

managed by the current "serving" satellite. As long as a terminal remains within the same Earth-fixed cell, it maintains the same channel assignment for the duration of a call, regardless of how many satellites and beams are involved. Channel reassignments become the exception rather than the normal case, thus eliminating much of the frequency management and hand-off overhead.

A database contained in each satellite defines the type of service allowed within each Earth-fixed cell. Small fixed cells allow Teledesic to avoid interference to or from specific geographic areas and to contour service areas to national boundaries. This would be difficult to accomplish with large cells or cells that move with the satellite.

B. Multiple Access

Teledesic uses a combination of space, time, and frequency division multiple access to ensure efficient spectrum utilization (Fig. 7). At any instant of time each fixed supercell is served by one of 64 transmit and one of 64 receive beams on one of the Teledesic satellites. The scanning beam scans the 9 cells within the supercell with a 23.111 msec scan cycle. Each scanning beam supports 1440 16-Kbps channels. FDMA is used for the uplinks and asynchronous TDMA (ATDMA) for the downlinks.

Satellite transmissions are timed to ensure that all supercells receives transmissions at the same time. Terminal transmissions are also timed to ensure that transmissions from the same numbered cell in all supercells in its coverage area reach that satellite at the same time. Physical separation and a checkerboard pattern of left and right circular polarization eliminate interference between cells scanned at the same time in adjacent supercells. Guard time intervals eliminate overlap between signals received from time-consecutive cells.

On the uplink, each active terminal is assigned one or more frequency slots for the call's duration and can send one packet per slot each scan period (23.111 msec). The number of slots assigned to a terminal determines its maximum available transmission rate. One slot corresponds to a Standard Terminal's 16 Kbps basic channel with its associated 2 Kbps signaling and control channel. A total of 1440 slots per cell scan interval are available for Standard Terminals.

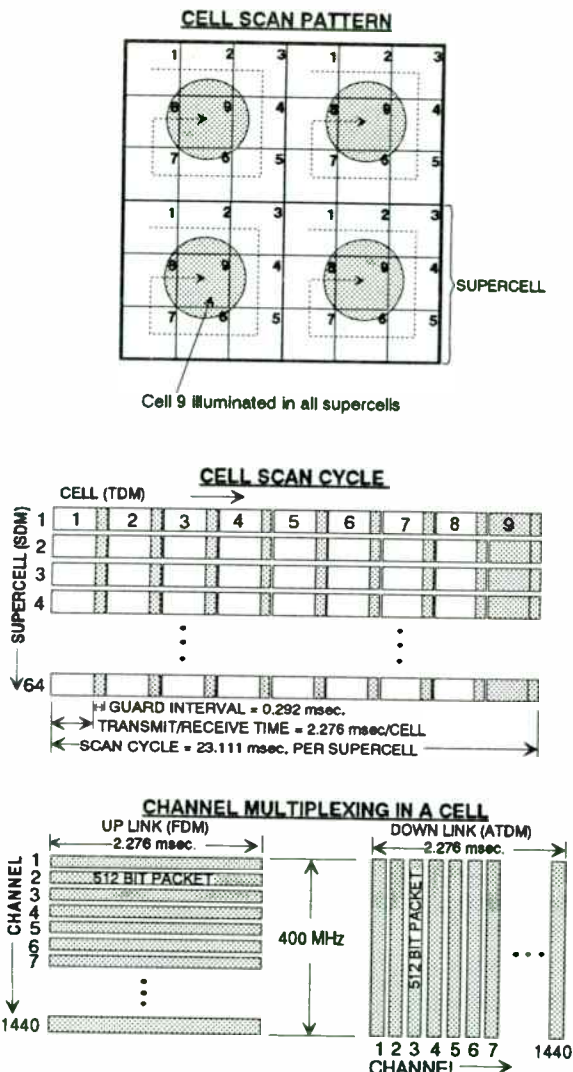


Fig. 7. Standard Terminal Multiple Access

The terminal downlink uses the packet's header rather than a fixed assignment of time slots to address terminals. During each cell's scan interval the satellite transmits a series of packets addressed to terminals within that cell. Packets are delimited by a unique bit pattern, and a terminal selects those addressed to it by examining each packet's address field. A Standard Terminal operating at 16 Kbps requires one packet per scan interval. The downlink capacity is 1440 packets per cell per scan interval. The satellite transmits only as long as it takes to send the packets queued for a cell.

The combination of Earth-fixed cells and multiple access methods results in very efficient use of spectrum. The Teledesic system will reuse its spectrum over 350 times in the

continental U.S. and 20,000 times across the Earth's surface.

IV. COMMUNICATIONS LINKS AND TERMINALS

All of the Teledesic communications links transport data, video, and voice as fixed-length 512 bit packets. The links are encrypted to guard against eavesdropping. Terminals perform the encryption/decryption and conversion to and from the packet format.

The uplinks use dynamic power control of the RF transmitters so that the minimum amount of power is used to carry out the desired communication. Minimum transmit power is used for clear sky conditions; transmit power is increased to compensate for rain.

The Teledesic Network supports a family of subscriber terminals providing on-demand data rates from 16 Kbps up to 2.048 Mbps (E1), and for special applications from 155.52 Mbps (OC-3) up to 1.24416 Gbps (OC-24). This allows a flexible, efficient match between system resources and subscriber requirements.

Standard Terminals include both fixed-site and transportable configurations that operate at multiples of the 16 Kbps basic channel payload rate up to 2.048 Mbps (the equivalent of 128 basic channels). These terminals use antennas with diameters from 16 cm to 1.8 m as determined by the terminal's maximum transmit channel rate, climatic region, and availability requirements. Their average transmit power varies from less than 0.01 W to 4.7 W depending on antenna diameter, transmit channel rate, and climatic conditions. All data rates, up to the full 2.048 Mbps, can be supported with an average transmit power of 0.3 W by suitable choice of antenna size.

Within its service area each satellite can support a combination of terminals with a total throughput equivalent to over 100,000 simultaneous basic channels.

The Network also supports a smaller number of fixed-site GigaLink Terminals that operate at the OC-3 rate (155.52 Mbps) and multiples of that rate up to OC-24 (1.24416 Gbps). Antennas for these terminals range in size from 28 cm to 1.6 m as determined by the terminal's maximum channel rate, climatic region and availability requirements. Transmit power varies from 1 W to 49 W depending on antenna diameter, data rate, and climatic conditions. Antenna site-diversity can be used to

reduce the probability of rain outage in situations where this is a problem.

GigaLink Terminals provide gateway connections to public networks and to Teledesic support and data base systems, as well as to privately owned networks and high-rate terminals. Each satellite can support up to sixteen GigaLink terminals within its service area.

Intersatellite Links (ISLs) operate in the 60 GHz band. They interconnect each satellite with its eight neighbor satellites. Each ISL operates at the OC-3 rate, and multiples of that rate up to OC-24 depending upon the instantaneous capacity requirement.

V. SATELLITES

The Teledesic satellites are specifically designed to take advantage of the economies that result from high volume production and launch. All satellites are identical and use technologies and components that allow a high degree of automation for both production and test. To minimize launch cost and the deployment interval, the satellites are designed to be compatible with over twenty existing international launch systems, and to be stacked so that multiple satellites can be launched on a single vehicle. Individual satellites, the constellation as a whole is designed to operate with a high degree of autonomy.

The on-orbit configuration of the Teledesic satellite, Fig. 8, resembles a flower with eight "petals" and a large boom-mounted square solar array. The deployed satellite is 12 m in diameter and the solar array is 12 m on each side. Each petal consists of three large panels containing the phase-array antennas. The octagonal baseplate also supports eight pairs of intersatellite link antennas, the two satellite bus structures that house the engineering subsystem components, and propulsion thrusters. A third satellite bus structure, containing power equipment and additional propulsion thrusters, is mounted at the end of the solar array boom. The solar array is articulated to point to the sun. A functional block diagram of the satellite is shown in Fig. 9.

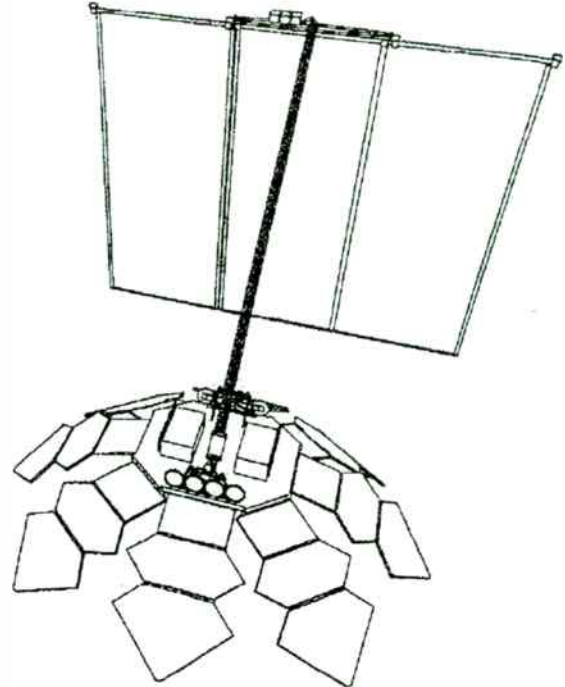


Fig. 8. Teledesic Satellite

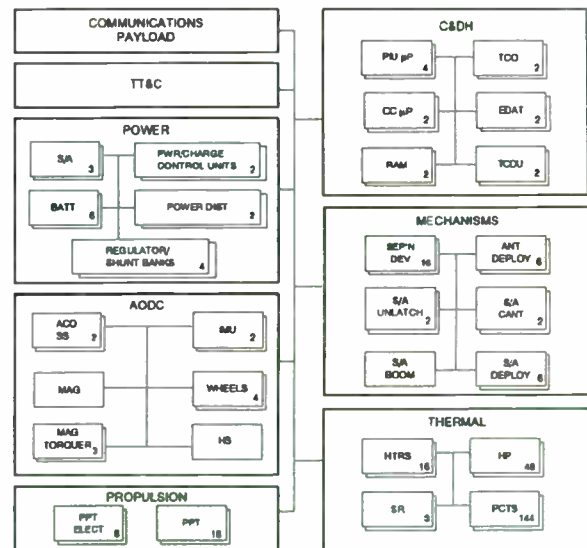


Fig. 9. Satellite Block Diagram

VI. COMMUNICATIONS PAYLOAD

A functional block diagram of the communications payload is shown in Fig. 10. The heart of the payload is the fast packet switch (FPS). It routes packets to and from the Scanning Beam (SB), GSL, and ISL transmitters and receivers. The FPS is essentially non-

blocking with very low packet delay, and a throughput in excess of 5 Gbps.

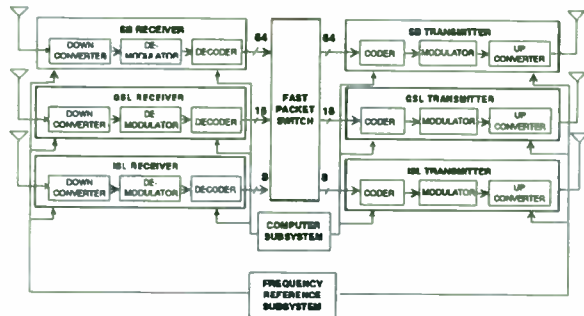


Fig 10. Communications Payload

The frequency reference subsystem provides stable frequency and time references to the SB, GSL, and ISL transmitters and receivers. The computer subsystem provides control information to the FPS and the SB, GSL, and ISL transmitters and receivers.

The SB subsystem consists of 64 transmit channels and 64 independent receive channels plus spares. Each transmit channel accepts digital data packets from the FPS. The packets are encoded and modulated to form an IF signal. The IF signal is upconverted and applied to an active-element phased-array antenna incorporating GaAs MMIC power amplifiers. The antenna converts the RF signal to a free-space propagated waveform with the proper polarization for the Earth-fixed cell that it is serving. The signal frequency is pre-compensated to eliminate the apparent Doppler shift at the center of the Earth-fixed cell.

Each SB receive channel uses an active-element phased-array antenna incorporating GaAs MMIC low-noise amplifiers (LNAs) to convert free space propagated waveforms into a RF signal. The antenna selects the signal polarization corresponding to the Earth-fixed cell that it is serving. The RF signal is downconverted to an IF signal, demodulated, and decoded. The decoded data packets are sent to the FPS.

The SB antenna arrays are located on panels that are oriented at angles to the Earth's surface that reduce the beam steering requirements of each array to a few degrees. The antenna arrays on the inclined panels are elliptical in shape and produce elliptical patterns that compensate for the distortion from circular encountered at antenna grazing angles less than 90° with the Earth's surface.

The GSL subsystem consists of 16 transmit channels and 16 independent receive channels plus spares. Each transmit channel accepts digital data packets from the FPS. The packets are encoded and modulated to form an IF signal. The IF signal is upconverted and applied to an active-element phased-array antenna incorporating GaAs MMIC power amplifiers. The antenna converts the RF signal to a free-space propagated waveform with the proper polarization for the GigaLink Terminal it is serving. The signal frequency is pre-compensated to eliminate the apparent Doppler shift at the GigaLink Terminal.

Each GSL receive channel uses an active-element phased-array antenna incorporating GaAs MMIC LNAs to convert free-space propagated waveforms into a RF signal. The phased-array antenna selects the signal polarization corresponding to the GigaLink Terminal it is serving. The RF signal is downconverted to an IF signal, demodulated, and decoded. The decoded data packets are sent to the FPS.

The ISL subsystem consists of eight transmit channels and eight independent receive channels plus spares. Each transmit channel accepts digital data packets from the FPS. The packets are encoded and modulated to form an IF signal. The IF signal is upconverted and applied to an active-element phased-array antenna incorporating GaAs MMIC power amplifiers. The antenna converts the RF signal to a free-space propagated waveform with the proper polarization for the satellite with which it is communicating. The signal frequency is pre-compensated to eliminate the apparent Doppler shift at the receiving satellite.

Each ISL receive channel uses an active-element phased-array antenna incorporating GaAs MMIC LNAs to convert free space propagated waveforms into a RF signal. The antenna selects the signal polarization corresponding to the satellite it is serving. The RF signal is downconverted to an IF signal, demodulated, and decoded. The decoded data packets are sent to the FPS.

The Teledesic constellation incorporates over 100,000 active-element phased-array antennas. Teledesic will be one of the major consumers of Ka-band GaAs MMICs in the late 1990's [4].

VII. ACKNOWLEDGMENTS

The author wishes to thank David Patterson, Dr. James Stuart, Russ Daggatt, Tren Griffin, David Montanaro, and the other members of the Teledesic team for their contributions to this paper.

VIII. REFERENCES

- [1] *Teledesic Company Overview*
- [2] George Gilder, "TELECOSM: Ethersphere", *Forbes ASAP*, 10 October 1994, pp. 133-148.
- [3] *Application of Teledesic Corporation for a Low Earth Orbit ("LEO") Satellite System in the Fixed Satellite Service ("FSS")*, 21 March 1994.
- [4] M. A. Sturza, "The Teledesic Satellite System", *IEEE National Telesystems Conference*, June 1994, pp. 123-126.

MCPC VSAT FOR RURAL COMMUNICATIONS

M.L.SHARMA

ITI Limited, BANGALORE, INDIA

ABSTRACT

The Multiple Channel Per Carrier Very Small Aperture Terminal-MCPC VSAT is ideally suited for trunk connections between a large Switching Centre and a Small Exchange in Rural/Remote inaccessible areas on a Point to Point basis in star connectivity utilising low bit rate encoding (LRE) techniques for Voice, the MCPC VSAT achieves economy in satellite resources while retaining circuit quality.

The MCPC-VSAT consists of an outdoor RF Unit (RF ODU) mounted below the 2.4M Antenna and interconnected by IF Cable to an indoor unit. The RF ODU consists of UP and DOWN converters with independent frequency synthesisers and a 5 watt SSPA. The 65 deg. K LNA is mounted at the feed of the antenna. The Indoor unit consists of Voice/Data multiplexer, a QPSK modem and the NMS for the monitoring and controls of the VSAT.

INTRODUCTION

The Department of Telecommunications, Government of India has planned to provide reliable telecommunication services to places located in rural/remote hills and inaccessible terrain, which are neither feasible nor technologically economically viable on terrestrial media. Such stations have been planned and engineered to be connected on Satellite media with their respective state capital or district headquarters. Most of such places are provided with small exchange of 64/128 lines depending upon the local telecommunication need. Thus through MCPC VSATs, manual trunk circuits as well as subscriber trunk dialling facility would be provided by connecting the station with respective. Digital Trunk Exchange and Point to Point leased circuits.

Presently about 250 VSATs have been planned to work with 15 HUB Stations in different parts of the country. The 28 VSATs have already been installed in the Northern parts of India. The VSATs should work with either our National Satellites INSAT-I and INSAT-II series.

SYSTEM CONFIGURATION

The MCPC-VSAT Network operates in a STAR Configuration with a hub either type A with $G/T > 31.7$ dB/K or type B with $G/T > 25.7$ dB/K, both of INSAT Network providing access to a large number of VSATs with public/private Voice/Data networks. A block schematic giving the system concept is given in Figure 1.

Based on the size of local telephone exchange as well as traffic needs, a low capacity satellite terminal of $G/T > 15$ dB/K may be adequate to meet the need. The VSAT Satellite terminal will be co-located with the local telephone exchange. The VSAT block schematic is shown in Figure 2. The MCPC VSAT consists of an outdoor RF unit mounted below the 2.4 M antenna and inter connected by IF cable to an indoor unit. The ODU consists of UP and DOWN converters with independent frequency synthesisers and a

5 watt solid state power amplifier. A 65 degree K LNA is mounted at the feed of the antenna. The SSPA is temperature compensated for stable output power.

The Indoor unit consists of a Voice/Data Multiplexer and a QPSK Modem. The multiplexer encodes voice at variable bit rate upto 16 Kbps and can support upto 7 voice channels. Additionally, an orderwire voice channel is also provided . The multiplexer can support upto 4 data channels. Three of the channels can support upto 19.2 Kbps and the fourth can support upto 112 Kbps. The aggregate data rate of the multiplexed signals is variable upto 128 Kbps including a 0.8 Kbps overhead. Modem working upto the information rate of 128 Kbps is designed utilising the latest digital signal processing techniques and provides total flexibility in selection of data rate.

The Network Management System (NMS) housed in the indoor unit monitors and controls all the active sub systems of the MCPC VSAT.

HUB STATION ELECTRONCS

The corresponding hub station electronics consists of identical MUXES, Modems in 8:1 configuration and independent frequency synthesiser controlled UP and DOWN converters in 1+1 configuration. The HUB station electronics can support several MCPC VSATs by gradual expansion of MUXES and Modems with associated switch over unit. AT the hub station, centralised NMS monitors all the remote VSATs. The NMS utilises an exclusive data channel for each link to the VSAT. The antenna and the HPA of the HUB are engineered based on the number of VSATs it has to support. The technical specifications are shown in Figure 3.

PERFORMANCE

The MCPC VSAT Network consisting of 28 terminals deployed in the Northern States of Himachal Pradesh and Utter Pradesh with its HUB at Delhi working satisfactorily and providing the Voice/Data communications in the rural/remote areas. Further 250 VSATs are being installed at the remote locations.

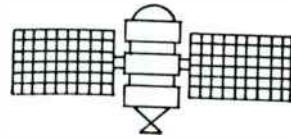
CONCLUSION

The MCPC VSATs system provides the best economy for this route application particularly in the remote areas where other types of transmission media are not economically viable. In India, about 80% of population lives in rural, remote, sparsely populated areas where presently there is no basic telephone service available. The geographic remoteness, hilly hostile terrain requires the installation of costly transmission lines to bring basic telephone services to these under developed areas.

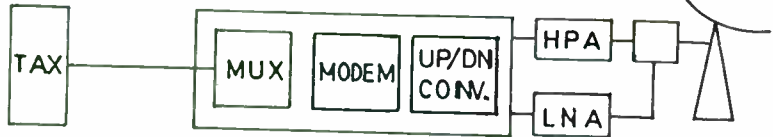
ACKNOWLEDGEMENT

The author wishes to thank Dr.A.Prabhakar, Director (R&D), ITI Limited, for his encouragement during the course of these development work. Also the very helpful discussions with Mr.T.K.Sridharan, Deputy General Manager and Mr.A.K.Sekhar, Chief Engineer are sincerely acknowledged.

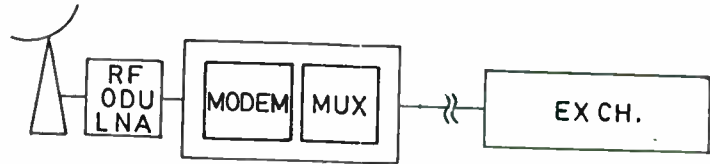
INSAT I/II



414



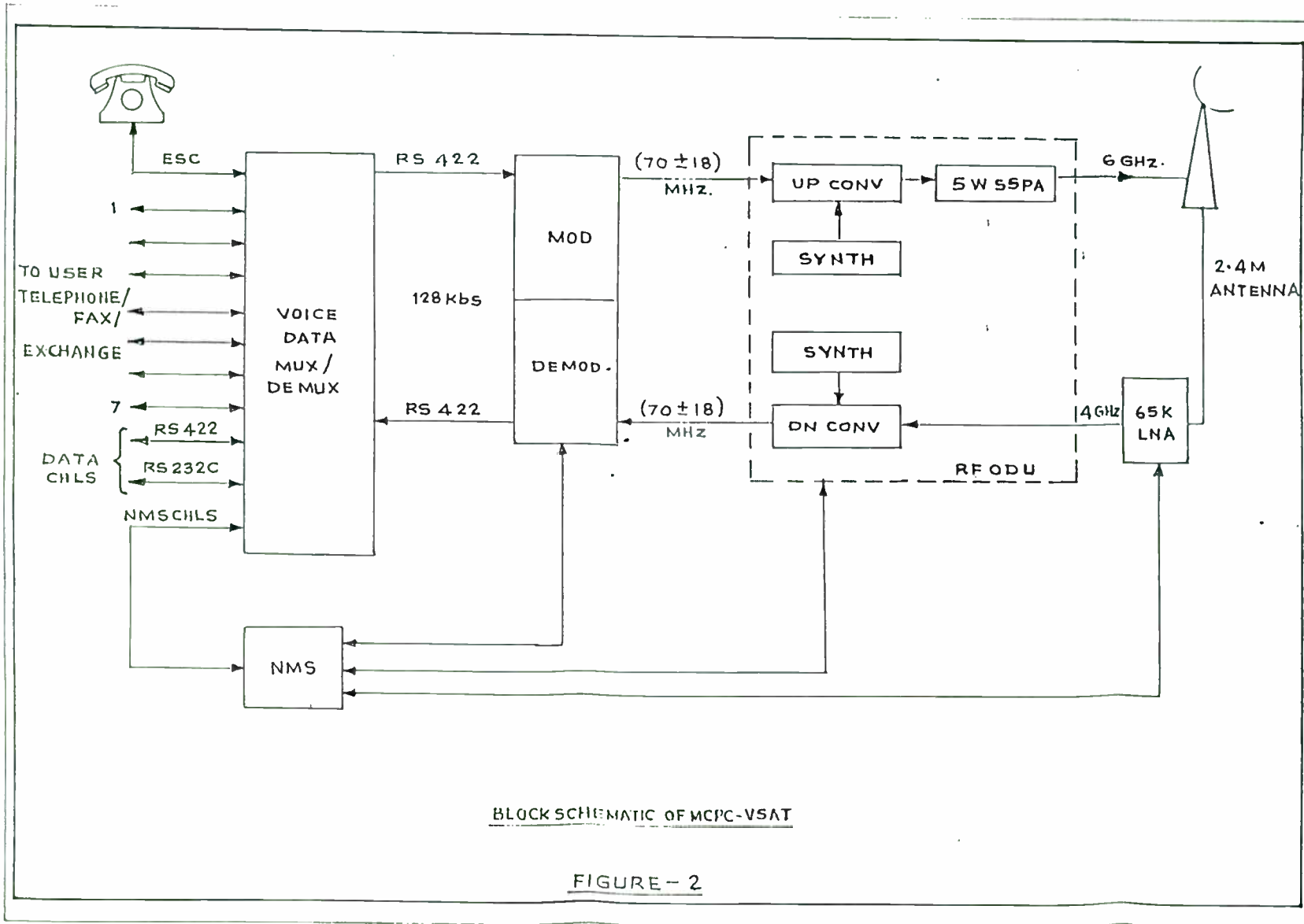
HUB STATION



MCPC V SAT

REMOTE STATION

FIGURE-1



BLOCK SCHEMATIC OF MCPC-VSAT

FIGURE - 2

MCPC VSAT
Technical Specifications

System Specifications

No. of Voice Channels	:	Seven apart from ESC
No. of Data Channels	:	Upto four in lieu of Voice
G/T	:	15dB/Deg. K.
EIRP	:	45dBW/46.5dbW @ 6GHz
Antenna Dia	:	1.8M/2.4M
Uplink Frequency	:	5.925-6.425 GHz
Downlink Frequency	:	3.7-4.2 GHz
Link error performance	:	1×10^{-6} at $E_b/N_o = 6.5\text{dB}(\text{Nom})$

Base Band Specifications

4W Trans.	:	-16 plus/minus 0.5dBm
4W Rec.	:	+7 plus/minus 0.5dBm
Impedance	:	600 ohms
Signalling	:	4W E&M
Voice Coding	:	16Kbps

IF Specifications

Modulation	:	QPSK
Frequency	:	70 MHz Plus/Minus 18MHz
Frequency Step size	:	2.5 KHz
FEC Coding	:	Rate 1/2 Convolution
Decoder	:	Viterbi
Information Data Rate	:	Upto 128 Kbps
Acquisition Range	:	Plus/Minus 30 KHz

RF Specifications

Converter Frequency	:	2.5 MHz
Stepsize		
Frequency Stability	:	1×10^{-8} /day @ 25 deg.C
Power Output of SSPA	:	+37 dBm minimum

Environmental Specifications

ODU	:	QM 333 Cat.D.
IDU	:	QM 333 Cat.B.

Power Supply

M CVSAT	:	-48V plus/minus 10% DC.
---------	---	-------------------------

Size.

RF ODU	:	458H x 305W x 229 D (Excluding LNA)
IDU	:	1703H x 545W x 900 D

B I O - D A T A

M.L.Sharma did his BE (Telecomm) from Birla College of Engineering, Pilani in 1963 and M.Sc.(Engg.) in Advanced Electronics from College of Engineering, Poona in 1964. He joined DRDO in 1965 and worked on the design and development of Feed for the Mono-pulse Tracking System, Battle Field Surveillance Radar, S-band Tropo Communication System, Solid State Transponder for Missile Target and State of the art Microwave Sub-systems.

In 1978 he joined the Transmission R&D division of the Indian Telephone Industries Ltd., Bangalore and has been working on the UHF and Microwave analog and digital LOS systems, Satellite Communication System. He has published/presented 25 technical papers in various journals/conferences.

At present, he is General Manager in the Transmission R&D Division of Indian Telephone Industries Ltd. Bangalore.

Automatic Frequency Control for VSAT Network

Cheol Sig Pyo, Jae Ick Choi, and Choon Sik Yim

Electronics and Telecommunications Research Institute,
Yusong P.O.Box 106, Taejon, 305-600, Korea

Abstract - This paper describes the automatic frequency control(AFC) technique to compensate for frequency errors in very small aperture terminal(VSAT) network. Such AFC module in the hub radio frequency(RF) subsystem uses outbound time division multiplexing(TDM) binary phase shift keying(BPSK) modulated carrier returned through the satellite. It compensates for not only the inherent frequency instability of the local oscillators of the hub station and satellite, but also the relative Doppler frequency shift on the inbound carriers received from the remote stations. It is designed so as to compensate for above $\pm 500\text{Hz}$ Doppler shift while its pull-in-range is above $\pm 40\text{kHz}$. The AFC module was tested and verified through the INTELSAT VA.

I. Introduction

Recent advances in technology have given a new thrust to the satellite communications industry by deploying low cost very small aperture terminal (VSAT) network for data, voice, and video communications. VSAT networks provide one-way or two-way data communications, video broadcast, etc.[1][2] The point-to-multipoint VSAT networks consist of a hub and many remotes. In this topology, the system designer foresees the need to minimize the complexity of the remote, small earth station at the expense of single hub station. One of these approaches is that the low cost oscillators of remote stations are to be phase-locked to the very

high stabilized oscillator of the hub station.[3]

In satellite communication systems, there are frequency errors as follows: 1) long term instability of local oscillator(LO) in transmitter, receiver and satellite, and 2) frequency shift due to the Doppler effects. To compensate for the frequency instability due to above item 1, the automatic frequency control(AFC) technique using one pilot has been generally utilized.[4] But, this AFC method might not compensate for the frequency error due to hub-remote satellite link Doppler effects at VSAT networks in which the reference oscillator of remote station is phase-locked to that of hub station. Therefore a new AFC technique with an additional function is required to compensate for these Doppler shift. One of these AFC methods is to use two pilot tones in hub station, which have two great demerits: power consumption and frequency occupation by transmitting two pilots.[5][6][7]

In this paper, frequency errors on inbound carrier are analyzed in the Ku-band VSAT system, in which remote station is synchronized with hub station, and a new AFC technique, which uses the time division multiplexing(TDM) binary phase shift keying(BPSK) modulated outbound signal, is presented. And then, described is the AFC technique for centering burst inbound carriers within acquisition range of the burst demodulator in our TDM-time division multiple access(TDMA) VSAT system of point to multipoint network, which is designed so as to operate with a Ku-band and/or inclined-orbit satellite. Finally the AFC module is experimentally verified by satellite loop tests through the INTELSAT VA satellite.

II. Frequency errors in our VSAT network

In our VSAT system, the reference oscillator of remote station is synchronized with that of hub and the sources of frequency error on inbound TDMA carriers at the burst demodulator input of hub station are as follows:[3]

- 1) long term frequency instability of satellite LO
- 2) long term frequency instability of the hub receive side LOs
- 3) Doppler effect of remote to hub satellite link
- 4) Doppler effect of hub to remote satellite link
- 5) jitter from clock recovery loop in remote station

The long term frequency instability of LOs (item 1, 2) used for frequency conversion causes the center frequency of carrier spectrum to be shifted.[3] Doppler effect (item 3, 4) due to the movement of satellite not only shifts the center frequency of spectrum, but also spread its bandwidth, and Doppler frequency shift becomes larger in the higher frequency and more inclined-orbit satellite. Table 1 shows the Doppler frequency shift versus the inclination for Ku-band INTELSAT satellite system.[3][8]

Table 1. Maximum Doppler frequency shift and rate of inclined INTELSAT Satellite

Parameter	Inclination (East/West Drift 0.1°)				
	0.1	0.5	1.0	1.5	2.0
Maximum deviation of Doppler frequency (@13.375GHz)*	±120 (Hz)	±267 (Hz)	±498 (Hz)	±624 (Hz)	±809 (Hz)
Maximum rate of Doppler frequency (@ 13.375GHz)	1.745 x10 ⁻²	3.891 x10 ⁻²	6.516 x10 ⁻²	9.141 x10 ⁻²	0.118 (Hz/s)

* Average operating frequency of up/down link for 14/12GHz satellite system.

On the other hand, in our VSAT network, the outbound TDM signal transmitted by hub station is recovered in remote station. The recovered clock is utilized as the reference frequency signal for the

transmit frequency of remote station. This clock may be drifted due to Doppler effect of the above item 4. Therefore the inbound carriers synchronized with the reference clock of hub station are shifted nearly as much as the Doppler frequency shift. Furthermore, other than frequency error is added to inbound carrier because there is jitter from the clock recovery process and the the transmit frequency of remote station is phase-locked to the recovered clock.

Table 2 shows all the frequency errors on burst carrier to be considered for the design of AFC loop in our Ku-band VSAT system. The frequency errors caused by items 1, 2 and 3 in Table 2 can be compensated for by the one pilot AFC technique in the intermediate frequency(IF) subsystem of hub station. But, there are still the frequency errors caused by items 4 and 5. That is: total amount of frequency errors may be above ±1kHz in any case. Therefore an additional AFC function is required to compensate for frequency error of item 4 or 5.

Table 2. Frequency errors on inbound carrier in our VSAT network

Items	Amount of frequency error(Max.)	Remarks
1) Satellite LO instability	±25kHz	INTELSAT
2) Receive LO instability of hub station	±1.4kHz	
3) remote to hub link Doppler shift	refer to Table 1	
4) hub to remote link Doppler shift	refer to Table 1	
5) frequency error by clock jitter	±420Hz	

III. Design of Automatic Frequency Control

A. AFC Module Architecture

Fig.1 shows AFC module within RF system of hub station in our VSAT system. The AFC module receives the IF band signal (70±18MHz) from the down converter(D/C). This signal is amplified by the automatic gain control(AGC) amplifier. The IF

band signal includes at least one outbound BPSK modulated carrier received from the satellite. The AFC module demodulates the outbound carrier, and then by using the outbound baseband signal to perform AGC, AFC, and Doppler frequency shift compensation functions. Therefore the center frequency of inbound carriers is maintained within ± 1 kHz by compensating for frequency errors of items 1 to 4, except items 5 in Table 2. To demodulate the outbound carrier, the AFC module uses a LO that is phase-locked to a 10MHz frequency reference, and that is frequency-synthesized over the IF band (70 ± 18 MHz) in 10kHz steps.

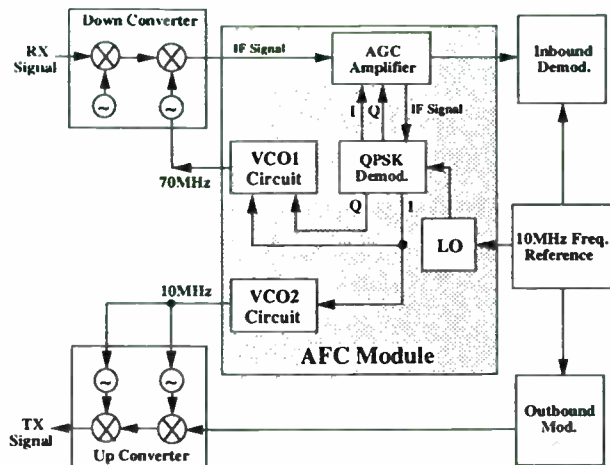


Fig. 1 AFC module architecture

The AFC module outputs a 70MHz signal from voltage controlled oscillator(VCO)1 circuit to the down converter to compensate for frequency errors of items 1, 2, and 3 in Table 2. The L-band phase-locked oscillator(PLO) at 1120MHz in the D/C is phase-locked to the 70MHz signal. This PLO is used to translate a 1050 ± 18 MHz band signal to 70 ± 18 MHz IF band. This forms a Costas loop [8] implemented with the AGC amplifier, quadrature phase shift keying(QPSK) demodulator, VCO1 circuit, L-band PLO and 2nd down converter. The LO that is phase-locked to 10MHz frequency reference provides the frequency reference for Costas loop. Also, the AFC module outputs a 10MHz signal from VCO2 circuit to the up converter(U/C) to compensate for frequency error of

item 4. The L-band PLO and Ku-band frequency synthesizer in the U/C is phase-locked to the 10MHz signal.

The 10MHz signal is locked to the clock frequency recovered from the outbound carrier. The clock signal was originally generated from the 10MHz frequency reference in hub station. Since the recovered clock has been transmitted over the satellite link, it will be Doppler-shifted. The result is that outbound carriers are transmitted with a frequency shift approximately equal to the Doppler shift. Since the remote stations also use the Doppler shifted reference, the hub and the remote stations will be transmitting at approximately the same frequency. This keeps relative channel spacing of hub transmitted -outbound carriers and remote station transmitted -inbound carriers constant at the satellite. Together with the VCO1 circuit's AFC loop it ensures the inbound carriers will be correctly centered at the hub demodulator input for quick acquisition of the burst carriers.

B. VCO1 circuit

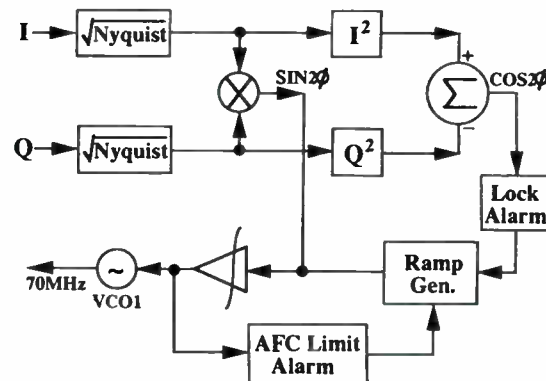


Fig. 2 VCO1 circuit block diagram

The in-phase(I) and quadrature(Q) channel output of QPSK demodulator in Costas loop are filtered with root Nyquist filters as shown in Fig. 2. The root Nyquist filtered I and Q signals are multiplied to detect the frequency difference between the center frequency of input signal and the LO frequency. The output signal is integrated to generate an AFC voltage which is applied to the

70MHz oscillator. When the AFC loop is not locked, the carrier lock alarm is generated and the sweep voltage is started. When the AFC loop locks up, the carrier lock alarm clears and the voltage sweep stops. If the frequency difference between the LO frequency and outbound center frequency is within the range of the VCO1 sweep circuit, $\pm 40\text{kHz}$, the outbound carrier will phase-lock to the LO signal.

C. VCO2 Circuit

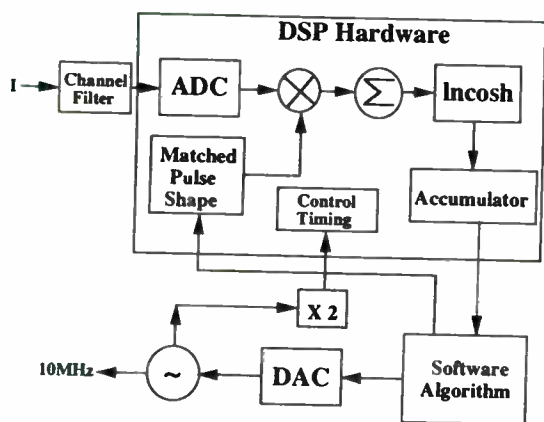


Fig. 3 VCO2 circuit block diagram

The VCO2 circuit uses a digital signal processing (DSP) and a tracking algorithm in microprocessor to implement the Doppler frequency shift compensation loop [9]. A functional diagram of the VCO2 circuit is shown in Fig. 3. The reference input to the circuit is the I signal from the QPSK demodulator. The analog input is converted to a digital signal with analog to digital converter (ADC). The VCO2 circuit outputs 10MHz signal to the U/C. The 10MHz signal is used to generate a digital representation of a "matched filter" pulse shape at $66 \frac{2}{3}$ kHz. An optimum synchronizer [10] implemented in DSP hardware compares this with the sampled input signal and outputs relative phase difference information. The algorithm, implemented in software, then reads in the phase difference information and processes it with loop filter, integrator and gain functions. The software calculates the frequency control voltage to control the 10MHz signal and outputs it through a DAC(digital to analog converter). In addition the software outputs a clock alarm when

synchronization is not achieved, and a frequency-control alarm when the rate of change of the phase exceeds a threshold.

IV. Verification by Satellite Loop Tests

A. Test Set-up

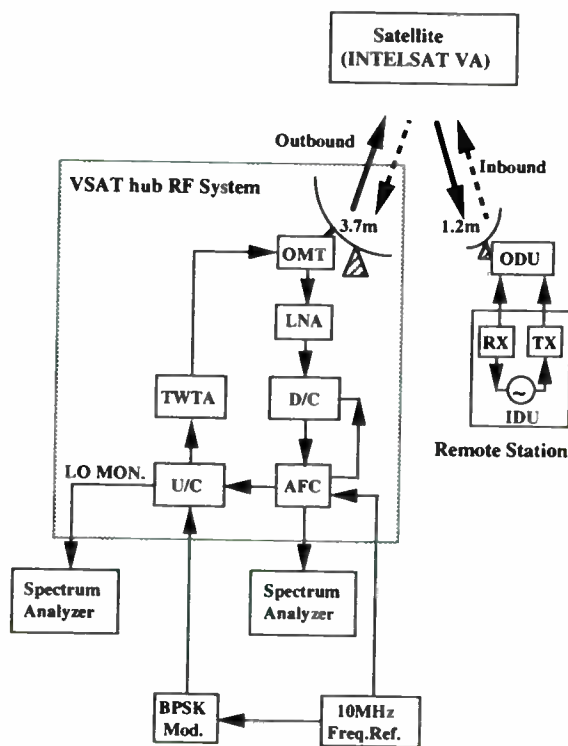


Fig. 4 Set-up for satellite loop tests

To verify experimentally the AFC module, satellite loop tests were carried out in January 1994 using a Ku-band hub station and VSAT terminals through the INTELSAT VA satellite operating in inclined orbit mode of about $\pm 0.95^\circ$. The configuration for tests is shown in Fig. 4. [11]

The hub station consists of a 3.7m antenna with tracking equipment, the Ku-band RF system, an outbound BPSK modulator, 10MHz reference oscillator and so on. The remote VSAT terminal consists of an outdoor unit (ODU) with 1.2m antenna diameter and indoor unit (IDU). For measurement, outbound BPSK modulated carrier of 67.89MHz center frequency and inbound pure carrier

of 68.37MHz are used. The experiments were carried out by using spectrum analyzer in Max. hold mode for 24 hours.

B. Test Results

The frequency offset on the inbound carrier measured without Doppler shift tracking loop is about ± 600 Hz at IF output port as shown in Fig. 5. This presents frequency errors of items 4 and 5 in Table 2.

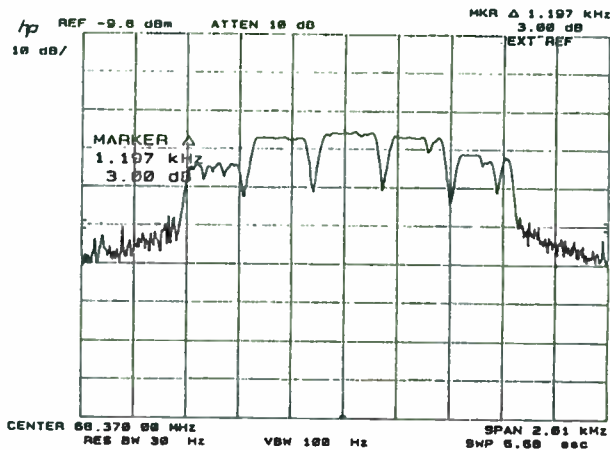


Fig. 5 Inbound carrier frequency error by Doppler effects

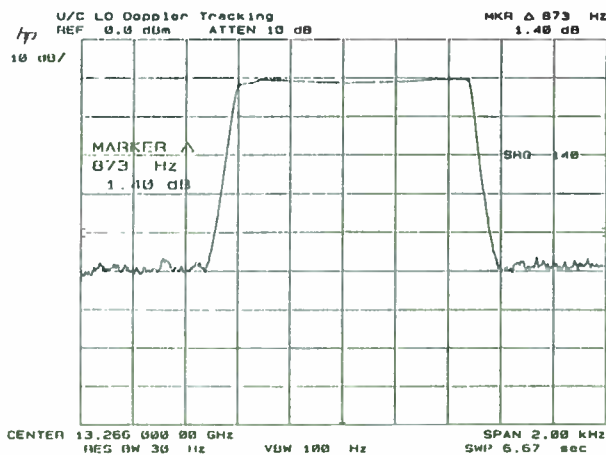


Fig. 6 Measured Doppler frequency shift

Fig. 6 shows the Doppler frequency shift measured at the Ku-band LO monitor port of U/C.

It is about ± 435 Hz, which has a close agreement with Doppler frequency shift shown in Table 1. After the Doppler frequency shift (item 4) is compensated for by the VCO2 circuit loop of AFC module, the frequency offset of inbound carrier is about ± 100 Hz as shown in Fig. 7. This shows the center frequency of inbound carriers is maintained within ± 1 kHz acquisition range of a burst demodulator.

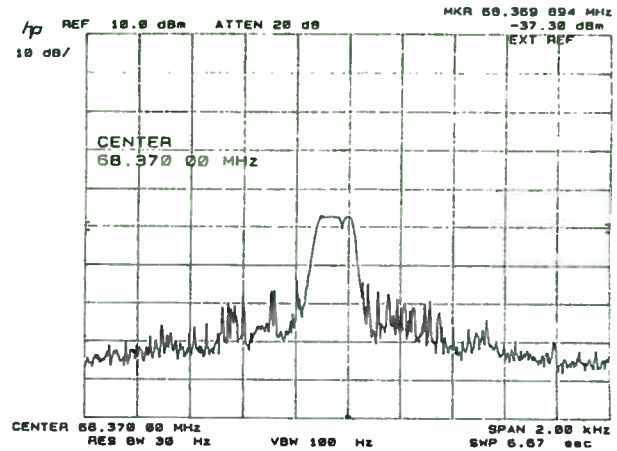


Fig. 7 Frequency error after AFC

V. Conclusions

An AFC module suitable for the low cost VSAT network is designed so as to compensate for both the relative Doppler frequency and the inherent frequency instability. It was tested with a hub and remote stations through the INTELSAT VA. The experimental results show that the proposed AFC circuit tracks very well the considered several frequency instabilities and is therefore maintained within ± 1 kHz of acquisition range required for general burst demodulators.

Reference

- [1] A. Hamid Rana, J. McCOSKY, and W. Check, "VSAT Technology, Trends, and Applications," Proceedings of the IEEE, Vol.78, No.7, July 1990, pp. 1087 - 1095.

- [2] Guillermo F. Bosch and Luigi Pagni, "Integrated VSAT Communications and Services," Proceedings of Intelcom'94, November 2 - 5, 1994 in Turin, pp. 217 - 221.
- [3] C.S. Pyo, J.I. Choi, C.S. Yim, and S.J. Chung, "A Study on Effects of Frequency Errors on System Performance and its Compensation Technologies in Satellite Communication Network," Proceedings of Fall 1993 Conference, Vol. 12-2, November 13, 1993 in Korea, pp. 565 - 569.
- [4] INTELSAT, "SCPC/QPSK and SCPC/PCM/QPSK System Specification," INTELSAT Earth Station Specification (IESS)-303, March 12, 1987.
- [5] Sewerinson Ake N, "Two Pilot Frequency Control for Communication Systems", U.S.A, Patent No. 1 193 674, 1985.9.17.
- [6] Marvin K. Simon, "Dual Pilot Tone Calibration Technique," IEEE Transactions on Vehicular Technology, Vol. VT-35, No.2, May 1986, pp. 63 - 70.
- [7] Christopher P. LaRosa and Todd K. Citron, "Performance Analysis of Dual-Pilot Tone Calibration Technique", Proceedings of ICC'87, 1987 in Seattle, pp. 1445 - 1449
- [8] Robert Gagliardi, Introduction to Communications Engineering, John Wiley & Sons, New York, 1978, pp. 427 - 432.
- [9] J.I. Choi and J.W. Park "Design of Doppler Frequency-tracking System by the Optimum Synchronization Techniques for the Digital Satellite Communication System," The Journal of the Korean Institute of Communication Sciences, Vol.19, No.12, December 1994. to be published.
- [10] P.A. Wintz, E.J. Luecke, "Performance of Optimum and Suboptimum Synchronizers," IEEE trans. Comm. Technologies, Vol. COM-17, June 1969, pp 380 -389.
- [11] C.S. Pyo, J.I. Choi, "The Doppler Frequency Shift of Inclined Orbit Satellite and Its Effects on System Performance," Proceedings of JCCI'94, April 29, 1994 in Korea, pp. 215 - 219.

Performance of a PM HEMT based LNA vs. temperature for VSAT applications

A. Caddemi, P. Livreri and M. Sannino

Dipartimento di Ingegneria Elettrica - Università di Palermo
Laboratorio di Elettronica delle Microonde
Viale delle Scienze - 90128-Palermo - ITALY

Abstract- For low-noise microwave applications, pseudomorphic (PM) and lattice-matched HEMTs exhibit outstanding noise and gain performances at both ambient and cryogenic temperatures. Due to these features, these devices are widely used for design of low-noise amplifiers in many applications such as satellite communication, radio astronomy, remote sensing, and so on, where maximum signal sensitivity is strictly required.

The trade-off performance of a PM HEMT-based LNA for VSAT receiver system applications has been investigated starting from the noisy model vs. frequency and temperature. The relevant results are reported and discussed in this paper.

INTRODUCTION

A careful investigation on the performance of an HEMT-based low-noise amplifier under change in ambient temperature requires knowledge of the active device's signal and noise properties vs. frequency and temperature. In this work,

an LNA design for VSAT applications has been carried out at room temperature (20°C) by accounting for all the optimum trade-off values (noise figure, operating power gain, input VSWR) obtained by means of two trade-off charts for a commercial pseudomorphic (PM) HEMT series (CFB001-03 by Celeritek) [1]. The performance of this LNA has then been analyzed as a function of frequency and temperature starting from the measured transistor behavior.

The measurements of the PM HEMT scattering (S-) parameters were carried out with the aid of a temperature controlled chamber in the $-50 \div +20$ °C range at 10°C steps. An equivalent circuit model was then fitted to the measured S-parameter sets by following an accurate modeling procedure to the aim of representing the *typical* device.

At room temperature, a complete characterization of the device series was also performed in terms of scattering, noise and gain parameters by means of a specialized computer-controlled instrument set-up developed in our Lab and extensively

used for testing and modeling several series of microwave low-noise transistors (MESFETs, HEMTs, PM HEMTs).

The noise performance has been associated to the HEMT equivalent circuit by using a noise temperature model which employs equivalent noise temperatures associated with the lossy circuit elements.

By using the noisy model, a careful investigation on the performance of the LNA under change in ambient temperature was carried out. The relevant results are reported in this paper.

DEVICE CHARACTERIZATION VS. TEMPERATURE

The S-parameter measurements were carried out with the aid of a thermostatic chamber to control the ambient temperature of the device under test (DUT). Semi-rigid coaxial cables connected the transistor test fixture (TTF) to the automatic network analyzer. The employed TTF consisted of three parts: two outer sections, which include the APC7 connections to the cables, and a middle insert, in which the DUT was located. The measurement set-up was calibrated at room temperature (20 °C), except for the cables whose performance had been characterized in terms of loss and electrical length at each temperature of interest. This led to the determination of a scattering matrix representing a lossy transmission

line with end discontinuities due to the APC7 transition.

The S-parameters of the devices were measured over the 2-18 GHz frequency range and over the -50 ÷ +20 °C range at 10°C steps. The tested device type was bonded in a 70 mil ceramic package.

At room temperature, a complete characterization of the device series was also performed in terms of noise, gain and scattering parameters by means of a specialized computer-controlled system, whose measuring procedure and relevant data processing techniques have been totally developed in our Lab [2-4 and references therein].

As far as the microwave noise performance is concerned, we refer to the representation in terms of the four noise parameters which appear in the following relationship

$$F(\Gamma_S) = F_{\min} + 4 r_n \frac{|\Gamma_S - \Gamma_O|^2}{|1 + \Gamma_O|^2 (1 - |\Gamma_S|^2)}$$

where F_{\min} (minimum noise figure), $|\Gamma_O|$ and r_n (optimum value of Γ_S) and r_n are the four parameters, F and Γ_S are the noise figure and the relevant input termination reflection coefficient of the DUT, respectively. A similar relationships holds for the four gain parameters.

By means of our automatic system, we perform measurements of either $F(\Gamma_S)$

for some properly selected values of Γ_S and $F(\Gamma_S)$, at each Γ_S value, for different values of system losses as introduced by a programmable step attenuator. From these noise data we derive both the noise and the gain parameter set through data processing techniques. The scattering parameters are then calculated by use of well-known relationships employing the gain parameters and, therefore, are not measured directly by a network analyzer.

The measuring system is presently operating over the 1-18 GHz range and over the $-100 \div 100$ °C temperature range by means of a thermocontrolled chamber. The implementation of a more compact version extended up to 40 GHz and to cryogenic temperatures directly on chip is in progress.

EXTRACTION OF THE NOISY MODEL

Since the characterization involved 10 samples, the S-parameter sets at each temperature have first undergone statistic evaluation in order to determine a single representative set of experimental values (say, a *typical* sample) to be employed in the subsequent model extraction vs. frequency and temperature .

As an example, Fig.1 shows the measurement results at different temperatures for the $|S_{11}|$ and $|S_{21}|$ parameters. While $|S_{21}|$ exhibits a clear trend for increasing upon cooling down the device, the other parameters show only

subtle changes which, however, affect the device modeling.

The equivalent circuit model was fitted to the measured S-parameter sets by following the subsequent steps: 1) fixing the basic circuit topology which includes package parasitics; 2) applying a decomposition approach for the optimization of the circuit variables at room temperature; 3) adding knowledge of the behavior of the chip model elements to provide physical consistency and additional constraints for the optimization at lower temperatures.

The network configuration, reported in Fig. 2 , is characterized by a symmetrical outer section which refers to the influence of the package parasitics plus bonding wires and by an internal structure related to the chip device. The model element values are shown in Tab.1.

The circuit elements which mainly affect the microwave performance of the chip device are the transconductance g_m , the gate-to-source capacitance C_{GS} and the output resistance R_{DS} . Their value trends are in accordance with the physics-based behavior. The pronounced increase in the value of g_m and the decrease of the C_{GS} value are related to the expected increase in the device gain and cutoff frequency as the temperature lowers.

The noise performance has been associated to the above circuit by using a noise temperature model which allows to simulate noise parameters upon assignment

of equivalent noise temperatures to the lossy circuit elements [5]. Typically, all the resistor temperatures follow the ambient temperature value, whereas the resistance R_{DS} is *overwarmed* at a temperature T_d of several thousands degrees centigrade.

To the aim of deriving this latter value and its rate of decrease with decreasing temperature, we have employed the noise measurements performed at room temperature. By fitting the values of the minimum noise figure F_{min} vs. frequency we have thus derived the value of T_d at 20 °C.

Since previous experimental results [6] have shown that the variation of T_d is quite similar to the rate of decrease of the ambient temperature, we could extrapolate the performance of F_{min} vs. temperature and frequency.

As expected, the F_{min} values decrease with decreasing temperature, while the other noise parameters are affected in a more complex way by the changes occurring in all the model element values.

DESIGN AND PERFORMANCE OF THE LNA

Recent advances in MMIC technology have resulted in substantial size and mass reduction in many types of solid state microwave equipment. However, the stringent electrical specifications in most microwave receivers require the use of MIC and hybrid technologies in the front-end LNA stages rather than MMICs. Where size

and mass are also critical parameters the optimum solution is to use MIC front-end stages followed by MMIC gain blocks. According to this solution a two-stages front-end LNA over the VSAT frequency range (10.95 GHz - 12.75 GHz) was designed and its performance vs. temperature was analysed.

Optimum noise figure, operating power gain, input VSWR and unconditional stability was the key parameters which have defined the LNA input matching network and its design. The circuit configuration was analysed using the Smith chart and the LIBRA™ CAD package. In order to obtain high performance and to avoid unfriendly procedures of trial and error during the process of loads selection, the low-noise sections were designed, according to a design methodology developed in our Lab., making use of the optimum trade-off values (noise figure, operating power gain, input VSWR) of the chosen PM HEMT.

Starting from the noisy model vs. frequency and temperature a careful investigation on the performance of the LNA under change in ambient temperature was carried out.

In Fig.3, the LNA noise figure and operating power gain as a function of frequency and temperature are reported.

DIRECT DIGITAL SYNTHESIS OF FM (CHIRP) WAVEFORMS

D.Cioppi^{}, P.Tortoli^{**}, F.Guidi^{**}*

^{*} *Micrel S.p.A.*

Via A.Einstein, 26 - 50013 Campi Bisenzio (Florence), Italy

^{**} *Electronic Engineering Department - University of Florence
Via S.Marta, 3 - 50139 Florence, Italy*

Direct Digital Synthesizers (DDS's) provide a wide variety of signals employed in radar, communication and test systems. High frequency agility, fine phase and frequency resolution, digital control of all operations, are inherent advantages of this waveform synthesis technique which allows complex modulated signals, such as n-bit PSK, FSK, FM, QAM, to be accurately generated. However, since most DDS's have limited bandwidth, i.e. limited clock frequency, they are often used in conjunction with mixing stages and/or phase locked loops to translate the output signal in a frequency range compatible with IF's typical of modern communication systems.

The possibility of avoiding the need for upconversion circuitry by exploiting alias images of the fundamental spectrum generated by a DDS is here discussed. The new method is also experimentally demonstrated in a complex frequency generator for a multimode radar pulse compression system, using one digital expander and SAW matched filters. The proposed approach is shown capable of extending the area of application of DDS's having limited bandwidth without sacrificing overall system performance.

1. Introduction

Advantages of modern Direct Digital Synthesizers [1] are well known: tight digital control of all operations; very fine frequency steps and, at the same time, high switching speed; excellent phase noise, usually better than that of reference oscillator; good spurs level at the digital output, except some cases of correlation between output frequency and clock frequency; reduced weight and size. By Taking advantage of these features, modern radar and communications transmitters with unprecedented accuracy and simplicity can now be built, even for generating complex modulation such as Fast Frequency Shift Keying (FFSK), n-bit Phase Shift keying (PSK), n-bit Quadrature Amplitude Modulator (QAM), conventional FM, AM, PM or their combination.

The maximum clock frequency, and therefore the maximum signal bandwidth, is one of most important factors limiting

the use of DDS's. Modern radar and communication systems, in fact, use Intermediate Frequencies (IF's), where direct synthesis is not feasible unless special and expensive components are employed. Improvements in design and manufacturing process of both DDS and Digital to Analog Converters (DAC's) are expected to contribute to overcome this limit but, in most current architectures, signals to be transmitted are synthesized at low frequencies and then translated to IF by means of one, or more, upconversion stages.

The possibility of reducing the need for upconversion circuitry by exploiting alias images of the fundamental spectrum generated by a DDS, is discussed in this paper. Theoretical features of aliased spectra in such application are discussed in the next section. Experimental tests of the proposed approach, shown in section 4, have been conducted within a multimode

radar pulse compression loop. The loop employs a DDS for generation of pulsed frequency modulated (chirp) waveforms and Surface Acoustic Wave (SAW) devices for matched filtering.

Chirp signals have a frequency spectrum well suited to the alias test to be carried out. The nearly rectangular amplitude shaping, in fact, gives evidence to any possible distortion. Moreover, compressed pulse sidelobes exhibit great sensitivity to any deviation of the synthesized chirp from ideality, namely the stronger the difference the higher the sidelobe level. Hence, the compressed pulse, may be used to indirectly evaluate the quality of synthesized signals.

Comparison of different compressed pulses obtained at the output of SAW matched filters, revealed that there are no performance degradations by using aliased DDS-based expander with respect to directly generated, i.e. no aliased, expanders. Accordingly, the area of application of DDS with limited clock frequency is significantly extended.

2. Direct digital synthesis of aliased signals

As known, in DDS operation the instantaneous output frequency depends on both the system clock, i.e. sampling, frequency F_{ck} and the digital control word set at the accumulator input. The actual

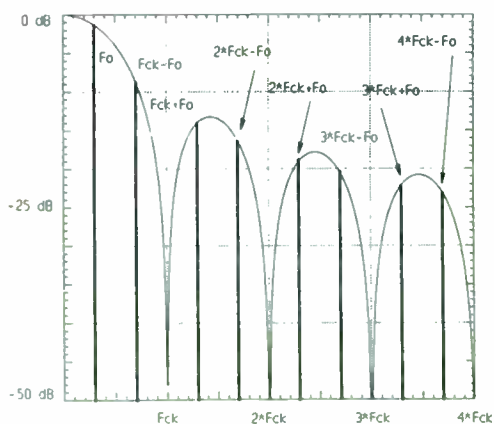


Fig. 1 Simulated wideband spectral plot of a cw signal generated by a DDS.

maximum output frequency which can be realistically synthesized is conditioned by a number of factors.

Classical Nyquist sampling theory dictates that the maximum output frequency is $F_{ck}/2$. Practical considerations on reconstruction filter limit the actual maximum frequency at about 30% + 40% of reference frequency.

System clock noise is another limiting factor. High analog output frequencies, in fact, require high clock rates which are difficult and expensive to obtain, especially if reference oscillators with excellent phase noise performance are needed. Moreover clock feedthrough is always present in the analog output, with a level related to the clock frequency itself and to the complexity of clock noise reduction techniques utilized in circuit layout.

Another limitation is represented by the relatively poor spectral purity of signals reconstructed by means of high speed DAC's, due to their differential non-linearity, integral non-linearity and glitch energy. Furthermore, the higher is the frequency of the signal being reconstructed, the lower is the DDS's and DAC's output resolution available.

To increase the output signal frequency, DDS based circuits are often used in conjunction with phase locked loop (PLL) or heterodyning mixer stages. Although most of the DDS features are preserved, disadvantages arise in terms of circuit complexity and critical trimming operations.

However, the DDS architecture can be used in such a way that PLL or mixer upconversion stages are unnecessary. As shown in Fig.1, the output spectrum of a cw signal of frequency F_0 generated by a DDS operating at F_{ck} rate, contains components at $N \cdot F_{ck} \pm F_0$, where N is an integer number. By bandpass filtering one of the aliased images instead of the fundamental spectral line, the additional upconversion circuitry may be avoided.

Design difficulties are connected to the fact that the output waveform, being originated from a DAC, is of the sample and hold type, i.e. yields a $\text{sinc}(\pi F_0/F_{ck})$

frequency roll-off, while spurious energy due to DAC's non-linearity and quantization noise do not have the same characteristics. Bandpass filtering may then be required to isolate the desired alias from adjacent harmonics and spurious. On the other hand, it has to be recalled that DDS's with 10-12 bits of output resolution are hardly capable of working at clock frequencies higher than 100 MHz. Hence, the proposed method significantly extends the range of application of devices where quantization noise is reduced at minimum levels.

This approach, so far discussed for continuous wave signals [2], may be extended to more sophisticated waveforms, including those where useful information is coded through modulation of the carrier frequency. A significant example is shown in the next section, where the generation of FM waveforms for radar pulse compression is presented.

3. Application to radar pulse compression

In the last few years, Radar pulse compression systems have evolved from a full analog implementation - typically based on SAW devices - to mixed Analog-Digital implementations [3]. While SAW technology is still unsurpassed for implementing wide-band matched filters (compressors), the digital approach is now particularly attractive for generating the frequency modulated (chirp) waveform to be transmitted, since it can guarantee a predictable high level of accuracy. Typically, the waveform is generated at baseband through the synthesis of in-phase (I) and quadrature (Q) components. Digital I/Q samples are converted to analog format and then frequency translated to an intermediate frequency (IF) using a conventional single-side-band modulator.

The major drawback of this approach is that, for obtaining proper matching between quadrature channels, critical trimming operations are usually needed. Advanced radar performances, in fact, can involve compressed pulse

sidelobe level as low as -40 dB: in order to reach this goal, the amplitude and phase ripple of transmitted waveform must be maintained within 0.2 dB and $\pm 0.5^\circ$, respectively [4], which calls for an accurate control of both I and Q channels.

Recent advances in the technology of DDS's have finally made feasible their use for directly generating the desired chirp waveform around a suitable frequency F_o . Advantages with respect to the I/Q approach lie in the reduction of necessary components (dimensions, weight, power consumption), and, overall, in the elimination of any trimming operation.

As already mentioned, Nyquist criteria and practical considerations on reconstruction filter limit the maximum output frequency to about 40% of clock frequency. This constitutes a drawback which can noticeably reduce the area of application of each device. In radar pulse compression systems, in fact, main specifications concern the bandwidth (B) and the duration (T) of the chirp waveform [5], since these parameters are related to the obtainable resolution and range, respectively. No significant system requirements are imposed to the value of the intermediate frequency, which is therefore fixed on the basis of possible receiver requirements. SAW implementation of matched filters is easier if narrow fractional bandwidth, i.e. low B/F_o ratios, are involved. Hence, even for moderate bandwidth, an IF of typically several tens of MHz is often used. According to the above mentioned limitation, a large class of DDS devices (e.g., all those which are TTL compatible and operate with maximum clock frequencies not higher than 100 MHz), would not be suitable for this application.

However, this limitation can be overcome just by exploiting the generation of aliased images of the fundamental chirp waveform (Fig.2), due to sampling at the F_{ck} rate. By properly choosing F_{ck} and the fundamental frequency F_o of the synthesized signal, the frequency of the first ($F_{ck}-F_o$), or second ($F_{ck}+F_o$) image can be made coincident with the desired IF. If the frequency difference is chosen, it must

be considered that a "mirror" image of the fundamental component is obtained. Namely, in order to select an "up" chirp signal (i.e., one with an increasing frequency vs time slope) around $F_{IF} = F_{ck} - F_o$, the DDS clocked at F_{ck} must be programmed to synthesize a "down" chirp around the frequency F_o .

The design difficulty in using first or higher order alias images is connected to the $\text{sinc}(\pi F_o/F_{ck})$ frequency roll-off of output spectrum. As a consequence, the selected image of the chirp spectrum always exhibits a non-flat frequency behavior due to the sampled system sinc response. Such distortion can be seen as an AM with a very low modulating frequency, which, according to the well-known paired-echo theory [5], yields only a pair of sidelobes well within the width of the compressed pulse main lobe. Usually, these close-in sidelobes do not constitute a problem, but, if necessary, they could be avoided by compensating for the sinc roll-off response with a suitable high-pass filter. However, it has also to be recalled that the chirp signal which is effectively transmitted by the radar system is often saturated, and this type of distortion is inherently avoided.

4. Experimental results

A "multimode" pulse compression system based on SAW filters operating in the VHF range and a single Direct Digital

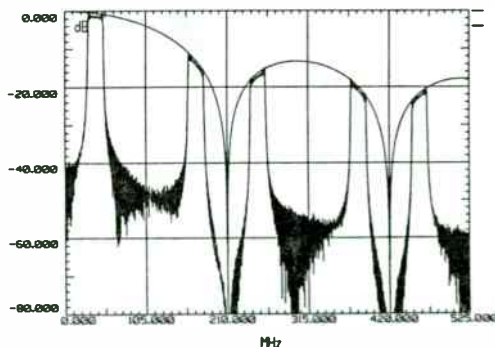


Fig. 2 Wideband spectral plot of a chirp signal with $T = 20 \mu\text{s}$, $B = 20 \text{ MHz}$, $F_o = 40 \text{ MHz}$ synthesized by SP2001 clocked at 210 MHz.

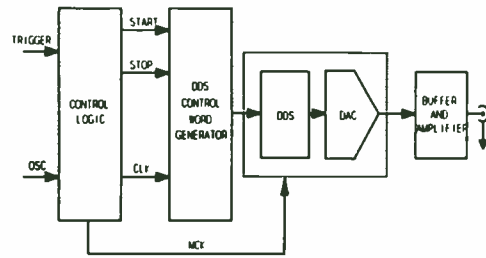


Fig. 3 DDS-based digital expander block diagram.

Synthesizer employing an SP2001 device, specified for generation of waveforms up to 100 MHz [6], has been implemented. The needed chirp signals have been obtained (Fig.3) by enabling the DDS output for a time T , corresponding to the signal duration. During this time, the output frequency was swept over the desired bandwidth by reading the DDS input from an EPROM, where samples corresponding to discrete frequencies of desired frequency vs time chirp characteristic have been stored. Different signals were generated by selecting different EPROM pages.

As an example, fig. 4 shows the fundamental, first and second alias spectral images of a chirp signal having bandwidth $B = 3.85 \text{ MHz}$ and duration $T = 60 \mu\text{s}$. They were obtained by operating the DDS at a clock frequency (210 MHz) such that the center frequency of the first alias image (180 MHz) was made coincident with the actual IF of the corresponding SAW compressor. Note that this IF is higher than the maximum output frequency (100 MHz) specified for the SP2001 device. Fig. 4 gives evidence to the fact that the selected spectrum represents a mirror image of the fundamental spectrum, with no appreciable distortions except the predicted slight frequency roll-off.

In order to demonstrate that no significant degradation of the synthesized waveform is involved, the compressed pulses obtained by means of the proposed approach have been compared with results obtained with conventional synthesis methods. First, the same device has been used with two different clock frequencies, $F_{1ck} = 210 \text{ MHz}$ and $F_{2ck} = 85 \text{ MHz}$, to

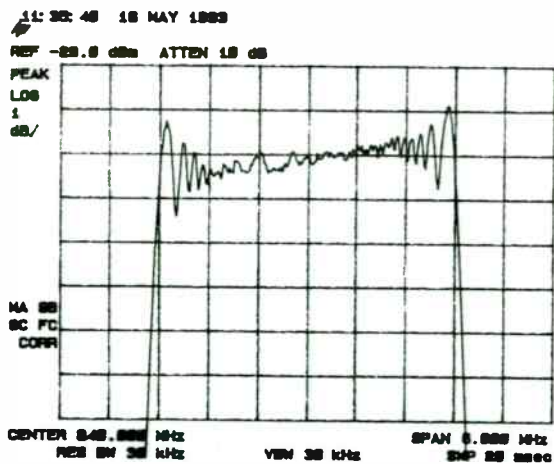
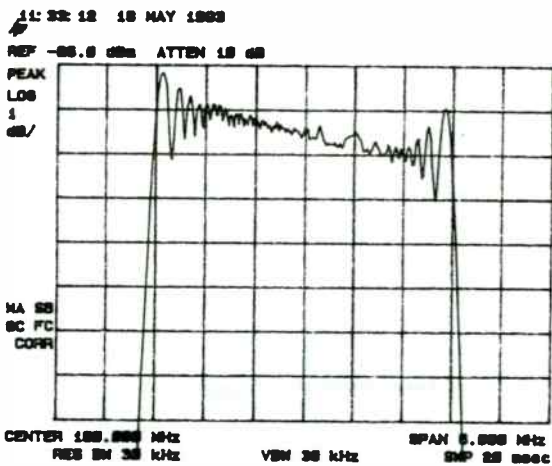
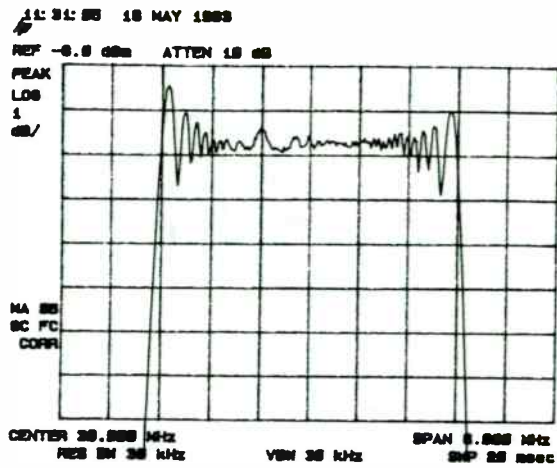


Fig.4 Fundamental spectrum ($F_0=30$ MHz, top), first ($F_1=180$ MHz, middle) and second ($F_2=240$ MHz, bottom) alias images obtained by clocking an SP2001 at 210 MHz.

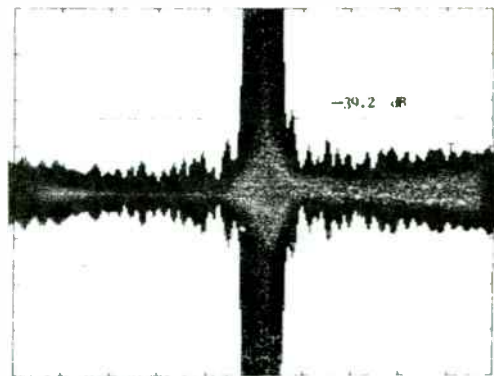
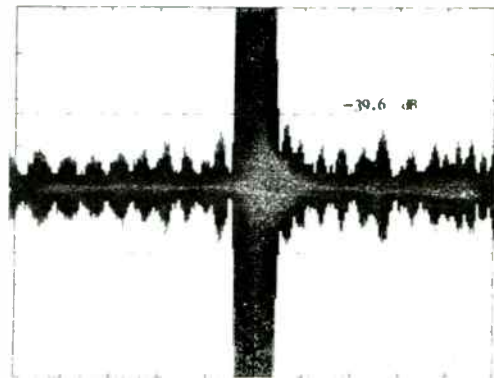


Fig.5 Compressed pulses with $B=5.6$ MHz, $T=20$ μ s, $F_0=60$ MHz obtained with an SP2001: conventional ($F_{ck}=210$ MHz, top) and alias mode ($F_{ck}=85$ MHz, bott.)

generate a fundamental spectral image and a first alias image, respectively, around $F_0 = 60$ MHz. As expected, the compressed pulses obtained in the two cases (Fig. 5) present equivalent sidelobe levels, thus demonstrating that there is no advantage in using a DDS operated in a conventional mode (and, therefore, at a higher clock frequency).

Similar conclusions are obtained by observing the output of a SAW filter operating at $F_0 = 120$ MHz, when the input chirp waveform was produced by a classical I/Q generator followed by a single sideband modulator. Accurate trimming between baseband I and Q channels yielded a sidelobe level in the -40 dB range, the same obtained by operating a DDS at $F_{ck} = 95$ MHz to select the first alias image at 120 MHz.

5. Conclusions

The possibility of using, in modern communication transmitters, aliased images of fundamental spectrum generated by a DDS has been discussed. Experimental results have been presented for frequency modulated pulsed (chirp) signals.

Main advantages of the proposed approach lie in the extension of the area of application of each device, as well as in the limitation of the clock frequency to values compatible with operations of low cost logic.

Acknowledgements

The authors wish to acknowledge the valid technical contribution of Mr. S.Fiumicelli in the implementation of the experimental system and the help of Mr. P.Lippi in preparing this paper.

References

- [1] P.Saul, T.Coffey, "Current achievements in direct digital synthesis", *Microwave Engineering Europe*, 1993, pp. 31-36.
- [2] A.Hill, J.Surber, "Using aliased-imaging techniques in DDS to generate RF signals", *RF Design*, 1993, pp. 31-36.
- [3] P.Tortoli et al., "Digital technology improves radar pulse compression", *Microwaves & RF*, Vol.32, March 1993, pp. 64-70.
- [4] J.R. Klauder et al., "The theory and design of chirp radars", *Bell Systems technical Journal*, Vol.34, n.4, 1960, pp. 781-789.
- [5] C.E. Cook, M. Bernfeld, *Radar Signals*, Academic Press, New York, 1967.
- [6] "Professional products handbook", GEC Plessey Semiconductors, May 1991.

Components For Wireless Design

Session Chairperson: Chris Fisher,
Microwave Technology, Inc. (Fremont, CA)

Design and implementation of low-noise discrete silicon bipolar transistors and GaAs FET devices in low-current commercial applications at 900 MHz and 2400 MHz. **Al Ward,** Hewlett-Packard Co., Communications Components Division (Richardson, TX).....**437**

A 1-W, Class A, hybrid surface-mountable amplifier for ultralinear multicarrier wireless applications. **Masa Omori, John Martin, and Chris Fisher,** Microwave Technology, Inc. (Fremont, CA).....**444**

Low-cost broadband GaAs RF IC amplifiers. **Leonard Reynolds, Jr.** RF Micro-Devices (Greensboro, NC).....**445**

Unique VCO design for wireless applications. **Shankar Joshi,** Synergy Microwave Corp (Paterson, NJ).....**452**

KTP: A new piezoelectric material for wireless communications. **David K.T. Chu,** EI DuPont, Central Research and Development Group (Wilmington, DE).....**453**

DESIGN AND IMPLEMENTATION OF LOW NOISE DISCRETE SILICON BIPOLAR TRANSISTORS IN LOW CURRENT COMMERCIAL APPLICATIONS AT 900 MHz AND 2400 MHz

Al Ward
Hewlett-Packard Communications Components Division
Richardson, Texas

ABSTRACT

Discrete bipolar transistors offer low cost solutions for commercial applications in the VHF through microwave frequency range. Today's silicon bipolar transistors offer state of the art noise figure and gain performance with low power consumption. Commercially available discrete NPN bipolar transistors optimized for maximum f_t at low voltages are the subject of this paper. Devices with sub 1 dB F_{min} s and associated gains greater than 10 dB at a V_{ce} of 2.7 volts at 1 to 2 mA of collector current will be discussed.

This paper will cover the design techniques and performance of silicon bipolar low noise amplifiers for use in the 900 MHz and 2400 MHz ISM bands. Typical applications include pagers, cellular telephones and spread spectrum systems.

I. INTRODUCTION

The pager and cellular markets are always looking for ways of increasing battery life. Lower current consumption translates to increased battery life and increased customer satisfaction. Although MMICs reduce the space required to implement a particular function, they generally don't offer an advantage over discrete devices in terms of current drain from the battery.

This paper will discuss the design and implementation of a new line of low current silicon bipolar transistors that have been optimized for maximum f_t at low voltage operation, making these devices ideal for low current battery operation in the pager and cellular markets. Low current devices will also find homes in other

markets such as GPS and in the 900 MHz and 2400 MHz ISM bands.

The new AT-3 series of silicon bipolar transistors are fabricated using an optimized version of Hewlett Packard's 10 GHz f_t Self-Aligned-Transistor (SAT) process. The die are nitride passivated for surface protection. Excellent device to device uniformity is guaranteed in fabrication by the use of ion-implantation, self aligned techniques, and gold metalization.

The AT-3 series of devices has a 3.2 micron emitter-to-emitter pitch and has been fabricated in a variety of geometries for various applications. The 20 emitter finger interdigitated geometry yields an easy to match device capable of moderate power at low to moderate current. The 10 emitter finger geometry offers higher gain at low current while the 5 emitter finger geometry offers the highest gain at lowest current consumption. The smaller devices at very low currents present very high impedances that can make them more of a challenge to design with. The impedances associated with very low current transistors at 900 MHz are very similar to those presented by 500 micron MESFETs at 900 MHz.

This paper will cover the design and implementation of two low noise amplifiers; one for use at 900 MHz and one at 2400 MHz. The 900 MHz amplifier uses the Hewlett Packard AT-32033 device which is available in the industry standard SOT-23 package. The 2400 MHz amplifier uses the AT-31011 device. The 2400 MHz amplifier uses a device in the SOT-143 package because of its reduced package parasitics and resultant higher gain at the higher frequency.

II GENERAL DESIGN CONSIDERATIONS

Achieving the lowest possible noise figure from either a silicon bipolar or GaAs FET device requires an input matching network that transforms the system impedance, generally 50Ω , to Gamma Optimum (Γ_o). Γ_o is the device input reflection coefficient required for the device to produce its rated noise figure. Impedance matching circuits must be chosen so that they have minimal loss, desired bandwidth, and tolerance to component variations in production. Losses of actual input matching circuits have been measured at nearly 0.5 dB at VHF frequencies when attempting to match the high impedances of MESFETS. Similar impedances can be encountered when using low current silicon bipolar transistors. Matching a device for lowest noise performance does not necessarily guarantee the best input VSWR and performance tradeoffs need to be made. A solution is the use of inductance in either the source or emitter to create negative feedback which can bring Γ_o and S_{11}^* closer in value. The amount of inductance must be carefully weighed against its effect on other circuit parameters such as gain and stability. An improperly chosen amount of inductance can cause out of band oscillations that can prohibit an amplifier from delivering its rated performance. Other techniques such as resistive feedback and resistive loading can improve stability but can limit power output capability.

An often overlooked part of an amplifier is the bias decoupling network that must be invisible to the RF matching networks. Generally they provide a low loss method of biasing the devices but in some situations can actually be used to provide some resistive loading for stability both in-band and out-of-band. Properly designed bias decoupling networks can also be used to provide some form of band pass or high pass filtering that could help reduce low frequency out-of-band gain. A poorly designed amplifier with very high low-frequency gain that maybe unconditionally stable according to the computer simulation may actually oscillate if mounted in a resonant enclosure. The enclosure that

houses the amplifier must be designed such that it offers enough isolation around the circuit such that it does not make the amplifier circuit unstable at any frequency.

The manner in which circuit elements are implemented will effect the overall amplifier performance. The use of etched circuit elements as opposed to surface mount discrete elements offers a cost benefit but may effect losses. Surface mount components offer small size but parasitics and device Q must be understood if their effect on circuit performance is to be properly analyzed.

III. 900 MHz AMPLIFIER

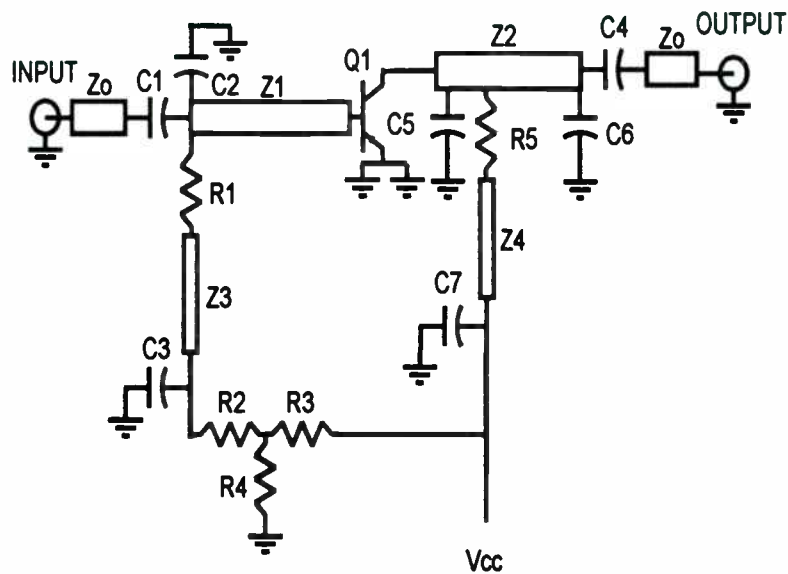
The 900 MHz AT-32033 amplifier is designed for a nominal 1 dB noise figure and 10 dB associated gain at 2 mA collector current. Although the device is capable of sub 1 dB noise figures, most applications don't require much below 1.5 dB. Starting out with a device that has such a low f_{min} allows the designer to make tradeoffs between noise figure, gain, stability, etc.

The schematic diagram of the 900 MHz amplifier is shown in Figure 1. The input noise match consisting of a low pass network in the form of C2 and Z1 provides a low Q broad band match. A small wound inductor could replace transmission line Z1. A value in the range of 15 to 20 nH would be a good substitute. In the actual circuit it was found that the input shunt capacitor was not required. Adding a shunt capacitor at this point will allow the designer to make tradeoffs between noise figure and input VSWR.

The output match consists of a 3 element low pass network. The 3 element network allowed a shorter length of series transmission line to be used as compared to a 2 element match. . The series inductive element can be etched onto the printed circuit board or a low cost wound inductor can be used if board space is limited. A suggested value would be in the range of 20 to 25 nH. The artwork and component placement guide are shown in Figures 2 and 3. A small amount of emitter inductance is used to improve in-band stability. This value

must be carefully chosen such that an excessive amount is not used, otherwise high frequency oscillations could be produced. Out of band oscillations will severely limit the ability of the device to produce it's rated performance. Resistor R1 provides very low frequency stability while resistor R5 enhances overall stability, including in-band performance. A current

source consisting of resistor R2 connected to the resistive divider consisting of resistor's R3 and R4 provide the necessary base current to produce the desired 2 mA collector current.



- C1 - 10 pF chip capacitor
- C2 - 1 pF chip capacitor (adj for NF/VSWR)
- C3, C7 - 1000 pF chip capacitor
- C4 - 100 pF chip capacitor
- C5 - 1 pF chip capacitor
- C6 - 2.7 pF chip capacitor
- Q1 - Hewlett-Packard AT-32033 Silicon Bipolar Transistor
- R1 - 50 ohm chip resistor
- R2 - 47 K ohm chip resistor (adjust for rated Ic)
- R3, R4 - 15 K ohm chip resistor
- R5 - 150 - 180 ohm chip resistor (adj for stability/Pout)
- Z0 - 50 ohm microstripline
- Z1 - Z2 - etched microstripline circuitry (may substitute inductor)
- Z3 - Z4 - microstrip bias decoupling lines

Figure 1. Schematic diagram of AT-32033 900 MHz amplifier

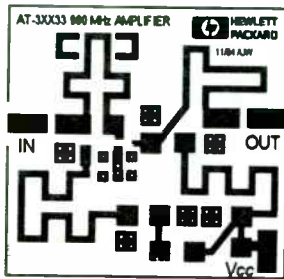


Figure 2. 1X artwork for 900 MHz amplifier using 0.062 inch thick FR-4

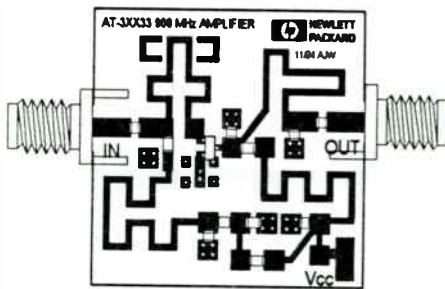
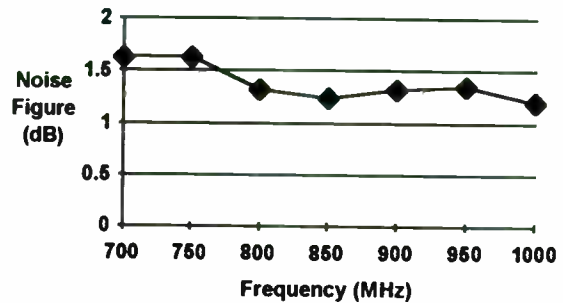


Figure 3. Component placement for 900 MHz amplifier using 0.062 inch thick FR-4

Actual measured noise figure of the amplifier with a microstripline input is shown in Figure 4. The amplifier provides a nominal 1.25 dB noise figure from 800 to 1000 MHz. The noise figure will improve slightly with the use of a wound inductor in place of the microstripline. Pay careful attention to the parasitic capacitance of the wound inductor as it could limit amplifier noise figure and effect out-of-band stability. Actual measurements of similar microstripline noise match circuits suggest losses as high as 0.4 dB depending on the device reflection coefficient to be matched. Subtracting 0.4 dB from the measured amplifier noise figure suggests a device noise figure of 0.8 dB. Measured losses of circuits using wound inductors are in the 0.2 to 0.25 dB range.

Figure 4. AT-32033 Amplifier Noise Figure



Actual measured amplifier gain is shown in Figure 5. The amplifier has a nominal 11 dB gain from 750 to 900 MHz.

Figure 5. AT-32033 Amplifier Gain

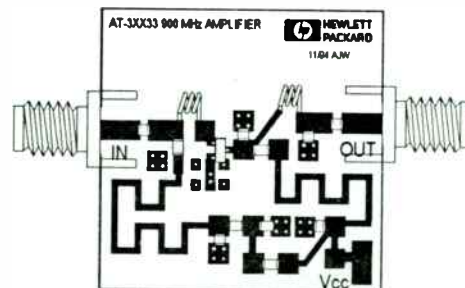
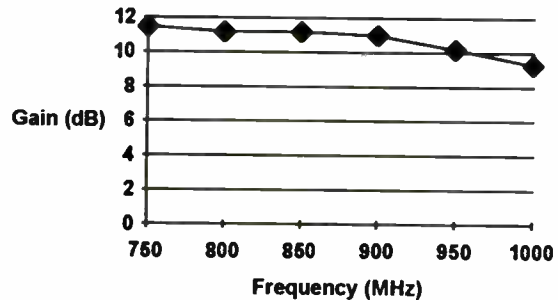


Figure 6. 900 MHz amplifier showing the placement of wound inductors in place of microstripline networks

Once the circuit has been optimized for best noise figure, gain and input/output VSWR, it is then necessary to take a look at output power. The 900 MHz amplifier was first tested for P1dB and then for IP3. Initial results for P1 dB were less

than those as specified on the data sheet. The major difference is that the amplifier being evaluated was conjugately matched at the output. Most device manufacturers specify P1dB at a "power match" and not a "conjugate match". This implies that tuners are used at the input and output of the device to maximize gain and power output. Maximum power output rarely occurs when any device's output port is conjugately matched. How much improvement can be achieved by power matching?

Initially, the 900 MHz amplifier was tuned for best output VSWR at 850 MHz. Greater than 20 dB return loss was obtained. The measured 1 dB compression point was -5.5 dBm with the device biased at a Vce of 2.7 volts and 2 mA Ic. Close examination of the output matching network suggested that possibly the 180 Ω resistor used in the output bias decoupling line might be absorbing some of the power. This resistor was placed in the circuit to raise in-band stability. Placing a short across this resistor and re-measuring the 1 dB compression point showed an improvement of 3.5 dB! Also observed was an increase in collector current when the device is driven toward compression. An increase in current causes an increase in the voltage drop across the 180 Ω resistor causing the collector voltage to sag. Minimizing the value of this resistor will tend to keep Vce high when the device is driven hard and will also minimize power absorption in the circuit. The drawback could be decreased stability. Some compromise with respect to output loads may have to be instituted if additional power output is desired.

A P1dB of -2 dBm is still slightly lower than the data sheet specification, however, the output is still conjugately matched and not power matched. In order to provide a power match, one must provide an alternative output match. In order to prove that a power match will provide greater power output, a lab exercise can be set up. A double stub tuner is connected in series with the existing conjugately matched amplifier output circuitry and the power meter. The tuner is then adjusted for greatest power output while driving the input circuit higher. A spectrum analyzer can be

useful here to determine that harmonics are not high enough in level to distort the power meter measurement. In small steps increase the input power and then retune the output tuner for maximum fundamental power. After retuning the output for a power match, it was found that the P1dB increased to nearly 2 dBm with a reduction in gain of 1 dB over the small signal conjugate match. In order to revise the output match to provide a power match would require breaking the circuit at the collector port of the device and measuring the new Gamma Load (Γ) presented by the existing circuit plus the external tuner. It is interesting to note that the output return loss which was greater than 20 dB at 850 MHz is now only 8.5 dB at the power match condition.

In addition to measuring P1dB at all output matches, the two tone third order intercept point (IP3) was also measured. For each test, two tones were introduced at the input to the amplifier which are separated by 10 MHz.. The resultant third order products were then measured and averaged and IP3 was calculated. The results are shown in Table 1.

Table 1. 900 MHz amplifier power output summary

Condition	P 1dB	IP3
Conjugate Match	-5.5 dBm	+16 dBm
Conjugate Match w/o resistor	- 2.0 dBm	+18 dBm
Power Match	+2 dBm	+23 dBm

The results show a consistent 20 to 21 dB of difference between P1dB and IP3. This is somewhat greater than has been measured on other larger geometry small signal devices but it does appear to be repeatable..

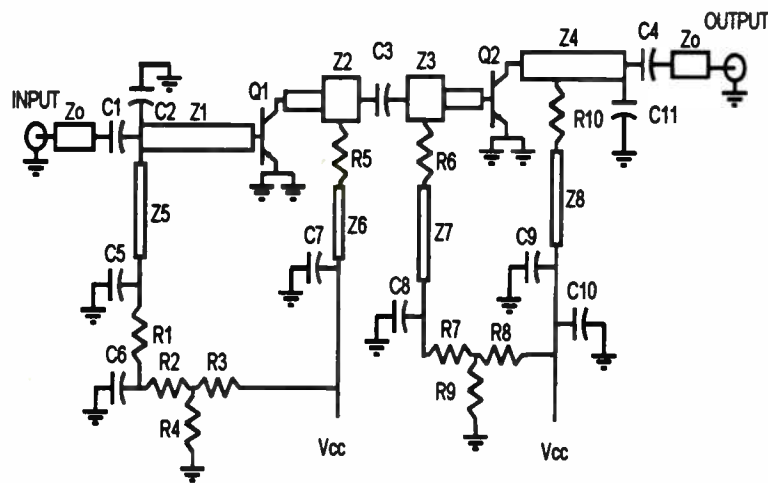
IV. 2400 MHz AMPLIFIER

The 2400 MHz amplifier is designed around the Hewlett Packard AT-31011. The 10 emitter finger geometry plus the SOT-143 package with the two emitter leads offers improved performance at frequencies above 2 GHz. At a rated current of 1 mA, the AT-31011 provides a device noise figure of 1.7 dB at 2400 MHz with an associated gain of 10 dB.

The schematic diagram of the 2400 MHz amplifier is shown in Figure 7. The input noise match consisting of a low pass network in the form of C2 and Z1 provides a low Q broad band match. The capacitor at C2 can be optimized for either a noise or conjugate match.

The output match consists of a 2 element low pass network while the interstage network consists of two short transmission lines and a series capacitor. The artwork and component placement guide are shown in Figures 8 and 9. Minimal

emitter inductance is used to preserve in-band gain without sacrificing stability. Resistor R1 provides low frequency stability while resistors R5 and R10 enhance overall stability, including in-band performance. Two current sources (resistor R2 connected to the resistive divider consisting of resistor's R3 and R4 and R7 connected to the resistive divider consisting of R8 and R9) provide the necessary base current to produce the desired 1 mA collector current in each device.



- C1, C4, C5, C9 - 10 pF chip capacitor
- C2 - 1.3 pF chip capacitor
- C3 - 1.5 pF chip capacitor
- C6, C7, C8, C10 - 1000 pF chip capacitor
- C11 - 2 pF chip capacitor (adjust for min output VSWR)
- Q1, Q2 - Hewlett-Packard AT-31011 Silicon Bipolar Transistor
- R1, R10 - 50 ohm chip resistor
- R2, R7 - 47 K ohm chip resistor (adjust for rated Ic)
- R3, R4, R8, R9 - 15 K ohm chip resistor
- R5 - 16 ohm chip resistor
- R6 - 1 K ohm chip resistor
- Z0 - 50 ohm microstripline
- Z1 - Z4 - etched microstripline circuitry
- Z5 - Z8 - microstrip bias decoupling lines

Figure 7. Schematic diagram of AT-31011 2400 MHz amplifier

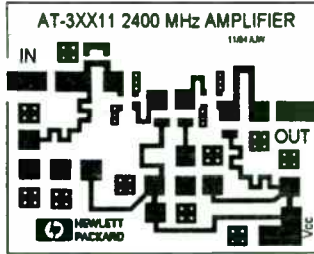


Figure 8. 1X artwork for 2400 MHz amplifier using 0.062 inch thick FR-4

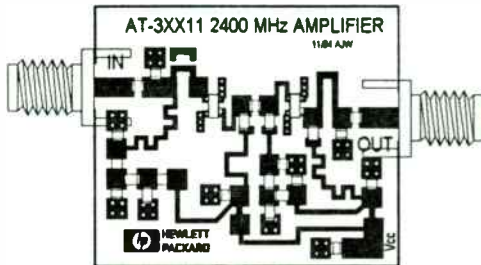


Figure 9. Component placement for 2400 MHz amplifier using 0.062 inch thick FR-4

The amplifier has a measured noise figure between 1.9 and 1.95 dB from 2400 to 2500 MHz with an nominal associated gain of 20 dB at a total current consumption of 2 mA for both devices. Measured output 1 dB gain compression point is -4.5 dBm with an associated IP3 of +7 dBm.

Figure 10. AT-31011 Amplifier Noise Figure

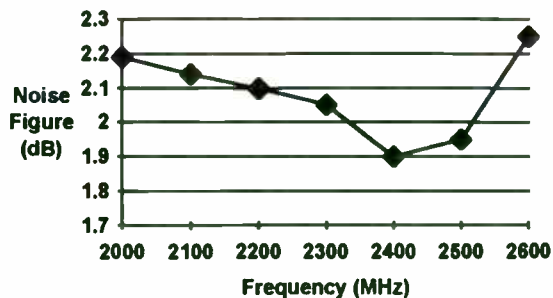
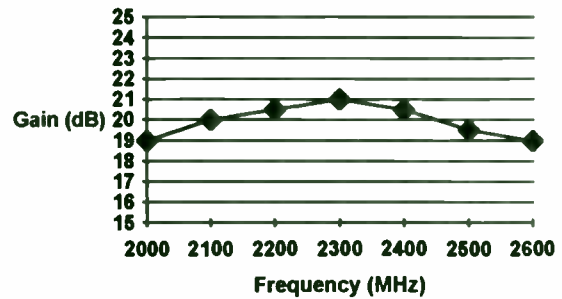


Figure 12. AT-31011 Amplifier Gain



V. OTHER APPLICATIONS

The low current bipolar transistors can also be used in frequency converter applications. Although not optimum, the 900 MHz amplifier circuit shown in Figure 3 can be used to demonstrate mixer operation. The amplifier circuit can be modified for use as a downconverter to a 10.7 MHz IF by simply coupling out the IF by attaching a .1 to .3 uH coil to the output circuit. The point to couple to should be at the junction of C4 and C6 (reference Figure 1). Ultimately the IF should also have dc blocking capacitor but it was not required for this simple test. The LO is injected into the output port of the amplifier and the amplifier input port is the RF input port. With a nominal +3 dBm LO, the circuit without any optimization provides a nominal 6 dB conversion gain and less than 12 dB noise figure. Optimization of the bias and matching structures will improve performance. Generally higher LO increases conversion gain but there is generally a nominal LO power that produces the lowest noise figure. Bias voltage and current can be critical especially for lowest noise operation.

VI. CONCLUSIONS

The AT-3 series of silicon bipolar transistors have demonstrated very good noise figure and gain performance at both 900 MHz and 2400 MHz while consuming a minimal amount of dc power. Sample circuits have been presented along with successful design techniques.

WIRELESS SYMPOSIUM AND EXPOSITION

Santa Clara Convention Center -- Santa Clara, CA

Masa Omori, Ph.D.
John Martin
Chris Fisher

Microwave Technology, Inc.
4268 Solar Way
Fremont, CA 94538

PH: (510) 651-6700
FAX: (510) 651-2208

A 1W Class A Hybrid Surface Mountable Amplifier for Ultra Linear Multi-Carrier Wireless Applications

Abstract

The need for mobile voice and data communications networks has never been greater. The growth in the numbers of subscribers has created an insatiable demand for capacity while concurrently putting downward pressure on infrastructure costs to in turn reduce the costs of providing service. The most obvious of these is the conversion from analog cellular technologies to digital cellular technologies. While many know the needs of and the opportunities for subscriber equipment, few in the semiconductor world have paid attention to the network radio system conversion taking place.

Traditional analog cell sites primarily use single channel feed forward amplifiers and a tunable cavity filter to achieve the desired level of adjacent channel intermodulation suppression. Some cell sites will use up to 20 of these amplifier/filter combinations. The result is a relatively large and a relatively expensive base station product to service a given number of users. With the advent of PCS and other digital cellular technologies, the need to move to a lower cost and micro-cell oriented environment is obvious. The easiest way to reduce these system costs is to replace the multiple amplifier/cavity filter systems with a single multiple carrier amplifier with enough linearity to provide the level of intermodulation performance the system requires.

This paper describes two low cost surface mountable hybrid module amplifiers which operate class A from 800 MHz to 1 GHz and 1.8 GHz to 2.1 GHz and exhibit extremely high IP3 performance (+45 dBm) for relatively low DC power consumption (3 W). The use of this amplifier is as a driver stage for high power feed forward single and multi-carrier amplifiers for digital cellular systems like IS-54C, IS-95 and GSM. It also serves as a final output stage for lower power micro-cell and pico-cell applications such as DECT and PHP. Frequency derivatives of these systems for wireless local loop usage in developing countries is also a primary use of these amplifiers.

The paper outlines the devices capability relative to more traditional GaAs and bipolar structures. Test data for two tone and "at-modulation" inputs is presented to demonstrate system performance. The customer benefits and technical considerations of integrating these low cost ceramic SO packaged amplifiers is also discussed.

Low-Cost Broad-band GaAs RFIC Amplifiers

Leonard D. Reynolds, Jr.

RF Micro Devices, Inc.
7341 West Friendly Avenue
Greensboro, NC 27410
(910) 855-8085

Summary

First offerings in a new family of low-cost RFIC amplifiers, the RF2301 and RF2304 are broad-band amplifiers operating over the 100 MHz to 3 GHz frequency range. These two new circuits are fabricated in an advanced GaAs MESFET process, resulting in lower power consumption and superior high frequency performance compared with existing silicon ICs. The amplifiers operate over a wide power supply range down to 2.7 volts without external bias stabilization circuitry. Intended for high-volume consumer products, the amplifiers are offered initially in plastic SO-8 packages, require no external matching circuitry, and are priced less than one dollar when purchased in large quantity.

I. Introduction

GaAs IC technology has a number of advantages over silicon for high-performance RF amplifiers, including superior performance at higher frequencies, lower noise, low circuit parasitics, high substrate isolation, and high efficiency. In addition, many silicon general-purpose RF amplifier ICs require an external resistor in series with the power supply to stabilize DC operating point over temperature, compromising or preventing operation in newer 3 volt equipment. Two new high-performance general-purpose amplifier ICs bring the performance advantages of GaAs MESFET IC technology to low-cost commercial and consumer systems. The RF2301 uses the excellent isolation of GaAs substrates to achieve high reverse isolation in a single low-cost plastic-packaged IC. The RF2304 achieves low noise and low distortion for high dynamic range

transmitter and receiver application. Each utilizes GaAs MESFET circuits to set a stable, efficient DC operating point for single-supply operation between 2.7 and 6 volts without external bias stabilization resistors.

II. RF2301 High Isolation Buffer Amplifier

The RF2301 is a three-stage buffer amplifier IC with high reverse isolation in an industry-standard plastic SO-8 package. The Figure 1 block diagram illustrates the circuit. Internal shunt feedback is used to set input impedance and gain. The output stage is an open drain transistor for maximum efficiency. The output impedance is set with an external resistor for simple broad-band circuits or with an inductor network for maximum gain and output power.

A typical broad-band application circuit is shown in Figure 2. The output impedance is set primarily by the 100 ohm external resistor. The external series capacitors can be eliminated if the connected component interfaces are open circuit at DC. Measured gain and reverse isolation with 5 volt V+ are plotted in Figure 3. Gain is greater than 20 dB between 500 and 2500 MHz. Small-signal 3 dB bandwidth is 100 to 3000 MHz. Reverse isolation is greater than 40 dB over the full frequency range, and is greater than 50 dB at 900 MHz. Reverse isolation is high enough to replace two silicon general-purpose amplifiers in many LO buffer applications. Figure 4 shows input and output return loss greater than 10 dB over the 500 to 3000 MHz range.

Figure 5 plots 900 MHz gain, power supply current, output power, and reverse isolation versus power supply voltage. Gain rises from 17 dB at 3 volts to 20 dB at 5 volts. DC current is

18.7 mA at 3 volts, rising to 23.1 mA at 5 volts. Output power 1-dB compression point is +1.8 dBm at 3 volts increasing to +4.1 dBm at 5 volts. Measured mid-band input IP_3 is -7 dBm at 3 volts, -5.5 dBm at 4 volts, and -6 dBm at 5 volts. Output power capability and intercept point are within +/- 0.9 dB of these figures to at least 2500 MHz.

An alternate application circuit is shown in Figure 6. The output pin inductor network improves gain and output power by about 3 dB over a 20 percent bandwidth compared with the broad-band circuit. Inductor values are shown for 900 MHz and 2500 MHz operation. The resulting +7 dBm output power is useful in transmitter driver applications as well as LO distribution.

III. RF2304 High Dynamic Range Amplifier

The RF2304 is a single-stage low-noise small-signal amplifier IC, shown in the Figure 7 block diagram. Shunt resistive feedback is used to set input and output impedance to 50 ohms over the full frequency range without external matching circuitry. The SO-8 package pin-out and typical application circuit is shown in Figure 8. Current to the RF output pin is fed through a choke inductor and the bias control Vb pin is tied to power supply. The choke value is not critical, but should have greater than 150 ohms reactance at the lowest frequency of interest. If the DC voltages present on the RF input and output pins are not compatible with connecting component interfaces, series capacitors are added to block DC. The Vb pin can be used to place the amplifier in a low-current standby mode by switching Vb to 0 volts.

Gain and noise figure of the packaged amplifier are plotted in Figure 9. Power supply voltage is 5 volts. Measured gain is 12 dB at 900 MHz and 8.4 dB at 2450 MHz. Noise figure is 1.8 to 2 dB below 1600 MHz, rising to just 2.3 dB at 2.7 GHz. No external matching elements are required to achieve this performance. Input and

output return loss are greater than 10 dB over the 500 to 3000 MHz frequency range. Output return loss is greater than 10 dB above 150 MHz. Reverse isolation is 20 dB at 900 MHz and -15.5 dB at 3 GHz.

Performance at 900 MHz is plotted against power supply voltage in Figure 10. Gain, output power capability, and DC current vary slightly with power supply voltage. Gain is 10 dB at 3 volts rising to 12 dB at 5 volts. DC current is 7 mA at 3 volts, rising to 17 mA at 5 volts. Output power 1-dB compression point is +5 dBm at 3 volts increasing to +8.5 dBm at 5 volts. Measured mid-band input IP_3 is +2.8 dBm at 3 volts and +8 dBm at 5 volts. Output power capability and intercept point are within +/- 0.5 dB of these figures to at least 2500 MHz. Noise figure is not affected by power supply voltage between 3 and 5 volts, as shown by the plot. Input and output impedance match are similarly not affected by power supply voltage.

This combination of low noise figure and highly linear amplification allow the RF2304 to be used for a variety of receive and transmit applications without degrading either noise figure or intermodulation distortion.

IV. Conclusions

First offerings in a new product family from RF Micro Devices, the RF2301 and RF2304 are low-cost high-performance amplifiers suitable for a variety of receiver and transmitter applications in wireless communication systems. Both utilize GaAs MESFET process technology for superior performance and efficient single-supply operation from 2.7 to 6 volts without external stabilization resistors. The RF2301 is well-suited for high-isolation LO buffer application with a minimum of board components. The RF2304 offers a unique combination of low noise figure, high linearity, and low cost. Initial packaging is the industry-standard plastic SO-8. Large volume price is under a dollar.

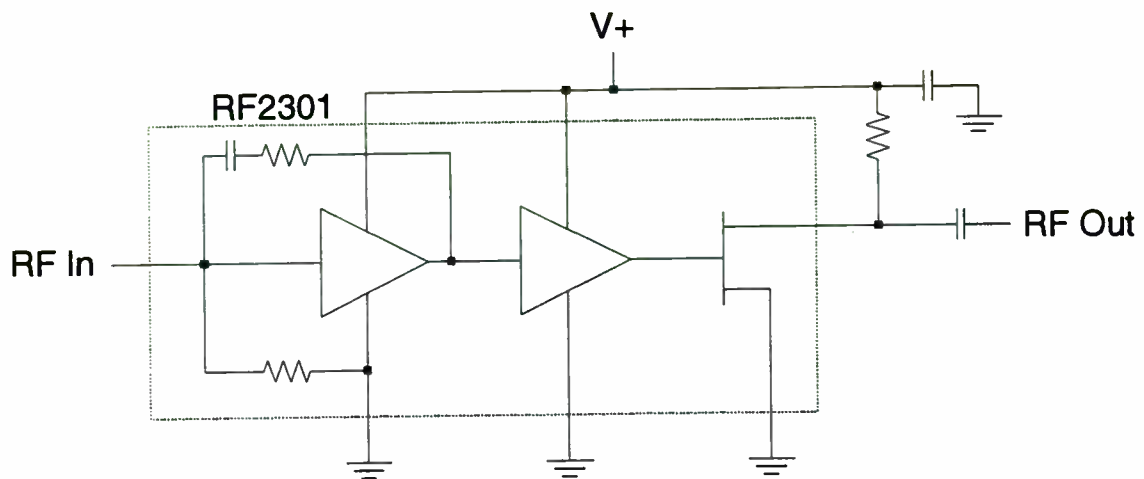


Figure 1. RF 2301 block diagram.

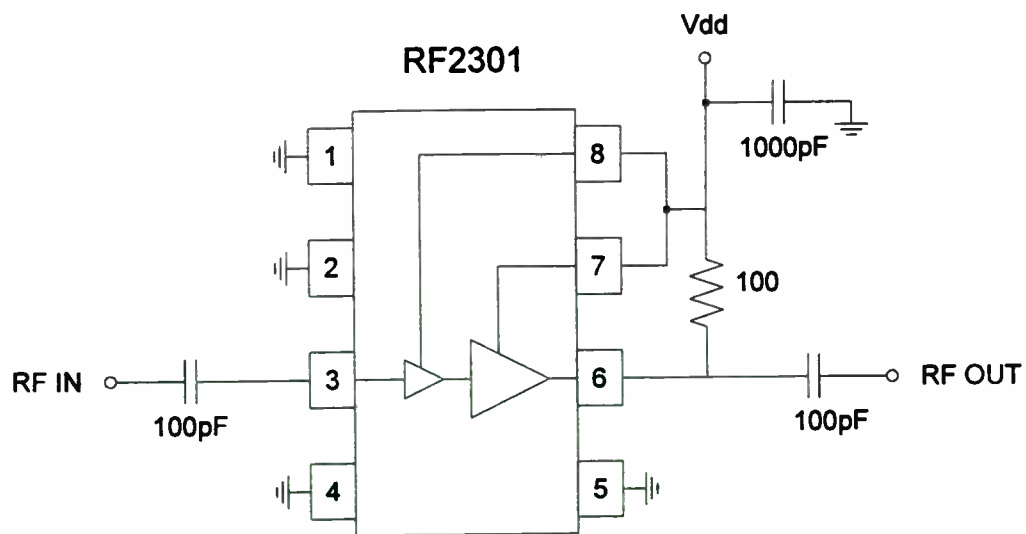


Figure 2. A broad-band RF2301 application circuit.

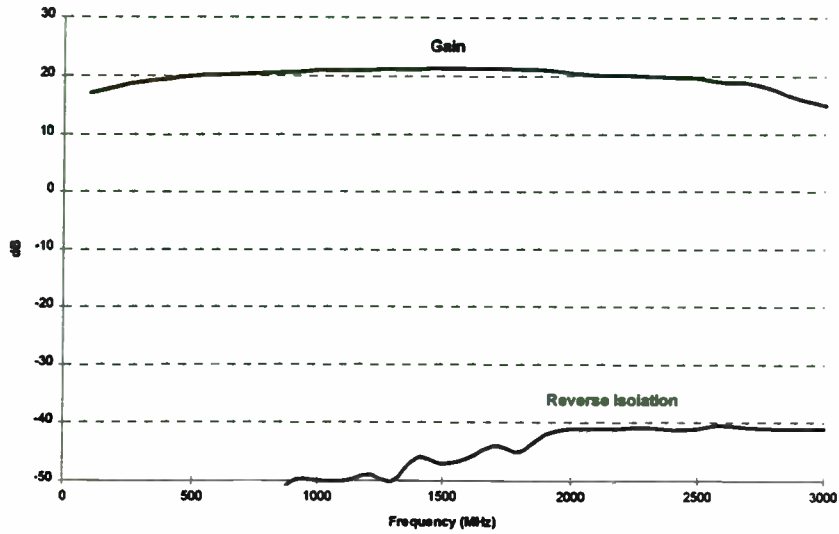


Figure 3. Measured RF2301 gain and reverse isolation, $V_+ = 5$ volts. Gain is greater than 20 dB between 500 and 2500 MHz. Reverse isolation is greater than 40 dB to 3 GHz.

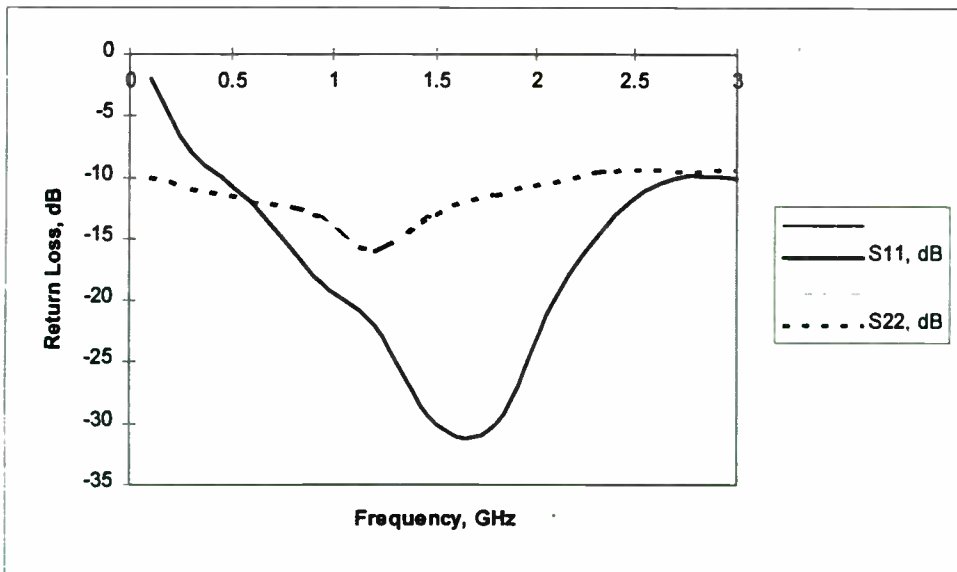


Figure 4. Measured RF2301 input and output return loss is greater than 10 dB between 500 and 3000 MHz.

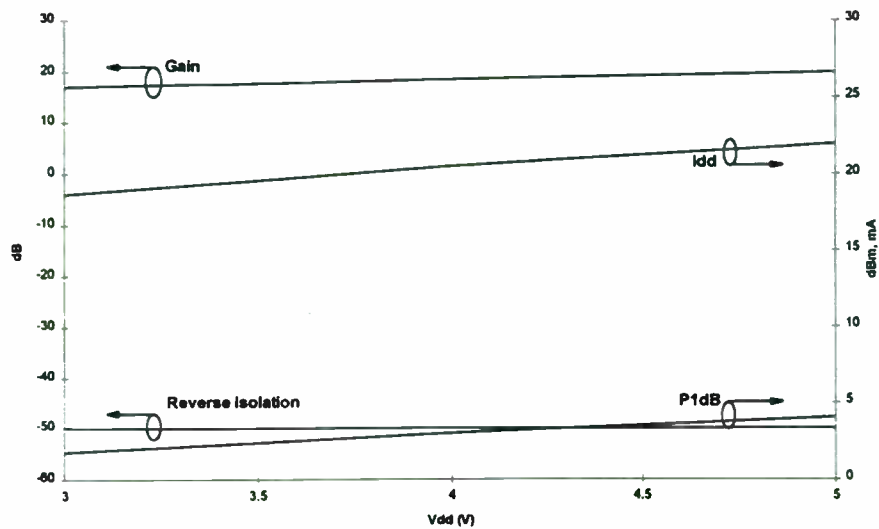


Figure 5. RF2301 performance plotted versus power supply voltage.

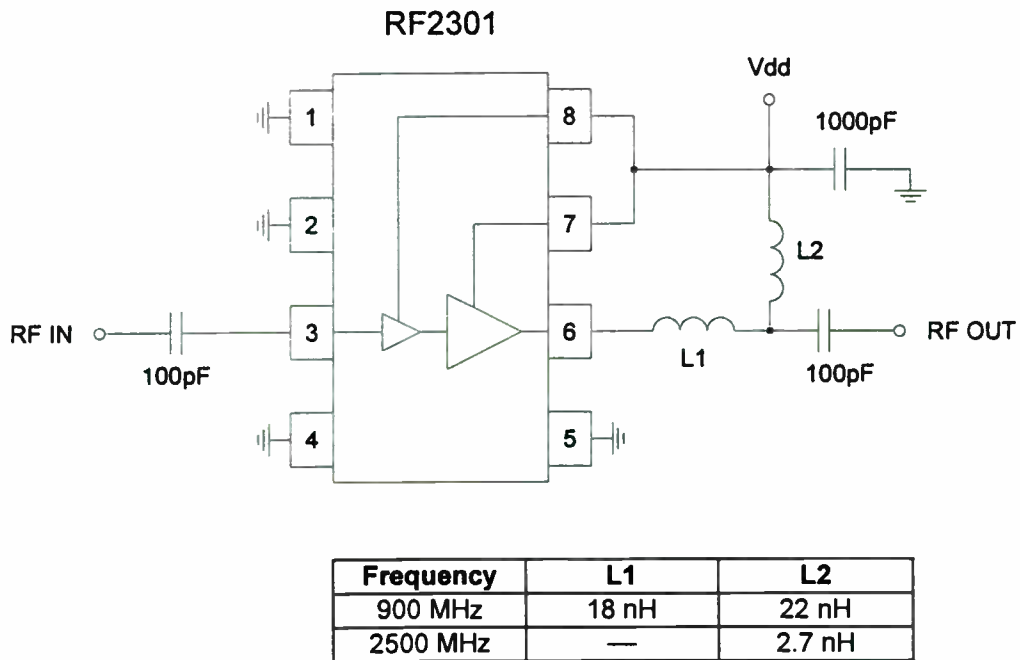


Figure 6. RF2301 alternate application circuit with component values for 900 MHz and 2500 MHz. Gain and output power are increased approximately 3 dB compared with the broad-band circuit

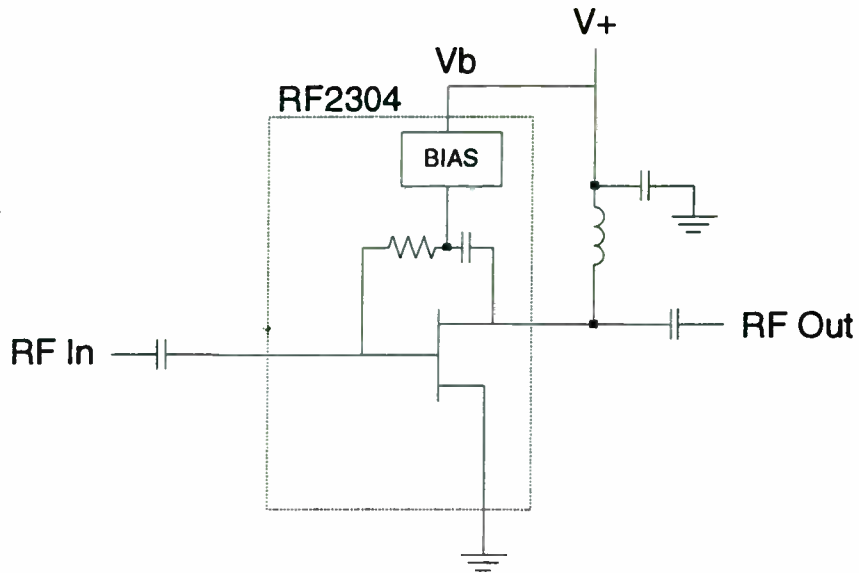


Figure 7. RF2304 block diagram.

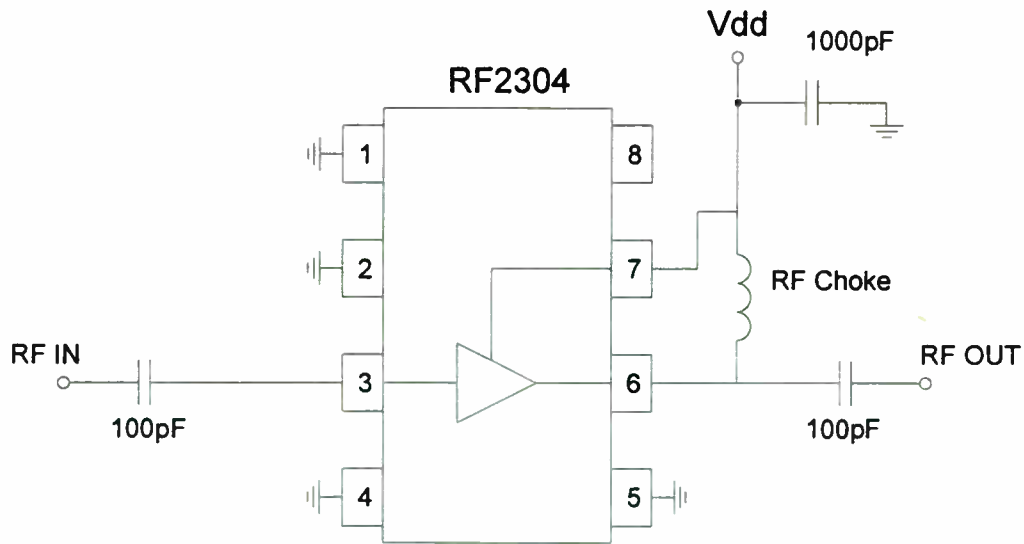


Figure 8. RF2304 application circuit.

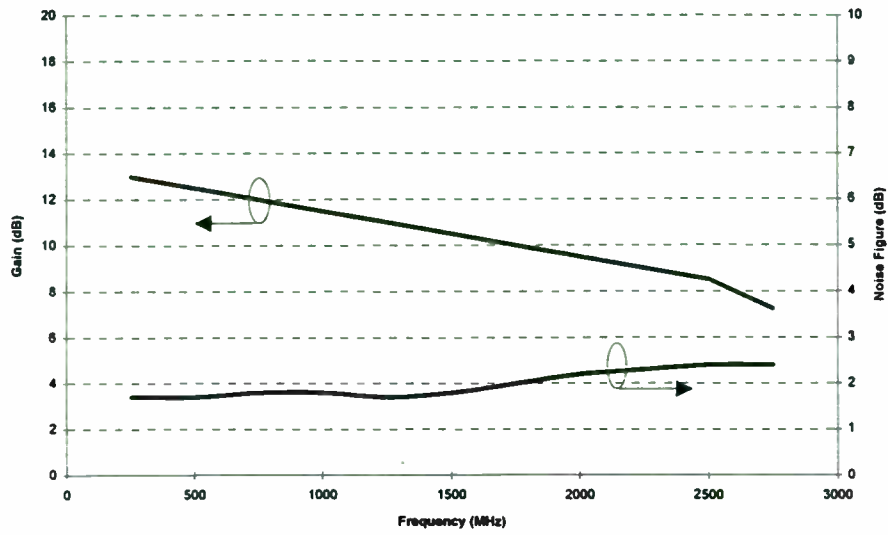


Figure 9. Measured RF2304 gain is 12 dB at 900 MHz and 8.5 dB at 2450 MHz. Noise figure is less than 2 dB to 1600 MHz, and only 2.3 dB at 2.7 GHz.

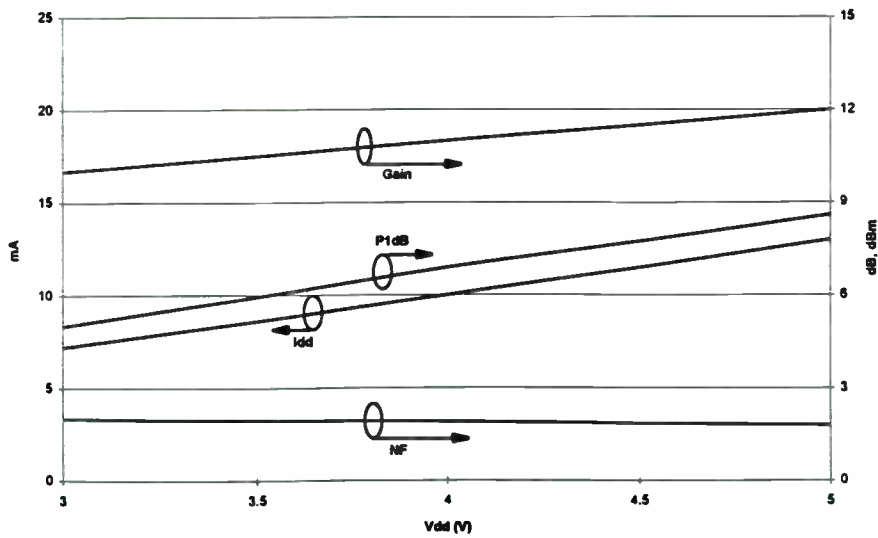


Figure 10. RF2304 gain, output power, noise figure and DC current drain plotted versus power supply voltage.

Unique VCO design for wireless applications

Shankar Joshi
Synergy Microwave Corporation
201 McLean Boulevard
Paterson, NJ 07504
Tel: (201) 881-8800
FAX: (201) 881-8361

Voltage-controlled oscillators (VCOs) are an essential part of virtually all tuned wireless receivers and transmitters. A new design has been developed that features high-performance operation with little power consumption, making it ideal for hand-held applications. This presentation will discuss the patented design as well as measured performance results.



CENTRAL RESEARCH AND DEVELOPMENT
 Experimental Station
 P.O. Box 80356
 Wilmington, Delaware 19880-0356

KTiOPO₄ (KTP): A New Piezoelectric Material For Wireless Communication

David K. T. Chu, E.I. DuPont, Central Science & Engineering, Wilmington, DE.
 Wei Gao, Electrical Engineering Dept., University Of Delaware, Newark, DE.

New spectrum allocated for wireless communications raise opportunities as well as challenges for acoustic frequency control applications. Challenges posed for acoustic devices operating at microwave frequencies such as the needs for higher acoustic velocity and better piezoelectric coupling materials to reduce the resolution requirement for photolithography and to simplify the device design are of strong interest to material science. In this article, information on piezoelectric and acoustic properties of potassium titanyl phosphate (KTiOPO₄:KTP) will be presented. Some important findings of KTP are summarized as followings. KTP has been identified as a material which possesses bulk properties of relatively high acoustic velocities (as high as 7600 m/sec of the longitudinal mode along y axis) as well as large electromechanical coupling coefficients ($k_t = 40\%$, k_{15} , $k_{24} \sim 20\%$). High surface acoustic wave (SAW) velocity (≈ 3900 m/sec) and medium coupling coefficient ($k^2 = 0.7\%$) were also obtained. Due to the crystal structure (mm2 point group), KTP also supports Bleustein-Gulyaev (B-G) waves (a pure shear surface mode) in a y (or x) cut substrate with propagation direction along x (or y) axis. The measured acoustic velocity of a x-cut y propagation B-G wave in KTP is about 4250 m/sec. B-G waves in KTP also exhibit large coupling coefficients ($k^2 \approx 4\%$). In addition to SAW and B-G waves, most importantly, surface skimming bulk waves (SSBW's) have been identified in KTP crystals as well. With a y-cut z propagation geometry, a SSBW's velocity of 6040 m/sec was obtained. High efficiency and large bandwidth were also observed. It is our belief that KTP should have some impact to the wireless communication due to its high acoustic velocities, large coupling coefficients and full compatibility to standard IC photolithography.

Millimeter-Wave Components and Technology For Commercial Communications

Session Chairperson: Paul Khanna,
Hewlett-Packard Co. (Santa Clara, CA)

Millimeter-wave communications: Current use and future trends.
George Bechtel, Strategies Unlimited (Mountain View, CA).....**455**

Microwave technology in 23- and 38-GHz PCN data-communication systems. **Roberto Alm**, Innova Corp. (Seattle, WA).....**458**

Low-phase-noise transmitter sources at 23 and 38 GHz for PCN radio links. **Roland Soohoo and Paul Khanna**, Hewlett-Packard Co. (Santa Clara, CA).....**464**

A heterostructure triple varactor device for a 40-GHz PCN radio source. **Kathiravan Krishnamurthy and Robert G. Harrison**, Department of Electronics, Carleton University (Ottawa, Ontario, Canada); **Erik Boch**, Lockheed Canada (Kanata, Ontario, Canada).....**468**

Digital transmission over a millimeter-wave fiber-digital radio link. **John Park and K.Y. Lau**, Department of Electrical Engineering and Computer Sciences, University of California (Berkeley, CA); **M.S. Shakouri**, Hewlett-Packard Co., Microwave Communications Group (Palo Alto, CA).....**471**

MILLIMETER WAVE COMMUNICATIONS: CURRENT USE AND FUTURE TRENDS

George Bechtel
Strategies Unlimited
201 San Antonio Circle
Mountain View, CA 94040
(415) 941-3438

ABSTRACT

The growing demand for wireless voice, data and video services is driving the need for broadband delivery systems. This paper reviews current services and requirements for millimeter-wave communications systems that are used to provide the broadband links. Millimeter wave frequency spectrum usage will be reviewed and recent FCC regulatory proposals to license services above 40 GHz will be discussed. The market growth and technology trends for millimeter wave components will be presented.

INTRODUCTION

Wireless services are requiring huge bandwidths to handle the quantity of information demanded by the consumer of today. Everyone wants to stay in touch; with the competitive world of today, providing and receiving the right information at the right time is extremely important.

This paper will describe the trends driving the growth in wireless services and will address the growing use of millimeter wave frequencies for the important interconnections between the service and consumer and within the service loop.

THE GROWTH OF WIRELESS SERVICES

The wireless subscriber services are considered to be:

- Cellular telephone
- Cordless telephone
- Business data transmission
- Paging
- Video distribution

In addition to the subscriber services, wireless technology is being used in local area networks (LANs). Data rates are increasing and Ethernet is no longer considered fast enough for video transfer.

A result of the growing information needs is the strong growth of the telecommunications industry. Factory sales of telecommunications reached \$40 billion in 1993, growing at a rate of 13 percent, three times the growth rate of the U.S. economy.

BROADBAND LINKS

Wireless services are distributed by networks of cells, interconnected by cable, optical fiber, microwave, or millimeter wave links. Millimeter wave (MMW) links offer advantages over cable or fiber in areas of high subscriber concentration and in areas with difficult terrain for cable or fiber. In rapid growth areas and for ad-hoc needs, microwave or MMW links can be deployed quickly. With the decreasing cost of RF components, microwave and MMW links have pay-back periods of less than a year, compared to leased lines.

Some examples of the uses of millimeter wave technology are listed in Table 1.

Table 1. Applications of Millimeter Wave Technology to Wireless Services

SERVICE	APPLICATION	FREQUENCY
Telephone/data	Base station transceivers	18, 23, 38 GHz
Television	Receiver/converter	28 GHz
Vehicular communications	In-vehicle transceiver, roadside beacon/transceiver	60 GHz

MMW FREQUENCY SPECTRUM ISSUES

The growing use of MMW frequencies is due in part to the lack of many users. Until recently, military applications dominated the use of frequencies above 30 GHz. Moreover, there are few licensed applications. The 28 GHz license for video distribution was only recently issued.

In an effort to promote the use of MMW frequencies, the Federal Communications Commission (FCC) issued a Notice of Proposed Rule Making in November, 1994, listing frequency allocations for various services above 40 GHz. The proposed frequency allocations are listed in Table 2. The FCC proposes to auction the licensed allocations (LMWS) in a similar fashion to the PCS frequency allocation auction for the 1.8 to 2.0 GHz band, initiated in December, 1994.

Table 2. Proposed FCC Frequency Allocations Above 40 GHz

FREQUENCY BAND (GHz)	USE	LIC OR UNLIC	FCC PART
40.5 - 42.5	LMWS	Lic	21
47.2 - 47.4	Vehicle radar	Unlic	
47.4 - 48.2	LMWS	Lic	21
59.0 - 64.0		Unlic	15
71.0 - 71.5	LMWS	Lic	21
71.5 - 72.0		Unlic	15

Table 2. (continued) Proposed FCC Frequency Allocations Above 40 GHz

FREQUENCY BAND (GHz)	USE	LIC OR UNLIC	FCC PART
76.0 - 77.0	Vehicle radar	Unlic	
84.0 - 84.5	LMWS	Lic	21
84.5 - 85.0		Unlic	15
94.7 - 95.7	Vehicle radar	Unlic	
103.0 - 103.5	LMWS	Lic	21
103.5 - 104.0		Unlic	15
116.0 - 116.5	LMWS	Lic	21
116.5 - 117.0		Unlic	15
122.0 - 122.5	LMWS	Lic	21
122.5 - 123.0		Unlic	15
126.0 - 126.5	LMWS	Lic	21
126.5 - 127.0		Unlic	15
139.0 - 140.0	Vehicle radar	Unlic	
152.0 - 152.5	LMWS	Lic	21
152.5 - 153.0		Unlic	15

Definition of terms:

LMWS: Licensed millimeter wave service

Part 15: Low power, unlicensed use

Part 21: FCC regulation reference for LMWS

Other agencies who control the use of MMW frequencies are:

- Canada: Department of Commerce (DOC)
- Europe: European Conference of Postal and Telecommunications (CEPT)
- Japan: Ministry of Posts and Telecommunications (MPT)

CURRENT MILLIMETER WAVE SYSTEMS

The principal use of MMW communications systems today is in short haul links for interconnecting base stations. Most of the systems in use today operate at 18 and 23 GHz. Newer systems are being deployed at 38 GHz. The distance between stations ranges from 10 to 28 miles.

These systems carry both voice and data channels. The MMW transceivers used in these systems typically sell for \$1,000 to \$2,000 and over 5,000 have been installed to date, mainly in Europe.

A second MMW system deployment example is the 28 GHz Cellularvision receiver/converter for video distribution to homes in areas with no cable coverage. These set-top converters sell for under \$200 and the potential volume is large.

The use of MMW communication systems for smart vehicle/highway applications has been studied in Europe. RACE - MBS (Mobile Broadband Service) would provide roadside -to-vehicle and vehicle-to-vehicle communication for road information, as well as personal data services.

In Japan, the use of 60 GHz for local area networks has been proposed. The development of systems is now underway by several Japanese companies, with support by Japan's MPT and MITI. The application is said to be driven by the high data rates needed by new multi-media services.

OUTLOOK FOR MMW TECHNOLOGY

Most of the MMW systems today are implemented in discrete device technology. Frequency generation uses Gunn diodes as fundamental oscillators; step-recovery diodes are used as frequency multipliers in some applications. Mixers use Schottky diodes; discrete FETs and PHEMTs are used for low noise amplifiers.

MMIC technology is now appearing for commercial applications above 20 GHz. Earlier MMIC development was directed toward military applications, such as radar for smart weapons. Now, chips are now being sampled to the communications market that provide the transmitter power, allowing the use of a low power

oscillator, (possibly a MMIC also). LNAs are also available in MMIC versions. The question is: can the MMIC technology become affordable?

THE MARKET FOR MMW COMMUNICATION COMPONENTS

Short-haul microwave radios, operating at 18, 23, and 38 GHz (and above), will be used to link cellular base stations back to the public switch sites. Microwave radios will also continue to be used in public telecommunications networks and private networks worldwide. The number of short-haul radios produced annually is expected to reach 78,000 units in 1997, with a compound annual growth rate of 29%. Most of growth is expected to occur at 38 GHz.

The growth of 28 GHz receivers for television distribution is dependent largely on achieving an acceptable subscriber base in non-cable areas. The rapid growth in direct broadcast satellite receiver sales in the U.S. in recent months, with stores reporting outstanding sales, may portend a good future for MMW video distribution for new subscribers.

Microwave Component Technology in 23 GHz and 38 GHz PCN Data Communication Systems

Dr. Roberto Alm

Innova Corporation; Seattle, Washington

As PCN systems move into the mm-wave frequency ranges, several important lessons are being learned by radio manufacturers as well as component suppliers. Many of the deleterious effects of microwave transmit and receive modules that were successfully ignored in the past cannot be ignored at these higher frequencies. The designers who best understand and can best predict the behavior of these higher-frequency mm-wave modules are those who will first succeed in manufacturing PCN systems in high volumes and at low cost.

There are many suppliers in the microwave industry that are anxious to embrace the fast-growing PCN marketplace. Some are making a good effort to move their products into a practical format and at cost levels that make application of the technology attractive to PCN manufacturers. As system requirements are defined, however, PCN designers must be very careful in specifying these components and in applying them to system architectures.

PCN Transmitters: The Old -vs- the New

From a historical perspective, microwave communications equipment has traditionally employed vacuum-tubes in transmitter applications and single-diode detectors in receivers. For lower power applications, solid-state bulk-effect devices such as Gunn and Impatt diodes have been utilized for some time as RF sources in transmitters.

Bulk-Effect Sources: The Choice of the Past:

Two-terminal bulk-effect devices such as Gunn and Impatt diodes are physically mounted in mechanical cavities which are resonant at the desired frequency, and oscillation depends on an inherent negative-resistance at certain bias conditions. Typical Gunn-diode oscillators generate up to 100 mW of useful output power, and Impatt-diode designs are typically used in applications requiring up to 500mW (typical). Impatt sources, are, however, usually somewhat noisy as compared to lower-power Gunn oscillators.

Although the advantages of solid-state RF sources such as a Gunn oscillators are obvious as compared to tube based designs, there are still numerous problems associated with two-terminal bulk-effect devices. First, the negative resistance associated with the I-V curve of the diode occurs over a fairly narrow bias region, and the behavior of the region varies with temperature and external load conditions. A Gunn-diode oscillator can thus be sensitive to temperature variations, and the spectral purity (spurious output and phase-noise performance) can also vary with temperature and external (RF) load conditions.

Another problem associated with fundamental-mode bulk-effect devices is that the output is generally unbuffered. The RF load, generally a filter or an antenna, is applied directly to the output port of the cavity, albeit sometimes through an isolator. The output impedance of the unbuffered oscillator seldom matches the load impedance,

and frequency pulling is a problem. If the mismatch is large enough, spurious outputs can occur, the phase-noise can be degraded, and stability with temperature can be reduced.

The frequency pulling problem can be overcome by incorporating an isolator and a varactor (tuning) diode into the oscillator cavity which can be used to electronically tune the oscillator in an operating system.

A tuning diode is excellent for "locking" the oscillator on the correct frequency, but care must be taken not to over-couple the tuning diode to the resonator or to in any other way reduce the operating Q of the oscillator. A lower operating Q will result in an increased sensitivity to temperature, an increase in uncompensated frequency pulling, and a degradation in the phase-noise of the output (carrier) signal.

A varactor diode can be used to tune a bulk-effect oscillator by a few percent of the center frequency, which is practical for frequency correction and/or modulation, but it is not practical as a broadband electrical tuning element.

The mechanical dimensions of the cavity can be adjusted (with a tuning screw) to provide a 10-20% frequency adjustment range, but this is seldom convenient, and it often leads to non-ideal coupling between the two-terminal device and the cavity. Care must be exercised here, because improper coupling to the cavity can result in spurious outputs, decreased output power, degraded phase-noise and marginal temperature stability.

It is important to note that the above applies equally to the RF output port of an unbuffered bulk-effect oscillator. The output port is generally set to couple $\approx 10\%$ of the energy stored within the resonator to the load. Attempting to couple more energy from the cavity will degrade the performance of the oscillator in the same manner as described above. This is usually the parameter which limits the output of a Gunn oscillator to less

than 100 mW (typical).

Bulk-effect devices have also had a historical reliability problem in the field. Although Gunn and Impatt diodes are solid-state devices, vacuum-tube like MTBF numbers have been associated with bulk-effect devices in the past for both military and commercial applications. Recent advances in semiconductor fabrication have eliminated many of the lifetime-associated failures with newer Gunn oscillator designs, but the poor reputation of bulk-effect devices lingers within the community of users.

Finally, bulk-effect oscillators are noted for their high-current requirements and their physical size and weight. Even though the diodes themselves are small, the associated cavity and heat-sinking requirements often result in brass "cubes" that are bulky, heavy and "hot" as compared to the surrounding circuitry. A typical Gunn oscillator will operate on +7 VDC with a current requirement of ≈ 500 mA. In addition, the operating voltage usually varies from unit to unit as well, which requires flexibility and additional complexity in the DC power supply design.

MMIC Technology: The Choice of the Future:

There are two basic approaches that PCN manufacturers are currently employing for generating mm-wave signals for transmission. The first technique uses a *synthesized* or frequency-multiplier approach, where a lower-frequency fundamental three-terminal oscillator is up-converted through non-linear circuits to generate harmonics in the mm-wave bands. (Figure 1). The desired harmonic is then filtered-off and amplified using Gallium-Arsenide (GaAs) MESFET devices at the mm-wave output frequency.

The second approach is to take Gallium-Arsenide MESFET technology one step farther, and to develop Monolithic

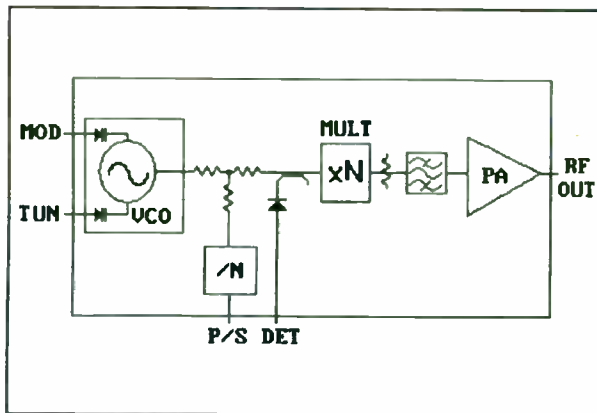


Figure 1 - Block Diagram of a Synthesized RF Source.

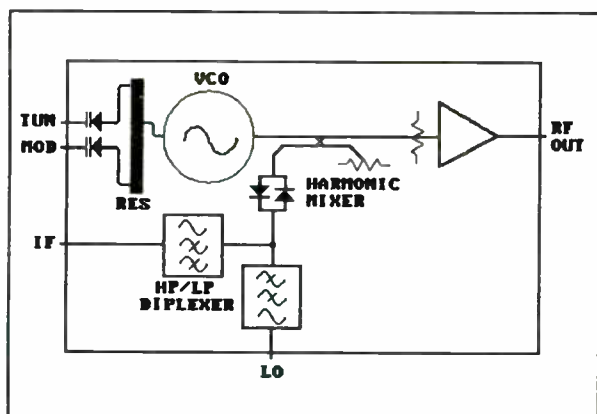


Figure 2 - Block Diagram of a Fundamental-Mode Transmitter Module

Microwave Integrated Circuits (MMICs) which integrate specific requirements into a fundamental-mode approach. (Figure 2). With this approach, there are no sub-harmonic RF signals, and the mm-wave output signal is generated directly within the MMIC device. The output is amplified to a level suitable for transmission in the same manner as above. As a further enhancement, rather than using discrete GaAs MESFET devices, a GaAs MMIC monolithic amplifier device can be used for the final output stage.

The advantage of using GaAs MMIC devices is that many discrete functions can be incorporated into one chip, which increases the level of integration and eliminates labor

and variability at the microelectronics level, which can be a big cost-driver. At mm-wave frequencies, the parasitic behavior of bondwires and chip-components is not straight forward, and great care must be taken to ensure success, especially at high-volume levels.

The multiplier-approach described above can also take advantage of GaAs MMIC technology. The multiplier and gain functions could easily be incorporated using available GaAs MMIC technology, but the filtering would remain as independent requirement.

Whether a fundamental-mode or multiplier-based VCO is developed as the transmitter source, a method must be available to tune and frequency-lock the transmitter signal in an operating system. If a fundamental-mode MMIC-based oscillator is employed, a sampling phase-gate can be employed which provides a DC output proportional to a reference frequency which can be used to control the VCO.

Alternatively, a harmonic-mixer can be included in the RF circuit which provides an output frequency which can be prescaled for use in a phase or frequency lock loop. (Figure 2) If a multiplier approach is selected, the lower-frequency source oscillator is usually prescaled directly to provide a signal to the frequency control circuits.

Fundamental-Mode -vs- Synthesized Transmitters:

Many manufacturers prefer to build mm-wave PCN transmitters using the *synthesizer* approach, where a lower-frequency C-Band or X-Band oscillator is multiplied-up to the desired mm-wave frequency. Often the reasons cited for selecting this approach relate to the cost and availability of components and equipment at lower frequencies, and an overall desire to reduce risk by not attempting to develop

components and techniques too far removed from present levels of expertise.

It is true that a wide variety of components and equipment exist at X-Band frequencies that are not available at mm-wave frequencies. For this reason, it is easier to develop prototype modules and brassboards at lower frequencies, and to minimize the component and testing requirements at higher frequencies by pursuing a multiplied-RF source approach.

Another reason that some manufacturers opt for a multiplied RF transmitter source relates to the resulting phase-noise of the transmitter.¹ Modern semiconductor devices allow for the construction of VCOs with very low phase-noise levels, especially at frequencies under 10 GHz. Phase-noise degrades at a rate of 6 dB per octave of frequency, thus a C-Band VCO operating at 6.33 GHz can be multiplied (X6) up to 38 GHz with only a 15 dB degradation in phase noise.

Alternatively, it may not be possible to build a MMIC-based fundamental-mode VCO with phase-noise performance as good as a multiplied C-Band source. This fundamental limitation, can, however, be circumvented through the use of wideband phase-lock loops which can average the phase-noise of the VCO itself and reduce the overall phase-noise requirement within the system.

A fundamental mode transmitter can be realized using discrete $\frac{1}{2}$ - μm or $\frac{1}{4}$ - μm epitaxial GaAs FET devices and a suitable

resonant structure. The resonator includes the varactor diodes necessary to tune and modulate the RF source, or the entire VCO can be fabricated as a Monolithic Microwave Integrated Circuit (MMIC), with the varactor diode fabrication being incorporated as part of the MMIC processing.

The advantage of using discrete components is that the resonator can be maintained as a high-Q structure and the coupling to the active device can be optimized for maximum performance. The disadvantages, however, essentially eliminate the discrete device approach from any practical consideration for even low-volume manufacturing of fundamental-mode sources. At mm-wave frequencies, the bond-wires and bias circuits in a discrete layout are of dimensions compatible with those of the resonant structures, and multiple-resonant behavior is almost a certainty. Tuning such structures to perform as desired is a nightmare, and each resulting unit is different from the next.

The advantage of the MMIC realization is that once the design is defined, all subsequent devices are nearly identical. The parasitic behavior is well controlled, and high-volume manufacturing can be cost-effective and repeatable. The disadvantage, however, is that it usually takes two or three design passes through a GaAs fabrication process before the design is available in production quantities, which usually means more than a year of development time.

It may seem that the long-development time associated with the fundamental RF source make it an impractical approach, but the MMIC based transmitter has the potential to be substantially cheaper than the synthesized (multiplier) approach in high volume, thus interest is high in applying available MMIC technology to PCN transmitter requirements.

One disadvantage associated with the synthesized approach relates to the need to

¹ In an FSK or PSK radio system, uncertainty in the absolute phase or frequency of the carrier due to noise competes with data modulation, which shifts the phase or frequency by prescribed amounts which are then demodulated to determine the input data stream. Phase / frequency errors are manifested as data errors. At the receive threshold level, the phase-noise competes with the received data to generate data errors. Once these errors exceed a certain statistical rate, i.e.; 10^{-9} S^{-1} , the receive threshold is defined, and this is a very competitive number among radio manufacturers.

eliminate the unwanted RF harmonic energy. Suitable filters must be developed, and some care must be taken to ensure that the harmonic energy does not in any way interfere with its surroundings -- including RFI leakage considerations. In addition, a synthesizer is inherently physically larger than an equivalent fundamental source, and due to its more complex nature, it may very well be more expensive to realize.

Receivers

It is important to keep the noise-figure of the receiver as low as possible, as this front-end value ultimately determines the threshold level of the receive channel and the overall sensitivity of the radio system. Some modern mm-wave PCN systems currently employ GaAs MMIC low-noise amplifiers (LNAs) in the front end to establish the base noise-figure for the receiver, some do not.

At mm-wave frequencies, LNA technology is very new. The most effective available technology resides with the pseudomorphic high-electron mobility transistor (PHEMT) process with gate lengths of $\frac{1}{4}$ - μm . Such devices are just now becoming available, but what is not available as a specific need can be designed and fabricated through one of several "GaAs foundries" that currently accept commercial work.

Obviously, it takes some experience to work with this technology. If design expertise in the area of GaAs MMICs is available to a PCN manufacturer, there may be a good opportunity to develop leading-edge front-end components. The only drawback with this approach is that it generally takes anywhere from six months to a year for an Engineering development cycle to finally result in the availability of production quantities of devices, and the Engineering runs are very expensive. Those who can afford to wait for the industry to

develop these "building blocks" may choose to wait until the availability is there, but those working to advance the state-of-the-art in PCN radio systems will need to become involved directly in the development of the needed PCN devices.

Once an LNA precedes the first down-converter, the requirements on the mixer are not as stringent as they are in an unbuffered system. At mm-wave frequencies, the down-converters are usually simple in topology, often a two-diode single-balanced mixer with simple IF filtering. If an LNA is employed, either an image-reject filter is inserted (Figure 3) or two mixers may be used in an image-reject configuration in order to reduce the noise contribution from the LNA, but each mixer is still a simple topology.

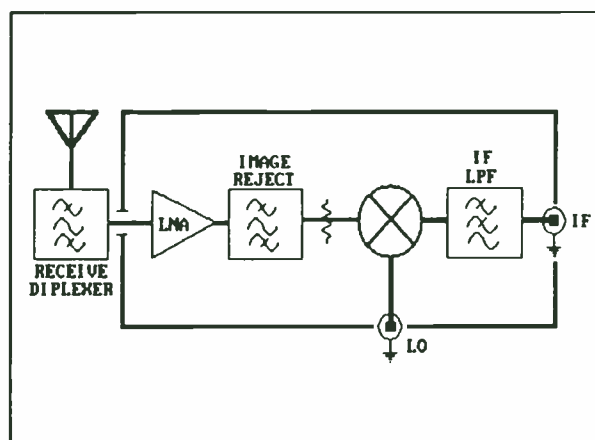


Figure 3 - A First Down-Converter which Employs an LNA and an Image-Reject Filter.

The IF systems in mm-wave PCN systems are typically in the UHF range. In an unbuffered system (no LNA), the mixer and the first IF gain stage will determine the noise-figure of the receiver. For this reason, it is often desired to use a first-stage IF amplifier with as low a noise-figure as possible. The Interconnection between the mixer and the first gain stage should be clean and well controlled. The input noise match to this device is important, and a poor match can

have the same effect as several more dB of conversion loss in the mixer.

The local oscillator that is used in the receiver is also an important microwave component. The IF signal that is processed from the first down-converter carries the attributes of the local oscillator in terms of phase-noise and frequency stability.

Traditionally, microwave radio systems have used klystrons, Gunn oscillators and synthesizers to create the LO signal for the receiver, and the transmitter has been considered to be the limiting factor for phase-noise in the system. In order for this assumption to be valid, the phase-noise performance of the receiver should be 10 to 15 dB better than the transmitter.

Conclusions

Designers of microwave and mm-wave subsystems for use in PCN radio applications must be very aware of available technologies and the tradeoffs between these technologies in order to achieve the most reliable, appropriate and cost-effective designs. The next generation of PCN products will begin to integrate many of the front-end functions through the use of GaAs MMIC technology. The designer must consider the advantages and applications of MMIC technology in future designs, and he or she must be willing to design at the IC level if necessary in order to realize the most cost-effective and reliable PCN products.

PCN front-end design is an area where a good understanding of new technology can affect overall system architecture decisions. An illustration of this point was presented through the description of the tradeoffs between synthesized and fundamental-mode transmitters. Other examples were presented as this concept was extended to the receiver side as well.

In general, many approaches are

available to the designer which can lead to good, reliable and cost-effective PCN front-end designs, but we should maintain a focus on where the next step of development will be.

In the area of PCN front end components, higher levels of integration will lead to greater cost savings, and in particular, GaAs MMIC based components will become the technology of choice in newer designs. In addition to the cost savings, the physical size, weight and power requirements will steer the future of PCN front-end component technology toward higher levels of GaAs MMIC integration in future PCN products.

Rev. 11-29-94 RWA

Low Phase Noise Transmitter Sources at 23 & 38GHz for PCN Radio Links

R.K. Soohoo and A.P.S. Khanna
Hewlett-Packard
Communication Components Division
3175 Bowers Ave., Santa Clara CA 95054-3292

Abstract

The 23 & 38 Ghz PCN Wireless Radio Link market is growing rapidly. There is a particular need for the microwave/millimeter wave portion of these links to be more highly integrated to reduce system integration times and costs. In the frequency source area there is a requirement to develop reliable, low phase noise compact sources at 23 and 38 Ghz which will allow 4-level or greater FSK modulation schemes to be implemented. This paper describes a microwave/millimeter wave source module architecture that delivers excellent phase noise and RF power levels, reduces integration complexities and is phase lockable for the transmit portion of PCN radio links.

I. Introduction

The typical transmission frequencies for PCN radio links are 21.2 to 23.6 Ghz and 37 to 40 Ghz. The maximum RF power level required for transmission is +20 dBm and +18 dBm respectively and varies with link installation distance. There are two primary uses for these links: to interconnect cellular/PCN cell sites to each other and with the BSC and MTSO and to establish private wireless high speed data links.

Frequency sources used in PCN Radio Links have historically used fundamental frequency Gunn Diode Oscillators or more recently GaAs based MMIC Oscillators. These oscillators are typically used as carriers in the millimeter transmit chains for transmission of digital data. A FSK modulation scheme is typically used for coding of information.

Although Gunn oscillators possess good phase noise and RF output power characteristics, they are known to have issues related to microphonics, power

consumption and mechanical tolerances. Gunns also can only be tuned over a narrowband due to their construction. Fundamental GaAs MMIC Oscillators suffer from poor phase noise performance, frequency pulling and tuning sensitivity linearity issues. The typical phase locking method for fundamental oscillators uses a harmonic sampler along with a high purity local oscillator which can be complex to implement.

Clearly a different approach was needed that addresses the historical difficulties and complexities of previous technologies. This paper describes a high performance implementation using a mix of Si and GaAs technologies that reduces system integration times and cost by providing the required phase noise, RF power levels and performance needed in modern radio links.

II. Design Approach

Figure 1 shows the integrated source module block diagram. A Silicon-based high-purity voltage controlled oscillator (VCO) is used as a source which is then multiplied by two GaAs PHEMT multipliers (a X4 and an X2) to create the appropriate MMW output frequency. A 20-40 GaAs PHEMT MMIC Amplifier provides the necessary gain and output power needed for PCN Radios which is usually +20 dBm at 23 Ghz and +18 dBm at 38 Ghz.

In addition, a Silicon prescaler is utilized to create a signal below 750 Mhz for phase locking the source and a detector circuit is supplied to monitor the output signal. The advantage of this implementation is that no high frequency mixers and LOs are required. The following describes a compact, highly integrated, low cost source module that integrates all microwave/milimeter wave functions described together in a single housing.

A. The Oscillator

The oscillator is a voltage controlled oscillator (VCO) that utilizes a Silicon device in a common base series feedback configuration. A schematic of the VCO is shown in Figure 2. A varactor diode is used to form a tunable resonator in the emitter of the device and the collector is the RF output port. Negative resistance is generated in the device by the use of a series inductive feedback in the base. RF output power exceeds +14 dBm. Phase noise is better than -102 dBc/Hz at the output of the oscillator before it is fed into the multipliers. The oscillator frequency for the 23 Ghz module is 2.65 to 2.95 Ghz and the output frequency of the oscillator for the 38 Ghz module is 4.625 to 5 Ghz.

Good tuning sensitivity linearity is desired for ease of phase locking. A linearity of 1.1:1 has been achieved over a narrowband (300 Mhz) and a 1.5:1 has been achieved over the entire communications band. A separate modulation input is available to modulate the oscillator and send data.

Some of the RF output power is coupled off to a silicon divide by four prescaler. In the case of the 23 Ghz source module one frequency divider is used whereas the 38 Ghz source utilizes 2 dividers in cascade to achieve an output frequency lower than 750 Mhz. This low frequency output is provided to phase lock the source to an external oscillator.

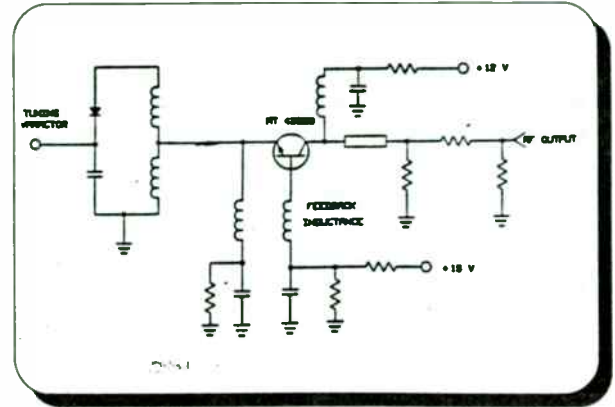


Figure 2 - VCO Schematic

B. Frequency Multipliers

The basic multiplier topology is shown in Figure 3. A bandpass filter is placed at the output of the device to extract the desired harmonic from the multiplier as several harmonics are generated in the device.

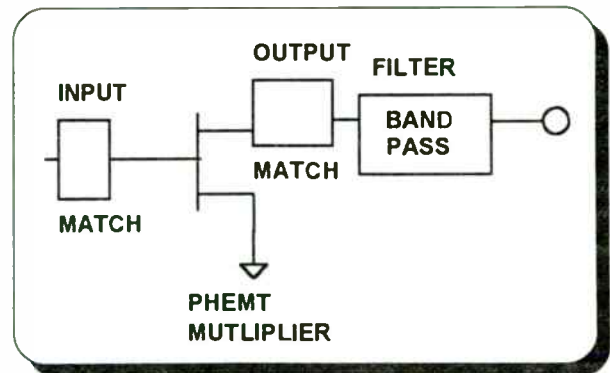


Figure 3 - Multiplier Configuration

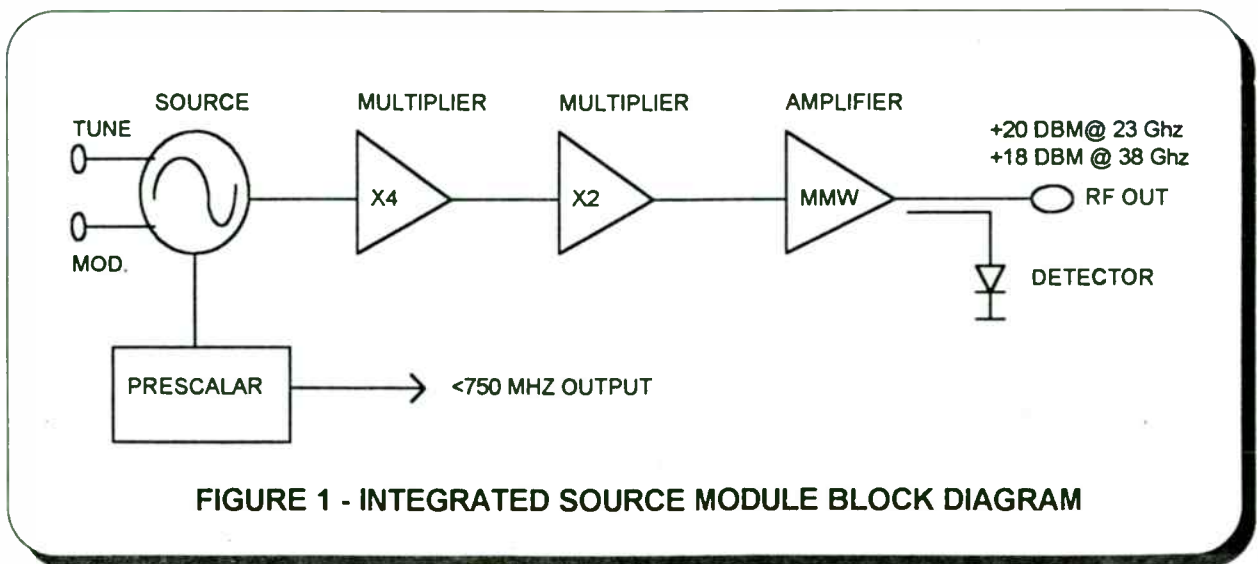


FIGURE 1 - INTEGRATED SOURCE MODULE BLOCK DIAGRAM

Both frequency multipliers utilize GaAs PHEMTs. The PHEMT devices allow for low conversion loss because of their high gain and non-linear transconductance as opposed to other devices such as varactor diodes. A 7-9 dB conversion loss has been achieved for the X4 multiplier and a conversion gain of 0-2 dB has been achieved for the X2 multiplier.

Oscillator phase noise is degraded in a multiplier based on Equation 1:

$$\phi_{NoiseDegradation} = 20 \log M \quad (1)$$

where M is the frequency multiplication factor.

The fundamental oscillator has -100 dBc/Hz phase noise at 100 KHz offset at 4.65 - 5 GHz for the 38 GHz module before entering the multiplier chain. It degrades by 12 dB after passing through the X4 multiplier. After passing through the second X2 multiplier the phase noise degrades by an additional 6 dB resulting in a phase noise of -82 dBc/Hz at 100 KHz. This phase noise number is satisfactory for four level FSK operation. This is at least 10 dB better than the phase noise of a fundamental MMIC oscillator².

c. PHEMT Power Amplifier

A 20-40 GHz Hewlett-Packard MMIC³ was used for gain and reaching the required power levels at the output. The chip was fabricated using a .25 micron PHEMT process and has over 20 dB of gain across the band and a saturated output power of 20 dBm. Typical gain and saturated power is shown in Figure 4. Input and Output return loss is better than 8 dB across the band.

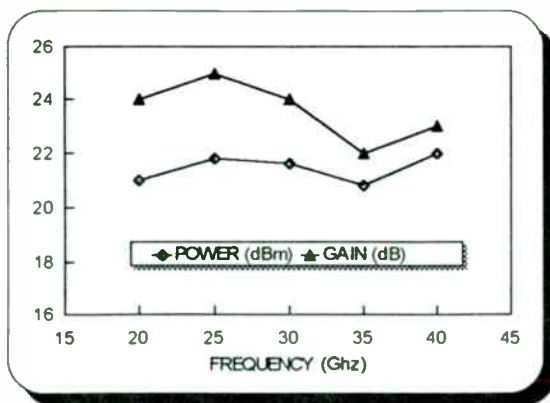


Figure 4 - Characteristics of MMW MMIC

D. Package Details

All circuits were realized on thin film Alumina substrates. They were housed in a aluminum housing measuring 2.25" (L) x 1.25" (W) x .4" thick. The output connector was designed to be either a feedthru pin, K-Connector or waveguide. All input/output connections were made by feedthrus soldered to the case and can be interfaced directly to a PCB.

III. Integrated Module Experimental Data

After integration the key parameters of the source module were measured including phase noise, linearity, power output, modulation bandwidth, and detector output. A mute function was also implemented where the output signal could be attenuated by over 50 dB.

Figure 5 shows the power output data at both 23 and 38 GHz. A power level of +20 dBm minimum was achieved at 23 GHz and +18 dBm minimum at 38 GHz.

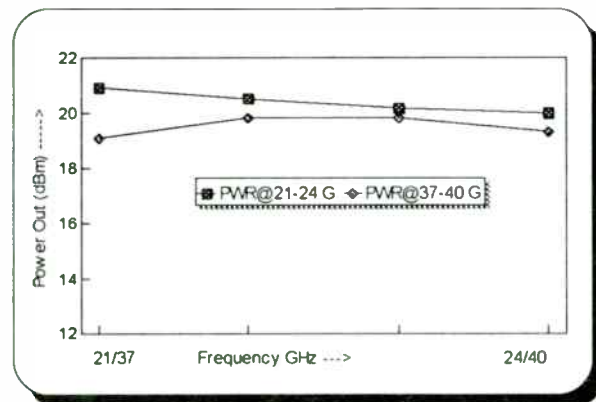


Figure 5 - Power Output at 23 and 38 GHz

Figure 6 shows the tuning sensitivity linearity and modulation sensitivity linearity at 37-40 GHz. An average of tuning sensitivity of 225 Mhz/V at 23 GHz and 300 Mhz/V at 38 GHz was achieved with a linearity of better than 1.1:1 over any 300 Mhz band and 1.5:1 over any 2.4 GHz band. Modulation sensitivity linearity was better than 1.5:1 with an average sensitivity of about 25 Mhz/V.

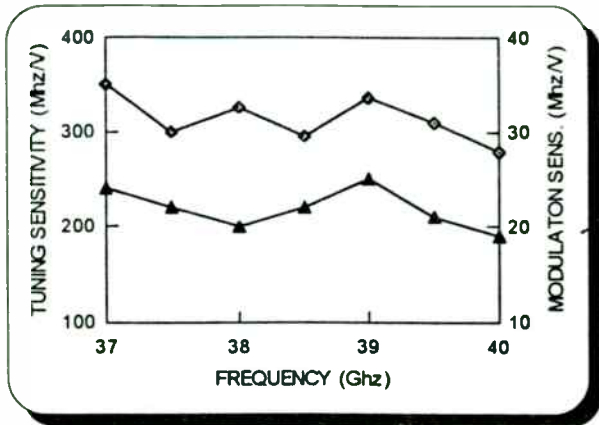


Figure 6 - Tuning Sensitivity Linearity

Figure 7 shows a free running phase noise plot of a 38 Ghz module. The phase noise was -82 dBc/Hz minimum at 37-40 Ghz and -88 dBc/Hz at 21.2 to 23.6 Ghz. The phase noise is adequate for four level FSK operation at both bands.

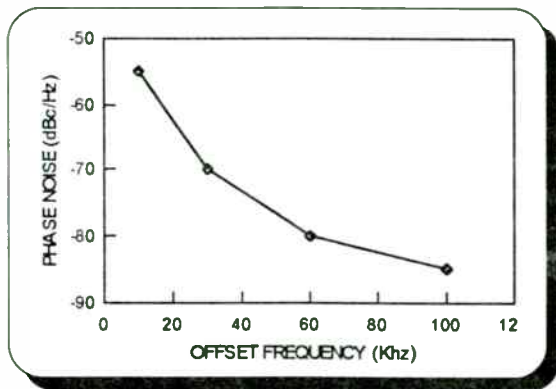


Figure 7 - Phase Noise Plot at 40 Ghz

The modulation bandwidth of the module was tested and was found to be in excess of 30 Mhz. This bandwidth can support all commonly used PCN data rates. A voltage variable attenuator was constructed and placed after the output MMIC in order to control the transmitter link power. The pin diode based attenuator gave in excess of 30 dB of dynamic range and insertion loss of less than 2 dB. The following table summarizes the integrated module results:

Frequency (Ghz)	21.2 - 23.6	37 -40
RF Power Out (dBm)	+20 min.	+18 min.
Phase Noise @100 KHz offset (dBc/Hz)	-88 typ.	-82 typ.

Harmonics	-30 dBc max.	-30 dBc max.
Prescaler Output (Mhz)	662.5 - 737.5	289 - 312.5
Detector Out (Volts)	.5 - 1.5	.5 - 1.5
Modulation BW (Mhz)	>30	>30
Tuning Voltage (Volts)	1 to 16	1 to 16
Tuning Sensitivity (Mhz/V) (Variation over 300 Mhz) (Variation over entire band)	250 typ. <1.1:1 <1.5:1	300 typ. <1.1:1 <1.5:1
Modulation Sens. (Mhz/V) (Variation over entire band)	25 typ. 1:5:1	25 typ. 1.5:1
Spurious (dBc)	-60	-60

Table 1 - Summary of Module Results

IV. Conclusion

A design methodology has been described where almost all microwave/mm-wave components of the transmitter were integrated in a single housing with excellent electrical characteristics. This was achieved by using a mix of Silicon and GaAs technologies. Experimental data was shown that validates this concept. The test module exhibited excellent phase noise characteristics, tuning and modulation sensitivity and power output. In addition, prescaling for phase locking, detection and variable attenuation functions were included. This type of module provides a high level of integration which can reduce system level test times and cost.

Acknowledgments

The authors would like to thank M. Duplaix, E. Topacio and B. Kunz for their valuable technical contributions.

References:

1. A.P.S. Khanna, M. Duplaix, B. Kunz & E. Topacio, "Low Phase Noise 38 Ghz 20 dBm Source for PCN Radio Links", 24th European Microwave Conference Proceedings, 1994, pp. 548 - 553.
2. Lamberto Rafaelli and Earle Stewart, "A standard Monolithic Transmitter for 38 Ghz PCN Applications", Microwave Journal, October 1992, pp. 24-30.
3. Hiroshi Kondoh and Alex Cognata, "A 20-50 Ghz MMIC Amplifier with 21 dBm Output Power and Its Application as a Frequency Doubler", IEEE 1993 Microwave and Millimeter-Wave Monolithic Circuits Symposium Digest, pp. 35-38.

A heterostructure tripler varactor device for 40 GHz PCN radio source

Kathiravan Krishnamurthi

Department of Electronics, Carleton University, Ottawa, K1S 5B6, ON, Canada

Erik Boch

Lockheed Canada, Solant Road, Kanata, K2K 2M8, ON, Canada

Robert G. Harrison

Department of Electronics, Carleton University, Ottawa, K1S 5B6, ON, Canada

November 30, 1994

Abstract

This paper describes a device that has potential to be used in a PCN source unit at 40 GHz. A 13 GHz stable fundamental oscillator-amplifier combination is used to drive an idler-free, bias-free tripler based on this device. A waveguide tripler with 20 dBm output and 7 dB conversion loss, and a planar tripler with 10.8 dBm output and 11 dB loss are reported.

1 Introduction

Signals of commercial interests for wireless communication are being allotted in the 38-40 GHz range. A source unit consisting of a low frequency source followed by GaAs pHEMT based resistive doublers/quadruplers and amplifiers has been demonstrated [1]. A viable low-phase-noise source can be designed using varactors to frequency multiply a low-frequency phase locked source. Conventional pn-junction, Schottky varactor-based planar multipliers have been traditionally limited to doublers because of the need for idlers. A new symmetric varactor device called the Single Barrier Varactor (SBV) which has a symmetric $C(v)$ characteristic around zero bias, was demonstrated to work in tripler circuits in the 200 GHz range [2]. Early SBV devices had excessive leakage currents and low

breakdown voltages. Further, the specific capacitance of such devices is high. Devices have to be smaller to realize low $C(0)$ but then they have high series resistance and become difficult to contact. Triplers constructed with these devices have efficiencies that are limited by power saturation at low input power levels. This is due to leakage currents.

All the above limitations can be overcome by stacking varactor layers, thereby reducing specific capacitance and increasing the power output capability of the varactors. This paper outlines the stacked heterostructure symmetric $C(v)$ varactor device. Its potential at an output frequency of 40 GHz is supported by results of a planar tripler and an experimental waveguide tripler.

2 Device

The device structure is described in [3]. The leakage characteristic is improved by choosing a pseudomorphic barrier $InAlAs/AlAs/InAlAs$ barrier. Three layers of the barrier and associated depletion layers are stacked by using the MBE technique. Low-leakage characteristics are indicated by the small signal-impedance measurements and $I(v)$ curves. A C_{max}/C_{min} ratio of 3, with $C(0)=0.6$ pF and $R_s = 0.37 \Omega$ is obtained for a 36 μm diameter device. This yields

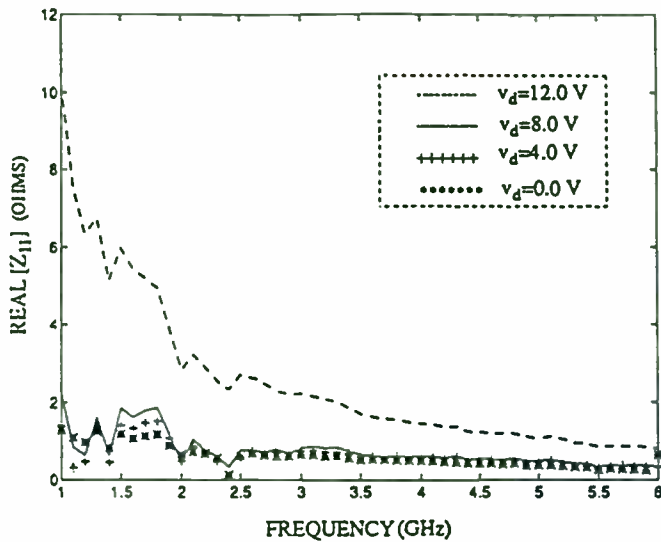


Figure 1: Low-leakage characteristics of stacked HBV.

a large-signal cutoff frequency of 1.4 THz and a convenient area for wirebonding the device to a package or a planar substrate. The growth and fabrication of these devices are described in [3].

3 Simulation

Many tripler experiments have been reported using SBV devices [2] [4] [5]. These experiments have demonstrated that triplers without idlers and bias circuits are possible using SBVs. But the triplers have been severely hampered by output power saturation at lower input power levels due to resistive tripling dominating over reactive tripling. We demonstrate here by large signal simulations of modelled stacked varactor that the resistive saturation effects are not present and higher efficiencies can be potentially realized. The tripler waveforms obtained by the program of Seigel and Kerr [6] applied to a fully pumped stacked HBV are shown in Figure 3. They indicate that the resistive current is low compared to the reactive current. A power output of 50 mW at 50 % intrinsic efficiency can be obtained at 39 GHz output when the diode voltage reaches the breakdown voltage of 14.25 V.

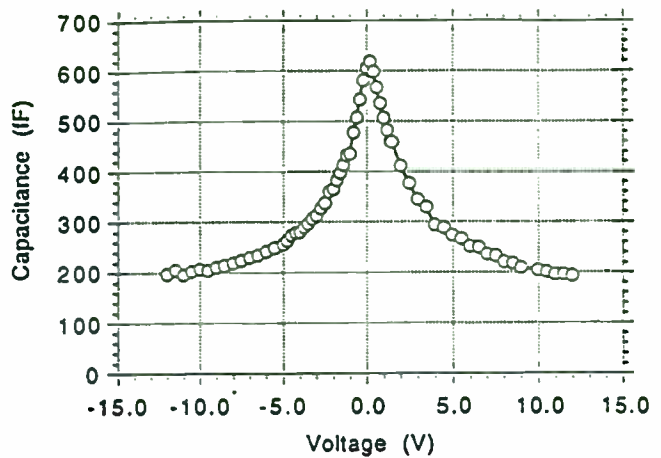


Figure 2: Symmetric $C(v)$ characteristic of stacked HBV.

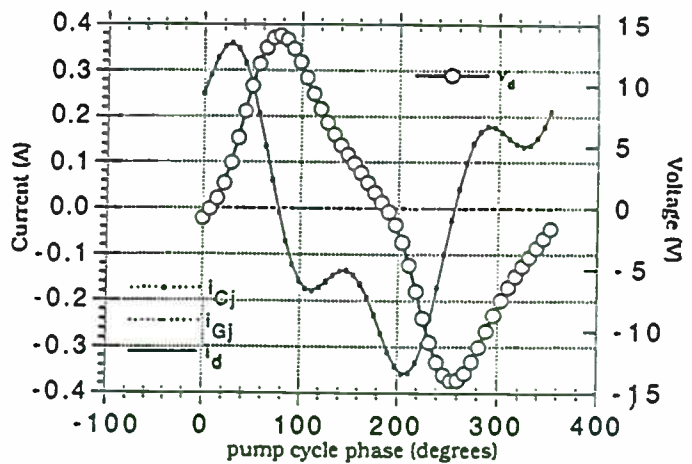


Figure 3: Tripler waveforms indicating pure reactive tripling when the device is pumped to breakdown, $v_d \approx 14$ V.

4 Waveguide and Planar tripler

A waveguide tripler was tested (at Philips Microwave, Hazel Grove, UK) using a packaged varactor with the described characteristics. An existing multiplier mount was used. The circuit performance did not depend on the position of the idler. The P_{out} vs P_{in} characteristic does prove the absence of saturation due to resistive tripling. An output of 100 mW with 7 dB return loss is obtained at 39 GHz [7]. The devices behaved like short circuits at higher input power. A planar tripler was tested at (Lockheed Canada) on alumina using the same device. It yields a 11 dB conversion loss and 10.8 dBm output. Again resistive multiplication is not observed. The output is limited by the available power at the input of the tripler [8].

5 Conclusions

A new improved tripler device has been demonstrated for potential use in a PCN source unit at 40 GHz. The symmetric heterostructure barrier varactor makes it possible to implement triplers without idlers or bias circuit [no battery] and makes the circuit design simpler. Careful circuit and device optimization will result in lower loss and higher power output.

Acknowledgements

We wish to acknowledge the help of Mr. Gary Smith of Philips Microwave, Hazel Grove, Stockport, Cheshire, UK; the help and hospitality of Prof. E. Kollberg at the Chalmers University of Technology, Gothenberg, Sweden; and the financial support of the Defence Research Agency, Malvern, UK and of Natural Sciences and Engineering Research Council of Canada.

References

- [1] A. Khanna, M. Duplaix, B. Kunz, and E. Topacio, "Low phase noise 38-GHz 20 dbm source for PCN radio links," *Proc. European Microwave Conf.*, pp. 548-551, 1994.
- [2] A. Rydberg, H. Grönqvist, and E. Kollberg, "Millimeter- and submillimeter-wave multipliers using quantum barrier varactor diodes (QBV)," *IEEE Electron Device Letters*, vol. 11, pp. 373-375, Sept. 1990.
- [3] K. Krishnamurthi, R. G. Harrison, C. Rogers, J. Ovey, S. M. Nilsen, and M. Missous, "Stacked heterostructure barrier varactors on InP for millimeter wave triplers," *Proceedings European Microwave Conference*, pp. 758-763, Sept. 1994.
- [4] T. Tolmunen, A. Räisänen, E. Brown, H. Grönqvist, and S. Nilsen, "Experiments with single barrier varactor tripler and quintupler at millimeter wavelengths," *Proceedings of Space Terahertz Technology Conference*, 1994.
- [5] D. Choudhury, M. Frerking, and P. Batelaan, "A 200 GHz tripler using a single barrier varactor," *IEEE Trans. Microwave Theory and Tech.*, vol. 41, pp. 595-599, Apr. 1993.
- [6] H. Seigel, A. Kerr, and W. Hwang, "Topics in the optimization of millimeter-wave mixers," NASA Tech. Paper 2287, 1984.
- [7] C. Rogers, "Stacked quantum barrier high power multiplier varactors," Technical Report RP6-127, Philips Microwave, Hazel Grove, U.K., 1993.
- [8] K. Krishnamurthi, "Heterostructure varactors on GaAs and InP for millimeter-wave triplers," PhD dissertation, Carleton University, 1995.

Digital Transmission Over a Millimeter-Wave Fiber-Digital Radio Link

J. Park, K. Y. Lau

*Department of Electrical Engineering and Computer Science, University of California at Berkeley
Berkeley, CA 94720*

M. S. Shakouri

*Hewlett Packard Company, Microwave Communication Group
Palo Alto, CA 94304*

Abstract--Due to the scarcity of available free-space communications bandwidth at radio frequencies, the demand for broadband mobile and personal communications has pushed technology requirements toward the millimeter-wave frequency band. High-capacity digital radio will require high bit rates and high spectral efficiencies. Optical fiber is a low loss, high bandwidth means of distributing millimeter-wave signals to radio base stations. We demonstrate transmission with high-level digital modulation formats on millimeter-wave frequency subcarriers (38 GHz) over an optical fiber-radio link using commercially available components.

I. INTRODUCTION

Digital communications offers the ability to use low cost VLSI technology and digital error correction techniques for voice and data transmission and reception. The desire for higher bit rates must be taken with the need to conserve communications bandwidth. The high spectral efficiencies of high-order digital modulation formats such as 16-QAM and 64-QAM assist both needs.

The millimeter-wave frequency band, covering frequencies over 26 GHz, offers a large supply of bandwidth for free-space communications. Components and technology are emerging for 38 GHz digital radio. At these small wavelengths antenna sizes become small, making them ideal for wireless mobile and personal communications applications. However, electrical signals at these frequencies must be delivered through metallic waveguides or rigid coaxial cables. For remote antenna applications in which the base station antenna may be tens of kilometers from the control station or central office, the high attenuation and cost of waveguide and coaxial cables together with the high cost of electrical repeaters are prohibitive.

For the distribution of millimeter-wave electrical signals over distances of tens of kilometers, a fiber-optic link is a superior option. The advantages of optical fiber are:

- Very low loss
- Very high bandwidth
- Immunity to electromagnetic interference
- Low cost transmission medium
- Flexibility and light weight

Millimeter-wave fiber-optic links offer the advantages of central control of signals and simplified base

station designs. Several methods for distributing mm-wave signals over fiber will be described and demonstrated. At the ends of a mm-wave fiber-optic link, mm-wave optical transmitters and receivers are required. For optical receivers, direct detection photodetectors with bandwidths of up to hundreds of gigahertz have been demonstrated and 60 GHz detectors are commercially available. For optical transmitters, the direct modulation bandwidth of semiconductor lasers is limited to 30 GHz [1]. External optical modulators can be used as mm-wave optical transmitters.

II. EXTERNAL OPTICAL MODULATORS

The operation of an external optical amplitude modulator (EOM) is based on the electro-optic effect of a nonlinear medium such as a lithium niobate crystal. The cosine-squared optical intensity transfer function of an ideal Mach-Zehnder EOM with an RF modulation of $V \cos \omega_{LO} t$ can be expanded using Bessel function identities to give (neglecting terms higher than second-order):

$$I_{out} = \frac{I_{in}}{2} \{ 1 - \sin \Phi [2J_1(m) \cos \omega_{LO} t \mp \dots] \quad (1) \\ + \cos \Phi [J_0(m) - 2J_2(m) \cos 2\omega_{LO} t \pm \dots] \}$$

where $J_n(x)$ is the n th-order Bessel function of the first kind, $\Phi = \pi V_{DC} / V_\pi$ is the modulator phase bias, $m = \pi V / V_\pi$ is the modulation index, V is the RF modulation voltage amplitude, and V_π is the modulator half-wave drive voltage.

With the phase bias set at $\Phi = \pi/2$ ($V_{DC} = V_\pi/2$), Eq. (1) reduces to:

$$I_{out} \cong \frac{I_{in}}{2} [1 - 2J_1(m) \cos \omega_{LO} t] \quad (2)$$

The modulator output intensity consists of a fundamental frequency term and a DC term. Therefore a high-speed EOM can be used to produce an optical carrier at a mm-wave frequency of, for example, $f_{LO} = 38 \text{ GHz}$. High-speed modulators have been demonstrated at frequencies well into the mm-wave frequency band [2]. Using direct detection, a

photodetector converts the intensity modulation to a mm-wave current modulation.

III. MM-WAVE FIBER LINKS

Several methods of transmitting data at millimeter-wave frequencies using an external optical modulator and direct detection are shown in Fig. 1. In Fig. 1(a), the data or IF carriers to be transmitted are upconverted electrically and the resulting mm-wave subcarrier provides the input to the EOM. The EOM must have a very flat electrical frequency response near the mm-wave carrier frequency to limit distortion of the data. The required linearization can complicate the EOM especially if the data is wideband or there are multiple channels. This method was tested in [3].

In Fig. 1(b), the EOM is biased according to the linear case of Eq. (2) and is driven by the mm-wave carrier. The data or IF carriers are used to intensity modulate a laser diode. The laser intensity with electrical modulation is given by:

$$I = I_o (1 + k \cos \omega_{IF} t) \quad (3)$$

where I_o is the optical intensity at the DC bias point. Substituting Eq. (3) for the EOM optical input intensity I_{in} in Eq. (2) gives:

$$I_{out} = \frac{I_o}{2} [1 + k \cos \omega_{IF} t - 2J_1(m) \cos \omega_{LO} t + kJ_1(m) \cos(\omega_{LO} - \omega_{IF}) t + kJ_1(m) \cos(\omega_{LO} + \omega_{IF}) t] \quad (4)$$

Eq. (4) shows that the optical intensity at the EOM output contains the upconverted laser modulation which appears as the sum and difference frequency components. The EOM acts as an optoelectronic upconverter. No separate electrical upconverter is needed, simplifying the downlink architecture. The original laser modulation and electrical frequency components also appear in the EOM optical output intensity. The detector converts the optical intensity to RF signals.

The IF input to the laser diode can either be baseband data or data on a subcarrier. Multiple low frequency subcarriers can intensity modulate the laser diode and linearized low-frequency laser diodes are commercially available. The advantage of using the laser as the IF data input and the EOM as the LO input is that it is the *laser* modulation response, *not* the EOM modulation response, that limits the bandwidth of the data that can be transmitted since the EOM simply multiplies by the LO. Because only a single frequency is used to drive the EOM, a narrowband EOM can be used. No linearization of the modulator is needed because the LO harmonics are at multiples of the mm-wave frequency.

The last type of mm-wave link was investigated and characterized as a method of distributing mm-wave signals

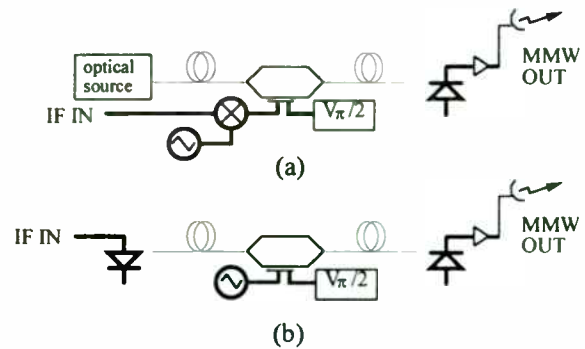


Fig. 1. EOM fiber-optic link configurations. a) electrical upconversion, b) optical upconversion with second harmonic carrier.

between a signal source and an antenna. Because there is a strong fundamental local oscillator component in the optical intensity according to Eq. (4), this method can also be used as a way of distributing the local oscillator signal to base station receiving antennas for future two-way links.

Instead of directly modulating the laser, an EOM can use the data or IF subcarriers to modulate an optical source. Then a second EOM with the mm-wave carrier can be used as the upconverter. Although the optical losses are high, a free-running high power optical source can be used. The use of these cascaded EOMs as a microwave optoelectronic mixer is described in [4].

IV. SYSTEM DESIGN

The experimental mm-wave fiber-digital radio system is shown in Fig. 2. The five blocks on the left-hand side of the figure comprise the digital modulator. A HP3762A Data Generator produces a $2^{15}-1$ pseudo-random binary sequence of NRZ pulses at a bit rate of 5 Mbps for BPSK and 20 Mbps for 16-QAM. The symbol rate for both digital modulation formats is 5 Mbaud. The PRBS is mapped into the desired digital modulation format by a HP8782B-KO3 Digital Video Source/Filter. The I and Q bit streams are filtered with raised-cosine programmable digital filters with $\alpha = 0.3$, and are used by a HP8782B Vector Signal Generator to modulate a 150 MHz carrier. The unfiltered and bandlimited signal spectra of the digitally modulated carrier are shown in Fig. 3.

The mm-wave fiber link consists of a laser, EOM and a high-speed photodiode. The laser transmitter is a commercially available Iptek FiberTrunk-900 1310nm linearized DFB laser transmitter with a bandwidth of 900 MHz. The laser RF input is the 150 MHz digitally modulated carrier. The EOM is a 50 GHz Mach-Zehnder LiNbO₃ optical amplitude modulator [2] that is biased at the half-intensity point and driven at 38 GHz by a HP83650A Synthesized Sweeper. The EOM is used to upconvert the 150 MHz digitally modulated carrier with a 38 GHz carrier. The modulator upconversion loss at 38 GHz compared to the detected power at 150 MHz was

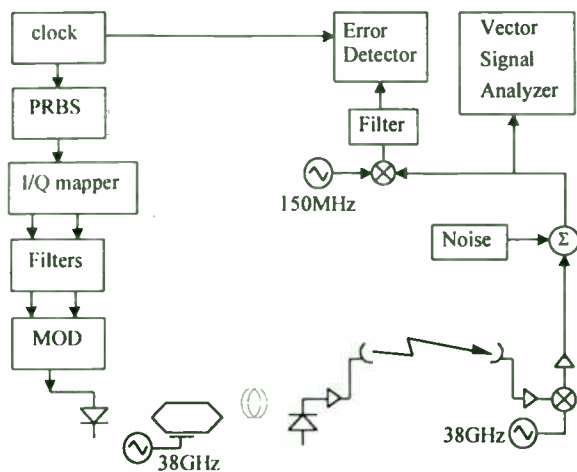


Fig. 2. The mm-wave fiber-digital radio system.

about 18 dB, which corresponds to an EOM modulation depth of $m=0.25$. Although this loss is rather high, Eq. (4) shows that it is dependent on the EOM modulation depth m which can be increased. For example, with $m=0.8$, the conversion loss will be $[J_1(m)]^2 = 8.7$ dB. A high modulation depth can be achieved because LO harmonics are out of the frequency band. Because the laser is linearized, the IF harmonics are low and consequently the intermodulation products will be low.

The mm-wave signals are sent through about 5 m of single mode fiber. The optical power at the fiber output was about 1 mW. The base station consists of the high-speed photodiode, a high-power mm-wave amplifier, and an antenna. The transmit subcarrier power of the sidebands is less than -30 dBm. The RF spectrum of the transmitted signal is shown in Fig. 4, showing the sum and difference products produced by the upconversion process. Because there is no image rejection by the upconverter, in a real system bandpass filters would be used to limit the spectrum to one of the sidebands of the 38 GHz carrier. 38 GHz bandpass filters were unavailable for this experiment.

The path from the transmitting antenna to receiving antenna is line-of-site. The radio link loss is about 34 dB at 38 GHz. For a terrestrial line-of-site link, the Friis free-space transmission formula[5] with high gain antennas of 35 dB gives a propagation distance of about 100 meters. Distances on the order of kilometers can be reached with a higher transmitter power. The transmitter power in this experiment was low due to a lack of amplification at 38 GHz.

The receiver downconverts the received 38 GHz signal back down to 150 MHz. It consists of a mm-wave antenna, a mm-wave mixer and amplifiers. The recovered digitally modulated carrier is demodulated and decoded by the HP89440A Vector Signal Analyzer or the HP8981A Vector Modulation Analyzer. It can also be downconverted to baseband, filtered and analyzed using the HP3763A

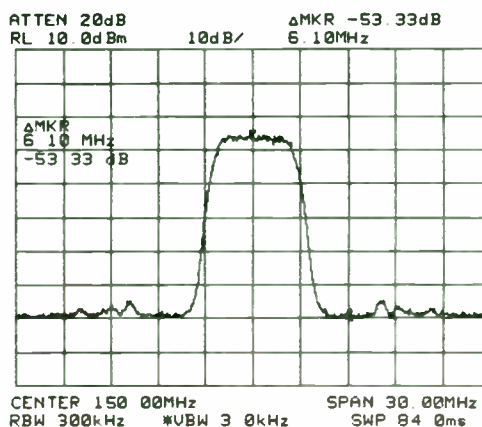
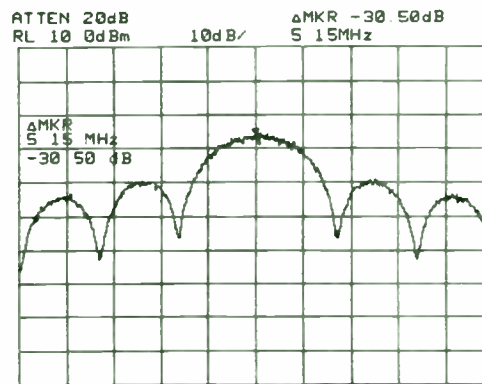


Fig. 3. The unfiltered (top) and bandlimited (bottom) spectra of the 150MHz digitally modulated carrier. (Symbol rate = 5 Mbaud, raised-cosine filter roll-off factor = 0.3, carrier power = 0 dBm.)

Error Detector. White noise can be added at the receiver end using the HP3708A Noise and Interference Test Set.

V. SYSTEM PERFORMANCE

The maximum received carrier-to-noise ratio measured at the downconverted IF frequency of 150 MHz was 32 dB. The bit-error rate for a 5 Mbps BPSK digital modulation format was measured as a function of carrier-to-noise ratio which was varied using the white noise generator. Square-root-raised-cosine filters corresponding to a roll-off factor of $\alpha = 0.3$ were used at the transmitter and receiver to provide Nyquist filtering. The results are shown in Fig. 5. The error rate measurements were subject to imperfect filtering and limited decision level sensitivity at the receiver.

High-order digital modulation formats were also sent across the mm-wave fiber-radio links. 16-QAM was successfully received as shown by the constellation, measured on the HP 8981A, in Fig. 6. The input bit stream was a PRBS of NRZ pulses at a bit rate of 20 Mbps, giving a symbol rate of 5 Mbaud. The I and Q streams were filtered using raised-cosine digital filters with a roll-off factor of $\alpha = 0.3$. This corresponds to a spectral efficiency

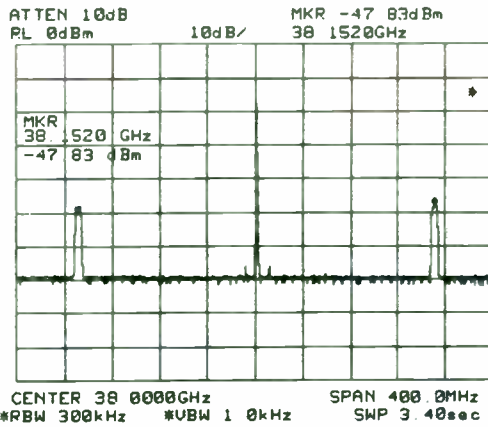


Fig. 4. The 38 GHz transmitted spectrum showing the upconverted sum and difference products. The frequency separation of the sidebands from the 38 GHz tone is 150 MHz which corresponds to the frequency of the digitally modulated carrier.

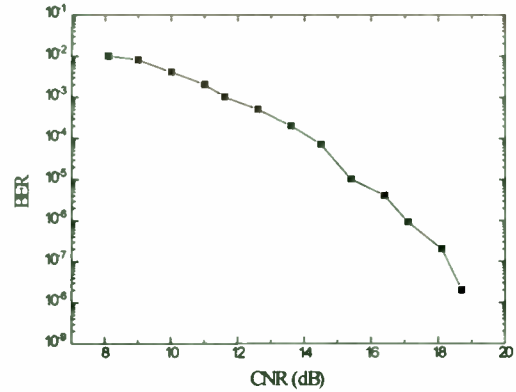


Fig. 5. BER for a 5 Mbps BPSK signal. The signal bandwidth is 6.5 MHz corresponding to the raised-cosine filter roll-off factor of 0.3.

of 3.1 b/s/Hz. As shown in Fig. 6, the I and Q closures were about 15% for the 16-QAM case. The carrier power at the input to the HP 8981A was -6 dBm with a carrier-to-noise density of about 96 dB/Hz. With low noise amplifiers, a higher power laser with a lower relative intensity noise, and a higher transmitter power the carrier-to-noise will improve and the closures will be reduced.

The highest spectral efficiency was achieved using the 64-QAM digital modulation format. Using a bit rate of 30 Mbps, 64-QAM was successfully transmitted at a symbol rate of 5 Mbaud. The same digital filters were used, giving a spectral efficiency of 4.6 b/s/Hz. The constellation as measured on the HP 8981A Vector Modulation Analyzer is shown in Fig. 7, with I and Q closures of about 36%. Clearly as the constellation becomes more complex, the signal-to-noise requirements increase.

To observe the effects of fiber, the fiber length was extended to 20 km. The total fiber loss for 20 km of single-mode fiber was 7 dB which corresponds to an electrical loss of 14 dB and there is no fiber dispersion at the 1310nm wavelength. The received optical power at the photodetector was 284μW. The detected signal was amplified to a transmission power of -36 dBm. As before, the link loss was about 34 dB. A CNR of 22 dB was obtained which was limited mainly by the low transmitter power. A BER of 3×10^{-5} for BPSK was measured which was limited by the sensitivity of the error detector. Again, a higher transmitter power should improve the system performance.

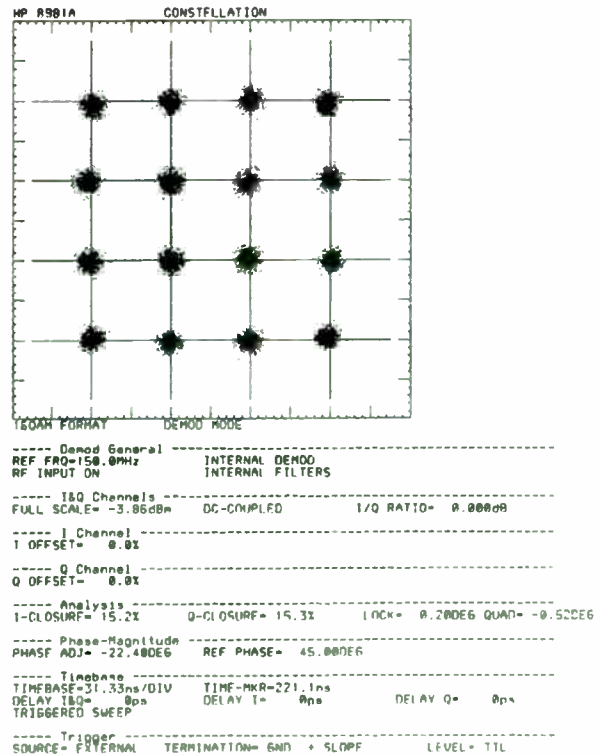


Fig. 6. The received constellation for 16-QAM.

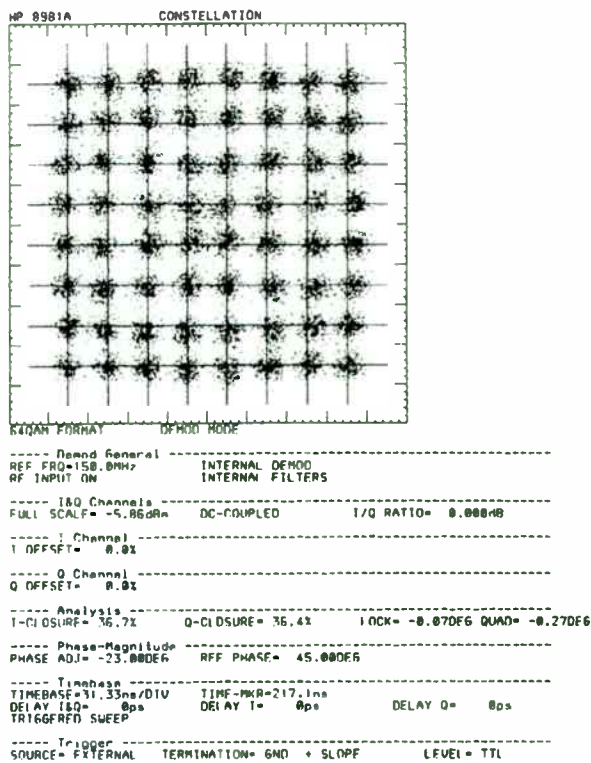


Fig. 7. The received constellation for 64-QAM.

VI. CONCLUSION

To demonstrate the distribution of mm-wave signals for antenna remoting applications and for 38 GHz digital radio links, a digital mm-wave fiber-optic link configuration was analyzed and tested. By using the EOM as an optoelectronic upconverter, no electrical upconverter is needed. Using direct modulation of a laser diode takes advantage of commercially available multi-channel linearized lasers. High spectral efficiency, high-order digital modulation formats were successfully transmitted over the mm-wave fiber-digital radio link. The highest spectral efficiency of 4.6 b/s/Hz was achieved with 64-QAM. In addition, digital transmission over a 20km fiber link was demonstrated. As 38 GHz millimeter-wave electrical and electro-optic components become more available, increased transmit powers and carrier-to-noise ratios are expected.

ACKNOWLEDGEMENTS

The authors would like to thank L.B. Aronson and D.W. Dolfi of Hewlett Packard Laboratories and D. Scherer of Hewlett Packard Company, MCG, for valuable discussions, assistance, and optoelectronic components.

REFERENCES

- [1] S.D. Offsey, L.F. Lester, W.J. Schaff, and L.F. Eastman, "High-speed modulation of strained-layer InGaAs-GaAs-AlGaAs ridge waveguide multiple quantum well lasers," *Appl. Phys. Lett.*, vol. 58, no. 21, pp.

2336-2338, May 27, 1991.

- [2] D.W. Dolfi and T.R. Ranganath, "50 GHz Velocity-Matched Broad Wavelength LiNbO₃ Modulator with Multimode Active Section," *Electronics Letters*, vol. 28, no. 13, June 18, 1992, pp.1197-1198.
- [3] H. Ogawa, D. Polifko and S. Banba, "Millimeter-Wave Fiber Optics Systems for Personal Radio Communication," *IEEE Trans. Microwave Theory Tech.*, vol. 40, no. 12, Dec. 1992, pp.2285-2293.
- [4] G.K. Gopalakrishnan, W.K. Burns, and C.H. Bulmer, "A LiNbO₃ Microwave-Optoelectronic Mixer with Linear Performance," in *IEEE MTT-S Int. Microwave Symposium Digest*, June 1993, vol.2, pp. 1055-1058.
- [5] M.D. Yacoub, *Foundations of Mobile Radio Engineering*, CRC Press, Boca Raton, FL, 1993, p. 68.

